

Topics in Organometallic Chemistry 50

Eike Bauer *Editor*

Iron Catalysis II

 Springer

Editorial Board

M. Beller, Rostock, Germany

J.M. Brown, Oxford, United Kingdom

P.H. Dixneuf, Rennes, France

J. Dupont, Porto Alegre, Brazil

A. Fürstner, Mülheim, Germany

Frank Glorius, Münster, Germany

L.J. Gooßen, Kaiserslautern, Germany

T. Ikariya, Tokyo, Japan

S. Nolan, St Andrews, United Kingdom

Jun Okuda, Aachen, Germany

L.A. Oro, Zaragoza, Spain

Q.-L. Zhou, Tianjin, China

Aims and Scope

The series *Topics in Organometallic Chemistry* presents critical overviews of research results in organometallic chemistry. As our understanding of organometallic structure, properties and mechanisms increases, new ways are opened for the design of organometallic compounds and reactions tailored to the needs of such diverse areas as organic synthesis, medical research, biology and materials science. Thus the scope of coverage includes a broad range of topics of pure and applied organometallic chemistry, where new breakthroughs are being achieved that are of significance to a larger scientific audience.

The individual volumes of *Topics in Organometallic Chemistry* are thematic. Review articles are generally invited by the volume editors. All chapters from *Topics in Organometallic Chemistry* are published OnlineFirst with an individual DOI. In references, *Topics in Organometallic Chemistry* is abbreviated as *Top Organomet Chem* and cited as a journal.

More information about this series at
<http://www.springer.com/series/3418>

Eike Bauer

Editor

Iron Catalysis II

With contributions by

E.B. Bauer · R.B. Bedford · P.B. Brenner · P.-A.R. Breuil ·
G.J.P. Britovsek · B. Burcher · C. Darcel · D.P. de Sousa ·
S. Gaillard · M. Grau · M. Itazaki · H. Keipour · L. Magna ·
C.J. McKenzie · H. Nakazawa · H. Olivier-Bourbigou ·
T. Ollevier · J.-L. Renaud · J.-B. Sortais



Springer

Editor

Eike Bauer

Dept. of Chemistry and Biochemistry

University of Missouri - St. Louis, One University Boulevard

St. Louis, Missouri

USA

ISSN 1436-6002

ISSN 1616-8534 (electronic)

Topics in Organometallic Chemistry

ISBN 978-3-319-19395-3

ISBN 978-3-319-19396-0 (eBook)

DOI 10.1007/978-3-319-19396-0

Library of Congress Control Number: 2015945936

Springer Cham Heidelberg New York Dordrecht London

© Springer International Publishing Switzerland 2015

This work is subject to copyright. All rights are reserved by the Publisher, whether the whole or part of the material is concerned, specifically the rights of translation, reprinting, reuse of illustrations, recitation, broadcasting, reproduction on microfilms or in any other physical way, and transmission or information storage and retrieval, electronic adaptation, computer software, or by similar or dissimilar methodology now known or hereafter developed.

The use of general descriptive names, registered names, trademarks, service marks, etc. in this publication does not imply, even in the absence of a specific statement, that such names are exempt from the relevant protective laws and regulations and therefore free for general use.

The publisher, the authors and the editors are safe to assume that the advice and information in this book are believed to be true and accurate at the date of publication. Neither the publisher nor the authors or the editors give a warranty, express or implied, with respect to the material contained herein or for any errors or omissions that may have been made.

Printed on acid-free paper

Springer International Publishing AG Switzerland is part of Springer Science+Business Media (www.springer.com)

Preface

Catalysis is a fundamental chemical principle with huge significance in both industry and academia. Catalysts save energy and resources, increase selectivities and yields, and make compounds accessible that are otherwise difficult or impossible to synthesize. The economic impact of catalysis is tremendous and difficult to quantify. The *Pacific Northwest National Laboratory* states that the economic impact of catalysis has been valued to be over 10 trillion dollars per year worldwide. The American Chemical Society estimates that *85% of all chemical products being produced use at least one catalytic step.*

The field of homogeneous catalysis has been dominated in the last 30 years by either early or precious transition metals such as titanium, osmium, rhodium, palladium, or ruthenium. This is well demonstrated by the Nobel prizes awarded for homogeneous catalysis in 2001, 2005, and 2010, which are all related to these metals and which underline the significance of the field. However, there are serious issues associated with these metals. Due to their low natural abundance, they are high and volatile in price, and they are present in metal rich ores in only small concentrations. Furthermore, these metals are also of interest in the automotive industry and in the consumer electronic sector, creating extra competition for their sources. Finally, the toxicity poses a serious problem, e.g., in the pharmaceutical industry, where only trace amounts of toxic metals can be present in the final product to meet quality standards set by authorities.

In turn, homogeneous iron catalysis was for many years a “Sleeping Beauty” and was not as extensively investigated compared to the other metals mentioned above. Heterogeneous iron catalysis, though, has been applied for at least a century for example as in the Haber–Bosch or Fischer–Tropsch processes. However, applications in the synthesis of fine chemicals were scarce to nonexistent. This changed around the turn of the century, when the chemical community started realizing that iron has a number of advantages compared to the other metals typically applied in homogeneous catalysis. Iron is relatively cheap, nontoxic, and tolerant to a number of functional groups, making it an interesting alternative to other transition metals typically applied in catalysis, especially for applications in pharmaceutical

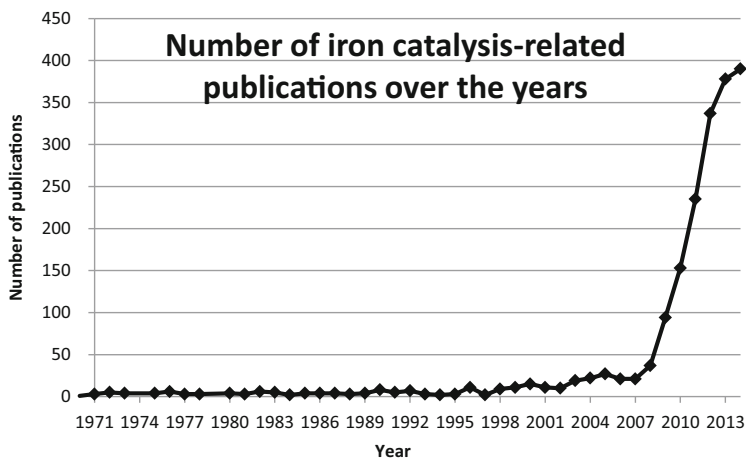


Fig. 1 Publication activity in iron catalysis over the years

industry. Its eco friendliness and catalytic activity are in line with two major principles of Green Chemistry, which calls for both catalytic processes and for chemicals that *pose little or no toxicity to human health and the environment*.

These aspects promoted increasing research activity in the field starting about 15 years ago. More and more research groups turned to iron as a basis for catalytic applications, as demonstrated by an increasing number of research articles published in the area. About 5 years ago, the field began a self-reflection. Matthias Beller raised the question of *Sustainable Metal Catalysis with Iron: From Rust to a Rising Star?* in an *Angewandte Chemie* article in 2008. In 2009, Carsten Bolm proclaimed a new *Iron Age* in a *Nature Chemistry* article. Alois Fürstner described iron as a *base metal for a noble task*. The journal *Organometallics* devoted a special issue in 2014 to the *Catalytic and Organometallic Chemistry of Earth-Abundant Metals*. The magazine *Science* published in the last 5 years 6 articles related to iron catalysis. Three of them were also highlighted in the *New York Times* in December 2013. In this article, Robert Morris, a player in the field, was quoted as saying *It shows that with the right organic molecules attached to it, we can make iron do things that weren't thought possible before*.

A look at the number of publications in the field corroborates the proclamation of a new *Iron Age*. I performed a Scopus® search in January 2015 for journal articles containing the phrase “iron catalysis”. The result is depicted in Fig. 1, where the number of publications is plotted against the year of their appearance. Before around 2000, only a single digit number of publications under the search phrase were published each year. An exponential increase of publications can be observed starting around 2009.

This book provides an overview of the increasing research activities in the field of homogeneous iron catalysis. It is organized under the aspect of synthetic applications of iron catalysis, mainly in the area of the production of fine chemicals

or polymers. The advances in coupling, oxidation, reduction, and polymerization reactions in the last 5 years are covered, and enantioselective as well as stoichiometric reactions of iron complexes (which play an important role in the development of catalytic processes) are also highlighted.

The book outlines new avenues for the production of a variety of organic compounds under iron catalysis. Challenges still remain. Iron complexes exhibit a number of features that are not prevalent for other transition metals. Iron is stable in a variety of oxidation states, with +2 and +3 being probably the most prevalent ones for precatalysts. Iron can undergo redox chemistry, which can be promoted by the ligands supporting a catalytically active iron complex. Many oxidation states of iron can produce paramagnetic iron complexes, which makes their investigation by NMR challenging.

Turning to iron is a smart move from both economic and environmental points of view. Still, it appears that homogeneous iron catalysis is not as common in the industrial production of fine chemicals compared to other transition metals. Some iron-catalyzed processes still require high reaction temperatures, which might be problematic for sensitive substrates as often encountered in pharmaceutical industry. However, it can be expected that the vigorous research activities in the field will provide solutions for these challenges. This book is meant to inspire chemists in the field of catalysis or chemical production to consider iron as a valuable alternative in the production of chemicals at all stages of the supply chain. Our knowledge of iron catalysis will grow as additional researchers begin investigating its potential from different perspectives. This will be important, because to say it with the words of Morris Bullock in relation to the aforementioned *Science* articles: *there is no exclusive single 'recipe' for success in developing catalysts based on cheap metals.*

St. Louis, MO, USA

Eike Bauer

Contents

Iron Catalysis: Historic Overview and Current Trends	1
Eike B. Bauer	
The Development of Iron Catalysts for Cross-Coupling Reactions . . .	19
Robin B. Bedford and Peter B. Brenner	
Iron-Catalyzed Cross-Dehydrogenative-Coupling Reactions	47
Masumi Itazaki and Hiroshi Nakazawa	
Iron-Catalyzed Carbon–Nitrogen, Carbon–Phosphorus, and Carbon–Sulfur Bond Formation and Cyclization Reactions	83
Jean-Luc Renaud and Sylvain Gaillard	
High-Valent Iron in Biomimetic Alkane Oxidation Catalysis	145
Michaela Grau and George J.P. Britovsek	
Iron-Catalyzed Reduction and Hydroelementation Reactions	173
Christophe Darcel and Jean-Baptiste Sortais	
Iron-Catalyzed Oligomerization and Polymerization Reactions	217
Benjamin Burcher, Pierre-Alain R. Breuil, Lionel Magna, and H�el�ene Olivier-Bourbigou	
Enantioselective Iron Catalysts	259
Thierry Ollevier and Hoda Keipour	
Molecular Iron-Based Oxidants and Their Stoichiometric Reactions	311
David P. de Sousa and Christine J. McKenzie	
Index	357

Iron Catalysis: Historic Overview and Current Trends

Eike B. Bauer

Abstract Iron catalysis is a growing area of research, as seen by an exponential increase in the publication activities on the topic. This introductory chapter provides a historic overview of the development of iron catalysis including some notable milestones. The advantages of iron, i.e., its abundance, low price, and relative nontoxicity, are discussed, and an overview of the main type of reactions catalyzed by iron is outlined. The advances of heterogeneous iron catalysis (which is not covered in this volume) are exemplified with a few notable cases. Finally, the potential impact of metal impurities in iron sources on the catalytic activity is discussed.

Keywords History of iron catalysis · Iron abundance · Iron catalysis · Iron toxicity · Metal Impurities in Iron Catalysis

Contents

1	Introduction	2
2	Abundance and Low Toxicity	2
3	Historic Development	4
4	Overview of Main Reactions That Are Catalyzed Under Homogeneous Conditions by Iron Complexes	6
4.1	C–C Bond-Forming Reactions	7
4.2	C–Heteroatom and Heteroatom–Heteroatom Bond-Forming Reactions	9
4.3	Oxidation Reactions	10
4.4	Reduction Reactions	11
4.5	Polymerization Reactions	12
4.6	Enantioselective Iron Catalysis and Stoichiometric Considerations	13

E.B. Bauer (✉)

Department of Chemistry and Biochemistry, University of Missouri – St. Louis, One University Boulevard, St. Louis, MO 63121, USA

e-mail: bauere@umsl.edu

5	Impurities in Iron Metal as the Actual Catalyst?	14
6	Recent Heterogeneous Applications of Iron	15
7	Outlook	16
	References	16

1 Introduction

As already outlined in the preface to this volume, increasing research activities are currently emerging in the area of iron catalysis. This is evidenced by an exponentially growing number of publications in the area as well as an increasing number of review articles, books, special issues, or some highlight articles in the mainstream press that appeared on the topic. This chapter outlines some of the advances of iron catalysis (i.e., the abundance and low toxicity of iron) and provides the reader with a historic overview and outlines some current trends in iron catalysis. The chapter is not meant to be comprehensive. It gives readers who lack familiarity with the topic the opportunity to learn some fundamental aspects of iron catalysis. For in-depth descriptions of some of the topics, the readers are referred to the subsequent chapters of this volume.

2 Abundance and Low Toxicity

Two major advantages of iron-based catalysts are regularly stated throughout the literature: the abundance (and, consequently, its low price) and the relative nontoxicity of iron. Both aspects have major impact on the practical applications of iron catalysis.

Iron is the fourth most abundant element in the Earth's crust, accounting for around 6% of its mass [1]. Only oxygen (47%), silicon (26%), and aluminum (8%) are more abundant on the surface of the earth. However, the core of the Earth is believed to be mainly composed of an iron–nickel alloy, and taking the composition of the Earth as a whole under consideration, it is made up of 32% by weight iron [1]. The geological composition and the occurrence of iron are linked to its nucleosynthesis. Iron is synthesized in dying stars through fusion of lighter elements. The nuclear fusion releases energy up to elements in the iron group (Fe, Co, Ni). The formation of heavier elements requires energy, giving iron a special status during its synthesis in dying stars and supernovae [1].

Its abundance makes iron a readily available, cheap metal. This is reflected in the world market price for iron compared to other, more precious metals. In February 2015, one troy ounce (28.3 g) of palladium was US\$ 788, and one ounce of platinum was US\$ 1230; one metric ton of iron ore was US\$ 62.

The abundance of iron might be responsible for the fact that iron is relatively nontoxic to humans. Indeed, iron is an essential nutrient for living systems, and the

human body contains 3–5 g iron [2]. Iron forms the basis for a number of metalloproteins that can be found in living cells and that play a major role in metabolism. Hemoglobin, the carrier of oxygen in red blood cells, is probably the best known example; it consists of an iron porphyrin prosthetic group, which also forms the base for other enzymes, such as cytochromes [3]. Extracellularly, iron is bound in the human body to transferrin, which serves as the iron carrier in the plasma [2]. It is transported into cells through transferrin receptors, where it is utilized in metabolism through iron-containing proteins. Intracellularly, iron is “detoxified” through binding to ferritin [2]. As can be seen, iron is essential for living systems. The human body has recognized transport and storage of iron, unlike for other, less abundant metals, which cannot be found in living systems. That contributes to the relative nontoxicity of iron.

However, it needs to be stated that an iron overload in the human body can cause severe health problems [2]. Mammals do not have the capability of active iron excretion [2]. An excess of iron in the human body can give rise to the formation of reactive oxygen intermediates (such as hydroxy radicals) through the Fe(II)/Fe(III) redox couple and Fenton chemistry (which is, from a synthetic point of view, further outlined by George Britovsek in [4]). Once the concentration of these reactive oxygen intermediates reaches a critical level, “oxidative stress” ensues, and the intermediates attack and cause degeneration of essential building blocks of the body such as enzymes or cell membranes [2]. Furthermore, iron has been related to atherosclerosis as well as Alzheimer’s disease [5]. Iron toxicity can also occur in plants when a toxic concentration of the metal is accumulated in their leaves [6].

Still, iron is far less toxic than other transition metals typically utilized in catalysis, and the issues described in the previous paragraph typically play no role in iron catalysis. The practical consequence of the relatively low toxicity of iron translates to a real bonus for the pharmaceutical industry. Final pharmaceutical products must only contain trace amounts of residual metals that might have been left over in the process of synthesizing the drug, generally through the catalysts utilized in synthetic steps. As suggested in 2013 in the United States Pharmacopeial Convention, the concentration limit for an oral drug with a maximum daily dose of 10 g/day is 10 µg/g for each of ruthenium, osmium, palladium, iridium, and platinum. By contrast, no value for the maximum level is presented for iron [7].

In 2007 the European Medicines Agency categorized iron as a *metal with minimal safety concern* [8]. The agency suggested a concentration limit of 10 ppm for Pt and Pd and of 10 ppm of any combination of Ir, Rh, Ru, and Os. A concentration limit of 1,300 ppm of iron in a final pharmaceutical product was suggested.

These values demonstrate the low toxicity of iron compared to other metals, when present in small amounts. This has an impact on the pharmaceutical industry. When toxic metals are employed in drug synthesis, pharmaceutical companies have to make special effort to remove these metals from the final product in order to meet quality standards, e.g., chemically [9] or through the application of supported catalysts [10]. Such efforts are not necessary (or at least not as extensive) when iron is used as a reagent or catalyst. This volume is intended to show catalytic

applications of iron in organic syntheses, and we think that its relatively low toxicity makes it a good candidate for industrial applications.

3 Historic Development

Historically, iron has been applied as a heterogeneous catalyst for more than a century. Milestones related to iron catalysis are compiled in Fig. 1. The Haber–Bosch process – the synthesis of ammonia from its elements nitrogen and hydrogen – was patented in 1910 [11]. It utilizes a heterogeneous iron catalyst, which promotes the kinetically determined cleavage of the $\text{N}\equiv\text{N}$ triple bond, a critical step in the catalytic cycle. The ammonia obtained through this process plays an enormous role in the synthesis of fertilizers. The search for more efficient iron-based catalysts for the reaction is ongoing [12, 13].

The Haber–Bosch process requires high temperatures and pressures (500°C, 200 bar), which is its major disadvantage. On the other hand, there are iron-containing nitrogenases known in nature which reduce nitrogen under ambient temperatures and pressures through a number of proton and electron transfer steps. Research in the area of “nitrogen fixation” is directed toward the development of transition metal catalysts to perform nitrogen reduction under

Iron Catalysis Timeline
1894 – Fenton oxidation chemistry published
1910 – Haber-Bosch process patented
1925 – Fischer-Tropsch process developed
1944 – First iron-catalyzed cross-coupling reported
1951 – First preparation of ferrocene
1953 – Reppe carbonylation of ethylene by a homogeneous iron catalyst
1959 – Determination of the structure of Hemoglobin
1971 – Kochi, further investigations on iron-catalyzed cross-coupling reactions
1979 – Iron porphyrin complexes catalyze epoxidation reactions
1983 – Catalytic enantioselective epoxidations with chiral iron-porphyrin complexes
1998 – Efficient iron catalysts for ethylene polymerization
2000s – Intensification of research in iron-catalyzed cross-coupling reactions and enantioselective transfer hydrogenations
Since 2010 – Rapid development in all fields of iron catalysis

Fig. 1 Iron catalysis timeline

homogeneous and ambient conditions [14]. Most nitrogenases consist of a Fe/Mo cofactor; artificial, molybdenum-based catalyst systems are currently the best performing ones. However, Peters showed in recent work that certain single site iron complexes can also be catalytically active for the reaction [15]. Still, there is currently no catalytic system known that performs nitrogen fixation under aerobic conditions at standard temperature and pressure [14].

The Fischer–Tropsch process, i.e., the conversion of a mixture of CO and H₂ (“synthesis gas”) to obtain hydrocarbons, was developed around 1925 [16]. The synthesis gas utilized in this process can be obtained from many carbon-containing sources such as coal or biomass and thus plays a role in energy supply that is independent from raw oil. As for the Haber–Bosch process, iron-based catalysts are utilized for the Fischer–Tropsch process and research is performed presently to optimize the system [17, 18]. Homogeneous Reppe chemistry (the hydroformylation of olefins using CO and water to obtain alcohols and aldehydes) was first reported in 1953 to be catalyzed by Fe(CO)₅, and similar optimization efforts as described above for other processes have also been reported for this system [19].

As for many industrial applications of catalysts, the iron systems for both Fischer–Tropsch and Haber–Bosch are heterogeneous. Homogeneous catalysis based on transition metals was significantly advanced in the second half of the twentieth century. This might be exemplified by the development of Wilkinson’s catalyst [RhCl(PPh₃)₃] for the hydrogenation of olefins around 1965 [20], the development of asymmetric rhodium-based catalysts for the same reactions around 1968 [21], and the extensive mechanistic investigations of these systems in the 1970s [22, 23]. Since then, homogeneous transition metal catalysis became a major branch of organometallic chemistry, and iron played only a minor role in the early stages of these developments. Following the pioneering work by Vavon and Mottez in the 1940s [24], Kochi reported in the early 1970s that the Kumada cross-coupling reaction of Grignard reagents with organic halides is catalyzed by iron salts. However, major advances in homogeneous catalysis were mainly reported for metals such as Rh, Pd, Ru, Pt, or Ti.

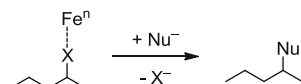
This changed somewhat in the late 1970s when the course of oxygen transfer from an iron porphyrin complex to a substrate was investigated, quickly leading to iron porphyrin catalysts for oxidation reactions [25], of which soon thereafter enantioselective versions were reported (this chemistry is further outlined by George Britovsek in [4]). In the late 1990s, Brookhart [26] and Gibson [27] discovered that bis(imino)pyridyl iron complexes were efficient catalysts for ethylene polymerization reactions, which initiated vigorous research activities in the field. Polymerization reactions are further discussed by H el ene Olivier-Bourbigou in [28]. The field of iron-catalyzed cross-coupling reactions – based on Vavon’s early work in the 1940s and Kochi’s findings in the early 1970s – was revitalized in the early 2000s, as described by Robin Bedford in [29]. Since then, increased research activities can be observed in all branches of the field [30–34].

4 Overview of Main Reactions That Are Catalyzed Under Homogeneous Conditions by Iron Complexes

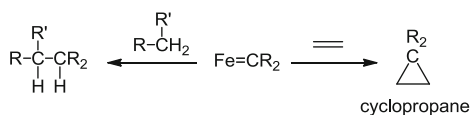
The volume is organized by reaction types that are catalyzed by a variety of iron-based catalyst systems. This section is meant to give readers who are not so familiar with iron chemistry an overview of the main types of iron-catalyzed processes. The compilation is not comprehensive, and readers are referred to the subsequent chapters for a more detailed account of the different reaction types.

The role of iron in catalytic cycles is multifaceted, as illustrated in Scheme 1. It can simply act as Lewis acid, and, for example, promote the formation of carbocation intermediates (Scheme 1a) [35]. Iron–nitrene or carbene intermediates $\text{Fe}=\text{NR}$ and $\text{Fe}=\text{CR}_2$ can transfer carbon or nitrogen species to double bonds, forming aziridines or cyclopropanes (Scheme 1b, c) [36, 37]. The intermediates can

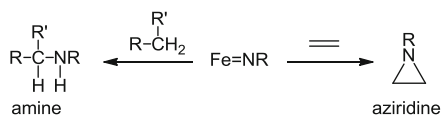
a Fe^n as Lewis acid.



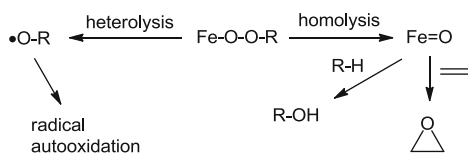
b $\text{Fe}=\text{CR}_2$ intermediates for carbene transfer and insertion.



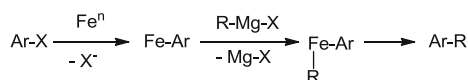
c $\text{Fe}=\text{NR}$ intermediates for nitrene transfer and insertion.



d Fe-O-O-R intermediates in oxidation chemistry (simplified).



e Low valent iron species Fe^n in cross coupling chemistry ($n < 2$), simplified.



Scheme 1 General reactivities of iron species

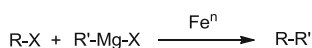
also insert a CR_2 or NR unit into a C-H bond (the latter one forming an amine upon insertion). Through single electron transfer processes and/or through the formation of $\text{Fe}^{\text{n}}\text{-O-O-R}$ or $\text{Fe}^{\text{n}} = \text{O}$ species, iron can activate peroxides and other oxidants for catalytic oxidation reactions (Scheme 1d) [38]. Low-valent iron complexes can be engaged in cross-coupling reactions, following oxidative addition, reductive elimination, or ligand exchange processes (Scheme 1e) [39]. The properties of iron can be tuned through their supporting ligands toward any of these processes, making it applicable in a variety of catalytic transformations.

4.1 C–C Bond-Forming Reactions

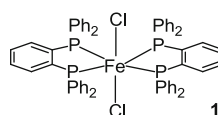
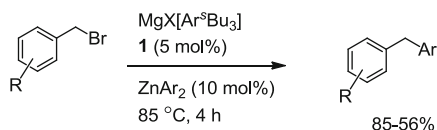
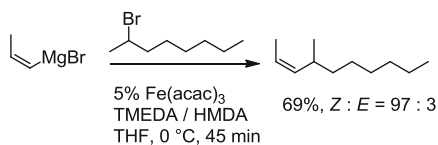
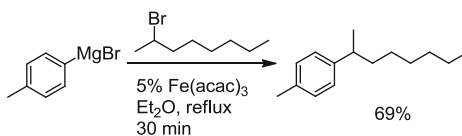
Coupling reactions to obtain larger units from small building blocks is the core challenge in many synthetic transformations. Numerous coupling reactions based on transition metals are known, and iron is increasingly utilized. Carbon–carbon bonds through iron catalysis are mainly formed either through coupling of a nucleophile with an electrophile (Scheme 2) or through cross dehydrogenative coupling (CDC, Scheme 3).

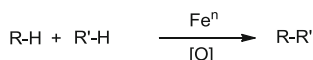
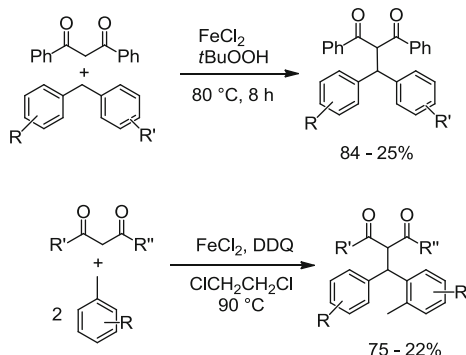
Scheme 2 Iron-catalyzed cross-coupling reactions [40–42]

a Generalized cross coupling reaction.



b Representative examples



Scheme 3 Dehydrogenative cross-coupling reactions [43, 44]**a Generalized cross dehydrogenative coupling****b Representative examples**

The general pattern of coupling a nucleophile with an electrophile is shown in Scheme 2 together with some notable iron-catalyzed examples [40–42]. This chemistry will be described further by Robin Bedford in [29]. As outlined above, it has been known for a while that Grignard reactions can be accelerated by the presence of small amounts of iron salts [45], and Vavon and Mottez reported iron-catalyzed cross coupling as early as 1944 [24]. Kochi expanded these findings in the early 1970s by publishing the Kumada couplings of alkenyl halides with Grignard reagents that were catalyzed by iron salts [46]. The coupling of Grignard reagents with electrophilic carbon atoms is most common, mainly those that contain a halogen leaving group. The discovery of the beneficial impact of NMP (*N*-methylpyrrolidone) as cosolvent or TMEDA as an additive [47] was only two milestones in the development of the reaction. As outlined by Robin Bedford in [29], some challenges still need to be addressed for the reaction. The role of cosolvents or additives is still not really well understood. Also, the employment of nucleophiles beyond Grignard reagents (e.g., based on zinc or boron) needs to be further pursued, and efforts in this direction appeared recently in the literature [48, 49]. Finally, further mechanistic investigations are necessary, as little is currently known concerning the nature (and especially the oxidation state) of the catalytically active iron species.

A different approach to carbon–carbon bond-forming reactions involves the cross dehydrogenative coupling (CDC, Scheme 3) of two C–H bearing units under the formal elimination of hydrogen [50]. This chemistry is further explained by Masumi Itazaki and Hiroshi Nakazawa in [51]. Two notable examples of the reaction are shown in Scheme 3 [43, 44]. Li pioneered the reaction catalyzed by iron in his work published in 2007 [43]. The reaction typically proceeds under oxidative conditions, with *t*BuOO*t*Bu, DDQ (2,3-dichloro-5,6-dicyano-1,4-benzoquinone), or $\text{K}_2\text{S}_2\text{O}_8$ commonly applied as oxidants. Carbon atoms of different

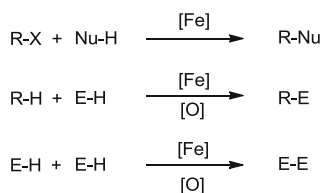
hybridizations can be connected, and a carbon–heteroatom and a heteroatom–heteroatom bond can also be formed through cross dehydrogenative coupling. The latter two types of cross dehydrogenative couplings are further discussed by Jean-Luc Renaud in [52].

4.2 C–Heteroatom and Heteroatom–Heteroatom Bond-Forming Reactions

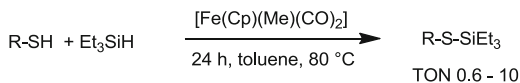
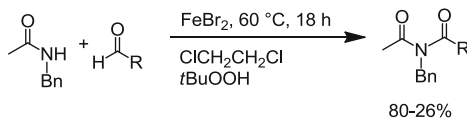
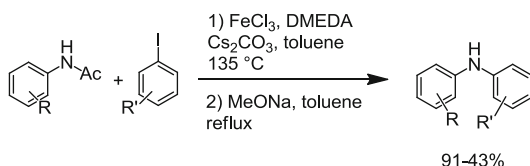
The generalized formation of carbon–heteroatom and heteroatom–heteroatom bonds is depicted in Scheme 4, along with some prototypical examples [53–55]. The chemistry is discussed in detail by Jean-Luc Renaud in [52]. Carbon–heteroatom bonds can be formed by the reaction of a heteroatom nucleophile with a carbon-based electrophile or through CDC. A variety of heteroatoms can be employed, and consequently the methodology is diverse. Intra- or intermolecular cyclization reactions to form heterocycles are also possible.

Scheme 4 Dehydrogenative cross-coupling reactions [53–55]

a Generalized C-heteroatom and heteroatom–heteroatom bond formation



b Representative examples



In many of the reactions employing a heteroatom nucleophile and a carbon-based electrophile, iron acts as a Lewis acid and bases are added to the reaction to help neutralize the H–X formed through the reaction. As outlined in [52], while some of the reactions require high reaction temperatures, intramolecular cyclization reactions often proceed under milder conditions. In a perspective drawn by Jean-Luc Renaud, simple iron salts could be replaced by iron complexes bearing supporting ligands, which might allow some of the reactions in [52] to proceed under milder conditions at a higher selectivity and potentially with a lower catalyst loading.

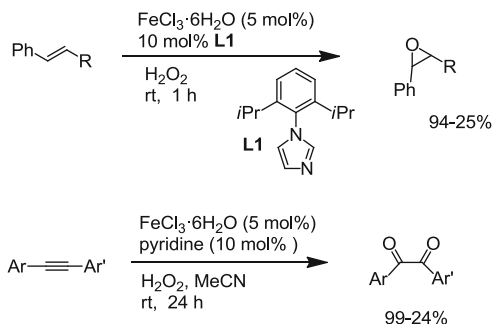
4.3 Oxidation Reactions

Fenton chemistry, i.e., the ability of iron salts in combination with hydrogen peroxide to oxidize substrates, has been known for over 100 years [56]. It is based on hydroxyl ($\cdot\text{OH}$) radicals and, as such, is not very chemo- and regioselective. Fenton chemistry is utilized in wastewater treatment to destroy organic contaminants [57]. Gif chemistry was introduced by Barton at the beginning of the 1980s and consists of a number of catalyst systems to selectively oxidize hydrocarbons to alcohols or ketones [58]. It utilizes iron complexes, a reducing agent, and oxygen or air or peroxides as the oxidant. Pyridine and carboxylic acids are the solvents and picolinic acid is often included as an additive. Barton's non-radical mechanistic pathway has subsequently been challenged [59]. As with Fenton chemistry, selectivity issues remain [60, 61].

The selective, iron-catalyzed oxidation of hydrocarbons or other functional groups remains an important goal. There are enzymes known in nature that activate dioxygen toward a variety of oxidation reactions in living systems [62]. These enzymes can roughly be divided into heme [3] and nonheme systems [63]. As further outlined by George Britovsek in [4] and Christine McKenzie in [64], synthetic efforts have been directed toward mimicking these efficient oxidation enzymes by artificial systems based on iron complexes [65]. The research activity in the field led to a number of iron-based catalytic systems that can oxidize a number of organic substrates, utilizing oxygen, peroxides, or other oxidizing agents as the oxidant. Only two representative examples of this rich chemistry are depicted in Scheme 5 [66, 67]. The field was pioneered by Grove, who, in 1979, found that iron porphyrin complexes can epoxidize alkenes and convert alkanes to alcohols, utilizing iodosylbenzene as the oxidant [25]. Since then, a number of heme and nonheme oxidation systems have been published that catalyze the oxidation of a variety of organic substrates such as alkanes, alkenes, aromatic ring systems, and sulfides, among others.

Iron-catalyzed oxidation chemistry can proceed either through radicals or through the intermediacy of the *ferryl* function, $\text{Fe}=\text{O}$ [68]. The latter species can also be found in natural oxidation processes and is more selective than oxidants based on free radicals [68]. The extensive investigations of iron oxo species $\text{Fe}=\text{O}$,

Scheme 5 Representative examples of iron-catalyzed oxidation reactions [66, 67]



their impact on selectivities, and their potential role in catalytic cycles are outlined in detail in [4, 64].

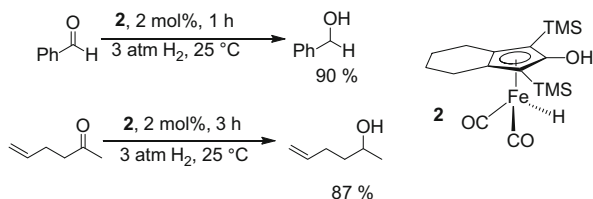
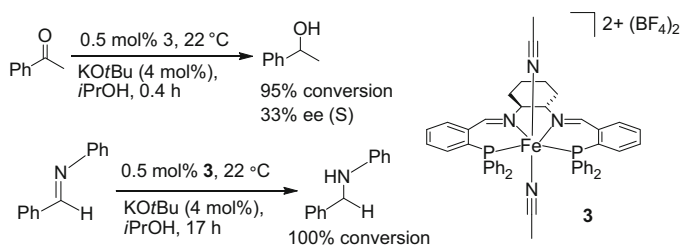
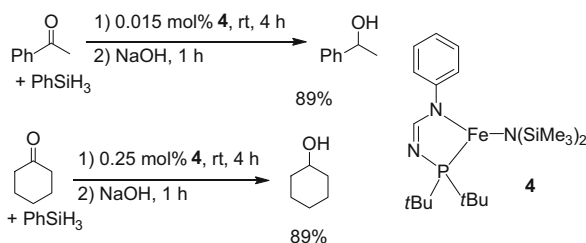
As further detailed in [64] by Christine McKenzie, the design of catalytically active iron complexes is complicated by the fact that under the oxidative reaction conditions, the ligand itself can get oxidized [69], and decomposition pathways have been investigated [70]. It is, thus, difficult to identify a catalytically active species in oxidation reactions. Furthermore, several catalytically active species and several oxidants may be operational at the same time under the reaction conditions, making characterization efforts even more difficult.

The latest trends in the field are toward the development of regio- [71] and enantioselective oxidation reactions [72]. Also, the application of “simple” oxidants (like oxygen or H_2O_2 compared to *t*BuOOH or iodobenzene) and of environmentally benign solvents (such as acetone or water) remains an ongoing topic of research.

4.4 Reduction Reactions

Significant progress has also been made in the iron-catalyzed hydrogenation and transfer hydrogenation of alkenes, alkynes, and carbonyl groups [73–75], which is further outlined by Christophe Darcel in [76]. Enantioselective versions of these reductions have been reported as well [77, 78], as highlighted by Thierry Ollevier in [79]. The hydrosilylation of alkenes is also a reduction reaction and allows access to a variety of silanes; the hydrosilylation of carbonyl units affords silyl ethers, which can subsequently be hydrolyzed to give the corresponding alcohols [80, 81].

Some notable examples are depicted in Scheme 6. Casey reported the iron hydride complex **2** to be an efficient catalyst in the hydrogenation of carbonyl compounds to obtain the corresponding alcohols (Scheme 6a) where an outer-sphere heterolytic activation of the hydrogen molecule was suggested [82]. Morris found a series of tetradentate, PNNP coordinating ligands such as **3** to be catalytically active in transfer hydrogenation reactions (Scheme 6b) [78]. Turculet recently reported that the (*N*-phosphinoamidinate)iron pre-catalyst **4** is highly

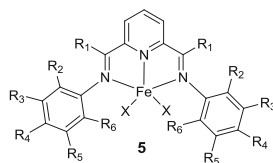
a Hydrogenation catalysis**b Transfer hydrogenation catalysis****c Hydrosilylation catalysis****Scheme 6** Iron-catalyzed reduction reactions [78, 82, 83]

active in hydrosilylation reactions (Scheme 6c) [83]. Many more recent examples are given in [76].

4.5 Polymerization Reactions

Polymerization reactions are of huge economic significance, as polymerization products find widespread applications as plastics and rubbers, e.g., in the automotive industry. Research in the area of iron-catalyzed polymerization reactions was significantly advanced when Gibson [27] and Brookhart [26] found independently that 2,6-bis(arylimino)pyridyl iron(II) complexes (**5** in Fig. 2) catalyze the oligomerization and polymerization of ethylene, as further described by Hélène Olivier-Bourbigou in [28]. As can be seen in Fig. 1, the complex can be modified at several positions on the ligand. Tuning of the 2,6-bis(arylimino)pyridine complexes has

Fig. 2 Iron(II),
polymerization catalyst
[26, 27]



had an influence on the course of the polymerization reactions, allowing for optimization of the system [84]. It turns out that bulky groups in the *ortho* position of the aryl ligands improve catalyst performance [85]. A major challenge facing the application of these systems is their thermal stability; the catalyst class appears to decompose at elevated temperatures, which results in polymers with shorter chain lengths and an increase in (unwanted) branched polymers [84].

4.6 *Enantioselective Iron Catalysis and Stoichiometric Considerations*

These two concepts are only briefly described here, and readers are referred to [64, 79] for an in-depth discussion.

Many of the reactions described above have enantioselective counterparts, and iron has also increasingly been investigated in catalysts for asymmetric syntheses, as described by Thierry Ollevier in [29, 86, 87]. One of the earliest examples was the enantioselective epoxidation of olefins using a chiral iron porphyrin catalyst and iodossylbenzene as the oxidant [88]. Some representative examples of enantioselective, iron-catalyzed reduction reactions can be found in Scheme 6a, b. Challenging areas in enantioselective iron catalysis are the asymmetric hydrogenation of unfunctionalized olefins and C–C bond-forming reactions [86]. On the other hand, as the number of achiral iron catalysts grows, so will the number of chiral iron catalysts. Many iron complexes described in this volume can easily be made chiral through their ancillary ligands.

Finally, a number of stoichiometric processes are known where iron is used as a substrate rather than a catalyst. A prototypical example is Davies' reagent, an iron-based chiral auxiliary, which can be employed in a number of enantioselective reactions, e.g., enolate alkylations [89]. Certain iron complexes and their stoichiometric reactions are currently intensely investigated, as outlined by Christine McKenzie in [64] with the example of iron-based oxidants. The understanding of the structure of oxygen-transferring species can help to develop catalytic systems for oxidation reactions. Other examples are $\text{Fe} \equiv \text{N}$ nitrido complexes that stoichiometrically transfer their nitrogen ligand to olefins [90].

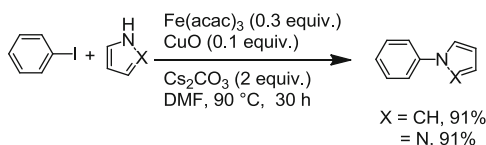
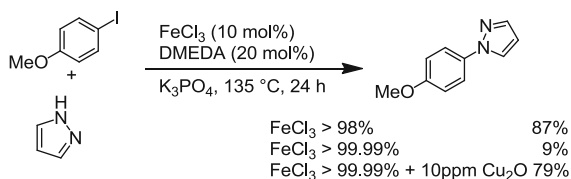
5 Impurities in Iron Metal as the Actual Catalyst?

In 2009, Buchwald and Bolm published a paper where the issue of impurities in iron metal or salts and their influence on the course of a catalyzed reaction was addressed [91]. Iron is often contaminated with trace amounts of copper or other metals. For certain reactions, it might actually be the copper or other impurities that form the catalytically active species or the presence of copper is essential in order for the iron catalyst to unfold its activity. In their paper, the authors pointed out iron-catalyzed cross-coupling reactions originally reported by Bolm [92] (and literature cited therein), for which they later found out that the efficiency of the catalyst systems depended on the iron source. Both authors reported that highly (>99.99%) pure FeCl₃ did show significantly reduced catalytic activity, whereas FeCl₃ with >98% purity (supplied by Merck) or highly pure FeCl₃ treated with Cu₂O showed high activity (Scheme 7, top) [91]. Metals other than iron can potentially be affected in the same way [94].

Since then, some iron-catalyzed processes have been revisited, and there are indeed examples, where “impure” iron salts produce better results than highly pure ones. Based on the findings of Buchwald and Bolm, authors regularly perform test reactions employing highly pure (and therefore expensive) iron salts in order to show that the catalytic process under investigation is actually iron catalyzed.

The following pattern seems to evolve. For processes known to be either copper catalyzed or copper/iron cocatalyzed, caution is advised. For example, the alkylation of aryl rings was reported by several authors to be catalyzed by Fe(III)/Cu(I) systems at high temperatures in the presence of a base [95–97]. A cooperative Fe/Cu catalyst was shown to arylate *N*-nucleophiles (Scheme 7, bottom) [93]. Consequently, in attempts to investigate “copper-free,” iron-catalyzed C–N coupling reactions, a dependency of the catalytic activity of the iron source was observed (such as in Scheme 7, top), which might be attributed to copper impurities that are present [94, 98]. Also, cross-coupling reactions involving alkynes can be critical, as copper forms copper acetylides, which might promote the reactions [99]. Finally, the iron-catalyzed analogs of Pd-catalyzed cross-

Scheme 7 Impact of impurities in an iron catalyst on an *N*-arylation reaction (top) [91] and copper-cocatalyzed example (bottom) [93]



coupling reactions might actually also be Pd catalyzed, as iron could contain palladium impurities. It has been shown that ppb quantities of Pd impurities can catalyze cross-coupling chemistry [100–102]. For example, a palladium-free, iron-catalyzed Suzuki reaction presented by Franzén [103] was later shown to be not reproducible [104], and the original paper has subsequently been retracted.

On the other hand, there are systems known where metal impurities in the iron source do not play a role. For example, Charette described an iron-catalyzed direct arylation of aryl halides, and in this case, an increasing purity of the iron source produced higher yields [105]. In many cases, no impact of the purity of the iron source on the catalytic activity was observed [106]. Also, it seems that the Kumada-type cross coupling of Grignard reagents and halides, further discussed by Robin Bedford in [29], is not due to metal contaminants; palladium-catalyzed Kumada reactions appear not to work ligand-free [107–109]. The lower efficiency of palladium-catalyzed Kumada-type couplings was attributed to the high reactivity of Grignard reagents compared to the nucleophiles typically employed in cross-coupling chemistry, such as boranes [109]. Also, Pd-alkyl species have a higher tendency to undergo β -hydride elimination, making them less suitable for Kumada couplings [109].

However, a clear trend cannot be given, and it is always advisable to test for the influence of impurities in the iron source through employment of highly pure iron salts.

6 Recent Heterogeneous Applications of Iron

In the previous sections, early examples of heterogeneous iron catalysis and some major trends in homogeneous iron catalysis were described. Beyond these applications, iron also shows great promise in heterogeneous reactions. Only two representative examples are given here.

The conversion of methane gas to liquid fuels is a major challenge in “gas to liquid” processes, which are important for raw oil-independent energy sources [110]. Current technology relies on metals such as copper, nickel, or molybdenum and requires high reaction temperatures [111]. Recently, a *Science* report showed a route for direct methane conversion to higher hydrocarbons to be catalyzed by single iron sites embedded in a silica matrix [112]. The catalyst produced ethylene, benzene, and naphthalene with a high selectivity for ethylene. Reaction temperatures were high, but the catalyst exhibited a high thermal stability.

Another challenge related to energy supply is the large-scale oxidation of water to obtain hydrogen gas [113], which can be utilized as fuel. Base metals are frequently investigated for this purpose [114]. Recently, an amorphous, heterogeneous iron oxide was reported to exhibit superior catalytic parameters for the reaction compared to other metals [115].

These are only two examples to demonstrate that iron shows potential beyond the homogeneous catalysis described in this book.

7 Outlook

As outlined above and throughout the whole volume, iron catalysis is advancing on all levels. Despite some challenges described in the subsequent chapters, research activities in iron catalysis are making great progress, and further breakthroughs can be expected in the future. The “New Iron Age” is dawning!

References

1. Frey PA, Reed GH (2012) *ACS Chem Biol* 7:1477–1481
2. Papanikolaou G, Pantopoulos K (2005) *Toxicol Appl Pharmacol* 202:199–211
3. McQuarters AB, Wolf MW, Hunt AP, Lehnert N (2014) *Angew Chem Int Ed* 53:4750–4752
4. Grau M, Britovsek GJP (2015) High-valent iron in biomimetic alkane oxidation catalysis. *Top Organomet Chem*. doi:10.1007/3418_2015_100
5. Brewer GJ (2010) *Chem Res Toxicol* 23:319–326
6. Sahrawat KL (2004) *J Plant Nutr* 27:1471–1504
7. U. S. Pharmacopeial Convention (2013) Elemental Impurities Limits <http://www.usp.org/usp-nf/key-issues/elemental-impurities>. Accessed 4 Mar 2015
8. European Medicines Agency (2008) Guideline On The Specification Limits For Residues Of Metal Catalysts Or Metal Reagents http://www.ema.europa.eu/ema/pages/includes/document/open_document.jsp?webContentId=WC500003586. Accessed 25 Feb 2015
9. French JM, Griffiths JR, Diver ST (2015) *Adv Synth Catal* 357:361–365
10. Bergbreiter DE, Tian J, Hongfa C (2009) *Chem Rev* 109:530–582
11. Schlögl R (2003) *Angew Chem Int Ed* 42:2004–2008
12. Kandemir T, Schuster ME, Senyshyn A, Behrens M, Schlögl R (2013) *Angew Chem Int Ed* 52:12723–12726
13. Vojvodic A, Medford AJ, Studt F, Abild-Pedersen F, Khan TS, Bligaard T, Nørskov JK (2014) *Chem Phys Lett* 598:108–112
14. Sivasankar C, Baskaran S, Tamizmani M, Ramakrishna K (2014) *J Organomet Chem* 752:44–58
15. Anderson JS, Rittle J, Peters JC (2013) *Nature* 501:84–88
16. Khodakov AY, Chu W, Fongarland P (2007) *Chem Rev* 107:1692–1744
17. Schulz H (2013) *Catal Today* 214:140–151
18. Jacobs G, Ma W, Gao P, Todici B, Bhatelia T, Bukur DB, Davis BH (2013) *Catal Today* 214:100–139
19. Massoudi R, Kim JH, King RB, King AD (1987) *J Am Chem Soc* 109:7428–7433
20. Osborn JA, Jardine FH, Young JF, Wilkinson GJ (1966) *J Chem Soc A* 88:1711–1732
21. Knowles WS, Sabacky MJ (1968) *Chem Commun* 1445–1446
22. Halpern J, Riley DP, Chan ASC, Pluth JJJ (1977) *J Am Chem Soc* 99:8055–8057
23. Tang W, Zhang X (2003) *Chem Rev* 103:3029–3069
24. Vavon G, Mottez P (1944) *C R Hebd Seances Acad Sci* 218:557–559
25. Groves JT, Nemo TE, Myers RS (1979) *J Am Chem Soc* 101:1032–1033
26. Small BL, Brookhart M, Bennett AMA (1998) *J Am Chem Soc* 120:4049–4050
27. Britovsek GJP, Gibson VC, Kimberley BS, Maddox PJ, McTavish SJ, Solan GA, White AJP, Williams DJ (1998) *Chem Commun* 849
28. Burcher B, Breuil P-AR, Magna L, Olivier-Bourbigou H (2015) Iron-catalyzed oligomerization and polymerization reactions. *Top Organomet Chem*. doi:10.1007/3418_2015_101
29. Bedford RB, Brenner PB (2015) The development of iron catalysts for crosscoupling reactions. *Top Organomet Chem*. doi:10.1007/3418_2015_99

30. Sun X, Li J, Huang X, Sun C (2012) *Curr Inorg Chem* 2:64–85
31. Czaplik WM, Mayer M, Cvangroš J, Jacobi von Wangelin A (2009) *ChemSusChem* 2:396–417
32. Sarhan AAO, Bolm C (2009) *Chem Soc Rev* 38:2730–2744
33. Bauer EB (2008) *Curr Org Chem* 12:1341–1369
34. Enthaler S, Junge K, Beller M (2008) *Angew Chem Int Ed* 47:3317–3321
35. Padrón JI, Martín VS (2011) *Top Organomet Chem* 33:1–26
36. Che C-M, Zhou C-Y, Wong EL-M (2011) *Top Organomet Chem* 33:111–138
37. Chow TW-S, Chen G-Q, Liu Y, Zhou C-Y, Che C-M (2012) *Pure Appl Chem* 84:1685–1704
38. Costas M, Mehn MP, Jensen MP, Que L (2004) *Chem Rev* 104:939–986
39. Mancheño OG (2011) *Angew Chem Int Ed* 50:2216–2218
40. Cahiez G, Duplais C, Moyeux A (2007) *Org Lett* 9:3253–3254
41. Bedford RB, Brenner PB, Carter E, Clifton J, Cogswell PM, Gower NJ, Haddow MF, Harvey JN, Kehl JA, Murphy DM, Neeve EC, Neidig ML, Nunn J, Snyder BER, Taylor J (2014) *Organometallics* 33:5767–5780
42. Nagano T, Hayashi T (2004) *Org Lett* 6:1297–1299
43. Li Z, Cao L, Li C-J (2007) *Angew Chem Int Ed* 46:6505–6507
44. Yang K, Song Q (2015) *Org Lett* 17:548–551
45. Kharasch MS, Tawney PO (1941) *J Am Chem Soc* 63:2308–2316
46. Tamura M, Kochi J (1971) *J Am Chem Soc* 93:1487–1489
47. Nakamura M, Yoshikai N (2010) *J Org Chem* 75:6061–6067
48. Bedford RB, Brenner PB, Carter E, Carvell TW, Cogswell PM, Gallagher T, Harvey JN, Murphy DM, Neeve EC, Nunn J, Pye DR (2014) *Chem Eur J* 20:7935–7938
49. Hatakeyama T, Hashimoto T, Kathriarachchi KKADS, Zenmyo T, Seike H, Nakamura M (2012) *Angew Chem Int Ed* 51:8834
50. Darcel C, Sortais J-B, Quintero Duque S (2014) Iron-catalyzed cross-dehydrogenative-coupling reactions. In: Li C-J (ed) *From C–H to C–C bonds: cross-dehydrogenative-coupling*. The Royal Society of Chemistry, Cambridge, pp 67–92
51. Itazaki M, Nakazawa H (2015) Iron-catalyzed cross-dehydrogenative-coupling reactions. *Top Organomet Chem*. doi:[10.1007/3418_2015_105](https://doi.org/10.1007/3418_2015_105)
52. Renaud J-L, Gaillard S (2015) Ironcatalyzed carbon-nitrogen, carbon-phosphorus and carbon-sulfur bond formation and cyclization reactions. *Top Organomet Chem*. doi:[10.1007/3418_2015_103](https://doi.org/10.1007/3418_2015_103)
53. Correa A, Carril M, Bolm B (2008) *Chem Eur J* 14:10919–10922
54. Wang J, Liu C, Yuana J, Lei A (2014) *Chem Commun* 50:4736–4739
55. Fukumoto K, Kasa M, Oya T, Itazaki M, Nakazawa H (2011) *Organometallics* 30:3461–3463
56. Fenton HJH (1894) *Chem Soc J Lond* 65:899–910
57. Garrido-Ramírez EG, Theng BKG, Mora ML (2010) *Appl Clay Sci* 47:182–192
58. Barton DHR, Doller D (1992) *Acc Chem Res* 25:504–512
59. Stavropoulos P, Çelenligil-Çetin R, Tapper AE (2001) *Acc Chem Res* 34:745–752
60. Labinger JA (2004) *J Mol Cat A* 220:27–35
61. Bordeaux M, Galarneau A, Drone J (2012) *Angew Chem Int Ed* 51:10712–10723
62. de Montellano PRO (2010) *Chem Rev* 110:932–948
63. Bruijninx PCA, van Koten G, Klein Gebbink RJM (2008) *Chem Soc Rev* 37:2716–2744
64. de Sousa DP, McKenzie CJ (2015) Molecular iron-based oxidants and their stoichiometric reactions. *Top Organomet Chem*. doi:[10.1007/3418_2015_108](https://doi.org/10.1007/3418_2015_108)
65. Talsi EP, Bryliakov KP (2012) *Coord Chem Rev* 256:1418–1434
66. Schröder K, Enthaler S, Bitterlich B, Schulz T, Spannenberg A, Tse MK, Junge K, Beller M (2009) *Chem Eur J* 15:5471–5481
67. Enthaler S (2011) *ChemCatChem* 3:1929–1934
68. Lawrence Q, Tolman WB (2008) *Nature* 455:333–340
69. Crabtree RH (2015) *Chem Rev* 115:127–150
70. Kumar D, de Visser SP, Shaik S (2005) *J Am Chem Soc* 127:8204–8213

71. Lenze M, Bauer EB (2013) *Chem Commun* 49:5889–5891
72. Shaw S, White JD (2014) *J Am Chem Soc* 136:13578–13581
73. Junge K, Schröder K, Beller M (2011) *Chem Commun* 47:4849–4859
74. Morris RH (2009) *Chem Soc Rev* 38:2282–2291
75. Gaillard S, Renaud J-L (2008) *ChemSusChem* 1:505–509
76. Darcel C, Sortais J-B (2015) Iron-catalysed reduction and hydroelementation reactions. *Top Organomet Chem*. doi:10.1007/3418_2015_104
77. Xie J-H, Bao DH, Zhou Q-L (2015) *Synthesis* 47:460–471
78. Sues PE, Demmans KZ, Morris RH (2014) *Dalton Trans* 43:7650–7667
79. Ollevier T, Keipour H (2015) Enantioselective iron catalysts. *Top Organomet Chem*. doi:10.1007/3418_2015_102
80. Zhang M, Zhang A (2010) *Appl Organomet Chem* 24:751–757
81. Trovitch RJ (2014) *Synlett* 25:1638–1642
82. Casey CP, Guan H (2007) *J Am Chem Soc* 129:5816–5817
83. Ruddy AR, Kelly CM, Crawford SM, Wheaton CA, Sydora OL, Small BL, Stradiotto M, Turculet L (2013) *Organometallics* 32:5581–5588
84. Xiao T, Zhang W, Lai J, Sun W-H (2011) *C R Chim* 14:851–855
85. Zhang Z, Chen A, Zhang X, Li H, Ke Y, Lu Y, Hu Y (2005) *J Mol Catal A* 230:1–8
86. Gopalaiah K (2013) *Chem Rev* 113:3248–3296
87. Darwish M, Wills M (2012) *Catal Sci Technol* 2:243–255
88. Groves JT, Myers RS (1983) *J Am Chem Soc* 105:5791–5796
89. Davies SG (1988) *Pure Appl Chem* 60:13–20
90. Lee W-T, Juarez RA, Scepaniak JJ, Muñoz SB, Dickie DA, Wang H, Smith JM (2014) *Inorg Chem* 53:8425–8430
91. Buchwald SL, Bolm C (2009) *Angew Chem Int Ed* 48:5586–5587
92. Correa A, Carril M, Bolm C (2008) *Chem Eur J* 14:10919–10922
93. Taillefer M, Xia N, Ouali A (2007) *Angew Chem Int Ed* 46:934–936
94. Thomé I, Nijs A, Bolm C (2012) *Chem Soc Rev* 41:979–987
95. Mao J, Xie G, Wu M, Guo J, Ji A (2008) *Adv Synth Catal* 350:2477
96. Rao Volla CM, Vogel P (2008) *Tetrahedron Lett* 49:5961
97. Huang H, Jiang H, Chen H, Liu H (2008) *J Org Chem* 73:9061
98. Correa A, Bolm C (2008) *Adv Synth Catal* 350:391–394
99. Chinchilla R, Nájera C (2011) *Chem Soc Rev* 40:5084–5121
100. Bedford RB, Welch SL (2001) *Chem Commun* 129–130
101. Bedford RB, Hazelwood, ZL, Norton PN, Hursthouse MB (2003) *Dalton Trans* 4164–4174
102. Arancon RAD, Lin CSK, Vargas C, Luque R (2014) *Org Biomol Chem* 12:10–35
103. Kymälä T, Valkonen A, Rissanen K, Xu Y, Franzén R (2008) *Tetrahedron Lett* 49:6679–6681
104. Bedford RB, Nakamura M, Gower NJ, Haddow MF, Hall MA, Huwe M, Hashimoto T, Okopie RA (2009) *Tetrahedron Lett* 50:6110–6111
105. Vallée F, Mousseau JJ, Charette AB (2010) *J Am Chem Soc* 132:1514–1516
106. Atack TC, Lecker RM, Cook SP (2014) *J Am Chem Soc* 136:9521–9523
107. López-Pérez A, Adrio J, Carretero JC (2009) *Org Lett* 11:5514–5517
108. Ackermann L, Potukuchi HK, Kapdi AR, Schulzke C (2010) *Chem Eur J* 16:3300–3303
109. Jana R, Pathak TP, Sigman MS (2011) *Chem Rev* 111:1417–1492
110. Zhang K, Kogelschatz U, Eliasson B (2001) *Energy Fuel* 15:395–402
111. Xu B-Q (2014) *Natl Sci Rev* 1:325–326
112. Guo X, Fang G, Li G, Ma H, Fan H, Yu L, Ma C, Wu X, Deng D, Wei M, Tan D, Si R, Zhang S, Li J, Sun L, Tang Z, Pan X, Bao X (2014) *Science* 344:616–619
113. Parent AR, Crabtree RH, Brudvig GW (2013) *Chem Soc Rev* 42:2247–2252
114. Parent AR, Saka K (2014) *ChemSusChem* 7:2070–2080
115. Smith RDL, Prévot MS, Fagan RD, Zhang Z, Sedach PA, Siu MKJ, Trudel S, Berlinguette CP (2013) *Science* 340:60–63

The Development of Iron Catalysts for Cross-Coupling Reactions

Robin B. Bedford and Peter B. Brenner

Abstract Cross-coupling between organometallic nucleophiles and organic electrophiles is currently one of the most widely investigated areas of organic homogeneous catalysis with iron. This overview charts the development and application of iron catalysts for cross-coupling reactions, focusing predominantly on findings over the last 5 years.

Keywords Cross-coupling · Iron · Iron catalysis

Contents

1	Introduction	20
1.1	Background	20
1.2	Scope	21
2	Iron Catalysts for the Cross-Coupling of Grignard Reagents	22
2.1	Oxygen, Nitrogen and Sulphur Donor Ligands	22
2.2	Phosphines and Related Ligands	30
2.3	<i>N</i> -Heterocyclic Carbene Ligands	32
3	Iron Catalysts for the Cross-Coupling of Softer Nucleophiles	35
3.1	Zinc-Based Nucleophiles	35
3.2	Boron-Based Nucleophiles	38
3.3	Aluminium-, Gallium-, Indium- and Thallium-Based Nucleophiles	41
4	Summary and Outlook	41
	References	42

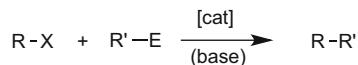
Abbreviations

acac	Acetylacetonate
Ar	Aryl
9-BBN	9-Borabicyclo[3.3.1]nonane
bmim	1-Butyl-3-methylimidazolium
cat	Catalyst
Cp	Cyclopentadienyl
dpbz	1,2-Bis(diphenylphosphino)benzene
dppe	1,2-Bis(diphenylphosphino)ethane
dppp	1,3-Bis(diphenylphosphino)propane
EPR	Electron paramagnetic resonance
Mes	Mesityl, 2,4,6-trimethylphenyl
NHC	<i>N</i> -heterocyclic carbene
NMP	<i>N</i> -methylpyrrolidone
salen	<i>N,N'</i> -ethylenebis(salicylimine)
Tf	Triflate
THF	Tetrahydrofuran
TMEDA	<i>N,N,N',N'</i> -tetramethyl-1,2-ethylenediamine
TMS	Trimethylsilyl
Ts	Tosyl
Xantphos	4,5-Bis(diphenylphosphino)-9,9-dimethylxanthene

1 Introduction

1.1 Background

Cross-coupling reactions between an organic electrophile, typically an organic halide or related species, and an appropriate organometallic or related nucleophile (Scheme 1) are widely exploited in the formation of carbon–carbon bonds. By far the most often used catalysts for such cross-coupling processes are based on palladium. However, the high and rising cost of palladium, coupled with its relatively low natural abundance, competition for its use from the automotive and consumer electronics sectors, the environmental impact of its extraction (around



R, R' = aryl, alkenyl, alkynyl, vinyl ...
 X = halide, pseudohalide leaving group ...
 E = MgY, ZnY, SnY₃, BY₂ ...

Scheme 1 Generalised cross-coupling reactions. Base is sometimes required, typically to activate the nucleophilic coupling partner

only 6 g of metal are produced from 1 t of palladium ore) and its toxicity all ultimately limit the medium to long-term use of the metal in cross-coupling. These limitations, combined with the potential for developing new or orthogonal reactivities and processes with other metals, have led to the search for catalysts based on more Earth-abundant elements. Iron is particularly well suited to be a potential replacement for palladium due to its high natural abundance, low cost, and low toxicity.

Iron-catalysed cross-coupling reactions are far from new; indeed, the seminal publication in this area dates back over 70 years: a paper published by Motez and Vavon on the iron-catalysed coupling of aryl Grignard reagents with alkyl halides [1]. Despite further pioneering work by Kochi in the early 1970s [2–6], much of which predates the use of palladium in cross-coupling reactions, the field lay largely dormant, with occasional sporadic publications, notably from the groups of Molander [7] and Cahiez [8–10], until the early 2000s. Triggered in particular by publications from the groups of Fürstner [11–14], Nakamura and Nakamura [15], Hayashi [16] and Bedford [17–19] in the early to mid 2000s, the renaissance of iron-catalysed cross-coupling reactions has been marked by an exponential growth in the number of publications on the topic since the beginning of the millennium.

1.2 Scope

This chapter summarises many of the important advances in the field of iron-catalysed cross-coupling chemistry over the last 5 years or so, focusing primarily on the types of iron-based catalysts that are currently available and selected examples of their applications. This is not intended to be a comprehensive review but rather an introduction to the most significant catalyst developments and an overview of the application of these catalysts in selected carbon–carbon bond-forming processes. While the literature discussed here predominately covers the last half decade, where appropriate, we have included some results that predate 2009 in order to give a better overview of the ‘state of the art’.

The chapter is primarily organised by the type of nucleophilic coupling partner exploited in the cross-coupling reactions. To date, the vast majority of the iron-catalysed cross-coupling reactions are those of Grignard reagents, and this area is addressed first, in Sect. 2. This section is broadly subdivided by catalyst type since most, if not all, of the relevant pre-catalysts used in iron-catalysed cross-coupling processes have been exploited at some stage in the coupling of Grignard reagents.

Obviously the high reactivity of organomagnesium reagents can place constraints on the substitution patterns of the electrophilic cross-coupling partner, and this had triggered the search for catalysts that can couple ‘softer’ organometallic nucleophiles such as those based on copper, zinc or boron, and this topic is covered in Sect. 3. Here the discussion is organised by class of organometallic nucleophile.

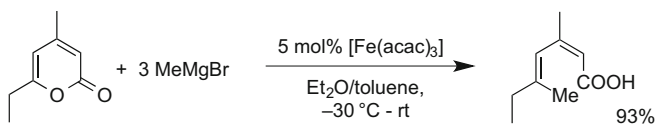
2 Iron Catalysts for the Cross-Coupling of Grignard Reagents

Many of the early iron-catalysed cross-coupling reactions, which typically exploited simple iron halide pre-catalysts, were plagued by competitive side reactions, such as homocoupling and, where alkyl halides were used, β -elimination processes. Accordingly, there has been a significant effort to develop ligand sets and/or conditions that give increased selectivity for the desired cross-coupled product. The following sections are organised according to catalyst type or ligand/additive sets used in Grignard cross-coupling reactions. The use of organoferrates [20] as pre-catalysts is not explicitly reviewed in this section but has been covered in detail in previous excellent accounts [21, 22].

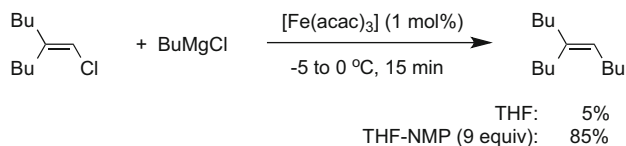
2.1 Oxygen, Nitrogen and Sulphur Donor Ligands

Iron(III) tris(acetylacetonate), $[\text{Fe}(\text{acac})_3]$, stands out as a very useful pre-catalyst in a range of selective cross-coupling reactions, not least because it is a free-flowing air- and moisture-stable, non-hygroscopic solid that is inexpensive and easily handled. Indeed, we recommend this as an ideal first catalyst to trial in any proposed new catalytic C–C bond-formation process based on iron. First exploited by Kochi in the coupling of alkyl Grignards with vinyl halides [4], $[\text{Fe}(\text{acac})_3]$ was subsequently shown by Hayashi to give good performance in the challenging coupling of primary and secondary alkyl halides with aryl Grignard reagents, without the need for additives, provided that the reaction was performed in diethyl ether, preferably at reflux temperature [16]. In a recent example, Fürstner developed a ring opening/cross-coupling reaction of 2-pyranones with methyl Grignard, using $[\text{Fe}(\text{acac})_3]$ as the pre-catalyst (Scheme 2) [23]. This protocol provides an attractive route to stereo-defined diene carboxylates.

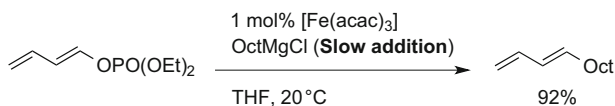
While $[\text{Fe}(\text{acac})_3]$ can often give excellent results on its own, its performance, like that of simple iron (II) or (III) halides, can often be enhanced by the inclusion in the reaction mixture of an appropriate ‘additive’. The first major success in the use of additives to improve the outcome of iron-catalysed cross-coupling was achieved by Cahiez and Avedissian who, in 1998, reported the use of NMP (*N*-methylpyrrolidone) as co-solvent with THF in the coupling of alkenyl halides and alkyl



Scheme 2 Example of the iron-catalysed ring opening/cross-coupling of 2-pyranones



Scheme 3 The beneficial role of NMP as an additive

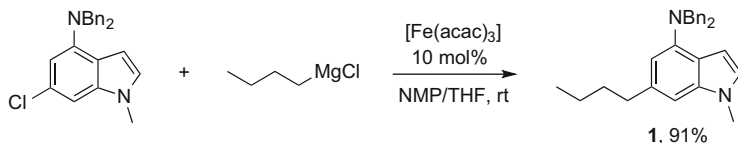


Scheme 4 Cross-coupling of dienyl phosphates

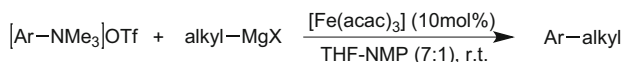
Grignard reagents [8]. They found that the presence of NMP could have a profound beneficial influence on the amount of cross-coupled product (e.g. Scheme 3).

The NMP-additive approach works particularly well with vinyl halides; however, access to these substrates can be problematic. To circumvent this, in 2008 Cahiez reported a protocol for the coupling of related enol phosphates with primary, secondary and tertiary Grignard reagents. These alkenylation reactions give high yields and good stereoselectivity [24]. Cahiez has extended this class of reaction to the coupling of dienyl substrates. The preparation of alkylated dienes from diene electrophiles and alkyl Grignard reagents is often plagued by oligomerisation of the dienyl halide substrates. By contrast dienol phosphates can be exploited as substrates in $[\text{Fe}(\text{acac})_3]$ -catalysed coupling with alkyl and aryl Grignards (Scheme 4) [25]. Interestingly in this case it appears that the presence of NMP is detrimental to the performance of the catalyst. The efficacy of this protocol was illustrated by the synthesis of the pheromone of *Diparopsis castanea*.

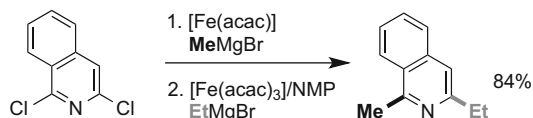
Vinyl halides and related species are not the only Csp^2 -based electrophilic substrates able to undergo iron-catalysed cross-coupling facilitated by the addition of NMP. Fürstner demonstrated that NMP could be used to good effect in the coupling of aryl and heteroaryl chlorides, tosylates and triflates with a range of alkyl Grignard reagents [11, 12]. In some cases, aryl Grignards could also be exploited, but this was limited to coupling of an electron-deficient aryl chloride (methyl-4-chlorobenzoate) or 2-chloro-*N*-heterocyclic substrates. The use of aryl bromides and iodides, substrates that are typically more amenable to palladium-catalysed cross-coupling reactions than aryl chlorides, led to the formation of significant amounts of the free arene, produced by a competitive hydrodehalogenation process. Cabri has recently exploited this methodology in the synthesis of **1**, a key intermediate in the synthesis of ST1535, a promising molecule for the treatment of Parkinson's disease (Scheme 5) [26]. In contrast to palladium coupling, this iron-based protocol proceeds very rapidly under mild conditions, generating comparatively little waste.



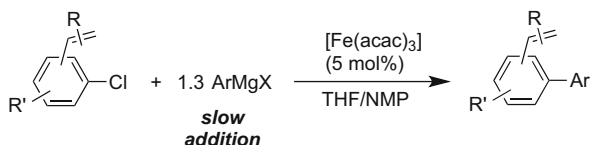
Scheme 5 Formation of an intermediate in the preparation of ST1535



Scheme 6 Cross-coupling of arylammonium triflate salts



Scheme 7 Selective one-pot difunctionalisation

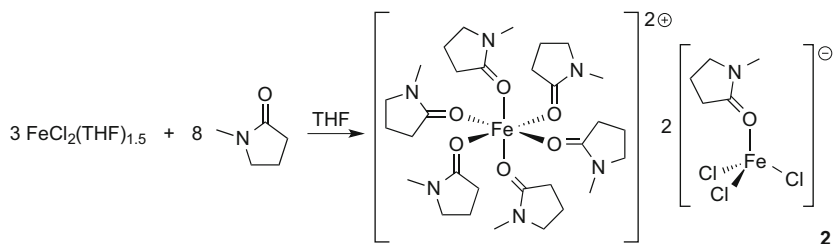


Scheme 8 Iron-catalysed cross-coupling of chlorostyrenes with aryl Grignard reagents

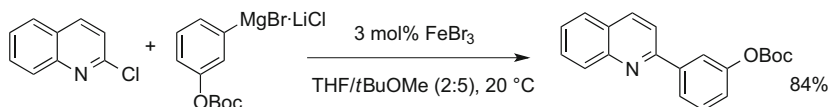
Wang and co-workers recently showed that the $[\text{Fe}(\text{acac})_3]/\text{NMP}$ systems could be applied to the coupling of arylammonium triflate salts with alkyl Grignard reagents (Scheme 6). Poorer performance was observed when phosphine, *N*-heterocyclic carbene or amine ligands were used in place of the NMP additive [27].

Interestingly, Malhotra and co-workers found that the presence or absence of NMP can be used to tune the site selectivity in the coupling of dihaloheteroaromatics with alkyl Grignard reagents allowing for one-pot sequential difunctionalisations, such as that shown in Scheme 7 [28].

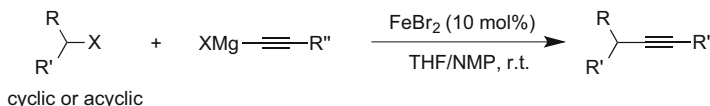
The cross-coupling of aryl halides with aryl Grignard reagents appears to be significantly more challenging for catalysts based on iron compared with those based on palladium and until quite recently was limited to the use of electron-deficient aryl chlorides or *N*-heterocyclic halides [11, 12]. Güllak and Jacobi von Wangelin provided an intriguing exception to this rule when they showed that chlorostyrenes could be coupled with aryl Grignards using $[\text{Fe}(\text{acac})_3]$ in THF/NMP, typically with slow addition of the Grignard reagent (Scheme 8) [29]. The authors proposed that the vinyl substituent coordinates to the iron centre, which then undergoes a haptotropic shift followed by activation of the C–Cl bond.



Scheme 9 Formation of an NMP-coordinated, Fe(II) ion pair



Scheme 10 Representative coupling of *N*-heterocyclic halides with aryl Grignards

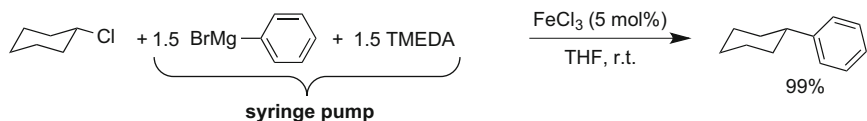


Scheme 11 Cross-coupling of alkyl halides with alkynyl Grignard reagents

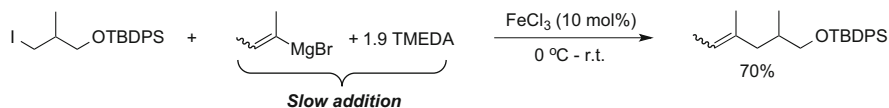
The use of NMP as an additive in iron-catalysed cross-coupling is, on occasion, somewhat misleadingly referred to as running the reactions under ‘ligand-free’ conditions. In an attempt to identify the possible role of NMP in iron-catalysed cross-coupling, Holland and co-workers not only confirmed the beneficial role played by NMP in the coupling of a representative aryl chloride with hexyl magnesium bromide using a variety of iron precursors, but they also isolated the mixed trinuclear iron(II)-NMP species **2** (Scheme 9) [30]. This demonstrated unequivocally the *O*-coordination of NMP to catalytically competent iron species.

It should be noted that NMP is by no means effective in every case. For instance, Knochel found NMP to be detrimental in a protocol for the cross-coupling between *N*-heterocyclic chlorides or bromides and various arylmagnesium reagents [31]. In this instance, the best performances were obtained by using a mixture of THF and the industrially attractive solvent *t*BuOMe using iron(III) bromide as the pre-catalyst (e.g. Scheme 10).

As can be seen in the preceding discussion, ever since the original report by Cahiez on the advantages of using NMP in iron-catalysed cross-coupling of vinyl halides, the majority of reports have focussed on the use of this additive in the coupling of Csp^2 -based electrophiles. A notable exception to this was provided very recently by Hu and co-workers, who showed that a simple $FeBr_2$ /NMP system is very effective in the coupling of a range of primary and secondary *alkyl* halides with alkynyl Grignard reagents (Scheme 11) [32].



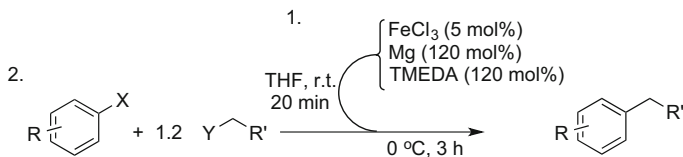
Scheme 12 An example of Nakamura and Nakamura's slow addition method, using stoichiometric TMEDA, for the coupling of alkyl halides with aryl Grignards



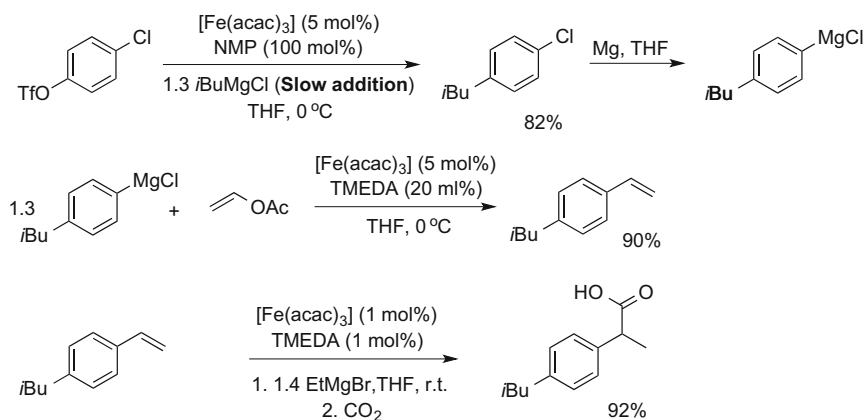
Scheme 13 Representative coupling of an alkenyl Grignard with an alkyl halide

While it is apparent that NMP can act as an excellent ligand/additive in a range of cross-coupling reactions, it is classified as a reprotoxin, and consequently there have been calls to limit its usage. Therefore, there is clearly a need for catalyst systems that do not require this additive, and amine donors have been found to play a particularly prominent role in this regard. In 2004 Nakamura, Nakamura and co-workers were the first to report the beneficial effects of amine additives, in particular TMEDA, on the coupling of primary and secondary alkyl halides with aryl Grignard reagents [15]. To ensure the best yields were obtained, it proved necessary to mix the aryl Grignard reagent with a greater than stoichiometric amount of TMEDA and then add this very slowly, using a syringe pump, to a mixture of the appropriate electrophile and catalytic amounts of FeCl_3 (e.g. shown in Scheme 12). Reactions with alkyl bromides and iodides are typically performed at 0°C to avoid unwanted olefin formation, while alkyl chlorides can be transformed at room temperature. This method is not limited to aryl Grignard reagents but can be extended to vinyl magnesium analogues, as demonstrated by Cossy and co-workers in 2007 (Scheme 13) [33]. Furthermore, Denmark recently found that alkyl thio-ethers and sulphones can be used as electrophilic coupling partners in the presence of a large excess of TMEDA [34].

In order to circumvent both the need to use stoichiometric amounts of amine additives and the use of a syringe pump, in 2005 Bedford and co-workers developed a more convenient and user-friendly procedure for the coupling of primary and secondary alkyls bearing β -hydrogen atoms with aryl Grignards using catalytic amounts of the added TMEDA or other amines [18]. Subsequently Cahiez also demonstrated that TMEDA could be used in catalytic quantities in similar reactions, either in the presence of an $[\text{Fe}(\text{acac})_3]$ /hexamethylenetetramine mixture or by the use of a preformed complex $'[(\text{FeCl}_3)_2(\text{tmeda})_3]'$ [35]. Some care needs to be taken in ascribing the structure of this complex as no spectroscopic or analytic data were presented in support of the formulation. Recently, Fox and co-workers found that catalytic quantities of TMEDA can be exploited in the cross-coupling of activated aryl chlorides with alkyl Grignard reagents [36].



Scheme 14 A ‘domino’ process for the coupling of alkyl and aryl halides



Scheme 15 Synthesis of ibuprofen by two sequential iron-catalysed cross-couplings and an iron-catalysed hydromagnesiation

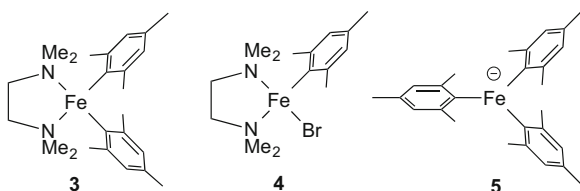
In 2009 Jacobi von Wangelin and co-workers reported a particularly attractive use for simple iron-TMEDA species, namely, a ‘domino’ reaction for the direct cross-coupling of aryl halides with alkyl halides using $\text{FeCl}_3/\text{TMEDA}$ as a pre-catalyst (Scheme 14). No preformed Grignard is required; rather, magnesium metal is added directly to the reaction, leading to in situ generation of the reagent [37]. Under these conditions, primary and secondary alkyl bromides couple with aryl and heteroaryl bromides bearing alkyl, alkoxy, fluoro, and amine substituents, whereas tertiary alkyls give very low yields.

This method was extended to aryl–alkenyl bond formation by the same authors in 2011 [38]. Activated aryl bromides readily form the Grignard reagent in the presence of FeCl_3 , whereas electron-rich aryl bromides, heteroaryl bromides and arenes bearing polar substituents require preformation of the aryl Grignard reagent.

In 2014 Thomas reported an elegant synthesis of ibuprofen using three sequential iron-catalysed processes (Scheme 15) [39]. In the first step, $[\text{Fe}(\text{acac})_3]$ was used in the presence of NMP to catalyse the coupling of 4-chlorophenyl triflate with isobutyl Grignard. Here the triflate reacts in preference to the aryl chloride function. The resultant aryl chloride was converted to the Grignard reagent, which was then coupled with vinyl acetate catalysed by $[\text{Fe}(\text{acac})_3]$ in the presence of cocatalytic amounts of TMEDA. In the final step, the resulting styrene undergoes an iron-catalysed hydromagnesiation process, previously developed in the Thomas group

[40], followed by in situ carboxylation of the resultant secondary benzyl Grignard to give ibuprofen.

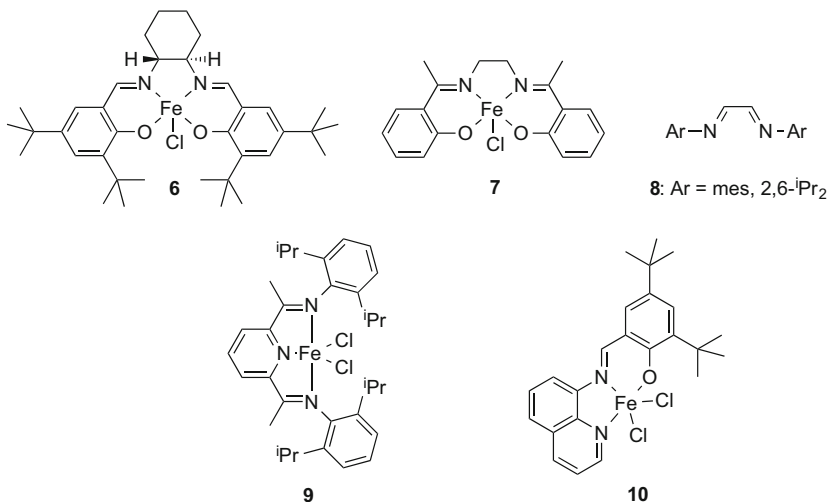
TMEDA is clearly a useful additive in iron-catalysed Grignard cross-coupling reactions, but what is its precise role in the reaction? It is tempting to conclude that it acts as a ligand for the iron centre during the catalytic cycle; indeed, Nagashima and co-workers [41] demonstrated that in the presence of excess TMEDA and *three* equivalents of mesityl Grignard, iron(III) chloride reacts to form the TMEDA bismesityl iron(II) complex **3**. Complex **3** is catalytically competent in the coupling of octyl bromide with mesityl Grignard and reacts with octyl bromide to generate the cross-coupled product and the mono-mesityl complex **4**, which in turn can regenerate **3** on reaction with mesityl Grignard. The authors concluded that the catalytic cycle therefore proceeds via the intermediates **3** and **4**. However, Bedford and co-workers subsequently showed this not to be the case [42]. In the presence of excess mesityl Grignard, as would be seen in catalytic reactions, complex **3** is converted to the TMEDA-free homoleptic iron complex **5**. Indeed during the catalytic reaction, only **5** is observed by ^1H NMR spectroscopy. Furthermore, complex **5** reacts far faster than **3** with octyl bromide, quashing the possibility that **3** has any role on the catalytic cycle. Thus, TMEDA does not appear to be coordinated to iron during the primary catalytic cycle. Instead, the authors suggested a possible role for the amine ligand was to stabilise off-cycle iron complexes with respect to the formation of iron nanoparticles, which are themselves catalytically active [43] but which may give lower selectivity.



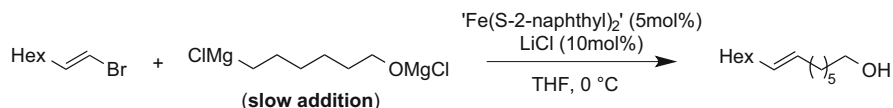
While useful in many cross-coupling reactions, TMEDA is by no means a panacea for all iron-catalysed cross-coupling processes and can indeed prove deleterious. For example, in 2013, Knochel reported that $\text{FeBr}_3 + \text{TMEDA}$ gave poorer performance in the iron-catalysed coupling of 2-halopyridines and pyrimidines with aryl Grignard reagents compared with the use of the iron bromide alone [44]. By contrast, adding isoquinoline gave a significant enhancement in activity. Presumably here both the substrate and the cross-coupled product can also act as ligands by coordination through the pyridyl nitrogen.

In view of the possible ligating role played by pyridyl-containing substrates, it is perhaps not surprising to discover that imine-based ligands in general can be used to good effect in a variety of iron-catalysed cross-coupling reactions. In particular Fe-salen complexes have proven to be useful, with Fürstner showing that complex **6** can be used, in the presence of NMP, in the coupling of secondary alkyl Grignard reagents with activated aryl chlorides [12], while Bedford showed that several

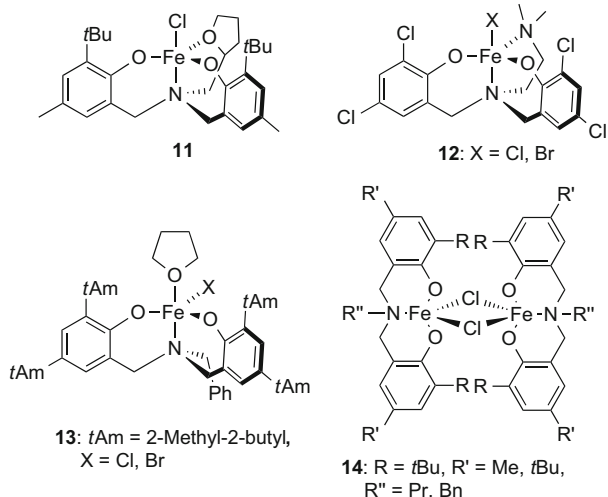
Fe-salen complexes, in particular **7**, can be exploited in the coupling of aryl Grignard reagents with primary and secondary alkyl halides, without the need for added NMP [17]. Under similar conditions, the simple diimine ligands **8** and the preformed imino-iron complexes **9** and **10** all showed good to excellent performance [43].



In a series of publications, Kozak and co-workers reported the application of a range of iron complexes **11–14** with aminophenolate ligands in cross-coupling reactions [45–49]. These pre-catalysts show reasonable to good activity in the coupling of aryl or allyl Grignard reagents with primary and secondary alkyl or benzyl halides. While the activity displayed by these complexes is interesting, the more synthetically elaborate nature of the ligands detracts somewhat from the appeal of these pre-catalysts in the face of competition from simpler catalyst systems that show similar or better activity.



Scheme 16 A representative iron-dithiolate-catalysed cross-coupling

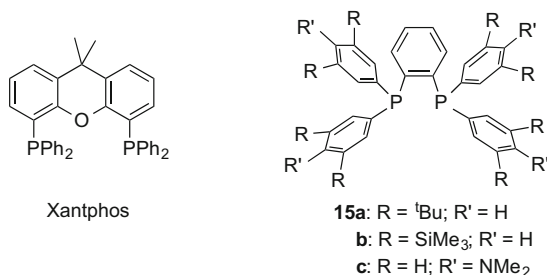


As discussed above, while NMP can be an excellent additive in iron-catalysed cross-coupling reactions, its reprotoxicity casts a shadow over its continued usage. Accordingly, Cahiez, who pioneered the use of this additive, sought to replace NMP with more benign ligands. In 2012 his group reported that the iron bis-thiolate complex, 'Fe(S-2-naphthyl)₂', formed in situ from FeCl₂ and the magnesium thiolate salt, could be used to replace the Fe–NMP system in the coupling of alkenyl halides with alkyl Grignard reagents (Scheme 16) [50].

2.2 Phosphines and Related Ligands

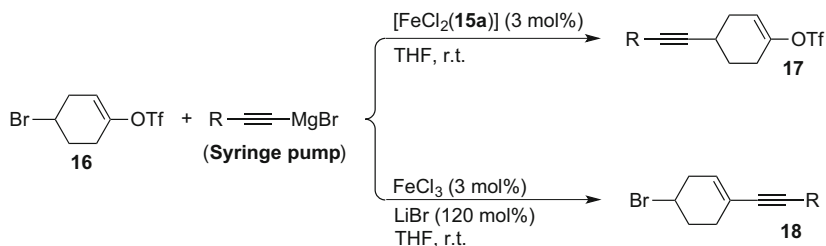
Sulphur donors are notably softer than *N*- and *O*-donor ligands, being more akin to phosphine donors; therefore, it comes as no surprise that phosphines can also act as excellent co-ligands in iron-catalysed cross-coupling reactions. In 2006 Bedford and co-workers reported a detailed investigation into the use of iron–phosphine complexes as pre-catalysts in cross-coupling processes [19]. They showed that a wide range of monodentate and chelating diphosphine ligands, as well as related phosphite and arsine ligands, could be used to good effect in the iron-catalysed coupling of aryl Grignard reagents with primary and secondary alkyl halides. Subsequently, Chai and co-workers showed that iron–phosphine catalysts,

particularly those containing a Xantphos ligand, could be exploited in the $\text{Csp}^3\text{-Csp}^3$ coupling of alkyl halides with alkyl Grignards [51].



In 2011, Nakamura reported that an iron dichloride adduct of the bisphosphine ligand **15a** is an efficient pre-catalyst for the cross-coupling of primary, secondary and tertiary alkyl halides with electron-poor, electron-rich and sterically hindered aryl Grignard reagents, provided that the Grignard reagent is added slowly, using a syringe pump [52]. Nakamura also investigated the cross-coupling of benzylic chlorides with aryl Grignards and found, in this case, that the electron-rich phosphine **15c** performed best, giving good yields of the desired diarylmethanes, whereas the use of **15a**, **b** or more electron-deficient analogues led to greater amounts of unwanted homocoupled products [53]. He also showed that the pre-catalyst $[\text{FeCl}_2(\mathbf{15a})]$ can be exploited in the cross-coupling of alkynyl Grignard reagents with alkyl halides [54]. Interestingly, changing the catalyst composition leads to a switch in selectivity in the coupling of the substrate **16**, which contains both alkyl bromide and vinyl triflate functions: the iron–phosphine complex favours coupling at the former to give **17**, while FeCl_3 , in the presence of greater than stoichiometric amount of LiBr, targets the latter site to give **18** (Scheme 17).

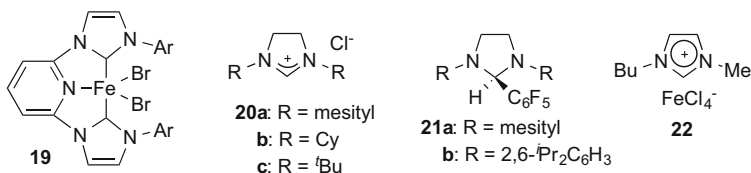
Recently, Fürstner and co-workers published a practical procedure for iron-catalysed cross-coupling reactions of sterically demanding aryls with primary alkyl halides. Here the best pre-catalyst proved to be one based on the commercially available chelating diphosphine bis(diethylphosphino)ethane [55].



Scheme 17 Tuning selectivity in iron-catalysed cross-couplings with alkynyl Grignard reagents

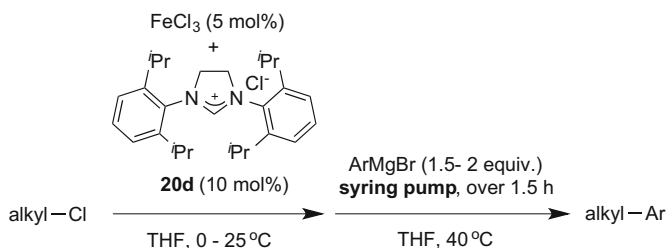
2.3 *N*-Heterocyclic Carbene Ligands

N-Heterocyclic carbene ligands can be excellent alternatives to phosphines in iron-catalysed cross-coupling, with the first examples provided by Bedford and co-workers in 2006 [19]. They showed that the preformed bis-NHC complex **19**, or species formed in situ from FeCl₃ and the carbene precursors **20** or **21**, shows good to excellent activity in the cross-coupling of primary and secondary alkyl bromides with tolyl Grignard.

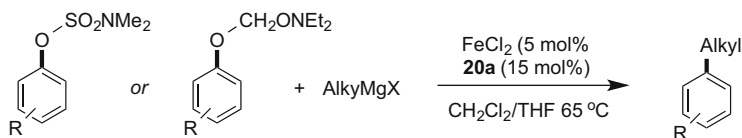


Shortly afterwards Bica and Gaertner reported the use of the ionic liquid [bmim][FeCl₄], **22**, as a pre-catalyst for the coupling of alkyl halides with aryl Grignards. This air-stable pre-catalyst reacts in a biphasic system and can be reclaimed with little loss in activity by simple decantation of the product [56]. It seems likely that the imidazolium salt is deprotonated by the Grignard reagent under the reaction conditions to give an *N*-heterocyclic carbene ligand. Interestingly, and somewhat unusually for Grignard reagents, the authors report that the reactions do not need to be performed under an inert atmosphere.

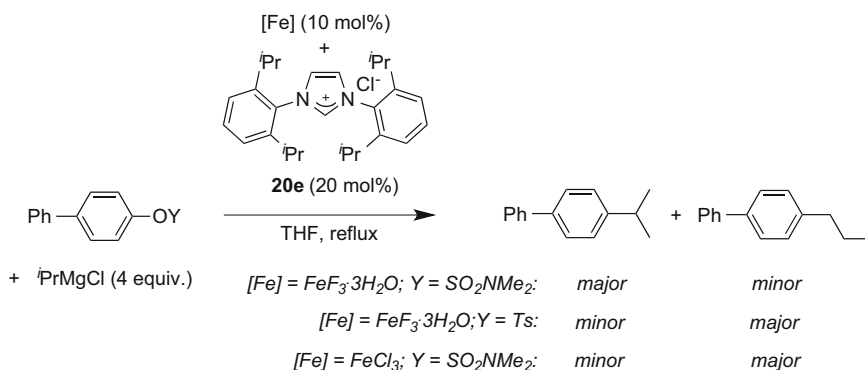
Alkyl chlorides are generally cheaper and more widely available than their bromide or iodide counterparts, but they can be more challenging substrates in cross-coupling. To address this problem, Nakamura and co-workers exploited NHC–iron pre-catalysts and a slow addition protocol [57]. The best results were obtained using the NHC precursor **20d** and the addition of excess (1.5–2 equivalents) of the aryl Grignard with a syringe pump over one and half hours (Scheme 18). Under these conditions, primary, secondary and even some tertiary alkyl chlorides coupled with ease. Substrates with more than one alkyl chloride function were smoothly converted to the corresponding di- and triarylated products.



Scheme 18 NHC–iron-catalysed coupling of alkyl chlorides with aryl Grignard reagents



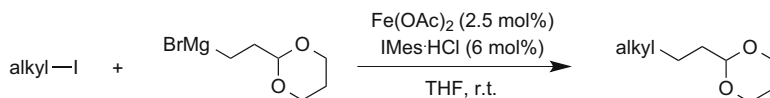
Scheme 19 NHC–iron-catalysed coupling of aryl sulphamates and tosylates with alkyl Grignard reagents



Scheme 20 Tuning branched–linear selectivity in the coupling of secondary alkyl Grignard reagents

NHC–Fe-catalysed Csp^2 – Csp^3 coupling is by no means limited to aryl nucleophiles and alkyl electrophiles, for example, in 2012 Garg and co-workers reported the iron-catalysed cross-coupling of alkyl Grignard reagents with aryl sulphamates and carbamates (Scheme 19), using the carbene precursor **20a** and $FeCl_2$ [58]. These electrophilic substrates are particularly attractive due to both the ease of their synthesis and their stability under a range of reaction conditions. *N*-Heteroaryl and aryl electrophiles can be coupled, and the reactions work well with both primary and secondary alkyl Grignard reagents. Similarly, Perry and co-workers showed that iron–NHC systems can also be used in the coupling of unactivated aryl chlorides with primary and secondary alkyl Grignard reagents [59]. Interestingly, they found that better activity was obtained with hydrated rather than anhydrous iron salt precursors.

More recently, Agrawal and Cook reported that an NHC– FeF_3 pre-catalyst can be used to realise the coupling of aryl sulphamates or tosylates with primary and secondary alkyl Grignard reagents [60]. Interestingly, they showed that an aryl sulphamate substrate couples with isopropyl magnesium chloride to yield predominantly the expected branched product, whereas the corresponding aryl tosylate favours the formation of the linear product (Scheme 20). In this instance, the alkyl nucleophile undergoes isomerisation prior to C–C bond formation. This difference in selectivity may be due to the coordination of different counterions to the iron centre, which implies that the system is very sensitive to changes in the

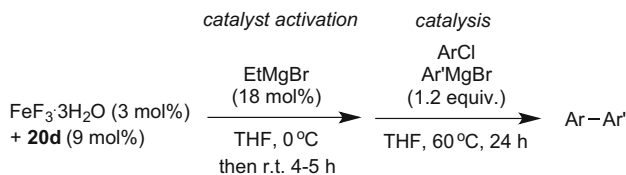


Scheme 21 Fe–NHC-catalysed alkyl–alkyl cross-coupling

coordination sphere of the iron. Indeed this appears to be borne out by the observation that changing the anionic ligands on the iron precursor can also have a significant influence on selectivity. For instance, changing from iron(III) fluoride to chloride leads to a reversal in selectivity in the coupling with an aryl sulphonate (Scheme 20).

Csp^3 – Csp^3 bond formation can also be accessed by iron–NHC-catalysed cross-coupling. Thus, Cárdenas and co-workers demonstrated the coupling of alkyl iodides with either the alkyl Grignard reagent shown in Scheme 21 or benzyl Grignard [61]. The authors provided EPR spectroscopic and mechanistic data in support of the formation of an Fe(I) intermediate under catalytically relevant conditions and proposed that this is likely the lowest oxidation state in the catalytic manifold, in line with early suggestions by Kochi [5, 6].

Aryl–aryl bond formation is one of the major successes of palladium-catalysed cross-coupling; indeed, such reactions are ubiquitous in the formation of biaryl motifs. By contrast this class of reaction has proven to be significantly more challenging for iron-based catalysts. Therefore, reports by Nakamura and co-workers in 2007 [62] and 2009 [63] detailing the use *N*-heterocyclic carbene-ligated iron catalysts in the cross-coupling of aryl Grignards with aryl chlorides represent a major breakthrough in the field. The reactions work best using **20d** as the carbene source and iron (II) or (III) fluoride precursors, ideally $FeF_3 \cdot 3H_2O$. Phosphine and amine ligands perform very poorly by comparison giving little or none of the desired product, while the use of either $FeCl_3$ or $[Fe(acac)_3]$ leads to substantial amounts of homocoupled product derived from the aryl Grignard. Interestingly, the addition of KF to the reaction catalysed by iron chloride led to a suppression in homocoupling and a good yield of the cross-coupled product. In stark contrast to the good activity obtained with aryl chloride substrates, poor performance was obtained with aryl bromides and iodides. In its simplest form, the reaction requires a large excess of the aryl Grignard to maximise the yield of the cross-coupled product, which the authors suggested may be due to slow deprotonation of the carbene precursor. To accelerate this deprotonation, the catalyst mixture can be pre-activated with sub-stoichiometric amounts of the more basic ethyl Grignard reagent; Scheme 22 outlines this optimised protocol. Very recently, Chua and Duong have shown that the dimeric alkoxide $[Fe_2(O^tBu)_6]$ can be used in place of iron fluorides, and NaO^tBu can replace the alkyl Grignard reagent as the activating agent in such reactions [64].



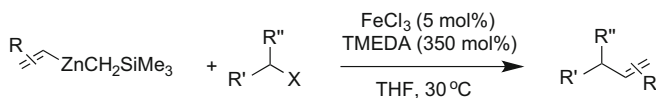
Scheme 22 Optimised conditions for the cross-coupling of aryl chlorides with aryl Grignard reagents

3 Iron Catalysts for the Cross-Coupling of Softer Nucleophiles

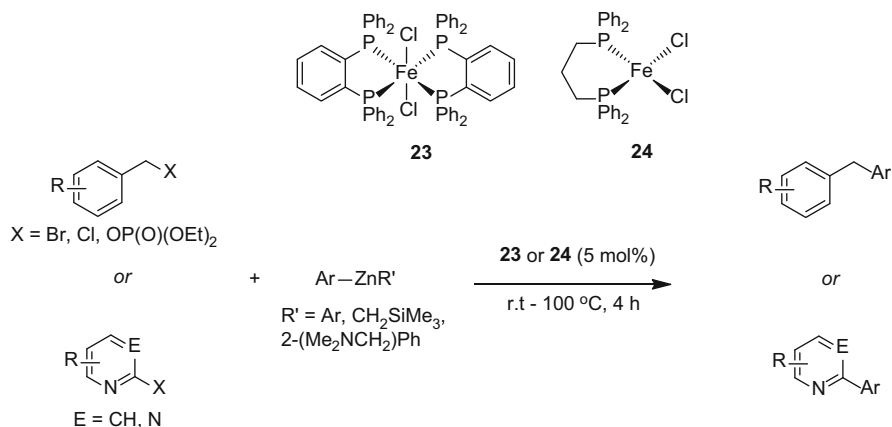
As can be seen in the preceding section, the development of iron-catalysed cross-coupling of aryl, alkyl and related Grignard reagents with electrophilic coupling partners has proceeded apace, and iron can be considered as a serious contender for application to a broad range of such processes. It should be noted, however, that Grignard cross-coupling is limited by the relatively high reactivity of the nucleophile with a range of common functional groups, which can impose constraints on the substitutional decoration of the substrates employed. High relative rates of coupling reactions compared with side reactions, low reaction temperatures or slow addition protocols may help alleviate some of the substrate tolerance problems, but ultimately, the use of less reactive, ‘softer’ nucleophiles provides a synthetically more viable approach. Accordingly, the study of iron-catalysed cross-coupling with softer nucleophiles is garnering increased attention, particularly over the last 5 years or so, although there were seminal reports before this period. Thus, both organocuprate [65–68] and organomanganese nucleophiles [9, 12, 69] have been exploited to good effect, but the majority of this work was reported before 2009 and falls outside of the scope of this review. In this section, we focus instead on zinc, boron and other group 13-based nucleophiles in iron-catalysed cross-coupling.

3.1 Zinc-Based Nucleophiles

An early example of the iron-catalysed cross-coupling of organozinc reagents was reported by Fürstner and co-workers who showed that the triethylzincate anion could be coupled with methyl-4-chlorobenzoate using an $[\text{Fe}(\text{acac})_3]/\text{NMP}$ catalyst system [11, 12]. Following on from this, Nakamura and co-workers showed that alkenylzinc reagents can be coupled with primary and secondary alkyl chlorides, bromides and iodides using FeCl_3 in the presence of excess TMEDA (Scheme 23) [70]. Simple vinyl zinc halides performed poorly; instead diorganozinc reagents with the desired vinyl residue and a non-transferable (trimethylsilyl)methyl group



Scheme 23 Cross-coupling of vinyl zinc reagents with alkyl halides



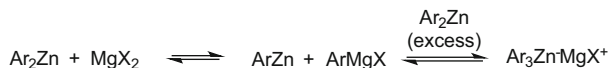
Scheme 24 Cross-coupling of arylzinc reagents with benzyl and 2-*N*-heteroaryl halides and related substrates

were found to work best. These are easily produced in situ by the reaction of zinc chloride with an appropriate vinyl Grignard reagent, followed by reaction with $\text{TMSCH}_2\text{MgCl}$.

Nakamura also found that primary and secondary alkyl sulphonates and arylzinc reagents, formed from ZnI_2 , can be coupled using FeCl_3 as the pre-catalyst and an excess of TMEDA [71]. Key to the success of the reaction is the in situ formation of alkyl iodides from the sulphonate substrates. Again the reaction requires two organic groups on the zinc centre, either a diarylzinc reagent or $\text{ArZnCH}_2\text{TMS}$. It was also found that the presence of cocatalytic amounts of magnesium halide salt is essential for activity.

Iron–phosphine complexes have also proved to be useful in the cross-coupling of arylzinc reagents. Thus, Bedford and co-workers demonstrated that the preformed complexes **23** and, to a lesser extent, **24** can be exploited in the coupling of arylzinc reagents with benzyl halides or phosphates [72] or 2-halopyridines and pyrimidines [73] (Scheme 24). Interestingly, when benzyl halides are used as substrates, then halo substitution on the benzyl ring is unaffected by the cross-coupling, selectivity that could be challenging for palladium catalysis. Shortly afterwards, Nakamura and co-workers demonstrated that the pre-catalyst **23** can be used in the Negishi coupling of electron-deficient fluoroaryl zinc reagents with alkyl halides [74].

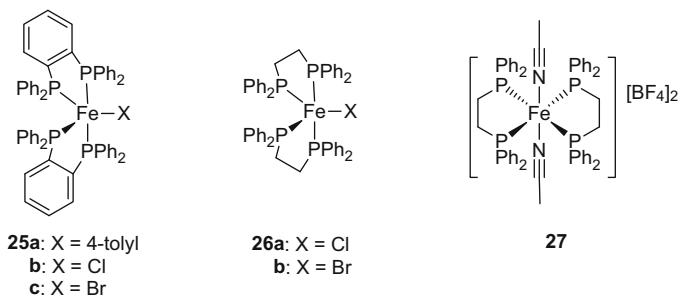
The need to use diorganozinc reagents and the requirement of magnesium halide in the reaction mixture is common to all of the cross-coupling reactions described



Scheme 25 Hetero-Schlenk equilibrium between diarylzinc and triarylzincate in the presence of magnesium salts

above. The (trimethylsilyl)methyl group can be used to good effect in all of the reactions as a non-transferable ‘dummy’ ligand and is easily prepared in situ; however, the precursor, $\text{TMSCH}_2\text{MgCl}$, is relatively expensive. Accordingly, Bedford and co-workers sought to replace it with a cheaper alternative and found that ortho-zincated *N,N*-dimethylbenzylamine worked well in this regard [72]. The authors suggested that the need for both a diorganozinc reagent and magnesium halide salts was most likely due to the establishment of a hetero-Schlenk equilibrium leading to the formation of far more nucleophilic triarylzincate species under the reaction conditions (Scheme 25).

As described above, complex **23** is a good catalyst for a range of organozinc cross-coupling reactions, but the chelating diphosphine employed, 1,2-bis(diphenylphosphino)benzene (dpbz), is reasonably expensive, offsetting some of the benefits of iron catalysis. During a study into the likely catalytic intermediates formed from pre-catalyst **23**, Bedford and co-workers isolated the iron (I) complexes **25a–c**. While **25a** proved to be an off-cycle species, the bromide complex **25c** behaves like a viable catalytic intermediate or resting state species [75]. Based on the findings from this study, it was concluded that cheaper, more readily available diphosphines such as dppe may be exploitable, provided they are introduced into the reaction in such a way as to maximise the chances of formation of bis(diphosphine) iron(I) complexes. Part of the problem here is that simple bis-dppe complexes of iron dichloride do not form. However, both the preformed Fe(I) bis-dppe complexes **26a** and **b** and the cationic iron(II) bis-dppe complex **27** show good activity in the coupling of arylzinc reagents with benzyl or alkyl halides [76].



In 2012, Quing and co-workers reported the cross-coupling of α -halo- β,β -difluoroethylene-containing compounds with arylzinc reagents using TMEDA and dppe as co-ligands. This methodology affords a wide range of *gem*-difluoromethylated compounds in moderate to good yields. The competitive

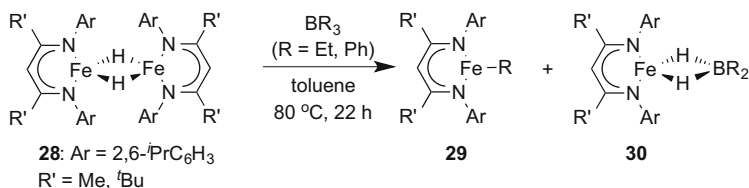
dehalodefluorination reaction typically observed upon treatment of such substrates with reductive metal reagents was largely suppressed in this case [77].

3.2 Boron-Based Nucleophiles

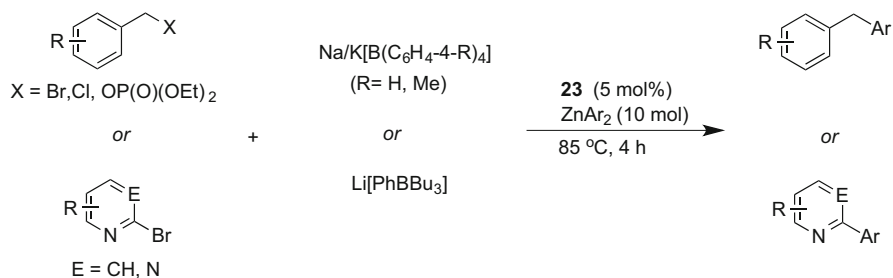
Boron-based nucleophilic coupling partners are especially attractive in cross-coupling reactions due to their stability, comparatively low toxicity and substrate and media tolerance. Indeed the palladium-catalysed Suzuki–Miyaura reaction is a mainstay of biaryl and related bond-forming processes. By contrast, analogous iron-catalysed processes remain in their infancy. An early report by Young and co-workers in 2008 showed that while no reaction was observed at atmospheric pressure, at 15,000 bar and 100 °C, phenylboronic acid could be coupled with either bromobenzene or 4-bromotoluene using a mixture of FeCl₃ and (2-pyridyl) diphenylphosphine as pre-catalyst [78]. While interesting, this methodology is synthetically limited by the extremely high pressures required. However, it remains the only example to date of an iron-catalysed Suzuki cross-coupling that exploits boronic acid substrates; the activity of simple iron-based catalyst systems reported to achieve the same results under mild conditions was subsequently shown to be most likely due to impurities in the reaction mixture [79], and the report was retracted [80], as was a similar publication shortly afterwards [81].

The development of straightforward, rapid transmetalation between boron and iron seems to be a major stumbling block in the development of routine iron-catalysed Suzuki cross-coupling reactions. For instance, in an early example of such a transmetalation process, Holland and co-workers showed that the complex **28** reacts only slowly with triethyl or triphenylboron to generate equimolar mixtures of the transmetalated product **29** and the dihydroborate complex **30** (Scheme 26) [82]. Interestingly, Ingleson and co-workers very recently showed that iron–NHC complexes react with representative borates ArB(OR)₃[−] by transfer of the alkoxide rather than the aryl group, a finding which suggests simple transmetalation with more traditional borate precursors may prove problematic [83].

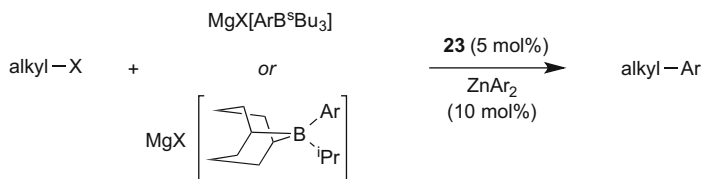
In an early attempt to circumvent the issues of B–Fe transmetalation, Bedford and co-workers exploited cocatalytic amounts of zinc additives in the coupling of tetraarylborates and, to a lesser extent, an aryltrialkylborate, with benzyl or 2-*N*-



Scheme 26 B–Fe transmetalation with triorganoboron reagents



Scheme 27 Iron-catalysed Suzuki coupling of benzyl and 2-*N*-heteroarylhalides with tetraorganoboron reagents



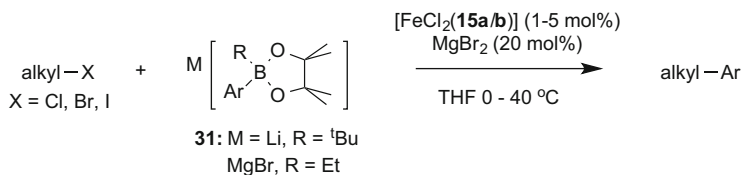
Scheme 28 Iron-catalysed Suzuki coupling of alkyl halides conveniently prepared aryl trialkylboronates

heteroarylhalides, catalysed by complex **23** (Scheme 27) [73]. They suggested that the reaction proceeds via a facile, sequential B–Zn/Zn–Fe transmetallation process. The chelating bisphosphine exploited in this case, dpbz, is expensive, and recently the authors have reported the application of complexes **26a** and **27**, based on the cheaper, more widely available bisphosphine dppe, in the couplings with benzyl halides [76].

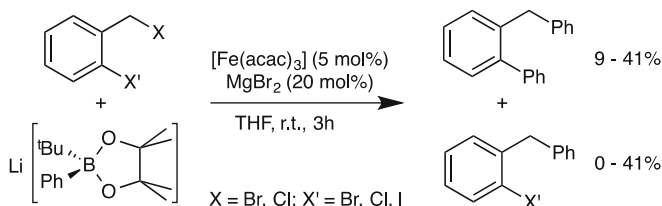
The two main drawbacks to the use of tetraarylborates as the nucleophilic coupling partner are the lack of commercially available reagents and the fact that only one of the four aryl groups is transferred. Bedford and co-workers recently reported that this problem can be circumvented by the use of aryltrialkylborates, which are readily synthesised in situ from the precursors tri-*sec*-butylborane or *i*Pr-9-BBN (Scheme 28) [84]. The diarylzinc cocatalyst can be conveniently prepared in situ by the reaction of zinc dichloride with the same aryl Grignard reagent used to prepare the arylboronate. Alternatively ZnCl₂ can be used as a cocatalyst albeit at higher (20 mol%) loading.

The use of tetraorganoborates as coupling partners can be extended to Csp³–Csp³ bond formation, as demonstrated by Nakamura and co-workers who showed that a pre-catalyst formed from [Fe(acac)₃] and Xantphos can be used to couple primary and secondary alkyl halides with tetraalkylboronates [85].

While the iron-catalysed coupling of tetraorganoborates with alkyl halides can generate a wide range of useful products, it is obviously desirable to be able to exploit the types of boron-based nucleophiles more typically associated with Suzuki cross-coupling, namely, those derived from boronic acids. The problem



Scheme 29 Iron-catalysed Suzuki coupling of primary and secondary alkyl halides with aryl alkyl pinacol boronate reagents



Scheme 30 Iron-catalysed Suzuki coupling of 2-halobenzylhalides with aryl alkyl pinacol boronate reagents

here is that, as described above, transfer of an oxygen-based group from the boron centre to the iron may be preferred over transmetalation of an organic function [83]. However, this can be prevented if the oxygen donors are held in a chelate ring, such as that found in the pinacol esters of boronic acids. Thus, Nakamura and co-workers reported the iron-catalysed Suzuki coupling of alkyl halides with the aryl alkyl pinacol ester boronates, **31**, formed in situ by the reaction of the parent arylboronic pinacol esters with *tert*-butyllithium or, to a lesser extent, EtMgBr (Scheme 29) [86]. The complexes [FeCl₂(**15a/b**)] serve as effective pre-catalysts, while magnesium halides act as cocatalysts. The reaction does not proceed in the absence of the magnesium halide, and although it is not yet clear what the role of the salt is in the transformation, the authors speculate that it may accelerate the transmetalation between boron and iron centres. Nakamura and co-workers also found that vinyl alkyl pinacol boronate analogues of **31** could be cross-coupled with alkyl, allyl and benzyl halides using [FeCl₂(**15a/b**)] as the pre-catalysts [87].

A major drawback in these reactions is the apparent requirement of the synthetically elaborate bisphosphine ligands **15a** or **b**. However, Bedford and co-workers recently showed that far simpler pre-catalysts such as [FeCl₂(dppe)], [FeCl₂(dppp)] or even, with more activated electrophilic coupling partners, the phosphine-free complex [Fe(acac)₃] can be exploited to excellent effect in such reactions [88]. Under these conditions, a range of primary and secondary alkyl, benzyl and allyl halides can be coupled with the aryl alkyl boronates **31**.

As discussed earlier, iron-catalysed biaryl bond formation remains challenging, and this appears to be particularly true of Suzuki biaryl bond formation. However, a recent paper by Bedford and co-workers shows that some biaryl bond formation can occur when using 2-halobenzylhalides as coupling partners with alkyl aryl boronates (Scheme 30) [89]. While not yet at a stage of being a synthetically viable

process, this holds the promise that routine, iron-catalysed Suzuki biaryl bond formation may well be achievable.

3.3 *Aluminium-, Gallium-, Indium- and Thallium-Based Nucleophiles*

In addition to the use of organoboron reagents described above, there have been a few reports that show that other group 13-based nucleophiles can be exploited in iron-catalysed cross-coupling reactions. The first example was reported by Nakamura and co-workers who demonstrated that primary and secondary alkyl halides can be coupled with $[AlAr_4]MgX$ salts using complex **23** as the catalyst [90]. The aluminate salt is easily prepared in situ by the reaction of $AlCl_3$ with the appropriate arylmagnesium chloride reagent (the use of $ArMgBr$ proved to be deleterious to catalyst performance). By contrast, no activity was observed with the salt-free, neutral $AlPh_3$, highlighting the importance of the more nucleophilic ‘ate’ complexes. Subsequently, Nakamura showed that arylaluminates could be coupled with non-protected halohydrins, catalysed by the complexes $[FeCl(15a/b)]$ [91]. These reactions most likely proceed via the in situ formation of aluminium alkoxide intermediates.

Again, simpler, less expensive phosphine ligands can be exploited in the coupling of organoaluminium species. Bedford and co-workers showed that complexes **26a** or **27** can be used to good effect in the coupling of tetraarylaluminates with alkyl and benzyl halides [76]. Under these conditions, the tetraarylindate $MgCl[In(tolyl)_4]$ can be used in place of the aluminate. The same authors recently showed that the complex **23** can be used as a pre-catalyst in the coupling of $MgX[MAr_4]$ ($M = Al, Ga, In$) or MAr_3 reagents ($M = Al, In, Tl$) with a range of alkyl, benzyl and allyl halides [84].

4 Summary and Outlook

The development of iron-catalysed cross-coupling processes has continued apace, with a substantial number of important publications appearing over the last 5 years or so. The majority of papers published during this time have concerned the coupling reactions of Grignard reagents, but there has been a noticeable shift towards developing catalyst systems that are capable of tackling more challenging but synthetically more useful ‘soft’ nucleophiles. Despite these advances, significant challenges remain, not least with regard to the types of soft nucleophiles that can participate in iron-catalysed coupling reactions. It is important that we develop new processes based on simpler nucleophiles, in particular those based on boron. Here the challenge is to achieve facile, rapid transmetallation between simple

organoboron reagents and the iron centre. Others challenges that still exist include the need to replace reprotoxic NMP in Grignard cross-coupling reactions. While slow addition of Grignard reagent, typically using a syringe pump, can sometimes circumvent the need for NMP, this in itself can limit a method's applicability and appeal. Consequently the development of catalysts that can tolerate the rapid addition of Grignard reagents to reaction mixtures remains a desirable, yet largely unmet target. Beyond NMP, several other 'additives' are used in iron-catalysed cross-coupling, often seemingly as part of some kind of 'witches brew', and it is becoming increasingly important to delineate what precise roles are played by these species. Finally there are still noticeable gaps in the coupling partners that can be routinely tolerated, for instance, there is a paucity of iron-catalysed biaryl bond-forming processes, and these gaps need to be filled in order for iron to be considered truly competitive with palladium in cross-coupling.

References

1. Vavon G, Mottez P (1944) Action des dérivés halogénés sur les magnésiens aromatiques en présence de chlorure ferrique. *C R Hebd Seances Acad Sci* 218:557–559
2. Tamura M, Kochi J (1971) Vinylation of Grignard reagents – catalysis by iron. *J Am Chem Soc* 93:1487–1489
3. Tamura M, Kochi J (1971) Coupling of Grignard reagents with organic halides. *Synthesis* 3:303–305
4. Neumann SM, Kochi JK (1975) Synthesis of olefins. Cross-coupling of alkenyl halides and Grignard reagents catalyzed by iron complexes. *J Org Chem* 40:599–606
5. Smith RS, Kochi JK (1976) Mechanistic studies of iron catalysis in the cross coupling of alkenyl halides and Grignard reagents. *J Org Chem* 41:502–509
6. Kochi JK (1974) Electron-transfer mechanisms for organometallic intermediates in catalytic reactions. *Acc Chem Res* 7:351–360
7. Molander GA, Rahn BJ, Shubert DC, Bonde SE (1983) Iron catalyzed cross-coupling reactions. Synthesis of arylenethenes. *Tetrahedron Lett* 24:5449–5452
8. Cahiez G, Avedissian H (1998) Highly stereo- and chemoselective iron-catalyzed alkenylation of organomagnesium compounds. *Synthesis* 8:1199–1205
9. Cahiez G, Marquais S (1996) Cu-catalyzed alkylation and Fe catalyzed alkenylation of organomanganese reagents. *Pure Appl Chem* 68:53–60
10. Dohle W, Kopp F, Cahiez G, Knochel P (2001) Fe(III)-catalyzed cross-coupling between functionalized arylmagnesium compounds and alkenyl halides. *Synlett* 12:1901–1904
11. Fürstner A, Leitner A (2002) Iron-catalyzed cross-coupling reactions of alkyl Grignard reagents with aryl chlorides, tosylates, and triflates. *Angew Chem Int Ed* 41:609–612
12. Fürstner A, Leitner A, Méndez M, Krause H (2002) Iron-catalyzed cross-coupling reactions. *J Am Chem Soc* 124:13856–13863
13. Fürstner A, Leitner A (2003) A catalytic approach to (R)-(+)-muscopyridine with integrated "self-clearance". *Angew Chem Int Ed* 42:308–311
14. Martin R, Fürstner A (2004) Cross-coupling of alkyl halides with aryl Grignard reagents catalyzed by a low-valent iron complex. *Angew Chem Int Ed* 43:3955–3957
15. Nakamura M, Matsuo K, Ito S, Nakamura E (2004) Iron-catalyzed cross-coupling of primary and secondary alkyl halides with aryl Grignard reagents. *J Am Chem Soc* 126:3686–3687
16. Nagano T, Hayashi T (2004) Iron-catalyzed grignard cross-coupling with alkyl halides possessing β -hydrogens. *Org Lett* 6:1297–1299

17. Bedford RB, Bruce DW, Frost RM, Goodby JW, Hird M (2004) Iron(III) salen-type catalysts for the cross-coupling of aryl Grignards with alkyl halides bearing β -hydrogens. *Chem Commun*:2822–2823
18. Bedford RB, Bruce DW, Frost RM, Hird M (2005) Simple iron-amine catalysts for the cross-coupling of aryl Grignards with alkyl halides bearing β -hydrogens. *Chem Commun*:4161–4163
19. Bedford RB, Betham M, Bruce DW, Danopoulos AA, Frost RM, Hird M (2006) Iron-phosphine, -phosphite, -arsine, and -carbene catalysts for the coupling of primary and secondary alkyl halides with aryl Grignard reagents. *J Org Chem* 71:1104–1110
20. Fürstner A, Martin R, Krause H, Seidel G, Goddard R, Lehmann CW (2008) Preparation, structure, and reactivity of nonstabilized organoiron compounds. Implications for iron-catalyzed cross coupling reactions. *J Am Chem Soc* 130:8773–8787
21. Sherry BD, Fürstner A (2008) The promise and challenge of iron-catalyzed cross coupling. *Acc Chem Res* 41:1500–1511
22. Jegelka M, Plietker B (2011) Catalysis by means of complex ferrates. *Top Organomet Chem* 33:177–213
23. Sun C-L, Fürstner A (2013) Formal ring-opening/cross-coupling reactions of 2-pyrones: iron-catalyzed entry into stereodefined dienyl carboxylates. *Angew Chem Int Ed* 52:13071–13075
24. Cahiez G, Gager O, Habiak V (2008) Iron-catalyzed alkenylation of Grignard reagents by enol phosphates. *Synthesis* 16:2636–2644
25. Cahiez G, Habiak V, Gager O (2008) Efficient preparation of terminal conjugated dienes by coupling of dienol phosphates with Grignard reagents under iron catalysis. *Org Lett* 10:2389–2392
26. Bartocchini F, Piersanti G, Armaroli S, Cerri A, Cabri W (2014) Development of a practical and sustainable strategy for the synthesis of ST1535 by an iron-catalyzed Kumada cross-coupling reaction. *Tetrahedron Lett* 55:1376–1378
27. Guo W-J, Wang Z-X (2013) Iron-catalyzed cross-coupling of aryltrimethylammonium triflates and alkyl Grignard reagents. *Tetrahedron* 69:9580–9585
28. Malhotra S, Seng PS, Koenig SG, Deese AJ, Ford KA (2013) Chemoselective sp^2 - sp^3 cross-couplings: Iron-catalyzed alkyl transfer to dihaloareomatics. *Org Lett* 15:3698–3701
29. Güлак S, Jacobi von Wangelin A (2012) Chlorostyrenes in iron-catalyzed biaryl coupling reactions. *Angew Chem Int Ed* 51:1357–1361
30. Ding K, Zannat F, Morris JC, Brennessel WW, Holland PL (2009) Coordination of *N*-methylpyrrolidone to iron(II). *J Organomet Chem* 694:4204–4208
31. Kuzmina OM, Steib AK, Flubacher D, Knochel P (2012) Iron-catalyzed cross-coupling of *N*-heterocyclic chlorides and bromides with arylmagnesium reagents. *Org Lett* 14:4818–4821
32. Cheung CW, Ren P, Hu X (2014) Mild and phosphine-free iron-catalyzed cross-coupling of nonactivated secondary alkyl halides with alkynyl Grignard reagents. *Org Lett* 16:2566–2569
33. Guerinot A, Reymond S, Cossy J (2007) Iron-catalyzed cross-coupling of alkyl halides with alkenyl Grignard reagents. *Angew Chem Int Ed* 46:6521–6524
34. Denmark SE, Cresswell AJ (2013) Iron-catalyzed cross-coupling of unactivated secondary alkyl thio ethers and sulfones with aryl Grignard reagents. *J Org Chem* 78:12593–12628
35. Cahiez G, Habiak V, Duplais C, Moyeux A (2007) Iron-catalyzed alkylations of aromatic Grignard reagents. *Angew Chem Int Ed* 46:4364–4366
36. Rushworth PJ, Hulcoop DG, Fox DJ (2013) Iron/tetramethylethylenediamine-catalyzed ambient-temperature coupling of alkyl Grignard reagents and aryl chlorides. *J Org Chem* 78:9517–9521
37. Czaplak WM, Mayer M, Jacobi von Wangelin A (2009) Domino iron catalysis: direct aryl-alkyl cross-coupling. *Angew Chem Int Ed* 48:607–610
38. Czaplak WM, Mayer M, Jacobi von Wangelin A (2011) Iron-catalyzed reductive aryl-alkenyl cross-coupling reactions. *ChemCatChem* 3:135–138

39. Greenhalgh MD, Kolodziej A, Sinclair F, Thomas SP (2014) Iron-catalyzed hydromagnesiation: synthesis and characterization of benzylic Grignard reagent intermediate and application in the synthesis of ibuprofen. *Organometallics* 33:5811–5819
40. Greenhalgh MD, Thomas SP (2012) Iron-catalyzed, highly regioselective synthesis of α -aryl carboxylic acids from styrene derivatives and CO₂. *J Am Chem Soc* 134:11900–11903
41. Noda D, Sunada Y, Hatakeyama T, Nakamura M, Nagashima H (2009) Effect of TMEDA on iron-catalyzed coupling reactions of ArMgX with alkyl halides. *J Am Chem Soc* 131:6078–6079
42. Bedford RB, Brenner PB, Carter E, Cogswell PM, Haddow MF, Harvey JN, Murphy DM, Nunn J, Woodall CH (2014) TMEDA in iron-catalyzed Kumada coupling: amine adduct versus homoleptic “ate” complex formation. *Angew Chem Int Ed* 53:1804–1808
43. Bedford RB, Betham M, Bruce DW, Davis SA, Frost RM, Hird M (2006) Iron nanoparticles in the coupling of alkyl halides with aryl Grignard reagents. *Chem Commun*:1398–1400
44. Kuzmina OM, Steib AK, Markiewicz JT, Flubacher D, Knochel P (2013) Ligand-accelerated iron- and cobalt-catalyzed cross-coupling reactions between *N*-heteroaryl halides and aryl magnesium reagents. *Angew Chem Int Ed* 52:4945–4949
45. Chowdhury RR, Crane AK, Fowler C, Kwong P, Kozak CM (2008) Iron(III) amine-bis(phenolate) complexes as catalysts for the coupling of alkyl halides with aryl Grignard reagents. *Chem Commun*:94–96
46. Hasan K, Dawe LN, Kozak CM (2011) Synthesis, structure, and C-C cross-coupling activity of (amine)bis(phenolato)iron(acac) complexes. *Eur J Inorg Chem* 29:4610–4621
47. Reckling AM, Martin D, Dawe LN, Decken A, Kozak CM (2011) Structure and C-C cross-coupling reactivity of iron(III) complexes of halogenated amine-bis(phenolate) ligands. *J Organomet Chem* 696:787–794
48. Qian X, Dawe LN, Kozak CM (2011) Catalytic alkylation of aryl Grignard reagents by iron(III) amine-bis(phenolate) complexes. *Dalton Trans* 40:933–943
49. Chard EF, Dawe LN, Kozak CM (2013) Coupling of benzyl halides with aryl Grignard reagents catalyzed by iron(III) amine-bis(phenolate) complexes. *J Organomet Chem* 737:32–39
50. Cahiez G, Gager O, Buendia J, Patinote C (2012) Iron thiolate complexes: efficient catalysts for coupling alkenyl halides with alkyl Grignard reagents. *Chem Eur J* 18:5860–5863
51. Dongol KG, Koh H, Sau M, Chai CLL (2007) Iron-catalysed sp³–sp³ cross-coupling reactions of unactivated alkyl halides with alkyl Grignard reagents. *Adv Synth Catal* 349:1015–1018
52. Hatakeyama T, Fujiwara Y, Okada Y, Itoh T, Hashimoto T, Kawamura S, Ogata K, Takaya H, Nakamura M (2011) Kumada-Tamao-Corriu coupling of alkyl halides catalyzed by an iron-bisphosphine complex. *Chem Lett* 40:1030–1032
53. Kawamura S, Nakamura M (2013) Ligand-controlled iron-catalyzed cross coupling of benzylic chlorides with aryl Grignard reagents. *Chem Lett* 42:183–185
54. Hatakeyama T, Okada Y, Yoshimoto Y, Nakamura M (2011) Tuning chemoselectivity in iron-catalyzed Sonogashira-type reactions using a bisphosphine ligand with peripheral steric bulk: selective alkynylation of nonactivated alkyl halides. *Angew Chem Int Ed* 50:10973–10976
55. Sun C-L, Krause H, Fürstner A (2014) A practical procedure for iron-catalyzed cross-coupling reactions of sterically hindered aryl-Grignard reagents with primary alkyl halides. *Adv Synth Catal* 356:1281–1291
56. Bica K, Gaertner P (2006) An iron-containing ionic liquid as recyclable catalyst for aryl Grignard cross-coupling of alkyl halides. *Org Lett* 8:733–735
57. Ghorai SK, Jin M, Hatakeyama T, Nakamura M (2012) Cross-coupling of non-activated chloroalkanes with aryl Grignard reagents in the presence of iron/*N*-heterocyclic carbene catalysts. *Org Lett* 14:1066–1069
58. Silberstein AL, Ramgren SD, Garg NK (2012) Iron-catalyzed alkylations of aryl sulfamates and carbamates. *Org Lett* 14:3796–3799

59. Perry MC, Gillett AN, Law TC (2012) An unprecedented iron-catalyzed cross-coupling of primary and secondary alkyl Grignard reagents with non-activated aryl chlorides. *Tetrahedron Lett* 53:4436–4439
60. Agrawal T, Cook SP (2013) Iron-catalyzed cross-coupling reactions of alkyl Grignards with aryl sulfamates and tosylates. *Org Lett* 15:96–99
61. Guisan-Ceinos M, Tato F, Bunuel E, Calle P, Cardenas DJ (2013) Fe-catalyzed Kumada-type alkyl-alkyl cross-coupling. Evidence for the intermediacy of Fe(I) complexes. *Chem Sci* 4:1098–1104
62. Hatakeyama T, Nakamura M (2007) Iron-catalyzed selective biaryl coupling: remarkable suppression of homocoupling by the fluoride anion. *J Am Chem Soc* 129:9844–9845
63. Hatakeyama T, Hashimoto S, Ishizuka K, Nakamura M (2009) Highly selective biaryl cross-coupling reactions between aryl halides and aryl Grignard reagents: a new catalyst combination of *N*-heterocyclic carbenes and iron, cobalt, and nickel fluorides. *J Am Chem Soc* 131:11949–11963
64. Chua Y-Y, Duong HA (2014) Selective Kumada biaryl cross-coupling reaction enabled by an iron(III) alkoxide-*N*-heterocyclic carbene catalyst system. *Chem Commun* 50:8424–8427
65. Sapountzis I, Lin W, Kofink CC, Despotopoulou C, Knochel P (2005) Iron-catalyzed aryl–aryl cross-couplings with magnesium-derived copper reagents. *Angew Chem Int Ed* 44:1654–1657
66. Dunet G, Knochel P (2006) Iron-catalyzed cross-coupling between alkenyl and dienyl sulfonates and functionalized arylcopper reagents. *Synlett* 3:407–410
67. Kofink CC, Blank B, Pagano S, Götz N, Knochel P (2007) Iron-catalyzed aryl–aryl cross-coupling reaction tolerating amides and unprotected quinolinones. *Chem Commun*:1954–1956
68. Castagnolo D, Botta M (2010) Iron-catalyzed cross-coupling between 1-bromoalkynes and Grignard-derived organocuprate reagents. *Eur J Org Chem* 2010(24):3224–3228
69. Cahiez G, Marquis S (1996) Highly chemo- and stereoselective Fe-catalyzed alkenylation of organomanganese reagents. *Tetrahedron Lett* 37:1773–1776
70. Hatakeyama T, Nakagawa N, Nakamura M (2009) Iron-catalyzed Negishi coupling toward an effective olefin synthesis. *Org Lett* 11:4496–4499
71. Ito S, Fujiwara Y, Nakamura E, Nakamura M (2009) Iron-catalyzed cross-coupling of alkyl sulfonates with arylzinc reagents. *Org Lett* 11:4306–4309
72. Bedford RB, Huwe M, Wilkinson MC (2009) Iron-catalysed Negishi coupling of benzyl halides and phosphates. *Chem Commun*:600–602
73. Bedford RB, Hall MA, Hodges GR, Huwe M, Wilkinson MC (2009) Simple mixed Fe-Zn catalysts for the Suzuki couplings of tetraarylborates with benzyl halides and 2-halopyridines. *Chem Commun*:6430–6432
74. Hatakeyama T, Kondo Y, Fujiwara YI, Takaya H, Ito S, Nakamura E, Nakamura M (2009) Iron-catalysed fluoroaromatic coupling reactions under catalytic modulation with 1,2-bis(diphenylphosphino)benzene. *Chem Commun*:1216–1218
75. Adams CJ, Bedford RB, Carter E, Gower NJ, Haddow MF, Harvey JN, Huwe M, Cartes MA, Mansell SM, Mendoza C, Murphy DM, Neeve EC, Nunn J (2012) Iron(I) in Negishi cross-coupling reactions. *J Am Chem Soc* 134:10333–10336
76. Bedford RB, Carter E, Cogswell PM, Gower NJ, Haddow MF, Harvey JN, Murphy DM, Neeve EC, Nunn J (2013) Simplifying iron-phosphine catalysts for cross-coupling reactions. *Angew Chem Int Ed* 52:1285–1288
77. Lin X, Zheng F, Qing F-L (2012) Iron-catalyzed cross-coupling reactions between arylzinc reagents and alkyl halides bearing β -fluorines. *Organometallics* 31:1578–1582
78. Guo Y, Young DJ, Hor TSA (2008) Palladium-free Suzuki-Miyaura cross-coupling at elevated pressures. *Tetrahedron Lett* 49:5620–5621
79. Bedford RB, Nakamura M, Gower NJ, Haddow MF, Hall MA, Huwe M, Hashimoto T, Okopie RA (2009) Iron-catalysed Suzuki coupling? A cautionary tale. *Tetrahedron Lett* 50:6110–6111
80. Kylmä T, Valkonen A, Rissanen K, Xu Y, Franzén R (2009) Retraction notice to “trans-Tetrakis(pyridine)dichloroiron(II) as catalyst for Suzuki cross-coupling in ethanol and water”. doi:10.1016/j.tetlet.2009.07.103

81. Bézier D, Darcel C (2010) Retraction: iron-catalyzed Suzuki–Miyaura cross-coupling reaction. *Adv Synth Catal* 2010(352):1081
82. Yu Y, Brennessel WW, Holland PL (2007) Borane B–C bond cleavage by a low-coordinate iron hydride complex and N–N Bond cleavage by the hydridoborate product. *Organometallics* 26:3217–3226
83. Dunsford JJ, Cade IA, Fillman KL, Neidig ML, Ingleson MJ (2014) Reactivity of $(\text{NHC})_2\text{FeX}_2$ complexes toward arylborane Lewis acids and arylboronates. *Organometallics* 33:370–377
84. Bedford RB, Brenner PB, Carter E, Clifton J, Cogswell PM, Gower NJ, Haddow MF, Harvey JN, Kehl JA, Murphy DM, Neeve EC, Neidig ML, Nunn J, Snyder BER, Taylor J (2014) Iron phosphine catalyzed cross-coupling of tetraorganoborates and related Group 13 nucleophiles with alkyl halides. *Organometallics* 33:5767–5780
85. Hatakeyama T, Hashimoto T, Kathriarachchi K, Zenmyo T, Seike H, Nakamura M (2012) Iron-catalyzed alkyl–alkyl Suzuki–Miyaura coupling. *Angew Chem Int Ed* 51:8834–8837
86. Hatakeyama T, Hashimoto T, Kondo Y, Fujiwara Y, Seike H, Takaya H, Tamada Y, Ono T, Nakamura M (2010) Iron-catalyzed Suzuki–Miyaura coupling of alkyl halides. *J Am Chem Soc* 132:10674–10676
87. Hashimoto T, Hatakeyama T, Nakamura M (2012) Stereospecific cross-coupling between alkenylboronates and alkyl halides catalyzed by iron–bisphosphine complexes. *J Org Chem* 77:1168–1173
88. Bedford RB, Brenner PB, Carter E, Carvell TW, Cogswell PM, Gallagher T, Harvey JN, Murphy DM, Neeve EC, Nunn J, Pye DR (2014) Expedient iron-catalyzed coupling of alkyl, benzyl and allyl halides with arylboronic esters. *Chem Eur J* 20:7935–7938
89. Bedford RB, Gallagher T, Pye DR, Savage W (2015) Towards iron-catalysed Suzuki Biaryl cross-coupling: unusual reactivity of 2-halobenzyl halides. doi:10.1055/s-0034-1380135
90. Kawamura S, Ishizuka K, Takaya H, Nakamura M (2010) The first iron-catalysed aluminium-variant Negishi coupling: critical effect of co-existing salts on the dynamic equilibrium of arylaluminium species and their reactivity. *Chem Commun* 46:6054–6056
91. Kawamura S, Kawabata T, Ishizuka K, Nakamura M (2012) Iron-catalysed cross-coupling of halohydrins with aryl aluminium reagents: a protecting-group-free strategy attaining remarkable rate enhancement and diastereoselection. *Chem Commun* 48:9376–9378

Iron-Catalyzed Cross-Dehydrogenative-Coupling Reactions

Masumi Itazaki and Hiroshi Nakazawa

Abstract Cross-dehydrogenative-coupling (CDC) reactions involving C–H bond activation are powerful tools for C–C bond formation and are highly significant from the perspective of atom economy. A variety of carbon–carbon bond-forming reactions utilizing various coupling partners are known today. Iron-catalyzed organic syntheses have attracted considerable attention because iron is an abundant, inexpensive, and environmentally benign metal. This chapter summarizes the development of iron-catalyzed CDC reactions, the reaction mechanism, and the role of the Fe species in the catalytic cycle in the period from 2007 to 2014.

Keywords Catalyst · Iron · Cross-dehydrogenative coupling · Oxidant · Radical

Contents

1	Introduction	48
2	Csp ³ –Csp ³ CDC Reaction	50
3	Csp ³ –Csp ² CDC Reactions	60
4	Csp ³ –Csp CDC Reaction	68
5	Other C–C CDC Reaction	72
6	E–E CDC Reaction	74
7	Conclusion	79
	References	80

M. Itazaki and H. Nakazawa (✉)

Department of Chemistry, Graduate School of Science, Osaka City University, 3-3-138
Sugimoto, Sumiyoshi-ku, Osaka 558-8585, Japan
e-mail: nakazawa@sci.osaka-cu.ac.jp

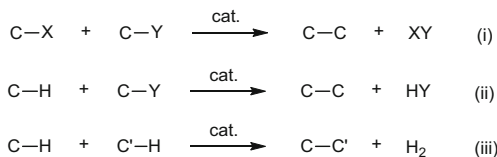
Abbreviations

Å	Ångström
acac	Acetylacetonone
Boc	<i>tert</i> -Butoxycarbonyl
cat.	Catalyst
CDC	Cross-dehydrogenative coupling
Cp	Cyclopentadienyl
dbm	Dibenzoylmethane
DCE	1,2-Dichloroethane
DDQ	2,3-Dichloro-5,6-dicyano- <i>p</i> -benzoquinone
<i>dr</i>	Diastereomeric ratio
equiv.	Equivalent(s)
Et	Ethyl
h	Hour(s)
Me	Methyl
min	Minute(s)
MS	Molecular sieves
Pr	<i>n</i> -Propyl
Ph	Phenyl
pin	Pinacol
rt	Room temperature
Bu	<i>tert</i> -Butyl
SET	Single-electron transfer
TEMPO	2,2,6,6-Tetramethylpiperidine-1-oxyl
TfO	Trifluoromethanesulfonate
TON	Turnover number
Ts	4-Toluensulfonyl

1 Introduction

C–C bond formation is one of the most important reactions in chemistry because organisms represented by a human being mainly consist of C–C bonds. Many reactions to create a C–C bond have been reported to date, and many transition metal complexes have been recognized to serve as useful and powerful catalysts for C–C bond formation (e.g., see [1–5]). Actually, they have attracted much attention from both academic and industrial points of view in the past two decades. These C–C bond formation reactions are roughly classified into three types (Scheme 1):

- (i) Reaction of a compound having a functional group (X) on carbon with that bearing another functional group (Y) on another carbon to form a C–C bond with the formation of X–Y. In some cases, the formation of X–Y is the driving force to promote this reaction. This method has disadvantages because two

Scheme 1 Typical modes of C–C bond formation

different functionalized starting materials have to be prepared from raw materials (usually hydrocarbons) prior to performing the desired C–C bond formation reaction.

- (ii) Reaction of a C–H compound with a functionalized compound (C–X). This is better than (i) because only one functionalized compound is required.
- (iii) Reaction between C–H compounds to form a C–C compound and H₂, which has been referred to as dehydrogenative coupling. This coupling reaction does not require the introduction of a functional group on C and thus shortens synthetic routes and is energy saving and is, thus, a highly recommended route.

However, this reaction has the difficulty of C–H bond activation even if a transition metal complex is used. Another difficulty of the dehydrogenative coupling catalyzed by a transition metal is selectivity which one encounters when he/she tends to perform the reaction of a C–H compound with a C'–H compound to give cross-coupling product (C–C'). In this reaction, C–C and C'–C' coupling products in addition to C–C' product are expected to form. Controlling the reaction to obtain only cross-coupling product without formation of homo-coupling products is a challenging topic.

Among many kinds of transition metals, iron is a highly abundant, cheap, and relatively nontoxic metal. These advantages of iron make it highly attractive as a catalyst. This chapter focuses on cross-dehydrogenative coupling (CDC) catalyzed by iron complexes or salts. Although many examples of transition metal-catalyzed CDC reaction have been reported, the first example of iron-catalyzed CDC reaction was achieved by Li and coworkers in 2007. This chapter summarizes the development of iron-catalyzed CDC reactions, their reaction mechanisms, and the role of the Fe species in the catalytic cycle reported in the period from 2007 to present (2014).

In order to introduce CDC reactions effectively, we classified their reactions using the type of carbon hybridization (sp³, sp², and sp hybridizations) involved in the coupling reactions: Csp³–Csp³ CDC reactions in Sect. 2, Csp³–Csp² CDC reactions in Sect. 3, Csp³–Csp CDC reactions in Sect. 4, and other C–C CDC reactions in Sect. 5. In addition, CDC reactions between main group elements other than carbon are summarized in Sect. 6. CDC reactions between carbon and main group element, such as C–N, C–P, and C–S bond formation, will be introduced in the following chapter of this book.

2 Csp³–Csp³ CDC Reaction

First row transition metal-catalyzed CDC reactions were developed by Li and coworkers in the past few years (for a review on CDC, see [6, 7] and references therein), and cheap copper salts were one of the most efficient and popular catalysts. It was considered that a radical process was involved in these reaction pathways.

In 2007, Li and coworkers reported the first example of selective CDC reaction of benzylic C–H bond catalyzed by iron salt FeCl₂ in the presence of ^tBuOO^tBu as the oxidant (Scheme 2) [8]. In this reaction, the catalytic activity of the iron salt was higher than those of Cu and Co salts. The yield decreased when *tert*-butyl hydrogen peroxide (TBHP) instead of ^tBuOO^tBu was used as an oxidant. In this reaction, only benzylic C–H bond and the C–H bond in the 2-position in the 1,3-dicarbonyl compound are activated to form the CDC product and not to form the homo-dehydrogenative-coupling products.

Table 1 summarizes the scope and limitation of substrates for this CDC reaction. The desired cross-coupling products were obtained in moderate to high yields. Reactions of the benzylic C–H bonds of both diphenylmethane derivatives and cyclic substrates with β -ketoesters and β -ketoamide afforded the desired cross-coupling products. The yields decreased when sterically bulky *tert*-butyl-substituted 1,3-diketone and *ortho*-substituted diphenylmethanes were used as a substrate. The reaction showed tolerance for functionalized diphenylmethanes with electron-withdrawing or electron-donating group on the aryl ring. The reactions of unsymmetrical 1,3-diketones with cyclic benzylic compounds afforded the corresponding CDC products with an approximately 1:1 mixture of diastereomers.

A plausible mechanism for this iron-catalyzed CDC reaction is shown in Scheme 3. The reaction is proposed to undergo a SET pathway. Reaction of ^tBuOO^tBu with Fe(II) affords a *tert*-butoxyl radical and an Fe(III)–O^tBu species. The abstraction of two different protons by the *tert*-butoxyl radical results in the formation of a benzyl radical and an Fe(III) enolate. Finally, the formation of the desired cross-coupling product through the electrophilic radical attack of the benzyl radical regenerates the Fe(II) species to complete the catalytic cycle.

The CDC reaction of activated methylene groups with cycloalkanes was reported by Li and Zhang in 2007. The desired CDC product, a 1,3-dicarbonyl compound, was obtained by the reaction of 1,3-dicarbonyl compounds, alkanes, and 2 equiv. of ^tBuOO^tBu as the oxidant in the presence of FeCl₂·4H₂O (Scheme 4) [9]. Use of other iron halides, for instance, FeCl₂, FeBr₂, FeCl₃, and FeCl₃·6H₂O, decreased the catalytic activity, and iron sources such as Fe(NO₃)₃·9H₂O, FeSO₄·xH₂O, Fe(C₂O₄)·6H₂O, and Fe(acac)₃ showed no activity.

Scheme 2 FeCl₂-catalyzed alkylation of the C–H bond of diphenylmethane

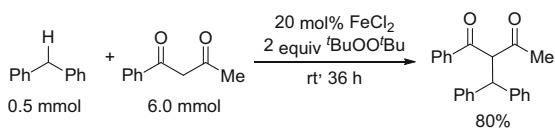
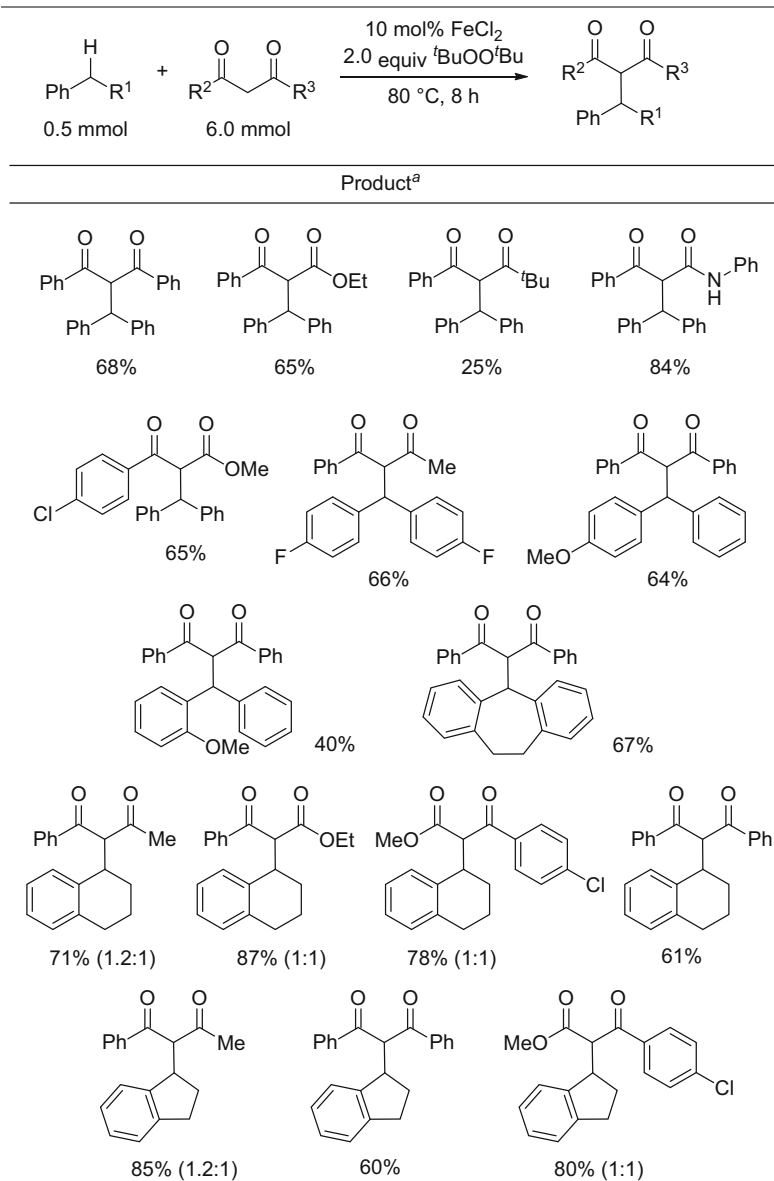
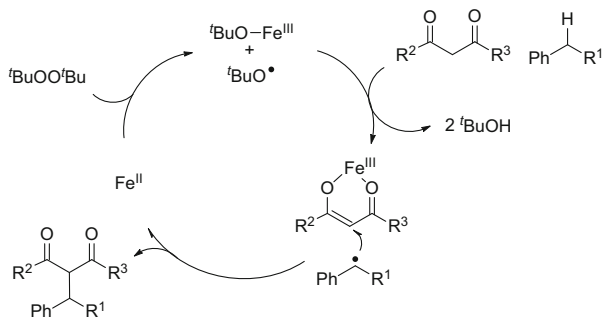


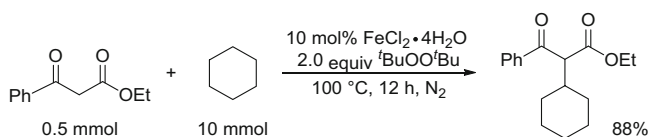
Table 1 FeCl₂-catalyzed selective CDC reaction of benzylic C–H bond

The ratio of the two diastereomers is given in parentheses

^aYield of isolated product



Scheme 3 A plausible mechanism for the iron-catalyzed CDC reaction of benzylic C–H bonds



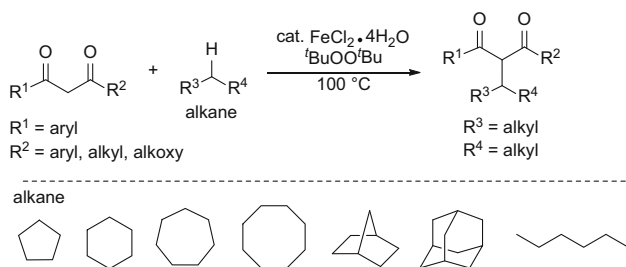
Scheme 4 FeCl₂-catalyzed alkylation of cyclohexane

In this reaction, various cycloalkanes (five-, six-, seven-, and eight-membered rings) were converted to the corresponding products. A mixture of two diastereoisomers in a 1:1 ratio was obtained in the reaction of norbornane with ethyl benzoylacetate. By using adamantane, a 4:1 mixture of regioisomers of the alkylation products was obtained with the major isomer corresponding to the coupling at the more-substituted carbon atom. When *n*-hexane was used, two regioisomers caused by the activation of the two types of methylene C–H bonds were obtained (Scheme 5).

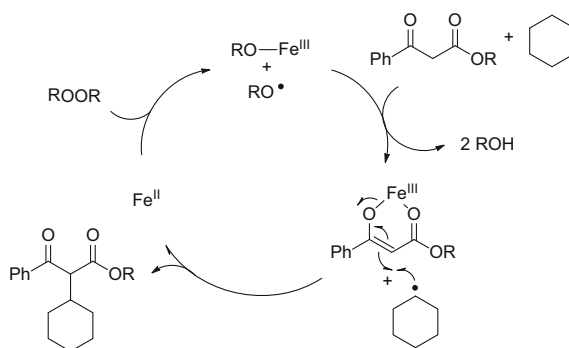
A tentative mechanism for the Fe-catalyzed alkylation of 1,3-dicarbonyl compounds by simple alkanes is depicted in Scheme 6 and is similar to the radical process in the iron-catalyzed CDC reaction of active benzylic C–H bond (see Scheme 2). This reaction process is considered to be a simple free-radical addition onto a C=C bond [10] of an iron benzoylacetate, although no product was obtained by using other metal salts such as CuCl·5H₂O, Cu(OAc)₂, CuSO₄·5H₂O, and CuCl₂ as a catalyst precursor.

An iron-catalyzed dehydrogenative C–C bond formation involving direct C–H bond cleavage adjacent to heteroatoms was reported by Li and coworkers in 2008 (Scheme 7) [11]. In the CDC reaction of THF and ethyl benzoylacetate, FeCl₂, FeBr₂, Fe(OAc)₂, and [Fe₂(CO)₉] acted as efficient catalysts, whereas group 6 carbonyl complexes [Cr(CO)₆] and [W(CO)₆] showed sluggish activity.

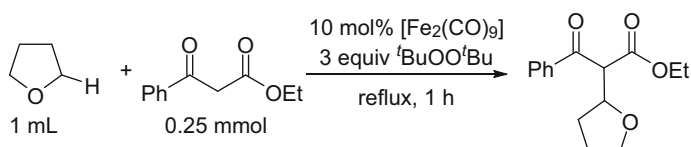
In the presence of Fe₂(CO)₉ as a catalyst, reactions of various acyclic and cyclic ether derivatives with ethyl benzoylacetate gave the corresponding products as a mixture of diastereoisomers in moderate to excellent yields. Tetrahydrothiophene and *N,N*-dimethylaniline were also suitable substrates (Table 2).



Scheme 5 $\text{FeCl}_2 \cdot 4\text{H}_2\text{O}$ -catalyzed, direct alkylation of 1,3-dicarbonyl compounds and alkanes



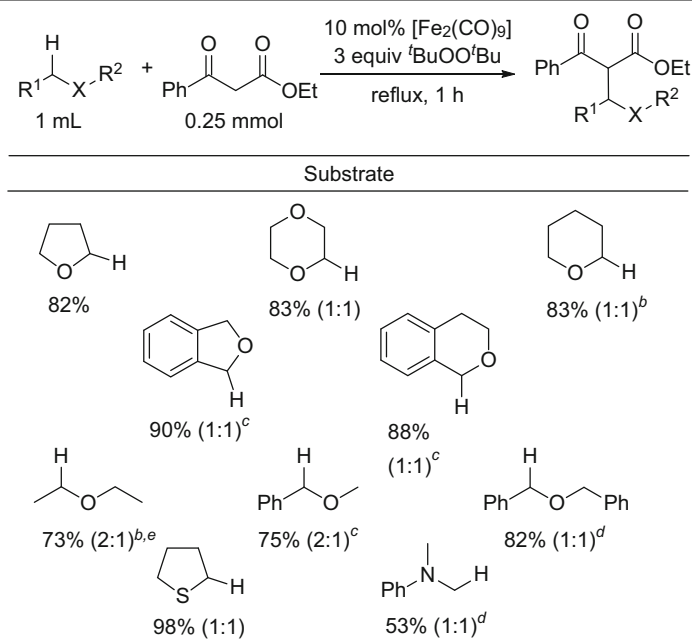
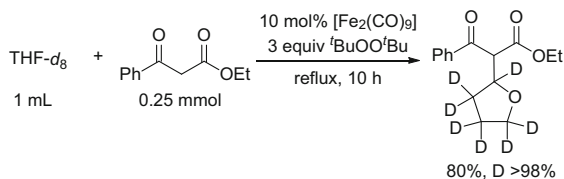
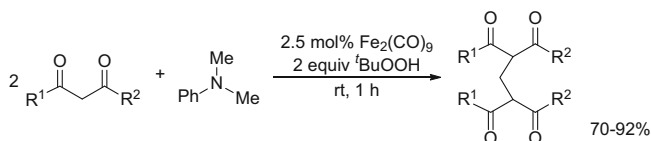
Scheme 6 A tentative mechanism for the Fe-catalyzed alkylation of 1,3-dicarbonyl compound by simple alkane



Scheme 7 An iron-catalyzed CDC reaction with the $\alpha\text{C-H}$ bond of THF

Reaction of $\text{THF-}d_8$ instead of THF with ethyl benzoylacetate afforded the corresponding deuterated product in 80% ($D > 98\%$, Scheme 8). Other possible products as a result of the scrambling of deuterium were not observed. Although details of the mechanism are not clear, it is considered that an iron–carbene species is not generated in the catalytic cycle [12, 13].

An unprecedented dialkylation of the methylene group of the methyl moiety of *N,N*-dimethylaniline was achieved by Li and coworkers in 2009 [14]. In this reaction, 2 equiv. of 1,3-dicarbonyl compounds and *N,N*-dimethylaniline in the presence of $\text{Fe}_2(\text{CO})_9$ were converted to methylene-bridged bis-1,3-dicarbonyl derivatives in high to excellent yield (Scheme 9). Initial screening reactions

Table 2 Fe-catalyzed CDC reactions with C–H bonds adjacent to heteroatoms^aYield of the isolated product; the ratios of the two diastereomers are reported in parentheses^bReaction time was 10 h^c100°C^d80°C^eUsing 30 mol% of the iron catalyst**Scheme 8** Iron-catalyzed CDC reaction of THF-*d*₈ with ethyl benzoylacetate**Scheme 9** Iron-catalyzed selective CDC reactions of *N,N*-dimethylaniline with 1,3-dicarbonyl compounds

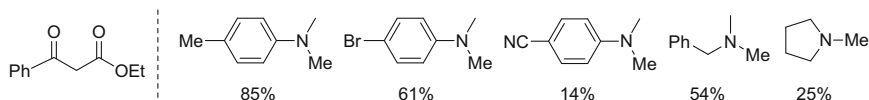
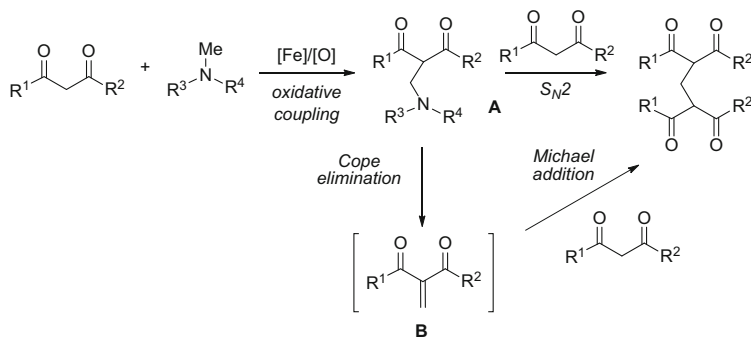


Fig. 1 CDC reactions of *N*-methyl amines with ethyl benzoylacetate



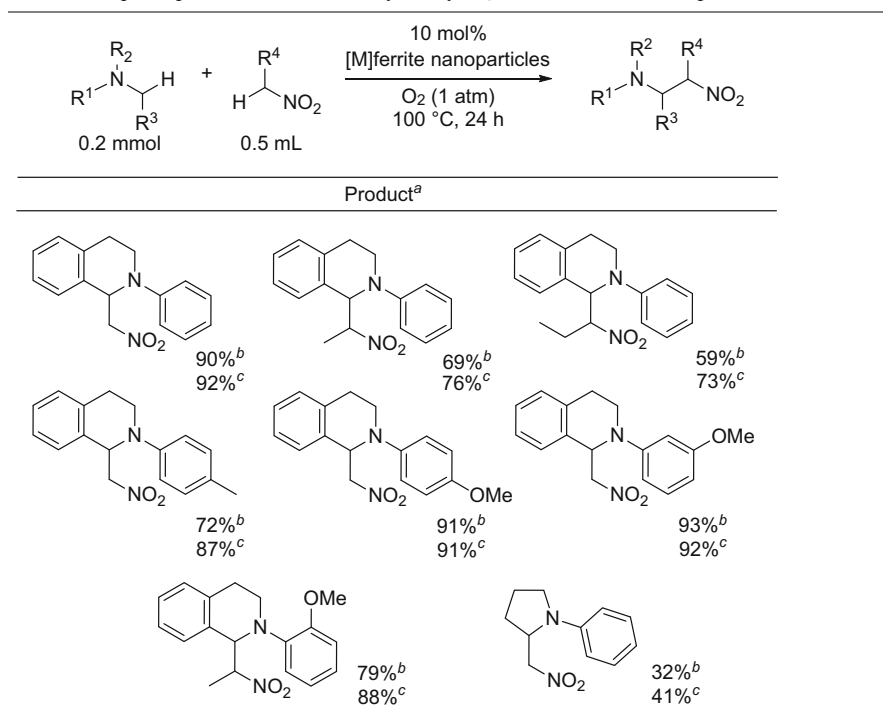
Scheme 10 Two possible pathways for the formation of methylene-bridged bis-1,3-dicarbonyl products

indicated that $\text{Fe}_2(\text{CO})_9$ was the best catalyst and $t\text{BuOOH}$ was the most efficient oxidant.

Other *N*-methyl amines shown in Fig. 1 also were suitable substrates for ethyl benzoylacetate in this catalytic system. Dimethylaniline derivatives with electron-withdrawing groups in the *para* position on the phenyl ring caused low conversions and yields, and aliphatic tertiary amines were not effective methylene sources.

The proposed reaction pathway for the formation of methylene-bridged bis-1,3-dicarbonyl product is shown in Scheme 10. Firstly, the reaction of *N*-methyl amine with 1,3-dicarbonyl compound takes place to give the oxidative coupling product **A**. Next, the following two possibilities are proposed to convert **A** into the final product: (i) the direct $\text{S}_{\text{N}}2$ substitution reaction of **A** with the second molecule of the 1,3-dicarbonyl compound and (ii) a tandem reaction of a Cope elimination from **A** to give **B** followed by the Michael addition of **B** with the second molecule of the 1,3-dicarbonyl compound.

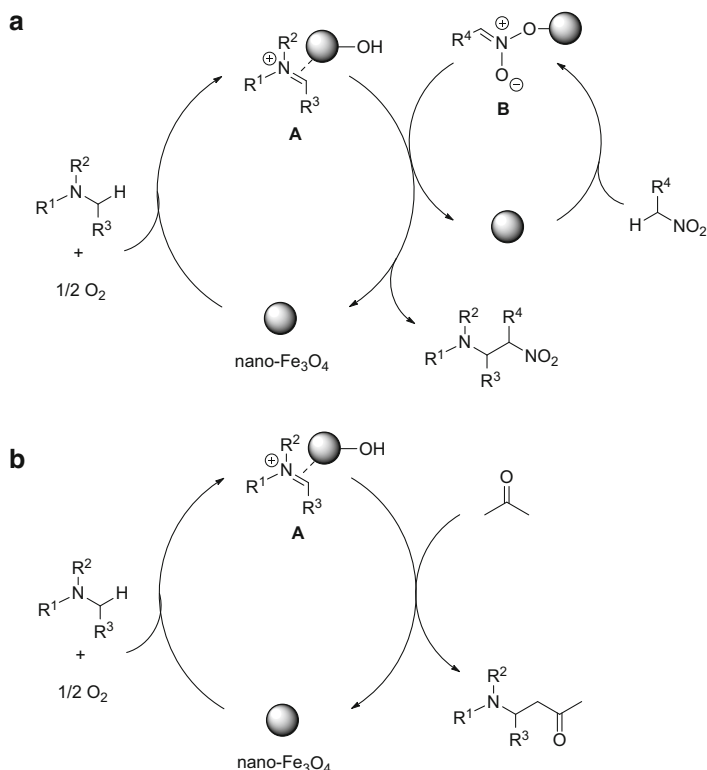
Not only iron halides and iron carbonyl compounds but also nanoparticles based on iron oxides such as Fe_3O_4 and CuFe_2O_4 have been reported to serve as catalyst for $\text{Csp}^3\text{-Csp}^3$ CDC reactions in 2010 and 2013 [15, 16]. The alkylated products summarized in Table 3 were obtained in the reaction of *N*-arylated analogues of tetrahydroisoquinoline with nitroalkanes in the presence of nanoparticles under oxygen. The yields of the product were slightly increased when CuFe_2O_4 instead of Fe_3O_4 was used. These nanoparticles have advantages because the Fe_3O_4 and CuFe_2O_4 can be easily recovered by using an external magnet and recycled up to ten times without significant decrease in activity. By using acetone instead of nitroalkane, the corresponding amino ketone was obtained in the presence of

Table 3 Csp³–Csp³ CDC reactions catalyzed by Fe₃O₄ and CuFe₂O₄ nanoparticles^aIsolated yield^bUsing Fe₃O₄ as a catalyst^cUsing CuFe₂O₄ as a catalyst

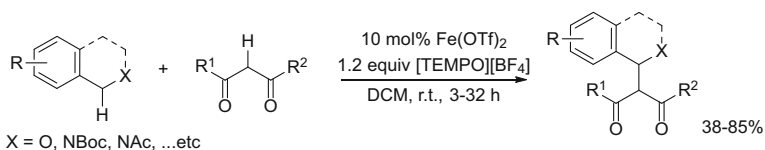
Fe₃O₄ in good yield. In addition, the copper ferrite (CuFe₂O₄) also acted as a catalyst for the Csp³–Csp³ CDC reaction of *N*-arylated analogues of tetrahydroisoquinoline with various aromatic alkynes (see: Sect. 4, Table 5).

The proposed CDC reaction mechanisms catalyzed by iron nanoparticles for (a) nitroalkanes and (b) acetone are shown in Scheme 11. An iminium cation is generated by the Fe₃O₄-catalyzed oxidation of the tertiary amine in situ [17, 18]. The coordination of an iminium cation to Fe₃O₄ nanoparticles affords the intermediate **A**. The Fe₃O₄ nanoparticles also act as a catalyst for deprotonation of nitroalkanes to generate intermediate **B** [19]. Subsequently, a coupling reaction of the two intermediates **A** and **B** yields the desired product and reinstalls the Fe₃O₄ nanoparticle to complete the catalytic cycle. Furthermore, the intermediate **A** also reacts with acetone to give the corresponding amino ketone [20].

In 2010, Richter and Mancheño reported an iron-catalyzed dehydrogenative functionalization of Csp³–H bonds adjacent to a heteroatom by using TEMPO oxoammonium salts (T⁺Y⁻) [21]. In this study, Fe(OTf)₂ was found to be an efficient catalyst in the presence of [TEMPO][BF₄] as a mild oxidant. Under



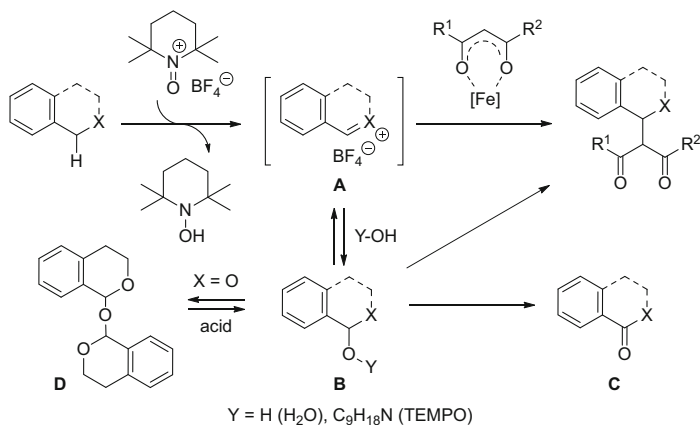
Scheme 11 The proposed CDC reaction mechanisms for (a) nitroalkanes and (b) acetone



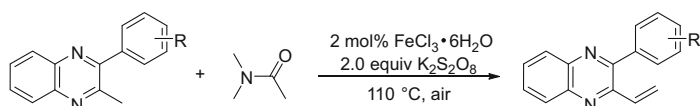
Scheme 12 Fe-catalyzed dehydrogenative functionalization of Csp³-H bonds adjacent to a heteroatom

optimized conditions, both isochromane and tetrahydroisoquinoline derivatives reacted smoothly with different 1,3-dicarbonyl substrates to give the desired products in moderate to high yield with accompanying trace amounts of isochromanone (Scheme 12).

Although the coupling products of this reaction are similar to that of Li's reaction [11], the reaction mechanisms are quite different. Reaction of isochromane and tetrahydroisoquinoline derivatives with [TEMPO][BF₄] affords oxonium or iminium intermediates **A** via hydride transfer to the oxygen of TEMPO⁺ (T⁺). Subsequently, the pronucleophile, which is generated by the iron catalyst and



Scheme 13 A possible reaction mechanisms via an ionic intermediate



Scheme 14 Fe-catalyzed direct vinylation of benzylic C–H bonds

1,3-dicarbonyl substrates, reacts with **A** to form the coupling product (Scheme 13). On the other hand, an intermediate **B** is generated by the nucleophilic attack of trace amounts of water or TEMPOH to the cationic intermediate **A**. Subsequent oxidation of **B** produces iso-chromanone **C** as a by-product. The oxygenated dimer **D** can form by the reaction of iso-chromanone with [TEMPO][BF₄] and can also be transformed to the desired product through the intermediate **B**. The cleavage of dimer **D** with acids is known [22]. In this reaction, the iron species acts as a simple Lewis acid.

The direct vinylation of the benzylic C–H bonds using the *N*-methyl group in amides was achieved by Xu and coworkers in 2012 (Scheme 14) [23]. The vinylated products were obtained by the reaction of various 2-methyl azaarene derivatives with *N,N*-dimethylformamide or *N,N*-dimethylacetamide in the presence of FeCl₃·6H₂O and K₂S₂O₈ as an oxidant in good to excellent yields. This reaction showed good functional group tolerance. Substrates with electron-withdrawing or electron-donating groups and sterically bulky groups such as F, Cl, Br, I, OMe, Me, NO₂, CF₃, Ph, and Ph(Me)₂-2,4 on the aryl ring could be employed in the reaction.

The carbon sources on the left side of the dashed line were highly effective as well as *N,N*-dimethylformamide, whereas those on the right side were not active in this catalytic system (Fig. 2).

A potential reaction mechanism for the vinylation of benzylic C–H bonds is depicted in Scheme 15. The reaction is initiated by formation of enamine **A** in situ [24–28]. Subsequently, the reaction of **A** with the iminium species **B** [29–32],

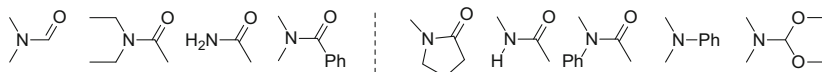
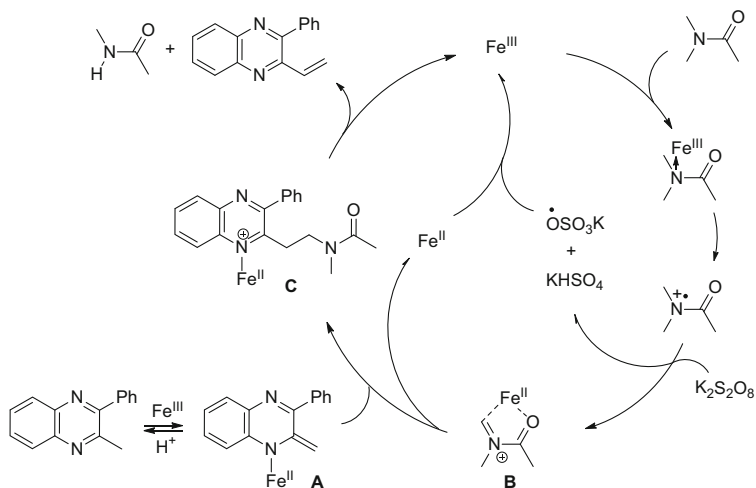


Fig. 2 Other amines as a carbon source for vinylation reaction



Scheme 15 A possible reaction mechanism for vinylation of the benzylic C-H bonds

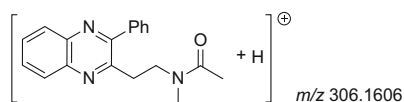


Fig. 3 A key intermediate coupled between 2-phenyl-3-methylquinoxaline and *N,N*-dimethylacetamide

which is generated by the Fe^{II} species, the amide compound, and K₂S₂O₈, gives the intermediate **C**. Then, elimination of *N*-methylacetamide from **C** affords the vinylated product and regenerates the Fe^{III} species. Addition of TEMPO (2 equiv.), a radical scavenger, to the system inhibited the formation of the desired product, suggesting that the reaction proceeds through a radical pathway.

Furthermore, a key coupling intermediate between 2-phenyl-3-methylquinoxaline and *N,N*-dimethylacetamide was detected (*m/z*: 306.1598) by mass spectrometry (Fig. 3).

3 Csp³–Csp² CDC Reactions

Csp³–Csp² CDC reactions were early reported by Minisci (for a review on Minisci radical alkylation and acylation, see [33–41]). The alkylation and acylation reactions involved the generation of an sp³-centered carbon radical, which added to olefins or to protonated heterocycles. Although a large number of the Csp³–Csp² CDC reactions have been reported since the 1970s, iron-catalyzed versions of the reaction were not discovered until recently.

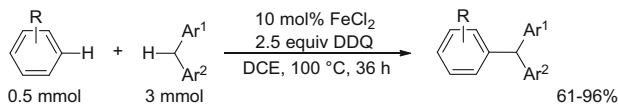
In 2009, Shi and coworkers reported an iron-catalyzed dehydrogenative cross-arylation of a benzylic C–H bond with arenes (Scheme 16) [42]. The desired coupling products were obtained by reactions of various electron-rich arenes with diarylmethanes in the presence of FeCl₂ and DDQ as the oxidant in good to excellent yields. This reaction was highly efficient but required relatively harsh conditions (100 °C for 36 h under N₂). The use of iron sources, for instance, FeBr₂ and Fe(OAc)₂, showed efficient catalytic activity, and other metal chlorides such as NiCl₂, CoCl₂, PdCl₂, and CuCl₂ showed only low activity. DDQ was the best oxidant for both efficient and safety considerations.

The double CDC product was obtained in an excellent yield when a more electron-rich arene, 1,2,3-trimethoxybenzene, was used (Fig. 4, left). Moreover, the dimerization of xylene forming a C(methyl)–C(aryl) bond took place at higher temperature (150 °C), and the turnover number was 11 (Fig. 4, right).

The proposed mechanism for the Fe-catalyzed cross-dehydrogenative arylation is shown in Scheme 17. In this catalytic cycle, a radical species, generated from the first step with DDQ, might be further oxidized to the benzyl cation. Subsequently, a Friedel–Crafts-type alkylation, followed by abstraction of the proton by the reduced hydroquinone, gives the coupling product and regenerates the catalytically active iron species.

Iron-catalyzed direct functionalization of benzylic C–H bonds with vinyl acetates was also achieved by Shi and coworkers in 2009 [43]. The reaction ran very smoothly to get the cross-coupling products in good to excellent yields in the presence of FeCl₂ and ^tBuOO^tBu. The yields decreased when other peroxides such as TBHP and ^tBuOOCOPh instead of ^tBuOO^tBu were used as an oxidant.

Table 4 summarizes the scope and limitation of substrates for this reaction. The system possesses a good degree of functional group tolerance for the functionalized diarylmethane with an electron-withdrawing group such as F or Cl in the *para* position on the aryl ring (entries 2–4), whereas electron-donating OMe group reduces the efficiency (Entry 6). The yield dramatically decreased by using an



Scheme 16 Iron-catalyzed cross-dehydrogenative arylation of aryl C–H bonds with benzylic C–H bonds

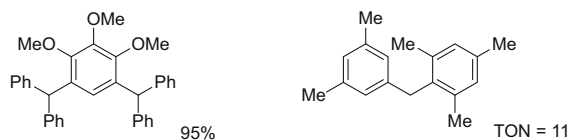
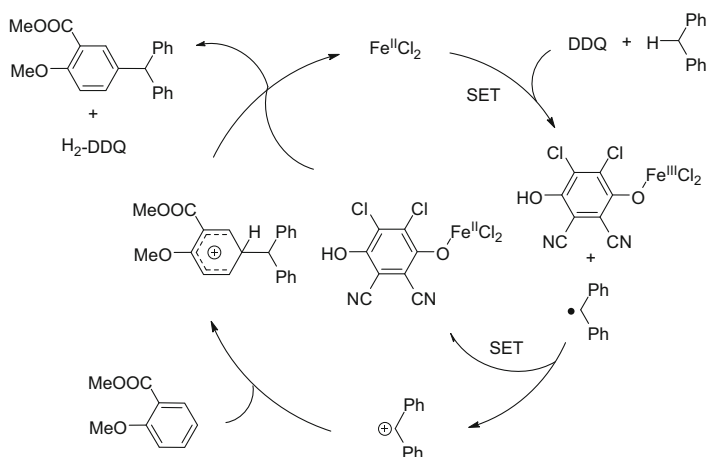
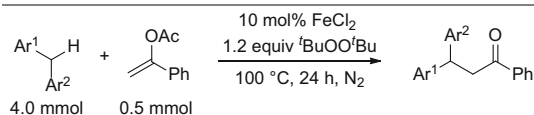


Fig. 4 The CDC coupling products



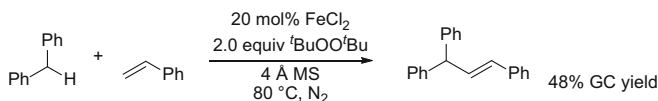
Scheme 17 A plausible mechanism for cross-dehydrogenative arylation

Table 4 C–C bond formation reaction via iron-catalyzed benzylic Csp³–H activation

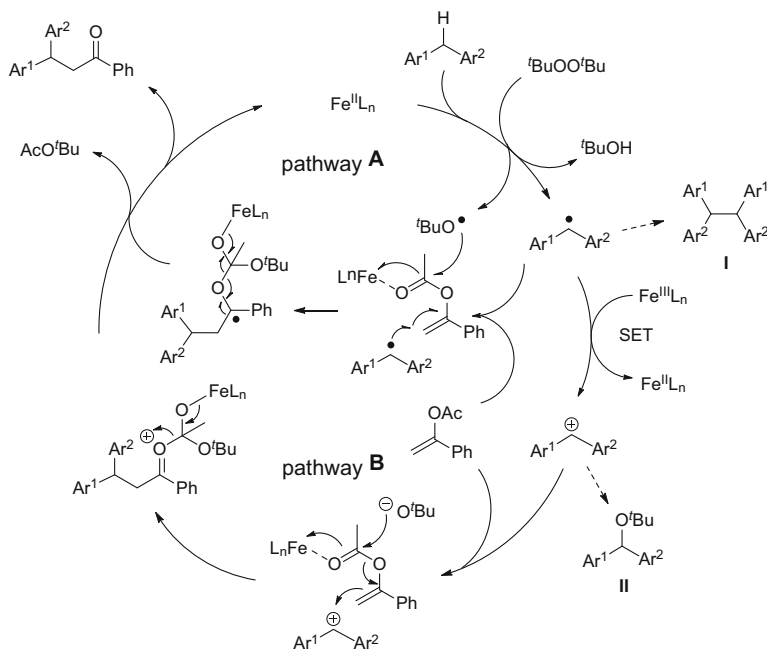


Entry	Ar ¹	Ar ²	Yield (%) ^a
1	Ph	Ph	74
2	4-FPh	4-FPh	62
3	4-FPh	Ph	73
4	4-ClPh	Ph	63
5	4-PhPh	Ph	77
6	4-MeOPh	Ph	45
7	2-MeOPh	Ph	13
8	2-Nap	Ph	69
9			77
10			59

^aIsolated yield



Scheme 18 Iron-catalyzed CDC reaction of olefinic C–H bond with benzylic C–H bond

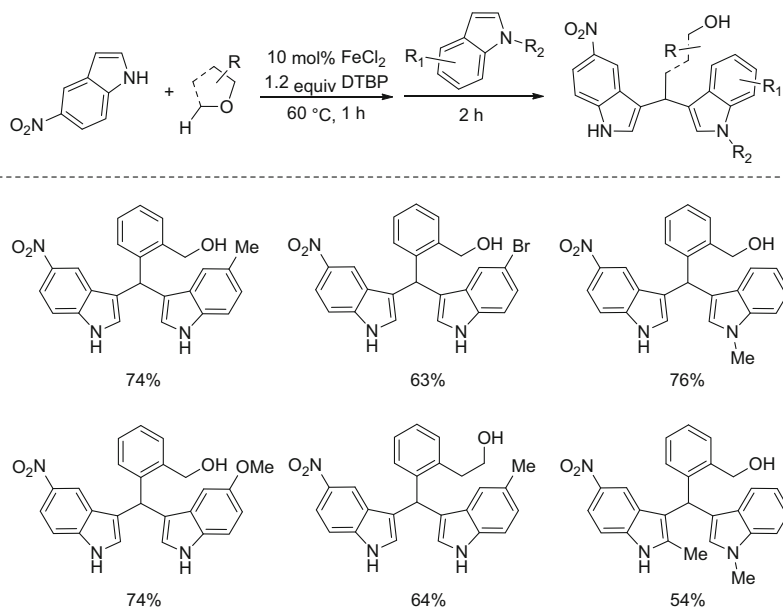


Scheme 19 The plausible mechanism on direct C–C bond formation via iron-catalyzed benzylic C–H activation via radical (path **A**) or cationic (path **B**) process

ortho-substituted substrate (entry 7). Furthermore, substituted phenyls, naphthyl, seven-membered cyclic diphenyl methane derivatives, and isochroman were also adaptable to this reaction (entries 5, 8–10).

This catalytic system is also adaptable to the Mizoroki–Heck-type reaction of styrene with diphenylmethane, although the catalytic activity is low and substrate scope is limited (Scheme 18). Other styrene derivatives with either an electron-rich or electron-deficient group on the phenyl ring cannot be applied with this system.

A plausible mechanism on direct C–C bond formation via iron-catalyzed benzylic C–H activation is shown in Scheme 19. Two pathways are conceivable and both reactions are initiated by iron-assisted SET oxidation to afford the benzylic radical and $t\text{BuO}^\bullet$ radical. Subsequently, electrophilic addition of the benzylic radical to vinyl acetate gives the iron-coordinated radical intermediate. The desired product is obtained by β -scission and then the catalytic active species $\text{Fe}^{\text{II}}\text{L}_n$ is regenerated and $\text{AcO}t\text{Bu}$ is formed as a by-product (pathway **A**). The other possibility for

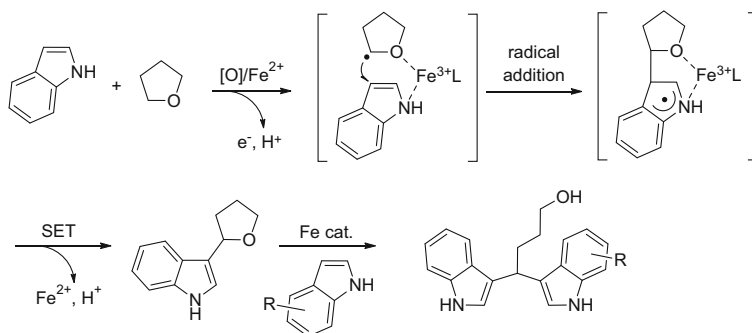


Scheme 20 Synthesis of unsymmetric bis-indolylmethanes catalyzed by an FeCl₂

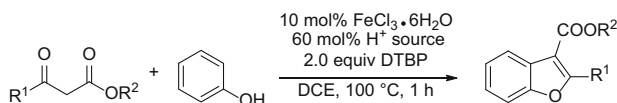
mechanism is a cationic pathway. The benzyl radical could be further oxidized to the benzyl cation. Subsequent electrophilic attack affords the desired product (pathway **B**). The generation of dimerized diphenylmethane **I** and *tert*-butyl ether **II** as major by-products gives evidence for the formation of benzyl radical species during the catalytic cycle.

In 2009, the iron-catalyzed conversion of indoles and ethers into a variety of symmetric and unsymmetric 1,1-bis-indolylmethane derivatives was achieved by Li and coworkers (Scheme 20) [44]. The reaction was carried out in the presence of FeCl₂ as a catalyst with *t*BuOO*t*Bu as an oxidant in excellent efficiency. The reaction of indole or COOMe substituted indole with 1,3-dihydroisobenzofuran gave a mixture of single- and double-indolation products. Selective single indolation took place when nitro substituted indole was used. The results show that the electronic effect of the nitro group on the indole plays an important role for a selective single-indolation reaction. Unsymmetric bis-indolylmethanes were selectively obtained by using NO₂ substituted indole in the first step and another substituted indole in the second step. The impact of nitro groups on the reactivity of indoles is well known in organic synthesis [45].

In this reaction, it is considered that the two different indoles are introduced in two different steps (Scheme 21). The first indolation step is likely a radical process, which is similar to other Fe-catalyzed CDC radical processes, and is less influenced by the electronic properties of indoles, whereas the second indolation step depends on the electronic effect of indoles, which is characteristic of Friedel–Crafts alkylations.



Scheme 21 A tentative mechanism for the formation of unsymmetric 1,1-bis-indolylmethane derivatives

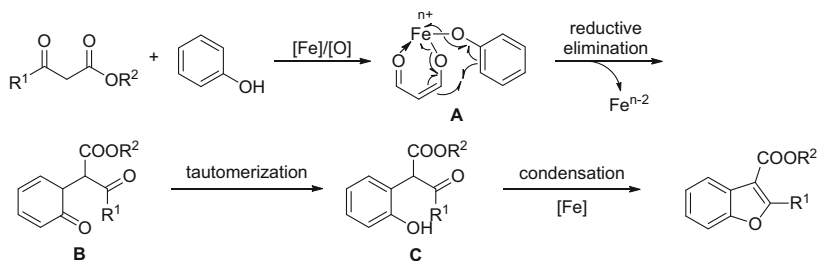


Scheme 22 Synthesis of polysubstituted benzofurans catalyzed by $\text{FeCl}_3 \cdot 6\text{H}_2\text{O}$

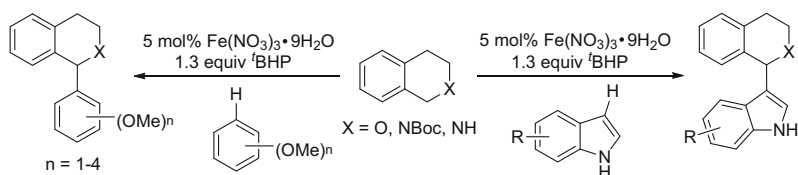
In the same year, Li and coworkers also reported the synthesis of polysubstituted benzofurans via Fe-catalyzed CDC reactions and subsequent annulation by using phenols and β -ketoesters (Scheme 22) [46]. The polysubstituted benzofuran derivatives were obtained in the presence of catalytic $\text{FeCl}_3 \cdot 6\text{H}_2\text{O}$ and $t\text{BuOO}t\text{Bu}$ in DCE at 100°C . Other iron salts such as $\text{Fe}_2(\text{CO})_9$, FeI_2 , $\text{Fe}(\text{acac})_2$, $\text{Fe}(\text{acac})_3$, $\text{Fe}(\text{OAc})_2$, $\text{Fe}(\text{dbm})_3$, $\text{FeSO}_4 \cdot 9\text{H}_2\text{O}$, $\text{Fe}_2(\text{SO}_4)_3 \cdot x\text{H}_2\text{O}$, FeF_3 , $\text{FeF}_3 \cdot 3\text{H}_2\text{O}$, and $\text{Fe}(\text{NO}_3)_3 \cdot 3\text{H}_2\text{O}$ were not effective. Interestingly, termination of the reaction system occurred when 4 Å MS for quenching of water was added to the reaction system. Solvent screening indicated that the use of DCE was very important and the yields decreased when another solvent such as MeNO_2 , PhMe, CHCl_3 , hexane, and MeCN was used. Recently, Nakamura's group reported that 1,2-dihalide such as 1,2-dichloroethane and 1,2-dichloro-2-methylpropane acted as an effective oxidant for iron-catalyzed C–H bond activation [47, 48].

The proposed reaction mechanism of Fe-catalyzed tandem oxidative coupling and annulation reaction of phenol and β -ketoesters is shown in Scheme 23. An intermediate **A** is generated in situ and then reductive elimination takes place to give an oxidative coupling product **B**. Subsequently, tautomerization of **B** yields the corresponding phenol **C** and then the desired benzofuran is formed by intramolecular condensation of **C** in the presence of an iron catalyst.

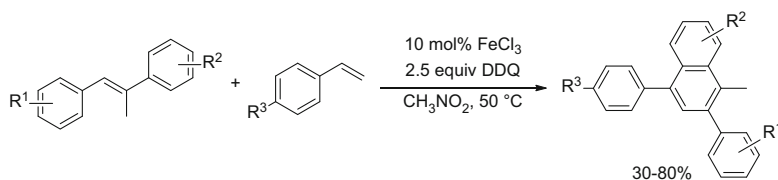
An effective method for an iron-catalyzed oxidative indolation and methoxyphenylation of *N*-protected tetrahydroisoquinolines and isochroman was reported by Schnürch and coworkers in 2010 (Scheme 24) [30]. The desired coupling products were obtained in good to excellent yields in the presence of $\text{Fe}(\text{NO}_3)_3 \cdot 9\text{H}_2\text{O}$ as catalyst and *tert*-butyl hydroperoxide ($t\text{BuOOH}$) as the oxidant. The yields



Scheme 23 The proposed mechanism of Fe-catalyzed tandem oxidative coupling and annulation



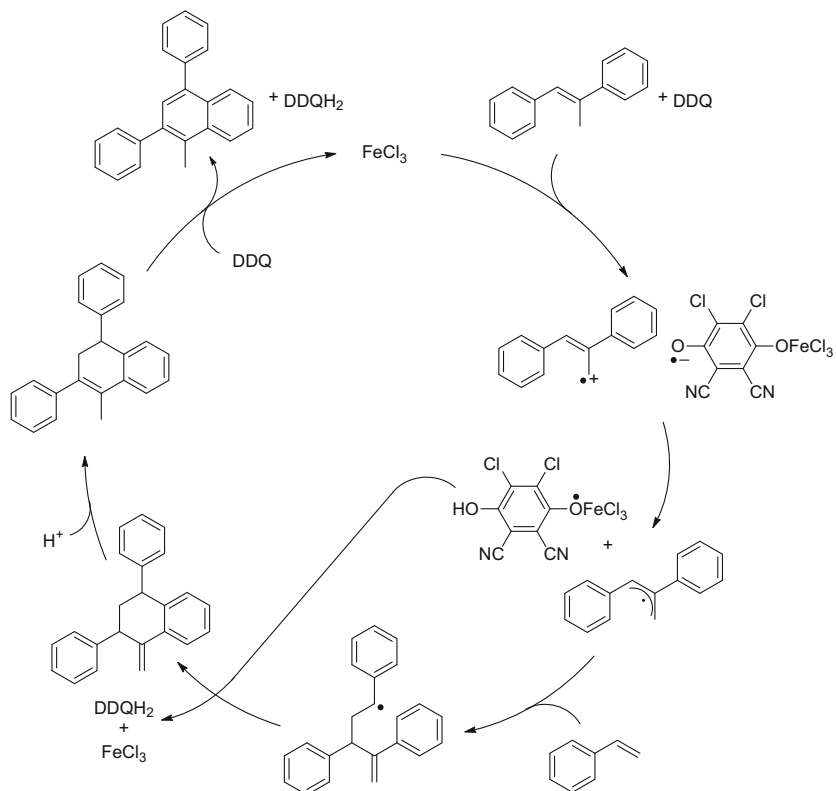
Scheme 24 Fe-catalyzed direct functionalization of *N*-protected tetrahydroisoquinolines and isochroman



Scheme 25 Fe-catalyzed tandem CDC reaction of terminal allylic Csp^3 with Csp^2 of styrene

decreased when iron halides such as $\text{FeCl}_2 \cdot 4\text{H}_2\text{O}$, $\text{FeCl}_3 \cdot 6\text{H}_2\text{O}$, and FeBr_2 were used. Molecular oxygen, with or without the radical initiator azobisisobutyronitrile (AIBN), was not an efficient oxidant in this system. The reaction mechanism is similar to other Fe-catalyzed CDC radical processes (see Scheme 20). The reaction failed when 1.5 equiv. of TEMPO as a radical scavenger was employed in the reaction system. This result suggests that reaction mechanism is not an ionic but a radical process.

The first example of iron-catalyzed CDC reactions of terminal allylic Csp^3 with Csp^2 of styrene followed by benzoannulation to give polysubstituted naphthalenes was reported by Deng and coworkers in 2012 (Scheme 25) [49]. In this reaction, a catalytic amount of FeCl_3 and 2.5 equiv. of DDQ were used in CH_3NO_2 at 50°C . The system possesses a good degree of functional group tolerance. Although substrates with a strong electron-donating OMe group on the aryl ring give no product, weakly electron-donating and electron-withdrawing substituents on the aryl ring afforded the corresponding naphthalenes in moderate to high yields. A reaction pathway according to previous reports was proposed (Scheme 26)

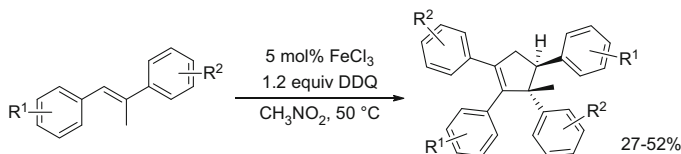
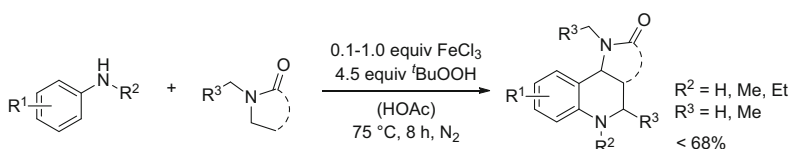
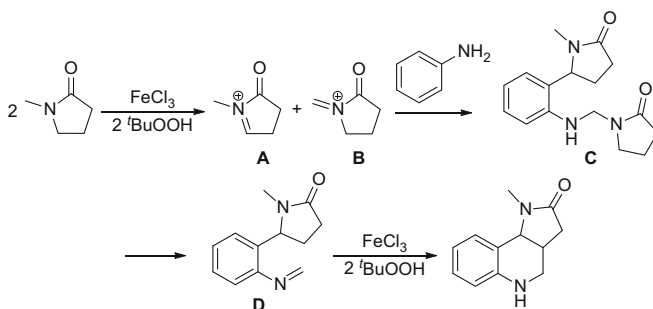


Scheme 26 A plausible reaction pathway for Fe-catalyzed tandem CDC reaction

[42, 50–52]. Although the important intermediates in this reaction pathway are not observed, it is considered that a radical process is involved in this reaction because termination of the reaction occurs when 2.0 equiv. of TEMPO is added to the reaction mixture.

Furthermore, Deng and coworkers reported in the same year the formation of highly substituted cyclopentenes via stereoselective tandem CDC and cyclization reactions when (*E*)-1,2-diarylprop-1-enes were used in the same reaction system (Scheme 27) [53]. In this reaction, the *trans*-configuration cyclopentanes were obtained exclusively. This transformation does not occur in other solvents such as toluene, acetonitrile, and 1,4-dioxane. The desired product is not obtained when substrates with a strong electron-donating group such as an OMe or an electron-withdrawing NO₂ group on the aryl ring were used. This tendency is similar to that for the naphthalene formation in the previous report [49].

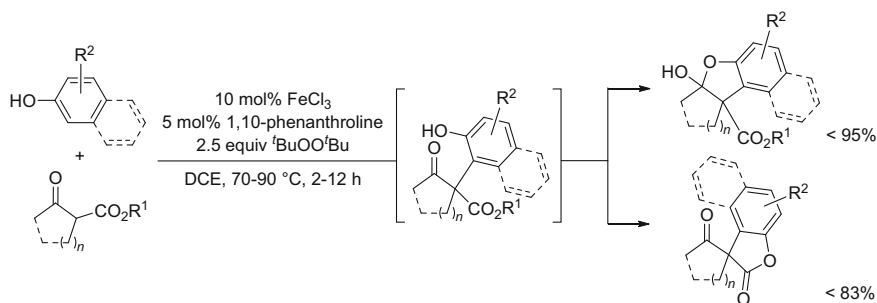
Bao and coworkers reported in 2013 that a ring-fused tetrahydroquinoline derivative was obtained in the reaction of arylamines with *N*-substituted lactams catalyzed by FeCl₃ in the presence of *t*BuOOH under a nitrogen atmosphere at 75°C (Scheme 28) [54]. The catalytic activity decreased by using other catalysts, for

**Scheme 27** Fe-catalyzed stereoselective tandem CDC reaction and cyclization**Scheme 28** Fe-catalyzed cascade cyclization**Scheme 29** The possible mechanism for synthesis of ring-fused tetrahydroquinoline derivatives

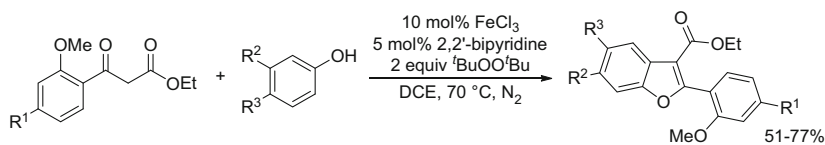
instance, FeBr₃, FeCl₃·6H₂O, FeCl₂·6H₂O, FeSO₄, CuI, Cu(OTf)₂, and ZrCl₂ and by using other peroxides such as ^tBuOO^tBu, 30% H₂O₂, and O₂ instead of ^tBuOOH as the oxidant.

A possible mechanism for synthesis of ring-fused tetrahydroquinoline derivatives is shown in Scheme 29. Iminium ions **A** and **B** are generated by the cleavage of the C(sp³)-H bond (α to the nitrogen) of the lactam. The intermediate **C** is formed by both a Friedel-Crafts-type reaction of the iminium ion **A** and a nucleophilic addition reaction of iminium ion **B** with the arylamine. Then **C** is converted to **D** via C-N bond cleavage [14, 55]. Finally, the SET oxidative process of **D** affords the desired product. Overall, this reaction consists of two C-C bonds and one C-N bond formation as well as one C-N bond cleavage.

In 2012, Pappo and coworkers reported an FeCl₃-catalyzed coupling of cyclic α -substituted β -ketoesters with phenols in the presence of 2.5 equiv. of ^tBuOO^tBu and a catalytic amount of 1,10-phenanthroline to produce polycyclic hemiacetals or polycyclic spirolactones (Scheme 30) [56]. Although the addition of 1,10-phenanthroline was not required in some cases, that ligand acted as an accelerator for the CDC reaction and a decelerator for side reaction.



Scheme 30 Fe-catalyzed CDC reaction of cyclic α -substituted β -ketoesters with phenols



Scheme 31 Fe-catalyzed coupling of ethyl 2-benzyl-oxyacetate derivatives with phenols

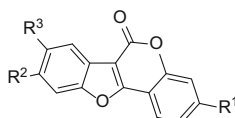
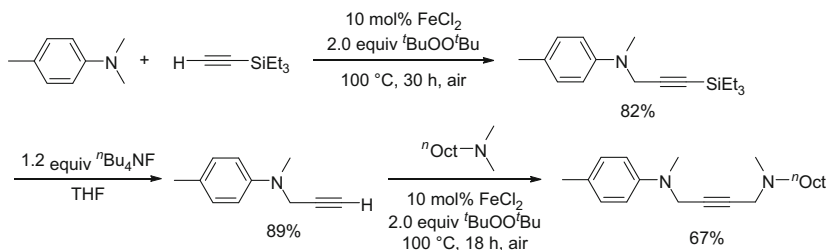


Fig. 5 Synthesized coumestan derivatives

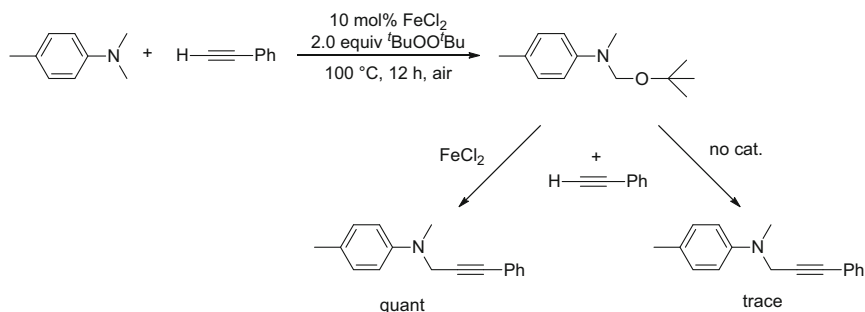
Furthermore, the combination of FeCl_3 and 2,2'-bipyridine with $t\text{BuOO}t\text{Bu}$ is also suitable for the reaction of phenols with ethyl 2-benzyl-oxyacetate derivatives instead of cyclic α -substituted β -ketoesters (Scheme 31) [57]. The corresponding benzofurans were obtained in good to high yields. The yields decreased when the reaction was carried out under aerobic conditions. The obtained benzofurans are easily converted to coumestan derivatives as selective estrogen receptor modulators (Fig. 5) [57].

4 Csp³-Csp CDC Reaction

In 2009, Volla and Vogel reported iron-catalyzed CDC reactions of tertiary amines and terminal alkynes to give propargylamines (Scheme 32) [58]. Screening reactions revealed that FeCl_2 without solvent in air was the best catalyst. The yields decreased when other iron compounds such as $\text{Fe}(\text{acac})_2$, $\text{Fe}_2(\text{CO})_9$, and $\text{Fe}(\text{CO})_5$ instead of FeCl_2 were used. In addition, $\text{Fe}(\text{OAc})_2$, $\text{Fe}(\text{acac})_3$, and $\text{Fe}(\text{ClO}_4)_2$



Scheme 32 Chemoselective FeCl_2 -catalyzed C–C cross-coupling reaction with two different tertiary amines

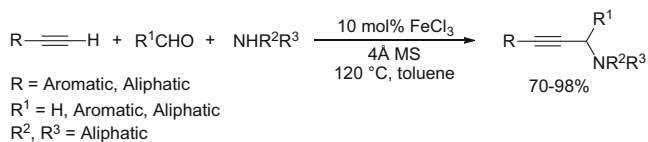


Scheme 33 Formation of α -aminoether $4\text{-MeC}_6\text{H}_4\text{N}(\text{Me})\text{CH}_2\text{-O}^t\text{Bu}$ and subsequent coupling with phenylacetylene

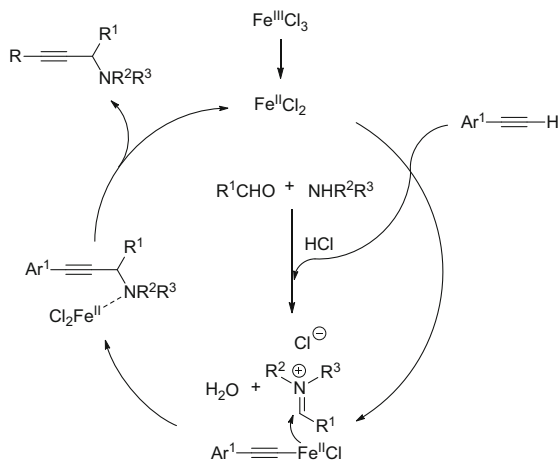
showed no activity. The reaction was applicable to a wide variety of aliphatic and aromatic amines and alkynes. In this reaction, a silyl group acted as a protecting group for the other side of the terminal alkyne.

The reaction was also proposed to proceed through an Fe-catalyzed SET process to generate an iminium ion intermediate. The coupling of the iminium ion intermediate and an alkynyl carbon anion afforded the desired product. The reaction mechanism via the formation of iminium ion intermediates is in good agreement with the well-known Horner mechanism [59, 60]. The reaction of $4,N,N$ -trimethylaniline with phenylacetylene in the presence of 10 mol% FeCl_2 and 2 equiv. of $t\text{BuOO}^t\text{Bu}$ afforded α -aminoether $4\text{-MeC}_6\text{H}_4\text{N}(\text{Me})\text{CH}_2\text{-O}^t\text{Bu}$, and subsequent coupling with phenylacetylene gave the corresponding propargylamine, whereas the desired product was not obtained in the absence of FeCl_2 (Scheme 33). This result shows that FeCl_2 acts as Lewis acid promoter and induces the $\text{S}_{\text{N}}1$ cleavage of the α -aminoether into iminium ion intermediate.

Shortly thereafter, Wang and coworkers reported FeCl_3 -catalyzed, ligand-free three-component coupling reactions of aldehydes, terminal alkynes, and amides to afford propargylamines (Scheme 34) [61]. The reaction ran very smoothly to afford the desired coupling products in good to excellent yields in the presence of FeCl_2



Scheme 34 FeCl₃-catalyzed, ligand-free three-component coupling reactions of aldehydes, terminal alkynes, and amides



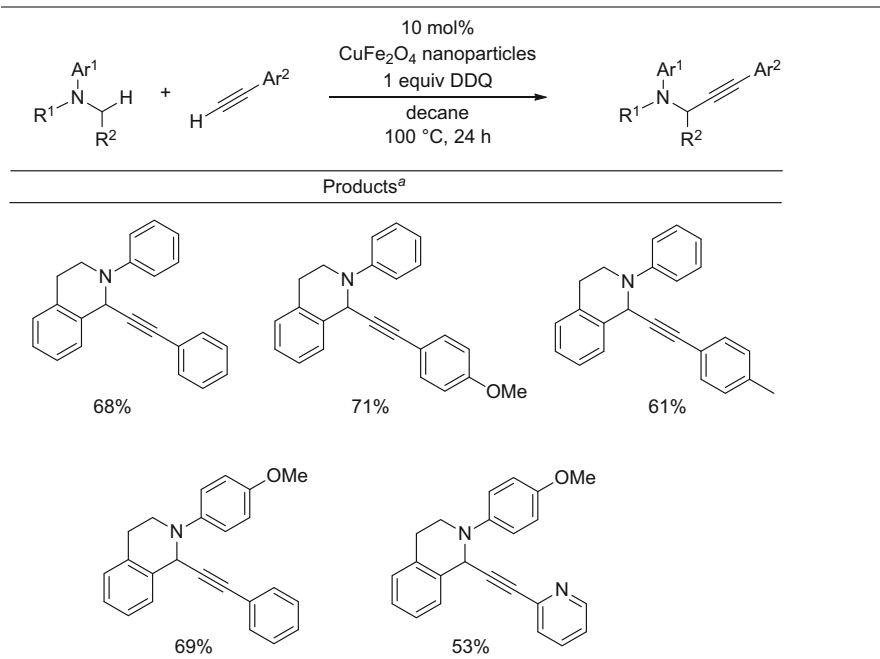
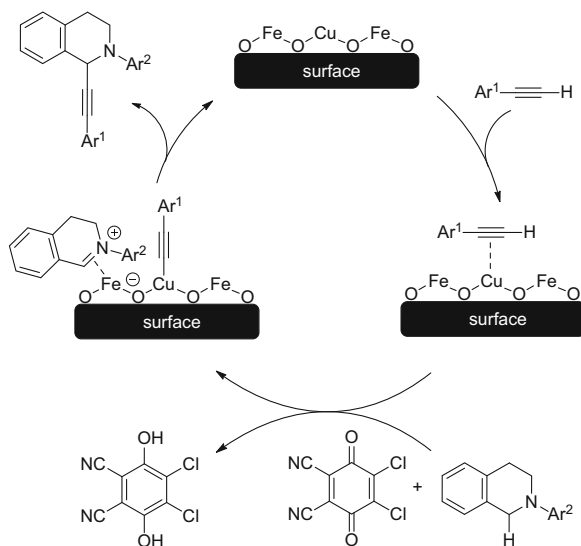
Scheme 35 A possible mechanism of FeCl₃-catalyzed three-component coupling of aldehyde, terminal alkyne, and amide

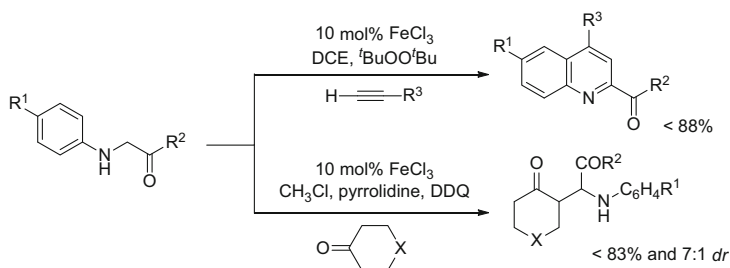
and 4 Å MS in toluene. The yields decreased when a phosphorus ligand such as PPh₃ or PCy₃ was added to the reaction system.

The possible mechanism of FeCl₃-catalyzed three-component coupling of aldehyde, terminal alkyne, and amine is shown in Scheme 35. Initially, an Fe^{II} salt, which is generated by reduction of an Fe^{III} salt, reacts with alkyne to produce an iron alkynyl complex and HCl. The formation of an iminium intermediate from an aldehyde and an amine is accelerated by the HCl generated. The subsequent reaction of the iron alkynyl complex with the iminium intermediate gives the desired propargylamine and regenerates the catalytically active Fe^{II} species to complete the catalytic cycle.

The Csp³-Csp CDC reaction catalyzed by CuFe₂O₄ nanoparticles in the presence of oxidant was reported by Li, Moores, and coworkers in 2013 [16]. CuFe₂O₄ nanoparticles were found to be an efficient catalyst for the Csp³-Csp CDC reaction of *N*-arylated analogues of tetrahydroisoquinoline with various aromatic alkynes in good yields (Table 5), whereas the catalytic activity of Fe₃O₄ was quite low. This result is understandable because it is known that copper salts activate alkynes.

The proposed mechanism for CuFe₂O₄ nanoparticles catalyzing Csp³-Csp CDC reaction is shown in Scheme 36. The mechanism is similar to that for Fe₃O₄

Table 5 Csp³-Csp CDC reaction catalyzed by CuFe₂O₄ nanoparticles^aIsolated yield**Scheme 36** A plausible mechanism for Csp³-Csp CDC reactions catalyzed by CuFe₂O₄ nanoparticles



Scheme 37 Iron-catalyzed CDC reaction of phenylglycine derivatives

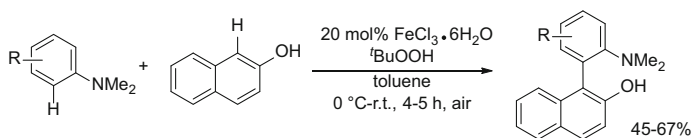
nanoparticles catalyzing CDC reaction of nitroalkanes with tertiary amines (see Sect. 2, Scheme 11). The Cu acetylide is generated by the reaction of the Cu center with an alkyne via the coordination of the alkyne. An iminium cation, which is generated from the oxidation of a tertiary amine by DDQ, coordinates to a neighboring Fe or Cu atom in the nanoparticle. Subsequently, a coupling reaction affords the desired product and regenerates the CuFe_2O_4 nanoparticle to complete the catalytic cycle.

In 2012, Hu and coworkers reported the construction of quinolines via an iron-catalyzed $\text{Csp}^3\text{-Csp}$ CDC reaction of phenylglycine derivatives with substituted acetylenes (Scheme 37) [62].

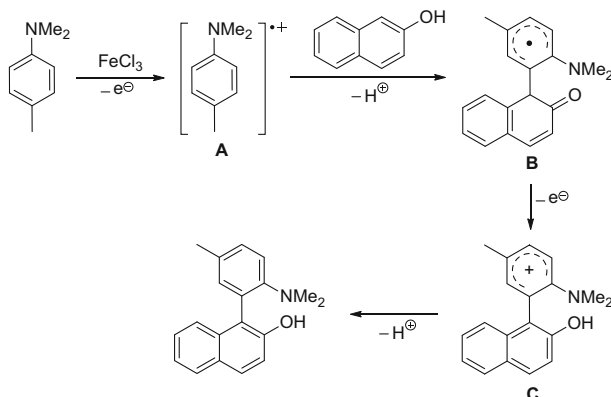
The desired products were obtained in the presence of a catalytic amount of FeCl_3 and $t\text{BuOO}^t\text{Bu}$ as the oxidant in good to high yields. Initial screening reactions indicated that DCE was the best solvent and both $t\text{BuOOH}$ and H_2O_2 as an oxidant showed lower or no activity. The desired quinoline was not obtained by using Cu_2O (10 mol%) as a catalyst. Therefore, iron plays an important role in this reaction. On the other hand, the reaction of phenylglycine derivatives with cyclic ketones instead of acetylene afforded the corresponding coupling products in good to high yields in the presence of pyrrolidine as organic catalyst, when a combination of DDQ and CH_3Cl was used. The addition of butylated hydroxytoluene as a radical scavenger resulted in a dramatic decrease of the yield of the desired product, implying that a radical species may be involved in each reaction.

5 Other C–C CDC Reaction

In 2011, Chandrasekharam and coworkers reported an iron-catalyzed regioselective direct oxidative $\text{aryl}(\text{Csp}^2)\text{-aryl}(\text{Csp}^2)$ CDC reaction (Scheme 38) [63]. The desired coupling products were obtained by the reaction of various N,N -dimethylaniline derivatives with 2-naphthol under mild conditions in the presence of $\text{FeCl}_3 \cdot 6\text{H}_2\text{O}$ and $t\text{BuOOH}$ as the oxidant in moderate to good yields. The C–C bond was formed selectively at the *ortho* position to the functional groups of the substrates. Other iron salts ($\text{FeSO}_4 \cdot 9\text{H}_2\text{O}$, $\text{NH}_4\text{Fe}(\text{SO}_4)_2 \cdot 12\text{H}_2\text{O}$, $\text{NH}_4\text{FeCl}_4 \cdot 6\text{H}_2\text{O}$), CuX ($\text{X} = \text{Cl}, \text{Br}, \text{I}$),



Scheme 38 Fe-catalyzed, regioselective, direct oxidative aryl(Csp²)–aryl(Csp²) CDC reaction



Scheme 39 Fe-catalyzed regioselective aryl(Csp²)–aryl(Csp²) CDC reaction

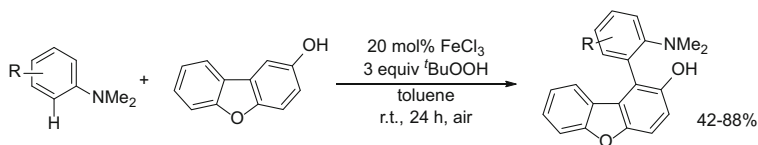
and NiCl₂ were not effective, whereas AlCl₃ acted as an efficient catalyst comparable to FeCl₃·6H₂O.

To investigate the reaction mechanism, the ESR (electron spin resonance) spectrum of the reaction mixture was recorded. No signals were detected at room temperature, whereas a sharp signal ($g = 2.01595$) was observed at -146°C . This result revealed that a radical species was generated from *N,N*-dimethylaniline during the reaction [64].

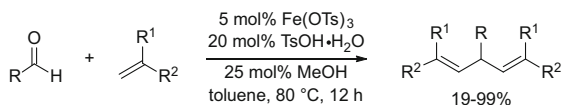
The proposed reaction mechanism for the iron-catalyzed aryl(Csp²)–aryl(Csp²) CDC reaction is shown in Scheme 39. A single-electron transfer from *N,N*-dimethylaniline to FeCl₃ affords a radical cationic intermediate **A** and an Fe²⁺ species. Subsequent nucleophilic attack of 2-naphthol on **A** at the *ortho* position gives the C–C bond coupling product **B**, and then an intermediate **C** is formed by losing one electron from **B**. Finally deprotonation of **C** affords the desired product. In this reaction, *t*BuOOH acts as an oxidant for the reduced catalyst.

Furthermore, 2-dibenzofuranol instead of 2-naphthol could also be employed for this reaction system and gave the corresponding 1-(2-aminophenyl)dibenzo[*b,d*]furan-2-ol derivatives in good to high yields (Scheme 40) [65]. Some of the compounds synthesized show *anti*-tubercular and cytotoxic activities.

In 2013, Huang and coworkers reported Fe-catalyzed cross-deoxygenative- and cross-dehydrogenative-coupling reactions of aldehydes and alkenes (Scheme 41) [66]. The reaction ran very smoothly to get skipped dienes in good to excellent yields in the presence of a catalytic amount of Fe(OTf)₃ as Lewis acid, TsOH·H₂O



Scheme 40 Fe-catalyzed aryl(Csp²)–aryl(Csp²) CDC reaction for the synthesis of 1-(2-aminophenyl)dibenzo[*b,d*]furan-2-ol derivatives



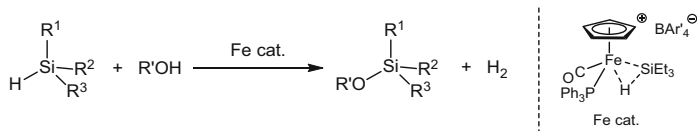
Scheme 41 Fe-catalyzed cross-deoxygenative and cross-dehydrogenative coupling of aldehydes and alkenes

as Brønsted acid, and MeOH. In this system, other Lewis acids such as FeCl₃, ZnCl₂, AlCl₃, Ni(OAc)₂, and Cu(OAc)₂ were not efficient and the yield dramatically decreased in the absence of TsOH·H₂O or MeOH. The reaction system showed great tolerance for functional groups such as halides or electron-withdrawing and electron-donating groups on the aromatic rings. Furthermore, paraformaldehyde instead of benzaldehyde was also applicable to this reaction and gave the corresponding skipped dienes in good yield.

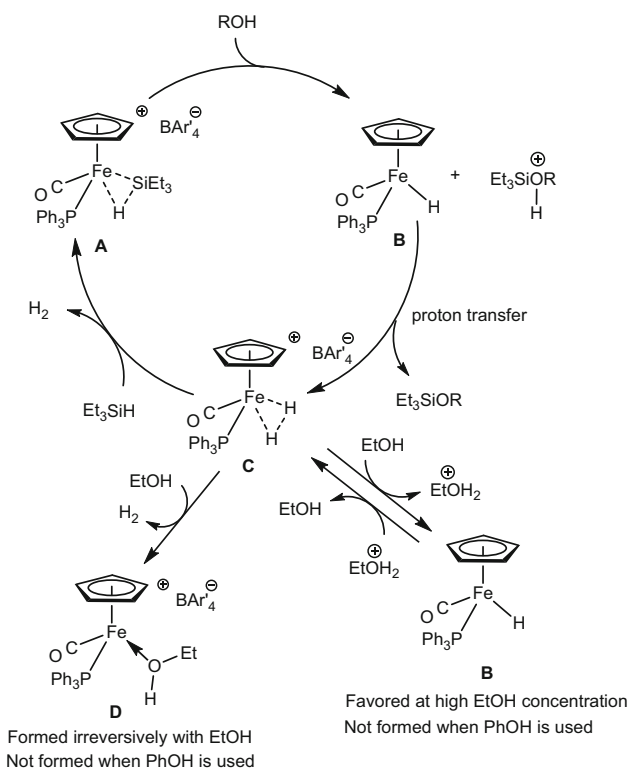
6 E–E CDC Reaction

The former sections summarized CDC reactions catalyzed by iron compounds to form a carbon–carbon bond. In this section, CDC reactions forming a bond between main group elements (E–E bond) other than carbon are introduced. C–E bond formations catalyzed by an iron compound are described in [67].

Silicon–oxygen bond formations through CDC reaction of hydrosilanes with alcohols have widely been reported, but reports on the formation catalyzed by an iron complex are quite limited. In 1998, Brookhart and coworkers reported the formation of silyl ethers and H₂ from hydrosilane and alcohols catalyzed by the cationic [Fe(Cp)(CO)(PPh₃)(Et₃SiH)]⁺[BAR'₄]⁻ (**A**) (Ar' = 3,5-(CF₃)₂C₆H₃) having η²-Si–H bond fashion (Scheme 42) [68]. When ethanol was used, catalyst deactivation rapidly took place. However, when phenol is utilized, catalytic activity is maintained until all of the phenol has been consumed. For example, 2,500 equiv. of Et₃SiH was added to a solution of CH₂Cl₂ containing [Fe(Cp)(Me)(CO)(PPh₃)] and 2 equiv. of [H(OEt₂)₂][BAR'₄], and then 2,500 equiv. of Et₃SiH and 2,000 equiv. of PhOH were added in this order. Subsequently, another 10,000 equiv. of Et₃SiH and



Scheme 42 CDC reaction of hydrosilanes with alcohols catalyzed by $[\text{Fe}(\text{Cp})(\text{CO})(\text{PPh}_3)(\text{Et}_3\text{SiH})][\text{BAR}'_4]$ affording silyl ethers



Scheme 43 The proposed catalytic cycle of CDC reaction of hydrosilane with alcohol catalyzed by a cationic Fe complex, $[\text{Fe}(\text{Cp})(\text{CO})(\text{PPh}_3)(\text{Et}_3\text{SiH})]^+$

PhOH were added to the solution. After workup, Et_3SiOPh was obtained in 99% yield.

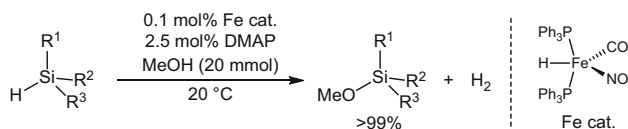
A reaction pathway has been proposed on the basis of VT-NMR (Variable Temperature-Nuclear Magnetic Resonance) measurements (Scheme 43). Complex **A** reacts with alcohol to give the iron hydride complex $[\text{Fe}(\text{Cp})\text{H}(\text{CO})(\text{PPh}_3)]$ (**B**) and the protonated silyl ether $\text{Et}_3\text{SiOHR}^+$, followed by proton transfer affording the cationic $\eta^2\text{-H}_2$ iron complex $[\text{Fe}(\text{Cp})(\text{H}_2)(\text{CO})(\text{PPh}_3)][\text{BAR}'_4]$ (**C**) and the silyl ether (Et_3SiOR). The next step is clearly dependent on the kind of alcohol utilized.

When phenol is used, the H_2 ligand in **C** is displaced by Et_3SiH to give **A** with H_2 gas evolution. Under these conditions, **C** is the resting state in the catalytic cycle and the rate-determining step appears to be the displacement of H_2 by Et_3SiH . In contrast, when ethanol, which is more basic and more nucleophilic than phenol, is used, **C** is readily deprotonated to give the neutral iron hydride complex $[\text{Fe}(\text{Cp})\text{H}(\text{CO})(\text{PPh}_3)]$ (**B**) with the formation of EtOH_2^+ . Complex **B** is the catalyst resting state in the presence of excess ethanol. When this complex is reprotonated by EtOH_2^+ to give **C**, displacement of the H_2 ligand by ethanol ultimately occurs and effectively terminates the catalytic cycle to form the cationic EtOH coordinating complex, $[\text{Fe}(\text{Cp})(\text{CO})(\text{EtOH})(\text{PPh}_3)] [\text{BAR}'_4]$ (**D**).

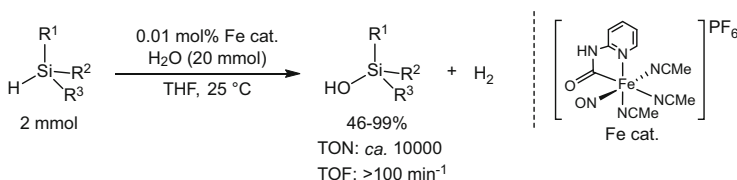
In 2014, Plietker reported the CDC reaction of hydrosilane and MeOH in the presence of iron hydrido complex $[\text{FeH}(\text{NO})(\text{CO})(\text{PPh}_3)_2]$ as a catalyst and *N,N*-4-dimethylaminopyridine (DMAP) as a co-catalyst (Scheme 44) [69].

In the above reaction, primary and secondary alkyl/aryl silanes such as PhSiH_3 and Ph_2SiH_2 and hydrosiloxane such as $(\text{MeO})_3\text{SiH}$ were converted to the corresponding silyl ethers and hydrogen gas in quantitative yields within seconds, whereas sterically hindered tertiary alkyl/aryl silanes such as Ph_3SiH , Et_3SiH , and $(\text{PhCH}_2)_2\text{SiH}$ proved unreactive. An excellent catalytic activity was observed in the CDC reaction of PhSiH_3 with MeOH catalyzed by $[\text{FeH}(\text{NO})(\text{CO})(\text{dppp})]$ (*dppp* = diphenylphosphinopropane) (0.1 mol%) and DMAP (2.5 mol%). The PhSiH_3 was completely converted to $\text{PhSi}(\text{OMe})_3$ within 18 s, showing that the TOF and TON were $600,000 \text{ h}^{-1}$ and 3,000 (per Si–H bond), respectively.

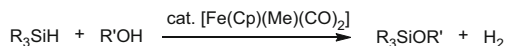
Shortly thereafter, iron-catalyzed CDC reaction of hydrosilane and H_2O was also achieved by Fan and Teo (Scheme 45) [70]. The reaction ran very smoothly to afford the silanol and hydrogen gas in excellent yields in THF (TON = *ca.* 10,000, TOF = $>100 \text{ min}^{-1}$). In the reaction using Ph_3SiH , the yield decreased to 46%.



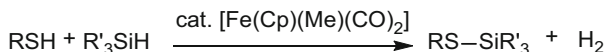
Scheme 44 CDC reaction of hydrosilanes with MeOH catalyzed by $[\text{FeH}(\text{NO})(\text{CO})(\text{PPh}_3)_2]$ affording silanols and H_2 gas



Scheme 45 CDC reaction of hydrosilanes with MeOH catalyzed by $[\text{FeH}(\text{NO})(\text{CO})(\text{PPh}_3)_2]$ affording silanol and H_2 gas



Scheme 46 CDC reaction of hydrosilane with alcohol catalyzed by $[\text{Fe}(\text{Cp})(\text{Me})(\text{CO})_2]$ affording silyl ethers



Scheme 47 CDC reactions of hydrosilanes with thioalcohols catalyzed by $[\text{Fe}(\text{Cp})(\text{Me})(\text{CO})_2]$ affording silyl thioethers

The siloxane was afforded when CHCl_3 instead of THF as a solvent was used, and the silanol was not obtained in the absence of H_2O .

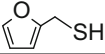
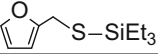
Nakazawa and coworkers reported that the neutral iron complex $[\text{Fe}(\text{Cp})(\text{Me})(\text{CO})_2]$ could serve as a catalyst for CDC reaction of hydrosilanes with alcohols (Scheme 46) [71]. Several alcohols such as EtOH, CyOH, t BuOH, PhOH, 4-MeO- $\text{C}_6\text{H}_4\text{OH}$, PhCH_2OH , and (furyl) CH_2OH reacted with Et_3SiH in the presence of a catalytic amount of $[\text{Fe}(\text{Cp})(\text{Me})(\text{CO})_2]$ and in the absence of $[\text{H}(\text{OEt}_2)_2]$ $[\text{BAR}'_4]$ (cf. Scheme 41). The catalytic activities (TON) were in the range of 3–21.

Catalytic activity of $[\text{Fe}(\text{Cp})(\text{Me})(\text{CO})_2]$ in the reaction of hydrosilanes with thioalcohols was also reported. This reaction selectively creates a Si–S bond (Scheme 47) [72]. Dehydrogenative coupling of hydrosilanes and thiols catalyzed by a transition metal complex has attracted less attention mainly because catalyst poisoning by sulfur was a major deterrence. Only Wilkinson's catalyst, Pd nanoparticles, and $\text{B}(\text{C}_6\text{F}_5)_3$ have been reported as catalysts for the CDC Si–S formation. The reaction shown in Scheme 47 is the first example of an iron-catalyzed CDC reaction forming a Si–S bond.

Several thiols and tertiary silanes were examined to explore the scope and limitation of the CDC reaction (Table 6). The results suggested that (i) thiols having an electron-donating substituent exhibited better TONs (entries 1, 2 vs. 4, 5), (ii) a bulky substituent on the thiol seemed to reduce the catalytic activity to some extent (entry 3), (iii) a thiol substituent capable of coordinating to the metal seemed unfavorable for this coupling (entries 6 and 7), and (iv) the substituents on the tertiary silane also affected the TONs (compare entries 4, 8, and 9), as bulky substituents seemed to reduce the catalytic activity.

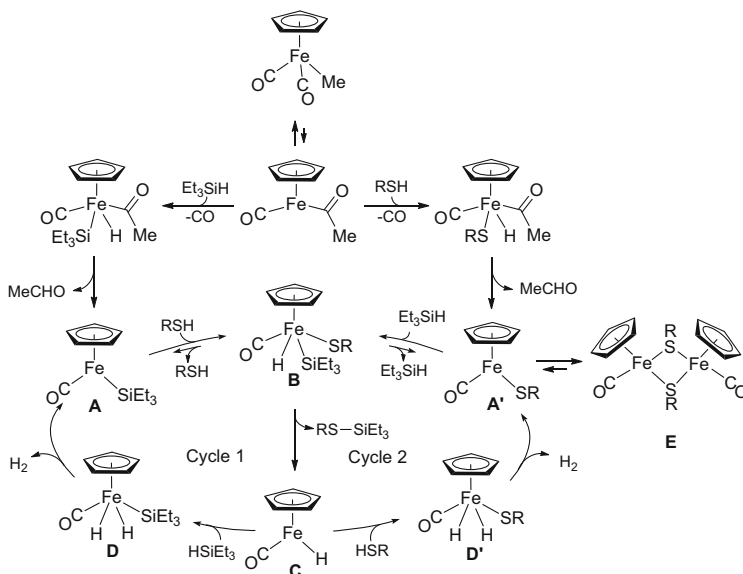
On the basis of the NMR experiments, two plausible catalytic cycles are conceivable (Scheme 48). $[\text{Fe}(\text{Cp})(\text{Me})(\text{CO})_2]$ is in equilibrium with $[\text{Fe}(\text{Cp})\{\text{C}(\text{O})\text{Me}\}(\text{CO})]$. This $16e^-$ species reacts with either Et_3SiH or RSH in solution. In the reaction with Et_3SiH , Si–H oxidative addition followed by reductive elimination of $\text{MeC}(\text{O})\text{H}$ yields $[\text{Fe}(\text{Cp})(\text{SiEt}_3)(\text{CO})]$ (**A**), which then reacts with RSH to give **B**. Complex **B** is alternatively produced by the reaction of $[\text{Fe}(\text{Cp})\{\text{C}(\text{O})\text{Me}\}(\text{CO})]$ with RSH, followed by $\text{MeC}(\text{O})\text{H}$ dissociation and oxidative addition of Si–H of Et_3SiH . As **B** has three different one-electron donor ligands, **B** may exhibit three kinds of couplings: coupling of H and SR to give **A**, coupling of H and SiEt_3 to

Table 6 CDC reactions of thiols and hydrosilanes

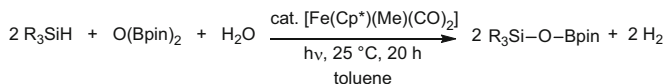
Entry	RSH	R ₃ SiH	RS-SiR ₃	TON
1	EtSH	Et ₃ SiH	EtS-SiEt ₃	8.4
2	CySH	Et ₃ SiH	CyS-SiEt ₃	10
3	^t BuSH	Et ₃ SiH	^t BuS-SiEt ₃	6.4
4	PhSH	Et ₃ SiH	PhS-SiEt ₃	5.8
5	MeO-C ₆ H ₄ -SH	Et ₃ SiH	MeO-C ₆ H ₄ -S-SiEt ₃	7.2
6	Ph-CH ₂ -SH	Et ₃ SiH	Ph-CH ₂ -S-SiEt ₃	0.6
7		Et ₃ SiH		N.R.
8	PhSH	Me ₂ PhSiH	PhS-SiPhMe ₂	7.6
9	PhSH	MePh ₂ SiH	PhS-SiPh ₂ Me	3.6

The TON value was based on the concentration of the iron complex and calculated from ¹H NMR data

^aReactions were carried out for 24 h at 80°C by using [Fe(Cp)(Me)(CO)₂] (0.112 mmol), RSH (1.02 mmol), and R₃SiH (11.2 mmol) in toluene



Scheme 48 The proposed catalytic cycle of CDC reaction of hydrosilane with thiol catalyzed by [Fe(Cp)(Me)(CO)₂]



Scheme 49 CDC reaction of hydrosilanes with bisboryloxiide to form Si–O–B bonds

give **A'**, and coupling of SR and SiEt₃ to give **C**. The first two couplings are reversible, but the last one is presumably irreversible. Complex **C** irreversibly formed reacts with Et₃SiH to give **D**, followed by reductive elimination of H₂ to reproduce **A** (Cycle 1). Alternatively, **C** reacts with RSH to give **D'**, followed by reductive elimination of H₂ to regenerate **A'** (Cycle 2). As **A'** was expected to form its dimer **E**, the reaction of Et₃SiH with PhSH in the presence of the isolated **E** as a catalyst was conducted, revealing that the catalytic activity was less than one-tenth of that when [Fe(Cp)(Me)(CO)₂] was used as a catalyst. Therefore, Cycle 1 rather than Cycle 2 was proposed to be more plausible.

Another interesting CDC reaction catalyzed by an iron complex is the formation of boryl silyl ether from bisboryloxiide, O(Bpin)₂ (pin = (OCMe₂)₂), and a tertiary silane. A toluene solution of O(Bpin)₂, two equiv. of Et₃SiH, one equiv. of H₂O, and 0.01 equiv. of [Fe(Cp*)(Me)(CO)₂] (Cp* = η⁵-C₅Me₅) was photoirradiated with a 400 W medium-pressure mercury arc lamp at 25°C for 20 h, affording Et₃Si–O–Bpin (Scheme 49) [73]. The TON was 110. The similar iron complex [Fe(Cp)(Me)(CO)₂] did not show catalytic activity in this case.

This is the second example of a catalytic Si–O–B bond formation using a transition metal complex and the first example using an iron catalyst. The only one precedence was reported using a Ru catalyst [74]. In terms of the Si–O–B bond formation reaction shown in Scheme 46, Mo(CO)₆ exhibited better catalytic activity (TON = 368). These catalytic systems were applicable for various hydrosilanes such as Et₃SiH, ⁿPr₃SiH, ^tBuMe₂SiH, Me₂PhSiH, MePh₂SiH, Ph₃SiH, MePh(CH₂=CH)SiH, O(SiMe₂H)₂, and Et₂SiH₂ and for several boron compounds such as O(Bpin)₂, HBpin, HOBpin, (MeBO)₃, MeB(OH)₂, and O(BPh₂)₂. As borosilicates bearing a Si–O–B unit have been widely used in many areas because of their excellent heat and chemical resistance (e.g., see [75–78]), the CDC reaction forming a selective Si–O–B bond by using transition metal catalyst is important and promising.

7 Conclusion

There is growing interest in the CDC reaction catalyzed by iron complexes including iron salts. Csp³–Csp³, Csp³–Csp², and Csp³–Csp bond-forming reactions were achieved by the great efforts to date. Reaction mechanism for some CDC reactions catalyzed by iron complexes has been proposed, but there are many unclear reactions from a mechanistic point of view. Therefore, more investigation concerning reaction mechanism is needed. Another remaining challenge is

Csp²–Csp bond-forming reaction. Development of more E–E' bond-forming reactions (E, E' = main group elements other than carbon) is important. Asymmetric synthesis by iron-catalyzed CDC reactions is also a challenging topic. We hope that these reactions will be achieved in the near future and make a great contribution to medicinal and material chemistry fields.

Acknowledgment We would like to show our respect for the great efforts of all authors, whose names were listed in the references. We wish to thank Dr. Yuji Suzuki for the reference collection.

References

1. Diederich F, Stang PJ (eds) (2004) Metal-catalyzed cross-coupling reactions. Wiley, Weinheim
2. Seechurn CCCJ, Kitching MO, Colacot TJ, Snieckus V (2012) *Angew Chem Int Ed* 51:5062
3. Beletskaya IP, Cheprakov AV (2009) In: Oestreich M (ed) *The Mizoroki-Heck reaction*. Wiley, Chichester
4. Torborg C, Beller M (2009) *Adv Synth Catal* 351:3027
5. Beller M (2011) *Chem Soc Rev* 40:4891
6. Li C-J (2009) *Acc Chem Res* 42:335, and the references therein
7. Guo X, Li Z, Li C-J (2010) *Prog Chem* 22:1434
8. Li Z, Cao L, Li C-J (2007) *Angew Chem Int Ed* 46:6505
9. Zhang Y, Li C-J (2007) *Eur J Org Chem* 4654
10. Huyser ES, Munson LR (1965) *J Org Chem* 30:1436
11. Li Z, Yu R, Li H (2008) *Angew Chem Int Ed* 47:7497
12. Mbuvi HM, Woo LK (2008) *Organometallics* 27:637
13. Li Y, Huang J-S, Zhou Z-Y, Che C-M, You X-Z (2002) *J Am Chem Soc* 124:13185
14. Li H, He Z, Guo X, Li W, Zhao X, Li Z (2009) *Org Lett* 11:4176
15. Zeng T, Song G, Moores A, Li C-J (2010) *Synlett* 13:2002
16. Hudson R, Ishikawa S, Li C-J, Moores A (2013) *Synlett* 24:1637
17. Li Z, Li C-J (2005) *J Am Chem Soc* 127:3672
18. Baslè O, Li C-J (2009) *Chem Commun* 4124
19. Evans DA, Seidel D, Rueping M, Lam HW, Shaw JT, Downey CW (2003) *J Am Chem Soc* 125:12692
20. Shen Y, Li M, Wang S, Zhan T, Tan Z, Guo C-C (2009) *Chem Commun* 953
21. Richter H, Mancheño OG (2010) *Eur J Org Chem* 4460
22. Xu YC, Lebeau E, Gillard JW, Attardo G (1993) *Tetrahedron Lett* 34:3841
23. Lou S-J, Xu D-Q, Shen D-F, Wang Y-F, Liu Y-K, Xu Z-Y (2012) *Chem Commun* 48:11993
24. Qian B, Guo S, Shao J, Zhu Q, Yang L, Xia C, Huang H-M (2010) *J Am Chem Soc* 132:3650
25. Rueping M, Tolstoluzhsky N (2011) *Org Lett* 13:1095
26. Komai H, Yoshino T, Matsunaga S, Kanai M (2011) *Org Lett* 13:1706
27. Song G-Y, Su Y, Gong X, Han K-L, Li X-W (2011) *Org Lett* 13:1968
28. Qian B, Xie P, Xie Y-J, Huang H-M (2011) *Org Lett* 13:2580
29. Tsuchimoto T, Ozawa Y, Negoro R, Shirakawa E, Kawakami Y (2004) *Angew Chem Int Ed* 43:4231
30. Ghobrial M, Harhammer K, Mihovilovic MD, Schnürch M (2010) *Chem Commun* 46:8836
31. Shirakawa E, Uchiyama N, Hayashi T (2011) *J Org Chem* 76:25
32. Wei Y, Ding H-Q, Lin S-X, Liang F-S (2011) *Org Lett* 13:1674
33. Minisci F (1973) *Synthesis* 1

34. Minisci F, Porta O (1974) In: Katritzky AR (ed) *Advances in heterocyclic chemistry*, vol. 16. Academic, New York, p 123
35. Minisci F (1976) *Top Curr Chem* 62:1
36. Minisci F, Porta O (1980) *Chim Ind* 62:769
37. Minisci F (1984) In: Graziani M (ed) *Fundamental research in homogenous catalysis*, vol 4. Plenum, New York, p 173
38. Minisci F (1986) In: Viehe HG (ed) *Substituent effects in radical chemistry*. Reidel, Boston, p 391
39. Minisci F, Vismara E (1987) In: Chizhov O (ed) *Organic synthesis: modern trends*. Blackwell Scientific, Oxford, p 229
40. Minisci F, Fontana F, Vismara E (1989) *Heterocycles* 28:489
41. Minisci F, Fontana F, Vismara EJ (1990) *Heterocycl Chem* 27:79
42. Li Y-Z, Li B-J, Lu X-Y, Lin S, Shi Z-J (2009) *Angew Chem Int Ed* 48:3817
43. Song C-X, Cai G-X, Farrell TR, Jiang Z-P, Li H, Gan L-B, Shi Z-J (2009) *Chem Commun* 6002
44. Guo X, Pan S, Liu J, Li Z (2009) *J Org Chem* 74:8848
45. Ono N (ed) (2001) *The nitro group in organic synthesis*. Wiley, New York
46. Guo X, Yu R, Li H, Li Z (2009) *J Am Chem Soc* 131:17387
47. Yoshikai N, Matsumoto A, Norinder J, Nakamura E (2009) *Angew Chem Int Ed* 48:2925
48. Norinder J, Matsumoto A, Yoshikai N, Nakamura E (2008) *J Am Chem Soc* 130:5858
49. Liu H, Cao L, Sun J, Fosseyab JS, Deng W (2012) *Chem Commun* 48:2674
50. Wang Z, Mo H, Cheng D, Bao W (2012) *Org Biomol Chem* 10:4249
51. Pan S, Liu J, Li H, Wang Z, Guo X, Li Z (2010) *Org Lett* 12:1932
52. Liu X, Chen Y, Li K, Wang D, Chen B (2012) *Chin J Chem* 30:2285
53. Li Y, Cao L, Luo X, Deng W (2012) *Chin J Chem* 30:2834
54. Sun M, Zhang T, Bao W (2013) *J Org Chem* 78:8155
55. Yang J, Wang Z, Pan F, Li Y, Bao W (2010) *Org Biomol Chem* 8:2975
56. Parnes R, Kshirsagar UA, Werbeloff A, Regev C, Pappo D (2012) *Org Lett* 14:3324
57. Kshirsagar UA, Parnes R, Goldshtein H, Ofir R, Zarivach R, Pappo D (2013) *Chem Eur J* 19:13575
58. Volla CMR, Vogel P (2009) *Org Lett* 11:1701
59. Horner L, Junkermann H (1955) *Ann Chem Justus Liebigs* 591:53
60. Horner L, Kirmse W (1955) *Ann Chem Justus Liebigs* 597:48
61. Li P, Zhang Y, Wang L (2009) *Chem Eur J* 15:2045
62. Liu P, Wang Z, Lin J, Hu X (2012) *Eur J Org Chem* 1583
63. Chandrasekharam M, Chiranjeevi B, Gupta KSV, Sridhar B (2011) *J Org Chem* 76:10229
64. Griffin BW (1978) *Arch Biochem Biophys* 190:850
65. Chiranjeevi B, Koyyada G, Prabusreenivasan S, Kumar V, Sujitha P, Kumar CG, Sridhar B, Shaik S, Chandrasekharam M (2013) *RSC Adv* 3:16475
66. Qian B, Zhang G, Ding Y, Huang H (2013) *Chem Commun* 49:9839
67. Grau M, Britovsek GJP (2015) High-valent iron in biomimetic alkane oxidation catalysis. *Top Organomet Chem*. doi:[10.1007/3418_2015_100](https://doi.org/10.1007/3418_2015_100)
68. Chang S, Scharre E, Brookhart M (1998) *J Mol Catal A* 130:107
69. Rommel S, Hettmanczyk L, Klein JEMN, Plietker B (2014) *Chem Asian J* 9:2140
70. Teo AKL, Fan WY (2014) *Chem Commun* 50:7191
71. Fukumoto K, Kasa M, Nakazawa H (2014) Accepted in *Inorg Chim Acta*. doi:[10.1016/j.ica.2015.02.019](https://doi.org/10.1016/j.ica.2015.02.019)
72. Fukumoto K, Kasa M, Oya T, Itazaki M, Nakazawa H (2011) *Organometallics* 30:3461
73. Ito M, Itazaki M, Nakazawa H (2014) *J Am Chem Soc* 136:6183
74. Marciniac B, Walkowiak J (2008) *Chem Commun* 2695
75. Soraru GD, Dallabona N, Gervais C, Babonneau F (1999) *Chem Mater* 11:910
76. Fujinami T, Mehta MA, Sugie K, Mori K (2000) *Electrochim Acta* 45:1181
77. Wang Q, Fu L, Hu X, Zhang Z, Xie Z (2006) *J Appl Polym Sci* 99:719
78. Peña-Alonso R, Mariotto G, Gervais C, Babonneau F, Soraru GD (2007) *Chem Mater* 19:5694

Iron-Catalyzed Carbon–Nitrogen, Carbon–Phosphorus, and Carbon–Sulfur Bond Formation and Cyclization Reactions

Jean-Luc Renaud and Sylvain Gaillard

Abstract The formation of carbon–heteroatom bonds (C–X bonds with X=N, S, P) upon addition of X-nucleophiles or X-electrophiles to unsaturated alkynes and alkenes, cross-coupling reactions, cycloadditions, tandem or consecutive reactions, or C–H functionalization is an attractive strategy in organic synthesis and is an intensive research area. Many organometallic species, more specifically palladium, nickel, and rhodium complexes, have paved the way to useful synthetic applications in this field. This chapter will cover iron-catalyzed bond-forming reactions between carbon and a heteroatom.

Keywords Iron catalysis · C–X bond formation · Cross-coupling reactions · Cycloaddition · C–H functionalization · Addition reactions

Contents

1	Introduction	84
2	Iron-Catalyzed C–N Bond Formations	85
2.1	Cross-Coupling Reactions	85
2.2	Allylic Substitution Reactions	88
2.3	C–H Functionalization	90
2.4	Synthesis of Nitrogenated Heterocycles	98
2.5	Miscellaneous	119
3	Iron-Catalyzed C–S Bond Formations	128
3.1	Michael Additions	128
3.2	Cross-Coupling Reactions	131
3.3	Addition on Alkynes	132
3.4	Allylic Substitution	133
3.5	Synthesis of Benzothiazoles	135
3.6	Miscellaneous Reactions	136

J.-L. Renaud (✉) and S. Gaillard
Laboratoire de Chimie Moléculaire et Thioorganique, UMR 6507, Normandie University,
University of Caen Basse Normandie, 14050, Caen, France
e-mail: jean-luc.renaud@ensicaen.fr

4 Iron-Catalyzed C–P Bond Formation	137
5 Conclusion	139
References	140

Abbreviations

AIBN	Azobisisobutyronitrile
BINAP	2,2'-Bis(diphenylphosphino)-1,1'-binaphthyl
cod	1,5-Cyclooctadiene
DCIB	1,2-Dichloroisobutane
DDQ	2,3-Dichloro-5,6-dicyano-1,4-benzoquinone
DMEDA	<i>N,N'</i> -Dimethylethylenediamine
DMSO	Dimethyl sulfoxide
dppe	1,2-Bis(diphenylphosphino)ethane
dppf	1,1'-Bis(diphenylphosphino)ferrocene
dppp	1,3-Bis(diphenylphosphino)propane
DTBP	Di- <i>tert</i> -butyl peroxide
4-F-dppbz	Bis(4-fluorophenyl)phosphinobenzene
HDA	Hetero-Diels–Alder reaction
HMDS	<i>Bis</i> (trimethylsilyl)amine
NBS	<i>N</i> -Bromosuccinimide
Pc	Phthalocyaninato
TBHP	<i>tert</i> -Butyl hydroperoxide, <i>t</i> BuOOH
TEMPO	(2,2,6,6-Tetramethylpiperidin-1-yl)oxyl
terpy	Terpyridine ligand
triflate	OTf, Trifluoromethanesulfonate, CF ₃ SO ₃ [−]
TMSCl	Trimethylsilyl chloride
TPP	Tetraphenylporphyrin
TTN	Total turnover number

1 Introduction

Many organic compounds used in biological, pharmaceutical, and material sciences contain C–X bonds. Reviews covering or including carbon–heteroatom bond formation reactions via metal-catalyzed additions to unsaturated molecules [1–5], cross-coupling reactions [6–8], and cycloadditions catalyzed by a wide range of metals have appeared during the last decade [9–12]. However, all these efficient catalysts are mainly based on expensive noble metals. Due to economic constraints and environmental concerns in chemistry, the demand for the replacement of noble metals by Earth-abundant ones is increasing. The development of environmentally friendly, metal-catalyzed C–X bond-forming reactions constitutes one of the major goals in modern chemistry and chemical industry. Iron is an excellent candidate,

thanks to its low price, its nontoxicity or low toxicity, and its environmentally benign character. While iron catalysts were initially used as Lewis acids, impressive progresses have been made in the fields of iron-catalyzed cross-coupling reactions, C–C bond formation, hydrogenation, and even C–H bond functionalization reactions. This chapter will be devoted to highlight some, but not all, bond-forming reactions between carbon and a heteroatom upon addition to unsaturated alkynes or alkenes, cross-coupling reactions, cycloadditions, tandem or consecutive reactions, and C–H functionalizations.

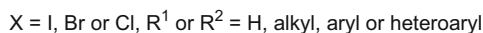
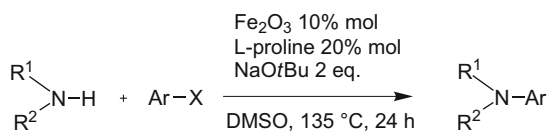
2 Iron-Catalyzed C–N Bond Formations

2.1 Cross-Coupling Reactions

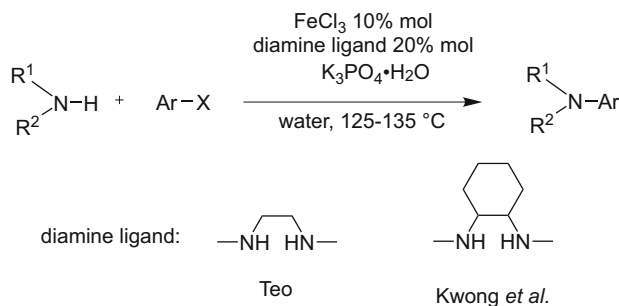
The *N*-arylation reaction is an important tool for the construction of building blocks being of interest in pharmaceutical and fine chemical industries. Many procedures reported to date involved palladium or copper catalysts [13–16]. Since the early work of Taillefer et al. on the cooperative catalysis of iron and copper for the arylation of pyrazoles with aryl iodides and bromides [17], several examples involving only iron catalysts have been reported.

In 2008, Liu and coworkers reported the use of Fe₂O₃ as catalyst and L-proline as ligand for the C–N bond formation between aryl halides and a broad range of amines (Scheme 1) [18]. It is worth mentioning that, in some cases, NaOtBu could lead to the expected products but the authors have shown that iron oxide improved the efficiency of the coupling reaction. Another key point of this procedure was the use of aryl chlorides as electrophiles, even if the yields were then lower than in the presence of aryl bromides or iodides. Thus, the amination of chlorobenzene by morpholine yielded the aniline derivative in 51%, while the yields were 82 and 85% from bromobenzene and iodobenzene, respectively. Finally, a *cine*-substitution effect [19] involving a benzyne intermediate was observed leading into a mixture of *para*- and *meta*-substituted arylamines (1:1 to 4:1 ratio) when substituted aryl halides were engaged under these reaction conditions.

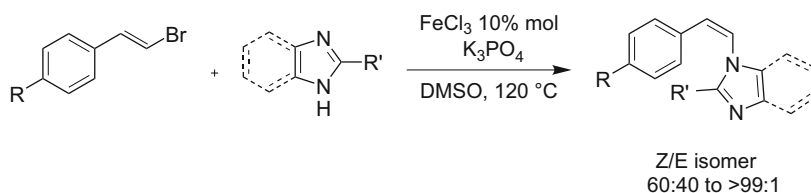
Two related reports appeared from the group of Teo [20] and the group of Kwong [21] on the use of FeCl₃ and diamine ligands for the *N*-arylation of amine in aqueous media under high temperatures (Scheme 2).



Scheme 1 *N*-Arylation of amines



Scheme 2 *N*-Arylation of amines catalyzed by iron(III) chloride



Scheme 3 Amination of (*E*)-vinyl bromides

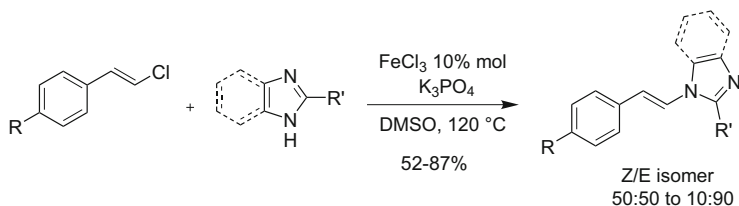
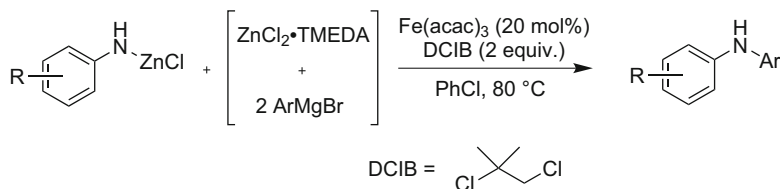
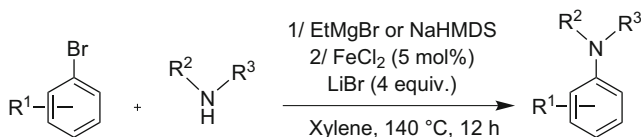
Several (hetero)aromatic halides were evaluated in this reaction. Under these reaction conditions, only the report of Teo mentioned a mechanism involving oxidative and reductive process via a mononuclear iron species but a dinuclear species was not excluded.

In addition to the aryl halide derivatives, Mao *et al.* reported the use of vinyl bromide for the C–N bond formation via cross-coupling reaction catalyzed by iron salts [22]. This reaction was carried out with FeCl_3 as catalyst in the presence of K_3PO_4 as base in DMSO at 120 °C. It is worth mentioning that starting from the (*E*)-vinyl bromide, the major stereoisomer obtained was the (*Z*)-vinylamine product (Scheme 3).

Interestingly, when the (*E*)-isomer was subjected to the same catalytic reaction conditions, no isomerization to the (*Z*)-isomer took place. This result may suggest that the (*E*)-isomer is not an intermediate during the formation of the (*Z*)-isomer. Nevertheless, the (*E*)-isomer product could be obtained using (*E*)-vinyl chloride as starting material for the amination (Scheme 4).

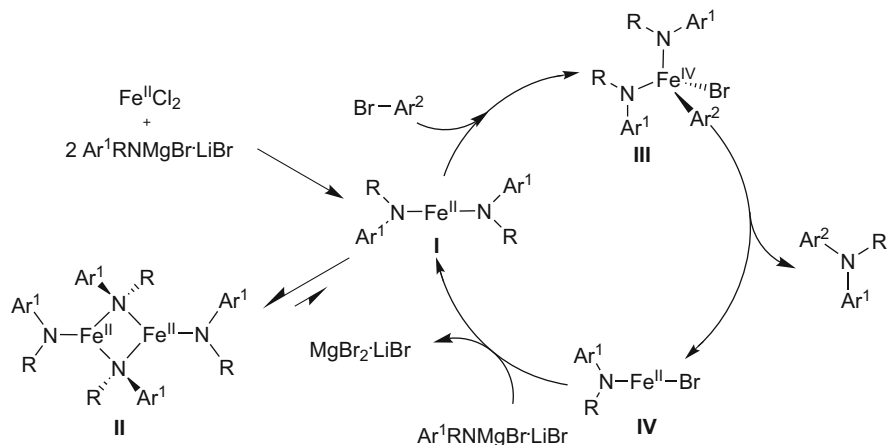
In 2011, Nakamura *et al.* reported an oxidative cross-coupling reaction involving zinc amide as nucleophile with aryl halides for monoarylation of primary amines (Scheme 5) [23]. The best iron source was found to be $\text{Fe}(\text{acac})_3$ (20 mol%) with 2 equivalents of 1,2-dichloroisobutane (DCIB) as re-oxidant. However, the scope of the reaction was limited to aniline derivatives. Alkylamines gave only very poor GC yields.

Later, a methodology was reported for the arylation of secondary amines [24]. For this second arylation, FeCl_2 (5 mol%) was the most active salt in the presence of LiBr (4 equiv.) and a base such as Grignard reagents or NaHMDS

**Scheme 4** Amination of a (*E*)-vinyl chloride**Scheme 5** Monoarylation of amines**Scheme 6** Arylation of secondary amines

(2 equiv.) in order to generate in situ magnesium or sodium amides (Scheme 6). In combination with Nakamura's methodology, this protocol opens an easy access to tertiary amines from simple anilines.

To obtain a better understanding of this reaction, stoichiometric reactions were carried out. Thus, a dinuclear iron species **II** was isolated and characterized by X-ray analysis, leading to the mechanism for the arylation of secondary amines depicted in Scheme 7. A disubstitution of the chloride by two amides on FeCl_2 could give the bis-amide iron species **I** in equilibrium with **II**. The intermediate **I** is comparable to the well-known $[\text{Fe}(\text{HMDS})_2]$. Then, an oxidative addition of aryl bromide, providing the iron(IV) intermediate **III**, followed by a reductive elimination could liberate the arylated amine and the iron species **IV**. The catalytic active species **I** could finally be regenerated by a substitution of the bromide with an amide (Scheme 7).



Scheme 7 Proposed mechanism for the arylation of secondary amines

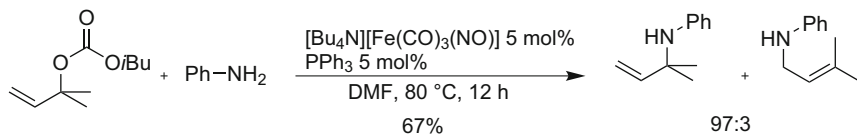
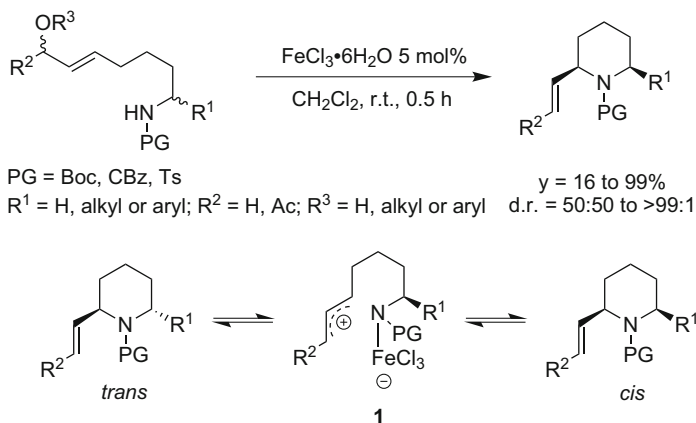
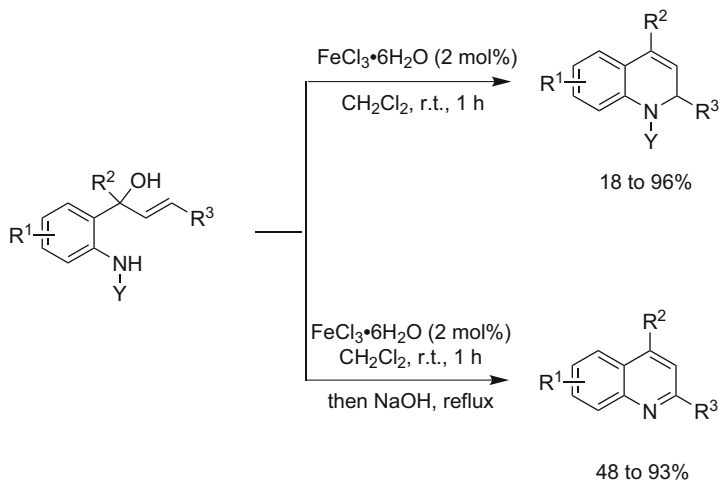
2.2 Allylic Substitution Reactions

Allylic amines are interesting building blocks in organic synthesis. The allylic amination is classically catalyzed by palladium [25]. However, there is a lack of selectivity. Indeed, in palladium catalysis, the nucleophile typically reacts at the less sterically encumbered allylic position [25]. Various noble metals, such as iridium or rhodium, were able to promote allylic substitution with amines as nucleophile. Regioselectivities (branched vs. linear isomers) were usually high. Recently, in order to replace the expensive metals, iron complexes offered new opportunities to this chemistry. Plietker reported in 2006 the use of $[\text{Bu}_4\text{N}][\text{Fe}(\text{CO})_3(\text{NO})]$ (5 mol%) with PPh_3 (5 mol%) as a catalytic system capable of regioselectively and selectively affording the branched allylic aminated products from allylic carbonates (Scheme 8) [26].

Interestingly, when chiral allylic carbonates were utilized, the chiral information was maintained with retention and only a slight loss of the enantiomeric excess was noticed. Concerning the mechanism of the reaction, Plietker proposed the formation of a σ -allyl metal intermediate which might explain the regio- and the stereoselectivities.

In 2010, Cossy, Reymond, and coworkers reported a diastereoselective synthesis of 2-vinyl-piperidines and tetrahydropyrans starting from acyclic allylic acetates and alcohols tethered with amine frameworks [27]. $\text{FeCl}_3 \cdot 6\text{H}_2\text{O}$ (5 mol%) without any ligand catalyzed these reactions at room temperature in high yields and high diastereoselectivities in favor of the *cis*-isomers (Scheme 9).

Interestingly, after 10 h in the presence of $\text{FeCl}_3 \cdot 6\text{H}_2\text{O}$, epimerization occurred and, from a 1:1 diastereoisomeric mixture, the *cis*-diastereoisomer was obtained as the main or exclusive isomer. The authors proposed the formation of a zwitterionic intermediate **1** to explain the sole formation of the *cis*-diastereoisomer (Scheme 9).

**Scheme 8** Regioselective allylic amination of allylic carbonates**Scheme 9** Diastereoselective synthesis of 2-vinyl-piperidines**Scheme 10** Synthesis of dihydroquinoline and quinolone derivatives

In 2012, Wang, Sun, and coworkers applied the same reaction conditions to the synthesis of dihydroquinolines from allylic alcohols tethered to anilines (Scheme 10) [28]. The authors developed further a one-pot procedure to quinoline derivatives in good to high yields. The judicious choice of the nitrogen-protecting

group allowed its easy cleavage under basic conditions and promoted the aromatization of the dihydroquinoline intermediate (Scheme 10).

2.3 C–H Functionalization

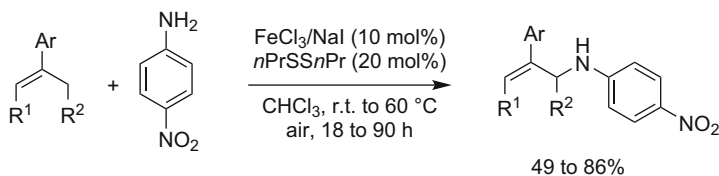
2.3.1 Cross-Dehydrogenative Coupling Reactions

The construction of C–C bonds is one of the most important tasks in organic synthesis. The selective and efficient functionalization of C–H bonds has attracted much attention from both industry and academia in the last decade [29–33], especially if this transformation occurs without any prefunctionalization. Among all the coupling reactions, the cross-dehydrogenative coupling (CDC) has appeared to be an efficient process to form C–C bonds directly from two different C–H bonds under oxidative conditions [34–36]. One of the challenging transformations is the formation of allylic amine derivatives via C–H functionalization. The first iron-catalyzed example was reported by Shi et al. using iron(III) chloride as catalyst under oxidative conditions [37]. The reaction was performed using a 1:2 mixture of FeCl₃/NaI (10 mol%) with dipropyl disulfide (20 mol%) in chloroform at 60 °C under air. However, only *para*-nitroaniline was used as nitrogen nucleophile in this report (Scheme 11).

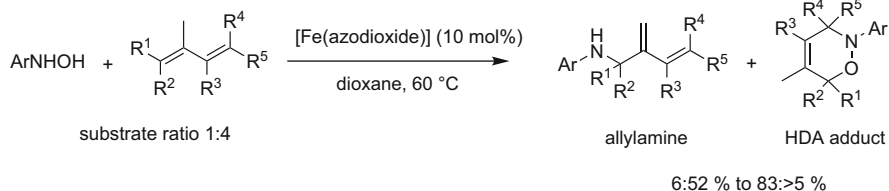
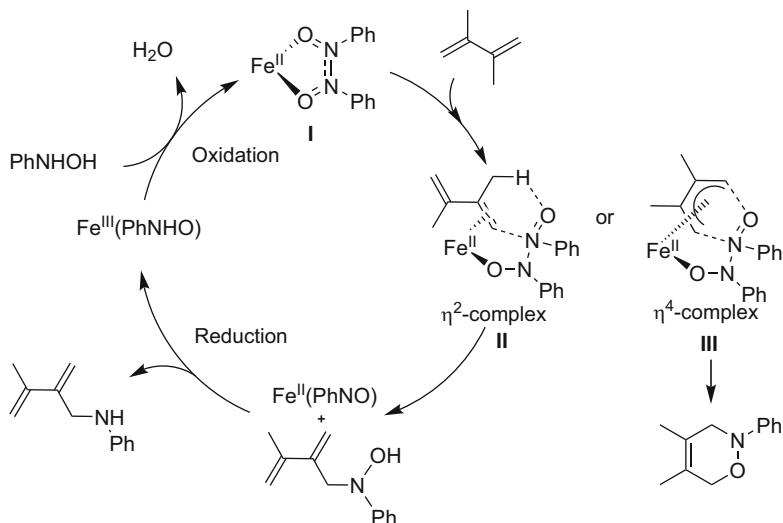
Srivastava reported the allylic C–H amination of 1,3-dienes using arylhydroxylamine as amine precursor [38]. In this reaction, not only the allylamine but also a competitive hetero-Diels–Alder (HDA) reaction was observed. The authors found that the iron azodioxide complex ([Fe{PhN(O)N(O)Ph}₃][FeCl₄]₂) was the most active and chemoselective in the model reaction. Nevertheless, the reaction appeared to be substrate dependent. Thus, with 2,3-disubstituted dienes, the allylamines were the major (or even the sole) products, whereas the HDA product was obtained as the major product from 2,3-unsubstituted dienes (Scheme 12).

The authors proposed for this transformation the mechanism shown in Scheme 13. The key intermediates, which might explain the chemoselectivity, are the η²- and η⁴-complexes **II** and **III** (Scheme 13).

The same group reported also another methodology to synthesize selectively the allylic amines, which are formally Baylis–Hillman adducts. This reaction occurred via a nitroso-ene reaction and was catalyzed by simple iron(II) salts (Scheme 14)



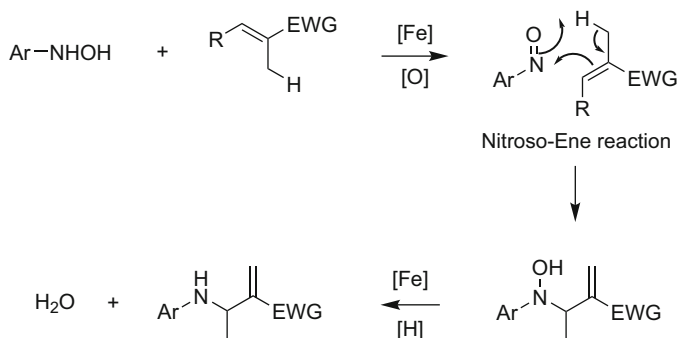
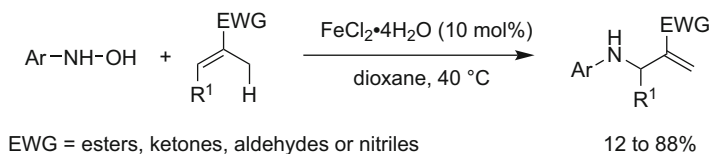
Scheme 11 Allylic amination reactions

**Scheme 12** Allylic C–H amination and HDA reactions**Scheme 13** Proposed mechanism for allylic C–H amination and HDA reactions

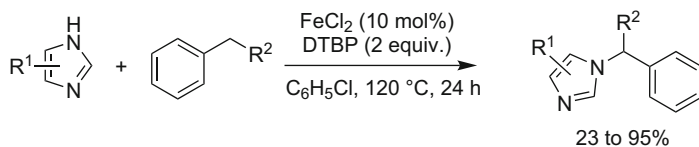
[39]. In this reaction, several electron-poor olefins, such as unsaturated esters, aldehydes, ketones, and nitriles, were tolerated.

Intermolecular oxidative C–H bond amination using benzylic derivatives and imidazole as nucleophiles catalyzed by FeCl₂ was reported by Qiu, Chen, and coworkers in 2011 (Scheme 15) [40]. In this work, the best oxidant was di-*tert*-butyl peroxide (DTBP) in chlorobenzene as solvent at 120 °C for 24 h. These reaction conditions afforded the benzylimidazole derivatives in moderate to high yields (23–95%). Noteworthy, in this reaction, electron-withdrawing groups, such as nitrile or nitro on the 4 and/or 5 position in the imidazole ring and also 2-substituted benzimidazoles, gave better results than unsubstituted benzimidazoles. Imidazole was totally inert under these reaction conditions.

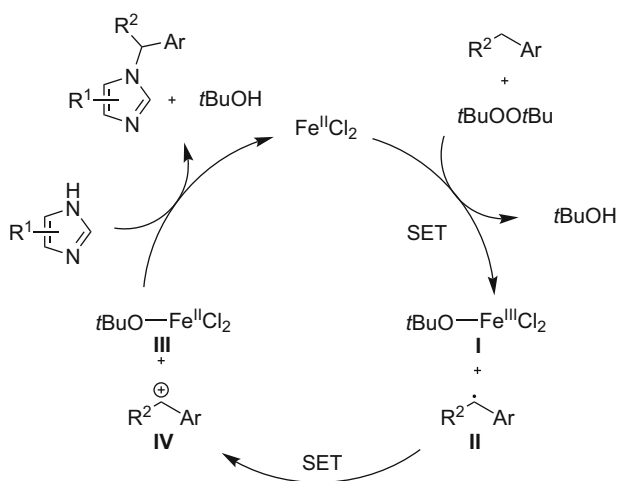
The proposed mechanism involves a radical process (Scheme 16) and starts with the generation of a benzylic radical **II** through hydrogen abstraction of the benzylic derivative by DTPB in the presence of the iron(II) salt. The radical could be further oxidized to the benzylic cation **IV** through a single-electron transfer assisted by the iron(III) alkoxide species **I** generated in the first step. Finally, a nucleophilic attack



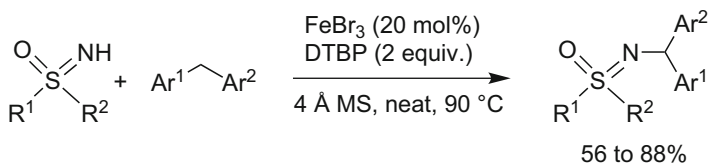
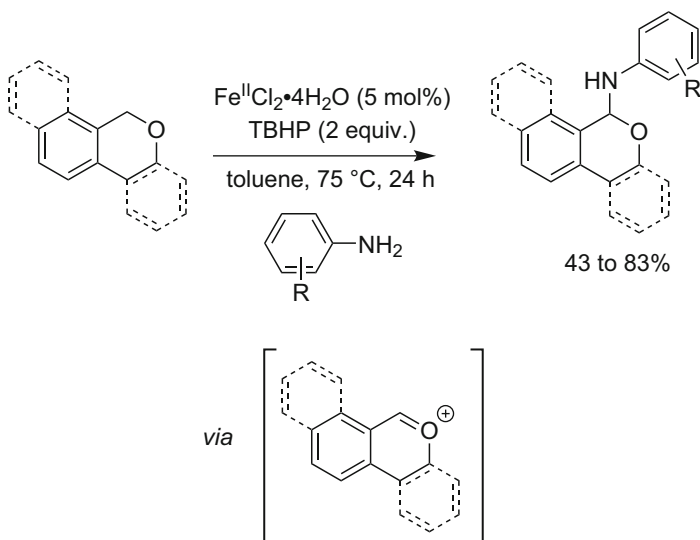
Scheme 14 A nitroso-ene reaction



Scheme 15 Synthesis of benzylic imidazoles



Scheme 16 Cross-dehydrogenative amination reaction

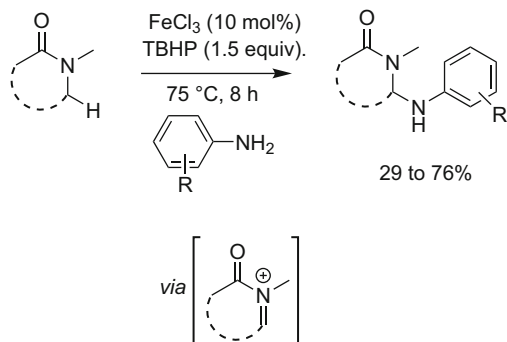
**Scheme 17** Synthesis of sulfoximines**Scheme 18** Synthesis of isochroman derivatives via benzylic C–H amination

of the imidazole derivative with deprotonation of the imidazole by the iron alkoxide **III** could liberate the product and regenerate the catalytic iron salt.

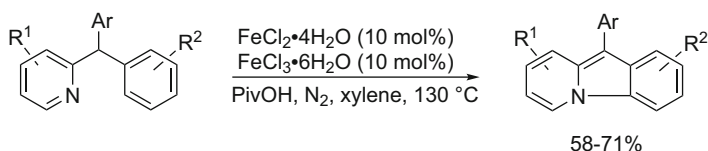
In 2014, Bolm and coworkers reported a similar reaction using sulfoximines as nucleophiles, but in this case, the best iron salt was iron(III) bromide [41]. Importantly, the reaction has to be carried out in the presence of molecular sieves without any solvent. *N*-Alkylated sulfoximines were obtained in moderate to high yields (56–88%, Scheme 17).

Yang and coworkers applied successfully this methodology for the C–H amination of isochromans [42]. The amino-isochroman derivatives were obtained in yields ranging from 43 to 83%, using iron(II) chloride as catalyst and TBHP as oxidant (Scheme 18). To explain this process, the authors proposed the following mechanism. The first step could be a hydrogen abstraction catalyzed by the iron salt and TBHP, as also reported by Qiu [40], but then the oxidation of the radical species could yield an oxonium intermediate (Scheme 18), which could react with amino nucleophiles.

Subsequently, thanks to the oxidability of the α -position of a heteroatom, Bao and coworkers reported the synthesis of aminal derivatives using cyclic and acyclic



Scheme 19 Synthesis of aminal derivatives via cross-dehydrogenative coupling reactions



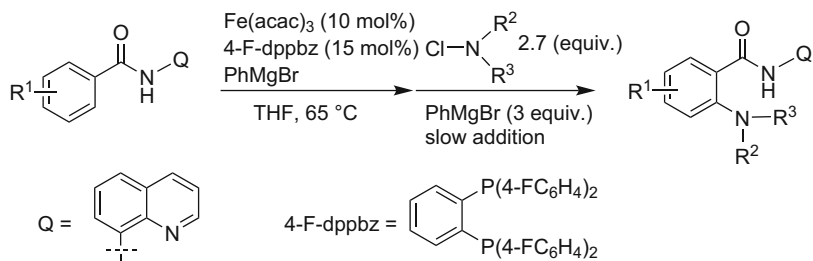
Scheme 20 Synthesis of pyrido[1,2-a] indoles

amides as electrophiles and aniline derivatives as nucleophiles (Scheme 19) [43]. The screening of iron salts, iron(II) chloride (10 mol%) and iron(III) chloride (3 mol%), showed that both were able to catalyze the coupling in 73 and 76% isolated yield, respectively. For the scope of the reaction, the authors selected iron (III) chloride for economic considerations, but for elucidation of the mechanism, they used an iron(II) to generate the active amidinium intermediate. The aminal derivatives were isolated in yields ranging from 29 to 76% (Scheme 19).

Pyrido[1,2-a]indoles were prepared from 2-benzhydrylpyridines through an intramolecular C–H amination reaction [44]. The syntheses of a broad range of Pyrido[1,2-a]indoles were achieved in quite good yields (58–71%) in the presence of iron(II) and iron(III) chloride (10 mol% each) and pivalic acid at 130°C under an inert atmosphere (Scheme 20). Both iron salts and pivalic acid were required to exhibit some activity but their role was not clear and no mechanistic clues were given.

2.3.2 N-Arylation via C–H Activation

In 2014, Nakamura et al. developed an *ortho*-amination of aromatic carboxamides using chloroamine reagents (Scheme 21) [45]. Importantly, this reaction requires a directing group. The nature of this group was studied and the quinolone framework was found to be the most selective and efficient. Under these conditions, in the presence of 10 mol% of $\text{Fe}(\text{acac})_3$, 15 mol% of bis(4-fluorophenyl)



Scheme 21 *Ortho*-amination reaction

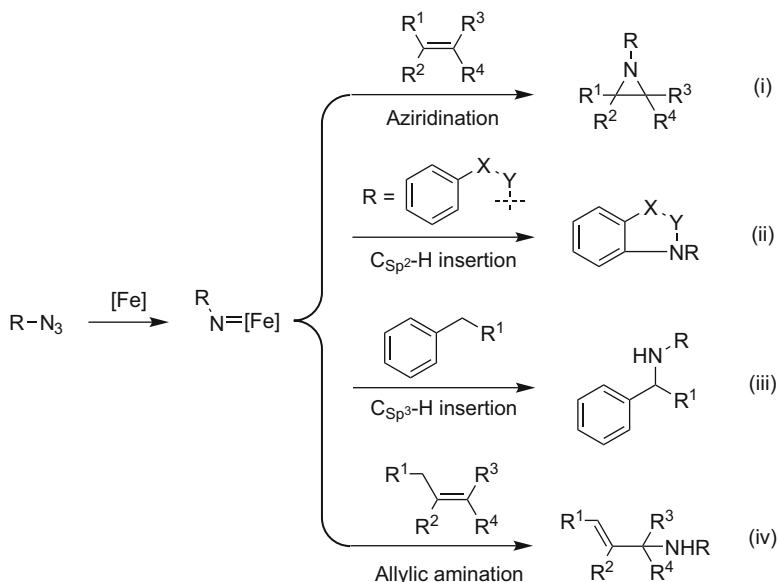
phosphinobenzene (4-F-dppbz), three equivalents of phenylmagnesium bromide, and 2.7 equivalents of various chloramines, several aniline derivatives were isolated in yields ranging from 0 to 100% depending of the aromatic substituents (Scheme 21). This C–H bond activation can also be achieved starting from heteroaromatic derivatives such as thiophene or indene.

2.3.3 Decomposition of Azide Generation of Nitrenes

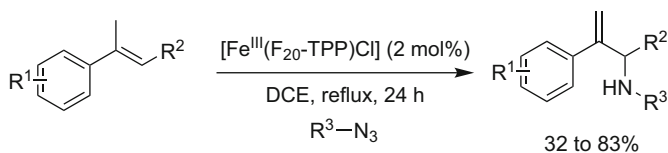
Iron salts or complexes are able to form nitrene iron species from azides, haloamines, and iminoiodanes. The chemical behavior of these nitrene iron species depends on the reaction partner: (1) aziridination reactions in the presence of an olefin (see Sect. 2.4.1) [46], (2) amination of aromatic compounds via an activation of aromatic $\text{Csp}^2\text{-H}$ bonds leading to indoles (vide infra, Sect. 2.4.2.7), (3) intramolecular amination of $\text{Csp}^2\text{-H}$ or $\text{Csp}^3\text{-H}$ bonds providing tetrahydroquinolines (vide infra, Sect. 2.4.3.2), and (4) allylic or benzylic amination. All these activations/transformations will be presented and discussed in this section and in the following ones (Scheme 22) [47, 48].

Allylic amination can also take place under similar reaction conditions as aziridination or $\text{Csp}^3\text{-H}$ functionalization reactions. Thus, the $[\text{Fe}^{\text{III}}(\text{F}_{20}\text{-TPP})\text{Cl}]$ complex and dipyrromethene iron complexes were respectively reported by the group of Che [49] and the group of Betley [50] to be catalytically active in allylic amination and amidation reactions. The scope of the reaction described by Che was limited to α -methylstyrene derivatives but gave the expected products in yields ranging from 17 to 83% (Scheme 23) [49]. Nevertheless, when α -methylhomoallylbenzene was utilized, aziridination of the olefin occurred instead of the allylic amidation. As mentioned by Che, the allylic amination products might result from an aziridination/ring-opening sequence and could, thus, be described as a formal direct allylic C–H bond insertion [49].

With dipyrromethene iron complex **2** as catalyst, allylic amination was also observed by Betley with a series of olefins and azide adamantane. Nevertheless, isolated yields were low to moderate with 20 mol% of the catalyst. The reactivity was also lower with cycloalkenes than with methylstyrene. Stoichiometric reactions were also performed and led in some cases to an improvement of the yields up to



Scheme 22 Reactivity of iron nitrene species

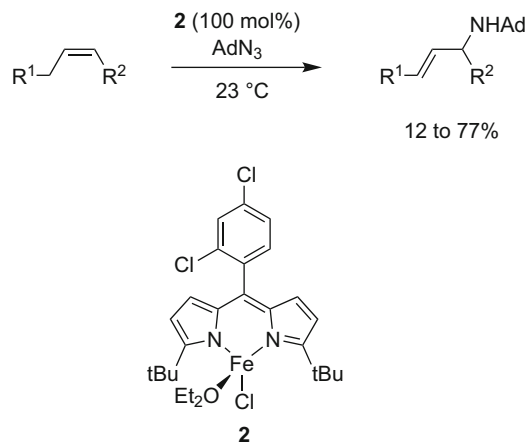
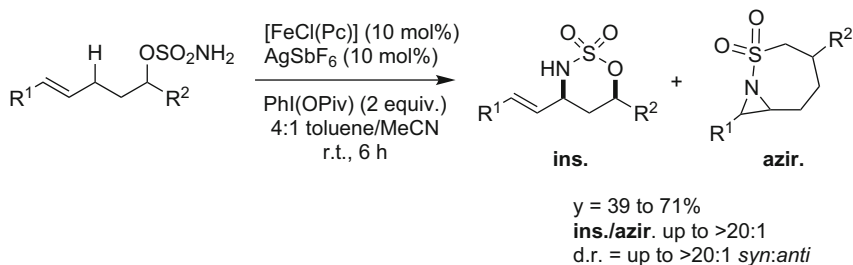
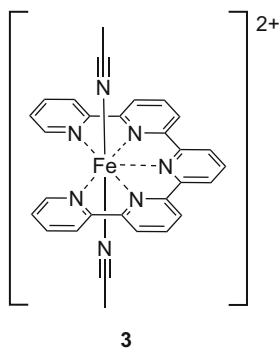
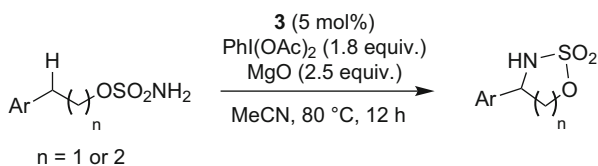


Scheme 23 $[Fe^{III}(F_{20}\text{-TPP})Cl]$ -catalyzed allylic amination and amidation

77% (Scheme 24) [50]. Importantly, intermolecular amination with unsaturated substrates led exclusively to allylic amination and not to the aziridine derivatives.

White et al. reported an intramolecular version of the allylic C–H amination with a sulfamate ester tethered to an olefin using $[FeCl(Pc)]$ ($Pc = \text{phthalocyaninato}$) as pre-catalyst and $PhI(OAc)_2$ as oxidant [51]. The use of silver salts to generate a cationic iron species improved the catalytic activities but was not absolutely necessary. The chemoselectivity (C–H amination vs. aziridination reaction) was very high and diastereoselectivities were moderate to high in favor of the *syn*-diastereoisomers (Scheme 25).

In 2008, Che et al. reported that $[Fe(Cl_3\text{-terpy})_2][ClO_4]_2$, a nonheme iron complex, was an effective catalyst for the intramolecular amination of benzylic C–H bonds at 80°C. The sulfamate ester products were isolated in 84–90% yields [52]. The same group also reported that an iron complex bearing a pentapyridine ligand was a nonheme iron complex active for inter- and intramolecular amination of various $Csp^3\text{-H}$ bonds (alkanes, cycloalkanes, benzylic and allylic derivatives (**3**, Scheme 26) [53]. As proposed on the basis of DFT calculations, the crucial

**Scheme 24** Dipyrromethene iron complex-mediated allylic amination**Scheme 25** Intramolecular allylic C–H amination**Scheme 26** Benzylic C–H amination catalyzed by a nonheme iron complex

intermediate is a cationic 7-coordinate intermediate $[\text{Fe}(\text{qpy})(\text{NR})(\text{X})]^{n+}$ ($\text{X} = \text{NR}$, solvent, anion).

2.4 Synthesis of Nitrogenated Heterocycles

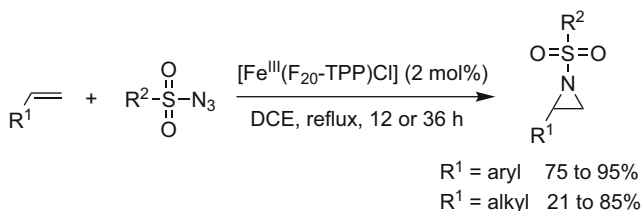
2.4.1 Aziridination of Olefins

Since the pioneering work of Mansuy [54] and Breslow [55] on the aziridination of olefins catalyzed by $[\text{Fe}^{\text{III}}(\text{TTP})\text{Cl}]$ with $\text{PhI}=\text{NTs}$ as nitrogen source, several catalytic systems based on porphyrin, corrole, and nonheme ligands have been developed [56–61]. To the best of our knowledge, in the last 5 years, only two new ligands have been developed for this useful organic transformation. The first one, reported by Che et al. [49], was based on a perfluorinated tetraphenylporphyrin ligand and the second one, reported by Betley et al. [62, 50], was based on a dipyrromethene ligand.

The perfluorinated tetraphenylporphyrin complex $[\text{Fe}^{\text{III}}(\text{F}_{20}\text{-TPP})\text{Cl}]$ exhibited higher activities than the original $[\text{Fe}^{\text{III}}(\text{TTP})\text{Cl}]$ complex used by Mansuy in the reaction between styrene and 2-phenyl-1-tosylaziridine. Good to excellent yields were obtained with styrene derivatives in the presence of several sulfonyl azides (Scheme 27). Poor to moderate conversions (21–41%) were obtained for the aziridination between more challenging aliphatic alkenes and arylsulfonyl azides bearing electron-donating substituents; but full conversions and good yields (75–85%) were reached with *para*-nitrobenzenesulfonyl azide (Scheme 24) and *para*-nitrophenyl azide.

As alternative to porphyrin chemistry, Betley et al. reported the synthesis of several dipyrromethene iron complexes (Fig. 1) and observed the aziridination of styrene with alkyl azide derivatives [62, 63].

Later, the scope of the reaction was evaluated with various styrene and azide derivatives [50]. Halides and ethers were well tolerated in the reaction between styrene and AdN_3 as azide. Yields between 75 and 85% were obtained. A dramatic decrease of the yield was noticed when phenyl azide was used (17%); however, the reactivity could be recovered by enriching the aromatic ring with an electron-donating group. Thus, the aziridine was isolated in 64% yield when *para-tert*-butyl-phenyl azide was engaged. Noteworthy, unlike the work of Che and



Scheme 27 $[\text{Fe}^{\text{III}}(\text{F}_{20}\text{-TPP})\text{Cl}]$ -catalyzed aziridination of olefins

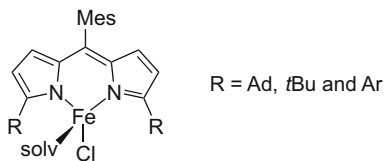
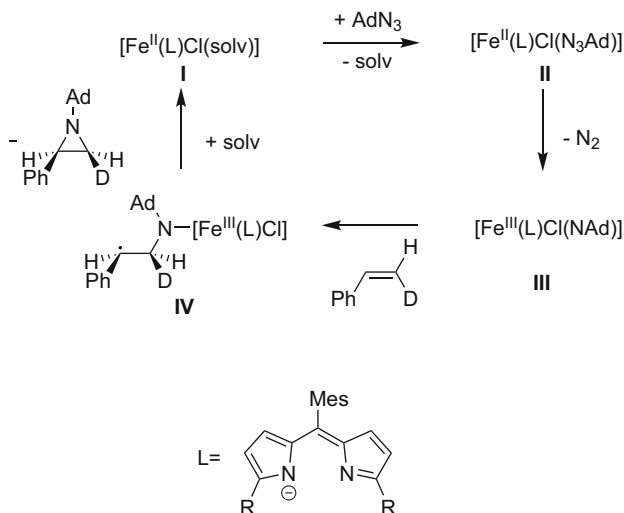


Fig. 1 Dipyrromethene iron complexes



Scheme 28 Proposed mechanism for the aziridination of styrene derivatives catalyzed by dipyrromethene iron complexes

coworkers [49], no reaction occurred with the *para*-nitrobenzenesulfonyl azide and TMSN_3 .

Catalytic aziridination was initially proposed to occur via a single-electron pathway [62]. Further experiments, based on labeling and Hammett studies, confirmed a radical intermediate, but no definitive mechanism was reported [50]. Indeed, while isomerization of a *cis*-olefin into a mixture of *cis*- and *trans*-aziridine suggested a stepwise mechanism, its lack was less informative. However, the following mechanism was suggested. After the formation of the nitrene iron species **III**, the radical intermediate **IV** might be formed and leads to radical cyclization, which would release the catalytic species **I** and the aziridine (Scheme 28).

2.4.2 Construction of Five-Membered Cycles Containing Nitrogen Atoms

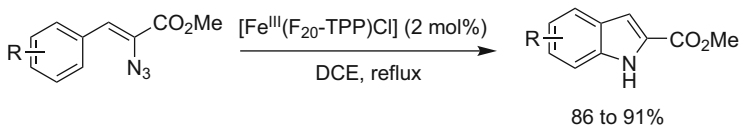
C_{sp²-H or C_{sp³-H Functionalization Reactions}}

As mentioned above, nitrene iron complexes own various reactivities. One of the most important transformations nowadays is the direct C–H functionalization. By decomposition of azide compounds, some iron complexes are able to catalyze either the amination of aromatic ring systems or even of C_{sp³-H bonds. Thus, the perfluorinated porphyrin iron complex [Fe^{III}(F₂₀-TPP)Cl], reported by Che et al., was able to catalyze an intramolecular amination reaction of aromatic rings after the decomposition of azides and furnished indole derivatives in high yields (Scheme 29) [64].}

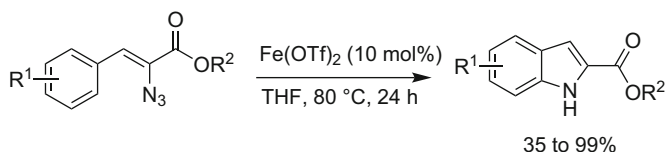
The mechanism of this cyclization was investigated by Li, Yan, and coworkers by DFT calculations [65]. First, while the perfluorinated ligand was replaced by a simple porphyrin ligand for the whole study, a comparison between these ligands in the transformation step “azide to nitrene complex” demonstrated that both electronic and steric effects of the complexes did not modify the relative energies. The study showed that the most favorable pathway involved the nitrene formation (after dinitrogen release), the homolytic cleavage of the C–H bond followed by a 1,2-hydrogen shift, and finally the C–N bond formation [65].

In 2011, the reaction was revisited by Bolm and Bonnamour with simple iron (II) triflate salt as catalyst. Indoles were isolated in yields between 35 and 99% (Scheme 30) [66]. The yields were certainly lower and the catalyst loading higher, but the catalytic system was much more simple than the one used by Che.

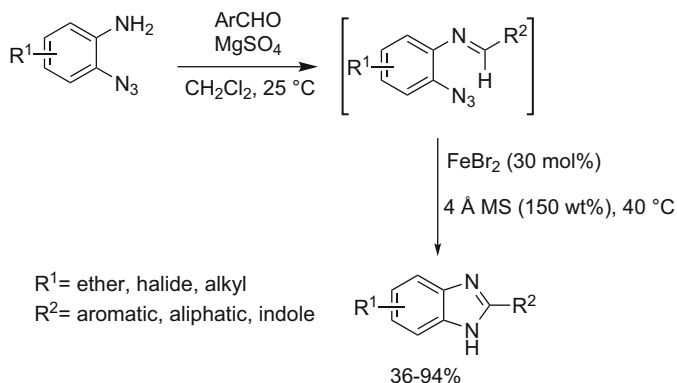
In addition to the indole synthesis, other nitrogen heterocycles could also be prepared by the decomposition of aromatic azides in the presence of iron salts or iron complexes. Driver et al. reported in 2008 an interesting two-step reaction with *ortho*-azido anilines and aromatic aldehydes [67]. The imines generated in situ from the condensation between aromatic or aliphatic aldehydes and *ortho*-azido aniline compounds reacted with the azide moiety. The intramolecular C_{sp²-H amination}



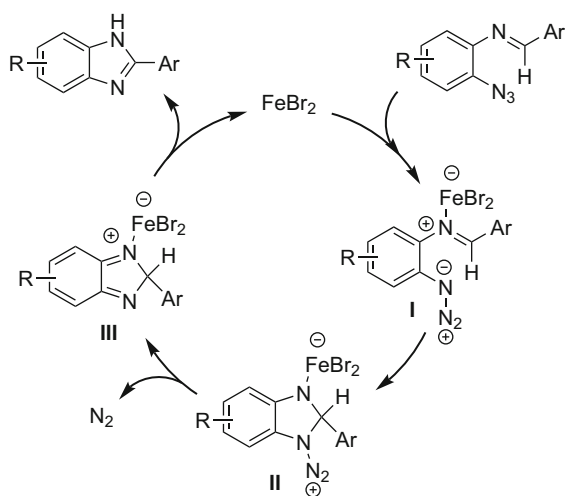
Scheme 29 [Fe^{III}(F₂₀-TPP)Cl]-catalyzed C_{sp²-H amination}



Scheme 30 Synthesis of indoles through C_{sp²-H amination}



Scheme 31 Synthesis of benzimidazoles through $\text{Csp}^2\text{-H}$ amination

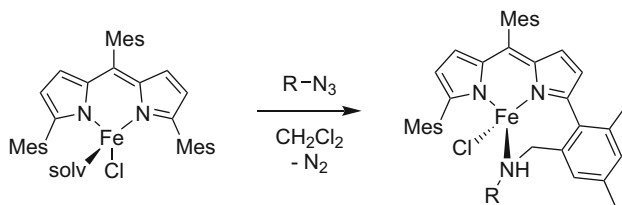


Scheme 32 Proposed mechanism for the synthesis of benzimidazoles

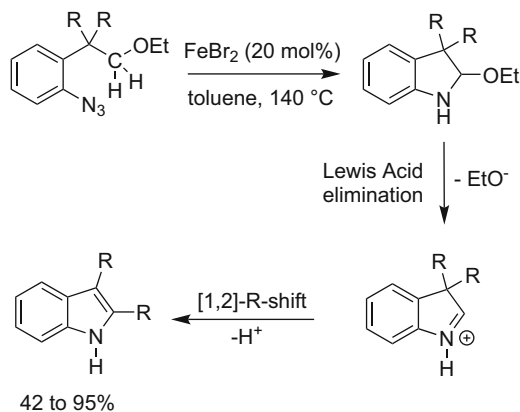
provided the corresponding C2-substituted benzimidazole derivatives in moderate to high yields (Scheme 31).

The authors postulated the following mechanism to explain the formation of the benzimidazoles. A Lewis acid activation of $\text{RC}_6\text{H}_3(\text{N}_3)\text{N}=\text{CHAR}$, followed by a nucleophilic attack of the internal nitrogen atom of the azide on the activated imine **I** to give **II**, and the elimination of a molecule of nitrogen could lead to a ferrate intermediate **III**. Finally, a 1,2-proton shift prototropy could liberate the iron salt and the benzimidazole (Scheme 32).

Betley et al. reported also the amination of less or nonreactive $\text{Csp}^3\text{-H}$ bonds. The group demonstrated that, first, organic azides could activate the benzylic position in the presence of stoichiometric amounts of the iron–dipyrrinato complex (Scheme 33) [62]. Then, amination of various toluene derivatives could be achieved



Scheme 33 Stoichiometric reaction between the dipyrromethene ligand and azide derivatives

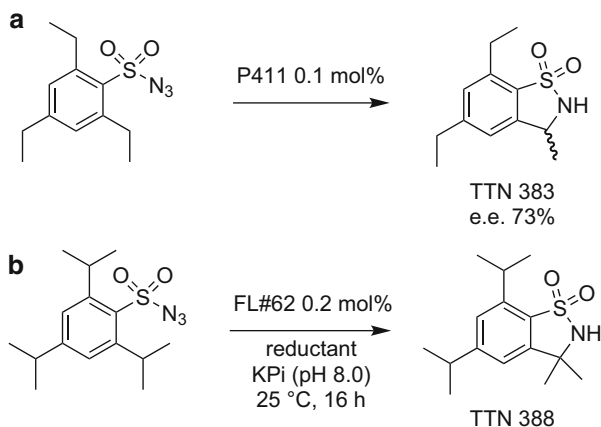


Scheme 34 Tandem Csp^3 -H amination and 1,2-alkyl shift

catalytically. They also showed that this catalytic system tolerated halides and ethers on the aromatic ring [50]. Finally, they nicely extended this process to the synthesis of pyrrolidine derivatives via an intramolecular insertion of alkyl azides into Csp^3 -H bonds [68].

Driver et al. reported a synthesis of indoles via a two-step procedure involving first an amination reaction of homobenzylic ethers in the presence of $FeBr_2$ and then ethanol elimination followed by a 1,2-alkyl migration. The indoles were isolated in moderate to high yields (42–95%, Scheme 34) [69].

Arnold et al. reported an enantioselective intramolecular Csp^3 -H amination in 2013 in the presence of a cytochrome P450 mutant as catalyst for the synthesis of chiral benzosultams from aromatic sulfonyl azides (Scheme 35) [70]. This reaction is still relatively substrate dependent, but it is also highly efficient when a matching substrate/enzyme combination is found. Indeed, a total turnover number (TTN) could reach 310 with enantiomeric excesses up to 73% (Scheme 35a). Noteworthy, when the reaction was performed *in vivo* with intact *E. coli* cells, TTNs reached up to 680 with 60% *e.e.* and an *e.e.* up to 89% but with a lower TTN of 250. This work was then implemented by Fasan et al. who evaluated new engineered P450_{BM3} variants.[71] The best mutant was FL#62 which gave the benzosultam derivatives with TTNs up to 388 (Scheme 35b). However, if selectivities are considered, the best results were obtained with 139-3(T268A), which provided benzosultams with



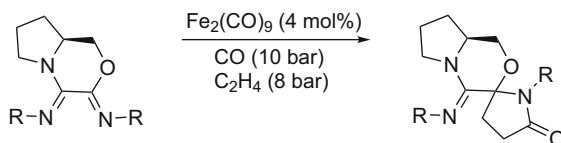
Scheme 35 Enantioselective intramolecular Csp³-H amination

enantiomeric excesses up to 91%. Noteworthy, depending on the mutant, opposite selectivities could also be observed. Finally, in this study, a scale up to 30 mg was successfully performed, leading to the corresponding sultam in 42% isolated yield.

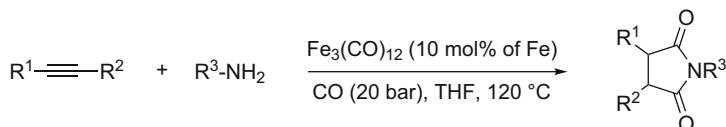
[2+2+1]-Cycloaddition

A hetero-[2+2+1]-cycloaddition between ketimines, carbon monoxide, and ethylene in the presence of catalytic amount of Fe₂(CO)₉ was reported by Imhof [72, 73]. The scope of this reaction was rather limited, as only one compound provided a good result (Scheme 36). Both one molecule of carbon monoxide and one of ethylene were inserted. DFT calculations demonstrated that the diimine acted as a bidentate ligand and the selectivity was due to a subtle substituent effect.

Beller and coworkers have developed a convenient one-pot method for the synthesis of various substituted succinimides. By starting from commercially available amines (or ammonia) and alkynes, several interesting succinimides were obtained selectively in the presence of catalytic amounts of either Fe(CO)₅ or Fe₃(CO)₁₂ (Scheme 37) [74, 75]. The *N*-substituted succinimides were obtained in moderate to good yields (37–84%). The authors demonstrated that these iron-catalyzed carbonylations proceeded smoothly in the presence of various heterocycles and that the carbonylation protocol is tolerant to different functional groups. However, it is worth to note that maleimides were isolated when diphenylacetylene and substituted amines were used. This result could be due to a facile aromatization. This iron-catalyzed double carbonylation, related to a palladium-catalyzed Sonogashira reaction, led to a straightforward synthesis of a library of *trans*-3,4-disubstituted succinimides and, after a further in situ oxidative dehydrogenation, to various 3,4-diarylmaleimides [75]. This strategy was used to a short synthesis of a natural arcyriarubin intermediate [75].



Scheme 36 Synthesis of functionalized lactams



Scheme 37 Synthesis of functionalized succinimides

Mathur and coworkers disclosed a related approach to maleimides from isocyanates and terminal acetylenes under a pressure of carbon monoxide [76]. However, selectivities and yields were lower than Beller's procedure.

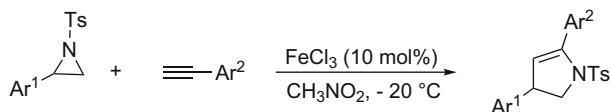
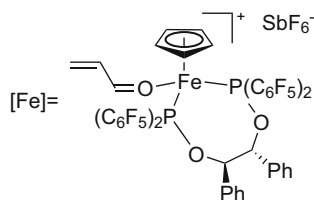
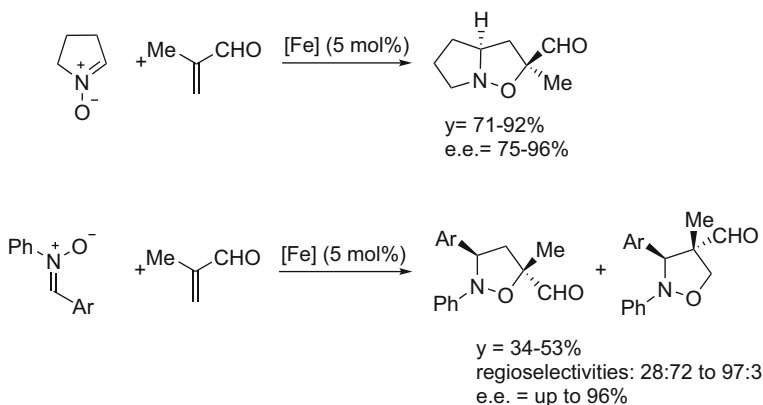
[3+2]-Cycloaddition Reactions

Iron is not only a transition metal but it is also a Lewis acid and several reactions have been reported in the literature to access five-membered nitrogenated cycles. Thus, Das et al. developed an efficient method for an access to 1,2,3,5-tetrasubstituted pyrroles by treatment of α -bromo aryl ketones or their derivatives with amines and dialkyl acetylenedicarboxylate using iron(III) chloride as a catalyst [77]. The pyrroles were obtained usually in high yields (84–89%).

The simple iron salt FeCl_3 was an efficient catalyst for the synthesis of dihydropyrroles from terminal aryl alkynes and aziridine derivatives [78]. The dihydropyrroles were obtained in yields between 48 and 82% (Scheme 38). However, this reaction was quite limited, as electron-deficient or unactivated aziridines and aliphatic alkynes were not good substrates for this reaction.

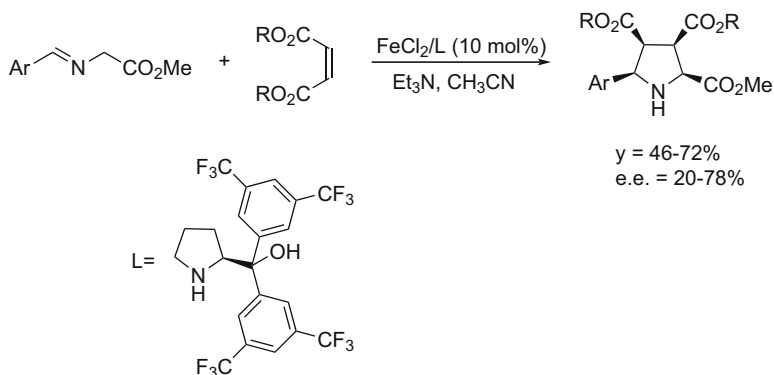
Asymmetric [3+2] cycloaddition reactions are a synthetic pathway to pyrrolidines. Kündig developed a protocol using a chiral Lewis acid based on the combination of a strong electron-deficient diphosphine ligand and a cyclopentadienyl iron framework [79, 80]. Good to high yields and enantioselectivities were obtained in the reaction between methacrolein and pyrrolidine *N*-oxide (Scheme 39). The use of diarylnitrones provided a mixture of regioisomers in moderate yields (34–53%). Moreover, even if the cycloaddition was completely *endo*-selective, the enantioselectivities depended on the electronic properties of the nitrones.

Wang et al. reported that FeCl_2 in combination with α,α -bis(3,5-bis(trifluoromethyl)phenyl)prolinol catalyzed the asymmetric [3+2] cycloaddition between

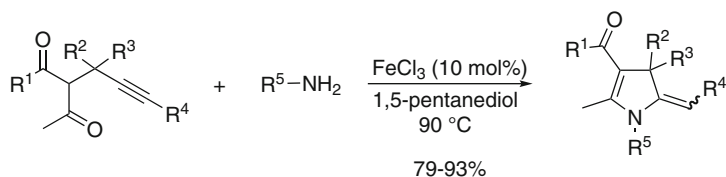
**Scheme 38** Synthesis of dihydropyrroles**Scheme 39** Enantioselective [3+2] cycloadditions

azomethine ylides and electron-poor alkenes (Scheme 40) [81]. The *endo*-adducts were isolated in moderate yields (46–72%) and enantioselectivities (up to 78%).

Feng reported the asymmetric synthesis of 1,2,4-triazoline derivatives via an enantioselective cyclization of α -isocyano esters and azodicarboxylates catalyzed by a *N,N'*-dioxide/ $\text{Fe}(\text{acac})_2$ complex [82]. High yields (up to 98%) and enantioselectivities (up to 94%) were reached.



Scheme 40 Enantioselective [3+2] cycloaddition



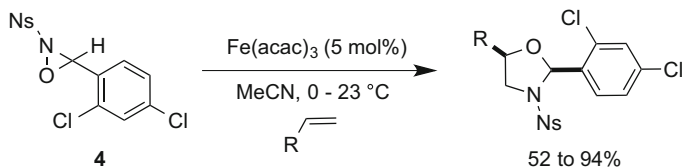
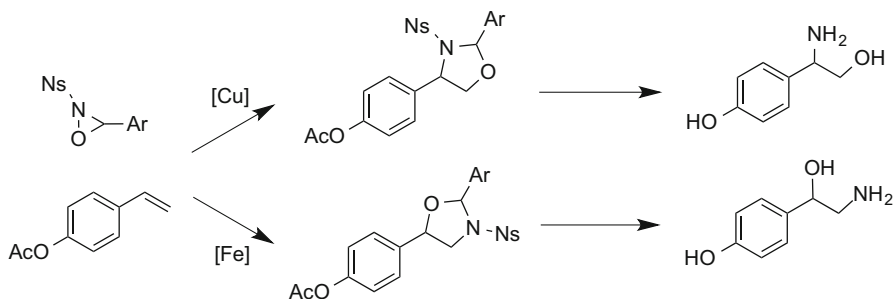
Scheme 41 Synthesis of 4,5-dihydropyrroles

[4+1]-Cycloaddition

An efficient synthesis of 4,5-dihydropyrroles was developed through an iron-catalyzed [4+1]-cyclization of 4-acetylenic ketones with primary amines [83]. The reaction conditions tolerated functional groups and allowed a straightforward approach to a wide range of substituted 4,5-dihydropyrroles in good to high yields (79–93%, Scheme 41). It is also worth to mention that the (*Z*)-isomer was the major or the exclusive isomer in this reaction.

Intermolecular Aminohydroxylation of Olefins

The aminohydroxylation of olefins is an interesting methodology via oxazolidinone or oxazole intermediates to obtain 1,2-aminoalcohols, a common structural motif in bioactive natural products and chiral reagents for stereoselective synthesis. Sharpless and coworkers disclosed first this reaction with an osmium catalyst [84]. Then, alternative transition metal-based complexes such as palladium [85, 86], platinum, rhodium, gold, and copper [87] have been found to avoid the toxicity of osmium complexes. In 2010, Yoon et al. reported first the aminohydroxylation of olefins using oxaziridine **1** with catalytic amount of iron(III) salts as pre-catalyst [88]. This powerful tool in organic chemistry is complementary to the previous methodologies reported by the same group in the presence of a copper catalyst [89–92]. In this

**Scheme 42** Aminohydroxylation of olefins**Scheme 43** Regioselective aminohydroxylation of olefins catalyzed by iron(III) or copper(II)

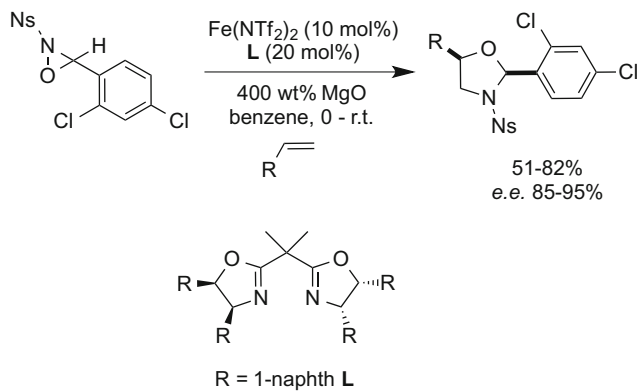
reaction, the isolated yields were moderate to high (52–94%) and the regioselectivities were up to >10:1 (Scheme 42) [88].

The authors have compared the regioselectivities obtained with the two metals and have demonstrated that both approaches are complementary. Indeed, the regioselectivities depended on the copper or iron catalyst to be used in the reaction (Scheme 43).

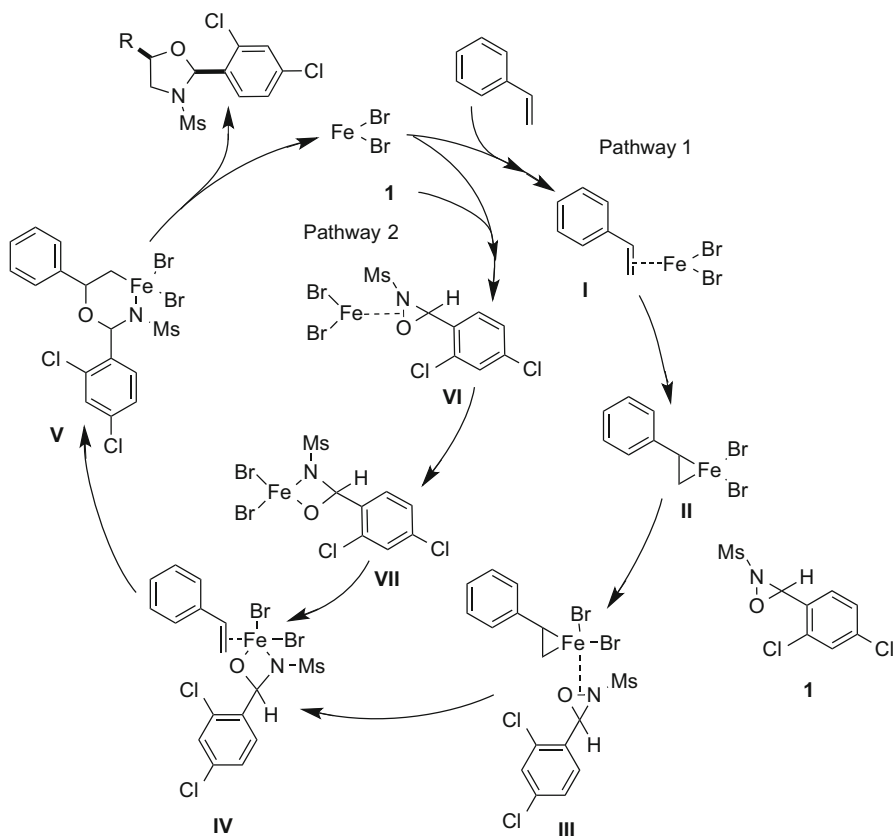
Yoon et al. reported the asymmetric version of this oxyamination catalyzed by an in situ generated iron(II) bis(oxazoline) complex starting from $\text{Fe}(\text{NTf}_2)_2$ and bis-oxazoline **L**. The oxaziridines were isolated in moderate to high yields and good enantiomeric excesses (85–95%, Scheme 44) [93].

Mechanistic studies and DFT calculations were recently reported by Ren et al. on the reaction between styrene and oxaziridines (Scheme 45) [94]. The mechanistic hypotheses were based on the activation of the styrene (intermediate **I**, pathway 1) or the oxaziridine (intermediate **VI**, pathway 2) for the first step of the catalytic cycle. The energetic profile of pathway 1 was found to be more favorable than the one of pathway 2. Based on these results, the first step could be the coordination of the styrene to the metal center **I** followed by the insertion of the iron(II) species into the N–O bond of the oxaziridine leading to the intermediate **IV**. Then, the insertion of the olefin could occur into the Fe–O bond yielding to a six-membered ring species **V**. This intermediate could liberate the final product and regenerate the catalytically active species after a final reductive elimination step.

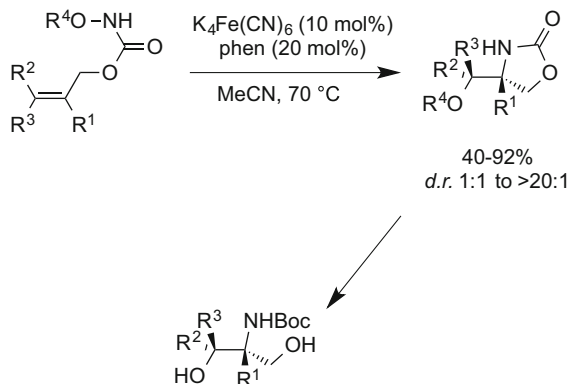
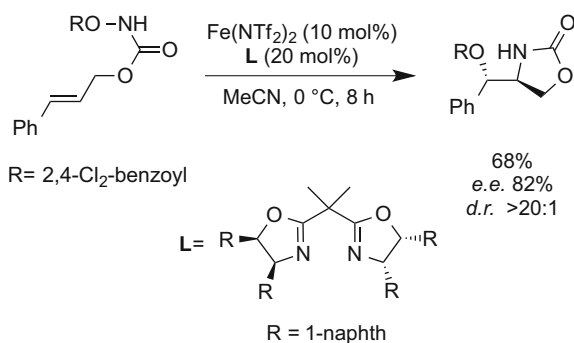
In 2013, Xu and coworkers developed the synthesis of oxazolidinones via an intramolecular aminohydroxylation of *trans*-olefins from functionalized hydroxylamines (Scheme 46) [95]. Diastereoselectivities ranged from 1:1 to >20:1. As



Scheme 44 Iron(II)-catalyzed asymmetric aminohydroxylation of olefins



Scheme 45 Mechanistic studies for the iron-catalyzed aminohydroxylation

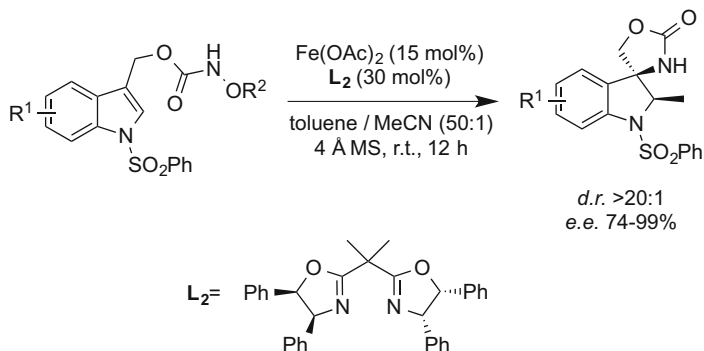
**Scheme 46** Synthesis of oxazolidinones**Scheme 47** Asymmetric synthesis of oxazolidinone

mentioned earlier by the authors, yields depended on the substitution of the olefin. The order of reactivity was the following: trisubstituted > disubstituted > monosubstituted olefins.

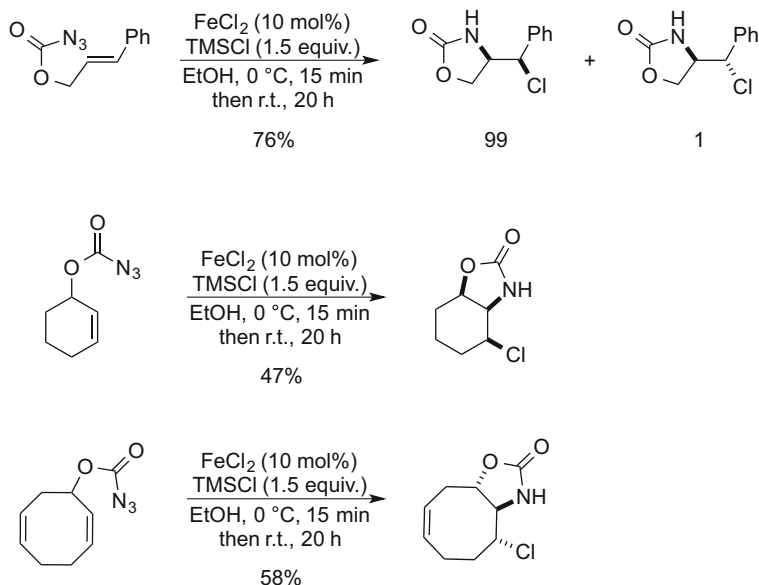
In the same report, the first intramolecular asymmetric version was successfully achieved using the same catalytic system than Yoon and coworkers ($\text{Fe}(\text{NTf}_2)_2$ and bis-oxazoline **L2**). The oxazolidinone was prepared in high diastereomeric ratio (*d.r.* >20:1), in enantiomeric excess (82%), and in 68% yield (Scheme 47).

The same group has extended the scope of the asymmetric aminohydroxylation to substrates like indole derivatives (Scheme 48) [96]. In the presence of 15 mol% of $\text{Fe}(\text{OAc})_2$ and 30 mol% of bis-oxazoline **L2**, the aminohydroxylated indoles were obtained in good yields (62–75%), high diastereomeric ratios (>20:1), and good to high enantiomeric excesses (74–99%).

Oxazolidinones could not only be synthesized via aminohydroxylation but also via a sequence “decomposition of an electron-poor azide/addition on an alkene” [97, 98]. Thus, cycloalkenoxycarbonyl and cinnamyloxycarbonyl azides, in the presence of iron(II) chloride and trimethylsilyl chloride, underwent an intramolecular amino chlorination (Scheme 49). No aziridine intermediates were detected in the presence of the $\text{FeCl}_2/\text{TMSCl}$ combination. The mechanism



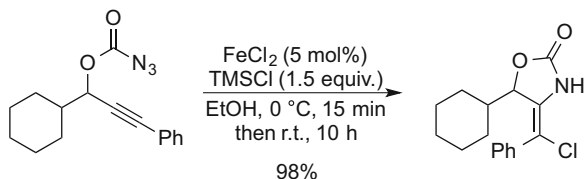
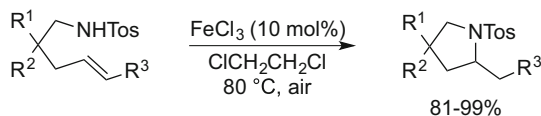
Scheme 48 Asymmetric intramolecular aminohydroxylation of indoles



Scheme 49 Aminochlorination of alkenes

of this reaction was then assumed to proceed through radical species. The stereoselectivities depended on the substrates and could be explained by the different conformations and the coordination of the iron center with the heteroatoms. More importantly, while the iron-catalyzed amino chlorination provided the *threo*-isomer from the cinnamyl azide derivative, the thermal non-catalyzed reaction furnished the *erythro*-isomer via the ring opening of the aziridine intermediate.

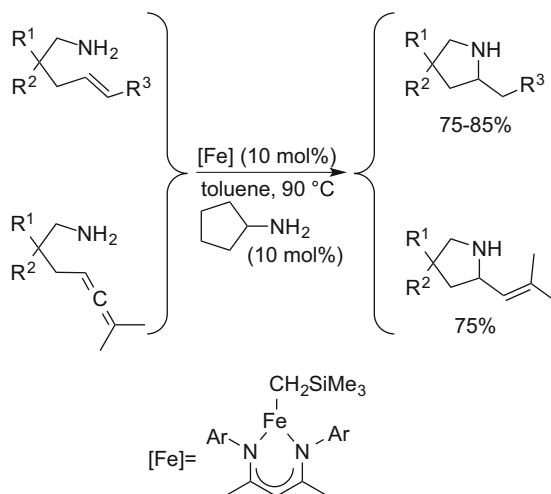
Finally, the intramolecular amino chlorination of alkynes was performed under the same reaction conditions and only the (*Z*)-isomers were detected (Scheme 50) [98, 99].

**Scheme 50** Aminochlorination of alkynes**Scheme 51** Hydroamination with electron-poor amines

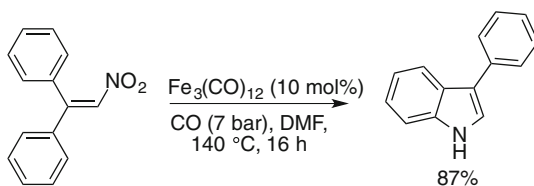
Hydroamination of Alkenes

Catalytic hydroamination is a 100% atom-efficiency process. Some iron-based catalysts have been described in the last 10 years [100–102]. Only the intramolecular hydroamination leading to pyrrolidines will be presented in this section; the intermolecular reaction will be presented in Chap. 7 of this book. The first efficient catalyst was the simple iron(III) chloride which was able to catalyze the intramolecular hydroamination of unactivated alkenes with electron-deficient amines at 80 °C under air (Scheme 51) [103]. Under these conditions, *gem*-disubstituted alkenes or 1,2-disubstituted alkenes reacted and were converted into pyrrolidines in high yields. Various functional groups, such as ethers, tosylates, or iodides, were also compatible.

Hannedouche and coworkers have disclosed a major breakthrough in the intramolecular hydroamination reaction [104]. A well-defined four-coordinate β -diketiminatoiron(II) alkyl complex was shown to be an excellent pre-catalyst for the selective cyclohydroamination of primary aliphatic alkenylamines at 70–90 °C (Scheme 52). Such amines were previously incompatible due to the strong binding affinity of these electron-rich amines toward the metal center. Good conversions were obtained with some primary amines in this intramolecular hydroamination. However, the cyclohydroamination does not proceed without a geminal disubstitution on the tether or with 1,2-dialkylsubstituted alkenes. The mechanism seems likely to proceed via a σ -bond metathesis between the pre-catalyst and the primary amine. This amido iron species could insert into the alkene and then, after aminolysis, could liberate the hydroamination product and (re)generate another iron-amido species.



Scheme 52 Hydroamination with primary amines



Scheme 53 Synthesis of indoles

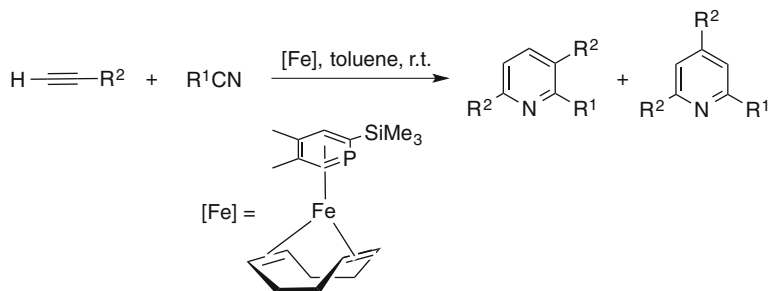
Synthesis of Indoles

Dong and coworkers have developed a new synthesis of indoles via a reductive cyclization of conjugated nitroalkenes in the presence of various metal salts, including iron ones [105]. $\text{Fe}_3(\text{CO})_{12}$ is an attractive catalyst due to its low cost in comparison to palladium or other noble metals, although higher temperatures and pressures were required to achieve good efficiency. Only one example was reported with the iron catalyst, but the indole was isolated in an excellent yield (Scheme 53).

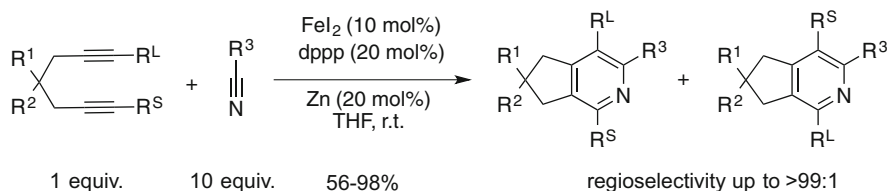
2.4.3 Construction of Six-Membered Cycles

Synthesis of Pyridines

Pyridine derivatives are one of the important classes of heterocyclic aromatic derivatives. They are present in pharmaceuticals, agrochemicals, natural products, and polymers [106] and have been used in some homogeneous catalytic applications as ancillary ligands [107, 108]. Several strategies have been developed for their synthesis [109]. Among them, the [2+2+2] cycloaddition between two alkynes and a nitrile molecule has emerged as a powerful tool and has been intensively



Scheme 54 Well-defined iron(0)-catalyzed [2+2+2] cycloaddition

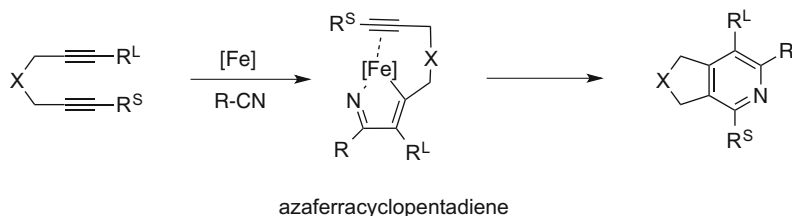


Scheme 55 Wan's approach to pyridines

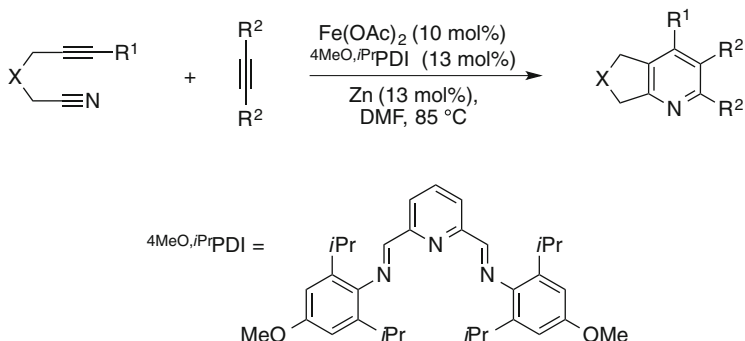
studied with various transition metal complexes as catalysts [110–115]. Besides complexes based on precious metals such as ruthenium [116], rhodium [117], and iridium [118], the most studied complex is the CpCo system [119–122]. However, this type of complex failed to fulfill the requirement of industrial use (such as toxicity of the complex, relative instability). Iron salts are usually nontoxic and very abundant on Earth and may be a good alternative to cobalt complexes. Only a few studies on iron-catalyzed [2+2+2] cycloaddition reactions have been reported. The seminal work of Zenneck et al. validated the proof of concept and demonstrated that the iron(0) complex ([Fe(cod)(2-(trimethylsilyl)-4,5-dimethylphosphinine)]) was able to catalyze the [2+2+2] cycloaddition between two alkynes and a nitrile (Scheme 54) [123]. A completely intermolecular reaction between four to ten equivalents of a nitrile and one equivalent of an alkyne led to the corresponding pyridine derivative, but without any control of the regioselectivity and with low chemoselectivity (benzene derivatives were the main products).

Improvements on this reaction appeared later in 2011 when the groups of Wan [124] and Louie [125] reported almost simultaneously [2+2+2] cycloaddition reactions either between tethered diynes and nitriles, diynes and cyanamides, or tethered alkynenitriles and alkynes.

In Wang's approach, a partially intramolecular process occurred between a diyne and a nitrile. In the presence of iron iodide (10 mol%), bis(diphenylphosphino)propane (20 mol%), and zinc (20 mol%) in THF at room temperature, the pyridine derivatives were obtained in 56–98% yield and in regioselectivities up to 99:1 (Scheme 55) [124]. The scope of the reaction revealed that under the optimized reaction conditions, (1) both aryl and alkyl nitriles reacted efficiently;



Scheme 56 Proposed mechanism by Wan



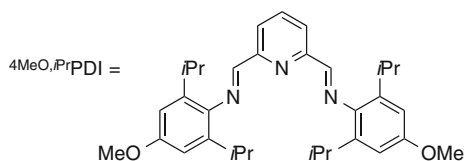
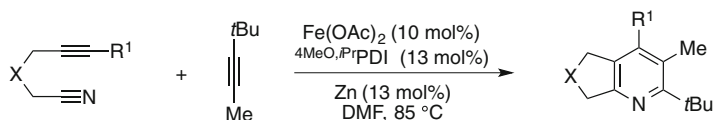
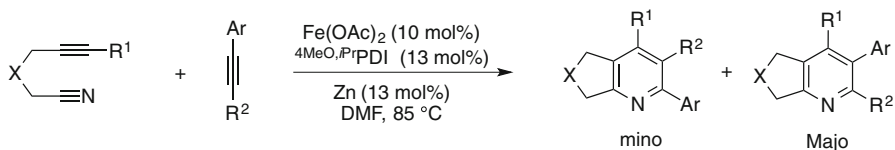
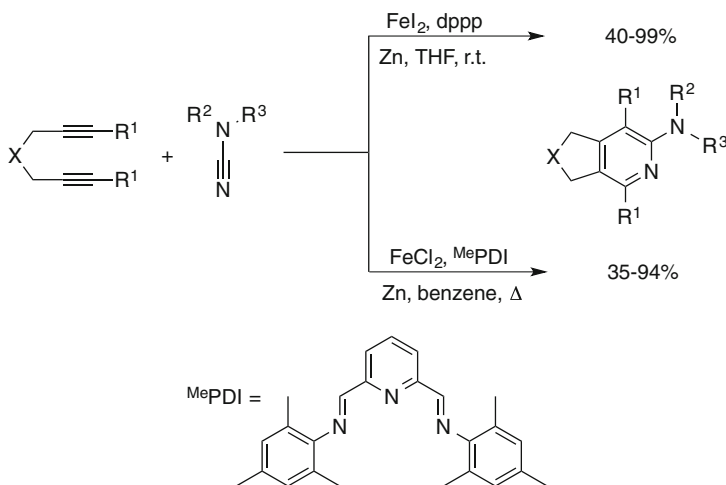
Scheme 57 Louie's procedure

(2) single regioisomers were produced from diynes bearing different terminal substituents. The smallest substituent was always in α -position to the nitrogen atom.

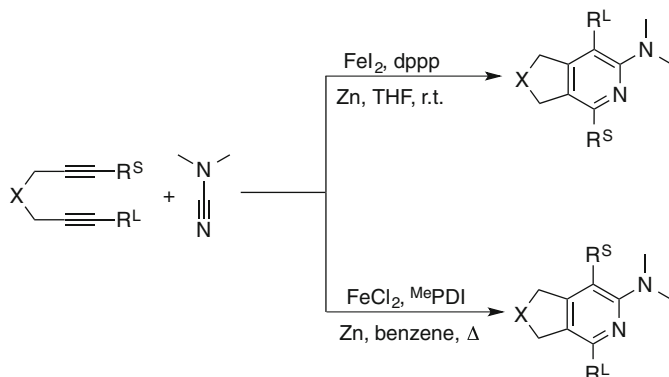
As the proposed mechanism, the authors hypothesized that an azaferrocyclopentadiene was initially produced to explain the regioselectivity. Indeed, this intermediate led to less unfavorable interactions between the terminal alkyne substituent and the iron ligand (Scheme 56).

Louie et al. developed a [2+2+2] cycloaddition reaction between tethered alkynenitriles and alkynes [85]. The catalytic system resulted from the combination of $\text{Fe}(\text{OAc})_2$ and a strong donating, sterically hindered ligand (and also a non-innocent ligand) [126–132]. The pyridines were isolated in moderate to high yields (30–86%, Scheme 57) from various aromatic and aliphatic alkynes and alkyne nitriles. As in the work of Wan, an in situ generated iron(0) was hypothesized. The steric and electronic effects on the bis-iminopyridine ligand had a profound impact on the reactivities. Thus, electron-donating groups at the *para*-position of the *N*-aryl ring and methyl substituent on the imine function led to higher yields.

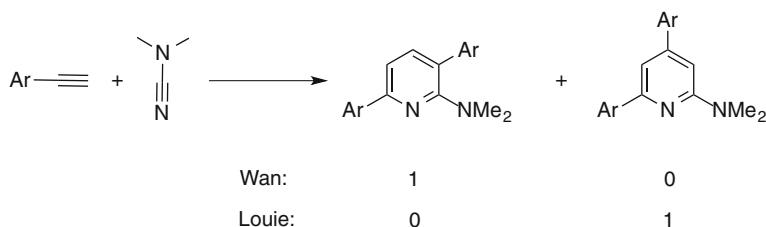
Unsymmetrical alkynes also reacted in the cycloaddition reactions. A mixture of regioisomers was isolated and modest control of the selectivity was observed, except with alkynes having a *t*-butyl group. Surprisingly, only one regioisomer was obtained from 4,4-dimethylpent-2-yne and the *t*-butyl group was in the product located proximal to the nitrogen atom (Scheme 58).

**Scheme 58** Regioselective cycloaddition**Scheme 59** Synthesis of aminopyridines

The group of Wan and the group of Louie extended these works to the synthesis of 2-aminopyridines (Scheme 59) [133, 134]. Dienes and cyanamides underwent cycloaddition reactions to form substituted 2-aminopyridines in 35–94% yields in the presence of $\text{FeCl}_2/\text{Me}^{\text{Mes}}\text{PDI}/\text{Zn}$ as the catalytic system (where $\text{Me}^{\text{Mes}}\text{PDI} = N,N$ -mesityl pyridinediimine) [133] and in 40–99% in the presence of $\text{FeI}_2/\text{dppp}/\text{Zn}$ as the catalytic system [134].



Scheme 60 Comparison of the regioselectivities



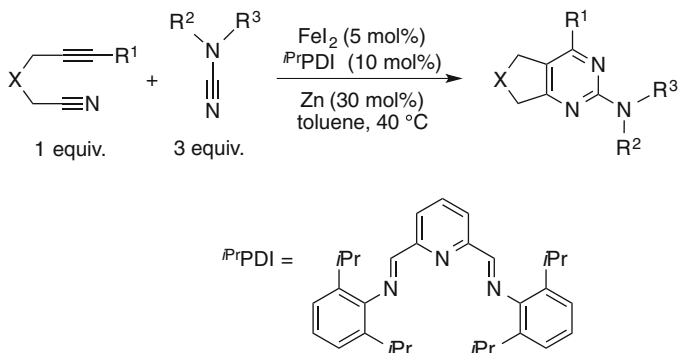
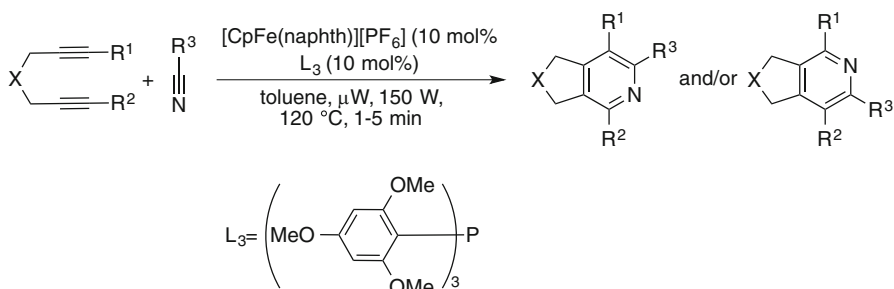
Scheme 61 Regioselective intermolecular [2+2+2] cycloadditions

More importantly, these catalytic systems provided additional regioselectivities. In the presence of the Louie's catalytic system, the larger substituent was proximal to the pyridine nitrogen of the product [133], unlike the Wan's in situ generated iron catalyst (Scheme 60) [134].

The same conclusions were also drawn when an intermolecular [2+2+2] cycloaddition between a cyanamide and two molecules of alkynes was carried out (Scheme 61). Thus, depending on the iron-based catalyst, both regioisomers could be prepared from the same starting materials.

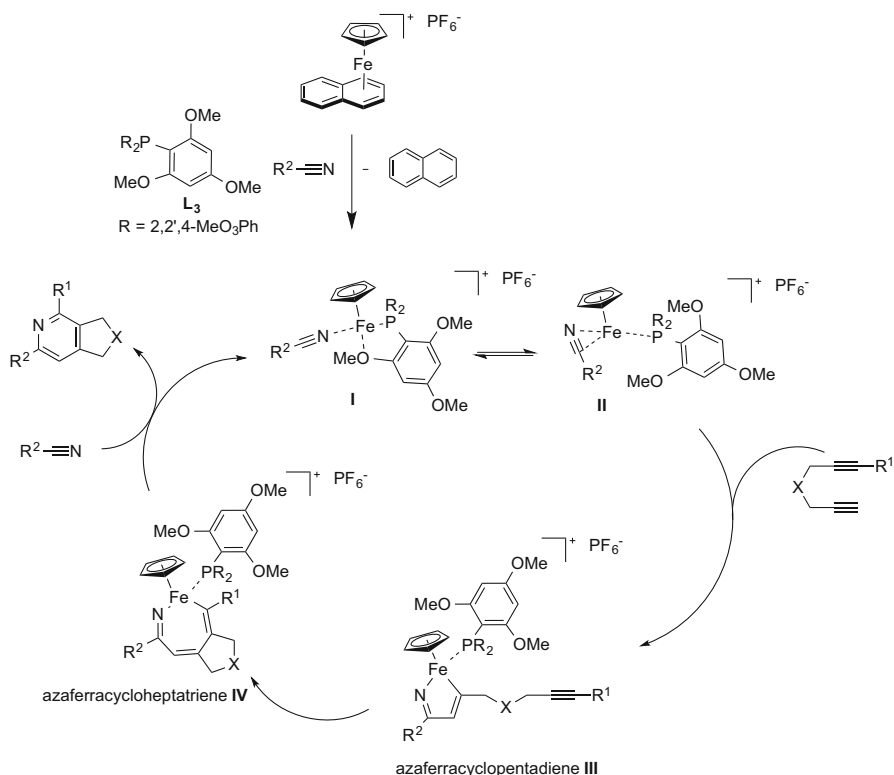
Finally, Louie reported also a related [2+2+2] cycloaddition between an alkynyl nitrile and a cyanamide. Catalytic amounts of FeI_2 , $^{\text{iPr}}\text{PDI}$, and Zn were found to effectively catalyze the cycloaddition to afford bicyclic 2-aminopyrimidines in moderate to excellent yields (27–90%, Scheme 62) [135]. Worth to mention is that catalysts usually efficient in cycloadditions, such as $\text{Rh}(\text{cod})_2\text{BF}_4/\text{BINAP}$, $\text{CoCp}(\text{CO})_2$, $[\text{Ir}(\text{cod})\text{Cl}]_2/\text{dppf}$, $\text{Ni}(\text{cod})_2/\text{ligand}$, and $\text{Cp}^*\text{RuCl}(\text{cod})$, were ineffective toward this strategy of the synthesis of 2-aminopyrimidine.

In 2002, Guerchais et al. reported an iron-mediated pyridine synthesis using the piano-stool iron complex $[\text{FeCp}^*(\text{PMe}_3)(\text{CH}_3\text{CN})_2][\text{PF}_6]$ [136]. As cyclopentadienyl ligands are well known to be strongly coordinated to metal center, Renaud and coworkers explored the catalytic ability of $[\text{CpFe}]$ complexes in [2+2+2] cycloadditions for pyridine syntheses without any reducing reagent

**Scheme 62** Synthesis of 2-aminopyrimidines**Scheme 63** In situ generated iron-catalytic system for the synthesis of pyridines

[137]. Then, they developed an in situ generated catalytic system, based on an air-stable iron(II) complex and a bidentate ligand bearing a phosphine and a hemilabile framework, for the [2+2+2] cycloaddition between diynes and alkyl, aryl, and vinyl nitriles. This reaction allowed a straightforward access to polyfunctionalized pyridines in good yields. Control of the regioselectivity was also possible when unsymmetrical diynes were employed and appeared to be complementary to the selectivities reported by Wan and coworkers in the presence of an iron(0) catalyst (Scheme 63).

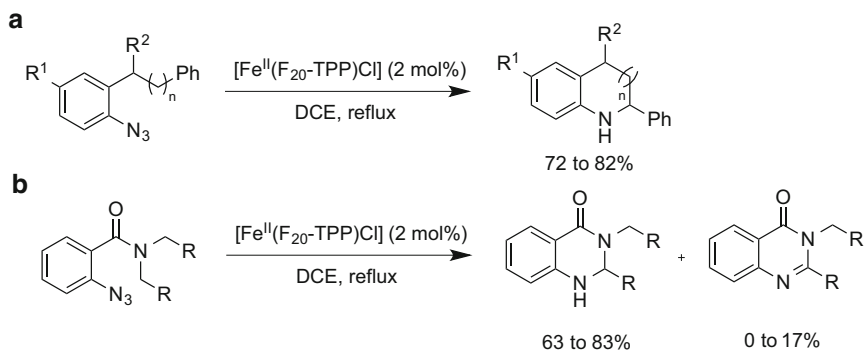
Based on previously reported mechanistic considerations [133] and on experimental data, Renaud et al. proposed the following mechanism (Scheme 64). Removal of the naphthalene ligand under heating in $[\text{CpFe}(\text{naphth})][\text{PF}_6]$ is followed by coordination of the phosphine and a nitrile molecule. The catalytically active species **I** with an edge-on coordinated nitrile might convert into its side-on bounded isomer **II** with the help of the hemilabile bidentate features of the phosphine L_3 . Moreover, **II** will facilitate the oxidative cyclization with the diyne to give the azaferracyclopentadiene intermediate **III** that subsequently might be converted into the azaferracycloheptatriene **IV** via intramolecular alkyne insertion. A reductive elimination starting from **IV** will provide pyridine, and the active catalyst **I** is regenerated through the coordination of a nitrile molecule.



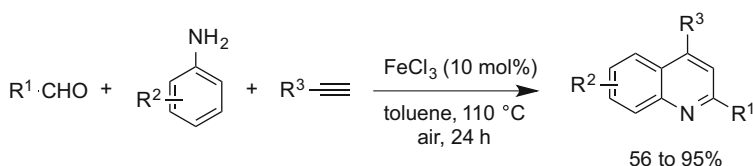
Scheme 64 Proposed mechanism by Renaud et al.

Synthesis of Tetrahydroquinolines and Dihydroquinazolines

The most challenging C–H amination reaction is the activation and functionalization of C_{sp^3} –H bonds. Recent work demonstrated the efficiency of iron complexes in such a process. Worth mentioning is that all the catalytic systems previously described for aziridination and C_{sp^2} –H amination were also reported to be active in C_{sp^3} –H amination reactions. Then, the perfluorinated porphyrin iron complex $[Fe^{III}(F_{20}\text{-TPP})Cl]$ was reported to catalyze the inter- or intramolecular C_{sp^3} –H amination in the presence of aryl azides and arylsulfonyl azides as nitrogen sources. Yields usually were relatively high (63–80%) for the intermolecular reaction. The authors noticed that, in the presence of the catalytic system, the amination of tertiary C–H bonds occurred preferentially, and the secondary C–H bonds remained untouched. Che et al. also reported the intramolecular version of this C–H amination reaction [64]. Indolines, tetrahydroquinolines, and dihydroquinazolines were isolated in high yields (63–83%, Scheme 65a and b).



Scheme 65 $[\text{Fe}^{\text{II}}(\text{F}_{20}\text{-TPP})\text{Cl}]$ -catalyzed $\text{Csp}^3\text{-H}$ aminations



Scheme 66 Multicomponent reaction for the synthesis of quinolines

Synthesis of Quinolines

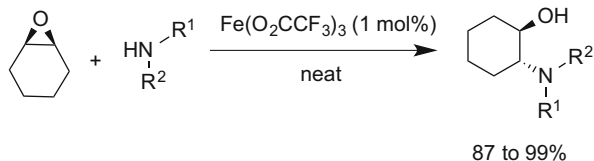
In 2009, Tu et al. reported a multicomponent reaction involving aldehydes, terminal alkynes, and primary amines for the formation of quinoline derivatives, catalyzed by FeCl_3 [138]. Concerning the scope of the reaction, aromatic and heteroaromatic terminal alkynes, aromatic and heteroaromatic aldehydes, and aromatic anilines were good candidates and afforded the quinoline derivatives in isolated yields ranging from 56 to 95% (Scheme 66).

2.5 Miscellaneous

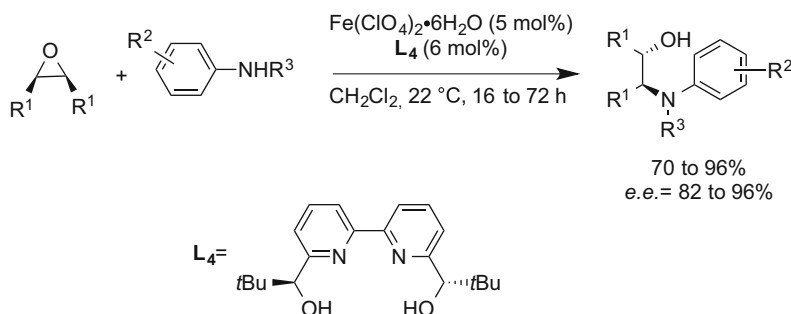
2.5.1 Ring Opening of Epoxides

In 2008, Demir et al. reported an epoxide-opening reaction by amines catalyzed by the iron salt $\text{Fe}(\text{O}_2\text{CCF}_3)_3$ [139]. The reaction can be performed with primary or secondary aromatic or aliphatic amines, leading to *trans*- β -amino alcohol derivatives in high yields (87–99%, Scheme 67).

When the reaction was performed with dissymmetric epoxides such as styrene oxides, the opening occurred preferentially at the most substituted position when primary anilines or benzylic amines were employed, whereas the nucleophilic attack occurred preferentially at the less hindered position when pyrrolidine was



Scheme 67 Iron-catalyzed ring opening of epoxides



Scheme 68 Enantioselective ring opening of *meso*-epoxides

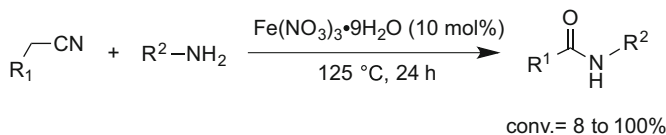
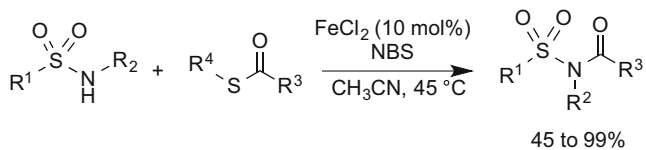
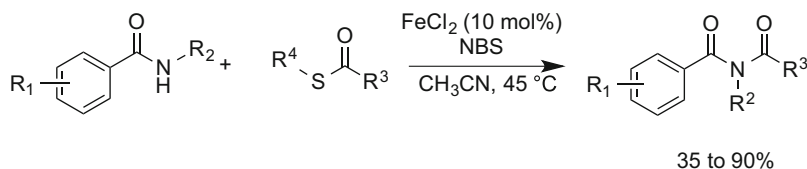
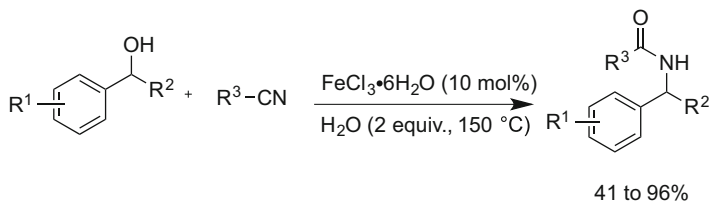
employed. Nevertheless, in the case of alkyl-substituted epoxides, the nucleophilic attack of anilines occurred at the less hindered position. Noteworthy, if the reaction is performed with enantiopure styrene oxides, the reaction proceeded without any loss of enantiopurity.

Then, a few years later, Ollevier and Plancq reported the enantioselective ring opening of *meso*-epoxides by anilines catalyzed by an iron complex generated in situ from $Fe(ClO_4)_2$ and Bolm's chiral bipyridine ligand L_4 (Scheme 68) [140]. The reaction occurred with good to high yields (70–96%) and with high enantioselectivities (e.e.s between 82 and 96%).

2.5.2 Amide Derivative Synthesis

In the last years, only a few methodologies have been reported for the synthesis of amides catalyzed by iron salts. In 2009, Williams et al. studied the formation of amides starting from nitriles and amines [141]. Several iron salts were evaluated and $Fe(NO_3)_3$ (10 mol%) was the most active to convert amines and nitriles into the expected amides (conversions between 8 and 100%, Scheme 69). The reaction was favored with linear primary amines and nitriles.

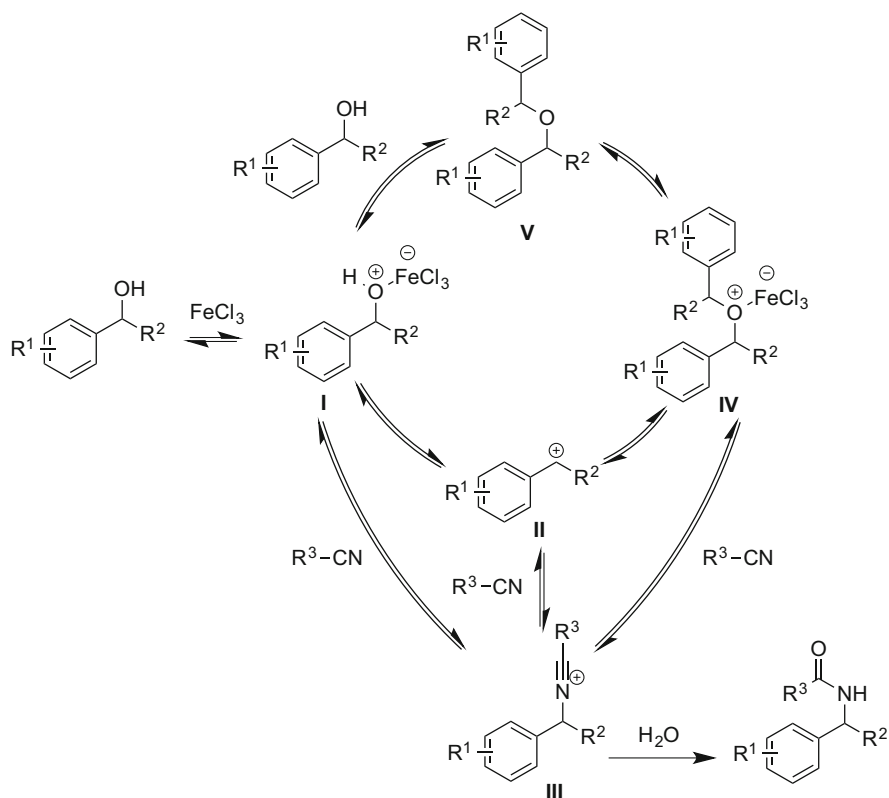
Jiang, Fu, and coworkers disclosed in the same year the synthesis of acylsulfonamides from sulfonamides and thioesters in the presence of NBS and a catalytic amount of $FeCl_2$ (10 mol%, Scheme 70) [142]. The reaction was performed with alkyl, aryl, and heteroaryl thioesters and sulfonamides in very good yields up to 99%. Only secondary sulfonamides gave moderate yields.

**Scheme 69** Amides formation from nitriles and amines**Scheme 70** Acylsulfonamides from sulfonamides and thioesters**Scheme 71** Imides from amides and thioesters**Scheme 72** Amide formation from benzylic alcohols

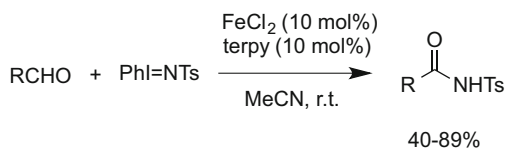
Following the same approach, imides were also synthesized from amides and thioesters in moderate to high yields (35–90%, Scheme 71) [142].

Cossy, Reymond, and coworkers disclosed a FeCl_3 -catalyzed Ritter reaction for the synthesis of amides [143]. Amides were obtained in moderate to high yields (41–96%) from aromatic or aliphatic nitriles with several functionalized benzylic alcohols (Scheme 72). Under these reaction conditions, *tert*-butyl acetate could also be used instead of benzylic alcohols.

The authors proposed a mechanism starting first with the formation of a benzylic cation **II** via the Lewis acid-activated species **I**. Then, the nitrile could attack the benzylic cation **II** to afford the amide through nucleophilic attack of water on the intermediate **III** (Scheme 73). An alternative pathway might proceed through the formation of a *bis*-benzyl ether **V** arising from the condensation of two molecules of



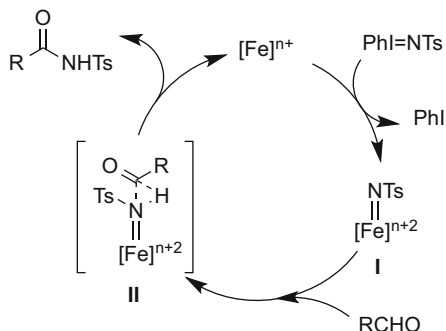
Scheme 73 Proposed mechanism for amide formation from benzylic alcohols



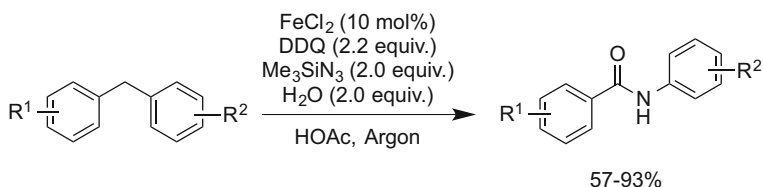
Scheme 74 Amides from aldehydes and PhI=NTs

benzylic alcohol. Then, this ether might be activated by the iron salt and attacked by the nitrile to form the adduct **III**.

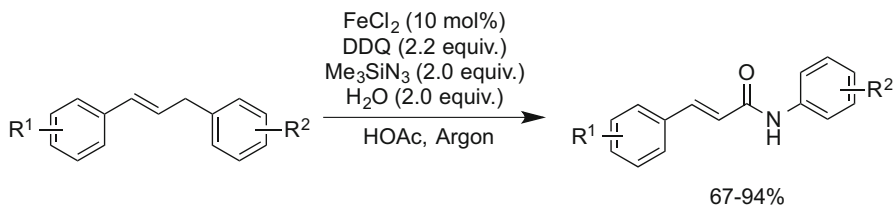
In 2011, Che et al. described the formation of amides from aldehydes and PhI=NTs . This reaction was catalyzed by an in situ generated iron complex from FeCl_2 and a terpyridine ligand (terpy) (Scheme 74) [144]. Aliphatic and aromatic aldehydes were well tolerated and led to the amides in moderate to high yield (40–89%). Compared to aromatic aldehydes, aliphatic aldehydes were more reactive and afforded the amides in higher yields. Other ligands or catalytic systems led also to lower activities.



Scheme 75 Proposed mechanism for amides formation from aldehydes and $\text{PhI}=\text{NTs}$



Scheme 76 Amide synthesis from diarylmethylene derivatives

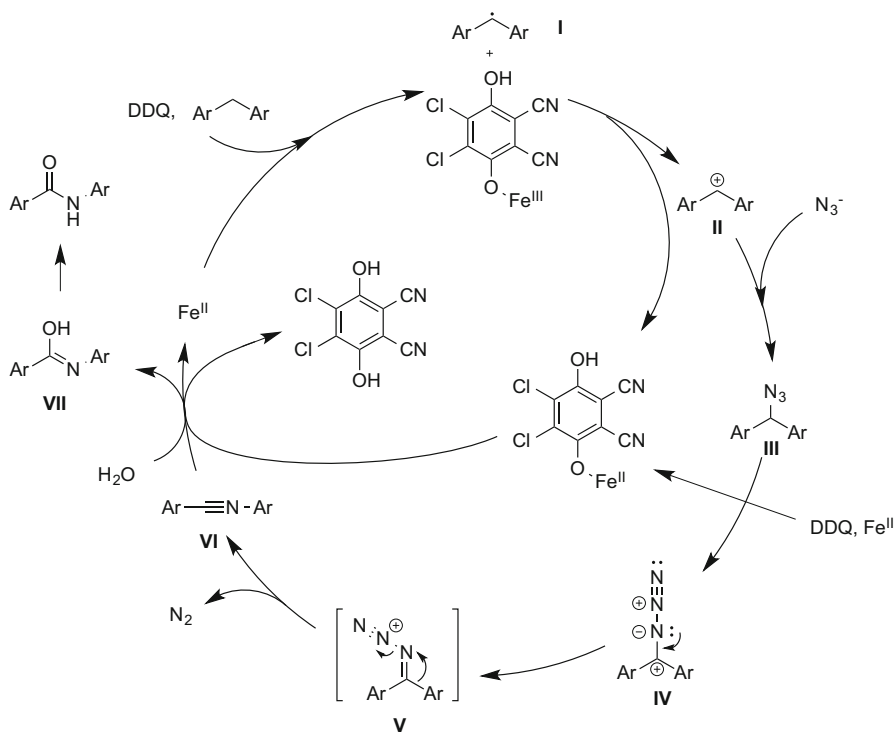


Scheme 77 Amides from 1,3-diarylpropenes

The mechanism reported by the authors was as follows: (1) formation of an iron nitrene species **I** from the iron salt and $\text{PhI}=\text{NTs}$, (2) then, insertion of the iron nitrene species into the C–H bond of the aldehydes **II**, (3) and finally liberation of the catalytically active species and the amides (Scheme 75).

More challenging was the reaction reported by Jiao et al. who described the formation of amides from bis-arylmethylene derivatives in the presence of DDQ, water, Me_3SiN_3 , and 10 mol% of FeCl_2 in acetic acid as solvent (Scheme 76) [145]. Remarkably, this reaction involves the cleavage of two C–H and one C–C bonds of the starting bis-arylmethylene.

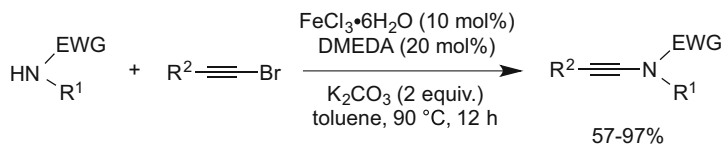
The reaction was also successfully extended to 1,3-diarylpropenes and the expected acrylamides were isolated in yields ranging from 67 to 94% (Scheme 77) [145].



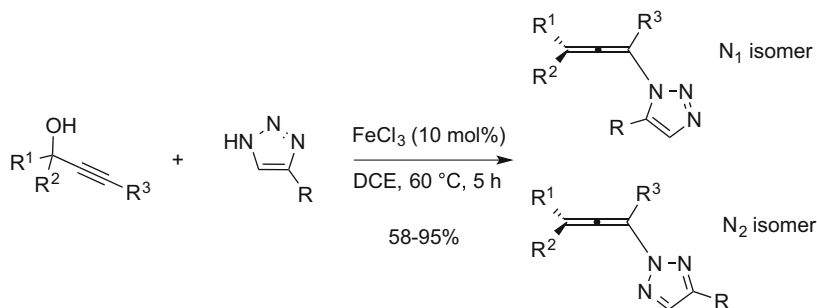
Scheme 78 Proposed mechanism for amide formation

Based on control and labeling experiments, the authors proposed the following mechanism (Scheme 78). The first step could be an iron-assisted single-electron-transfer oxidation with DDQ to form the *bis*-arylmethane radical **I**. This radical could be oxidized again to generate a *bis*-arylmethane cation **II**. Substitution of the cation by the azide anion would lead to a *bis*-benzyl azide **III**, which could be oxidized into the intermediate **IV** by the iron-assisted DDQ oxidative system. Subsequent isomerization of the *bis*-arylmethyl azide cation **IV** would lead to the loss of molecular nitrogen and a nitrilium intermediate **V**, which could be attacked by a molecule of water to give **VII**. After tautomerization, this intermediate **VII** could afford the observed amide. The catalytically active iron species would be regenerated at this stage thanks to the remaining proton.

Among the amides, ynamides occupy a pivotal role in organic chemistry nowadays [146]. These derivatives were, for example, synthesized from amides and bromoalkynes in the presence of a catalytic amount of $\text{FeCl}_3 \cdot 6\text{H}_2\text{O}$ (10 mol%) and DMEDA as ligand (20 mol%) [147]. This reaction was performed with sulfonamides, lactams, and oxazolidinones with aromatic and aliphatic bromoalkynes in good to high yields (57–97%, Scheme 79).



Scheme 79 Ynamides synthesis from amides and bromoalkynes



Scheme 80 Synthesis of allenyl triazoles

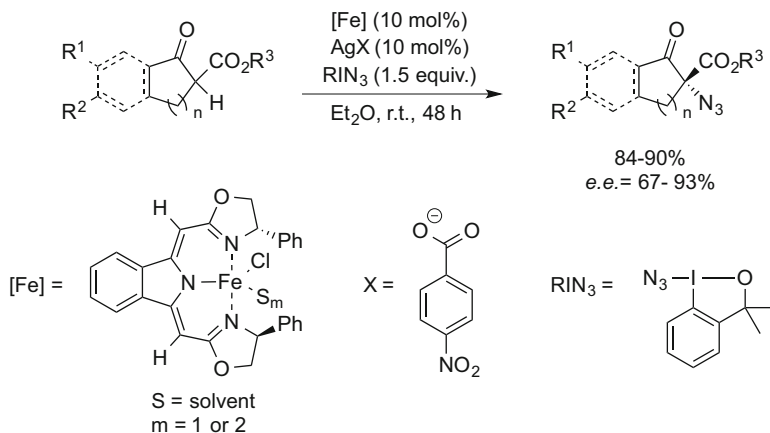
2.5.3 Synthesis of Allenyl Triazoles

In 2012, Shi et al. reported the synthesis of allenyl triazoles from propargylic alcohols and triazoles catalyzed by FeCl_3 [148]. Several other salts were catalytically active but only FeCl_3 presented the best selectivities in favor of the formal $\text{S}_{\text{N}}2'$ type products and the best yields. The scope of the reaction was then extended to benzotriazoles, substituted triazoles, and propargylic acetates, and various functionalized allenes were prepared in good to high yields (58–95%, Scheme 80). Noteworthy, in the case of non-symmetrically substituted triazoles, N_1 or N_2 isomers were detected with a ratio varying from 4:1 to 10:1 in favor of the N_2 isomer.

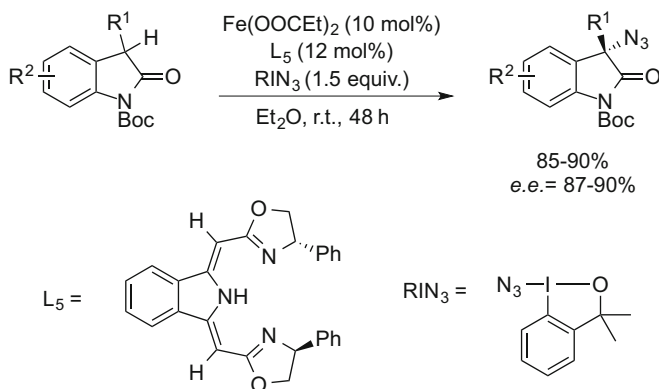
2.5.4 Azidation of β -Ketoesters

In 2013, Gade et al. reported an interesting enantioselective azidation of β -ketoesters and oxindoles using Togni's reagent [149] and a well-defined iron complex bearing chiral bis-oxazoline-amide ligand ("boxmi" ligand) [150, 151]. This combination, activated by silver carboxylate salts, was the most active with β -ketoesters (84–90%) and gave the highest enantiomeric excesses (67–83%, Scheme 81).

The screening of the reaction conditions with oxindoles as activated methylene compounds demonstrated that an in situ generated iron complex from iron (II) propanoate and a chiral "boxmi" ligand, without any further activation by a



Scheme 81 Enantioselective azidation of β -ketoesters

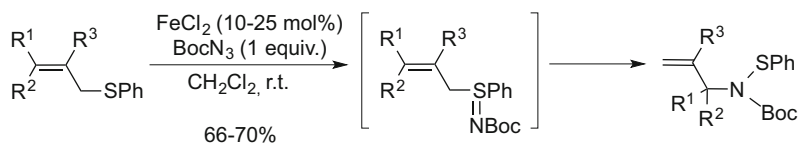


Scheme 82 Enantioselective azidation of oxindoles

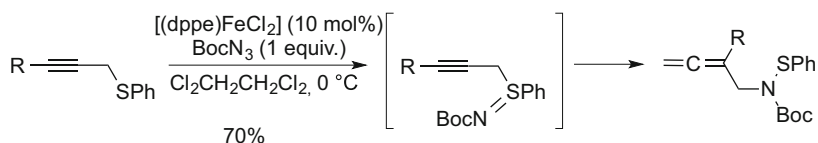
silver salt, was the most active (85–90%) and furnished the highest enantiomeric excesses (87–90%, Scheme 82).

2.5.5 Rearrangement of Allyl and Propargyl Sulfides

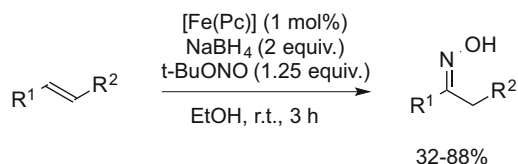
Allylic aryl sulfides underwent a [2,3]-sigmatropic rearrangement in the presence of a $FeCl_2/BocN_3$ combination [152]. The allyl amines protected by a Boc and a phenylsulfenyl group were isolated in good to high yields (66–70%, Scheme 83). It is worth mentioning that the phenylsulfenyl group can be removed using either $Bu_3SnH/AIBN$ or $P(OEt)_3/Et_3N$ to afford cleanly the Boc-protected allyl amines. This rearrangement with α -branched allyl sulfides furnished the corresponding



Scheme 83 Synthesis of allylic amines via a [2,3]-sigmatropic rearrangement



Scheme 84 Proposed mechanism



Scheme 85 Synthesis of oximes

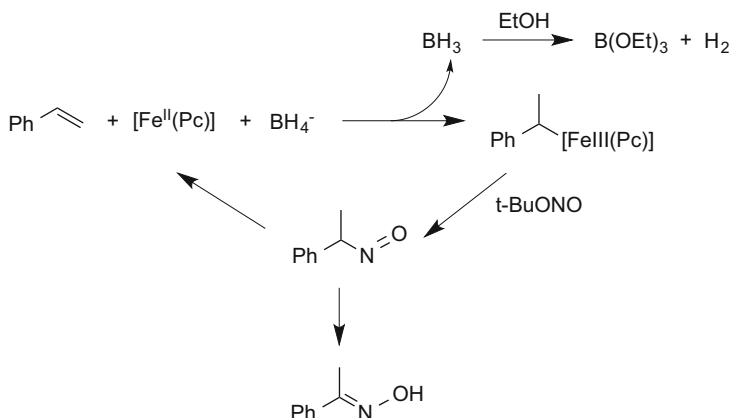
amines in low yields and in low enantiomeric excess (from enantiomerically pure α -branched allylic sulfides).

Van Vranken extended this work to propargyl aryl sulfides (Scheme 84) [153]. The corresponding allenic amines were prepared in good yields using $[\text{FeCl}_2(\text{dpppe})]$ as catalyst.

2.5.6 Synthesis of Oximes

In 2009, Beller et al. reported the synthesis of oximes from styrenes catalyzed by an iron phthalocyanine complex [154]. Other metal phthalocyanine complexes and in situ generated iron complexes with nitrogen-based ligands were evaluated but were less effective than the iron phthalocyanine complex. Under these reaction conditions, only styrene derivatives were good substrates and afforded oximes in yields ranging from 32 to 88% (Scheme 85). Nevertheless, only the reduction of the C=C bond was observed when the olefin was substituted by an ester group.

The authors proposed for the mechanism as a first step a hydrometallation assisted by NaBH_4 . Then, *t*-BuONO could react with the alkyl iron species yielding the nitroso intermediate, which could isomerize to an oxime (Scheme 86).



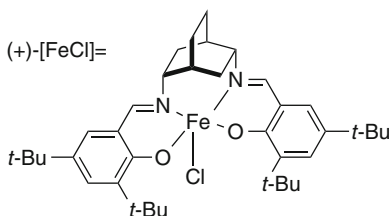
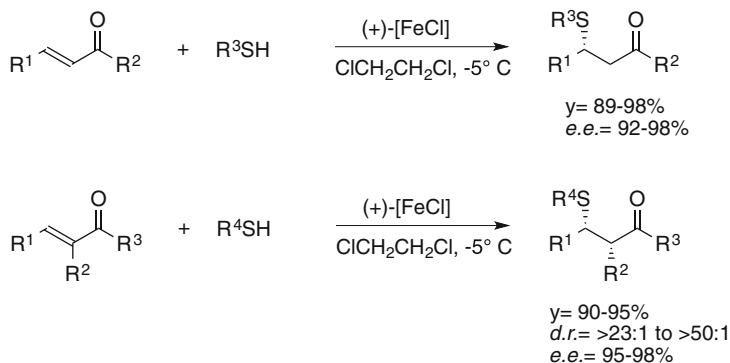
Scheme 86 Mechanism proposed for the synthesis of oximes

3 Iron-Catalyzed C–S Bond Formations

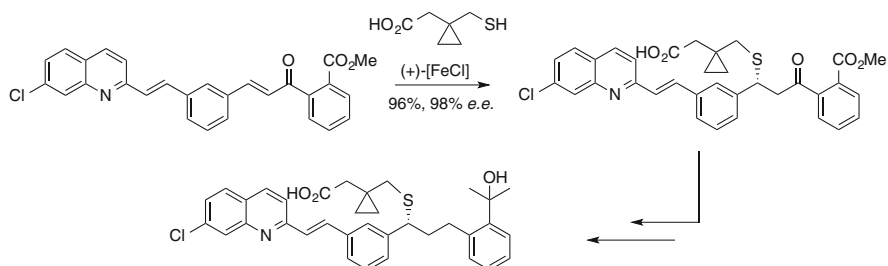
Compared to C–N bond formations, transition metal-catalyzed formation of sulfur–carbon bonds (or more generally C–S bonds) has been less studied. Indeed, this reaction, especially when sulfur atoms in low oxidation states are used, is quite challenging as sulfur atoms are known to bond to metallic centers irreversibly, leading to deactivation of the catalyst. Another challenge with thio-compounds is their sensitivity toward oxidation, leading to undesired disulfide coupling products. However, C–S bonds are prevalent in a wide range of pharmaceutically active compounds and polymeric materials. Thus, efficient C–S bond formation has to be designed with cost-efficient procedures. Recent works demonstrated the progress in the development of novel and practical iron-catalyzed transformations.

3.1 Michael Additions

The Michael addition is the addition of a nucleophile to an activated alkene and is often catalyzed by Lewis acids. Yao and coworkers published the first iron-catalyzed 1,4-addition in 2006 [155]. The Michael adducts, corresponding to the addition of various aromatic and aliphatic thiols to cyclic and acyclic enones, were isolated in high yields. Surprisingly, the authors noticed that the reaction rate and the selectivity were enhanced by the use of FeCl_3 compared to other metal salts. Kawatsura and Itoh reported the first enantioselective addition 1 year later [156]. A combination of $\text{Fe}(\text{BF}_4)_2 \cdot 6\text{H}_2\text{O}$ and a pybox-type ligand catalyzed the addition of various thiophenols to (*E*)-3-crotonoyloxazolidin-2-one and gave the products in 53–99% yields and 24–95% enantiomeric excesses. The sulfa-Michael addition with the highest enantioselectivity to date was communicated by White in 2014



Scheme 87 Enantioselective Michael addition

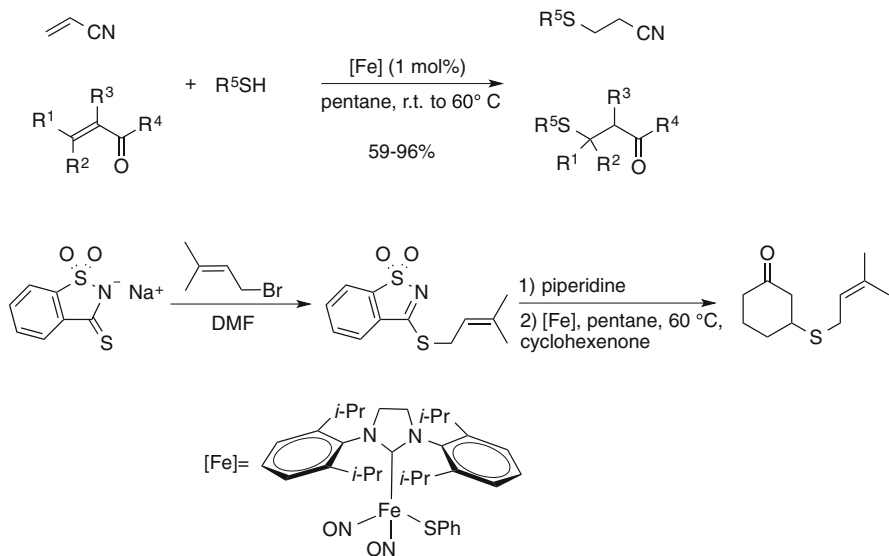


Scheme 88 Synthesis of (*R*)-Montelukast

[157]. The well-defined salen-iron(III) catalyst, based on a chiral *cis*-2,5-diaminobicyclo[2.2.2]octane, gave β -thio ketones in excellent yields (89–98%) and enantioselectivities (92–98%) from a wide range of aliphatic and aromatic thiols and chalcones or acyclic enones as Michael acceptors (Scheme 87). With α -substituted α,β -conjugated enones, the *syn*-diastereomer was produced over the *anti*-isomer (Scheme 87).

Finally, this methodology was applied to a short synthesis of (*R*)-Montelukast, the sodium salt of which is an anti-asthma drug (Scheme 88) [157].

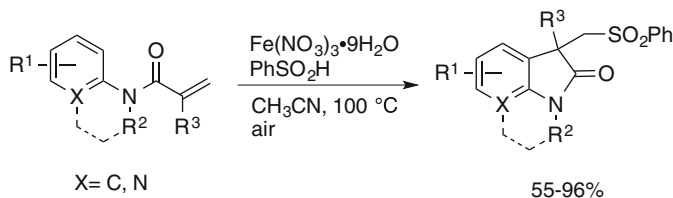
Plietker et al. demonstrated recently that iron complexes could also catalyzed Michael additions of various thiols to activated olefins (α,β -unsaturated ketones or vinyl nitriles) under low catalyst loading (1 mol%) and mild reaction conditions (room temperature to 60 °C) [158]. The corresponding thio-derivatives were



Scheme 89 Thio-Michael additions

isolated in 59–96% yields (Scheme 89). To avoid olfactory disagreements when handling thiol derivatives, an odorless alternative was addressed. The thioether of saccharose, known as an efficient thiol synthon, was prepared by treating thiosaccharose with an allyl bromide. The *in situ* liberation of the thiol in the presence of piperidine, followed by the addition of cyclohexanone and the iron catalyst, furnished the Michael product (Scheme 89). From a mechanistic point of view, the authors excluded both a simple anionic addition and a radical pathway (addition of radical scavengers did not slow down or inhibit the reaction), but favored a concerted, neutral metallosulfenylation mechanism, followed by hydrothiolysis of the C–Fe bond.

Jiao developed an aerobic difunctionalization of alkenes for the construction of C–S and C–C bonds catalyzed by a simple and inexpensive iron salt ($\text{Fe}(\text{NO}_3)_3 \cdot 9\text{H}_2\text{O}$) [159]. Other salts (such as FeCl_3 , AgNO_3 , $\text{Cu}(\text{NO}_3)_2$, $\text{Pd}(\text{OAc})_2$, and AuCl_3) led to lower efficiencies. The sulfur-containing oxindoles were obtained in good to excellent yields (58–96%) from benzenesulfinic acid via a radical process (Scheme 90). Tetrahydroquinolines or other polycyclic oxindoles could also be prepared through this methodology.

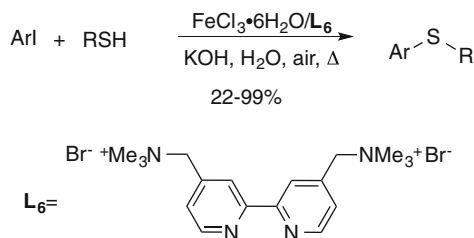
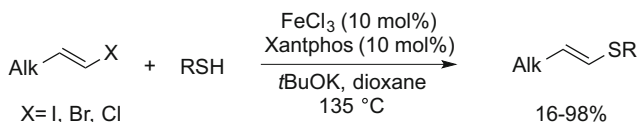


Scheme 90 Synthesis of oxindoles

3.2 Cross-Coupling Reactions

As reported with amines and alcohols, thiols could react with aryl halides to yield the corresponding aryl thioethers. Bolm mentioned the reaction first in a report in 2008 [160]. In the presence of 10 mol% of iron(III) chloride and *N,N'*-dimethylethylenediamine (DMEDA, 20 mol%) under basic conditions at 135 °C a *S*-arylation reaction occurred between (hetero)aromatic thiols and substituted aryl iodides and provided the thioethers in moderate to high yields (32–91%). Worth to note is that (1) no reaction took place with aliphatic thiols or with aryl bromide or chloride and (2) the DMEDA was crucial to prevent the formation of undesired disulfides. This work was further extended by Tsai and coworkers who described the development of a water-soluble and reusable iron complex for the coupling of aromatic or benzylic thiols and aryl iodides (Scheme 91) [161]. Yields were low to high (22–99%). The recycling of the catalyst was also evaluated and the activity was maintained for at least six runs. The coupling product was then isolated in 74% yield after the sixth run (92% after the first one) with this catalyst system. The slight drop of the yield was due to some catalyst leaching during the extraction, leading to a lower catalyst concentration in the aqueous phase. Without any ligand, the yield decreased run after run and no reaction was noticed after the fifth one.

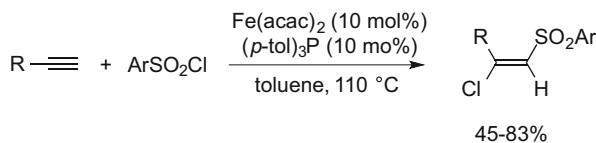
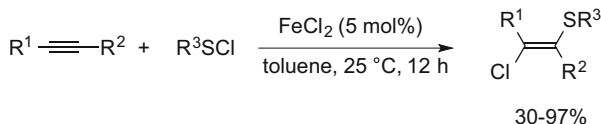
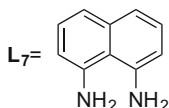
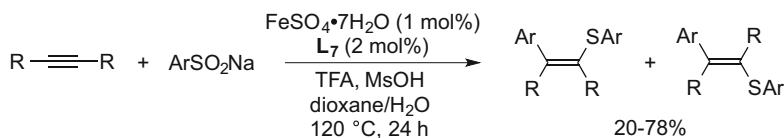
Alkenylation of thiols catalyzed by iron complexes was less studied and only one work by Lee and coworkers mentioned such a cross-coupling reaction [162]. The catalytic system employed was iron(III) chloride and the bidentate xantphos ligand (Scheme 92). Both alkyl vinyl iodides and bromides were shown to be suitable in the coupling reaction, giving the corresponding alkenyl thioethers in moderate to good yields (33–98%). The sole alkyl vinyl chloride reactive enough as vinyl coupling partner in this reaction was 1-(chloromethylidene)-4-*tert*-butylcyclohexane. The corresponding vinyl thioethers were then isolated in low to reasonable yields (16–62%).

**Scheme 91** Thioarylation in water**Scheme 92** Thiovinylation reactions

3.3 Addition on Alkynes

The group of Nakamura performed the first regio- and stereoselective chlorosulfonylation reaction of terminal alkynes in the presence of a catalytic amount of iron(II) (10 mol%) and *tris*-tolyl phosphine (10 mol%) in refluxing toluene (Scheme 93) [163]. Various other salts and other combinations were evaluated but only the combination of $\text{Fe}(\text{acac})_2$ with a monophosphine afforded the corresponding functionalized alkenes. Substituted aromatic sulfonyl chloride and aliphatic or (hetero)aromatic terminal alkynes were employed in this process and yields ranging from 45 to 83% were obtained. A radical mechanism was proposed based on the addition/cyclization sequence observed with a 1,6-enyne. However, no clues were given to explain the perfect control of the stereoselectivity and no attempts to employ internal alkynes were mentioned.

Nishihara recently reported a related reaction. The addition of sulfonyl chloride to various internal and terminal alkynes has been achieved in the presence of iron (II) chloride without any ligand in toluene at room temperature (Scheme 94) [164]. Electron-poor and electron-rich aryl or alkyl sulfonyl chlorides could be engaged in this process. More interestingly, with internal alkynes, regio- and stereoselective addition occurred, and, whatever the substituents on the alkyne were, the (*E*)-isomer was exclusively isolated in moderate to high yields (30–97%). The stereoselectivity complemented the palladium-catalyzed chlorothiolation of terminal alkynes, which afforded the (*Z*)-adducts with high regio- and stereoselectivities. From a mechanistic point of view, a radical process was proposed. After the homolytic cleavage of the S–Cl bond by iron(II) chloride, the sulfur-centered radical could add to the less sterically hindered carbon atom of the alkyne. This step may account for the control of the regioselectivity. The newly formed carbon-centered radical could then react with the sulfonyl chloride, generate again the

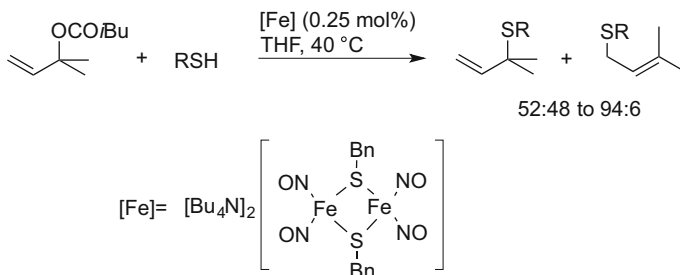
**Scheme 93** Chlorosulfonation of alkynes**Scheme 94** Chlorosulfonation of alkynes**Scheme 95** Arylsulfonation of alkynes

S-radical, and liberate the product. The (*E*)-selectivity could arise from the most stable carbon-centered radical intermediate, namely, the one having less steric repulsion.

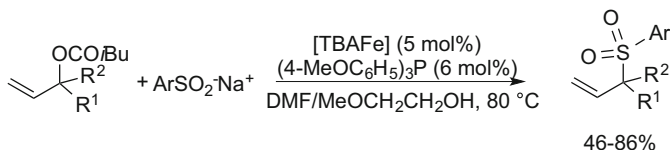
Deng and coworkers published an iron-catalyzed sulfenylation and arylation of internal alkynes with an aryl sulfinic sodium salt [165]. A combination of $\text{FeSO}_4 \cdot 7\text{H}_2\text{O}$ (1 mol%) and 1,8-naphthalene diamine **L**₇ (2 mol%) in acidic medium gave the best catalytic system (Scheme 95). Various tetrasubstituted alkenes were prepared in low to good yields (20–78%) as a mixture of isomers when the R and Ar groups were different.

3.4 Allylic Substitution

Iron complexes prepared by treatment of $[\text{Bu}_4\text{N}][\text{Fe}(\text{CO})_3(\text{NO})]$ with thiols or from iron salts under reductive conditions are active catalysts for the regioselective allylic sulfenylation [166]. The binuclear complex, also known as “reduced Roussin’s red ester,” afforded the allylic thioethers in high yields and moderate to



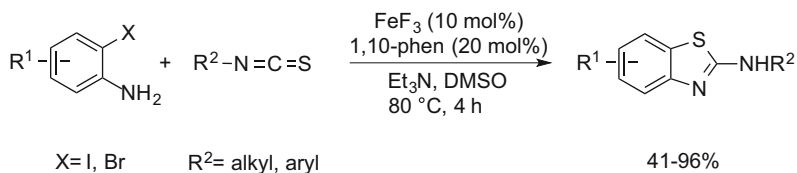
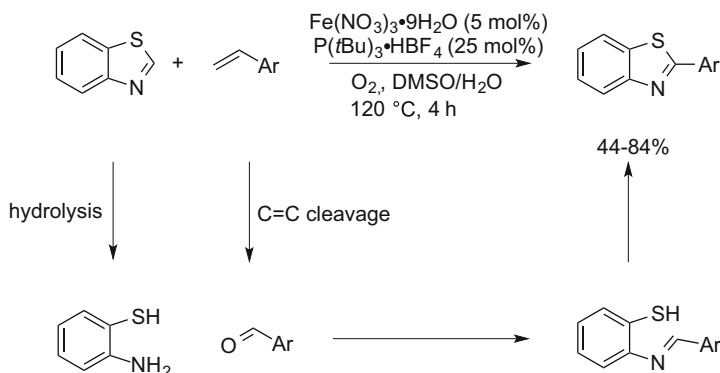
Scheme 96 Synthesis of allylic thioethers



Scheme 97 Synthesis of allylic sulfones

high regioselectivities (Scheme 96) at low catalyst loading (0.25 mol%). The addition of ligands did not improve the catalytic activity of this complex. Not only aromatic or benzylic thiols could be employed but also, and more importantly, less acidic and more nucleophilic aliphatic mercaptans. Selectivities in favor of the branched isomers were obtained, except with 2-thiopyridine. Finally, the stereoselective course of this sulfenylation was also investigated and the C–S bond was formed with almost a perfect retention of the configuration. To explain this outcome, the authors proposed a σ -enyl pathway and not a π -allyl intermediate.

Sulfones are important reagents in organic chemistry. They are, for example, starting materials in Ramberg–Bäcklund or in Julia reactions. To complement the well-known allylic sulfonation catalyzed by palladium complexes, Plietker communicated a regioselective iron-catalyzed allylic sulfonation for the preparation of aryl allyl sulfones [167]. In the presence of the ferrate $[\text{Bu}_4\text{N}][\text{Fe}(\text{CO})_3(\text{NO})]$ (also abbreviated as TBAFe) and tris-(*para*-methoxyphenyl)phosphine at 80 °C, aryl sulfonates reacted regioselectively with branched allylic carbonates to furnish the branched allylic sulfones in good yields (46–86%, Scheme 97). A variety of substituents both on the aryl group and on the allylic carbonates was well tolerated under the reaction conditions. However, this method was limited to tertiary allylic carbonates. Again, as with thiols, a σ -enyl pathway was postulated to explain the stereochemical course of this sulfonation.

**Scheme 98** Synthesis of *N*-substituted 2-aminobenzothiazoles**Scheme 99** Synthesis of *N*-substituted 2-arylbenzothiazoles

3.5 Synthesis of Benzothiazoles

Functionalized benzothiazoles are a relevant motive in organic chemistry because they are found in bioorganic and medicinal chemistry; they are also contained in drugs and in antitumor, antiviral, and antimicrobial agents. Therefore, many efforts have been devoted to their efficient synthesis. In 2009, Li and coworkers reported the synthesis of various 2-aminobenzothiazoles via an iron-catalyzed tandem C–S and C–N bond formations (Scheme 98) [168]. In the presence of an in situ generated FeF₃/1,10-phenanthroline catalytic system and a base, substituted 2-bromo or 2-iodoaniline reacted with various aliphatic or substituted aromatic isothiocyanates to furnish the corresponding *N*-substituted 2-aminobenzothiazoles in moderate to good yields (41–96%).

A novel synthesis of 2-arylbenzothiazoles was recently proposed from benzothiazoles and vinyl styrene derivatives [169]. This formal C–H arylation reaction was catalyzed by a combination of Fe(NO₃)₂·9H₂O and P(*t*Bu)₃·HBF₄ in a DMSO/H₂O solvent mixture at 120 °C under an atmosphere of oxygen. Compared to previous methodologies, this approach avoided multistep syntheses, stoichiometric amounts of organic oxidants, or an inert atmosphere. This economically and environmentally friendly reaction allowed the synthesis of a variety of 2-arylbenzothiazoles in moderate to high yields (44–84%, Scheme 99). Benzothiazole was the sole active reagent, unlike dimethylthiazole. After several

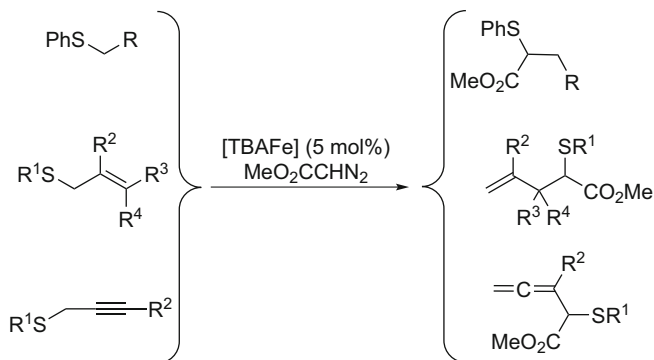
control experiments, a mechanism was proposed. First benzothiazole could be hydrolyzed into 2-aminophenol. Next, styrene derivatives could be oxidized to aromatic aldehydes. Then, a condensation step between the aldehydes and 2-aminothiophenol, followed by an intramolecular cyclization and an oxidative dehydrogenation, could deliver the final product (Scheme 99). A radical mechanism was not excluded, because the aryl benzothiazoles were not formed in the presence of TEMPO as radical scavenger.

3.6 Miscellaneous Reactions

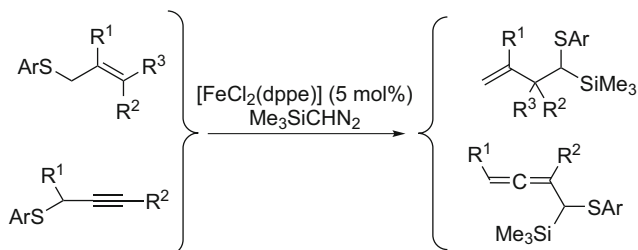
Plietker demonstrated in 2012 that the electron-rich ferrate $[\text{Bu}_4\text{N}][\text{Fe}(\text{CO})_3(\text{NO})]$ could activate a diazoester and transfer the carbenoid to electron-rich sulfides (Doyle–Kirmse reaction, Scheme 100) [170]. The products of this rearrangement were isolated in good yields from allylic thioethers (49–92%), propargylic thioethers (48–80%), and thiophenol (69%). Many functional groups (such as alcohols, amines, boronates, chlorides, and alkenes) were well compatible. Diazo compounds other than diazoester were also investigated. Both electron-rich and electron-poor diazo compounds were reactive in the Doyle–Kirmse reaction. However, the reaction conditions depended on the nature of the diazo compound and have to be adjusted.

This reaction can also take place in the presence of iron(II) or iron(III) and trimethylsilyl diazomethane [171, 172]. Even if FeCl_2 and FeCl_3 were active in this reaction, iron complexes bearing phosphine, such as $[\text{FeCl}_2(\text{dppe})]$, were preferentially used because they are more soluble in chlorinated solvent and are less hygroscopic. Both allylic and propargylic aryl sulfides were introduced as substrates (Scheme 101) and the corresponding sulfide products were formed in high yields.

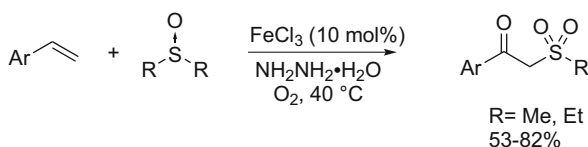
Huang et al. reported a simple protocol for the synthesis of β -oxosulfones from styrene derivatives and dimethyl sulfoxide (Scheme 102) [173]. In the presence of



Scheme 100 Doyle–Kirmse reaction



Scheme 101 Iron(II)-catalyzed Doyle–Kirmse rearrangement

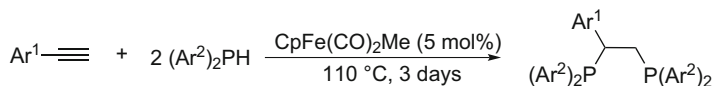
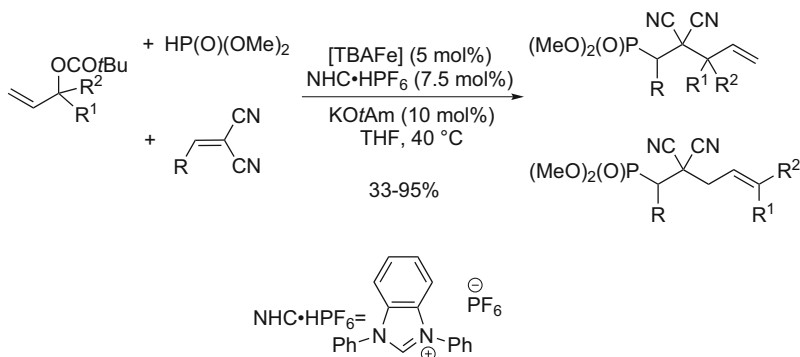
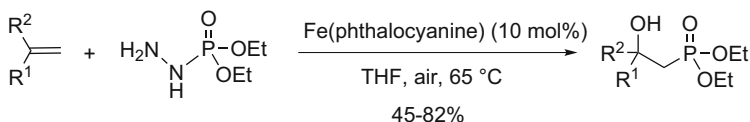


Scheme 102 Synthesis of β -oxosulfones

iron(III) chloride (10 mol%) and hydrazine and oxygen as oxidant, modest to high yields were obtained. Electronic properties of the substituents on the aromatic ring have a deep influence on the formation of the products. Electron-donating or electron-withdrawing substituted styrene derivatives exhibited reactivities, but better results were observed with electron-donating groups and no reactivity with strong electron-withdrawing groups (such as *para*-nitro, *para*-sulfonate, or pyridyl). A radical mechanism was proposed for this reaction, which involved successive C–S bond cleavage and C–S bond formation as key steps. The authors proposed that, under oxygen atmosphere, DMSO could generate methanesulfinic acid through an oxidative cleavage and a concomitant release of a CH₃ group. In the presence of an iron salt and hydrazine, this acid could afford a sulfonyl radical, which could add to the styrene derivative. Oxidation of the generated radical by oxygen could then furnish the β -oxosulfones.

4 Iron-Catalyzed C–P Bond Formation

The seminal works of Beleskaya and Dixneuf demonstrated that transition metals such as palladium and nickel can catalyze the hydrophosphination of alkynes [174–178]. However, examples of hydrophosphination catalyzed by transition metals are still limited, probably because of the possible coordination of the reactant (PR₂H) and/or the product to the metal center. In 2012, Nakazawa and coworkers described the first and, to the best of our knowledge, sole example of catalytic double hydrophosphination of various alkynes promoted by an iron catalyst (Scheme 103) [179]. Among the iron complexes, the most active was [FeCpMe(CO)₂]. The

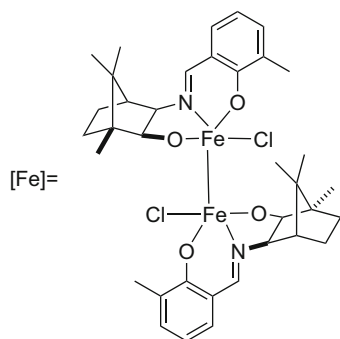
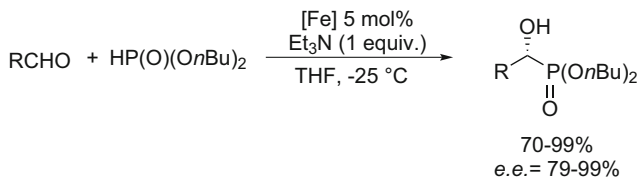
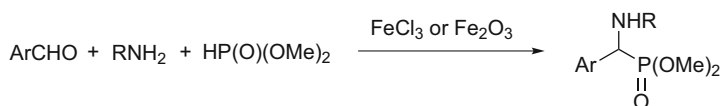
**Scheme 103** Diphosphorylation of alkynes**Scheme 104** Michael addition/allylic substitution sequence**Scheme 105** Addition of phosphorous atoms to alkenes

bis-addition occurred in the presence of two equivalents of a secondary aromatic phosphine, one equivalent of an (hetero)aromatic alkyne, and 5 mol% of the complex, at 110 °C without any organic solvent. The bis-adducts were obtained in yields ranging from 27 to 95%. With aliphatic reagents (phosphine or alkyne), no reaction took place. Moreover, disubstituted alkynes were not reported in this work.

$[\text{Bu}_4\text{N}][\text{Fe}(\text{CO})_3(\text{NO})]$ in association with an NHC: N-heterocyclic carbene ligand could also be applied in a C–P bond formation via a cascade reaction, namely, a Michael addition/allylic substitution sequence (Scheme 104) [180]. Various functionalized phosphonates could be synthesized in moderate to high yields and with a reasonable control of the regioselectivity in favor of the branched isomer.

The treatment of alkenes by phosphoryl hydrazides in the presence of iron (II) phthalocyanine in THF at 65 °C under air led to the hydroxyphosphonates in moderate to good yields (45–82%, Scheme 105) [181].

The enantioselective Pudovik reaction, i.e., the addition of a dialkyl phosphonates to aldehydes catalyzed by a camphor-based dinuclear iron(III), was recently reported by Chen et al. (Scheme 106) [182]. The hydroxyphosphonates were obtained in high yields (70–99%) and enantiomeric excesses (79–99%) from aromatic and aliphatic aldehydes.

**Scheme 106** Enantioselective Pudovik reaction**Scheme 107** Kabachnik–Fields reaction

The Kabachnik–Fields reaction is an analog of the Pudovik reaction. This is a three-component reaction between an aromatic aldehyde, a primary amine, and a dialkyl phosphonate (Scheme 107). The amino-phosphonates were isolated in high yields either in the presence of FeCl_3 [183] or nanoparticles of Fe_2O_3 [184]. In the latter example, the catalyst could be reused several times without any variation of the reactivity.

5 Conclusion

This review clearly demonstrated the potential of the cheap, abundant, and bio-compatible iron metal to perform major transformations under relatively mild conditions along with some quite good functional group tolerances and numerous potential applications for the academic community. Nevertheless, this chemistry is still in infancy for the formation of C–X bonds (X=N, S and P) and the iron complexes do not yet outperform the activities of noble metals. Even though iron complexes can be an alternative to noble transition metal such as palladium,

iridium, and rhodium, there are still some challenges to tackle and improvements to perform. Indeed, most of the transformations described in this chapter involved iron salts, which are certainly not expensive and easily available, but are still used at high catalyst loading (10–20 mol% in a lot of reactions). In order to render this chemistry more attractive, the introduction of inexpensive ligands or the synthesis of new ligands might allow a decrease of the catalyst loading and also of the reaction temperatures and consequently a higher chemoselectivity (e.g., like in the iron nitrene chemistry). The introduction of new ligands might also increase the functional group tolerance, enhance the range of substrates, and improve the regio- or enantioselectivities. A deeper understanding of the mechanism details will be also crucial to achieve higher efficiencies.

References

1. Bruneau C (2013) *Top Organomet Chem* 43:203
2. Evano G, Gaumont A-C, Alayrac C, Wrona IE, Giguere JR, Delacroix O, Bayle A, Jouvin K, Theunissen C, Gatignol J, Silvanus AC (2014) *Tetrahedron* 70:1529
3. Chemler SR, Bovino MT (2013) *ACS Catal* 3:1076
4. Hesp KD (2014) *Angew Chem Int Ed* 53:2034
5. Yim JC-H, Schafer LL (2014) *Eur J Org Chem* 6825
6. Evano G, Toumi M, Coste A (2009) *Chem Commun* 2009:4166
7. Li Y-M, Yang S-D (2013) *Synlett* 1739
8. Rossi R, Bellina F, Lessi M (2010) *Synthesis* 4131
9. Stanley LM, Sibi MP (2008) *Chem Rev* 108:2887
10. Adrio J, Carretero JC (2011) *Chem Commun* 47:6784
11. Chopade PR, Louie J (2006) *Adv Synth Catal* 348:2307
12. Neely JM, Rovis T (2014) *Org Chem Front* 1:1010
13. Aubin Y, Fischmeister C, Thomas CM, Renaud J-L (2010) *Chem Soc Rev* 39:4130
14. Evano G, Blanchard N, Toumi M (2008) *Chem Rev* 108:3054
15. Surry DS, Buchwald SL (2011) *Chem Sci* 2:27
16. Surry DS, Buchwald SL (2010) *Chem Sci* 1:13
17. Taillefer M, Xia N, Ouali A (2007) *Angew Chem Int Ed* 46:934
18. Guo D, Huang H, Xu J, Jiang H, Liu H (2008) *Org Lett* 10:4513
19. Suwiński J, Świerczek K (2001) *Tetrahedron* 57:1639
20. Teo YC (2009) *Adv Synth Catal* 351:720
21. Lee HW, Chan ASC, Kwong FY (2009) *Tetrahedron Lett* 50:5868
22. Mao J, Xie G, Zhan J, Hua Q, Shi D (2009) *Adv Synth Catal* 351:1268
23. Nakamura Y, Ilies L, Nakamura E (2011) *Org Lett* 13:5998
24. Hatakeyama T, Imayoshi R, Yoshimoto Y, Ghorai SK, Jin M, Takaya H, Norisuye K, Sohrin Y, Nakamura M (2012) *J Am Chem Soc* 134:20262
25. Johannsen M, Jørgensen KA (1998) *Chem Rev* 98:1689
26. Plietker B (2006) *Angew Chem Int Ed* 45:6053
27. Guérinot A, Serra-Muns A, Gnam C, Bensoussan C, Reymond S, Cossy J (2010) *J Org Lett* 12:1808
28. Wang Z, Li S, Yu H, Wang Y, Sun X (2012) *J Org Chem* 77:8615
29. Kozhushkov SI, Potukuchi HK, Ackermann L (2013) *Catal Sci Technol* 3:562
30. Mousseau JJ, Charette AB (2013) *Acc Chem Res* 46:412
31. Huang Z, Dong G (2014) *Tetrahedron Lett* 55:5869

32. Ferreira EM (2014) *Nature Chem* 6:94
33. Yu D-G, de Azambuja F, Glorius F (2014) *Angew Chem Int Ed* 53:7710
34. Yeung CS, Dong VM (2011) *Chem Rev* 111:1215
35. Wu Y, Wang J, Mao F, Kwong FY (2014) *Chem Asian J* 9:26
36. Jia F, Li Z (2014) *Org Chem Front* 1:194
37. Huang D, Wang H, Xue F, Shi Y (2011) *J Org Chem* 76:7269
38. Murru S, Srivastava RS (2014) *Eur J Org Chem* 2174
39. Murru S, Gallo AA, Srivastava RS (2012) *J Org Chem* 77:7119
40. Xia Q, Chen W, Qiu H (2011) *J Org Chem* 76:7577
41. Cheng Y, Dong W, Wang L, Parthasarathy K, Bolm C (2014) *Org Lett* 16:2000
42. Chen D, Pan F, Gao J, Yang J (2013) *Synlett* 2085
43. Sun M, Zhang T, Bao W (2014) *Tetrahedron Lett* 55:893
44. Karthikeyan I, Sekar G (2014) *Eur J Org Chem* 8055
45. Matsubara T, Asako S, Ilies L, Nakamura E (2014) *J Am Chem Soc* 136:646
46. Correa A, García Mancheño O, Bolm C (2008) *Chem Soc Rev* 37:1108
47. Zhang L, Deng L (2012) *Chinese Sci Bull* 57:2352
48. Chow TWS, Chen GQ, Liu Y, Zhou CY, Che CM (2012) *Pure Appl Chem* 84:1685
49. Liu Y, Che CM (2010) *Chem Eur J* 16:10494
50. Hennessy ET, Liu RY, Iovan DA, Duncan RA, Betley TA (2014) *Chem Sci* 5:1526
51. Paradine SM, White CM (2012) *J Am Chem Soc* 134:2036
52. Liu P, Wong EL-M, Yuen AW-H, Che C-M (2008) *Org Lett* 10:3275
53. Liu Y, Guan X, Wong EL-M, Liu P, Huang JS, Che CM (2013) *J Am Chem Soc* 135:7194
54. Mansuy D, Mahy JP, Dureault A, Bedi G, Battioni PJ (1984) *Chem Soc Chem Commun* 1161
55. Breslow R, Gellman SHJ (1982) *Chem Soc Chem Commun* 1400
56. Nam W (2007) *Acc Chem Res* 40:522
57. Sorokin AB (2013) *Chem Rev* 113:8152
58. Gross Z, Gray HB (2004) *Adv Synth Catal* 346:165
59. McDonald AR, Que L Jr (2013) *Coord Chem Rev* 257:414
60. Talsi EP, Bryliakov KP (2012) *Coord Chem Rev* 256:1418
61. de Visser SP, Rohde J-U, Lee Y-M, Cho J, Nam W (2013) *Coord Chem Rev* 257:381
62. King ER, Hennessy ET, Betley TA (2011) *J Am Chem Soc* 133:4917
63. King ER, Betley TA (2009) *Inorg Chem* 48:2361
64. Liu Y, Wei J, Che CM (2010) *Chem Commun* 46:6926
65. Li J, Wu C, Zhang Q, Yan B (2013) *Dalton Trans* 42:14369
66. Bonnamour J, Bolm C (2011) *Org Lett* 13:2012
67. Shen M, Driver TG (2008) *Org Lett* 10:3367
68. Hennessy ET, Betley TA (2013) *Science* 340:591
69. Nguyen Q, Nguyen T, Driver TG (2013) *J Am Chem Soc* 135:620
70. McIntosh JA, Coelho PS, Farwell CC, Wang ZJ, Lewis JC, Brown TR, Arnold FH (2013) *Angew Chem Int Ed* 52:9309
71. Singh R, Bordeaux M, Fasan R (2014) *ACS Catal* 4:546
72. Imhof W, Anders E, Göbel A, Görls H (2003) *Chem Eur J* 9:1166
73. Imhof W, Anders E (2004) *Chem Eur J* 10:5717
74. Driller KM, Klein H, Jackstell R, Beller M (2009) *Angew Chem Int Ed* 48:6041
75. Prateptongkum S, Driller KM, Jackstell R, Spannenberg A, Beller M (2010) *Chem Eur J* 16:9606
76. Mathur P, Joshi RK, Rai DK, Jha B, Mobin SM (2012) *Dalton Trans* 41:5045
77. Das B, Reddy GC, Balasubramanyam P, Veeranjaneyulu B (2010) *Synlett* 2010:1625
78. Fan JM, Gao LF, Wang ZY (2009) *Chem Commun* 5021
79. Viton F, Bernardinelli G, Kündig EP (2002) *J Am Chem Soc* 124:4968
80. Badoiu A, Bernardinelli G, Mareda J, Kündig EP, Viton F (2008) *Chem Asian J* 3:1298
81. Wu H, Wang B, Liu H, Wang L (2011) *Tetrahedron* 67:1210

82. Wang M, Liu X, He P, Lin L, Feng X (2013) *Chem Commun* 49:2572
83. Sun B, Ma Q, Wang Y, Zhao Y, Liao P, Bi X (2014) *Eur J Org Chem* 75:52
84. Sharpless KB, Chong AO, Oshima J (1976) *J Org Chem* 41:177
85. Alexanian EJ, Lee C, Sorensen EJ (2005) *J Am Chem Soc* 127:7690
86. Szolcsányi P, Gracza T (2005) *Chem Commun* 3948
87. Noack M, Göttlich R (2002) *Chem Commun* 536
88. Williamson KS, Yoon TP (2010) *J Am Chem Soc* 132:4570
89. Michaelis DJ, Shaffer CJ, Yoon TP (2007) *J Am Chem Soc* 129:1866
90. Michaelis DJ, Ischay MA, Yoon TP (2008) *J Am Chem Soc* 130:6610
91. Michaelis DJ, Williamson KS, Yoon TP (2009) *Tetrahedron* 65:5118
92. Benkovics T, Du J, Guzei I, Yoon TP (2009) *J Org Chem* 74:5545
93. Williamson KS, Yoon TP (2012) *J Am Chem Soc* 134:12370
94. Ren Q, Guan S, Shen X, Fang J (2014) *Organometallics* 33:1423
95. Liu G-S, Zhang Y-Q, Yuan Y-A, Xu H (2013) *J Am Chem Soc* 135:3343
96. Zhang Y-Q, Yuan Y-A, Liu G-S, Xu H (2013) *Org Lett* 15:3910
97. Bach T, Schlummer B, Harms K (2000) *Chem Commun* 287
98. Bach T, Schlummer B, Harms K (2001) *Chem Eur J* 7:2581
99. Bach T, Schlummer B, Harms K (2000) *Synlett* 1330
100. Michaux J, Terrasson V, Marque S, Wehbe J, Prim D, Campagne J-M (2007) *Eur J Org Chem* 2601
101. Cheng X, Xia Y, Xei H, Xu B, Zhang C, Li Y, Qian G, Zhang X, Li K, Li W (2008) *Eur J Org Chem* 1929
102. Dal Zotto C, Michaux J, Zarate-Ruiz A, Gayon E, Campagne J-M, Terrasson V, Pieters G, Virieux D, Gaucher A, Prim D (2011) *J Organomet Chem* 696:296
103. Komeyama K, Morimoto T, Takaki K (2006) *Angew Chem Int Ed* 45:2938
104. Bernoud E, Oulii P, Guillot R, Mellah M, Hannedouche J (2014) *Angew Chem Int Ed* 53:4930
105. Hsieh THH, Dong VM (2009) *Tetrahedron* 65:3062
106. For selected examples of drugs containing ring pyridines, see: Kodimuthali A, Lal Jabaris SS, Pal M (2008) *J Med Chem* 51:5471
107. For reviews on pyridine as ligand in homogeneous catalysis, see: Gibson VC, Redshaw C, Solan GA (2007) *Chem Rev* 107:1745
108. Wurz RP (2007) *Chem Rev* 107:5570
109. For a recent review on pyridine synthesis, see: Hill MD (2010) *Chem Eur J* 16:12052
110. For recent reviews on transition metal-catalysed [2+2+2] cycloaddition for pyridine synthesis, see: Weding N, Hapke M (2011) *Chem Soc Rev* 40:4525
111. Sugiyama Y-K, Okamoto S (2011) *Synthesis* 2247
112. Shaaban MR, El-Sayed R, Elwahy AHM (2011) *Tetrahedron* 67:6095
113. Domínguez G, Pérez-Castells J (2011) *Chem Soc Rev* 40:3430
114. Broere DLJ, Ruijter E (2012) *Synthesis* 2639
115. For applications of the metal-catalysed [2+2+2] cycloaddition reaction in natural product synthesis, see: Witulski B, Grand J (2013) in *Application to the Synthesis of Natural Products, in Transition-Metal-Mediated Aromatic Ring Construction* (ed K. Tanaka), John Wiley & Sons, Inc., Hoboken, NJ, USA. doi: 10.1002/9781118629871.ch7
116. For a recent example, see: Xu F, Wang C, Li X, Wan B (2012) *ChemSusChem* 5:854 and references cited therein
117. Komine Y, Tanaka K (2010) *Org Lett* 12:1312 and references cited therein
118. Onodera G, Shimizu Y, Kimura J-n, Kobayashi J, Ebihara Y, Kondo K, Sakata K, Takeuchi R (2012) *J Am Chem Soc* 134:10515
119. For a selected recent example, see: Garcia P, Evanno Y, George P, Sevrin M, Ricci G, Malacria M, Aubert C, Gandon V (2011) *Org Lett* 13:2030 and references cited therein
120. Sugiyama Y-k, Okamoto S (2011) *Synthesis* 2247 and references cited therein
121. Zou Y, Liu QY, Deiters A (2011) *Org Lett* 13:4352 and references cited therein

122. Weding N, Jackstell R, Jiao H, Spannenberg A, Hapke M (2011) *Adv Synth Catal* 353:3423 and references cited therein
123. Knoch F, Kremer F, Schmidt U, Zenneck U, Le Floch P, Mathey F (1996) *Organometallics* 15:2713
124. Wang C, Li X, Wu F, Wan B (2011) *Angew Chem Int Ed* 50:7162
125. D'Souza BR, Lane TK, Louie J (2011) *J Org Lett* 13:2936
126. For reviews on non-innocent ligands and related complexes, see: van der Vlugt JI (2012) *Eur J Inorg Chem* 363
127. Blanchard S, Derat E, Desage-El Murr M, Fensterbank L, Malacria M, Mouriès-Mansuy V (2012) *Eur J Inorg Chem* 376
128. Schauer PA, Low PJ (2012) *Eur J Inorg Chem* 390
129. Schneider S, Meiners J, Askevold B (2012) *Eur J Inorg Chem* 412
130. Lyaskovskyy V, de Bruin B (2012) *ACS Catal* 2:270
131. Chirik PJ, Wieghardt KW (2010) *Science* 327:794
132. Caulton KG (2012) *Eur J Inorg Chem* 435
133. Lane TK, D'Souza BR, Louie J (2012) *J Org Chem* 77:7555
134. Wang C, Wang D, Xu F, Pan B, Wan B (2013) *J Org Chem* 78:3065
135. Lane TK, Nguyen MH, D'Souza BR, Spahin NA, Louie J (2013) *J Chem Commun* 49:7735
136. Ferré K, Toupet L, Guerschais V (2002) *Organometallics* 21:2578
137. Richard V, Ipouck M, Mérel DS, Gaillard S, Whitby RJ, Witulski B, Renaud J-L (2014) *Chem Commun* 50:593
138. Cao K, Zhang FM, Tu YQ, Zhuo XT, Fan CA (2009) *Chem Eur J* 15:6332
139. Ertürk E, Demir AS (2008) *ARKIVOC* 160
140. Plancq B, Ollevier T (2012) *Chem Commun* 48:3806
141. Allen CL, Lapkin AA, Williams MJ (2009) *Tetrahedron Lett* 50:4262
142. Wang F, Liu H, Fu H, Jiang Y, Zhao Y (2009) *Adv Synth Catal* 351:246
143. Anxionnat B, Guérinot A, Reymond S, Cossy J (2009) *Tetrahedron Lett* 50:3470
144. Chen GQ, Xu ZJ, Liu Y, Zhou CY, Che CM (2011) *Synlett* 1174
145. Qin C, Zhou W, Chen F, Ou Y, Jiao N (2011) *Angew Chem Int Ed* 50:12595
146. Evano G, Jouvin K, Coste A (2013) *Synthesis* 17
147. Yao B, Liang Z, Niu T, Zhang Y (2009) *J Org Chem* 74:4630
148. Yan W, Ye X, Weise K, Petersen JL, Shi X (2012) *Chem Commun* 48:3521
149. Eisenberger P, Gishig S, Togni A (2006) *Chem Eur J* 12:2579
150. Deng QH, Bleith T, Wadepohl H, Gade LH (2013) *J Am Chem Soc* 135:5356
151. Deng QH, Wadepohl H, Gade LH (2011) *Chem Eur J* 17:14922
152. Bach T, Körber C (2000) *J Org Chem* 65:2358
153. Bacci JP, Greenman KL, Van Vranken DL (2003) *J Org Chem* 68:4955
154. Prateptongkum S, Jovel I, Jackstell R, Vogl N, Zeckbecker C, Beller M (2009) *Chem Commun* 1990
155. Chu C-M, Huang W-J, Lu C, Wu P, Liu J-T, Yao C-F (2006) *Tetrahedron Lett* 47:7375
156. Kawatsura M, Komatsu Y, Yamamoto M, Hayase S, Itoh T (2007) *Tetrahedron Lett* 48:6480
157. White JD, Shaw S (2014) *Chem Sci* 5:2200
158. Alt I, Rohse P, Plietker B (2013) *ACS Catal* 3:3002
159. Shen T, Yuan Y, Song S, Jiao N (2014) *Chem Commun* 50:4115
160. Correa A, Carril M, Bolm C (2008) *Angew Chem Int Ed* 47:2880
161. Wu W-Y, Wang J-C, Tsai F-Y (2009) *Green Chem* 11:326
162. Lin Y-Y, Wang Y-J, Lin C-H, Cheng J-H, Lee C-F (2012) *J Org Chem* 77:6100
163. Zeng X, Ilies L, Nakamura E (2012) *Org Lett* 14:954
164. Iwasaki M, Fujii T, Yamamoto A, Nakajima K, Nishihara Y (2014) *Chem Asian J* 9:58
165. Liu S, Tang L, Chen H, Zhao F, Deng G-J (2014) *Org Biomol Chem* 12:6076
166. Holzwarth MS, Frey W, Plietker B (2011) *Chem Commun* 47:11113
167. Jegelka M, Plietker B (2009) *Org Lett* 11:3462
168. Qiu J-W, Zhang X-G, Tang R-Y, Zhong P, Li J-H (2009) *Adv Synth Catal* 351:2319

169. Khemnar AB, Bhanage BM (2014) *RSC Adv* 4:8939
170. Holzwarth MS, Alt I, Plietker B (2012) *Angew Chem Int Ed* 51:5351
171. Carter DS, Van Vranken DL (2000) *Org Lett* 2:1303
172. Prabharasuth R, Van Vranken DL (2001) *J Org Chem* 66:5256
173. Shi X, Ren X, Ren Z, Li J, Wang Y, Yang S, Gu J, Gao Q, Huang G (2014) *Eur J Org Chem* 5083
174. Kazankova MA, Efimova IV, Kochetkov AN, Afanas'ev VV, Beletskaya IP, Dixneuf PH (2001) *Synlett* 497
175. Kazankova MA, Efimova IV, Kochetkov AN, Afanas'ev VV, Beletskaya IP (2002) *Russ J Org Chem* 38:1465
176. Alonso F, Beletskaya IP, Yus M (2004) *Chem Rev* 104:3079
177. Delacroix O, Gaumont AC (2005) *Curr Org Chem* 9:1851
178. Mimeau D, Delacroix O, Gaumont AC (2003) *Chem Commun* 2928
179. Kamitani M, Itazaki M, Tamiya C, Nakazawa H (2012) *J Am Chem Soc* 134:11932
180. Rommel S, Dieskau AP, Plietker B (2013) *Eur J Org Chem* 2013:1790
181. Taniguchi T, Idota A, Yokoyama S-i, Ishibashi H (2011) *Tetrahedron Lett* 52:4768
182. Boobalan R, Chen C (2013) *Adv Synth Catal* 355:3443
183. Wu J, Sun W, Wang W-Z, Xia H-G (2006) *Chin J Chem* 24:1054
184. Reddy BVS, Krishna AS, Ganesh AV, Kumar GGKSN (2011) *Tetrahedron Lett* 52:1359

High-Valent Iron in Biomimetic Alkane Oxidation Catalysis

Michaela Grau and George J.P. Britovsek

Abstract The combination of iron salts or complexes with strong oxidants such as hydrogen peroxide results in the formation of high-valent iron oxo species, the nature of which has been under discussion in the chemical literature for more than a century. Recent advances in the design and development of molecular iron-based oxidation catalysts and their mechanistic understanding are summarised in this chapter, in particular iron complexes featuring tetradentate and pentadentate ligands. Inspired by enzymatic systems based on heme and nonheme ligand environments, the development of biomimetic iron-based catalysts for the selective oxidation of alkanes and alkenes can potentially be applied in a range of areas, from late stage functionalisation of natural product synthesis to large-scale oxidation of hydrocarbons.

Keywords Biomimetic · Catalysis · Iron · Nonheme · Oxidation

Contents

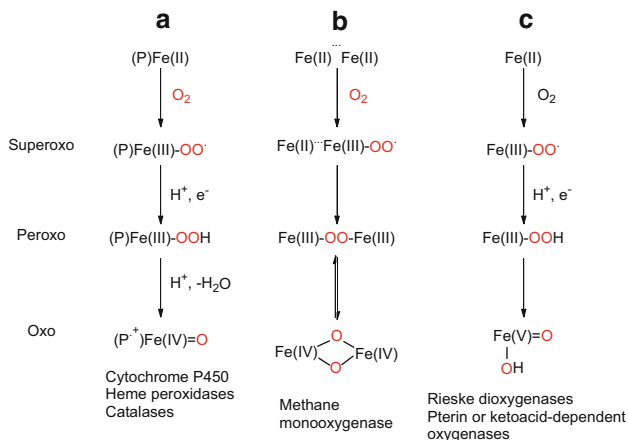
1	Iron-Based Enzymes	146
2	Metal-Ion Catalysed Autooxidation	153
3	Fenton Chemistry	153
4	Oxidation Catalysis with Synthetic Mononuclear Nonheme Fe(II) Complexes	154
4.1	Tetradentate Ligands	155
4.2	Pentadentate Ligands	159
5	Mechanistic Discussions	162
6	Summary and Conclusions	166
	References	167

Abbreviations

BLM	Bleomycin
DFT	Density functional theory
DNA	Deoxyribonucleic acid
EPR	Electron paramagnetic resonance
HAT	Hydrogen atom transfer
His	Histidine
KIE	Kinetic isotope effect
MMO	Methane monooxygenase
NMR	Nuclear magnetic resonance
PCET	Proton-coupled electron transfer
RC	Retention of configuration

1 Iron-Based Enzymes

Iron and copper are abundant metals in the geosphere and exhibit several accessible redox potentials. They are the metal ions of choice for enzymatic oxidation catalysis of organic substances. Nature uses catalytic oxidation reactions to combust carbohydrates and fatty acids in biosynthesis and many metabolism reactions or for the detoxification of harmful compounds. Excellent catalysts for these oxidations are metalloenzymes featuring either iron, copper, or manganese ions as the central atom at the active site of the enzyme [1, 2]. When featuring iron at the active site, these metalloenzymes can be divided into heme and nonheme systems. Heme systems are defined as iron-containing molecules that bind with proteins as a cofactor or prosthetic group to form the heme proteins. These are haemoglobin, myoglobin and the cytochromes. Essentially, heme comprises a porphyrin with its four nitrogen atoms coordinating the iron(II) atom as a macrocycle. The definition of nonheme systems is even broader; they are enzymes containing iron centres that are not coordinated within a porphyrin ring. To form the active oxidant, both systems (heme and nonheme) activate dioxygen or derivatives of dioxygen such as superoxide radical anions or hydrogen peroxide [3–5]. Furthermore, they exhibit substrate specificity, regio- and stereoselectivity and operate under mild conditions. To understand the mechanisms and to emulate the high efficiency of these metalloenzymes, their structure and function during the oxidation process has been extensively investigated. The oxidation of the substrate (e.g. alkane) is thermodynamically favoured, but slow in the absence of a catalyst. For example, the oxidation of methane to methanol is thermodynamically favoured due to a negative reaction enthalpy but is kinetically inert due to the strong C–H bonds. It has been found that iron(II) species react readily with dioxygen to form oxidants including iron(III)-superoxo (Fe(III)-O_2^-), iron(III)-peroxo (Fe(III)-O_2^{2-}), iron(IV)-oxo and iron(V)-oxo species (Scheme 1). There has been a long-standing

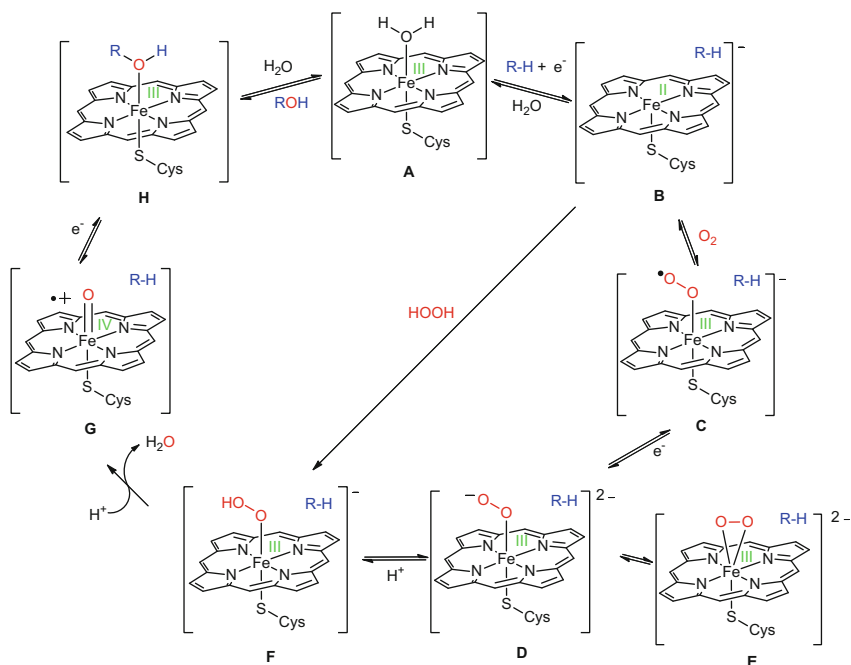


Scheme 1 Metallo-oxygenase mechanisms: (a) heme paradigm, (b) proposed mechanism for dioxygen activation by various dinuclear metallo-oxygenases, (c) proposed mechanism for dioxygen activation by mononuclear nonheme metalloenzymes (*P* porphyrin)

debate on whether high-valent iron species such as Fe(IV)-oxo and Fe(V)-oxo can be formed and stabilised in mononuclear and binuclear nonheme iron enzymes without the support of a porphyrin ligand. However, several enzymatic nonheme iron(IV)-oxo intermediates have been characterised during the last 15 years [1, 3, 6–8]. The mechanism proposed for the activation of oxygen by nonheme iron enzymes is therefore believed to be similar to the one proposed for cytochrome P450 (Scheme 2). Furthermore, the increasing number of isolated and characterised biomimetic nonheme iron(IV)-oxo complexes bearing tetradentate and pentadentate *N*-donor ligands supports the proposal that nonheme ligands can stabilise these highly reactive species [9–11]. The reaction pathways (a, b, c) illustrated in Scheme 1 emphasise the similarity between the proposed formation of the active oxidant for heme and nonheme systems. All involve the formation of an initial O₂-adduct (superoxo), conversion to a metal-peroxide (peroxo), and subsequent O–O bond cleavage to yield a high-valent oxidant (oxo).

For heme systems, the porphyrin ligand is responsible for the pathway by which dioxygen is activated. It makes the low-spin states of the iron centre accessible and stabilises highly oxidised iron intermediates through its redox activity [12]. In general, cytochrome P450, heme peroxidases and catalases belong to the class of heme iron enzymes. Cytochrome P450, whose reactivity has been summarised by Meunier et al., is one of the most studied and best understood heme systems [13]. These cysteinato-heme enzymes are able to oxidise a large variety of substrates. For instance, they can activate dioxygen and hydrogen peroxide to hydroxylate aliphatic C–H bonds and epoxidise C=C bonds with high regio- and stereoselectivity [12, 13].

The widely accepted mechanism of dioxygen activation by heme iron enzymes, here illustrated for P450 (Scheme 2), involves the initial reaction of an iron(II)



Scheme 2 Proposed mechanism for the activation of dioxygen by cytochrome P450

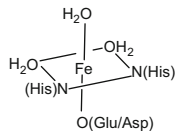
high-spin species **B** with molecular oxygen to form an end-on iron(III)-peroxyl radical **C**. Upon addition of an electron, an end-on iron(III)-peroxo species **D** is formed, which is in equilibrium with a side-on peroxide **E** [14]. Intermediate **E** is the only possible species to activate both oxygen atoms.

The first X-ray structure of a side-on peroxide complex was reported by Karlsson et al. [15] A proton subsequently adds to the iron(III) side-on peroxide **E** to form the more reactive end-on iron(III) hydroperoxide **F**. Intermediate **F** is believed to act as the key catalytic oxidant in these systems [16, 17]. The polarised O–O bond in intermediate **F** could undergo a heterolytic or homolytic bond cleavage to afford a high-valent iron(V)-oxo or iron(IV)-oxo species, respectively. In the case of cytochrome P450, it is proposed that, together with an additional protonation, a heterolytic O–O bond cleavage takes place to yield a highly reactive iron(V)-oxo intermediate, which subsequently reacts with the redox active porphyrin ligand to form the more stable iron(IV)-oxo porphyrin radical species **G**. This key intermediate oxidises the substrate by the rebound mechanism [18]. The coordinated product is replaced by a labile water ligand, which allows another substrate to diffuse into the enzyme pocket. Additionally, the high-spin iron(II) species **B** in cytochrome P450 is able to activate hydrogen peroxide via the so-called peroxide shunt, which allows the formation of the iron(III)-hydroperoxo species **F** in one step.

Similar to heme systems, the main role of nonheme enzymes is the activation of dioxygen in order to oxidise a certain substrate. In contrast, nonheme systems show a larger variety in their ligand structures. In most cases, the ligand is not fully conjugated or fully aromatic, but contains aromatic *N*-donors such as pyridine or pyrazoles, *N*-donors such as amines and *O*-donors such as carboxylate groups. Additionally, there can be mono- and binuclear active sites. The lack of conjugated ligands is proposed to make low-spin states less accessible, but the geometry of the active site is much more flexible. This often results in the formation of two accessible *cis* sites, which are proposed to be crucial for the oxidation mechanism. In contrast, heme systems such as cytochrome P450 exhibit only one labile site. These electronic and structural differences open up reaction pathways unavailable to heme iron enzymes [19–23]. During the last decade, more information on the oxidation catalysis of nonheme iron oxygenases has been obtained. A large variety of nonheme metalloenzymes and model complexes has been structurally characterised [3, 24–26]. The most studied examples for natural nonheme systems are methane monooxygenase (MMO), Rieske dioxygenases, pterin and α -keto acid-dependent oxygenases, all featuring iron at the active site [1, 27, 28]. Although these enzymes belong to the class of nonheme iron enzymes, they are quite different in certain ways. For instance, MMO contains two iron(II) atoms at the active site, while Rieske dioxygenases, pterin and α -keto acid-dependent oxygenases feature only one. Furthermore, MMO, pterin and α -keto acid-dependent oxygenases are monooxygenases and therefore incorporate only one oxygen atom from molecular oxygen into the substrate, whereas dioxygenases such as Rieske dioxygenases are the most atom-efficient metalloenzymes since they incorporate both oxygen atoms into the substrate. It should also be noted that most nonheme enzymes are substrate specific and some of them require a cofactor to operate, which increases their variety.

Nonheme iron(II) species can be divided into several subclasses and some enzymes fit into more than one of these. They can be divided into mono- and dioxygenases, both of which can feature either a mono- or binuclear active site. Additionally, they can be intradiol- or extradiol-cleaving enzymes, which include an iron(III) and an iron(II)-activating species, respectively. One motif which seems to occur in most nonheme enzymes is the so-called 2-His-1-carboxylate facial triad [29]. This class of enzymes features an iron(II) centre which is invariably coordinated by three protein residues, two histidine (His) and one asparagine (Asp) or glutamine (Glu), coordinating one face of the octahedron (Fig. 1) [23, 29, 30]. The three remaining sites on the opposite face of the octahedron are available for exogenous ligands, usually solvent molecules such as water. This class of dioxygenases is capable of different biological transformations, such as the oxidative ring cleavage of aromatic molecules and the *cis*-hydroxylation of arenes. Some of these enzymes need an α -keto acid or pterin as a cofactor. Comparisons among this superfamily of enzymes show that the 2-His-1-carboxylate triad is conserved within each subgroup, which strongly suggests convergent evolution towards a particularly favoured metal-binding site that is useful for promoting oxidation

Fig. 1 Illustration of the 2-His-1-carboxylate facial triad



reactions. This structural ligand motif allows the metal centre to activate both substrate and dioxygen for subsequent reaction [23, 29, 30].

This coordination flexibility of three vacant sites enables a mechanistic diversity, different from any other metalloenzyme class. Despite the large variety of transformations catalysed, a general mechanism at the iron(II) centre has been proposed on the basis of spectroscopic and crystallographic studies [25, 29, 31]. The iron (II) centre is typically six-coordinate at the start of the catalytic cycle and relatively unreactive towards dioxygen. Substrate binding or cofactor binding to the active site makes the metal centre five-coordinate and increases its affinity for dioxygen. The binding of dioxygen initiates the oxidative mechanism specific for each subclass. Some well-understood examples of nonheme iron enzymes are shown in Table 1, which illustrates the diversity of reactions these enzymes are capable of. The field of mononuclear nonheme iron active sites including enzymes, models and intermediates has been reviewed by Costas et al. in 2004 and the field of dinuclear iron nonheme enzymes by Lipscomb et al. in 1996 [3, 48].

Of particular importance is glycopeptide-derived antibiotic bleomycin (BLM), which is a monooxygenase with antitumour activity because of its ability to oxidatively cleave DNA. It features a square-pyramidal coordinated iron (II) complex at the active site with a pentadentate ligand (Fig. 2). The vacant axial position *trans* to the primary amine can be either occupied by a part of the sugar side chain of BLM or by a solvent molecule. This position is also the assumed coordination site for dioxygen or hydrogen peroxide [46]. The most extensively studied iron(III) hydroperoxo intermediate for nonheme enzymes is that of activated bleomycin. The properties of activated BLM have been reviewed comprehensively [46, 49–51]. In analogy to cytochrome P450, activated BLM is formed by reacting dioxygen or hydrogen peroxide with iron(II)BLM [50]. This similarity, as well as high kinetic isotope effect (KIE) values, have led to the proposal that activated BLM may serve as the precursor to an iron(V)-oxo species responsible for substrate oxidation [52]. However, analytical data obtained for the activated BLM only show evidence for a low-spin iron(III) hydroperoxo complex, suggesting this species acts as the active oxidant, achieving O–O bond homolysis concomitant with the C–H bond cleavage [51, 53]. An excellent structural model for the ligand environment around the iron centre in BLM is the linear pentadentate ligand HPMA (see Fig. 4) published by Mascharak et al., since [(BLM)Fe(II)] and [(PMA)Fe(II)] react with dioxygen to generate a low-spin iron(III) intermediate with nearly identical EPR parameters [54–56].

Dinuclear nonheme iron enzymes are typically coordinated by a histidine nitrogen, several carboxylate oxygens and one or more oxo/hydroxo bridges. These complexes are characterised by a relative symmetric ligand environment for both

Table 1 Examples of natural nonheme mono- and diiron metalloenzymes

Enzyme class	Characteristics and function	Scheme for conversion
α -Keto acid-dependent oxygenases – e.g. clavaminic synthase 2 (CAS)	Mononuclear high-spin iron (II) monooxygenase to oxidise C–H bonds [3]	
Aromatic amino acid hydroxylases (cofactor: pterin)	Mononuclear high-spin iron (II) monooxygenase to hydroxylate aromatic amino acids [32]	
Intradiol cleaving catechol dioxygenase	Mononuclear iron(III) dioxygenase to oxidise catechols [33, 34]	
Extradiol cleaving catechol dioxygenases	Mononuclear high-spin iron (II) dioxygenases to oxidise catechols [35]	
Fe-superoxide dismutase	Mononuclear iron(II/III) dioxygenase to dismutate superoxide radicals to hydrogen peroxide and oxygen [36]	$2 \text{O}_2^{\cdot -} + 2 \text{H}^+ \xrightarrow{[\text{Fe}], \text{O}_2} \text{H}_2\text{O}_2 + \text{O}_2$
Isopenicillin N synthase	Mononuclear high-spin iron (II) oxidase to form isopenicillin N [37–42]	
Lipoxygenases	Mononuclear high-spin iron (II) dioxygenases to peroxidise unsaturated fatty acids [43, 44]	
Rieske oxygenase	Mononuclear high-spin iron (II) dioxygenases to <i>cis</i> -dihydroxylate arenes [45]	
Bleomycin	Mononuclear high-spin iron (II) monooxygenase to cleave DNA [46]	$\text{DNA} \xrightarrow{[\text{Fe}], \text{O}_2} \text{base propenals}$
Methane monooxygenase	Dinuclear high-spin iron (II) monooxygenase to oxidise methane to methanol [47]	$\text{CH}_4 + 2 \text{H}^+ \xrightarrow{[\text{Fe}], \text{O}_2} \text{CH}_3\text{OH} + \text{H}_2\text{O}$

iron centres with a flexible ligand coordination that allows for rearrangements upon reduction. Dioxygen activation by enzymes containing a dinuclear nonheme iron site has been reviewed by Lipscomb and Friesner [48, 57]. A review on synthetic structural models for nonheme carboxylate-bridged diiron metalloproteins has been presented by Lippard et al. [58]. Methane monooxygenase (MMO) is a dinuclear nonheme iron enzyme that catalyses the oxidation of methane to methanol using

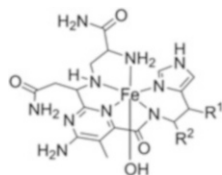
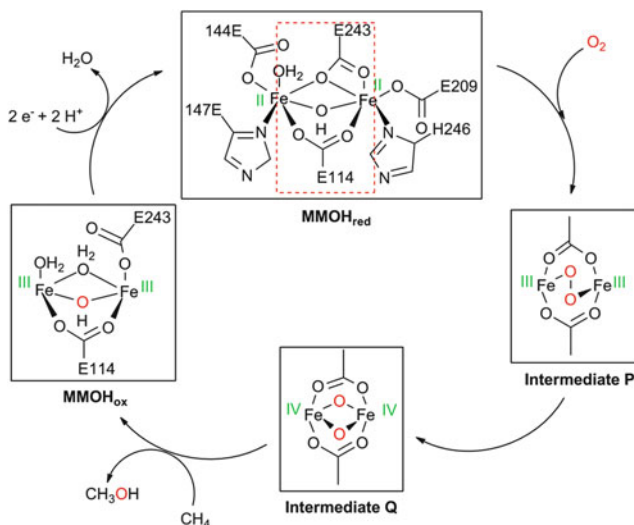
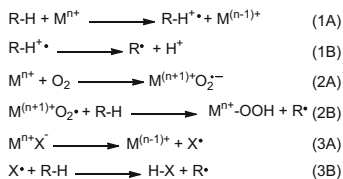


Fig. 2 Active site in bleomycin



Scheme 3 Proposed mechanism for methane monooxygenase

dioxygen as the primary oxidant [59]. Similar to the mechanism described for cytochrome P450 (Scheme 2), the high-spin iron(II) species **MMOH_{red}** reacts with molecular oxygen as shown in Scheme 3. In contrast to cytochrome P450, MMO features a dinuclear iron(II) active site. The oxidation of **MMOH_{red}** with molecular oxygen leads to the formation of a (μ -1,2-peroxo)diron(III) species **Intermediate P**, which subsequently rearranges to form a high-valent bis- μ -oxo-diron(IV) species **Intermediate Q**, which is believed to be the active oxidant. A dinuclear diiron(IV) intermediate has been identified with Mössbauer spectroscopy in the catalytic cycle of MMO and has also been supported by extended X-ray absorption fine structure (EXAFS) measurements [60]. One oxygen atom of **Intermediate Q** is involved in the oxidation of methane to methanol, while the other is converted to water (or hydroxide), resulting in an diiron(III) species **MMOH_{ox}**, which is then further reduced by a cofactor to the reactive high-spin iron(II) species **MMOH_{red}** and water.



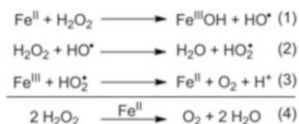
Scheme 4 Different pathways of how metal salts promote the autooxidation of hydrocarbons. (1) Proton-coupled electron transfer (PCET) from the substrate to the metal catalyst. (2) Reaction of primary oxidant (oxygen) with metal catalyst followed by hydrogen atom abstraction (HAT) from the substrate. (3) Decomposition of catalyst followed by HAT from the substrate to the initiator radical

2 Metal-Ion Catalysed Autooxidation

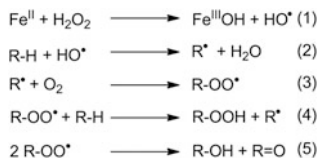
Liquid-phase oxidations proceeding via a radical chain mechanism with dioxygen as the oxidant are known as autooxidation. In uncatalysed autooxidations, a significant induction period can be observed, as a sufficient concentration of radicals needs to be generated before the chain reaction starts. Metal salts can promote the formation of radicals in three different ways: firstly, by proton-coupled electron transfer (PCET) from the substrate to the metal catalyst (Scheme 4, 1A and 1B); secondly, by hydrogen atom abstraction (HAT) from the substrate by a metal peroxo radical species (2A and 2B); and, thirdly, by catalyst decomposition into an initiator radical, which then reacts with the hydrocarbon (3A and 3B). In order to be a good catalyst, the metal ions need to be stable in at least two oxidation states. Some of the most effective metals capable of activating oxygen are manganese, iron, cobalt and copper. They can react with dioxygen due to its paramagnetic triplet ground state, which can accommodate one or two more electrons in the π^* -orbitals to form either superoxide ($\text{O}_2^{\bullet-}$) or a peroxide ion (O_2^{2-}), respectively. The activation described in Eqs. (1A) and (1B) is less common for hydrocarbon autooxidation but can be found for catalysts with high oxidation state metals. The mechanism described in Eqs. (2A) and (2B) is the most commonly proposed initiation path for metals in low oxidation states which can activate oxygen, e.g. M(II) salts of manganese, iron and cobalt. The initiation due to catalyst decomposition (3A) and (3B) has been proposed for metal carboxylates, but has yet to be proven. However, it has also been suggested for catalyst systems where metal halides act as initiators, for example, in the Amoco Process for the oxidation of *p*-xylene [61].

3 Fenton Chemistry

It has been known for more than a century that iron(II) salts can catalyse the decomposition of hydrogen peroxide to form highly reactive hydroxyl radicals (Scheme 5, (1)) [62–64]. This process triggers a chain reaction, which eventually converts hydrogen peroxide into water and dioxygen if no substrate is present. This



Scheme 5 Mechanism of hydrogen peroxide decomposition in the presence of an iron (II) compound according to Fenton [62]



Scheme 6 Radical chain mechanism for substrate oxidation with iron(II) compounds and hydrogen peroxide as the primary oxidant (Fenton chemistry). Further side reactions such as radical termination steps by the combination of two radicals (e.g. $\text{R} + \text{R} \rightarrow \text{R-R}$), or reactions between the iron(II) and iron(III) species with radicals are not included, since they have no significant influence on the product ratio ($A/K = 1$)

catalytic cycle is known as ‘Fenton chemistry’ and is mostly carried out in aqueous acidic conditions ($\text{pH} < 2$), for example, in aqueous perchloric acid with an excess of hydrogen peroxide and a catalytic amount of the iron(II) salt. As for iron(II) salts, it has also been shown by Drago et al. that cobalt(II) salts, in particular with weakly coordinating anions such as that found in $[\text{Co}(\text{NCMe})_4](\text{PF}_6)_2$, also catalyse the decomposition of peroxides [65].

If a substrate (R-H) is present, the highly reactive hydroxyl radicals promote a series of reactions that lead to substrate oxidation via a radical chain mechanism (Scheme 6) [63]. This metal-catalysed autooxidation of hydrocarbons with hydrogen peroxide was first found for iron(II) and has been explained with the Haber-Weiss mechanism [66]. In the presence of dioxygen, the initially produced radical (R) forms a peroxide radical, which either reacts with the large excess of substrate or reacts with another equivalent of peroxide radicals to yield one equivalent of alcohol (A) and one equivalent of ketone (K). Equation (5) in Scheme 6 is also known as the Russell termination step [67]. This reaction sequence leads to A/K ratios of approximately one, which is indicative of Fenton chemistry [68]. Apart from iron(II) salts, cobalt(II) and manganese(II) salts can also oxidise hydrocarbons in this manner [69].

4 Oxidation Catalysis with Synthetic Mononuclear Nonheme Fe(II) Complexes

This section focuses on nonheme systems and therefore synthetic heme systems will not be covered, but it should be noted that there are many metalloporphyrin catalysts that mimic the reactivity of cytochrome P450 [70–74]. The major

drawback of these catalysts is that they mostly require difficult, multiple-step syntheses and achieve only relatively low turnover numbers due to oxidative decomposition of the ligand system [73, 75–78]. It has been shown that sterically hindered and fluorinated porphyrin ligands are more stable under harsh oxidation conditions, but their synthesis is often too expensive for any large-scale industrial application [79–81].

To mimic or to model nonheme iron systems found in nature, a growing area of research focuses on the synthesis of so-called biomimetic nonheme oxidation catalysts and investigates their reactivity towards oxygen, hydrogen peroxide, alkyl peroxides or peracids, as well as their potential as alkane oxidation catalysts. Hydrogen peroxide is the most attractive primary oxidant in terms of costs, ease and safety of handling. It has a high oxygen content, can be safely handled in concentrations up to 60% and leaves only water as a by-product [82].

A large number of biomimetic systems have been investigated, such as the Gif systems developed by Barton [83, 84], the Fenton-like systems by Sawyer [85, 86] and nonheme iron complexes pioneered by Fish, Que, Ménage and Mascharak [87–94]. One advantage with respect to synthetic nonheme systems is that these systems are available in few synthetic steps and their synthesis is relatively cheap. Early investigations failed to find a catalyst system for stereospecific hydroxylation comparable to naturally occurring ones such as cytochrome P450, MMO, Rieske dioxygenases or any α -keto acid-dependent enzyme. In the past 15 years, intensive investigations have taken place to find nonheme iron catalysts capable of selectively oxidising alkanes [59]. A large variety of so-called bioinspired complexes have been reported and covered in several reviews [59, 68, 95, 96]. Examples include (μ -oxo)diiron(III) complexes with bi- and tridentate *N*-donor ligands and monoiron(II) complexes of tetradentate *N*-donor ligands [90, 91, 97–102]. Additionally, evidence for iron(III)-peroxo, iron(III)-hydroxo, iron(IV)-oxo, iron(V)-oxo and iron(IV)-oxo-hydroxo species, which could all serve as active oxidants in the catalytic cycle, has increased, suggesting that synthetic nonheme systems are capable of stabilising these highly reactive intermediates [9, 10, 16, 90, 91, 100, 103–109].

In the following sections, mononuclear nonheme iron complexes will be discussed, with a focus on their ligand structure and their catalytic performance in alkane oxidation. Two main classes of nonheme iron-based catalysts can be discerned featuring either tetradentate or pentadentate ligands.

4.1 Tetradentate Ligands

Iron(II) complexes with tetradentate *N*-donor ligands have been extensively investigated for the oxidation of alkanes with hydrogen peroxide as the primary oxidant [90, 91, 100–102]. The various ligands can be classified according to their binding mode, of which there are four principle types: tetracyclic ligands (**A**), tricyclic (**B**), tripodal (**C**) and linear (**D**), as shown in Fig. 3. In order to compare the catalytic

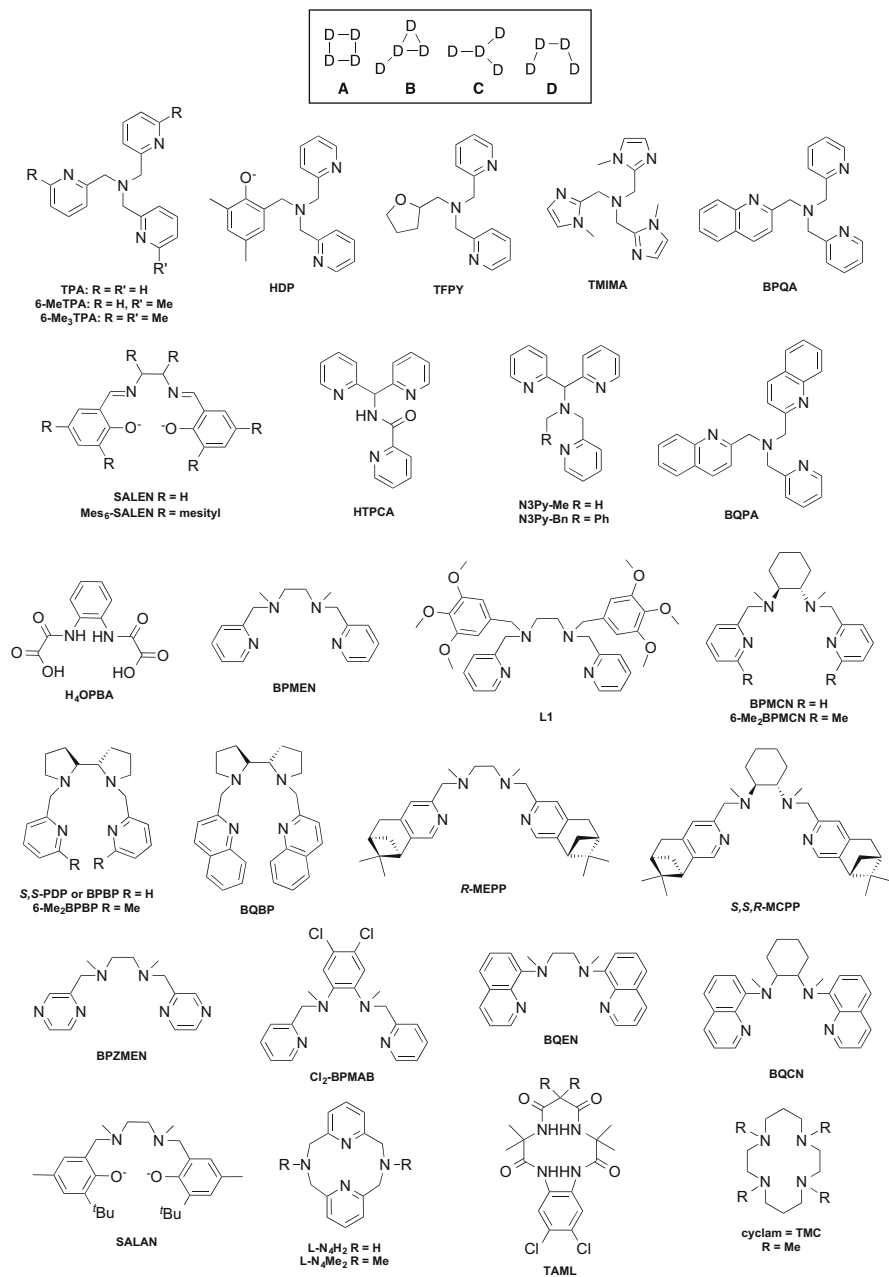


Fig. 3 Classes **A–D** and examples of tetradentate ligands used to form mononuclear biomimetic iron(II) complexes

Table 2 Catalytic oxidation of cyclohexane in acetonitrile catalysed by mononuclear iron (II) complexes bearing tetradentate ligands using H₂O₂ as the primary oxidant

Catalyst	A/K ^a	KIE ^b	Eff.(%) ^c	References
[(TPA)Fe(CH ₃ CN) ₂](ClO ₄) ₂	12.0	3.5	37	[90, 110]
[(5-Me ₃ TPA)Fe(CH ₃ CN) ₂](ClO ₄) ₂	9.0	3.8	40	[91]
[(3-Me ₃ TPA)Fe(CH ₃ CN) ₂](ClO ₄) ₂	14.0	3.7	–	[91]
[(6-MeTPA)Fe(CH ₃ CN) ₂](ClO ₄) ₂	7.0	3.6	–	[91]
[(6-Me ₂ TPA)Fe(CH ₃ CN) ₂](ClO ₄) ₂	2.0	4.0	–	[91]
[(3-Me ₃ TPA)Fe(CH ₃ CN) ₂](ClO ₄) ₂	1.0	3.3	–	[91]
[(BPQA)Fe(CH ₃ CN) ₂](ClO ₄) ₂	10.0	3.4	–	[91]
[(BQPA)Fe(CH ₃ CN) ₂](ClO ₄) ₂	2	3.5	–	[91]
[(HDP)FeCl ₂]	1.2	–	3	[111]
[(BPMEN)Fe(CH ₃ CN) ₂](ClO ₄) ₂	9.5	3.2	63	[91, 100, 110]
[(L ₁)Fe(CH ₃ CN) ₂](ClO ₄) ₂	8.0	–	38	[102]
[(N3Py-Me)Fe(CH ₃ CN) ₂](ClO ₄) ₂	4.6	3.5	19	[112]
[(N3Py-Bn)Fe(CH ₃ CN) ₂](ClO ₄) ₂	5.8	2.4	19	[112]
[(HTPCA)Fe(CH ₃ CN) ₂](ClO ₄) ₂	7	–	6	[113]
[(S,S'-PDP)Fe(CH ₃ CN) ₂](SbF ₆) ₂	9.7	–	67	Kyriacou and Britovsek (unpublished results)
[(S,S',R-MCPP)Fe(CH ₃ CN) ₂](OTf) ₂	0.15	–	42	[114]
[(BQEN)Fe(CH ₃ CN) ₂](OTf) ₂	5.0	–	51	[115]
[(BQCN)Fe(CH ₃ CN) ₂](OTf) ₂	1.1	–	16	[115]

For ligand abbreviations, see Fig. 3

^aA/K = cyclohexanol to cyclohexanone ratio

^bKinetic isotope effect of cyclohexanol formation

^cEfficiency based on conversion of H₂O₂

activity of these complexes, the oxidation of cyclohexane with hydrogen peroxide in acetonitrile often serves as a reference reaction and results are presented in Table 2.

One of the first nonheme mononuclear iron(II) complexes catalysing a stereoselective alkane hydroxylation with hydrogen peroxide as the primary oxidant was [(TPA)Fe(CH₃CN)₂](ClO₄)₂, reported by Que et al. in 1997 [90]. The oxidation of *cis*- and *trans*-1,2-dimethylcyclohexane with hydrogen peroxide affords the tertiary alcohol with 99% retention of stereochemistry [90, 91], while the oxidation of alkenes yields epoxide and *cis*-diol [90, 116]. In 1999, Que et al. published the iron(II) complex [(BPMEN)Fe(CH₃CN)₂](ClO₄)₂, which is highly stereospecific for alkane hydroxylation with a conversion of 70% based on hydrogen peroxide, in comparison to 40% conversion with complex [(TPA)Fe(CH₃CN)₂](ClO₄)₂ [100]. The oxidation of *cis*-1,2-dimethylcyclohexane affords only *cis*-1,2-dimethylcyclohexanol and no isomeric *trans*-alcohol product is observed. When performing the oxidation in the presence of labelled water (H₂¹⁸O), it was found that 26% of the *cis*-alcohol product is ¹⁸O-labelled, indicating that the oxidant responsible for stereospecific alkane hydroxylation can undergo oxygen atom exchange with water. The incorporation of ¹⁸O from H₂¹⁸O into the

oxidation product provided the first evidence that a nonheme iron catalyst can hydroxylate alkanes stereospecifically via a high-valent iron oxo species [100].

Jacobsen demonstrated that the use of acetic acid as an additive (30 mol%) together with $[(\text{BPMEN})\text{Fe}(\text{CH}_3\text{CN})_2]^{2+}$ converts alkenes into epoxides with high yields and that even terminal alkenes can be epoxidised [117]. Mas-Ballesté and Que showed that for $[(\text{BPMEN})\text{Fe}(\text{CH}_3\text{CN})_2]^{2+}$ and $[(\text{TPA})\text{Fe}(\text{CH}_3\text{CN})_2]^{2+}$, in an acetonitrile/acetic acid solvent mixture at 0°C, the effect of acetic acid can be used to convert cyclooctene nearly quantitatively to the epoxide [118]. The binding of acetic acid to the iron(III) peroxo intermediate was supported by spectroscopic and kinetic measurements. Que et al. suggested that the binding of a proximal proton donor is important to promote the heterolytic cleavage of the O–O bond to form a $[(\text{L})\text{Fe}(\text{V})(\text{O})(\text{OAc})]$ species as the active oxidant [118, 119]. The presence of acetic acid also improved the catalytic hydroxylation of unactivated tertiary C–H bonds as shown by White et al. with $[(S,S\text{-PDP})\text{Fe}](\text{SbF}_6)_2$ [120, 121].

The success of the BPMEN system encouraged the synthesis of a variety of BPMEN-derived ligands [114, 115, 120, 122, 123]. Chiral ligands such as BQBP, 6-Me₂BPBP, BPMCN and 6-Me₂BPMCN have been used to obtain complexes that give the *cis*-diol product with up to 97% enantiomeric excess when oxidising different alkenes [124]. Complexes containing the BPMCN ligand have also been used recently for the site-specific oxidation of methylenic sites in alkanes [125]. Gómez and Costas used the iron(II) complexes with the *R*-MEPP and *S,S,R*-MCPP ligands to perform stereospecific alkane oxidation. The complex $[(S,S,R\text{-MCPP})\text{Fe}(\text{OTf})_2]$ was the most active and efficient nonheme iron hydroxylation catalyst, and it was suggested that the combination of steric isolation and an oxidatively robust site may lead to even more active catalysts [114].

A possible deactivation pathway that has been invoked in a number of related nonheme catalyst systems is the formation of inactive dinuclear μ -oxo iron(III) complexes [114, 126]. However, certain dinuclear μ -oxo iron(III) complexes are active alkane hydroxylation catalysts [91, 102, 116], which suggests that dinuclear μ -oxo iron(III) complexes could be in equilibrium with mononuclear iron(III) hydroxo complexes (probably together with other dinuclear μ -oxo/ μ -hydroxo intermediates) [127–130]. The formation of dinuclear complexes may be minimised by steric congestion around the metal centre [102]. One approach has been to attach bulky substituents to the pyridine donor, for example, a pinene moiety or bis(trifluoromethyl)phenyl substituents in the five-position of the pyridine donors [114, 131, 132].

A large variety of tetradentate BPMEN-type ligands and their iron and some manganese and cobalt complexes have been investigated for cyclohexane hydroxylation [110, 115, 122, 123, 133, 134]. Whereas the iron(II) complexes showed different activities dependent on the ligand system, no or only very small amounts of oxidation products were generally obtained with the manganese(II) and cobalt (II) complexes under the same conditions. In addition to the catalyst systems already mentioned above, a notable example is $[(\text{BQEN})\text{Fe}(\text{CH}_3\text{CN})_2](\text{OTf})_2$ which yielded 51% of oxygenated product when oxidising cyclohexane with an A/K ratio of 5 [115]. As the major findings for all complexes with linear

tetradentate ligands, it can be summarised that their catalytic activity and selectivity depend on the coordination mode of the ligand and the ligand field strength. Linear tetradentate ligands coordinate to the metal centre in three different modes, *cis- α* , *cis- β* and *trans*, and those complexes which exhibit a *cis- α* geometry are generally better oxidation catalysts. It should be noted that it is difficult to determine the active species in solution, and in a number of cases, it was found that there can be temperature-dependent dynamic equilibria between different coordination modes [123, 135]. The studies on [Fe(BPMEN)(OTf)₂] have shown that changes to the BPMEN ligand framework that lead to a change in ligand flexibility have the effect that different coordination modes (*cis- β* and *trans*) become accessible. An increase in ligand flexibility generally results in complexes that show inferior catalytic activity in alkane oxidation [115, 123, 133]. As a result of these studies, it has become increasingly clear that catalyst stability, under the harsh oxidising conditions required to oxidise alkanes, is a major factor that determines the catalytic efficiency of a given catalyst. Ligand rigidity, a strong ligand field and low chemical reactivity of the ligand appear to be critically important for the stability and lifetime of nonheme catalysts [134].

4.2 Pentadentate Ligands

A large variety of pentadentate ligands have been used to prepare mononuclear nonheme iron(II) complexes, which have been evaluated in oxidation catalysis. From the studies of tetradentate systems, it was proposed that two labile *cis* sites are required for good catalytic activity. However, nature shows that active sites also feature pentadentate ligands, as, for example, in activated bleomycin (Fig. 2). Increasing research efforts are being carried out to determine how these species activate oxygen or hydrogen peroxide and whether an increase in the ligand denticity might improve the catalyst stability. Pentadentate ligands can be classified into eight classes: pentacyclic (**A**), tetracyclic (**B**), tricyclic (**C**, **D**, **E**), tetrapodal (**F**), tripodal (**G**) and linear (**H**). In Fig. 4, an overview of pentadentate ligands that have been used to form Mn(II), Fe(II) and Co(II) complexes is displayed. Most of these complexes with those pentadentate ligands have been used for mechanistic studies, for example, to investigate their reactivity towards different oxidants. A number of iron complexes with pentadentate ligands have been applied in the catalytic oxidation of cyclohexane, which are shown in Table 3.

In 1999, Feringa and Que et al. reported a nonheme mononuclear iron (II) complex of the pentadentate ligand N4Py to gain more information about the formation and stability of nonheme iron(III) hydroperoxo intermediates [141]. Experimental results, as well as theoretical studies, suggest an iron(IV)-oxo species and hydroxyl radicals as active oxidants, which are formed during the homolytic cleavage of the iron(III) hydroperoxo intermediate [136, 142]. Substitution of one picolyl group in [(N4Py)Fe(CH₃CN)](ClO₄)₂ with a non-coordinating moiety (Me, Ph) has led to iron(II) complexes which are able to perform

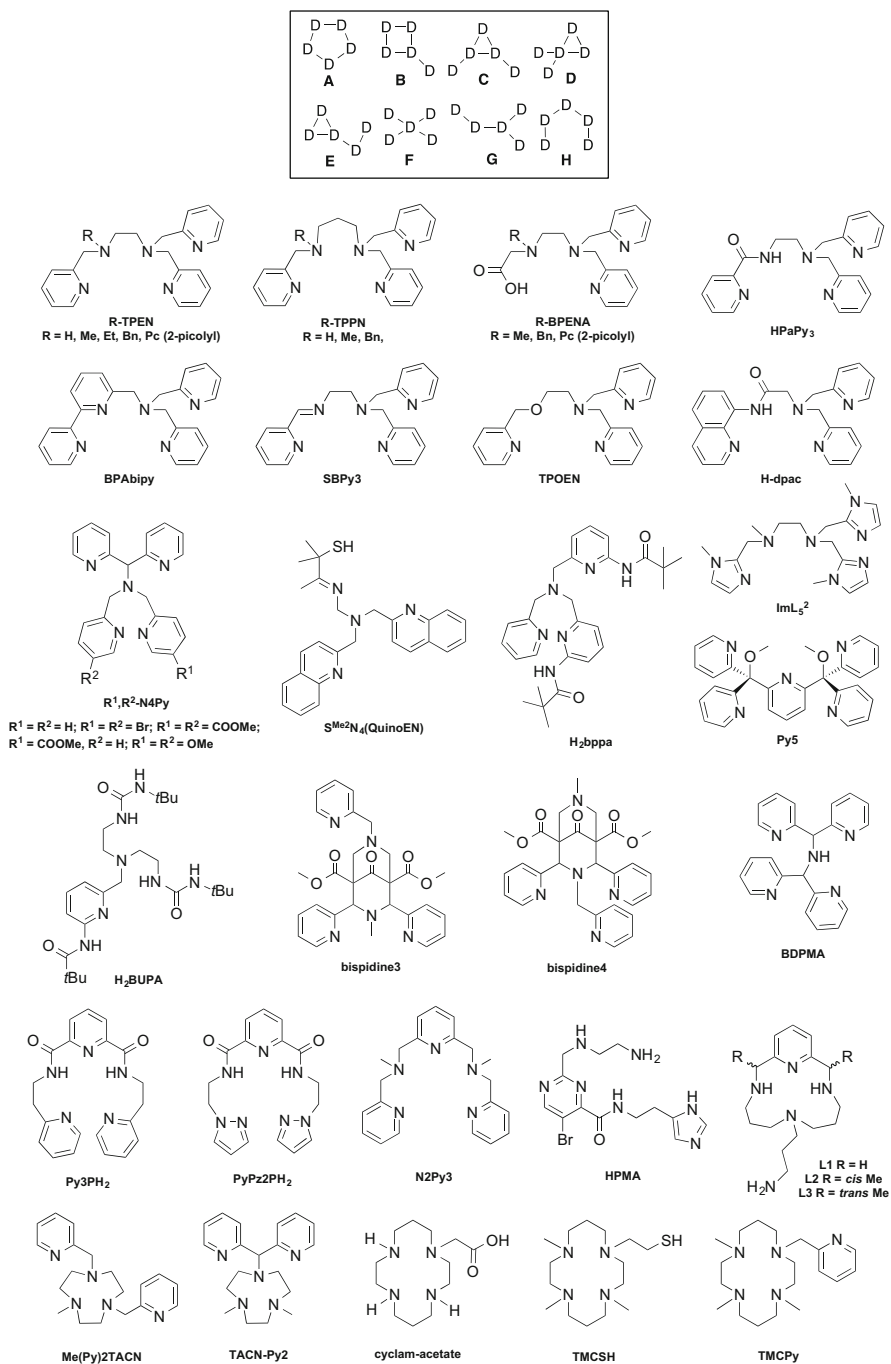


Fig. 4 Classes A–H and examples of different pentadentate ligand types used to prepare mono-nuclear biomimetic Mn(II), Fe(II) and Co(II) complexes

Table 3 Catalytic oxidation of cyclohexane in acetonitrile catalysed by mononuclear complexes bearing pentadentate ligands using H₂O₂ as the primary oxidant

Catalyst	A/K ^a	KIE ^b	Eff.(%) ^c	References
[(N4Py)Fe(CH ₃ CN)](ClO ₄) ₂	1.4	1.5	31	[136]
[(PaPy ₃)Fe(CH ₃ CN)](ClO ₄) ₂	1	–	12	[137]
[(H ₂ bppa)Fe(HCOO)](ClO ₄) ₂	Only A	–	7	[138]
[(Bispidine3)Fe(CH ₃ CN)](OTf) ₂	1.1	–	24	[139]
[(Bispidine4)Fe(CH ₃ CN)](OTf) ₂	0.8	–	21	[139]
[(BPAbipy)Fe(CH ₃ CN)]	1.2		23	[140]
[(N2Py3)Fe(OTf) ₂]	2.0		25	[134]

For ligand abbreviations, see Fig. 4

^aA/K = cyclohexanol to cyclohexanone ratio

^bKinetic isotope effect of cyclohexanol formation

^cEfficiency based on conversion of H₂O₂

stereoselective hydroxylation, but show less activity compared to [(N4Py)Fe(CH₃CN)](ClO₄)₂ [112]. A difference in kinetic isotope effect values (KIE, vide infra) was observed when comparing the oxidation of cyclohexane with hydrogen peroxide as the primary oxidant in acetonitrile and acetone. NMR studies of the complexes in both solvents showed that acetone replaces acetonitrile as the sixth donor ligand, resulting in a change of the redox potential of the iron centre. In the case of the complex with the N4Py ligand, the KIE value is 2.4–3.5 in acetonitrile, compared to 4.4–5.0 in acetone [112]. The oxidation of *cis*-1,2-dimethylcyclohexane and *trans*-1,2-dimethylcyclohexane afforded the tertiary alcohol with 50–85% retention of configuration at the tertiary carbon [112]. For the oxidation of alkenes, this was the first example of an iron-based catalyst that can either give *cis*- or *trans*-dihydroxylation simply by switching the solvent from acetonitrile to acetone [112]. The N4Py iron(IV)-oxo complex exhibits exceptional thermal stability, with $t_{1/2} = 60$ h at 25°C [143].

In 2002, Wada and Masuda published the synthetic isolation of an iron(III)-hydroperoxo complex using the pentadentate ligand H₂bppa, which contains pyridines as well as amido groups (see Fig. 4) [138]. The complex [(H₂bppa)Fe(OOH)]²⁺ was used as oxidant in the absence of hydrogen peroxide. Warming an acetone solution of this species from –70°C to 20°C accelerated the oxidation of cyclohexane to cyclohexanol and only traces of cyclohexanone were observed [138]. Another pentadentate ligand bearing pyridines, amines and amido groups (HPaPy₃), as well as its iron(III) complex [(PaPy₃)Fe(CH₃CN)](ClO₄)₂, was reported by Mascharak [137]. In the presence of 150 eq. of hydrogen peroxide as the primary oxidant, [(PaPy₃)Fe(CH₃CN)](ClO₄)₂ oxidises cyclohexane with a resulting A/K ratio of one, suggesting the involvement of hydroxyl radicals [137, 144]. Rybak-Akimova and co-workers reported several tetracyclic ligands with a pendant aminopropyl donor [145]. These [(L1-3)Fe(OTf)₂] complexes have been used to model the square-pyramidal coordination geometry of iron-BLM. In the presence of small amounts of weakly coordinating acids such as triflic acid, the pendant arm reversibly dissociates. It has been proposed that the aminoalkyl ‘tail’ is

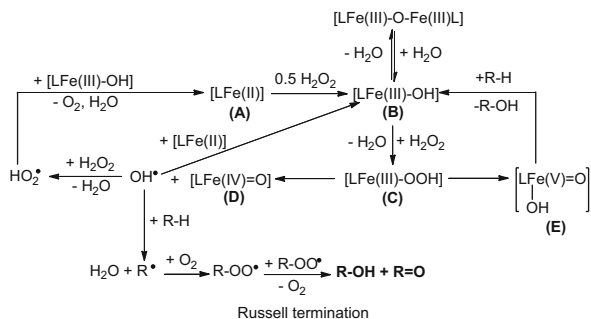
protonated by the acid and generates an ammonium group. [(L1-3)Fe(OTf)₂] (L1-3, see Fig. 4) complexes have been reported to activate hydrogen peroxide, forming a metal-based oxidant, capable of oxidising alkenes to the corresponding epoxides in good yield (up to 89%) and with good selectivity (90–98%) [145]. An excellent structural model for the ligand environment of BLM around the iron centre is the iron HPMA complex reported by Mascharak et al. [54–56].

5 Mechanistic Discussions

The oxidation of a substrate catalysed by nonheme metal complexes in the presence of hydrogen peroxide is believed to proceed by two competing mechanisms: a metal-based oxidation mechanism and a radical mechanism (metal-catalysed autooxidation) (Scheme 7). One way to minimise radical formation is to perform the reaction in a suitable organic solvent [146]. Therefore, the oxidation of alkanes is carried out preferentially in acetonitrile, pyridine or acetone. However, acetone and hydrogen peroxide can form an acetone peroxide, a primary explosive; for this reason acetone cannot be used on an industrial scale [147]. As most alkane oxidation studies with nonheme ligands have been reported for iron(II) systems, the mechanistic discussion will be illustrated for iron, but is similar for cobalt and manganese complexes. The key intermediate in this proposed mechanism is the transient iron(III)-hydroperoxo intermediate **C** (Scheme 7). Depending on its O–O and Mⁿ⁺–O bond strength, homolytic or heterolytic O–O bond cleavage can occur. Heterolytic bond cleavage yields an iron(V)-oxo-hydroxo species **E**, which would be an analogue to the proposed intermediate species for the heme paradigm. This species is believed to selectively oxidise alkanes to the corresponding alcohol. The homolysis of the O–O bond in the iron(III) hydroperoxo species **C** would lead to an iron(IV)-oxo species **D** and highly reactive hydroxyl radicals, which in turn can promote alkane oxidation via a radical chain mechanism yielding similar amounts of alcohol and ketone as the products [91]. If the concentration of primary oxidant is low, the development of free hydroxyl radicals is negligible due to their subsequent reaction with the iron(II) starting complex **A** to form a new iron(III) hydroxo species **B**. The iron(IV)-oxo complex may also act as the active oxidant, but recent research suggests that iron(IV)-oxo species only oxidise weak C–H bonds (<80 kcal/mol) and are certainly less reactive than the proposed iron(V)-oxo species [16, 148, 149]. A significant number of studies have focussed on the isolation and characterisation of iron(III) hydroperoxo and iron(III) alkylperoxo intermediates, mainly containing pyridine-based ligands [150–152].

To determine which of these reactions dominates the oxidation process, the following catalytic tests can be performed. Certain substrates and reaction conditions have been established in the literature to compare the catalytic reactivity of published complexes [68].

Scheme 7 Proposed mechanism for the formation of metal-based oxidants and radicals for nonheme-catalysed alkane oxidation



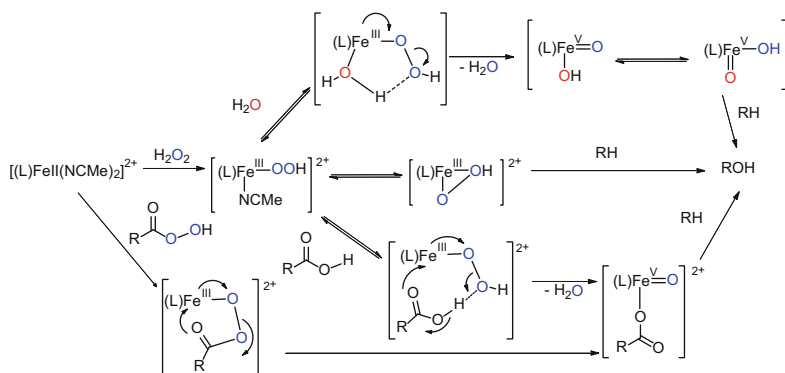
1. Cyclohexane is used as a substrate to determine the alcohol to ketone ratio (A/K) during the oxidation of the substrate. The A/K ratio is used as a first indicator of the lifetime of the alkyl radicals produced during the oxidation process. An A/K ratio of 1 suggests that long-lived alkyl radicals such as the cyclohexyl radicals are trapped by dioxygen at a diffusion-controlled rate to form alkylperoxy radicals, which will undergo a Russell-type termination step [67], which in turn leads to the formation of equimolar amounts of cyclohexanol (CyOH) and cyclohexanone (CyO) (Scheme 7). Larger A/K ratios (>3) suggest a metal-based oxidant, which selectively oxidises alkanes.
2. Another method to determine which mechanism dominates the oxidation of an alkane is to measure the kinetic isotope effect (KIE). This can be done by comparing the oxidation reaction for protio- and deuterioalkanes. Since the C–D bond is stronger than the C–H bond ($\Delta E = 1.7$ kcal/mol), the KIE values for oxidation reactions involving hydroxyl radicals are expected to range between 1 and 2 [153]. Therefore, if there is the same amount of protio- and deuterioalkane in the reaction mixture, both species are expected to undergo oxidation with the same probability. For less reactive alkoxy radicals such as *tert*-butyloxy radicals, KIE values of 4–5 are more common [154]. Larger KIE values are typical for oxidations that involve metal-based oxidants, as these are believed to be more selective [59, 153].
3. The regioselectivity of the oxidation reaction, namely, the comparison of the oxidation of the secondary and tertiary C–H bonds, can also reveal whether the reaction is dominated by hydroxyl radicals or by a metal-based oxidant. For example, in the oxidation of adamantane, which has both secondary and tertiary C–H bonds, the ratio of oxidised C–H bonds gives values of about 2 in the case of a radical mechanism. The participation of metal-based oxidants affords tertiary to secondary ratios higher than 15 [155].
4. The retention of configuration (RC) for the oxidation of a tertiary C–H bond to yield a tertiary alcohol also indicates whether the predominantly operating species is a metal-based oxidant or long-lived radicals. The ‘oxygen-rebound’ mechanism or C–O formation step is extremely fast when an iron oxo species serves as oxidant, which would result in RC, whereas a radical mechanism

would lead to epimerisation. For this class of catalytic tests, mainly *cis*-1,2-dimethylcyclohexane is used [59].

Detailed mechanistic studies on alkane and alkene oxidation have been reported for the complexes [(TPA)Fe(CH₃CN)₂](ClO₄)₂ and [(BPMEN)Fe(CH₃CN)₂](ClO₄)₂. In the 1990s, Que et al. reported several nonheme iron catalysts capable of stereospecific alkane hydroxylation in combination with hydrogen peroxide or alkyl peroxides [90, 156, 157]. The highest selectivity was observed when cyclohexane was oxidised in the presence of [(TPA)Fe(CH₃CN)₂](ClO₄)₂ in 15 min to a mixture of cyclohexanol and cyclohexanone with a A/K ratio of 4.2. It was concluded that the oxidant must be distinct from that typically associated with the radical mechanism, as the major product was the alcohol and the reaction was not influenced by the presence of air. Furthermore, when oxidising *cis*- or *trans*-1,2-dimethylcyclohexane, the tertiary alcohol product was obtained with >99% retention of configuration, and the KIE for cyclohexanol formation was 3.5, a value more indicative of an oxidant that is more selective than hydroxyl radicals (KIE = 1–2). These results started an investigation into gathering evidence for the active oxidant in these reactions. By reacting this complex at –40°C with hydrogen peroxide, the low-spin iron(III) hydroperoxo complex [(TPA)Fe(OOH)](ClO₄)₂ was identified by UV/Vis and EPR spectroscopy as well as ESI mass spectrometry [90].

When [(TPA)Fe(CH₃CN)₂](ClO₄)₂ is reacted with ^tBuOOH under the same conditions, the low-spin iron(III)-alkylperoxo complex [(TPA)Fe(OO^tBu)](ClO₄)₂ is formed, but the oxidation catalysis results are remarkably different. The system [(TPA)Fe(CH₃CN)₂](ClO₄)₂/^tBuOOH has been shown to generate long-lived alkyl radicals which can be trapped by O₂, and epimeric tertiary alcohol products are formed when oxidising *cis*-1,2-dimethylcyclohexane [90, 157]. Furthermore, unlike the [(TPA)Fe(CH₃CN)₂](ClO₄)₂/H₂O₂ system, [(TPA)Fe(CH₃CN)₂](ClO₄)₂/^tBuOOH is not able to epoxidise olefins.

As the reactivity of the peroxo complex appears to be crucial for the oxidation catalysis, the effect of the spin state of the iron complexes has been investigated by introducing one, two or three 6-methyl substituents on the pyridines of the TPA ligand [158]. In contrast to [(L)Fe(OOH)](ClO₄)₂ (L = TPA and 6-MeTPA), which are low-spin iron(III) complexes, [(L)Fe(OOH)](ClO₄)₂ (L = 6-Me₂TPA and 6-Me₃TPA) are high spin. Introducing more than one 6-methyl substituent serves as a simple but effective tool to tune the electronic properties of the metastable iron (III) alkylperoxo species [158]. This proposal was further supported by Raman spectroscopy data that has shown that low-spin complexes [(TPA)Fe(OOH)]²⁺ and [(N4Py)Fe(OOH)]²⁺ have a weaker O–O bond in comparison to high-spin species such as oxyhemerythrin [Fe(OOH)], as their $\nu(\text{O}–\text{O})$ signal is at least 50 cm^{–1} lower than that of a high-spin peroxo complex [103]. The weakened bond is believed to aid O–O bond cleavage to form either an iron(IV) or an iron(V)-oxo species as active oxidants. This theory was further supported by oxidation results showing that complexes [(TPA)Fe(CH₃CN)₂]²⁺ and [(N4Py)Fe(CH₃CN)₂]²⁺, which form low-spin peroxo species, are capable of oxidising relatively inert alkanes such as cyclohexane [90, 156].



Scheme 8 Different reaction paths for the formation of iron oxo species [91, 149]

Que and Solomon expanded this investigation by comparing the electronic structure obtained from DFT calculations and spectroscopic data of the low-spin complex $[(TPA)Fe(OH_2)(OO^tBu)]^{2+}$ and high-spin complex $[(6-Me_3TPA)Fe(OH_2)(OO^tBu)]^{2+}$ [159, 160]. In the high-spin Fe-OOR complexes, the Fe–O bond is cleaved, whereas in low-spin Fe-OOR complexes, homolytic O–O bond cleavage is the favoured pathway [159]. However, in the same year it was reported that depending on the spin state of the peroxo complex, even an iron(V)-oxo species could be formed and act as the active oxidant [91].

The O–O bond in high-spin complexes $[(L)Fe(OOH)](ClO_4)_2$ ($L = 6-Me_2TPA$ and $6-Me_3TPA$) cleaves homolytically, generating alkyl radicals, whereas O–O bond heterolysis occurs in low-spin species such as $[(L)Fe(OOH)](ClO_4)_2$ ($L = TPA$ and $6-MeTPA$) and is promoted by two factors: (a) the low-spin iron (III) centre and (b) the adjacent binding of a water ligand [91]. The formation of hydrogen bonds with the terminal oxygen of the peroxo group helps to form water, which is a better leaving group. In other words, a proximal proton donor, which can be water or acetic acid, supports the O–O bond heterolysis (Scheme 8) [91, 118, 119].

Low-temperature spectroscopy and room temperature ^{18}O -labelling experiments during the catalytic oxidation of cyclohexane with hydrogen peroxide in the presence of $H_2^{18}O$ suggest a stepwise mechanism involving a species that allows an oxygen atom from the $H_2^{18}O$ to be incorporated [91, 116, 161]. The retention of stereochemistry concomitant with ^{18}O incorporation into the products argues against a planar carbocation intermediate that would give epimerised tertiary alcohol products. Therefore, a high-valent iron oxo-hydroxo species showing an ‘oxo-hydroxo tautomerisation’ mechanism has been proposed (Scheme 8) [91].

In addition to studies on alkane hydroxylation with BPMEN and TPA-based iron (II) complexes, the reactivity of these catalysts for epoxidation and *cis*-dihydroxylation of alkenes was investigated [116]. Dependent on whether the iron(II) complex forms a high-spin or low-spin Fe-OOH species, different oxidation products are observed. Complexes forming a low-spin Fe-OOH species (category

A) yield mainly epoxides, whereas with complexes forming a high-spin Fe-OOH species (category B), *cis*-hydroxylation products are mainly observed. Furthermore, ^{18}O -labelling experiments have shown that category A complexes incorporate ^{18}O from H_2^{18}O , suggesting *cis*- $\text{H}^{18}\text{O}-\text{Fe}(\text{V})=\text{O}$ as the active oxidant, whereas the oxygen atoms in the *cis*-diol product derive exclusively from hydrogen peroxide, suggesting a putative Fe(III)- η^2 -OOH species [116]. Even though an iron(V)-oxo species has been evoked as the active metal-based oxidant, to date only Fe(III)OOR and Fe(IV)=O complexes have been isolated and characterised for ligands from the BPMEN and TPA family [116, 162]. Direct reactivity studies have revealed that Fe(III)OOR complexes are sluggish oxidants and Fe(IV)oxo complexes only oxidise weak C–H bonds (<80 kcal/mol). Therefore, they cannot be responsible for the selective oxidation of alkanes such as cyclohexane [118, 161, 163–166]. In 2007, Collins et al. reported the first spectroscopic evidence for an iron(V)-oxo complex [(TAML)Fe(O)]⁻, as previous evidence by ^{18}O -labelling experiments has been indirect [109, 167].

EPR spectroscopy analysis of several highly reactive iron-oxygen intermediates has been reported [168]. When [(L)Fe(CH₃CN)₂](ClO₄)₂ (L = BPMEN or TPA) is reacted with peracetic acid or hydrogen peroxide, an iron(V)-oxo species is presumably formed, which is subsequently responsible for cyclohexene epoxidation [168]. The iron-oxygen intermediates have been investigated, and their reactivity was studied towards cyclohexene epoxidation using EPR, ^1H and ^2H NMR spectroscopy and various oxidants: H₂O₂, H₂O₂/CH₃COOH, CH₃CO₃H, m-CPBA, PhIO, ^tBuOOH and ^tBuOOH/CH₃COOH [149]. This systematic study supports that [(L)Fe(CH₃CN)(O)]²⁺ and [(L)Fe(CH₃CN)(OOR)]²⁺ (L = BPMEN or TPA) are poor oxidants. EPR signals for iron(V)-oxo species were only observed for the following combination of complex [(L)Fe(CH₃CN)₂](ClO₄)₂ (L = BPMEN **A** or TPA **B**) and oxidant: **A**/H₂O₂, **A** or **B**/H₂O₂/CH₃COOH, **A** or **B**/CH₃CO₃H, **A** or **B**/m-CPBA and **A**/^tBuOOH/CH₃COOH. Only these systems were capable of selective olefin epoxidation, and the combinations **B**/H₂O₂, **A** or **B** PhIO, **A** or **B**/^tBuOOH and **B**/^tBuOOH/CH₃COOH showed no EPR evidence for an iron(V)-oxo intermediate and failed to epoxidise olefins. The combination **A**/^tBuOOH/CH₃COOH is a rare example of an iron nonheme system capable of selective olefin epoxidation with ^tBuOOH, but the addition of CH₃COOH promoted the formation of the iron(V)-oxo species [149]. These developments strongly suggest a highly reactive iron(V)-oxo species as the active metal-based oxidant. The formation of this species seems to be dependent on several factors such as the ligand and the primary oxidant used.

6 Summary and Conclusions

This chapter has given an overview of enzymatic and synthetic oxidation systems, which are of interest in the context of the development of nonheme iron-based alkane oxidation catalysts. The characterisation and application of iron complexes with tetradentate and pentadentate ligands have been reviewed as well as their

reactivity towards different primary oxidants such as H_2O_2 , $t\text{BuOOH}$ and O_2 and their application in hydrocarbon oxidation. In solution, complexes are able to attain more than one geometry and/or spin state, which has been of interest as some complexes investigated in this work show very interesting solution dynamics. The mechanism by which these oxidative transformations are believed to occur has been described, and the key intermediates that have been identified are iron(III) hydroperoxo complexes and iron(IV)-oxo complexes. The active oxidant in these nonheme iron-catalysed alkane oxidations is believed to be a high-valent iron(V)-oxo complex. Efforts to detect and characterise such high-valent iron complexes are ongoing and will hopefully shed further light on the nature of the active oxidants in these nonheme systems.

Fenton's early report in 1876 of a violet colour observed upon reacting iron (II) sulphate with hydrogen peroxide was rather optimistically ascribed to the formation of a high-valent ferrate $[\text{FeO}_4]^{2-}$ ion [169]. While the violet colour is attributable to a ferric tartrate complex, the notion of generating high-valent iron oxo species from iron(II) and hydrogen peroxide was not that far-fetched after all.

References

1. Merckx M, Kopp DA, Sazinsky MH, Blazyk JL, Muller J, Lippard S (2001) *Angew Chem Int Ed* 40:2782
2. Balasubramanian R, Rosenzweig AC (2007) *Acc Chem Res* 40:573
3. Costas M, Mehn MP, Jensen MP, Que L Jr (2004) *Chem Rev* 104:939
4. Sono M, Roach MP, Coulter ED, Dawson JH (1996) *Chem Rev* 96:2841
5. Law NA, Caudle MT, Pecoraro VL (1999) *Adv Inorg Chem* 46:305
6. Krebs C, Fujimori GD, Walsh CT, Bollinger JM Jr (2007) *Acc Chem Res* 40:484
7. Abu-Omar MM, Loaiza A, Hontzeas N (2005) *Chem Rev* 105:2227
8. Neidig ML, Solomon EI (2005) *Chem Commun* 41:5843
9. Nam W (2007) *Acc Chem Res* 40:522
10. Que L Jr (2007) *Acc Chem Res* 40:493
11. MacBeth CE, Golombok AP, Young VG, Kuczera K, Hendrich MP, Borovik AS (2000) *Science* 289:938
12. Kovacs JA (2003) *Science* 299:1024
13. Meunier B, de Visser SP, Shaik S (2004) *Chem Rev* 104:3947
14. Harris DL, Loew GH (1998) *J Am Chem Soc* 120:8941
15. Karlsson A, Parales JV, Parales RE, Gibson DT, Eklund H, Ramaswamy S (2003) *Science* 299:1039
16. Chen K, Costas M, Que Jr L (2002) *J Chem Soc Dalton Trans*: 672
17. Solomon EI (2001) *Inorg Chem* 40:3656
18. Groves JT (1985) *J Chem Educ* 62:928
19. Que L Jr, Ho YNR (1996) *Chem Rev* 96:2607
20. Ho RYN, Que L Jr, Roelfes G, Feringa BL, Hermant R, Hage R (1999) *Chem Commun* 21:2161
21. Neese F, Solomon EI (1998) *J Am Chem Soc* 120:12829
22. Decker A, Solomon EI (2005) *Curr Opin Chem Biol* 9:152
23. Hegg EL, Que L Jr (1997) *Eur J Biochem* 250:625
24. Lehnert N, DeBeer George S, Solomon EI (2001) *Curr Opin Chem Biol* 5:176

25. Solomon EI, Brunold TC, Davis MI, Kemsley JN, Lee SK, Lehnert N, Neese F, Skulan AJ, Yang YS, Zhou J (2000) *Chem Rev* 100:235
26. Solomon EI, Randall DW, Glaser T (2000) *Coord Chem Rev* 200–202:595
27. Bugg TDH, Ramaswamy S (2008) *Curr Opin Chem Biol* 12:134
28. Ullrich R, Hofrichter M (2007) *Cell Mol Life Sci* 64:271
29. Que L Jr (2000) *Nat Struct Biol* 7:182
30. Moelands MAH, Nijssse S, Folkertsma E, de Bruin B, Lutz M, Spek AL, Klein Gebbink RJM (2013) *Inorg Chem* 52:7394
31. Solomon EI, Decker A, Lehnert N (2003) *Proc Natl Acad Sci U S A* 100:3589
32. Hufton SE, Jennings IG, Cotton RGH (1995) *Biochem J* 311:353
33. Ohlendorf DH, Orville AM, Lipscomb JD (1994) *J Mol Biol* 244:586
34. Ohlendorf DH, Lipscomb JD, Weber PC (1988) *Nature* 336:403
35. Eltis LD, Bolin JT (1996) *J Bacteriol* 178:5930
36. Miller AF (2001) *Handbook of metalloproteins*. Wiley, Chichester
37. Roach PL, Clifton IJ, Fulop V, Harlos K, Barton GJ, Hajdu J, Andersson I, Schofield CJ, Baldwin JE (1995) *Nature* 375:700
38. Schofield CJ, Zhang Z (1999) *Curr Opin Struct Biol* 9:722
39. Schenk WA (2000) *Angew Chem Int Ed* 39:3409
40. Roach PL, Clifton IJ, Hensgens CMH, Shibata N, Long AJ, Strange RW, Hasnain SS, Schofield CJ, Baldwin JE, Hajdu J (1996) *Eur J Biochem* 242:736
41. Orville AM, Chen VJ, Kriauciunas A, Harpel MR, Fox BG, Munck E, Lipscomb JD (1992) *Biochemistry* 31:4602
42. Baldwin JE, Bradley M (1990) *Chem Rev* 90:1079
43. Nanda S, Yadav JS (2003) *J Mol Catal B: Enzym* 26:3
44. Minor W, Steczko J, Stec B, Otwinowski Z, Bolin JT, Walter R, Axelrod B (1996) *Biochemistry* 35:10687
45. Kauppi B, Lee K, Carredano E, Parales RE, Gibson DT, Eklund H, Ramaswamy S (1998) *Structure* 6:571
46. Stubbe J, Kozarich JW, Wu W, Vanderwall DE (1996) *Acc Chem Res* 29:322
47. Rosenzweig AC, Frederick CA, Lippard SJ, Nordlund P (1993) *Nature* 366:537
48. Wallar BJ, Lipscomb JD (1996) *Chem Rev* 96:2625
49. Sam JW, Tang XJ, Peisach J (1994) *J Am Chem Soc* 116:5250
50. Stubbe J, Kozarich JW (1987) *Chem Rev* 87:1107
51. Neese F, Zaleski JM, Zaleski KL, Solomon EI (2000) *J Am Chem Soc* 122:11703
52. Absalon MJ, Wu W, Kozarich JW, Stubbe J (1995) *J Am Chem Soc* 34:2076
53. Westre TE, Loeb KE, Zaleski JM, Hedman B, Hodgson KO, Solomon EI (1995) *J Am Chem Soc* 117:1309
54. Guajardo RJ, Hudson SE, Brown SJ, Mascharak PK (1993) *J Am Chem Soc* 115:7971
55. Loeb KE, Zaleski JM, Westre TE, Guajardo RJ, Mascharak PK, Hedman B, Hodgson KO, Solomon EI (1995) *J Am Chem Soc* 117:4545
56. Guajardo RJ, Chavez F, Farinas ET, Mascharak PK (1995) *J Am Chem Soc* 117:3883
57. Baik MH, Newcomb M, Friesner RA, Lippard SJ (2003) *Chem Rev* 103:2385
58. Tshuva EY, Lippard SJ (2004) *Chem Rev* 104:987
59. Costas M, Chen K, Que L Jr (2000) *Coord Chem Rev* 200–202:517
60. Shu L, Nesheim JC, Kauffmann KE, Munck E, Lipscomb JD, Que L Jr (1997) *Science* 275:515
61. Partenheimer W (1995) *Catal Today* 23:69
62. Fenton HJH (1894) *J Chem Soc Trans* 65:889
63. Gozzo F (2001) *J Mol Catal A Chem* 171:1
64. Dunford HB (2002) *Coord Chem Rev* 233–234:311
65. Goldstein AS, Drago RS (1991) *Inorg Chem* 30:4506
66. Haber F, Weiss J (1934) *Proc R Soc London Ser A* 147:332
67. Russell GA (1957) *J Am Chem Soc* 79:3871

68. Tanase S, Bouwman E (2006) *Adv Inorg Chem* 58:29
69. Talsi EP, Chinakov VD, Babenko VP, Sidelnikov VN, Zamaraev KI (1993) *J Mol Catal* 81:215
70. Meunier B (1992) *Chem Rev* 92:1411
71. Nam W, Oh S-Y, Sun YJ, Kim J, Kim W-K, Woo SK, Shin W (2003) *J Org Chem* 68:7903
72. Srinivas KA, Kumar A, Chauhan SMS (2002) *Chem Commun* 38:2456
73. Stephenson NA, Bell AT (2005) *J Am Chem Soc* 127:8635
74. Sorokin AB, Kudrik EV, Bouchu D (2008) *Chem Commun* 44:2562
75. Cunningham ID, Danks TN, Hay JN, Hamerton I, Gunathilagan S (2001) *Tetrahedron* 57:6847
76. Cunningham ID, Danks TN, Hay JN, Hamerton I, Gunathilagan S, Janczak C (2002) *J Mol Catal* 185:25
77. Cunningham ID, Danks TN, O'Connell KTA, Scott PW (1999) *J Chem Soc Perkin Trans 2*: 2133
78. Serra AC, Marçalo EC, Rocha Gonsalves AMdA (2004) *J Mol Catal* 215:17
79. Nappa MJ, Tolman CA (1985) *Inorg Chem* 24:4711
80. Goh YM, Nam W (1999) *Inorg Chem* 38:914
81. Nam W, Jin SW, Lim MH, Ryu JY, Kim C (2002) *Inorg Chem* 41:3647
82. Hill CL, Prosser-McCartha CM (1995) *Coord Chem Rev* 143:407
83. Barton DHR, Doller D (1992) *Acc Chem Res* 25:504
84. Barton DHR (1996) *Chem Soc Rev* 25:237
85. Sawyer DT, Sobkowiak A, Matsushita T (1996) *Acc Chem Res* 29:409
86. Sawyer DT (1997) *Coord Chem Rev* 165:297
87. Vincent JB, Huffman JC, Christou G, Li Q, Nanny MA, Hendrickson DN, Fong RH, Fish RH (1988) *J Am Chem Soc* 110:6898
88. Rabion A, Buchanan RM, Seris JL, Fish RH (1997) *J Mol Catal A Chem* 116:43
89. Neimann K, Neumann R, Rabion A, Buchanan RM, Fish RH (1999) *Inorg Chem* 38:3575
90. Kim C, Chen K, Kim J, Que L Jr (1997) *J Am Chem Soc* 119:5964
91. Chen K, Que L Jr (2001) *J Am Chem Soc* 123:6327
92. Leising RA, Norman RE, Que L Jr (1990) *Inorg Chem* 29:2553
93. Ménage S, Vincent JM, Lambeaux C, Chottard G, Grand A, Fontecave M (1993) *Inorg Chem* 32:4766
94. Nguyen C, Guajardo RJ, Mascharak PK (1996) *Inorg Chem* 35:6273
95. Lane BS, Burgess K (2003) *Chem Rev* 103:2457
96. Talsi EP, Bryliakov KP (2012) *Coord Chem Rev* 256:1418
97. Ménage S, Vincent JM, Lambeaux C, Fontecave M (1996) *J Mol Catal A Chem* 113:61
98. Kulikova VS, Gritsenko ON, Shteinman AA (1996) *Mendeleev Commun* 6:119
99. Duboc-Toia C, Ménage S, Lambeaux C, Fontecave M (1997) *Tetrahedron Lett* 38:3727
100. Chen K, Que L Jr (1999) *Chem Commun* 35:1375
101. Costas M, Que L Jr (2002) *Angew Chem Int Ed* 41:2179
102. Mekmouche Y, Ménage S, Toia-Duboc C, Fontecave M, Galey J-B, Lebrun C, Pécaut J (2001) *Angew Chem Int Ed* 40:949
103. Ho RYN, Roelfes G, Feringa BL, Que L Jr (1999) *J Am Chem Soc* 121:264
104. Bassan A, Blomberg MRA, Siegbahn PEM, Que L Jr (2002) *J Am Chem Soc* 124:11056
105. Duboc-Toia C, Menge S, Ho RYN, Que L Jr, Fontecave M (1999) *Inorg Chem* 38:1261
106. Hummel H, Mekmouche Y, Duboc-Toia C, Ho RYN, Que L Jr, Thomas F, Trautwein A, Lebrun C, Fontecave M, Ménage S (2002) *Angew Chem Int Ed* 41:617
107. Mekmouche Y, Hummel H, Ho RYN, Que L Jr, Schunemann V, Thomas F, Trautwein AX, Lebrun C, Gorgy K, Lepretre J-C, Collomb M-N, Deronzier A, Fontecave M, Menage S (2002) *Chem Eur J* 8:1196
108. Jensen MP, Costas M, Ho RYN, Kaizer J, Payeras AM, Muenck E, Que L Jr, Rohde J-U, Stubna A (2005) *J Am Chem Soc* 127:10512

109. Tiago de Oliveira F, Chanda A, Banerjee D, Shan X, Mondal S, Que L Jr, Bominaar EL, Muenck E, Collins TJ (2007) *Science* 315:835
110. Britovsek GJP, England J, White AJP (2005) *Inorg Chem* 44:8125
111. Ito S, Suzuki M, Kobayashi T, Itoh H, Harada A, Ohba S, Nishida Y (1996) *J Chem Soc Dalton Trans*: 2579
112. Klopstra M, Roelfes G, Hage R, Kellogg RM, Feringa BL (2004) *Eur J Inorg Chem*: 846
113. Gutkina EA, Rubtsova TB, Shteinman AA (2003) *Kinet Catal* 44:106
114. Gómez L, Garcia-Bosch I, Company A, Benet-Buchholz J, Polo A, Sala X, Ribas X, Costas M (2009) *Angew Chem Int Ed* 48:5720
115. England J, Britovsek GJP, Rabadia N, White AJP (2007) *Inorg Chem* 46:3752
116. Chen K, Costas M, Kim J, Tipton AK, Que L Jr (2002) *J Am Chem Soc* 124:3026
117. White MC, Doyle AG, Jacobsen EN (2001) *J Am Chem Soc* 123:7194
118. Mas-Ballesté R, Que L Jr (2007) *J Am Chem Soc* 129:15964
119. Mas-Ballesté R, Fujita M, Que L Jr (2008) *Dalton Trans* 37:1828
120. Chen MS, White MC (2007) *Science* 318:783
121. Chen MS, White MC (2010) *Science* 327:566
122. England J, Gondhia R, Bigorra-Lopez L, Petersen AR, White AJP, Britovsek GJP (2009) *Dalton Trans* 38:5319
123. England J, Davis CR, Banaru M, White AJP, Britovsek GJP (2008) *Adv Synth Catal* 350:883
124. Suzuki K, Oldenburg PD, Que L Jr (2008) *Angew Chem Int Ed Engl* 47:1887
125. Canta M, Font D, Gómez L, Ribas X, Costas M (2014) *Adv Synth Catal* 356:818
126. Vermeulen NA, Chen MS, Christina White M (2009) *Tetrahedron* 65:3078
127. Kurtz DM Jr (1990) *Chem Rev* 90:585
128. Poussereau S, Blondin G, Cesario M, Guilhem J, Chottard G, Gonnet F, Girerd J-J (1998) *Inorg Chem* 37:3127
129. Taktak S, Kryatov SV, Rybak-Akimova EV (2004) *Inorg Chem* 43:7196
130. Hazell R, Jensen KB, McKenzie CJ, Toftlund H (1995) *J Chem Soc Dalton Trans*: 707
131. Gómez L, Canta M, Font D, Prat I, Ribas X, Costas M (2013) *J Org Chem* 78:1421
132. Gormisky PE, White MC (2013) *J Am Chem Soc* 135:14052
133. Britovsek GJP, England J, White AJP (2006) *Dalton Trans* 35:1399
134. Grau M, Kyriacou A, Cabedo Martinez F, de Wispelaere I, White AJP, Britovsek GJP (2014) *Dalton Trans* 43:17108
135. Whiteoak CJ, Torres Martin de Rosales R, White AJP, Britovsek GJP (2010) *Inorg Chem* 49:11106
136. Roelfes G, Lubben M, Hage R, Que L Jr, Feringa BL (2000) *Chem Eur J* 6:2152
137. Rowland JM, Olmstead M, Mascharak PK (2001) *Inorg Chem* 40:2810
138. Wada A, Ogo S, Nagatomo S, Kitagawa T, Watanabe Y, Jitsukawa K, Masuda H (2002) *Inorg Chem* 41:616
139. Comba P, Maurer M, Vadivelu P (2009) *Inorg Chem* 48:10389
140. Wong E, Jeck J, Grau M, White AJP, Britovsek GJP (2013) *Catal Sci Technol* 3:1116
141. Roelfes G, Lubben M, Chen K, Ho RYN, Meetsma A, Genseberger S, Hermant RM, Hage R, Mandal SK, Young VG, Zang Y, Kooijman H, Spek AL, Que L Jr, Feringa BL (1999) *Inorg Chem* 38:1929
142. Lehnert N, Neese F, Ho RYN, Que L Jr, Solomon EI (2002) *J Am Chem Soc* 124:10810
143. Kaizer J, Klinker EJ, Oh NY, Rohde JU, Song WJ, Stubna A, Kim J, Muenck E, Nam W, Que L Jr (2004) *J Am Chem Soc* 126:472
144. Bukowski MR, Zhu S, Koehntop KD, Brennessel WW, Que L Jr (2004) *J Biol Inorg Chem* 9:39
145. Taktak S, Ye W, Herrera AM, Rybak-Akimova EV (2007) *Inorg Chem* 46:2929
146. Sheu C, Richert SA, Cofre P, Ross B, Sobkowiak A, Sawyer DT, Kanofsky JR (1990) *J Am Chem Soc* 112:1936
147. Tanase S, Foltz C, Gelder R d, Hage R, Bouwman E, Reedijk J (2005) *J Mol Catal A Chem* 225:161

148. Yoon J, Wilson SA, Jang YK, Seo MS, Nehru K, Hedman B, Hodgson KO, Bill E, Solomon EI, Nam W (2009) *Angew Chem Int Ed* 48:1257
149. Lyakin OY, Bryliakov KP, Talsi EP (2011) *Inorg Chem* 50:5526
150. Girerd J-J, Banse F, Simaan AJ (2000) *Metal-oxo and Metal-peroxo species in catalytic oxidations*, vol 97. Springer, Berlin, p 145
151. Balland V, Banse F, Anxolabéhère-Mallart E, Nierlich M, Girerd J-J (2003) *Eur J Inorg Chem*: 2529
152. Balland V, Mathieu D, Pons-Y-Moll N, Bartoli JF, Banse F, Battioni P, Girerd J-J, Mansuy D (2004) *J Mol Catal A Chem* 215:81
153. Buxton GV, Greenstock CL, Helman PW, Ross AB, Tsang W (1988) *J Phys Chem Ref Data* 17:513
154. MacFaul PA, Ingold KU, Wayner DDM, Que L Jr (1997) *J Am Chem Soc* 119:10594
155. Groves JT, Nemo TE (1983) *J Am Chem Soc* 105:6243
156. Lubben M, Meetsma A, Wilkinson EC, Feringa BL, Que L Jr (1995) *Angew Chem Int Ed* 34:1512
157. Kim J, Harrison RG, Kim C, Que L Jr (1996) *J Am Chem Soc* 118:4373
158. Zang Y, Kim J, Dong Y, Wilkinson EC, Appelman EH, Que L Jr (1997) *J Am Chem Soc* 119:4197
159. Lehnert N, Ho RYN, Que L Jr, Solomon EI (2001) *J Am Chem Soc* 123:12802
160. Lehnert N, Ho RYN, Que L Jr, Solomon EI (2001) *J Am Chem Soc* 123:8271
161. Lim MH, Rohde J-U, Stubna A, Bukowski MR, Costas M, Ho RYN, Muenck E, Nam W, Que L Jr (2003) *Proc Natl Acad Sci U S A* 100:3665
162. Duban EA, Bryliakov KP, Talsi EP (2007) *Eur J Inorg Chem*: 852
163. Lobanova MV, Bryliakov KP, Duban EA, Talsi EP (2003) *Mendeleev Commun* 13:175
164. Duban EA, Bryliakov KP, Talsi EP (2005) *Mendeleev Commun* 15:12
165. Park MJ, Lee J, Suh Y, Kim J, Nam W (2006) *J Am Chem Soc* 128:2630
166. Makhlynets OV, Rybak-Akimova EV (2010) *Chem Eur J* 16:13995
167. Que L Jr, Tolman WB (2008) *Nature* 455:333
168. Lyakin OY, Bryliakov KP, Britovsek GJP, Talsi EP (2009) *J Am Chem Soc* 131:10798
169. Fenton HJH (1876) *Chem News*: 190

Iron-Catalyzed Reduction and Hydroelementation Reactions

Christophe Darcel and Jean-Baptiste Sortais

Abstract During the last two decades, iron has proved to be an interesting transition metal which is a highly valuable alternative to classical precious ones for catalyzing organic transformations including the reduction of unsaturated C–C or C–heteroatom bonds. This chapter summarizes the rapid development of iron catalyzed selective reductions of alkene, alkyne, carbonyl and carboxylic derivatives. The emerging topic of hydroboration of alkenes and alkynes is also described.

Keywords Alkenes · Alkynes · Carbonyl derivatives · Carboxylic acid derivatives · Hydroboration · Hydrogen transfer · Hydrogenation · Hydrosilylation · Iron · Reduction

Contents

1	Reduction of Alkynes and Alkenes	175
1.1	Hydrogenation and Transfer Hydrogenation	175
1.2	Hydrosilylation	178
2	Reduction of Aldehydes and Ketones	183
2.1	Hydrogenation Reactions	183
2.2	Transfer Hydrogenation	187
2.3	Hydrosilylation Reactions	192
3	Reduction of Imines and Nitro-derivatives and Reductive Amination of Carbonyl Compounds	198
3.1	Reduction of Imines	198
3.2	Reduction of Nitrile and Nitro-compounds En Route to Primary Amines	200
3.3	Direct Reductive Amination (DRA)	201

4	Reduction of Carboxylic Acid Derivatives and Carbon Dioxide	202
4.1	Amides	202
4.2	Nitriles	203
4.3	Carboxylic Esters	204
4.4	Carboxylic Acids	206
4.5	Ureas	207
4.6	Carbon Dioxide and Formic Acid	207
5	Reduction of Sulfoxides	209
6	Hydroboration of Alkenes and Alkynes	210
7	Conclusion	211
	References	212

Abbreviations

cat	Catechol
cod	1,5-Cyclooctadiene
Cp	Cyclopentadienyl
dcpe	1,2-Bisdicyclohexylphosphinoethane
DBU	1,8-Diazabicyclo[5.4.0]undec-7-ene
DFT	Density functional theory
Dipp	2,6-Diisopropylphenyl
DMC	Dimethyl carbonate
DRA	Direct reductive amination
EDTA-Na ₂	Ethylenediaminetetraacetic acid disodium salt
IMes	1,3-Bis(2,4,6-trimethylphenyl) imidazole-2-ylidene
IPr	1,3-Bis(2,6-diisopropylphenyl) imidazole-2-ylidene
MD ⁺ M	[(MeO) ₂ MeSiH]
Mes	2,4,6-Trimethylphenyl
NHC	<i>N</i> -Heterocyclic carbene
NPs	Nanoparticles
pin	Pinacol
PMHS	Polymethylhydrosiloxane
<i>t</i> -PBO	<i>trans</i> -4-Phenyl-but-3-en-2-one
terpy	2,2':6',2''-Terpyridine
TFA	Trifluoroacetic acid
TMDS	1,1,3,3-Tetramethyldisiloxane
TMEDA	<i>N,N,N',N'</i> -Tetramethylethylenediamine
TMPP	Tris(2,4,6-trimethoxyphenyl)phosphine
TOF	Turnover frequency
TON	Turnover number

During the last two decades, iron has proved to be an interesting transition metal which is a highly interesting alternative to classical precious ones such as rhodium, ruthenium, platinum, or palladium for catalyzing organic transformations (for representative recent reviews and books on iron catalysis, see [1–7]), including

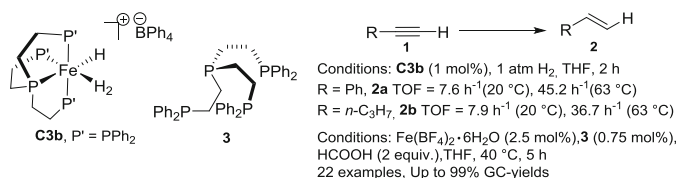
the reduction of unsaturated C–C or C–heteroatom bonds (for representative reviews on iron-catalyzed reductions, see [8–12]). Indeed, until recently, there were only scarce examples of applications of iron catalysts for such purposes, except for the classical Fischer–Tropsch and Haber–Bosch processes. In this chapter, the rapid development of numerous efficient iron-based systems able to perform selective reduction of alkenes, alkynes, and carbonyl and carboxylic acid derivatives will be reviewed. Lastly, the emerging topic of hydroboration of alkenes and alkynes will be described. Enantioselective reduction reactions, which will occasionally be illustrated in this chapter, will be discussed in detail in Chap. 8 of this volume.

1 Reduction of Alkynes and Alkenes

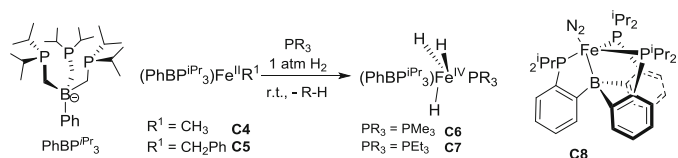
1.1 Hydrogenation and Transfer Hydrogenation

Even though pioneering contributions on the hydrogenation of alkenes and alkynes were reported starting in the early 1960s using iron species as catalysts, including $\text{Fe}(\text{CO})_5$ (**C1**), these reactions often suffered from drastic reaction conditions, lack of chemoselectivity, and a rather narrow scope of application (for representative examples, see [13–18]). In addition to hydrogenation reactions using molecular hydrogen, transfer hydrogenation using easy-to-handle and inexpensive liquid hydrogen donors such as alcohols or formic acid constitutes valuable alternative procedures for the reduction of carbonyl compounds. In the area of iron-catalyzed transfer hydrogenation, the first attempts were reported in the early 1970s using $[\text{FeCl}_2(\text{PPh}_3)_2]$ (**C2a**) and $[\text{FeBr}_2(\text{PPh}_3)_2]$ (**C2b**), respectively, as catalysts for the hydrogenation of the 1,5-cyclooctadiene (1,5-COD). Catechol derivatives served as hydrogen sources under harsh conditions (160–240°C), making them less attractive [19, 20].

The first breakthrough in this area was achieved by Bianchini et al. in the early 1990s, reporting the selective hydrogenation of terminal alkynes to the corresponding alkenes using iron(II) hydride catalyst precursors with tetraphosphine ligands $[(\mathbf{3})\text{FeH}(\text{N}_2)]\text{BPh}_4$ (**C3a**) and $[(\mathbf{3})\text{FeH}(\text{H}_2)]\text{BPh}_4$ (**C3b**) [$\mathbf{3}=\text{P}(\text{CH}_2\text{CH}_2\text{PPh}_2)_3$] under mild conditions (rt, 1 atm of H_2 , Scheme 1) [21, 22]. The selectivity of the reaction is rationalized mechanistically by the insertion of the coordinated alkyne into the Fe–H bond leading to a Fe–vinyl species which was then cleaved via an intramolecular protonolysis. It must be noted that the same catalyst (**C3b**) can be used for the reduction of α,β -unsaturated ketones in hydrogen transfer reactions using cyclopentanol as the hydrogen donor with unpredictable selectivity [23]. In 2012, Beller et al. reported an in situ generated active catalytic system obtained from $\text{Fe}(\text{BF}_4)_2 \cdot 6\text{H}_2\text{O}$ and the tetraphosphine ligand **3** for the selective catalytic transfer hydrogenation of terminal arylalkynes to styrenes by hydrogen transfer with formic acid as the hydrogen source under base-free



Scheme 1 Selective iron-catalyzed hydrogenation of alkynes to alkenes

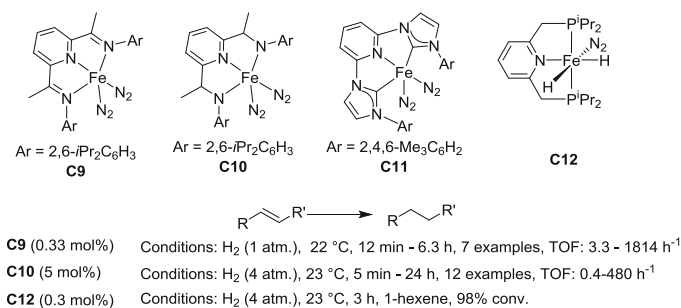


Scheme 2 Iron complexes bearing multidentate ligands for the hydrogenation of alkenes and alkynes

conditions at 40 °C for 5 h [24]. A wide scope of phenylacetylene derivatives can be selectively reduced to the corresponding styrenes, and remarkable chemoselectivities can be achieved with arylethyne bearing potentially reducible functional groups such as ketones or esters. The catalytic system can be also applied to heteroarylethyne and aliphatic terminal alkynes but not to internal alkynes. A fluoro-iron intermediate [Fe(F)(3)]⁺ was proposed as an active catalytic species which leads to the [Fe(3)(η²-H₂)(F)]⁺ intermediate after elimination of CO₂.

Similarly, several multidentate ligands have been used in combination with iron to perform such a hydrogenation reaction. Peters et al. developed a series of tri(phosphino)borate-supported iron(II) alkyl (**C4–C5**) and iron(IV) trihydride complexes (**C6–C7**) which can be used as pre-catalysts (10 mol%) for the hydrogenation of various unfunctionalized olefins and 2-pentyne under 1–4 atm H₂ at room temperature leading to the corresponding alkanes with a TOF up to 24 h⁻¹ [25]. Using similar complexes (**C8**) (3.33 mol%), the hydrogenation of alkenes and phenylacetylene led to the respective alkanes, under 1 atm of hydrogen in *d*⁶-benzene, at room temperature with TOFs up to 15 h⁻¹ for ethylene (Scheme 2) [26].

Another important breakthrough in this area was achieved by Chirik who reported a series of highly active iron(0,II) complexes bearing tridentate pyridinylidene pincer-type ligands, diimine ligands [27] and pyridine-di(NHC) ligands in the hydrogenation of alkenes and alkynes. Using 0.3 mol% of [(^tPrPDI)Fe(N₂)₂] (**C9**), at 22 °C under 4 atm of H₂, olefins can be efficiently reduced with TOFs up to 1,814 h⁻¹ (Scheme 3). The hydrogenation of 1-hexene took only 12 min. Notably, with internal alkenes, longer reaction times were required and only the *gem*-disubstituted C=C bond of (+)-(*R*)-limonene was selectively reduced. Alkynes such as diphenylacetylene can be also reduced to 1,2-diphenylethane via the initial formation of *cis*-stilbene [28]. It was shown that the ligand plays the role of an electron reservoir, able to accept up to three electrons from the iron center. Using the diamidopyridine pincer-type complex (**C10**, 5 mol%), at 23 °C under 4 atm of



Scheme 3 Chirik's catalytic systems for the hydrogenation of alkenes

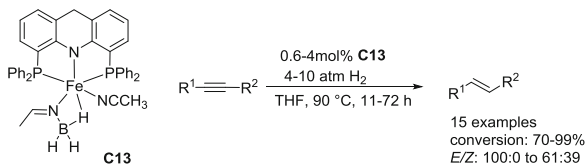
H₂, excellent functional group tolerance was observed for the hydrogenation of alkenes bearing reducible functional groups such as ketones, esters, amides, ethers, or unprotected amines. Unlike α,β -unsaturated ketones that led to the decomposition of the iron complex, α,β -unsaturated esters were selectively reduced to the corresponding saturated esters with TOFs up to 240 h⁻¹ [29].

For the more challenging hydrogenation of hindered C=C bond, Chirik developed pyridine-di(NHC)-based iron complexes such as **C11** and succeeded to hydrogenate unfunctionalized, trisubstituted alkenes (Scheme 3) [30]. Complex **C11** also was shown to hydrogenate tetra-substituted alkenes such as 2,3-dimethyl-1*H*-indene but with moderate conversion (68%) after 48 h and a 3:1 ratio of *cis*-/*trans*-diastereomers of the alkane. For the hydrogenation of ethyl 3,3-dimethylacrylate, the best catalyst was the 2,6-diisopropylphenyl-substituted analog which gave 95% conversion after 1 h of reaction, similar to the result obtained with [(^{Me}PDI)Fe(N₂)₂]₂(μ -N₂).

Chirik also described the analogous bis(diisopropylphosphino)pyridine pincer-type ligand (^{*i*}PrPNP) iron(II) hydride complexes *cis*-[(^{*i*}PrPNP)Fe(H)₂N₂] **C12**, which was active in the hydrogenation of 1-hexene under mild conditions (rt, 4 atm. H₂, Scheme 3) [31]. Similarly, Milstein et al. reported the use of a new iron pincer complex **C13** based on an acridine-based PNP ligand as the catalyst (0.6–4 mol%) to perform semi-hydrogenation of terminal alkynes to produce *E*-alkenes in THF at 90°C for 11–72 h under 4–10 atm of H₂, with small amounts of over-reduced alkanes as the by-product [32]. Noteworthy, this catalytic system tolerated functional groups such as esters, nitriles, ketones, and trimethylsilyl groups. Starting from terminal alkynes such as phenylacetylene, the corresponding styrenes were obtained quantitatively (Scheme 4).

Recently, using diphosphine iron dialkyl complexes and more particularly [Fe(L)(CH₂SiMe₃)₂] (**C14**, L = (*R*)-1{(*SP*)-2-[di-(2-furyl)phosphine]ferrocenyl} ethyldi-*tert*-butylphosphine) as the catalysts, Chirik succeeded to hydrogenate unfunctionalized alkenes using 5 mol% of (**C14**) under 4 atm of H₂ at 23°C for 24 h. However, no significant enantioselectivity was observed when prochiral olefins were employed, suggesting a heterogeneous process [33].

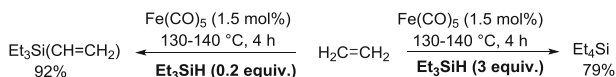
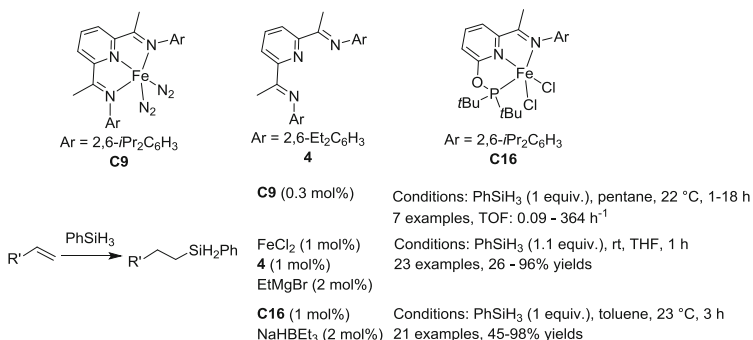
Scheme 4 Iron-catalyzed hydrogenation of alkynes to *E*-alkenes



Interestingly, some scarce examples of iron nanoparticle-catalyzed hydrogenation reactions were also reported. De Vries described the catalytic hydrogenation of alkenes and alkynes using Fe nanoparticles [34, 35] prepared by the method developed by Bedford by reducing a solution of FeCl_3 with 3 equiv. of EtMgCl in THF or Et_2O [36]. Terminal, 1,2-*cis*- and 1,1-disubstituted alkenes were reduced quantitatively after 15 h at rt under 1 atm. of H_2 . More drastic conditions (100°C) were necessary to hydrogenate 1,2-*trans*-disubstituted and cyclic *cis*-alkenes. Usually, tri- and tetra-substituted alkenes cannot be reduced. To perform the full reduction of alkynes to alkanes, more drastic conditions were required (20 atm of H_2 at 25°C for 15 h). Fe nanoparticles supported on chemically derived graphene can also be efficient for similar hydrogenations (20 atm of H_2 , 100°C , 24 h) and the catalyst can easily be separated by magnetic decantation [37]. Uozumi et al. developed amphiphilic, polymer-stabilized $\text{Fe}(0)$ nanoparticle catalysts for the hydrogenation of alkenes, styrenes, and alkynes in ethanol under 20–40 atm of H_2 at 80– 100°C in a flow reactor. Note the high chemoselectivity of the reduction as ketones, esters, arenes, and nitro-functionalities were tolerated [38]. Beller and Chaudret also described the use of well-defined ultrasmall iron(0) nanoparticles (NPs) as catalysts for the selective hydrogenation of various alkenes and alkynes to alkanes under mild conditions (2.4 mol% NPs, rt, 10 bar H_2 for 20 h). Monodisperse iron nanoparticles (about 2 nm size) were prepared by the decomposition of $\{\text{Fe}[\text{N}(\text{SiMe}_3)_2]_2\}_2$ under 3 bar of H_2 at 150°C for 2 h [39].

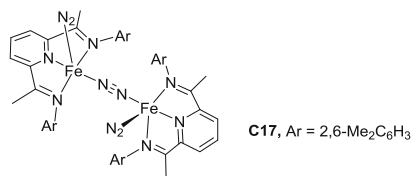
1.2 Hydrosilylation

The catalyzed hydrosilylation of alkenes is of great importance in the production of silicon derivatives [40]. Accordingly, there are numerous methods to perform such transformations including the use of Speier's catalyst [41] $[\text{H}_2\text{PtCl}_6] \cdot 6\text{H}_2\text{O}/i\text{PrOH}$ and the more active and selective Karstedt catalyst, $\{\text{Pt}_2[\text{Me}_2\text{SiCH}=\text{CH}_2)_2\text{O}_3\}$ [42, 43]. The last decades have also seen the development of iron-based catalysts. In a pioneering contribution in 1962, Nesmeyanov et al. [44] reported reactions of olefins with hydrosilanes in the presence of $\text{Fe}(\text{CO})_5$ (**C1**) or colloidal iron as the catalysts to yield a mixture of alkylsilanes (resulting from hydrosilylation reactions) and vinylsilanes (from dehydrogenative silylation processes). Only when the reaction was performed with ethylene and triethylsilane, a selective reaction occurred, depending on the amount of triethylsilane: when performed with 0.2 equiv. of triethylsilane, triethylvinylsilane was obtained specifically with 92% yield. With

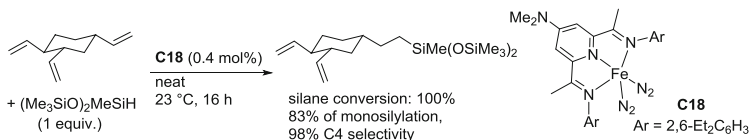
**Scheme 5** Fe(CO)₅-catalyzed hydrosilylation of alkenes**Scheme 6** Iron-catalyzed hydrosilylation of alkenes

3 equiv. of triethylsilane, tetraethylsilane was produced with 79% yield as the sole product (Scheme 5). Noticeably, under photoirradiation conditions, Fe(CO)₅ can catalyze reactions of alkenes with trialkylsilanes and lead to mixtures of alkanes, alkylsilanes, and alkenylsilanes [45]. Using Fe₃(CO)₁₂ (**C15**) as the catalyst, the reaction of styrene with triethylsilane led selectively to (*E*)-β-(triethylsilyl)styrene Ph-CH=CH-SiEt₃ with yields up to 89%. No traces of products resulting from the hydrosilylation of the styrenes were observed [46].

In 2004, during his studies on well-defined diimino-pyridine iron(0) dinitrogen complexes, Chirik also described their use as effective pre-catalysts for hydrosilylations of alkynes and alkenes (see reference [27]; [47]). The hydrosilylation of terminal or cyclic alkenes using 1 equiv. of phenylsilane as the hydrosilane source led exclusively to the anti-Markovnikov products with TOFs up to 364 h⁻¹. The low loading of the pre-catalyst (**C9**) used (0.3 mol%) and the mild reaction conditions (22 °C for 1–18.5 h, Scheme 6) must be pointed out. During the hydrosilylation of internal alkenes such as *trans*-2-hexene, mixtures of hexylsilanes were obtained due to the isomerization of the C=C bond after 70 h at 22 °C. Diphenylacetylene can also react with phenylsilane to give selectively the corresponding (*E*)-vinylsilane in quantitative yield. Similar results were obtained utilizing an in situ iron(0) catalytic species generated from the bis-iminopyridine ligand (**4**) (1 mol%), FeCl₂ (1 mol%) and NaBHEt₃ (2 mol%) [48]. Notably, a nice tolerance toward functional groups such as anilines, esters, ketones, aldimines, and nitriles was observed, and the catalytic system can be used for the hydrosilylation of internal alkynes to produce (*E*)-vinylsilanes and terminal alkynes to lead to (*Z*)-vinylsilanes.



Scheme 7 Nitrogen-bridged diiron complex **C17**



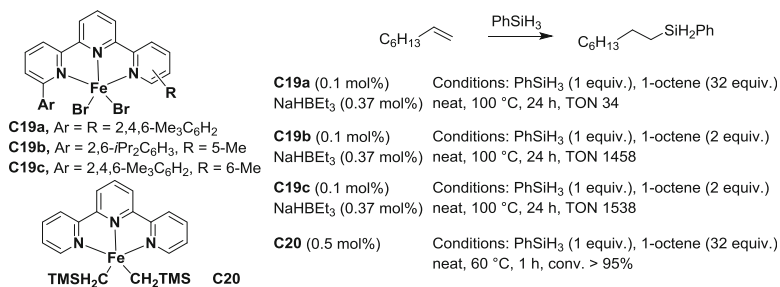
Scheme 8 Iron-catalyzed selective hydrosilylation of 1,2,4-trivinylcyclohexane

Importantly, the stoichiometric reaction of the complex (**C9**) with phenylsilane led to the bis-(σ -silane) iron(0) complex, whose structure was established by X-ray analysis. This complex was also very active in the hydrosilylation of 1-hexene [28].

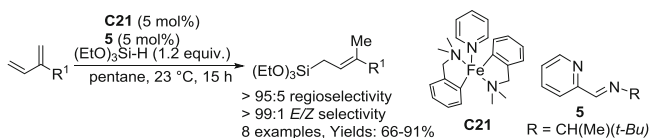
Using the nitrogen-bridged complex **C17**, a highly increased activity for the hydrosilylation of terminal alkenes was observed, as 0.004 mol% of **C17** was able to perform the complete hydrosilylation of 1-octene under neat reaction conditions at 23 °C after only 15 min using MD'M [(MeO)₂MeSiH] as the tertiary hydrosilane (Scheme 7). Only 0.007 mol% of **C17** was necessary to obtain full conversion with (OEt)₃SiH in 15 min and only 0.02 mol% of **C17** with Et₃SiH gave full conversion after 45 min [49]. This complex also allowed for the anti-Markovnikov hydrosilylation of styrene, *N,N*-dimethylallylamine, and allylpolyethers.

The complex **C9** is also active for the hydrosilylation of 1,2,4-trivinylcyclohexane with tertiary alkoxy silanes, an important process used in the manufacture of tires with low rolling resistance, involving the hydroelementation of only one of the three C=C bonds (Scheme 8). Notably, **C9** exhibited unprecedented regioselectivity for the monohydrosilylation of the desired 4-vinyl moiety (conversion of MD'M: 70%, 33% of monosilylated compound with 98% of C4 selectivity after 3 h at 23 °C). Interestingly, the modified complex **C18** gave a better result under similar conditions (conversion of MD'M: 83%, 60% of monosilylated compound with 98% of C4 selectivity) [50]. Prolonging the reaction for 16 h gave full conversion of the silane and afforded the desired C4-silylated product in 83% yield (Scheme 8). It must be pointed out that these iron complexes gave results which exceed the ones obtained with commercially used platinum compounds.

Interestingly, Huang developed a new family of phosphinite-iminopyridine-based iron complexes for the chemoselective hydrosilylation of functionalized olefins [51]. Using 1 mol% of **C16** in the presence of 2 mol% of NaBHET₃, various alkenes can be reduced in toluene at 23 °C for 3 h with 1 equiv. of either PhSiH₃ or Ph₂SiH₂ (Scheme 6). Notably, the unprecedented functional group tolerance must be outlined, as ketones, esters, and amides did not react, which differs from the



Scheme 9 Terpyridine-based iron complex for hydrosilylation of alkenes



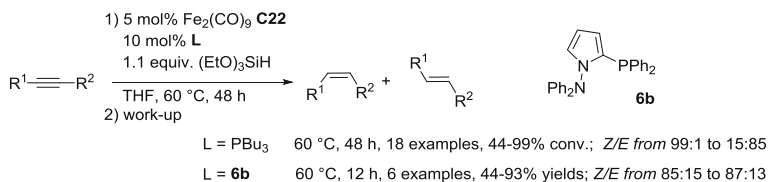
Scheme 10 Iron-catalyzed hydrosilylation of 1,3-dienes

chemoselectivity observed with Chirik's catalysts. By contrast, styrenes and internal C=C bond were not hydrosilylated.

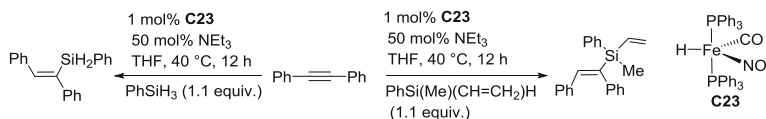
Terpyridine ligands have also been successfully applied in the hydrosilylation of olefins. Nakazawa et al. reported a series of substituted terpyridine iron halide complexes and identified some active ones such as **C19a–c**: the catalytically active species generated in situ by reaction of **C19a–c** with NaHBET₃ catalyzed the hydrosilylation of 1-octene with phenylsilane under neat reaction conditions at 100 °C for 24 h (Scheme 9). Unsymmetrically substituted terpyridine iron complexes revealed to be more active than the symmetrical one with moderate TONs at 100 °C (up to 1,530, **C19b–c** vs. **C19a**, Scheme 9) [52]. Simultaneously, Chirik described the terpyridine iron dialkyl complex (**C20**) as catalyst (0.5 mol%) for the hydrosilylation of 1-octene with tertiary hydrosilanes (Et₃SiH, MD'M) at 60 °C for 1 h. Notably, this catalyst can perform the chemoselective hydroelementation of vinylcyclohexene oxide without the alteration of the oxirane moiety [53].

Using a well-defined iron pre-catalyst (**C21**) (5 mol%) in combination with the iminopyridine ligand **5** (5 mol%), Ritter described the first 1,4-hydrosilylation of 1,3 dienes, affording allyl silanes in high regio- and stereoselectivities (linear/branch ratio from 95:5 to 99:1, and *E/Z* ratio >99:1) by reaction of 1,3-dienes with 1.2 equiv. of triethoxysilane at 23 °C for 15 h (Scheme 10) [54].

Specific iron complexes were also developed for the hydrosilylation of alkynes leading to the corresponding vinylsilanes. In 2011, Enthaler et al. published a selective reduction of alkynes to alkenes using iron–phosphine-based catalysts. Indeed, using an in situ generated catalyst from Fe₂(CO)₉ (**C22**, 5 mol%) and tributylphosphine (10 mol%) in the presence of 1.1 equiv. of (EtO)₃SiH, at 60 °C



Scheme 11 $\text{Fe}_2(\text{CO})_9$ /phosphine-catalyzed hydrosilylation of alkynes to alkenes



Scheme 12 Stereoselective $\text{Fe}(\text{H})(\text{CO})(\text{NO})(\text{PPh}_3)_2$ -catalyzed reduction of alkynes

for 48 h, the corresponding alkenes were obtained in high yields. Starting from internal alkynes, (*Z*)-alkenes were obtained as the major stereoisomers, except when substituted by carboxylate groups (Scheme 11). Notably, this catalytic system led to highly chemoselective reductions as numerous functional groups such as aldimines, esters, amides, alkenes, nitriles, and even epoxides can be tolerated [55].

Similarly, Enthaler also described catalytic systems based on $\text{Fe}_2(\text{CO})_9$ (**C22**) and a monodentate pyrrole–phosphine ligand (*N,N*-diphenyl-1*H*-pyrrol-1-amine-2-di-*R*-phosphine; $\text{R} = ^t\text{Bu}$, **6a**; $\text{R} = \text{Ph}$, **6b**), in the presence of $(\text{EtO})_3\text{SiH}$ as the reducing reagent (Scheme 11) [56]. It is important to note that two iron(0) tetracarbonyl–phosphine complexes were synthesized and characterized from the reaction of $\text{Fe}_2(\text{CO})_9$ (**C22**) with **6a** and **6b**, affording new iron complexes $[\text{Fe}(\text{CO})_4(\mathbf{6})]$. Nevertheless, under optimized conditions, the in situ regenerated catalyst gave higher yields and better selectivities than the direct use of the preformed, well-defined complexes.

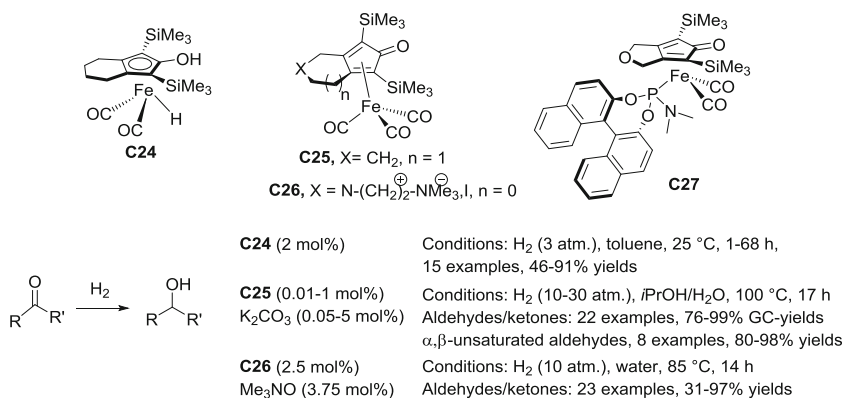
Plietker reported the use of the complex $[\text{Fe}(\text{H})(\text{CO})(\text{NO})(\text{PPh}_3)_2]$ (**C23**, 1 mol%) in the presence of triethylamine as an additive (50 mol%) for the selective hydrosilylation of internal alkynes to vinylsilanes (Scheme 12) [57]. It must be pointed out that the nature of the silane had a strong influence on the observed *E*- or *Z*-selectivity. For the hydrosilylation of diphenylacetylene, phenylsilane gave the best selectivity toward *Z*-vinylsilanes (*E/Z* up to 1/20; yields up to 98%), whereas tertiary silanes such as methylphenylvinylsilane $[\text{Ph}(\text{Me})(\text{CH}=\text{CH}_2)\text{Si-H}]$ gave the *E*-vinylsilane with a *E/Z* ratio of >20:1 (yields up to 97%). The nature of the internal alkyne is also crucial for the regioselectivity: as an example, the *E*-product was obtained from dialkylacetylene independently from the nature of the silane $[\text{PhSiH}_3$ or $\text{Ph}(\text{Me})(\text{CH}=\text{CH}_2)\text{Si-H}]$ (Scheme 12).

2 Reduction of Aldehydes and Ketones

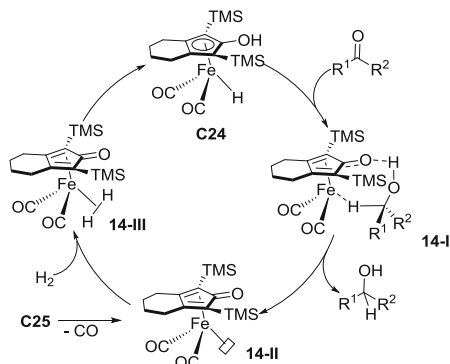
2.1 Hydrogenation Reactions

Selective hydrogenation and hydrogen transfer reactions of carbonyl derivatives are important reactions in both bulk and fine chemistry. Indeed, there is an increasing interest in the substitution of well-established noble transition metal catalysts with iron-based ones. In 1983, Markó described the first iron-catalyzed hydrogenation using $\text{Fe}(\text{CO})_5$ as the catalyst under drastic conditions (150°C – 100 bar of H_2 in triethylamine as the solvent) [58, 59]. In 2007, Casey et al. [60] reported one of the first efficient iron catalysts for the hydrogenation of aldehydes and ketones under mild conditions (3 atm of H_2 at room temperature) using a Knölker-type complex **C24** as the catalyst (Scheme 13) [61]. Nonconjugated $\text{C}=\text{C}$ and $\text{C}\equiv\text{C}$ are tolerated, but α,β -unsaturated ketones led to a mixture of derivatives due to the concomitant reduction of the $\text{C}=\text{C}$ bond.

Beller et al. developed a series of Knölker-type complexes such as **C25** which are air stable and able to catalyze the hydrogenation of aldehydes and ketones under 30 atm of H_2 at 100°C in a mixture of isopropanol/water as solvent. The reaction can tolerate esters, amides, and heterocycles and, more impressively, α,β -unsaturated aldehydes can be selectively reduced to the corresponding allylic alcohols [62]. The same complex **C25** can be also used as a catalyst for the reduction of aldehydes under water–gas shift conditions (10 atm of CO in DMSO/water at 100°C) [63]. Renaud et al. simultaneously developed Knölker-type complexes bearing ionic fragments such as ammonium salts **C26** which were able to perform the catalytic hydrogenation in water under 10 atm of H_2 at 85°C. Using this system, cyano-moieties can be tolerated, but the hydrogenation of α,β -unsaturated ketones led in the majority of the cases to a mixture of compounds resulting of concomitant reduction of the $\text{C}=\text{C}$ and $\text{C}=\text{O}$ bonds [64].



Scheme 13 Knölker-type complexes for the hydrogenation of ketones



Scheme 14 Outer-sphere mechanism for an iron-catalyzed hydrogenation reaction

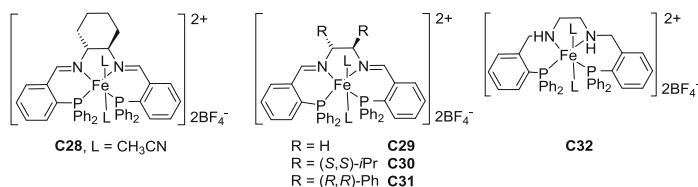


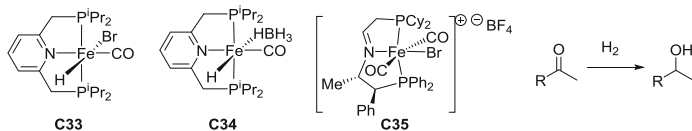
Fig. 1 Tetradentate diiminophosphine (PNNP) iron(II) complexes for hydrogenation reactions

In 2011, Berkessel et al. reported an asymmetric version of the hydrogenation of acetophenone using the modified Casey's catalyst **C27**, where one carbonyl ligand was substituted by a chiral phosphoramidite ligand under UV light irradiation [65], albeit only moderate enantiomeric excesses were obtained (up to 31% ee).

Noticeably, an outer-sphere mechanism was proposed to rationalize the catalytic cycle (Scheme 14) [66, 67]. Via a concerted hydride/proton transfer from the hydroxyl and the iron hydride to the carbonyl moiety, the intermediate **14-I** is formed and releases the alcohol and the 16 electron species **14-II** which can be also generated from (**C25**) by the nonreductive elimination of CO. The active species **C24** is then regenerated by heterolytic H₂ cleavage. This mechanism was supported by density functional theory (DFT) calculations and kinetic studies [68].

Based on their previous results with ruthenium complexes [69], Morris et al., in 2008, developed a series of chiral tetradentate diiminophosphine (PNNP) iron (II) complexes [70]. The complex [Fe(NCMe)₂{(R,R)-cyP₂N₂}](BF₄)₂ (**C28**, 0.44 mol%), in the presence of 6.7 mol% of ^tBuOK, was active in the hydrogenation of acetophenone to 1-phenylethanol (TOF = 5 h⁻¹ at 50°C) but with a moderate conversion (40%) and ee (27%) after 18 h under 25 atm of H₂ in *i*PrOH (Fig. 1).

The modification of the nature of the hydrocarbon bridge (N-CHR-CHR-N) of the ligand in chiral iron(II)-PNNP complexes showed that the activity was dependent on the substituents on the diamine moieties [71]. With an ethylene bridge (R = H) under similar experimental conditions, the corresponding complex **C29**



C33 (0.05 mol%)
KOtBu (0.1 mol%)

Conditions: PhCOMe, H₂ (4.1 atm.), EtOH, rt, 94% conv.
TON^(rt) = 1880; TOF^(rt) = 89 h⁻¹; TON^(40°C) = 1700; TOF^(40°C) = 425 h⁻¹

C34 (0.05 mol%)
no base

Conditions: PhCOMe, H₂ (4.1 atm.), EtOH, 40 °C, 89% conv.
TON = 1780; TOF = 296 h⁻¹

C35 (0.1 mol%)
LiAlH₄, *t*AmylOH

Conditions: *t*BuOK (1 mol%), H₂ (5 atm.), THF, 50 °C, 0.5–24 h,
21 examples, 20–99% conv., ee up to 85%; TON up to 990; TOF up to 1980 h⁻¹

Scheme 15 Hydrogenation of acetophenone catalyzed by the iron pincer complex **C33**

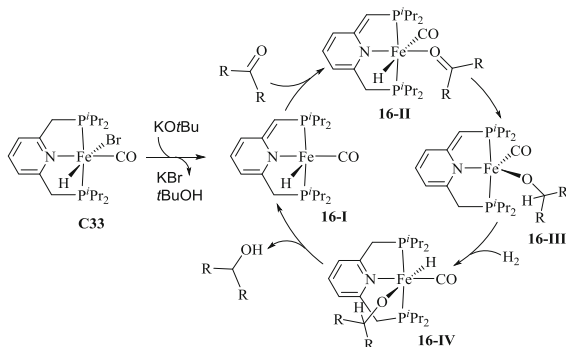
showed comparable moderate catalytic activities (conv. = 70–95%), even though the diaminodiphosphino iron complex (**C32**) exhibited slightly better activity than the corresponding diiminodiphosphino iron complex **C29** (conversion = 99%, TOF = 12 h⁻¹). By contrast, the complexes bearing more steric hindered substituents on the bridge (R = *i*Pr or Ph), such as the chiral complexes **C30** or **C31**, exhibited very low activity (conversion up to 4%). Under a mechanistic point of view, both catalysts based on an imine-type ligand (e.g., **C29**) and an amine-type one (e.g., **C32**) gave comparable activity, suggesting a similar, common active iron hydride intermediate in an outer-sphere mechanism via a secondary amino moiety of the ligand and the iron hydride [11].

In 2011, based on their previous reports on ruthenium-pincer complexes involving a new mode of cooperation between the ligand and the metal center via aromatization–dearomatization of the ligand [72–75], Milstein et al. published an elegant study about the hydrogenation of ketones catalyzed by a new iron(II) - diphosphino-pyridine pincer complex [Fe(Br)(H)(CO)(*i*PrPNP)] (**C33**) [76]. The complex **C33** was highly active in the hydrogenation of ketones, with a TOF of 425 h⁻¹ at 40 °C under 4.1 atm of hydrogen in ethanol. A good scope of several aromatic and aliphatic ketones was reported with 39–97% conversion and TONs up to 1,880 (Scheme 15). Nonetheless, functional groups such as cyano or amino seemed to inhibit the reduction, whereas no chemoselectivity was obtained for the reduction of α,β -unsaturated ketones.

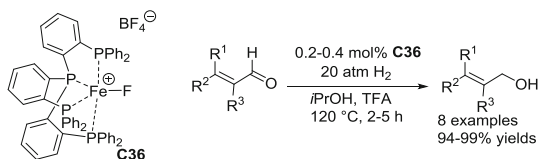
A plausible mechanism via an aromatization–dearomatization process of the diphosphine pyridine ligand was proposed, which aids with the activation of dihydrogen in a synergistic metal–ligand way (Scheme 16). A reactive, dearomatized species (**16-I**) was first produced and then coordinated the ketone leading to the intermediate **16-II**. After insertion of the coordinated ketone into the Fe–H bond, the obtained species **16-III** is capable of activating H₂, producing the hexacoordinate aromatic hydrido-alkoxy complex **16-IV**. The elimination of the alcohol finally regenerated the dearomatized species **16-I** [77].

Milstein et al. also reported an iron(II) pincer complex bearing both a hydride and a borohydride ligand [Fe(η^1 -BH₄)(H)(CO)(*i*PrPNP)] (**C34**) which showed catalytic activity similar to **C33** in the hydrogenation of acetophenone, even at a lower catalytic load (0.05 mol%) [78]. Noticeably, no additional base was necessary to

Scheme 16 Proposed reaction mechanism for the hydrogenation of ketones catalyzed by **C33**



Scheme 17 Iron-catalyzed chemoselective hydrogenation of α,β -unsaturated aldehydes

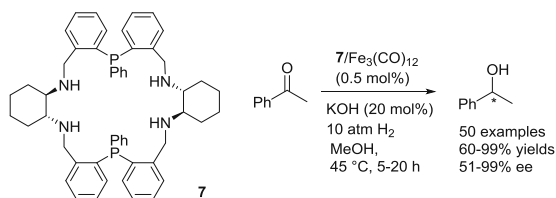


promote the hydrogenation of ketones. Complex (**C34**) exhibited the highest turnover number reported to date for iron-catalyzed hydrogenation of ketones (TON = 1,780 for 2-acetylpyridine, Scheme 15).

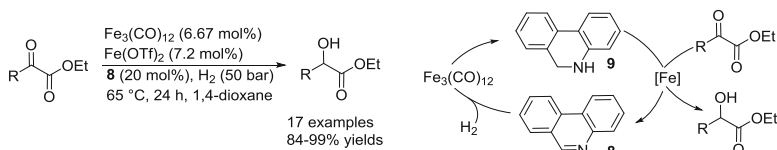
Recently, Morris described the use of chiral unsymmetrical P–N–P' iron pincer complexes, *mer-trans*-[Fe(Br)(CO)₂(P–CH=N–P')][BF₄] (**C35**), for the asymmetric hydrogenation of ketones in THF at 50 °C and 5 atm H₂ with *t*BuOK as a catalytic additive (Scheme 15) [79]. Starting from the bromo-iron complex (**C35**), by reaction with LiAlH₄ followed by the reaction with an alcohol ROH, a mixture of iron hydride complexes *mer*-[Fe(OR)(H)(CO)(Cy₂P–CH₂–NH–PPh₂)] were obtained as the pre-catalysts. A large variety of (hetero)arylalkylketones were hydrogenated with 20–90% conversion and ees up to 85%. Notably, high activities were observed as TONs up to 990 and TOFs up to 1,980 h⁻¹ were obtained.

Iron complexes bearing multidentate ligands can also be used for the hydrogenation of carbonyl compounds. The cationic iron–tetraphos fluoride complex **C36** (0.2–1.0 mol%), in the presence of 1–5 mol% of trifluoroacetic acid (TFA) in isopropanol under 20 atm of hydrogen at 120 °C for 2–5 h, was able to reduce aromatic and aliphatic aldehydes to give the corresponding alcohols in 95–99% yields [80]. Noticeably, reducible functional groups such as esters, sulfides, C=C bonds, and even ketones were tolerated. Notably, α,β -unsaturated aldehydes were chemoselectively hydrogenated leading to the corresponding allylic alcohols in 94–99% yields (Scheme 17). In a plausible mechanism supported by NMR and DFT investigations, the catalytically active species [(P₄)Fe–H][BF₄] was proposed to be generated from the iron fluoride complex **C36** by oxidative addition of H₂ followed by reductive elimination of HF.

Using the chiral N₄P₂ 22-membered macrocyclic ligand **7** associated to Fe₃(CO)₁₂ (**C15**) as an in situ generated catalyst (0.5 mol%), J. Xiao, J. Gao



Scheme 18 $\text{Fe}_3(\text{CO})_{12}/\mathbf{7}$ -based catalyst for asymmetric hydrogenation of ketones



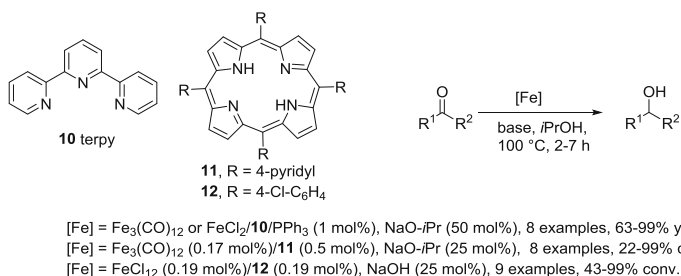
Scheme 19 Iron-catalyzed hydrogenation of α -ketoesters

et al. reported an asymmetric hydrogenation of various (hetero)arylalkyl ketones with ees up to 99% and with good functional group tolerance (cyano, iodo, bromo, and α,β -C=C, Scheme 18) [81]. Interestingly, under 50 bar of hydrogen at 65°C for 30 h in ethanol, β -ketoesters can be also reduced to afford the corresponding chiral hydroxyesters.

Using two different iron complexes, $\text{Fe}_3(\text{CO})_{12}$ (6.67 mol%) and $\text{Fe}(\text{OTf})_2$ (7.2 mol%), in a consecutive way in the presence of phenanthridine **8** as the ligand (20 mol%), the reduction of α -ketoesters gave the corresponding α -hydroxyesters (Scheme 19) [82]. Indeed, $\text{Fe}_3(\text{CO})_{12}$ catalyzed the hydrogenation of phenanthridine **8** to the corresponding hydrogenated reagent **9** which then acts as a direct hydride source to selectively reduce the α -keto C=O unit in a hydrogen transfer process catalyzed by $\text{Fe}(\text{OTf})_2$ (Scheme 19).

2.2 Transfer Hydrogenation

In the 1980s, Vancheesen et al. described a catalytic transfer hydrogenation of ketones using iron carbonyl complexes including the most effective $\text{Fe}_3(\text{CO})_{12}$ (**C15**, 4 mol%) in the presence of 1-phenylethanol or isopropanol as the hydride source and benzyltriethylammonium chloride and 18-crown-6 as phase transfer catalysts at 28°C for 2.5 h with moderate 20–60% conversions and TOFs up to 13 h⁻¹ [83, 84]. The use of the simple triphenylphosphine in combination with 2,2':6',2''-terpyridine (terpy, **10**) and $\text{Fe}_3(\text{CO})_{12}$ (**C15**) or FeCl_2 led to an efficient catalytic system for the transfer hydrogenation of aliphatic and aromatic ketones, in the presence of *i*PrONa (2 mol%) and isopropanol as the hydrogen source (Scheme 20) [85]. In situ catalysts prepared from either $\text{Fe}_3(\text{CO})_{12}$ (**C15**) or FeCl_2 in combination with porphyrins (**11–12**) also showed very good activity in



Scheme 20 Transfer hydrogenation of ketones

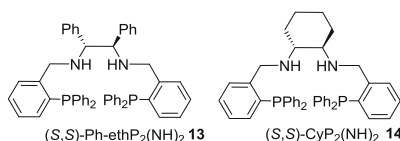


Fig. 2 Gao's P-NH-NH-P ligands for asymmetric transfer hydrogenation of ketones

the reduction of a large variety of ketones including α -substituted alkoxyketones in 22–99% conversions and TOFs of up to 642 h^{-1} [86, 87]. Unfortunately, the system exhibited some drawbacks such as a base-dependent reactivity and high reaction temperatures (100°C) as it has been shown before that simple bases can promote the reduction of aldehydes and ketones by transfer hydrogenation at lower temperatures [88].

Using diaminodiphosphine ligands (P_2N_2), this reaction can be performed under milder conditions, even at room temperature. The first example by Gao et al. in 2004 described the asymmetric transfer hydrogenation of ketones using an in situ generated active catalyst (1 mol%) from $[\text{NHEt}_3][\text{Fe}_3\text{H}(\text{CO})_{11}]$ (**C37**) and tetradentate P-NH-NH-P ligands, namely, (*S,S*)-Ph-ethP₂(NH)₂ (**13**) and (*S,S*)-CyP₂(NH)₂ (**14**) (Fig. 2) [89]. Using 80 mol% of KOH in isopropanol at 65°C for 21 h, the best results were obtained for the reduction of $\text{Ph}_2\text{CHCOCH}_3$, with ees up to 98% but with low yields (18%). For the reduction of classical ketones such as acetophenone, 56% ee and 92% yield were obtained.

Using the same type of ligands, Morris et al. reported in 2008 the asymmetric transfer hydrogenation of ketones to alcohols using well-defined iron(II) complexes *trans*-(*R,R*)-[Fe(CyP₂N₂)(NCMe)(CO)](BF₄)₂ **C38** and *trans*-(*R,R*)-[Fe(CyP₂N₂)(NCMe)(*t*BuCN)](BF₄)₂ **C39** (which were found to be inactive for hydrogenation reactions), with 18–61% ees (Fig. 3) [70]. Complex **C38** was an efficient catalyst for the reduction of benzaldehyde (94% conversion, rt, 2.4 h) and *N*-benzylideneaniline (>99%, rt, 17 h), but more difficult substrates such as ketimine ($\text{PhC}(\text{Me})=\text{CPh}$) were only reduced with conversion <5% after 17 h, while cyclohexanone showed no reactivity. By contrast, the reduction of aromatic ketones led to the corresponding alcohols with good conversions but moderate enantiomeric excesses. Complex **C38** also works for the transfer hydrogenation of α - β -unsaturated

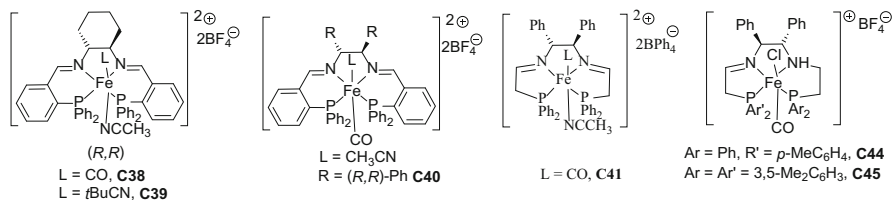
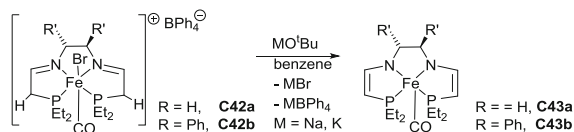


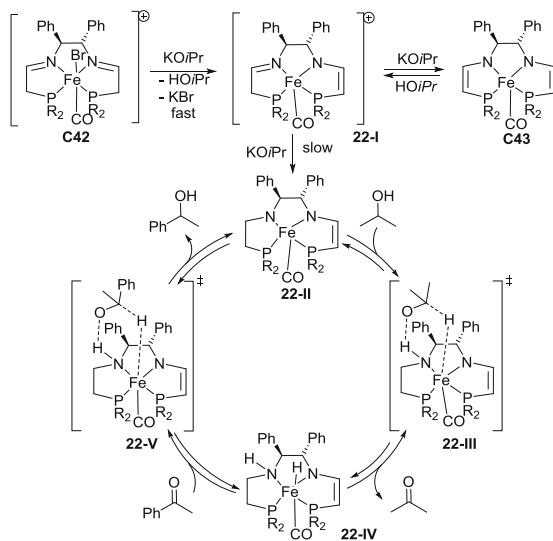
Fig. 3 Morris' catalysts active in catalytic transfer hydrogenation from 2-propanol



Scheme 21 Synthesis of neutral pentacoordinate Fe(II)-N₂P₂ complexes

ketones (*E*-PhCH=CHCOMe) leading to a mixture of the α,β -unsaturated alcohol (18% conversion, 45% ee) and the saturated alcohol (82% conversion, 27% ee). The complex **C39** showed better enantioselectivity but lower activity. Noticeably, the activity of **C38** is significantly better than those previously reported at rt (2,600 h⁻¹ TOF for acetophenone, 35% ee at 24°C) [90].

The same group then developed numerous analogs of **C38** in order to improve the enantiomeric induction. With **C40** (0.17–0.5 mol%), ees up to 96% were obtained, in particular with more sterically hindered ketones, with similar catalytic activity (TOF up to 2,000 h⁻¹) under mild conditions [90]. Following these preliminary results, Morris reported a systematic study involving a new family of diiminophosphine iron(II) complexes (17 examples, Fig. 3) [91–95]. The complex **C41** exhibited a higher activity and selectivity compared to the previously reported complexes **C38–40**. As a representative example, the reduction of acetophenone led to 90% conversion and ees up to 82%, (22°C, 30 min, 0.05 mol% catalyst loading) with a TOF of 3,600 h⁻¹. For other ketones, at rt for 8–200 min, 35–90% conversion and 14–99% ees were obtained. Notably, the reduction of *E*-PhCH=CHCOMe showed a high chemoselectivity and led to the α,β -unsaturated alcohol (82% conversion, 60% ee) with trace amount of the saturated alcohol (4% conversion, 25% ee). With **C41**, an optimized TOF of 21,000 h⁻¹ was observed at 28°C. One obvious character of these systems is the high amount of base (8 equiv. of KO^tBu with respect to [Fe]) required for the activation of the catalyst. In order to rationalize the role of base in the reaction, Morris and co-workers prepared a new family of neutral ene-amido pentacoordinate iron(II)-N₂P₂ complexes **C43a–b** by deprotonation with KO^tBu at the carbon α to the phosphorus center of the complexes **C42a–b** (Scheme 21). Under base-free conditions, transfer hydrogenation of acetophenone (**C43a–b**) showed similar behavior compared to their parent complexes. This is a clue that ene-amido compounds are intermediates in the base activation of iron(II)-N₂P₂ complexes in catalytic transfer hydrogenations [96].



Scheme 22 Proposed outer-sphere mechanism for the transfer hydrogenation of ketones

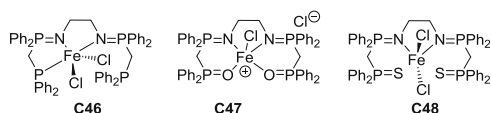
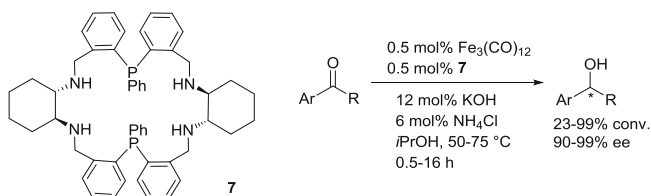


Fig. 4 Iminophosphorane diorganophosphorus-based iron complexes for catalytic hydrogen transfer of acetophenone

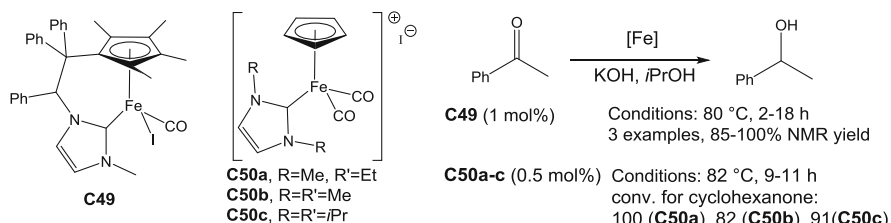
Via detailed kinetic [76] and DFT [77] studies, it was shown that starting from **C42** or **C43**, an imino/enamido intermediate complex **22-I** was formed and reacted slowly with $\text{KO}i\text{Pr}$ to generate the active catalytic species **22-II** (Scheme 22). Presumably via an outer-sphere process with isopropanol, the iron hydride species **22-IV** was generated and reacted with acetophenone to produce the 1-phenylethanol.

Morris also reported a family of amine(imine)diphosphine chloro-iron complexes for the efficient asymmetric transfer hydrogenation of ketones. Using 0.016–0.05 mol% of complexes (**C44–45**) in isopropanol in the presence of 0.033–0.4 mol% of KO^tBu , acetophenone can be reduced with ees up to 90% and TOFs up to 119 s^{-1} (for **C45**, Fig. 3) [97].

Le Floch et al. developed a series of related iron complexes bearing tetradentate ligands bearing two iminophosphorane moieties with two phosphines and thiophosphino and phosphine oxide groups (Fig. 4) [98]. The versatile coordination of these ligands to iron(II) metal centers such as the $[\text{FeCl}_2(\text{THF})_{1.5}]$ precursor led to the corresponding complexes $[\text{FeCl}_2(\text{P}_2\text{N})]$ (**C46**), $[\text{FeCl}_2(\text{O}_2\text{N}_2)]$ (**C47**), and $[\text{FeCl}_2(\text{N}_2)]$ (**C48**). Using 0.1 mol% of the three complexes **C46–C48** and 4 mol%



Scheme 23 In situ catalyst obtained from $\text{Fe}_3(\text{CO})_{12}$ and the N_4P_2 22-membered macrocyclic ligand **7** for enantioselective transfer hydrogenation of ketones



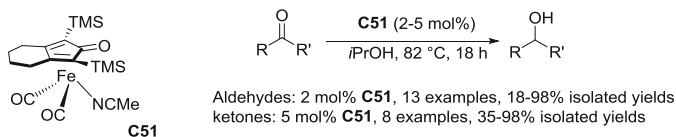
Scheme 24 NHC–Fe piano-stool for transfer hydrogenation of ketones

NaO^iPr for 6–8 h in isopropanol, acetophenone can be reduced at 82 °C in 80–91% conversions.

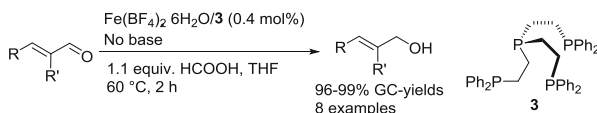
Similarly to hydrogenation reactions, using 0.5 mol% of a catalyst generated in situ from the chiral 22-membered macrocycle P_2N_4 ligand **7** in combination with $\text{Fe}_3(\text{CO})_{12}$ (**C15**), an asymmetric transfer hydrogenation of ketones was reported at 65 °C in isopropanol in the presence of 12 mol% of KOH and 6 mol% of NH_4Cl (Scheme 23) [99]. High activities (TOFs up to $1,940 \text{ h}^{-1}$), high conversions (up to 99%) and excellent enantioselectivities (up to 99% ee) were obtained.

Using cyclopentadienyl-functionalized *N*-heterocyclic carbene ligands, Royo reported tethered Cp–NHC–iron complexes such as (**C49**) as efficient catalysts for transfer hydrogenation of acetophenone, benzophenone, and cyclohexanone in the presence of a stoichiometric amount of KOH in isopropanol at 80 °C for 2–18 h [100]. $[\text{Fe}(\text{Cp})(\text{NHC})(\text{CO})_2][\text{I}]$ complexes (**C50a-c**) bearing 1,3-dialkylated *N*-heterocyclic carbene ligands can be also used as efficient catalysts for the transfer hydrogenation of cyclohexanone at 82 °C for 9–11 h in the presence of KOH as a base. Noticeably, the active species (0.5 mol%) can be generated in situ from imidazolium salts and $\text{CpFe}(\text{CO})_2\text{I}$ and allowed for the reduction of various ketones in 21–99% conversions under similar conditions (Scheme 24) [101].

Funk described a series of air-stable, nitrile-ligated Knölker-type complexes to be efficiently used in transfer hydrogenation. The acetonitrile complex **C51** exhibited the best activity in the transfer hydrogenation of aldehydes (2 mol% of **C51**, 80 °C, 18 h) and ketones (5 mol% of **C51**, 80 °C, 18 h). The catalyst **C51** exhibited similar activities than the air-sensitive iron hydride complex **C24** (1 mol%, 75 °C, 16 h, Scheme 25).



Scheme 25 Knölker-type catalyst for transfer hydrogenation of ketones



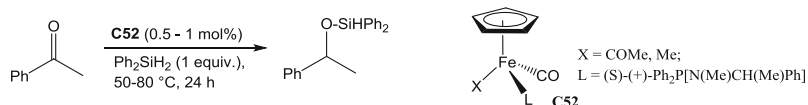
Scheme 26 Catalyst obtained from $\text{Fe}(\text{BF}_4)_2 \cdot 6\text{H}_2\text{O}$ and **3** for the selective transfer hydrogenation of aldehydes

Recently, Beller et al. reported an efficient and highly selective transfer hydrogenation of aromatic, heteroaromatic, and aliphatic aldehydes using in situ generated catalytically active species (0.4 mol%) from $\text{Fe}(\text{BF}_4)_2 \cdot 6\text{H}_2\text{O}$ /tris[2-(diphenylphosphino)ethyl]-phosphine [$\text{P}(\text{CH}_2\text{CH}_2\text{PPh}_2)_3$] (**3**) in the presence of 1.1 equiv. of formic acid as the hydrogen source in THF at 60°C for 2 h (20 examples, GC yields: 96–99%, Scheme 26) [102]. Notably, chloro-, bromo-, ketone, ester, and styryl moieties were well tolerated under these conditions. Furthermore, the unprecedented chemoselective reduction of α,β -unsaturated aldehydes to the corresponding allylic alcohols can be performed under base-free conditions.

2.3 Hydrosilylation Reactions

For chemoselectivity reasons, the hydrosilylation of alkenes is always an interesting alternative in reduction reactions, in particular with very inexpensive hydrogen sources such as PMHS (polymethylhydrosiloxane) and TMDS (1,1,3,3-tetramethyldisiloxane). In the iron-catalyzed realm, hydrosilylation has seen a huge development during the last decade. The very first example of the hydrosilylation of ketones with iron complexes as the catalysts was described in 1990 by Brunner and Fish. Using $[\text{Fe}(\text{Cp})(\text{CO})(\text{X})(\text{L})]$ (**C52**, 0.5–1 mol%) in the presence of 1 equiv. of diphenylsilane at 50 – 80°C for 24 h, the silylated ether was obtained quantitatively, without the formation of silylated enol ethers (Scheme 27) [103].

One of the first generally applicable iron catalyst systems for the hydrosilylation of carbonyl compounds was reported by Beller et al. in 2007: using an in situ generated catalyst from $\text{Fe}(\text{OAc})_2$ (5 mol%) and PCy_3 (10 mol%) in the presence of PMHS (3 equiv.) as the hydride source in THF at 65°C for 16 h, the reduction of functionalized aromatic, heteroaromatic, and alkyl aldehydes was efficiently performed (35 examples, 60–99% yields) [104]. The same catalytic system was



Scheme 27 Pioneering iron-catalyzed hydrosilylation of acetophenone by H. Brunner

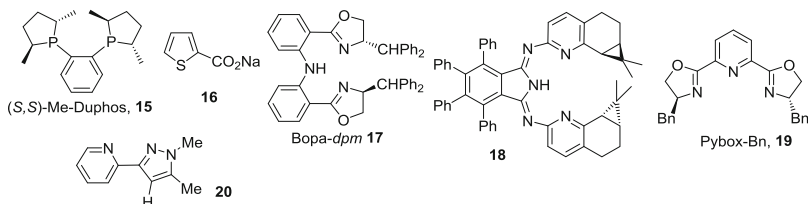


Fig. 5 Ligands for iron-catalyzed hydrosilylation of ketones

also able to reduce ketones (21 examples, 60–96% yields) after 20 h at 65°C [105]. Notably, ester, amino-, cyano-, and $\alpha,\beta\text{-C}=\text{C}$ moieties were tolerated under these conditions. An enantioselective version was then developed using an in situ generated catalyst from $\text{Fe}(\text{OAc})_2$ and (*S,S*)-Me-Duphos **15** as a chiral diphosphine (Fig. 5) using $(\text{EtO})_2\text{MeSiH}$ or PMHS as a hydride source at room temperature or 65°C, affording yields up to 99% and ees up to 99% in the reduction of aromatic ketones [106]. Simultaneously, Nishiyama et al. reported that the combination of $\text{Fe}(\text{OAc})_2$ (5 mol%) and nitrogen-based ligands such as *N,N,N',N'*-tetramethylethylenediamine (TMEDA, 10 mol%) as the catalyst can efficiently promote the hydrosilylation of ketones in the presence of 2 equiv. of $(\text{EtO})_2\text{MeSiH}$ at 65°C for 20–24 h to give the corresponding alcohols in 50–94% yields [107]. The combination of $\text{Fe}(\text{OAc})_2$ (5 mol%) and sodium thiophenecarboxylate **16** (10 mol%) as the ligand led also to an efficient catalyst system and gave similar results under the same conditions [108]. The group also reported an iron-catalyzed asymmetric hydrosilylation of ketones using *N,N,N*-bis(oxazolinyphenyl)-(bopa) ligands such as Bopa-dpm **17** (3 mol%) in combination with $\text{Fe}(\text{OAc})_2$ (2 mol%) as a catalyst and $(\text{EtO})_2\text{MeSiH}$ as the hydride source (88–99% yields and 50–88% ees) [109]. Other chiral ligands can be used such as tetraphenyl-carbpi **18** [110] or pybox-Bn **19** (Fig. 5) [111].

*N*1-Alkylated 2-(pyrazol-3-yl)pyridines such as **20** in combination with iron octanoate [$\text{Fe}(\text{O}_2\text{C}_8\text{H}_{15})_2$] were also suitable catalyst precursors for the hydrosilylation of aldehydes and ketones in heptane at 80°C for 20 h in the presence of PMHS as the hydride source [112].

Using a catalyst obtained in situ from PCy_3 and the widely used air- and moisture-stable complex $\text{Bu}_4\text{N}[\text{Fe}(\text{CO})_3(\text{NO})]$ **C53** [113], (which is a potent catalyst in allylic substitution [114]), Plietker et al. reported a highly active system for the mild hydrosilylation of a variety of functionalized aldehydes and ketones using PMHS as the hydrogen source. The corresponding alcohols were obtained in

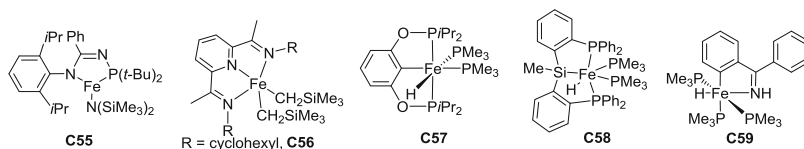
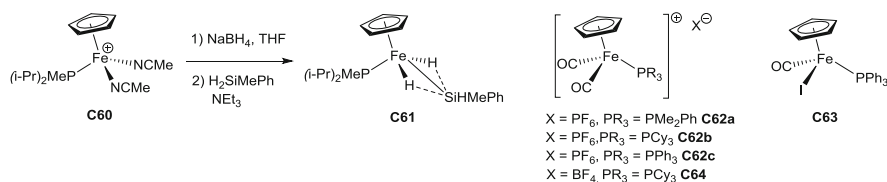


Fig. 6 Various iron complexes for hydrosilylation of carbonyl derivatives

moderate to excellent yields {aldehydes (65–99%); ketones (92–99%)} at low catalyst loadings (1–2.5 mol% **C53** and 1.1 mol% PCy₃) at 30–50°C for 14 h [115].

Using the simple but highly air-sensitive iron silylamide catalyst [Fe(N(SiMe₃)₂)] **C54**, Tilley succeeded to perform efficiently the hydrosilylation of various aldehydes and ketones using 1.6 equiv. of Ph₂SiH₂. Notably, he performed the reaction at 23°C for 0.3–20 h using low catalyst loading (0.01–2.7 mol%) with TOFs of up to 2,400 h⁻¹ for the reduction of 3-pentanone. Such mild conditions allowed for tolerating functional groups such as nitriles, cyclopropyl units, or olefins [116]. The well-defined iron(II) bis-(trimethylsilyl)amido complexes **C55** bearing a *N*-phosphinoamidate ligand (Fig. 6) can also be used as a catalyst (0.015–1 mol%) for the hydrosilylation of a large range of aldehydes and ketones in the presence of 1 equiv. of phenylsilane. It must be noted that TOFs up to 23,600 h⁻¹ can be reached at rt for the reduction of acetophenone, showing the beneficial influence of the ligand (compared to 1,266 h⁻¹ with **C54**).

Pincer-type iron complexes, which are usually more stable, were also extensively studied in the hydrosilylation of carbonyl derivatives. First, in 2008, Chirik developed a series of highly active bis(imino)pyridine(PDI) iron complexes such as [Fe(*i*PrPDI)(N₂)₂] (**C9**) for the hydrogenation and hydrosilylation of alkenes (vide supra) which was also catalytically active in the hydrosilylation of *p*-tolualdehyde and acetophenone with Ph₂SiH₂ at 23°C within 1 h. Interestingly, using the more active iron dialkyl complex **C56** (0.1 mol%) in the presence of 2 equiv. of diphenylsilane at 23°C for 3 h, a large variety of ketones can be efficiently reduced (Fig. 6). Noticeably, cyclohexenones were chemoselectively reduced within 12 h, leading to the corresponding unsaturated alcohols without hydrosilylation of the C=C bond, whereas the reduction was less chemoselective with acyclic enones, which gave the allylic alcohols as the major product [117]. In 2011, Guan et al. reported the synthesis of new iron hydride complexes bearing phosphinite-based pincer ligands (POCOP) such as **C57** (Fig. 6) and their application in the catalytic hydrosilylation of aldehydes and ketones [118]. For the reduction of benzaldehyde, full conversions were obtained at 50°C within 1 h using 1 mol% of catalyst **C57** in the presence of 1.1 equiv. of (EtO)₃SiH. With ketones such as acetophenone, a higher temperature (80°C) for 4.5 h was required to reach full conversion and the corresponding alcohols were isolated in up to 88% yield. This system can reduce different aromatic and aliphatic aldehydes in good yields (80–92% at 50–65°C for 1–36 h) and aromatic ketones in low to moderate yields (0–88% at 50–80°C for 4.5–48 h). Even though the mechanism for this reaction is not



Scheme 28 Cyclopentadienyl iron–phosphine–based complexes

clear, the decoordination of PMe₃ or CO as first step in order to generate the active catalyst seems a crucial step.

Most recently, H. Sun et al. described a similar silyl iron pincer complex **C58** (Fig. 6) bearing a tridentate bis(phosphine)silyl ligand whose catalytic activity was evaluated in the hydrosilylation of aldehydes such as benzaldehyde: using 1 mol% of **C58** in the presence of 1.5 equiv. (EtO)₃SiH in THF at 60°C for 1 h, benzyl alcohol was obtained quantitatively, whereas the reduction of ketones such as acetophenone and cyclohexanone required a longer reaction time (6 h) to give the corresponding alcohols with 89 and 99% yields, respectively [119]. Additionally, cyclometallated iron complexes can also be used as catalyst in hydrosilylation reactions: X. Li reported the use of the hydrido-iron complex **C59** (Fig. 6) as a catalyst (0.3–0.6 mol%) in the presence of 1.2 equiv. of (EtO)₃SiH in THF at 55°C for 1–4 h for aldehydes and 4–12 h for ketones leading to the alcohols in 65–92% isolated yields [120].

Cyclopentadienyl piano-stool iron(II) complexes are another family of well-defined iron complexes which were also widely studied in hydrosilylation reactions. Since the pioneering work of Brunner [103], Nikonov et al. in 2008 reported a nonclassical iron silyl dihydride complex (**C60**, 5 mol%) for the hydrosilylation of benzaldehyde with H₂SiMePh at 50°C for 12 h. The parent cationic complex **C61** (5 mol%) was also active in hydrosilylation of benzaldehyde with PhSiH₃ at 22°C for 3 h (Scheme 28) [121].

In our group, we have developed the analogous series of carbonyl complexes [Fe(Cp)(CO)₂(PR₃)]X (**C62–C63**, Scheme 28). These cationic complexes could be successfully used as catalysts for hydrosilylation of both aldehydes and ketones. Using 5 mol% of catalysts **C62a–c** and 1.1 equiv. of phenylsilane at 30°C under visible-light irradiation for 16 h, excellent conversions were obtained either in THF (92–98%) or under neat conditions (91–97%) for the reduction of benzaldehyde derivatives. Interestingly, PMHS (4 equiv.) as the hydrosilane could also be used in the presence of 5 mol% of complexes **C62a–b**, which gave the best conversions (95%) under similar conditions in THF. The best catalyst for the reduction of acetophenone was the neutral iron complex [Fe(Cp)(CO)(I)(PPh₃)] **C63** in the presence of 1.2 equiv. of phenylsilane under neat conditions and visible-light activation and slightly harsher conditions (70°C for 30 h). Interestingly, the tetrafluoroborate complexes **C64** exhibited similar or superior activities compared to the iodo- or hexafluorophosphate analogs such as **C64** (5 mol%). It gave 98% conversion for the reduction of acetophenone under visible-light activation at 70°C,

either with 1.2 equiv. of phenylsilane for 16 h or with 4 equiv. of PMHS for 72 h. It must be underlined that visible-light activation is necessary in order to facilitate the decoordination of one CO ligand and generate an unsaturated active species [122].

Similarly, piano-stool iron–NHC complexes (NHC = *N*-heterocyclic carbene) can efficiently play the role of catalysts in such reductions. In 2010, Royo reported the use of tethered Cp–NHC iron complexes such as **C49** (1 mol%) for the hydrosilylation of activated aldehydes (six examples) in the presence of 1.2 equiv. of (EtO)₂MeSiH in acetonitrile at 80°C for 1–18 h [100]. In our group, we have developed a family of piano-stool iron–NHC complexes [Fe(Cp)(CO)₂(NHC)][X] for the hydrosilylation of aldehydes and ketones. Using the cationic complex [Fe(Cp)(CO)₂(IMes)][I] (**C65**) and the neutral complex [Fe(Cp)(I)(CO)(IMes)] (**C66**) obtained by visible photoirradiation of **C65** in CH₂Cl₂, an efficient reduction of both aldehydes and ketones using 1 equiv. of phenylsilane was performed [123]. Good to excellent conversions (88–99%), and isolated yields were obtained for a variety of aldehydes (THF, 30°C, 3 h), albeit lower activities were observed with ketones (toluene, 70°C, 16 h, conversion = 50–99%) and electron-deficient acetophenone derivatives being easier to hydrosilylate. Notably, the visible-light activation is mandatory to generate the active catalyst from the cationic complex **C65**, whereas neutral complex **C66** works at 30°C without any activation. When conducting the hydrosilylation under solvent-free conditions and light irradiation, significant rate acceleration and better activities were obtained with acetophenone derivatives substituted by electron-donating groups which were then fully hydrosilylated. Noticeably, in most of the examples, the reactions proceed with higher conversions and yields than similar reactions conducted in THF or toluene and at lower temperatures (50 versus 70°C) [124]. Furthermore, nitrile, amine, and alkene groups were tolerated. NHC ligands such as IMes exhibited a significant influence on the activity as a huge difference of activity was observed when using [Fe(Cp)(IMes)(CO)₂][I] versus [Fe(Cp)(CO)₂]₂ or [Fe(Cp)(I)(CO)₂] precursors as the catalysts (for benzaldehyde, after 3 h at 30°C, the conversions are >97 versus <10%). The nature of the NHC ligand has an influence on the activity of the corresponding [Fe(Cp)(NHC)(CO)₂][I] pre-catalyst (Fig. 7). A series of piano-stool iron complexes comprising 1,3-disubstituted imidazolidin-2-ylidene ligands [Fe(Cp)(CO)₂(NHC)]I such as **C67** can be also used as catalysts but have shown moderate activity as hydrosilylation of aldehydes and ketones were conducted at 100°C for 0.5–4 h using phenylsilane under solvent-free conditions and in the absence of light activation [125]. With anionic six-membered-ring *N*-heterocyclic carbene ligands incorporating a malonate backbone, the corresponding [Fe(Cp)(NHC)(CO)₂] (**C68**, 1 mol%) is an active catalyst for the hydrosilylation of

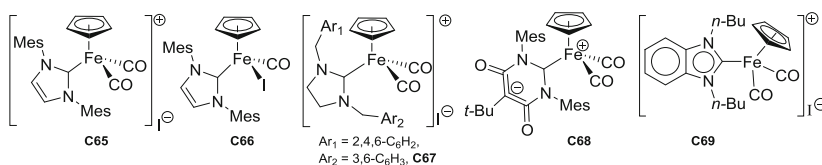
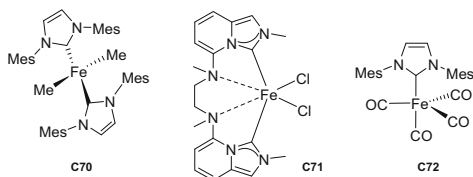


Fig. 7 Representative, catalytically active Cp–NHC iron complexes for hydrosilylation reactions

Fig. 8 Representative iron–NHC complexes catalytically active in hydrosilylation reactions



aromatic aldehydes using 1 equiv. of diphenylsilane at 30°C for 1–3 h (full conversions) and for the reduction of acetophenone derivatives using 1 equiv. of phenylsilane at 70°C for 16 h (37–98% conversions), similar to **C65** [126]. Similarly, in the presence of 1.2 equiv. of phenylsilane under visible-light irradiation and neat conditions, benzimidazole-based NHC iron complexes such as **C69** (2 mol%) catalyzed the hydrosilylation of benzaldehyde at 30°C within 3 h and acetophenone at 70°C within 17 h [127].

Adolfsson et al. described lately the hydrosilylation of ketones with PHMS as the hydrosilane by using in situ generated iron complexes, starting from iron(II) acetate and the imidazolium salt precursor IPr·HCl or *N*-hydroxyethylimidazolium in the presence of a base such as *n*-BuLi [128, 129]. It must be noted that the stoichiometry between the base and the imidazolium salts is important, as simple alkoxide salts are also able to promote such catalytic hydrosilylations with trisubstituted silanes.

The well-defined, low-valent iron–NHC complex [Fe(Me)₂(IMes)₂] (**C70**) was reported by F. Glorius, Y. Ohki, and K. Tatsumi (Fig. 8) [130]. Complex **C70** (0.1 mol%) was able to promote the hydrosilylation of 2'-acetonaphthone in THF with 1.1 equiv. of (EtO)₃SiH at 25°C for 5 h or with 1.1 equiv. of Ph₂SiH₂ at 40°C for 5 h. Noticeably, **C70** (1 mol%) is also efficient in transfer hydrogenation at 70°C in the presence of 1.2 equiv. of *i*PrOLi in *i*PrOH. Using the iron complex **C71** bearing a diamine-bridged bis-*N*-heterocyclic carbene (1 mol%) in combination with MeLi (2 mol%, in order to generate a Fe–Me species), the hydrosilylation of acetophenone was performed with 95% conversion in THF at 60°C for 16 h in the presence of 1.1 equiv. of Ph₂SiH₂ [131]. Royo described that the iron (0) complex [Fe(CO)₄(IMes)] **C72** (1 mol%) can reduce aromatic aldehydes using 1.2 equiv. of phenylsilane at room temperature for 4 h in THF, and remarkably reducible functional groups such as ketones, nitriles, or nitro groups were tolerated under these mild conditions [132].

Finally, in the area of iron hydrosilylation, Campagne succeeded to discover an unusual chemoselective reduction. The combination of PMHS (2.7 equiv.) and FeCl₃·6H₂O (10 mol%) in 1,2-dichloroethane under microwave irradiation at 120°C for 1 h efficiently reduced aldehydes and ketones to the corresponding methylene compounds in 62–98% yields [133].

3 Reduction of Imines and Nitro-derivatives and Reductive Amination of Carbonyl Compounds

3.1 Reduction of Imines

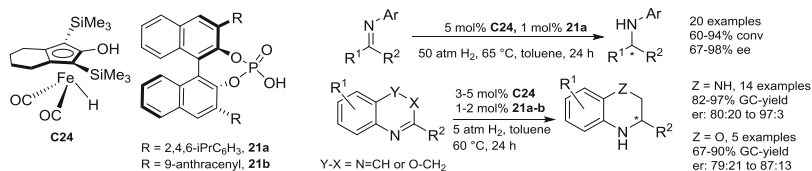
Until today, only scarce examples of reduction of imines catalyzed by iron-based catalysts have been described in the literature. Beller et al. reported the first catalytic hydrogenation of imines to amines [134]. Combining the Knölker complex **C24** and the chiral phosphoric Brønsted acid **21a** in a synergistic way, the resulting in situ catalyst can perform the hydrogenation of various *N*-aryl ketimines, leading to the corresponding amines in 60–94% isolated yields and 67–98% ees (Scheme 29). Using the same methodology, the group described that the enantioselective reductive hydroamination of terminal alkynes with primary anilines by hydrogenation via a sequential one-pot procedure involving a gold-catalyzed hydroamination {using 1 mol% of [Au(*o*-BiPh)(*t*Bu)₂P][BF₄]}, followed by an enantioselective hydrogenation of the in situ formed imines [**C24** (5 mol%)/**21** (2 mol%)] under the same conditions, yields up to 93%, ees of 70–94% [135].

The same catalytic system (3–5 mol% of **C24** and 1–2 mol% of **21a–b**) was also active in the enantioselective hydrogenation of quinoxalines and 2*H*-1,4-benzoxamines, leading to the corresponding tetrahydroquinoxalines with enantiomeric ratios (ers) up to 97:3 and to 3,4-dihydro-2*H*-1,4-benzoxamines with ers up to 87:13 (Scheme 29) [136].

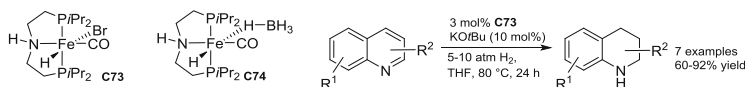
Interestingly, using a water-soluble Knölker-type complex **C26** (Scheme 13, 2.5 mol%) in the presence of Me₃NO (3.75 mol%) in water under 10 bar of H₂ at 100°C for 24 h, water-stable and water-soluble imines can be reduced in 91–98% yields [64].

Recently, Jones described the hydrogenation of *N*-heterocycles such as tetrahydroquinoxalines using the bifunctional iron pincer complex **C73** as the catalyst (3 mol%), under 5–10 atm of H₂, in the presence of 10 mol% of KO^tBu as a base in THF at 80°C for 24 h (60–92% isolated yields) [137]. It must be pointed out that using the same type of pincer complex as the catalyst, the reverse dehydrogenation of *N*-heterocycles can be performed in refluxing xylene for 30 h. The complex **C74** gave the best performance, whereas **C73** was inactive (Scheme 30).

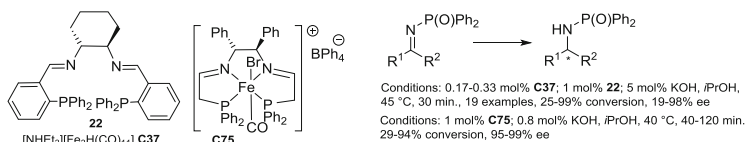
Imines can be also reduced under hydrogen transfer conditions. In 2011, the first iron-catalyzed enantioselective transfer hydrogenation of activated ketimines was



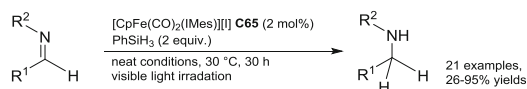
Scheme 29 Knölker complex/chiral phosphoric Brønsted acid for the catalytic asymmetric hydrogenation of C=N bonds



Scheme 30 Pincer complex **C73** for the catalytic hydrogenation of *N*-heterocycles



Scheme 31 Asymmetric transfer hydrogenation of imines



Scheme 32 Iron-catalyzed hydrosilylation of imines

described [138]. Using 0.33 mol% of [NHET₃][Fe₃H(CO)₁₁] (**C37**) combined with the diimino-phosphine tetradentate chiral ligand CyN₂P₂ (**22**) at 45 °C for 30 min in isopropanol in the presence of a catalytic amount of a base, numerous aromatic and heteroaromatic *N*-phosfonyl ketimines were reduced in 67–98% yields and 89–98% ees (Scheme 31).

Morris et al. reported a family of diimino-diphosphine iron complexes for the transfer hydrogenation of *N*-(diphenylphosphinoyl)- and *N*-(tolylsulfonyl)-ketimines: with the most effective complex **C75** (1 mol%) in combination with 0.8 mol% of *t*BuOK in *i*PrOH at 40 °C for 40–120 min, the corresponding amines were obtained with 29–94% conversion and 95–99% ees for the reduction of various *N*-(diphenylphosphinoyl)-ketimines [139].

In the hydrosilylation field, only one general methodology of iron-catalyzed hydrosilylation of aldimines and ketimines was reported up to date: using 2 mol% of the complex [Fe(Cp)(IMes)(CO)₂]I (**C65**, Fig. 7), a large range of aldimines were reduced under light irradiation at 30 °C for 30 h using 2 equiv. of phenylsilane under solvent-free conditions, and the corresponding amines were obtained after treatment with a base (Scheme 32) [140]. Various functional groups were tolerated, in particular halogenides (I, Br, Cl), ketones, esters, and alkenes which were not altered under these smooth catalytic conditions.

Compared with aldimines, slightly harsher conditions were used to hydrosilylate ketimines, as 24 h at 100 °C under neat conditions with 5 mol% of the pre-catalyst, and 2 equiv. of PhSiH₃ were required to obtain the corresponding amines in 57–95% yields.

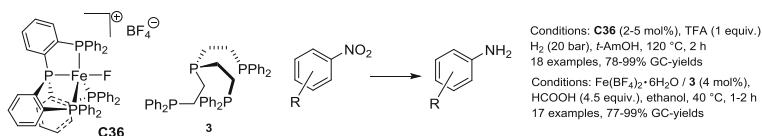
3.2 Reduction of Nitrile and Nitro-compounds *En Route* to Primary Amines

The preparation of primary amines via reduction processes is still a challenging area of research. Only a few protocols describing iron-catalyzed hydrogenation of nitroarenes are reported. In 1976, Knifton used $[\text{Fe}(\text{CO})_3(\text{PPh}_3)_2]$ as a catalyst (0.5 mol%) for the hydrogenation of nitrobenzene under 80 bar of H_2 at 125°C for 9 h in benzene/ethanol leading to the corresponding aniline in 87% [141]. With an in situ generated catalyst from $\text{FeSO}_4 \cdot 7\text{H}_2\text{O}$ (0.75 mol%) and Na_2EDTA (3.75 mol%), Chaudhari et al. succeeded to hydrogenate nitroarenes in water under 28 bar of H_2 at 150°C for 2–9 h [142]. Ketone, carboxylic acid and cyano-functionalities can be tolerated.

Using the iron-tetraphos complex **C36** (2–5 mol%) in the presence of 1 equiv. of trifluoroacetic acid (TFA) in *t*-AmylOH under 20 atm of hydrogen at 120°C for 2 h, nitroarenes were hydrogenated to the corresponding aniline derivatives in 78–99% yields (Scheme 33) [143]. The in situ generated catalysts from $\text{Fe}(\text{BF}_4)_2 \cdot 6\text{H}_2\text{O}$ and the corresponding tetraphos ligand **3** gave similar results. The interesting chemoselectivities observed toward nitriles, esters, styryl units, or α,β -unsaturated esters and halides (even iodides) must be underlined.

The same authors succeeded also to reduce nitroarenes by hydrogen transfer using formic acid (4.5 equiv.) as the reducing agent in the absence of additional base using the in situ generated catalyst (4 mol%) from a 1/1 mixture of $\text{Fe}(\text{BF}_4)_2 \cdot 6\text{H}_2\text{O}$ and the tris[2-(diphenylphosphino)ethyl]-phosphine $[\text{P}(\text{CH}_2\text{CH}_2\text{PPh}_2)_3]$ (**3**) [144]. At 40°C in ethanol for 1–2 h, various functionalized nitroarenes were reduced in full conversions and good to excellent yields (86–99%, Scheme 33).

Finally nitroarenes can also be reduced to anilines via hydrosilylation reactions. The in situ generated catalyst from FeBr_2 (10 mol%) and a phosphine $\{\text{PPh}_3, \text{P}(\text{Ph}-4\text{-OMe})_3 \text{ or } \text{PPh}_2\text{Me}\}$, 12 mol%} in the presence of 2.5 equiv. of PhSiH_3 as the hydride donor at 110°C for 16 h led to the chemoselective reduction of various nitro-substituted arenes and heteroarenes with 25–99% GC yields [145]. Later, Lemaire et al. described a simple system based on $\text{Fe}(\text{acac})_3$ (10 mol%) in the presence of TMDS (1.5 equiv.) for the selective reduction of nitroarenes to aniline derivatives in 20–99% yields after 24–48 h at 60°C . Notably, functional groups such as esters, carboxylic acids or cyano were tolerated. Under these conditions, nitroalkanes did not give the corresponding amines [146, 147].

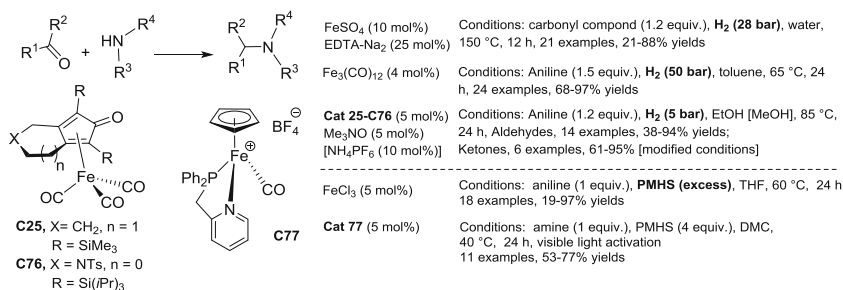


Scheme 33 C36-catalyzed hydrogenation of nitroarenes to anilines

3.3 Direct Reductive Amination (DRA)

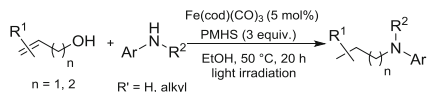
Among the preparative methodologies for the synthesis of amines, direct reductive amination is certainly one of the most versatile and useful pathways. Even though this reaction has been widely studied with stoichiometric alkali-reducing agents, applications of transition metals including iron for this reaction have been developed over the last decade. In 2008, Bhanage et al. described the DRA of aldehydes and ketones under 28 bar of hydrogen in the presence of primary and secondary amines at 150 °C for 12 h in water using a catalytic amount of $\text{FeSO}_4 \cdot 7\text{H}_2\text{O}$ (10 mol %) and ethylenediaminetetraacetic acid disodium salt (EDTA- Na_2 , 25 mol %) [148]. It must be underlined that under these conditions, small amounts of alcohols resulting from the hydrogenation of the carbonyl compounds were also obtained. Using $\text{Fe}_3(\text{CO})_{12}$ (4 mol %) under 50 bar of H_2 in toluene at 65 °C for 24 h, anilines can be efficiently transformed to the corresponding alkylated anilines in good yields (68–97%) by reaction with both aldehydes and ketones. Notably, molecular sieves are necessary for the DRA with ketones in order to completely shift the equilibrium of its condensation reaction with anilines. The reaction can be chemoselective with aldehydes bearing ketone or ester moieties [149]. Well-defined Knölker-type complexes can be also used efficiently for this transformation under mild conditions: in the presence of 5 mol % of the complex **C25** and 5 mol % of trimethylamine *N*-oxide as the catalytic system, under low hydrogen pressure (5 bar) at 85 °C in ethanol, aldehydes can react with various alkylamines leading to the corresponding alkylated amines in moderate to good yields. For the reaction of ketones, a slight modification of the conditions is necessary, as the reaction was performed in methanol with a catalytic amount of NH_4PF_6 (Scheme 34) [150, 151].

DRA at iron can be also performed by hydrosilylation. Enthaler reported in 2010 the first DRA of aldehydes by aniline derivatives using FeCl_3 (5 mol %) as the catalyst in the presence of a large excess of PMHS in THF at 60 °C for 24 h. Notably, the reaction did not take place with alkylamines such as benzylamine [152]. Still, using PMHS as the hydrosilane and well-defined cyclopentadienyl phosphanyl-pyridine piano-stool iron complexes such as **C77** (5 mol %) can promote DRA of benzaldehyde derivatives by secondary amines in dimethyl carbonate



Scheme 34 Iron-catalyzed direct reductive amination

Scheme 35 Cascade reaction involving and iron-catalyzed DRA



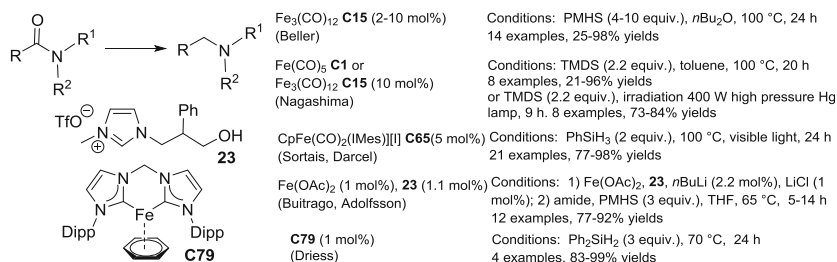
(DMC) at 40°C for 24 h under visible-light irradiation, leading to the corresponding tertiary amines in 53–93% isolated yields [153]. Esters, nitriles, ketones, and halides can be tolerated under such mild conditions. Interestingly, the phosphanyl-pyridine ligand seems to have a beneficial influence on the activity, as with monophosphine complexes $[\text{Fe}(\text{Cp})(\text{CO})_2(\text{PR}_3)][\text{BF}_4]$ such as **C64**, only moderate conversions (35–58%) were obtained. Recently, in a cascade fashion, DRA was performed starting from allylic or homoallylic alcohols and secondary and primary anilines using $[\text{Fe}(\text{cod})(\text{CO})_3]$ (**C78**, 5 mol%) as the catalyst and cheap and abundant PMHS as the hydrosilane reagent. Thus, the selective synthesis of tertiary and secondary aniline derivatives was achieved by reaction in ethanol under mild conditions (50–70°C under visible-light activation). This process corresponds to a formal DRA of (homo)allylic alcohols via a tandem isomerization/condensation/hydrosilylation reaction (Scheme 35) [154].

4 Reduction of Carboxylic Acid Derivatives and Carbon Dioxide

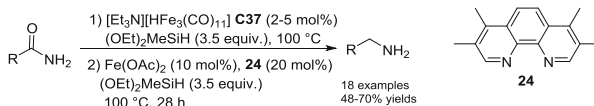
4.1 Amides

Among the carboxylic acid derivatives, carboxamides are certainly among the most difficult ones to reduce, and numerous transition metals have already been described for their catalytic reduction, in particular in hydrosilylation reactions. One of the challenges is to selectively cleave the C–N bond to give the resulting alcohols and amines or the C=O bond leading to the corresponding amines. Pioneering reports were published simultaneously by Beller [155] and Nagashima [156, 157] on iron-catalyzed reduction of secondary and tertiary amides yielding the corresponding amines, using $\text{Fe}_3(\text{CO})_{12}$ (**C15**) or $\text{Fe}(\text{CO})_5$ (**C1**) as pre-catalysts (2–10 mol%). Notably, the groups used either PMHS (4–10 equiv.) or TMDS (2.2 equiv.) as inexpensive silanes to perform the reduction at 100°C for 24 h. Interestingly, Nagashima showed that such reactions can also be efficiently promoted by irradiation using a 400 W high-pressure mercury lamp for 9 h at rt (Scheme 36).

Using well-defined iron(II) NHC complexes such as $[\text{Fe}(\text{Cp})(\text{CO})_2(\text{IMes})][\text{I}]$ (**C65**, 5 mol%) in the presence of 2 equiv. of phenylsilane at 100°C for 24 h, the reduction of tertiary and secondary amines can also be conducted under visible-light irradiation (24 W compact fluorescent lamps) under neat conditions [158]. Using the carefully in situ prepared iron *N*-heterocyclic carbene complex obtained from a THF mixture of $\text{Fe}(\text{OAc})_2$ (1 mol%), $([\text{PhHEMIM}][\text{OTf}])$ **23** (1.1 mol%) and LiCl (1 mol%) treated by 2.2 mol% of *n*-BuLi, the hydrosilylation can be conducted at



Scheme 36 Iron-catalyzed hydrosilylation of tertiary and secondary amides



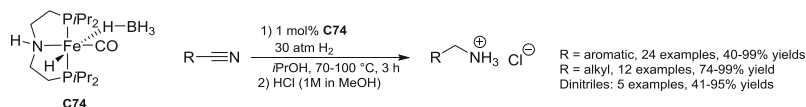
Scheme 37 Two consecutively applied, iron-based catalytic systems for the reduction of primary amides to primary amines

65 °C in the presence of PMHS as the hydride source. Notably, the presence of LiCl is crucial to obtain good chemoselectivities [159]. The reduction of tertiary amides can also be performed with the well-defined NHC-Fe(0) complex bis-(*N*-Dipp-imidazole-2-ylidene)methylene Fe(η^6 -benzene) (**C79**, 1 mol%) in the presence of 3 equiv. of diphenylsilane at 70 °C in THF for 24 h [160].

Reductions of primary amides under hydrosilylation conditions are more difficult to realize as under the reaction conditions mentioned above, with the major reaction being the dehydration leading to nitrile derivatives [161]. However, using two different iron complexes in a consecutive way, the reduction of primary amides led efficiently to primary amines [162] by using $[\text{Et}_3\text{NH}][\text{HFe}_3(\text{CO})_{11}]$ (**C37**, 2–5 mol%, which promotes the dehydration of primary amides to nitriles) and the combination of $\text{Fe}(\text{OAc})_2$ (20 mol%) and the terpyridine ligand **24** (20 mol%, which catalyzes the reduction of nitrile derivatives to primary amines) in the presence of $(\text{EtO})_2\text{MeSiH}$ (3 equiv.) in toluene at 100 °C for additional 28 h (Scheme 37).

4.2 Nitriles

The catalytic hydrogenation of nitriles leading to the corresponding primary amines is still a challenging reaction to be catalyzed by iron. Recently, Beller et al. reported the use of the iron PNP pincer complex **C74** for the hydrogenation of nitriles to lead selectively to the primary amines under 30 bar of H_2 in isopropanol at 70–100 °C for 3 h. Notably, aromatic, heteroaromatic, and alkyl nitriles, and dinitriles (including adiponitrile) can be reduced in 40–95% yields. Under these conditions, halides,



Scheme 38 Iron PNP pincer complex catalyzed hydrogenation of nitriles

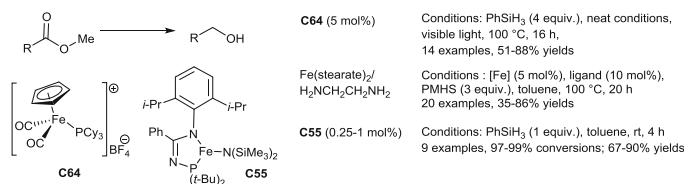
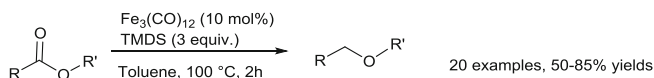
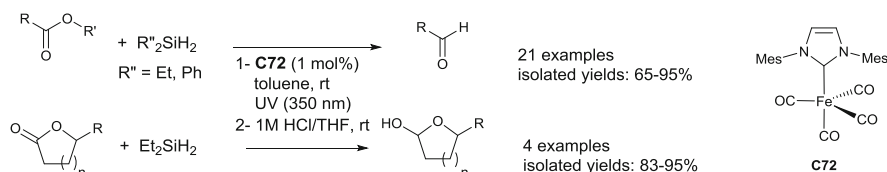
esters, ethers, acetamido-groups, and α,β -unsaturated C=C bonds were tolerated during the reduction of the nitrile (Scheme 38) [163].

4.3 Carboxylic Esters

In molecular synthesis, one of the most important, but also the most difficult task, is the efficient and chemoselective reduction of carboxylic acid derivatives such as carboxylic acids or esters to alcohols, ethers, or aldehydes. With iron, there are only a few reports dealing with that challenging task. The first iron-catalyzed reduction of esters was reported in 2012: using $[\text{Fe}(\text{Cp})(\text{CO})_2(\text{PCy}_3)][\text{I}]$ (**C80**, 5 mol%) under neat conditions and visible-light activation at 100°C for 16 h in the presence of 4 equiv. of phenylsilane, methyl phenylacetate was converted in 85% to a mixture of 2-phenylethanol and methyl 2-phenylethyl ether in a ratio of 6:1. With $[\text{Fe}(\text{Cp})(\text{CO})_2(\text{PCy}_3)][\text{BF}_4]$ (**C64**, 5 mol%) under similar conditions, the corresponding 2-phenylethanol was obtained specifically in 97% conversion and 88% isolated yield. Complex **C64** as the catalyst was able to perform efficiently the reduction of aliphatic carboxylic esters to give the corresponding alcohols in 51–88% isolated yields (Scheme 39) [164]. Chemoselectively catalyzed hydrosilylation reactions of aromatic and aliphatic esters to alcohols can also be conducted with a catalytic system consisting of $\text{Fe}(\text{stearate})_2$ and $\text{H}_2\text{NCH}_2\text{CH}_2\text{NH}_2$ in the presence of 3 equiv. of PMHS at 100°C for 20 h [165]. Furthermore, using the three-coordinate iron(II) *N*-phosphinoamidinate complex **C55** in low catalytic loading (0.25–1 mol%), the reduction of esters to alcohols is possible at room temperature within 4 h [166].

Modifying the nature of the catalytic system, different chemoselectivities can be reached. To obtain selectively ethers from esters, $\text{Fe}_3(\text{CO})_{12}$ (**C15**, 10 mol%) was used as the catalyst in the presence of TMDS (3 equiv.) as the hydride source in toluene at 100°C for 2 h [167]. This methodology can be applied to reduce aliphatic and alicyclic esters and even steroid esters (Scheme 40).

To obtain specifically aldehydes from aromatic, aliphatic, and heteroaromatic esters, the combination of $[\text{Fe}(\text{CO})_4(\text{IMes})]$ (IMes = 1,3-bis(2,4,6-trimethylphenyl)imidazole-2-ylidene) (**C72**, 5 mol%) as the catalyst and R_2SiH_2 (R = Et, Ph) as the silane allowed for the efficient reduction at room temperature under UV irradiation (350 nm) [168]. Notably, this catalyst system can also be applied for the chemoselective reduction of lactones to lactols in good isolated yields. Interestingly, experimental evidence was given which proved that the hydrosilylation

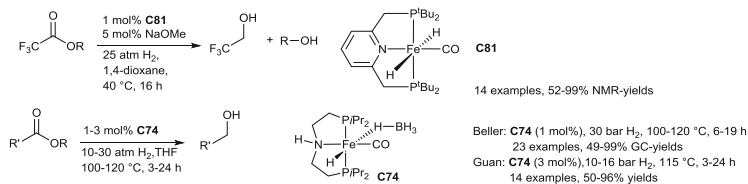
**Scheme 39** Selective iron-catalyzed hydrosilylation of esters to alcohols**Scheme 40** Selective iron-catalyzed hydrosilylation of esters to ethers**Scheme 41** Selective iron-catalyzed hydrosilylation of esters to aldehydes and lactones to lactols

occurs by an oxidative addition of the hydrosilane to an unsaturated NHC–Fe species yielding a hydride–silyl iron complex (Scheme 41).

Aldehydes can be also obtained by reduction, starting from more reactive acyl chlorides. Indeed, a catalytic system based on FeO (20 mol%) and tris(2,4,6-trimethoxyphenyl)phosphine (TMPP, 5.0 mol%) in the presence of phenylsilane (1.12 equiv.) allowed for the selective transformation of alkanoyl chlorides to the corresponding aldehydes when performing the reaction in toluene at 60–120°C for 20 h [169].

In terms of large-scale and industrial applications, the reduction of esters to alcohols via hydrogenation is a more interesting goal. Several complexes as catalysts were reported in early 2014. First, Milstein described an iron-catalyzed, selective hydrogenation of activated trifluoroacetic esters leading to 2,2,2-trifluoroethanol and the alcohols corresponding to the ester alkoxy groups in 52–99% NMR yields. The iron dihydrido-pincer complex **C81** (1 mol%) was utilized as catalyst in the presence of 5 mol% of NaOMe as the base in dioxane under 25 bar of hydrogen at 40°C for 16 h (Scheme 42) [170]. Notably, no activity was observed with difluoroacetic ester derivatives.

Later, in two simultaneous contributions, Beller [171] and Guan [172] described the use of the bifunctional PNP iron pincer complex **C74** as catalyst for the hydrogenation of a wide variety of esters under base-free conditions (Scheme 42). This catalytic system is suitable for the reduction of both aliphatic and aromatic esters. It can tolerate carboxylic amides, heteroaromatic motifs such as furans,

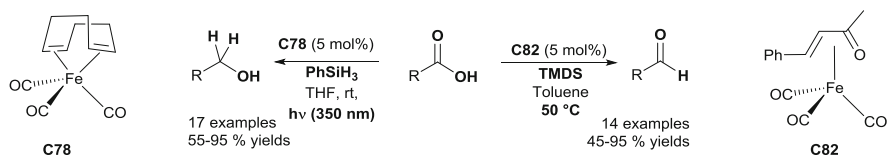
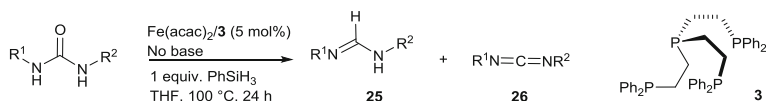
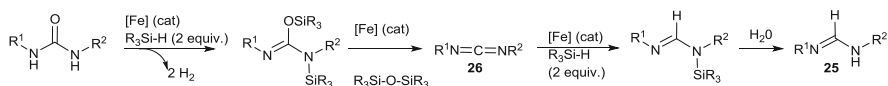


Scheme 42 Iron dihydrido-pincer complexes for the hydrogenation of esters to alcohols

pyridines, benzothiazoles, and nonconjugated alkenyl moieties. In contrast, cyano-groups were reduced to the corresponding amines. Lactones can be also efficiently reduced leading to the corresponding diols. Industrial samples of a mixture of C12–C16 esters can also be reduced under neat conditions. A mechanistic study showed that the –NH moiety on the PNP pincer backbone is crucial for the activity of the catalyst as no activity was observed with the NH replaced by a methyl group: a cooperative interaction involving the NH unit of the pincer ligand and the Fe–H group is proposed to rationalize the reactivity.

4.4 Carboxylic Acids

The chemoselective reduction of carboxylic acids to either alcohols or aldehydes is also an important challenge and can be achieved using a one-pot procedure based on an iron-catalyzed hydrosilylation reaction, using well-chosen silane–iron complex partners. Indeed, using 4 equiv. of phenylsilane as the hydride donor and 5 mol% of [Fe(CO)₃(cod)] catalyst (**C78**) under UV irradiation (350 nm) at rt for 24 h, carboxylic acids were converted after acidic hydrolysis to the corresponding alcohols (67–97% yields). When the reaction was performed in the presence of 5 mol% of [Fe(*t*-PBO)(CO)₃] (**C82**, *t*-PBO = *trans*-4-phenyl-but-3-en-2-one) as the catalyst and 2 equiv. of TMDS at 50 °C for 24 h, alkanolic acids led to the corresponding aldehydes in 45–95 isolated yields [173]. The chemoselectivity is due to the formation of a disilylacetal intermediate which is stable under the reaction conditions and which afforded the aldehydes after an acidic quench step (Scheme 43).

**Scheme 43** Chemoselective hydrosilylation of carboxylic acids**Scheme 44** Iron-catalyzed hydrosilylation of ureas**Scheme 45** Proposed mechanistic pathway for the reduction of ureas

4.5 Ureas

The selective reduction of ureas to formamidines is a challenging goal, when performed without further reduction to amins, methanol, and amines. Using an in situ generated iron catalyst (5 mol%) from $\text{Fe}(\text{acac})_2$ and tetraphos $[\text{P}(\text{CH}_2\text{CH}_2\text{PPh}_2)_3]$ **3** in the presence of 1 equiv. of phenylsilane in THF at 100°C for 24 h, a mixture of formamidines **25** and carbodiimides **26** was obtained with ratios ranging from 98:<1 to 29:69, strongly depending of the nature of the urea substituents, with 69–98% conversions (Scheme 44) [174].

Under a mechanistic point of view, the formation of carbodiimides **26** results from the iron-catalyzed dehydration of ureas in the presence of silane via a dehydrogenative silylation of the NH bonds, which are intermediates for the production of formamidines (Scheme 45).

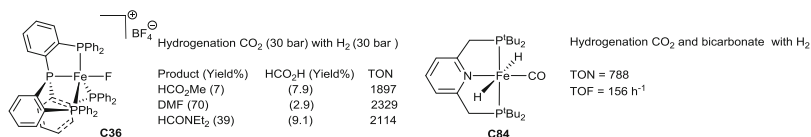
4.6 Carbon Dioxide and Formic Acid

Under a sustainability point of view, carbon dioxide is a very attractive, nontoxic, abundant, and environmentally friendly C_1 feedstock to produce bulk chemicals (urea, formic acid, formaldehyde, methanol, etc.) (for selected reviews, see [175, 176]). In the area of reduction reactions, the direct hydrogenation of CO_2 to formaldehyde, methanol, and methane is an important and challenging goal, in particular the CO_2 hydrogenation to afford formic acid (for selected leading reviews, see [177–180]). In 2003, using a high-pressure combinatorial catalyst

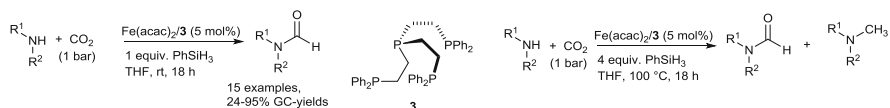
discovery technique, Jessop et al. described that the combination of FeCl_3 and dcppe (1,2-bisdicyclohexylphosphinoethane) in the presence 0.5 equivalents of DBU (1,8-diazabicyclo[5.4.0]undec-7-ene) can catalyze the direct hydrogenation of CO_2 to formic acid with molecular hydrogen with a TON of 113 and a TOF of 15.1 h^{-1} under 40 bar H_2 and 60 bar CO_2 at 50°C for 7.5 h [181]. In 2010, Beller, Laurenczy et al. reported the hydrogenation of carbon dioxide and bicarbonates (HCO_3^-) to formates, alkyl formates (in the presence of alcohols) and formamides (in the presence of amines), using an in situ generated well-defined complex $[\text{Fe}(\mathbf{3})\text{BF}_4]$ (**C83**) obtained from $\text{Fe}(\text{BF}_4)_2 \cdot 6\text{H}_2\text{O}$, $[\text{P}(\text{CH}_2\text{CH}_2\text{PPh}_2)_3]$ (**3**) and molecular hydrogen [182]. The catalytic reduction of sodium bicarbonate led to the formate with 88% yield and a TON of 610 using a combination of $\text{Fe}(\text{BF}_4)_2 \cdot 6\text{H}_2\text{O}$ and **3**, at 80°C , under 60 bar H_2 for 20 h. With the same catalyst, methyl formate can be also produced by the hydrogenation of CO_2 in the presence of methanol (and an excess of triethylamine), with 56% yield and a TON of 585, and dimethylformamide from dimethylamine with 75% yield and a TON of 727 [$\text{P}_{\text{H}_2/\text{CO}_2} = 60/30 \text{ bar}$, 100°C , 20 h]. Starting from ethanol, propanol and diethylamine, ethyl, and propyl formates and diethylformamide were obtained, respectively, in lower yields (9–28%). Notably, the in situ generated catalyst from $[\text{P}(\text{CH}_2\text{CH}_2\text{PPh}_2)_3]$ (**3**) and FeCl_2 can also be utilized in the hydrogenation of CO_2 [183]. The air- and thermally stable complex $[\text{Fe}(\mathbf{27})\text{BF}_4]$ (**C36**), resulting from the tetradentate tris[2-(diphenylphosphino)phenyl]-phosphine **27** and $\text{Fe}(\text{BF}_4)_2 \cdot 6\text{H}_2\text{O}$, is one of the most active iron-based systems for the hydrogenation of carbon dioxide and bicarbonates to afford formates and formamides with TONs up to 7,500 for the hydrogenation of sodium bicarbonate (Scheme 46) [184].

Interestingly, the in situ catalytic system $\text{Fe}(\text{BF}_4)_2 \cdot 6\text{H}_2\text{O}/\mathbf{3}$ can also catalyze the reversible reaction by dehydrogenation of formic acid to CO_2 and H_2 without base in high catalytic activity (TOFs up to $9,425 \text{ h}^{-1}$ and TONs up to 92,417 at 80°C and 0.005 mol% of catalyst) [185, 186]. Milstein et al. reported another iron catalyst, *trans*- $[\text{Fe}(\text{H})_2(\text{CO})]$ (*t*^{Bu}PNP) (**C84**, 0.1 mol% loading) to be active for the hydrogenation of CO_2 and sodium bicarbonate to formate salts in $\text{H}_2\text{O}/\text{THF}$ 10:1 media at 80°C under low pressures (6–10 bar, TONs up to 788 and TOFs up to 156 h^{-1}) [187, 188].

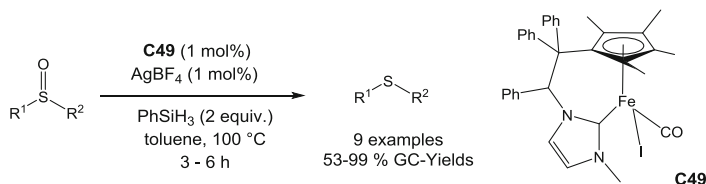
Using an in situ generated catalyst from $\text{Fe}(\text{acac})_2$ and $\text{P}(\text{CH}_2\text{CH}_2\text{PPh}_2)_3$ (**3**, 5 mol%), the reductive functionalization via the hydrosilylation of carbon dioxide can lead selectively to formamide and methylamine derivatives [189]. By the reaction of primary and secondary amines with 1 equiv. of phenylsilane in THF at rt for 18 h, CO_2 (1 bar) was transformed to the corresponding formamides



Scheme 46 Iron-catalyzed hydrogenation of carbon dioxide



Scheme 47 Fe(acac)₂/P(CH₂CH₂PPh₂)₃ catalyzed reductive functionalization of CO₂ via hydrosilylation



Scheme 48 Hydrosilylation of sulfoxides to sulfides using the Cp-NHC iron complex **C49**

in 24–95% GC yields (Scheme 47). With challenging primary amines, the reaction led to the mono-formylated compounds starting from primary aniline derivatives and a mixture of mono- and di-formyl compounds with primary alkylamines. It must be pointed out that this transformation can tolerate functional groups such as ketones and esters. It must be underlined that using 4 equiv. of phenylsilane in THF at 100°C for 18 h under 1 bar of CO₂, the catalytic system was able to perform the methylation of methylarylamines to give a mixture of formamides and tertiary methylated amines.

5 Reduction of Sulfoxides

Examples of iron-catalyzed hydrosilylation of sulfoxides to sulfides are rare. In 2011, Enthaler described the use of Fe₂(CO)₉ (**C22**, 5–10 mol%) as catalyst and either PMHS (5 equiv.) or PhSiH₃ (1 equiv.) in toluene at 100°C for 24 h to reduce sulfoxides to sulfides [190]. A good functional group tolerance was observed with this catalytic system as cyano-groups, esters and sulfonyl, alkenyl, and epoxide groups were not reduced. In 2012, Royo reported the same reaction using a combination of the well-defined tethered cyclopentadienyl–NHC iron complex **C49** (1 mol%) and a silver salt (1 mol%) with 2 equiv. of phenylsilane as the hydride source in toluene at 100°C for 3–6 h (Scheme 48) [191].

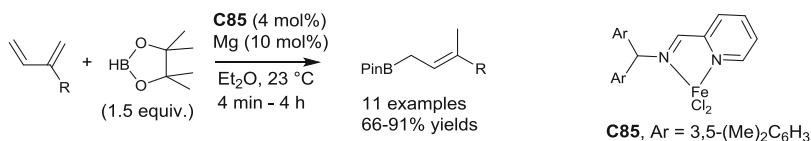
The reduction is suitable for aromatic and aliphatic sulfoxides. Interestingly, sulfoxides bearing functional groups such as chloride or vinyl can be reduced chemoselectively. In contrast, with a methyl acetate moiety, the reduction did not proceed under these conditions.

6 Hydroboration of Alkenes and Alkynes

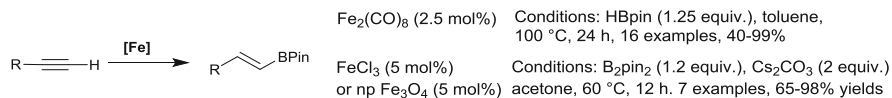
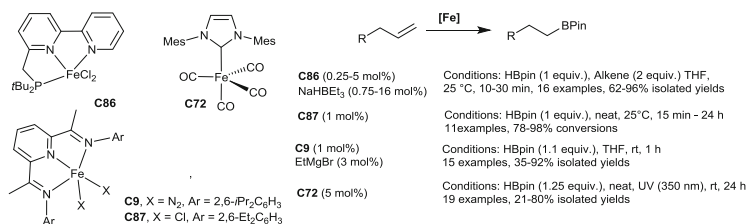
Transition metal-catalyzed hydroelementation processes represent nowadays an efficient and greener approach for the introduction of heteroelements such as boron (for selected reviews on hydroboration reactions, see [192–195]) into unsaturated carbon-based structures. More precisely, in the field of transition metal-catalyzed hydroboration, organoboronates have emerged as a significant class of organic reagents due to their good stability toward atmospheric oxidation, associated with their widespread use as synthons in selective transformations such as carbon–carbon or carbon–heteroatom bond formations (for selected reviews, see [196–199]). To perform such transformations, rhodium is usually the metal of choice (for selected reviews, see [200, 201]). Reports utilizing iron are scarce. In 1990s, Hartwig reported a pioneering stoichiometric activation of arenes leading to arylcatecholborane using the complex $[\text{Fe}(\text{Cp})(\text{Bcat})(\text{CO})_2]$ as the promoter (cat = catechol) [202, 203]. Then, two decades later, in 2010, Ritter described the first iron-catalyzed hydroboration of 1,3-dienes in the presence of pinacolborane, HBpin, using a catalyst generated from a well-defined (iminopyridine)FeCl₂ complex (**C85**) in the presence of magnesium [204]. Interestingly, the reaction can tolerate isolated C=C double bonds and esters; furthermore, it is highly chemo- and regioselective as only 1,4-addition adducts and (*E*)-C=C bonds were exclusively obtained (Scheme 49).

In 2013, Enthaler succeeded in hydroboration of alkynes using the $\text{Fe}_2(\text{CO})_9$ complex **C22** as the catalyst (2.5 mol%), yielding vinylboronate derivatives with high stereoselectivity when performing the reaction in the presence of 1.25 equiv. of HBpin at 100°C for 24 h. Starting from terminal alkynes, under similar conditions, (*E*)-vinylboronate derivatives were obtained selectively (17 examples), whereas more complex mixtures of regioisomers were obtained starting with terminal alkynes [205]. Using FeCl₃ or np Fe₃O₄ (5 mol%) in the presence of 1.2 equiv. of B₂pin₂ and 2 equiv. of Cs₂CO₃, terminal alkynes led to (*E*)-vinylboronates in 65–98% yields. Notably, np Fe₃O₄ can be reused up to six times without loss of activity (Scheme 50) [206].

Recently, the hydroboration of alkenes was competitively studied utilizing iron catalysts (Scheme 51). Huang described the use of an in situ generated catalyst prepared from the bipyridyl-based phosphine iron complex **C86** (0.25–5 mol%) and NaHBET₃ (3 equiv., 0.75–15 mol%) for the hydroborylation of terminal alkenes using 0.5 equiv. of HBpin at rt for 10–30 min. The reaction is chemoselective as only terminal C=C bond of a polyene is hydroborated [207]. Simultaneously,



Scheme 49 Chemo- and regioselective hydroboration of 1,3-dienes

**Scheme 50** Iron-catalyzed hydroboration of alkynes**Scheme 51** Iron-catalyzed hydroborylation of alkenes

Chirik reported that the bis(imino)pyridine iron dinitrogen complex **C9** (1 mol%) was also efficient for the hydroboration of terminal and disubstituted alkenes under neat conditions at 25 °C for 15 min to 24 h. Notably, the reaction also succeeded regioselectively with styrene derivatives [208]. Using a similar system, generating the active catalyst from the dichloro-iron complex **C87** or from FeCl₂ and the corresponding bis-iminopyridine ligand **4** (1 mol%) and EtMgBr (3 mol%), hydroboration of functional alkenes can be efficiently performed at rt for 1 h using 1.1 equiv. of HBpin. Notably, esters, amides, imines, amines, and alcohols are tolerated [209].

Using a well-defined iron-NHC complex, [Fe(CO)₄(IMes)] **C72** (5 mol%) under UV irradiation (350 nm) and neat conditions in the presence of 1.25 equiv. of HBpin, functionalized terminal alkenes can be hydroborated in moderate to good yields. The good functional group tolerance with ester, acetal, ether, silyl ether, epoxide, and nitrile moieties must be underlined [210].

7 Conclusion

In this chapter, we showed the major advances in the growing area of iron-catalyzed, chemoselective reduction of alkenes, alkynes, carbonyl derivatives, carboxylic compounds, and CO₂. Notably, the accurate design of the catalytic system also permitted to achieve highly chemoselective transformations. The topical reduction of carbon dioxide is also an exciting field of research, and iron starts to show promising performance. These initial achievements, in particular for challenging reductions of carboxylic acid derivatives, have already allowed very impressive advances and should stimulate the use of such methodologies in large-scale synthesis and fine chemistry.

References

1. Bolm C, Legros J, Le Paih J, Zani L (2004) *Chem Rev* 104:6217
2. Plietker B (2008) *Iron catalysis in organic chemistry*. Wiley-VCH Verlag, Weinheim
3. Bauer EB (2008) *Curr Org Chem* 12:1341
4. Sun CL, Li BJ, Shi ZJ (2011) *Chem Rev* 111:1293
5. Bézier D, Sortais JB, Darcel C (2013) *Adv Synth Catal* 355:19
6. Gopalaiah K (2013) *Chem Rev* 113:3248
7. Riener K, Haslinger S, Raba A, Högerl MP, Cokoja M, Herrmann WA, Kühn FE (2014) *Chem Rev* 114:5215
8. Junge K, Schröder K, Beller M (2011) *Chem Commun* 47:4849
9. Le Bailly BAF, Thomas SP (2011) *RSC Adv* 1435
10. Zhang M, Zhang A (2010) *Appl Organomet Chem* 24:751
11. Morris RH (2009) *Chem Soc Rev* 38:2282
12. Gaillard S, Renaud JL (2008) *ChemSusChem* 1:505
13. Frankel EN, Emken EA, Peters HM, Davison VL, Butterfield RO (1964) *J Org Chem* 29:3292
14. Frankel EN, Emken EA, Davison VL (1965) *J Org Chem* 30:2739
15. Schroeder MA, Wrighton MS (1976) *J Am Chem Soc* 98:551
16. Inoue H, Suzuki M (1980) *J Chem Soc Chem Commun* 817
17. Inoue H, Sato M (1983) *J Chem Soc Chem Commun* 983
18. Lynch TJ, Banah M, Kaesz HD, Porter CR (1984) *J Org Chem* 49:1266
19. Nishiguchi T, Fukuzumi K (1971) *J Chem Soc D Chem Commun* 139
20. Nishiguchi T, Fukuzumi K (1972) *Bull Chem Soc Jap* 45:1656
21. Bianchini C, Meli A, Peruzzini M, Vizza F, Zanolini F, Frediani P (1989) *Organometallics* 8:2080
22. Bianchini C, Meli A, Peruzzini M, Frediani P, Bohanna C, Esteruelas MA, Oro LA (1992) *Organometallics* 11:138
23. Bianchini C, Farnetti E, Graziano M, Peruzzini M, Polo A (1993) *Organometallics* 12:3753
24. Wienhöfer G, Westerhaus FA, Jagadeesh RV, Junge K, Junge H, Beller M (2012) *Chem Commun* 48:4827
25. Daida EJ, Peters JC (2004) *Inorg Chem* 43:7474
26. Fong H, Moret ME, Lee Y, Peters JC (2013) *Organometallics* 32:3053
27. Bart SC, Hawrelak EJ, Lobkovsky E, Chirik PJ (2005) *Organometallics* 24:5518
28. Bart SC, Lobkovsky E, Chirik PJ (2004) *J Am Chem Soc* 126:13794
29. Trovitch RJ, Lobkovsky E, Bill E, Chirik PJ (2008) *Organometallics* 27:1470
30. Yu RP, Darmon JM, Hoyt JM, Margulieux GW, Turner ZR, Chirik PJ (2012) *ACS Catal* 2:1760
31. Trovitch RJ, Lobkovsky E, Chirik PJ (2006) *Inorg Chem* 45:7252
32. Srimani D, Diskin-Posner Y, Ben-David Y, Milstein D (2013) *Angew Chem Int Ed* 52:14131
33. Hoyt JM, Shevlin M, Margulieux GW, Krska SW, Tudge MT, Chirik PJ (2014) *Organometallics* 33:5781
34. Phua P, Le Fort L, Boogers JAF, Tristany M, de Vries JG (2009) *Chem Commun* 3747
35. Rangheard C, de Julian FC, Phua PH, Hoorn J, Lefort L, de Vries JG (2010) *Dalton Trans* 39:8464
36. Bedford R, Betham M, Bruce D, Davis S, Frost R, Hird M (2006) *Chem Commun* 1398
37. Stein M, Wieland J, Steurer P, Toelle F, Muelhaupt R, Breit B (2011) *Adv Synth Catal* 353:523
38. Hudson R, Hamasaka G, Osako T, Yamada YMA, Li CJ, Uozumi Y, Moores A (2013) *Green Chem* 15:2141
39. Kelsen V, Wendt B, Werkmeister S, Junge K, Beller M, Chaudret B (2013) *Chem Commun* 49:3416
40. Ojima I, Li Z, Zhu J (1998) In: Rappoport Z, Apeloig Y (eds) *The chemistry of organosilicon compounds*, vol 2. Wiley, New York, p 1687

41. Speier JL (1979) *Adv Organomet Chem* 17:407
42. Karstedt BD (1973) US Patent 3 715 334
43. Hitchcock PB, Lappert MF, Warhurst NJW (1991) *Angew Chem Int Ed Engl* 30:438
44. Nesmeyanov AN, Freidlina RK, Chukovskaya EC, Petrova RG, Belyavsky AB (1962) *Tetrahedron* 17:61
45. Schroeder MA, Wrighton MS (1977) *J Organomet Chem* 128:345
46. Kakiuchi F, Tanaka Y, Chatani N, Murai S (1993) *J Organomet Chem* 456:45
47. Archer AM, Bouwkamp MW, Cortez MP, Lobkovsky E, Chirik PJ (2006) *Organometallics* 25:4269
48. Greenhalgh MD, Frank DJ, Thomas SP (2014) *Adv Synth Catal* 356:584
49. Tondreau AM, Hojilla Atienza CC, Weller KJ, Nye SA, Lewis KM, Delis JGP, Chirik PJ (2012) *Science* 335:567
50. Hojilla Atienza CC, Tondreau AM, Weller KJ, Lewis KM, Cruse RW, Nye SA, Boyer JL, Delis JGP, Chirik PJ (2012) *ACS Catal* 2:2169
51. Peng D, Zhang Y, Du X, Zhang L, Leng X, Walter MD, Huang Z (2013) *J Am Chem Soc* 135:19154
52. Kamata K, Suzuki A, Nakai Y, Nakazawa H (2012) *Organometallics* 31:3825
53. Tondreau AM, Hojilla Atienza CC, Darmon JM, Milsmann C, Hoyt HM, Weller KJ, Nye SA, Lewis KM, Boyer J, Delis JGP, Lobkovsky E, Chirik PJ (2012) *Organometallics* 31:4886
54. Wu JY, Stanzl BN, Ritter T (2010) *J Am Chem Soc* 132:13214
55. Enthaler S, Haberberger M, Irran E (2011) *Chem Asian J* 6:1613
56. Haberberger M, Irran E, Enthaler S (2011) *Eur J Inorg Chem* 2797
57. Belger C, Plietker B (2012) *Chem Commun* 48:5419
58. Markó L, Radhi MA, Örvös I (1981) *J Organomet Chem* 218:369
59. Markó L, Palágyi J (1983) *Trans Met Chem* 8:207
60. Casey CP, Guan H (2007) *J Am Chem Soc* 129:5816
61. Knölker HJ, Baum E, Goesmann H, Klauss R (1999) *Angew Chem Int Ed* 38:2064
62. Fleischer S, Zhou S, Junge K, Beller M (2013) *Angew Chem Int Ed* 52:5120
63. Tlili A, Schranck J, Neumann H, Beller M (2012) *Chem Eur J* 18:15935
64. Mérel DS, Elie M, Lohier JF, Gaillard S, Renaud JL (2013) *ChemCatChem* 5:2939
65. Berkessel A, Reichau S, von der Höh A, Leconte N, Neudörfl JM (2011) *Organometallics* 30:3880
66. Casey CP, Guan H (2009) *J Am Chem Soc* 131:2499
67. Bullock RM (2007) *Angew Chem Int Ed* 46:7360
68. Zhang H, Chen D, Zhang Y, Zhang G, Liu J (2010) *Dalton Trans* 39:1972
69. Rautenstrauch V, Hoang-Cong X, Churlaud R, Abdur-Rashid K, Morris RH (2003) *Chem Eur J* 9:4954
70. Sui-Seng C, Freutel F, Lough AJ, Morris RH (2008) *Angew Chem Int Ed* 47:940
71. Sui-Seng C, Haque FN, Hadzovic A, Pütz AM, Reuss V, Meyer N, Lough AJ, Zimmer-De Iuliis M, Morris RH (2009) *Inorg Chem* 48:735
72. Zhang J, Leitus G, Ben-David Y, Milstein D (2005) *J Am Chem Soc* 127:10840
73. Zhang J, Leitus G, Ben-David Y, Milstein D (2006) *Angew Chem Int Ed* 45:1113
74. Balaraman E, Gnanaprakasam B, Shimon LJW, Milstein D (2010) *J Am Chem Soc* 132:16756
75. Gunanathan C, Milstein D (2011) *Acc Chem Res* 44:588
76. Langer R, Leitus G, Ben-David Y, Milstein D (2011) *Angew Chem Int Ed* 50:2120
77. Yang X (2011) *Inorg Chem* 50:12836
78. Langer R, Iron MA, Konstantinovski L, Diskin-Posner Y, Leitus G, Ben-David Y, Milstein D (2012) *Chem Eur J* 18:7196
79. Lagaditis PO, Sues PE, Sonnenberg JF, Wan KY, Lough AJ, Morris RH (2014) *J Am Chem Soc* 136:1367
80. Wienhöfer G, Westerhaus FA, Junge K, Ludwig R, Beller M (2013) *Chem Eur J* 19:7701
81. Li Y, Yu S, Wu X, Xiao J, Shen W, Dong Z, Gao J (2014) *J Am Chem Soc* 136:4031

82. Lu LQ, Li Y, Junge K, Beller M (2013) *Angew Chem Int Ed* 52:8382
83. Jothimony K, Vancheesen S (1989) *J Mol Catal* 52:301
84. Jothimony K, Vancheesen S, Kuriacose JC (1985) *J Mol Catal* 32:11
85. Enthaler S, Hagemann B, Erre G, Junge K, Beller M (2006) *Chem Asian J* 1:598
86. Enthaler S, Erre G, Tse MK, Junge K, Beller M (2006) *Tetrahedron Lett* 47:8095
87. Enthaler S, Spilker B, Erre G, Junge K, Tse MK, Beller M (2008) *Tetrahedron* 64:3867
88. Polshettiwar V, Varma RS (2009) *Green Chem* 11:1313
89. Chen JS, Chen LL, Xing Y, Chen G, Shen WY, Dong ZR, Li YY, Gao JX (2004) *Huaxue Xuebao* 62:1745
90. Meyer N, Lough AJ, Morris RH (2009) *Chem Eur J* 15:5605
91. Mikhailine AA, Lough AJ, Morris RH (2009) *J Am Chem Soc* 131:1394
92. Lagaditis PO, Lough AJ, Morris RH (2010) *Inorg Chem* 49:10057
93. Mikhailine AA, Morris RH (2010) *Inorg Chem* 49:11039
94. Sues PE, Lough AJ, Morris RH (2011) *Organometallics* 30:4418
95. Mikhailine AA, Kim E, Dingels C, Lough AJ, Morris RH (2008) *Inorg Chem* 47:6587
96. Lagaditis PO, Lough AJ, Morris RH (2011) *J Am Chem Soc* 133:9662
97. Zuo W, Lough AJ, Feng Y, Morris RH (2013) *Science* 342:1080
98. Buchard A, Heuclin H, Auffrant A, Le Goff XF, Le Floch P (2009) *Dalton Trans* 1659
99. Yu S, Shen W, Li Y, Dong Z, Xu Y, Li Q, Zhang J, Gao J (2012) *Adv Synth Catal* 354:818
100. Kandepi VVKM, Cardoso JMS, Peris E, Royo B (2010) *Organometallics* 29:2777
101. Bala MD, Ikhile MI (2014) *J Mol Catal A Chem* 385:98
102. Wienhöfer G, Westerhaus FA, Junge K, Beller M (2013) *J Organomet Chem* 744:156
103. Brunner H, Fisch K (1990) *Angew Chem Int Ed Engl* 29:1131
104. Shaikh NS, Junge K, Beller M (2007) *Org Lett* 9:5429
105. Addis D, Shaikh NS, Zhou S, Das S, Junge K, Beller M (2010) *Chem Asian J* 5:1687
106. Shaikh NS, Enthaler S, Junge K, Beller M (2008) *Angew Chem Int Ed* 47:2497
107. Nishiyama H, Furuta A (2007) *Chem Commun* 760
108. Furuta A, Nishiyama H (2008) *Tetrahedron Lett* 49:110
109. Inagaki T, Phong LT, Furuta A, Ito JI, Nishiyama H (2010) *Chem Eur J* 16:3090
110. Langlotz BK, Wadepohl H, Gade LH (2008) *Angew Chem Int Ed* 47:4670
111. Tondreau AM, Darmon JM, Wile BM, Floyd SK, Lobkovsky E, Chirik PJ (2009) *Organometallics* 28:3928
112. Muller K, Schubert A, Jozak T, Ahrens-Botzong A, Schünemann V, Thiel WR (2011) *ChemCatChem* 3:887
113. Plietker B, Dieskau A (2009) *Eur J Org Chem* 775
114. Holzwarth M, Dieskau A, Tabassam M, Plietker B (2009) *Angew Chem Int Ed* 48:7251
115. Dieskau A, Begouin JM, Plietker B (2011) *Eur J Org Chem* 5291
116. Yang J, Tilley TD (2010) *Angew Chem Int Ed* 49:10186
117. Tondreau AA, Lobkovsky E, Chirik PJ (2008) *Org Lett* 10:2789
118. Bhattacharya P, Krause JA, Guan H (2011) *Organometallics* 30:4720
119. Wu S, Li X, Xiong Z, Xu W, Lu Y, Sun H (2013) *Organometallics* 32:3227
120. Zuo Z, Sun H, Wang L, Li X (2014) *Dalton Trans* 43:1176
121. Gutsulyak DV, Kuzmina LG, Howard JAK, Vyboishchikov SF, Nikonov GI (2008) *J Am Chem Soc* 130:3732
122. Zheng J, Misal Castro LC, Roisnel T, Darcel C, Sortais JB (2012) *Inorg Chim Acta* 380:301
123. Jiang F, Bézier D, Sortais JB, Darcel C (2011) *Adv Synth Catal* 353:239
124. Bézier D, Jiang F, Roisnel T, Sortais JB, Darcel C (2012) *Eur J Inorg Chem* 1333
125. Demir S, Gökçe Y, Kaloğlu N, Sortais JB, Darcel C, Özdemir İ (2013) *Appl Organomet Chem* 27:459
126. César V, Misal Castro LC, Dombray T, Sortais JB, Darcel C, Labat S, Miqueu K, Sotiropoulos JM, Brousses R, Lugan N, Lavigne G (2013) *Organometallics* 32:4643
127. Kumar D, Prakasham AP, Bheeter LP, Sortais JB, Gangwar M, Roisnel T, Kalita A, Darcel C, Ghosh P (2014) *J Organomet Chem* 762:81

128. Buitrago E, Zani L, Adolfsson H (2011) *Appl Organomet Chem* 25:748
129. Buitrago E, Tinnis F, Adolfsson H (2012) *Adv Synth Catal* 354:217
130. Hashimoto T, Urban S, Hoshino R, Ohki Y, Tatsumi K, Glorius F (2012) *Organometallics* 31:4474
131. Grohmann C, Hashimoto T, Fröhlich R, Ohki Y, Tatsumi K, Glorius F (2012) *Organometallics* 31:8047
132. Warratz S, Postigo L, Royo B (2013) *Organometallics* 32:893
133. Dal Zotto RC, Virieux D, Campagne JM (2009) *Synlett* 276
134. Zhou S, Fleischer S, Junge K, Beller M (2011) *Angew Chem Int Ed* 50:5120
135. Fleischer S, Werkmeister S, Zhou S, Junge K, Beller M (2012) *Chem Eur J* 18:9005
136. Fleischer S, Zhou S, Werkmeister S, Junge K, Beller M (2013) *Chem Eur J* 19:4997
137. Chakraborty S, Brennessel WW, Jones WD (2014) *J Am Chem Soc* 136:8564
138. Zhou S, Fleischer S, Junge K, Das S, Addis D, Beller M (2010) *Angew Chem Int Ed* 49:8121
139. Mikhailine AA, Maishan MI, Morris RH (2012) *Org Lett* 14:4638
140. Misal Castro LC, Sortais JB, Darcel C (2012) *Chem Commun* 48:151
141. Knifton JF (1976) *J Org Chem* 41:1200
142. Deshpande RM, Mahajan AN, Diwakar MM, Ozarde PS, Chaudhari RV (2004) *J Org Chem* 69:4835
143. Wienhöfer G, Baseda-Krüger M, Ziebart C, Westerhaus FA, Baumann W, Jackstell R, Junge K, Beller M (2013) *Chem Commun* 49:9089
144. Wienhöfer G, Sorribes I, Boddien A, Westerhaus F, Junge K, Junge H, Llusar R, Beller M (2012) *J Am Chem Soc* 133:12875
145. Junge K, Wendt B, Shaikh N, Beller M (2010) *Chem Commun* 46:1769
146. Pehlivan L, Métay E, Laval S, Dayoub W, Demonchaux P, Mignani G, Lemaire M (2010) *Tetrahedron Lett* 51:1939
147. Pehlivan L, Métay E, Laval S, Dayoub W, Demonchaux P, Mignani G, Lemaire M (2011) *Tetrahedron* 67:1971
148. Bhor MD, Bhanushali MJ, Nandurkar NS, Bhanage BM (2008) *Tetrahedron Lett* 49:965
149. Fleischer S, Zhou S, Junge K, Beller M (2011) *Chem Asian J* 6:2240
150. Pagnoux-Ozherelyeva A, Pannetier N, Diagne Mbaye M, Gaillard S, Renaud JL (2012) *Angew Chem Int Ed* 51:4976
151. Moulin S, Dentel H, Pagnoux-Ozherelyeva A, Gaillard S, Poater A, Cavallo L, Lohier JF, Renaud JL (2013) *Chem Eur J* 19:17881
152. Enthaler S (2010) *ChemCatChem* 2:1411
153. Jaafar H, Li H, Misal Castro LC, Zheng J, Roisnel T, Dorcet V, Sortais JB, Darcel C (2012) *Eur J Inorg Chem* 3546
154. Li H, Achard M, Bruneau C, Sortais JB, Darcel C (2014) *RSC Adv* 4:25892
155. Zhou S, Junge K, Addis D, Das S, Beller M (2009) *Angew Chem Int Ed* 48:9507
156. Sunada Y, Kawakami H, Motoyama Y, Nagashima H (2009) *Angew Chem Int Ed* 48:9511
157. Tsutsumi H, Sunada Y, Nagashima H (2011) *Chem Commun* 47:6581
158. Bézier D, Venkanna GT, Sortais JB, Darcel C (2011) *ChemCatChem* 3:1747
159. Volkov A, Buitrago E, Adolfsson H (2013) *Eur J Org Chem* 2066
160. Blom B, Tan G, Enthaler S, Inoue S, Epping JD, Driess M (2013) *J Am Chem Soc* 135:18108
161. Zhou S, Addis D, Das S, Junge K, Beller M (2009) *Chem Commun* 4883
162. Das S, Wendt B, Moeller K, Junge K, Beller M (2012) *Angew Chem Int Ed* 51:1662
163. Bornschein C, Werkmeister S, Werndt B, Jiao H, Alberico E, Baumann W, Junge H, Junge K, Beller M (2014) *Nat Commun* 5:4111
164. Bézier D, Venkanna GT, Misal Castro LC, Zheng J, Sortais JB, Darcel C (2012) *Adv Synth Catal* 354:1879
165. Junge K, Wendt B, Zhou S, Beller M (2013) *Eur J Org Chem* 2061
166. Ruddy AJ, Kelly CM, Crawford SM, Wheaton CA, Sydora OL, Small BL, Stradiotto M, Turculet L (2013) *Organometallics* 32:5581
167. Das S, Li Y, Junge K, Beller M (2012) *Chem Commun* 48:10742

168. Li H, Misal Castro LC, Zheng J, Roisnel T, Dorcet V, Sortais JB, Darcel C (2013) *Angew Chem Int Ed* 52:8045
169. Cong C, Fujihara T, Terao J, Tsuji Y (2014) *Catal Commun* 50:25
170. Zell T, Ben-David Y, Milstein D (2014) *Angew Chem Int Ed* 53:4685
171. Werkmeister S, Junge K, Wendt B, Alberico E, Jiao H, Baumann W, Junge H, Gallou F, Beller M (2014) *Angew Chem Int Ed*. doi:10.1002/anie.201402542
172. Chakraborty S, Dai H, Bhattacharya P, Fairweather NT, Gibson MS, Krause JA, Guan H (2014) *J Am Chem Soc*. doi:10.1021/ja405034
173. Misal Castro LC, Li H, Sortais JB, Darcel C (2012) *Chem Commun* 48:10514
174. Pouessel J, Jacquet O, Cantat T (2013) *ChemCatChem* 5:3552
175. Quadrelli EA, Centi G, Duplan JL, Perathoner S (2011) *ChemSusChem* 4:1194
176. Wang W, Wang S, Ma X, Gong J (2011) *Chem Soc Rev* 40:3703
177. Jessop PG, Ikariya T, Noyori R (1995) *Chem Rev* 95:259
178. Leitner W (1995) *Angew Chem Int Ed Engl* 34:2207
179. Jessop PG, Joó F, Tai CC (2004) *Coord Chem Rev* 248:2425
180. Federsel C, Jackstell R, Beller M (2010) *Angew Chem Int Ed* 49:6254
181. Tai CC, Chang T, Roller B, Jessop PG (2003) *Inorg Chem* 42:7340
182. Federsel C, Boddien A, Jackstell R, Jennerjahn R, Dyson PJ, Scopelliti R, Laurency G, Beller M (2010) *Angew Chem Int Ed* 49:9777
183. Drake JL, Manna CM, Byers JA (2013) *Organometallics* 32:6891
184. Ziebart C, Federsel C, Anbarasan P, Jackstell R, Baumann W, Spannenberg A, Beller M (2012) *J Am Chem Soc* 134:20701
185. Boddien A, Mellmann D, Gärtner F, Jackstell R, Junge H, Dyson PJ, Laurency G, Ludwig R, Beller M (2011) *Science* 333:1733
186. Yang X (2013) *Dalton Trans* 42:11987
187. Langer R, Diskin-Posner Y, Leitus G, Shimon LJM, Ben-David Y, Milstein D (2011) *Angew Chem Int Ed* 50:9948
188. Yang X (2011) *ACS Catal* 1:849
189. Frogneux X, Jacquet O, Cantat T (2014) *Catal Sci Technol* 4:1529
190. Enthaler S (2011) *ChemCatChem* 3:666
191. Cardoso JMS, Royo B (2012) *Chem Commun* 48:4944
192. Burgess K, Ohlmeyer MJ (1991) *Chem Rev* 91:1179
193. Miyaura N (2001) In: Togni A, Grützmacher H (eds) *Catalytic heterofunctionalization*. Wiley-VCH, Weinheim, pp 1–46
194. Hartwig JF (2011) *Chem Soc Rev* 40:1992
195. Mkhaliid IAI, Barnard JH, Marder TB, Murphy JM, Hartwig JF (2010) *Chem Rev* 110:890
196. Hall DG (2005) *Boronic acids*. Wiley-VCH, New York
197. Miyaura N, Suzuki A (1995) *Chem Rev* 95:2457
198. Doucet H (2008) *Eur J Org Chem* 2013
199. Jana R, Pathak TP, Sigman MS (2011) *Chem Rev* 111:1417
200. Brown JM (2005) In: Evans PA (ed) *Modern rhodium-catalysed organic reactions*. Wiley-VCH Verlag, Weinheim, pp 33–54
201. Coyne AG, Guiry PJ (2008) In: Andersson PG, Munslow IJ (eds) *Modern reduction methods*. Wiley-VCH Verlag, Weinheim, pp 65–86
202. Hartwig JF, Huber S (1993) *J Am Chem Soc* 115:4908
203. Waltz KM, He X, Muhoro C, Hartwig JF (1995) *J Am Chem Soc* 117:11357
204. Wu JY, Moreau B, Ritter T (2009) *J Am Chem Soc* 131:12915
205. Haberberger M, Enthaler S (2011) *Chem Asian J* 8:50
206. Rawat VS, Sreedhar B (2014) *Synlett* 1132
207. Zhang L, Peng D, Leng X, Huang Z (2013) *Angew Chem Int Ed* 52:3676
208. Obligacion JV, Chirik PJ (2013) *Org Lett* 15:2680
209. Greenhalgh MD, Thomas SP (2013) *Chem Commun* 49:11230
210. Zheng J, Sortais JB, Darcel C (2014) *ChemCatChem* 6:763

Iron-Catalyzed Oligomerization and Polymerization Reactions

Benjamin Burcher, Pierre-Alain R. Breuil, Lionel Magna, and Hélène Olivier-Bourbigou

Abstract Having the tremendous industrial importance of thermoplastics and elastomers in mind, it is not surprising to see a proliferation of studies on a variety of catalytic systems for polymerization and oligomerization of unsaturated hydrocarbons. Over the last 15 years, the development of mid- to late transition metal catalysts has provided significant advances in this area. The availability of iron combined with its low environmental impact and its tolerance to heteroatom functions attracts significant interest from both academia and industry. In the late 1990s, key milestones have been the development of well-characterized bulky bis(imino)pyridine-Fe(II) precatalysts, mainly for the polymerization or oligomerization of ethylene. This chapter provides a brief overview of the key developments reported in the last 5 years in the literature in the field of iron-catalyzed olefin and diolefin polymerization and oligomerization. Emphasis has been placed on ethylene oligomerization and polymerization, with a particular interest in ligand architecture modifications. The advances in characterization and understanding of catalytically active iron species and the corresponding mechanisms are reported. Heterogenization of bis(imino)pyridine iron catalytic systems has been considered for ethylene transformation and will also be covered in this chapter. The interest of iron catalysts for multiple single-site approaches such as reactor blending and tandem catalysis is also described. Finally, iron catalyst systems also present interesting features for diene polymerization even though both activities and selectivities remain far from those observed for conventional catalysts.

Keywords Diolefins · Iron · Olefins · Oligomerization · Polymerization

B. Burcher, P.-A.R. Breuil, L. Magna, and H. Olivier-Bourbigou (✉)
IFP Energies Nouvelles, Molecular Catalysis Department, Rond point de l'échangeur
de Solaize, 69360 Solaize, France
e-mail: helene.olivier-bourbigou@ifpen.fr

Contents

1	Introduction and Scope	219
2	Ethylene Oligomerization and Polymerization	221
2.1	Nitrogen-Based Architectures for Ligand Development	221
2.2	Comprehension and Characterization	229
2.3	Supported Homogeneous Iron Catalysts for Oligomerization and Polymerization of Ethylene	231
3	Multiple Single-Site Catalysis	234
3.1	Reactor Blending	235
3.2	Tandem Catalysis	237
4	Diene Polymerization	240
4.1	Iron-Based Catalysts for Polymerization of Conjugated Dienes	241
4.2	Iron-Based Catalysts for Homo- and Copolymerization of Olefins and Nonconjugated Dienes	246
5	Conclusion and Outlook	248
	References	249

Abbreviations

DSC	Differential scanning chromatography
EASC	Ethylaluminum sesquichloride $\text{Et}_3\text{Al}_2\text{Cl}_3$
EPR	Electron paramagnetic resonance
GPC	Gel permeation chromatography
HDPE	High-density polyethylene
<i>i</i> Pr	Isopropyl
K	Schulz–Flory coefficient
LAO	Linear alpha olefin
LLDPE	Linear low-density polyethylene
MAO	Methylaluminoxane
MMAO	Modified methylaluminoxane
M_n	Number-average molecular weight
M_w	Weight-average molecular weight
MW	Molecular weight
MWD	Molecular weight distribution
NMR	Nuclear magnetic resonance
Oct	Octyl
PP	Polypropylene
SHOP	Shell higher olefin process
TEA	Triethylaluminum = AlEt_3
THF	Tetrahydrofuran
TIBA	Triisobutylaluminum = $\text{Al}(i\text{Bu})_3$
TMA	Trimethylaluminum = AlMe_3
UHMWPE	Ultrahigh molecular weight polyethylene

1 Introduction and Scope

In the category of thermoplastics, polyolefins produced by polymerization of olefins, namely, ethylene and propylene (polyethylene including LDPE, LLDPE, HDPE, and polypropylene PP), represent more than 50%. More than 130 million tons of polyolefins were produced and utilized globally in 2012, making them by far the largest type of plastic [1]. Polyethylene (PE), produced by metal-catalyzed ethylene polymerization processes, is the most widely used thermoplastic worldwide [1].

Besides polymers, linear alpha olefins (LAOs) are versatile chemical intermediates for a wide range of industrial and consumer products. The major use of LAO is as a PE comonomer (for C4–C8 α -olefins) but also as starting materials for plasticizers (for C6–C10 α -olefins), surfactants, or lubricant oil additives (for C10–C20 olefins). Oligomerization of ethylene is one of the major processes for the production of LAOs. The catalysts used in industry are either alkylaluminum compounds, a combination of alkylaluminum with early transition metal complexes (Ti, Zr, or Cr), or with nickel and a monoanionic bidentate ligand (SHOP/Shell process).

Synthetic polymers are the newcomers among the bulk materials used in modern chemistry. In the category of synthetic elastomers, their demand is driven by both the need for tires and the automotive industry. Conjugated dienes, such as 1,3-butadiene, are still the most widely used feedstock for synthetic elastomer production. The development of various catalysts for diene polymerization processes, targeting these products, remains of deep interest.

Among the factors that significantly impact the properties of polymers or oligomers, the nature of the catalytic systems plays a key role. The search for new catalysts remains an important target and is pivotal for the industry, aiming to produce new polymers with improved properties or oligomers (mainly LAOs) with a better control of selectivity. Early transition metal-based catalysts were the most developed during the last 30 years as the Group IV metallocenes combined with methylaluminoxane (MAO) are highly efficient for polymerization reactions [2, 3]. However, over the last 15 years, the development of mid- to late transition metal catalysts has provided significant advances in these areas [4].

Having in view the tremendous importance of these industrial products, it is not surprising to see a proliferation of studies on a variety of catalytic systems, but what has been the role played by iron-based catalysts in this area and what can be expected? Of course, the availability of iron combined with its low environmental impact attracts significant industrial interest. Moreover, another interest that has appeared progressively is the tolerance of late transition metal complexes to heteroatom functions. This may open the possibility of copolymerization of olefins with polar comonomers [5] although this application is still in its infancy. However, this cannot be the only reasons to explain the rapid development of iron-based polymerization catalysts.

If we return to the early history, iron catalysis has had the potential to form carbon–carbon bonds starting from simple unsaturated compounds. This work was historically described in the 1960s by Hata who investigated the reactivity of diolefins (butadiene and isoprene alone or with ethylene) with Ziegler–Natta type catalytic systems based on the combination of Fe(III), typically Fe(acac)₃, and an alkylaluminum, typically AlEt₃, eventually in the presence of an additional electron donor ligand [6–8]. In the case of butadiene, the reaction afforded a mixture of branched and linear products. Cyclodimerization of butadiene to cyclooctadiene and vinylcyclohexene was achieved by using bipyridine as stabilizing ligand associated with iron(II)-diethyl or iron(0) complexes [9]. Later on, in the 1980s, iron–diimine complexes were reported by Tom Dieck [10, 11]. Nitrosyl iron-based systems were the most interesting systems to direct the reaction toward the selective formation of vinylcyclohexene [12]. In all these homogeneous systems, it seems that the active species arose from a zerovalent iron, to which the olefin to be oligomerized coordinates. Unfortunately, the lack of characterization hampered the full interpretation of reaction mechanisms.

Then, until the late 1990s, iron did not play a dominant role in the field of olefin polymerization or oligomerization, and to the best of our knowledge, the reactivity of iron complexes toward low molecular weight monoolefins (namely, ethylene or propylene) was not actually reported.

In the late 1990s, key milestones have been the development of the isolated bulky bis(imino)pyridine-Fe(II) precatalysts for the polymerization/oligomerization of olefins (mainly ethylene) [13]. The reactivity of these iron complexes was proclaimed as the start of the “Iron age”. The most attractive features were the modularity of the ligand and the exceptionally high activities achieved using MAO derivatives as activators. Modifying the ligand structure allows access to a wide range of products, such as high molecular weight and strictly linear polyethylenes or low molecular weight oligomers. Significant effort has been devoted to the fine tuning of catalyst ligands and full reviews cover the recent progress [14, 15]. However, many problems still remained to be solved to make these catalysts a reality for industry. The thermal instability of bis(imino)pyridyl iron complexes and their deactivation during the course of the reaction are some of the main issues associated with by-product formation. This motivates ongoing research on these systems.

Nevertheless, as a consequence of the unique features of these iron complexes in olefin polymerization and oligomerization, the catalytic performances of bis(imino)pyridine iron complexes on polymerization of polar monomers (such as methyl acrylate, methyl methacrylate, or *tert*-butyl acrylate) have been investigated [16]. We will not discuss this aspect in this chapter as the recent literature has not been extensive in this area.

This chapter will provide a brief overview of the key developments reported in the last 5 years in the literature in the field of iron-catalyzed ethylene polymerization and oligomerization with an emphasis on the issues encountered for these systems and the solutions proposed particularly in modifying the ligand architecture. Although reaction conditions reported in the different examples are generally not equivalent, the catalyst activities mentioned in this article may be ranked as

follows: high (10^7 g/(mol h) and above), good (10^6 g/(mol h)), and moderate (10^5 g/(mol h) and below). The ability of bis(imino)catalysts to polymerize other alkenes such as propylene, 1-butene, 1-hexene, or norbornene has been recently reviewed [17]. In the case of propylene, isotactic polypropylenes are obtained with a substantial effect of steric bulk of the aryl *o*-substituent on the polymer molecular weight. Oligomerization of 1-butene or 1-hexene with the less encumbered iron complexes leads to dimers consisting, interestingly, of mainly linear products [18]. However, these results have not been the object of significant developments in the last 5 years and will not be discussed in more detail in this chapter.

The immobilization of the iron complexes on various supports, organic or inorganic, through non-covalent and covalent interactions has been investigated and is discussed in this chapter, although no significant breakthrough has been achieved recently in this area. Studies devoted to the understanding of the catalytically active species generated in solution when the iron precatalysts are activated with MAO and research to clarify some aspects of the mechanism have been conducted. Unfortunately, despite these investigations, a gray area remains. The recent spectroscopic investigations directed toward the identification of the active species will be covered in this chapter.

Iron catalysts have been used in tandem catalytic systems (also named dual catalysis with an association of an oligomerization or a polymerization catalyst) for the production of specific PEs. Iron has also been used as polymerization catalysts in reactor blending to produce PE with better control of molecular weight distribution. The latest results will be documented in the chapter.

Finally, the latest achievements concerning the reactivity of tridentate or bidentate iron complexes for diene transformations will be discussed.

2 Ethylene Oligomerization and Polymerization

2.1 Nitrogen-Based Architectures for Ligand Development

2.1.1 Neutral Tridentate Ligands

Modifying the steric hindrance of the *ortho* positions of the imine aryl moieties has been recently investigated. Wu and coworkers described $[\text{FeCl}_2(\mathbf{L1})]$ complexes bearing *sec*-phenethyl-substituted aryl groups (Fig. 1) affording highly active systems upon MAO activation at 30°C and 1 bar of ethylene (up to 10^7 g/(mol h)) [19]. High M_w were obtained, above 10^6 g/mol with extremely broad and bimodal distributions (M_w/M_n up to 260). Under 10 bar of ethylene, excellent activities could be maintained at 70°C leading to polymers with high melting points (around 136°C), which were non-soluble for further analyses. Benzhydryl substitution on the aryl groups was recently proposed, leading to effective precatalysts $[\text{FeCl}_2(\mathbf{L2})]$ in the presence of MAO or MMAO at industrially relevant temperatures (60–80°C) and 10 bar of ethylene with high activities up to 10^7 g/(mol h)

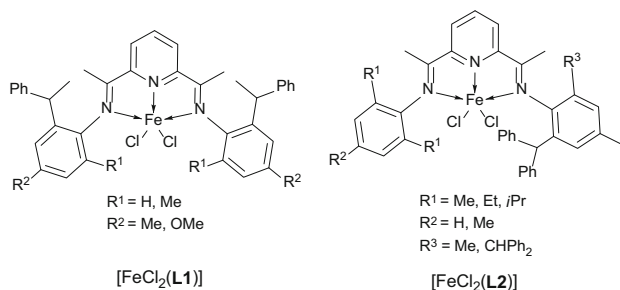


Fig. 1 Iron pre-catalysts bearing sterically hindered bis(imino)pyridine ligands

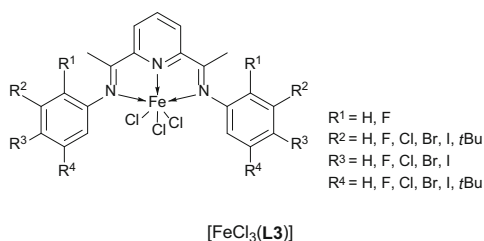


Fig. 2 Halogen-substituted bis(imino)pyridine complexes

[20]. At these temperatures, low MW polyethylenes having a broad molecular weight distribution were, however, obtained compared to PEs obtained at 20°C (10^4 vs 10^5 g/mol, respectively).

Görl et al. studied bis(imino)pyridine iron(III) complexes $[\text{FeCl}_3(\text{L3})]$ bearing halogen groups (Fig. 2) [21, 22]. These iron(III) catalytic systems appeared to be highly active in the presence of MAO (10^7 g/(mol h)) at 60°C and 10 bar of ethylene, even in the absence of substitution in *ortho* positions of the imine aryl rings, known to be a feature leading to rapid degradation. Indeed, the formation of the inactive ion pair $[\text{FeL}_2]^{2+}[\text{FeCl}_4]^{2-}$ may be a degradation pathway when no sterically hindered ligands are used. Short Schulz–Flory distributions were observed ($K = 0.2\text{--}0.4$), along with the presence of internal and branched olefins in the hexene fraction for some examples. This suggests that the limited steric hindrance around the metal center favors isomerization processes but also co-oligomerization processes of light alpha olefins such as 1-butene, opening avenues for desired copolymerization of ethylene and an alpha olefin with iron-based catalysts.

The modification of the central ring was investigated in detail by several research groups [23–27]. Additional nitrogen atoms as in pyrimidine or pyrazine led to a noticeable decrease of activity for the corresponding iron(II) catalysts compared to their bis(imino)pyridine analogues. Moreover, coordination of bis(imino)triazine ligands to iron was reported to be unsuccessful. With tridentate ligands having a central five-membered heterocycle, no coordination was observed

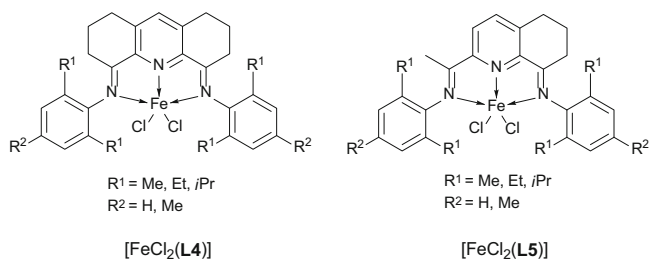


Fig. 3 Rigid and semirigid tridentate backbones for iron complexes

with 1-methylpyrrole, thiophene, or furan derivatives, while thiazole derivatives coordinate on iron(II) precursors leading to catalysts with low activity when MAO was added, affording short-chain oligomers [25, 28].

More recently, Kim et al. investigated the effect of a more rigid backbone compared to bis(imino)pyridine ligands by introducing 2,3,7,8-tetrahydroacridine-4,5-(1H,6H)-diimine through complexes [FeCl₂(L4)] in the presence of MAO (250 eq.) at 30°C and 1.3 bar of ethylene (Fig. 3) [29]. Increasing the bulkiness at *ortho* positions of the imine moieties (from Me to *i*Pr groups) generally led to slightly lower catalyst activity (10⁶ g/(mol h)) and higher but still low PE molecular weight. The 2,6-diisopropyl-substituted complex afforded a polyethylene with a *M_w* of 18,000 g/mol and broad distribution, a more than tenfold lower *M_w*, compared to the analogous bis(imino)pyridine catalyst [30]. Increasing the Al/Fe ratio or the temperature led to PE with decreased *M_w*, the catalyst being still active at 70°C. Related semirigid structures [FeCl₂(L5)] were reported by Redshaw and coworkers [31]. At 50°C and 10 bar of ethylene, high activities were obtained with MAO, affording moderate to high MW polyethylene (from 20,000 to 200,000 g/mol) with broad distribution. Surprisingly, increasing the temperature afforded a narrower and unimodal distribution (*M_w*/*M_n* from 35 at 30°C to 2.8 at 60°C) with an enhanced activity that may be indicative for single-site active species.

The groups of Gibson [32] and Chirik [33] reported the introduction of substituents at the imine carbon atom of bis(imino)pyridine backbone, leading to highly active catalyst in ethylene polymerization. Additional results by Britovsek, Gibson et al. at 25°C and 1 bar of ethylene showed that thioether-substituted complexes [FeCl₂(L6)] lead to higher activities (10⁷ g/(mol h)) compared to those with ether substituents (10⁶ g/(mol h)), while functionalization of the imine carbon atom by amino moieties or the methyl ether group afforded inactive catalysts (Fig. 4) [34]. Linear polyethylenes having a broad distribution were generally obtained. Enriching the steric hindrance at the imine carbon position or at the *ortho* positions of the imino aryl groups tends to decrease the catalyst activity and to afford PE with higher *M_w* (up to 430,000 g/mol).

Structural analogues of bis(imino)pyridine ligands, functionalized phenanthroline ligands, have been widely investigated by the group of Sun for the oligomerization of ethylene [35]. Their tedious synthesis allowed structural diversification of

Fig. 4 Substitution at the imine carbon atoms

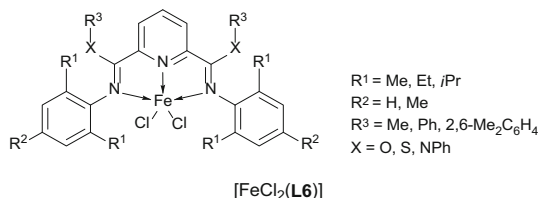
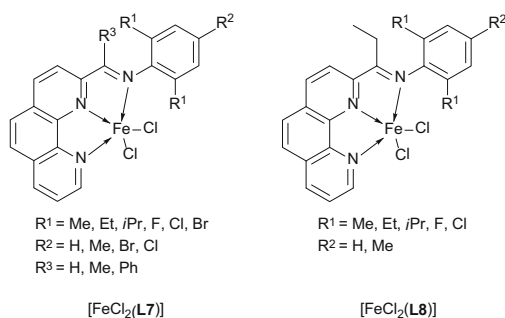


Fig. 5 Phenanthroline-derived iron complexes



iron(II) precursors $[\text{FeCl}_2(\text{L7})]$ leading to wax-free oligomer distribution when combined with MAO at 40°C and 10 bar of ethylene with activities up to 10^7 g/(mol h). Attempts to circumvent thermal instability led to the design of precatalyst $[\text{FeCl}_2(\text{L8})]$ having an ethyl-ketimine group and two electron-withdrawing halogen groups in R^1 position (Fig. 5) [36]. At 50°C, these catalysts exhibited good activity; however, rapid deactivation was observed above this temperature.

Nonsymmetrical tridentate ligands were developed by replacing one of the imino groups by a heterocyclic moiety (Fig. 6) [37 and references herein]. Evaluated at 30°C and under 10 bar of ethylene in the presence of MAO or MMAO, benzothiazolyl-derived precatalysts (with $\text{X}=\text{S}$) $[\text{FeCl}_2(\text{L9})]$ presented higher activities than benzoxazolyl functionalized (with $\text{X}=\text{O}$) or benzimidazolyl functionalized (with $\text{X}=\text{NH}$) in ethylene oligomerizations (up to 10^7 g/(mol h) vs 10^6 g/(mol h), respectively). Fine tuning of these catalytic systems allowed to access a range of Schulz–Flory distribution of oligomers from $K=0.4$ to $K=0.7$. However, in all cases, the olefin distribution was accompanied by a non-negligible amount of polyethylene wax. Evaluated at higher temperature, a rapid deactivation of these systems was reported. A series of ferric complexes $[\text{FeCl}_3(\text{L10})]$ (Fig. 6) were prepared from benzimidazolyl-functionalized ligands and led to active catalytic systems in the presence of MAO (10^6 g/(mol h)) at 20°C and 10 bar [38]. Interestingly, no wax or polymer was reported with Schulz–Flory distribution around $K=0.4$ – 0.5 . At higher temperature, the catalytic systems are inactive. Tenza et al. reported the use of bis(pyrazole) and bis(benzimidazole)pyridine iron (II) complexes $[\text{FeBr}_2(\text{L11})]$ and $[\text{FeBr}_2(\text{L12})]$ in ethylene oligomerizations (Fig. 6) [28]. All the precatalysts evaluated, activated by MMAO or $\text{AlEt}_3/[\text{Ph}_3\text{C}][\text{Al}(\text{O}t\text{Bu}^{\text{F}})_4]$, showed poor activities and rapid deactivation. Similarly, Britovsek

Fig. 6 Iron complexes coordinated by nonsymmetrical tridentate ligands

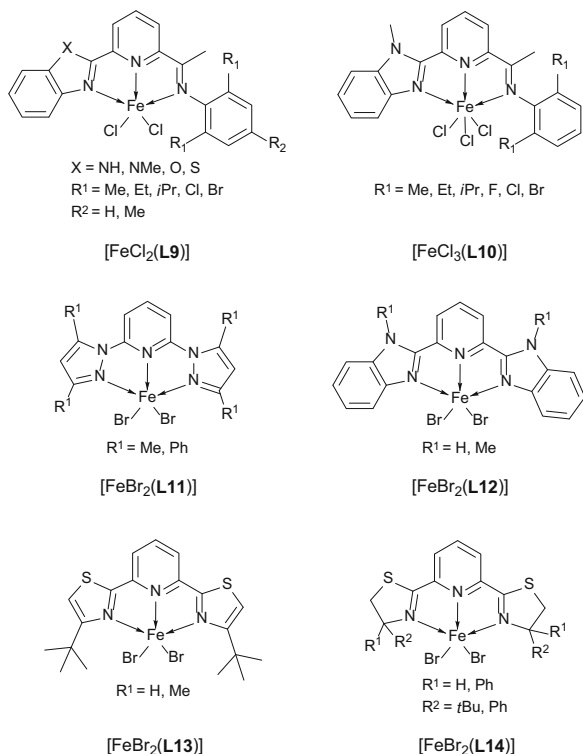
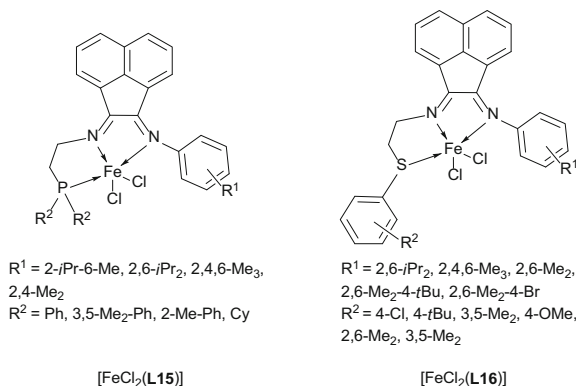


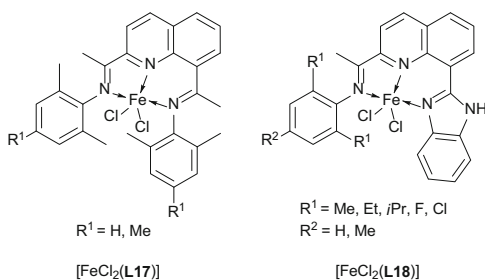
Fig. 7 Pendant donor-functionalized diimine iron precatalysts



and coworkers reported the preparation of (bis)thiazolylpyridine complexes $[\text{FeBr}_2(\text{L13})]$ and $[\text{FeBr}_2(\text{L14})]$ (Fig. 6) [39]. None of the complexes evaluated in the presence of MAO proved to be active in ethylene oligomerization or polymerization.

Small et al. described pendant donor-functionalized iron(II) complexes $[\text{FeCl}_2(\text{L15})]$ and $[\text{FeCl}_2(\text{L16})]$ for ethylene oligomerization (Fig. 7) [40, 41].

Fig. 8 Quinoline-derived ligands coordinated to iron (II)



Highly active catalytic systems were obtained upon activation by MMAO, up to 10^7 g/(mol h). $[\text{FeCl}_2(\text{L16})]$ complexes bearing the thioether-functionalized diimine proved to be slightly more active than their phosphine counterparts. Excellent selectivities of greater than 99% for α -olefins were obtained with such catalytic systems, with no polyethylene formed. Introducing methyl groups in *ortho* or *meta* positions of the aryls of the pendant donor groups led to lower catalyst activity. A cyclohexylphosphino group in $[\text{FeCl}_2(\text{L15})]$ (with $R^2 = \text{Cy}$) had also a detrimental effect on the catalytic behavior. Electronic tuning of complex $[\text{FeCl}_2(\text{L16})]$ through the *para* position of the thiophenol moiety showed that enhanced activity was obtained with a *t*Bu group compared to chloro or methoxy groups.

2,8-Bis(imino)quinoline iron(II) complexes $[\text{FeCl}_2(\text{L17})]$ were also reported as catalysts for ethylene polymerization (Fig. 8) [42]. While at room temperature or 40°C , only traces of polymer were observed after activation with MAO, and at ambient or elevated pressure of ethylene, these catalytic systems gave good activities (10^6 g/(mol h)) between 60°C and up to 100°C . No oligomeric products were reported, and the molecular weights of the polymers characterized are about 10^5 g/mol and present a relatively narrow distribution ($M_w/M_n = 2.3\text{--}4.8$). Benzimidazole-derived complexes $[\text{FeCl}_2(\text{L18})]$ were described and, upon MAO activation, were found to be inactive at room temperature [43]. Low productivities were observed at higher temperatures ($60\text{--}100^\circ\text{C}$).

2.1.2 Neutral Bidentate Ligands

Compared to catalysts bearing tridentate ligands, those containing bidentate N,N' ligands generally gave lower activities in ethylene oligomerization or polymerization. The groups of Wang [44] and Kempe [45] reported pyridine-imine iron (II) complexes giving moderate to low activities in ethylene oligomerization in the presence of MMAO ($10^5\text{--}10^3$ g/(mol h)). Chirik [46] and Bouwkamp [47] described conjugated and nonconjugated diimine-based complexes that, upon MAO activation, led to catalytic systems with low to no activity, respectively. Similarly, pyridine- and imidazole-imine iron(II) complexes developed by Stephan et al. led to poorly active catalytic systems [48]. Recently, Sun et al. reported a

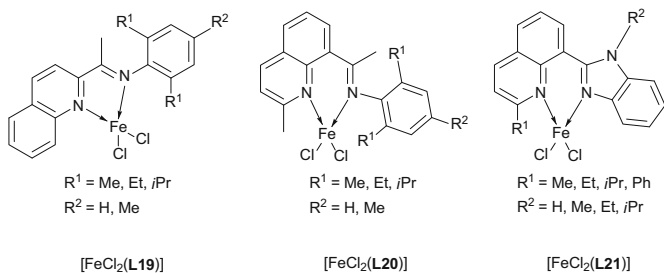


Fig. 9 Iron complexes coordinated by bidentate ligands

limited series of quinoline-based bidentate ligands coordinated to iron(II) centers (Fig. 9). With [FeCl₂(L19)] and [FeCl₂(L20)], activated by modified methylaluminumoxane (Al/Fe = 1,500), low activities were obtained at room temperature under 10 bar of ethylene, affording mainly short-chain oligomers such as butenes and hexenes [49]. At temperatures above 60°C, the systems became inactive. Introducing a benzimidazole moiety such as in [FeCl₂(L21)] and increasing the steric hindrance at the 2-position of the quinoline led to active catalysts at high temperature in polymerization conditions (100°C, 30 bar) [50]. These lowly productive catalysts led to the formation of polyethylenes having wide or bimodal distributions, suggesting multiple active species and chain transfer to aluminum, supported by the use of MAO/Fe ratio of 3,000.

2.1.3 Anionic Ligands

Examples of anionic ligands evaluated in iron-catalyzed ethylene oligomerization or polymerization are scarce, and only relatively inactive systems were reported until 2009 [23–27]. We reported the use of an anionic *N,N,N* ligand obtained from *n*-BuLi deprotonation associated to FeCl₃ as iron precursor [51]. The iron(III) precatalyst [FeCl₂(L22)] formed (Fig. 10) proved to steadily oligomerize ethylene at 80°C and 30 bar in the presence of MAO (10⁵ g/(mol h)) leading to 66 wt% of butenes with a selectivity of 98% for 1-butene, along with 12 wt% of polyethylene. Recently, Darkwa et al. described tridentate anionic imidazolyl phenoxy-imine ligands coordinated to iron(III) to afford [FeCl₂(L23)] (Fig. 10) [52]. Upon activation with ethylaluminum dichloride at moderate temperatures (30°C) and pressures (10 bar), good activities were obtained (10⁶ g/(mol h)) over 1 h affording C₄–C₁₂ oligomers, waxes, and alkyl-chlorobenzene or alkyl-toluene products from Friedel–Crafts alkylations of the solvent.

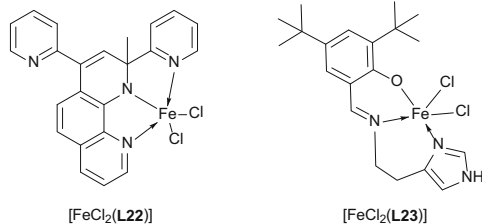


Fig. 10 Iron complexes based on anionic ligands

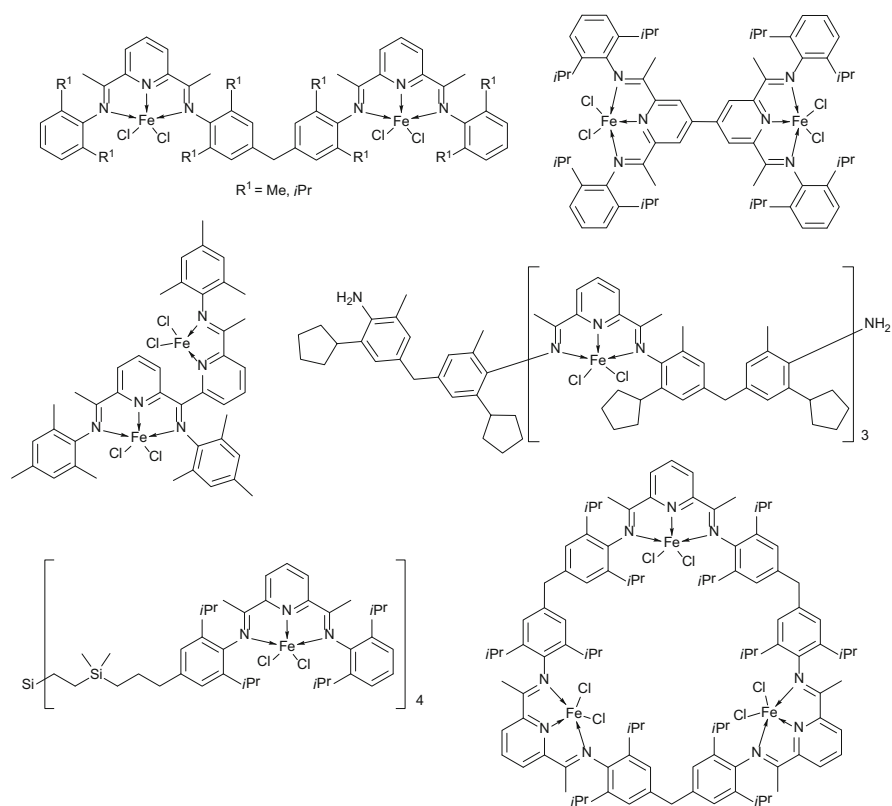


Fig. 11 Polynuclear iron complexes

2.1.4 Repeated Unit Ligands

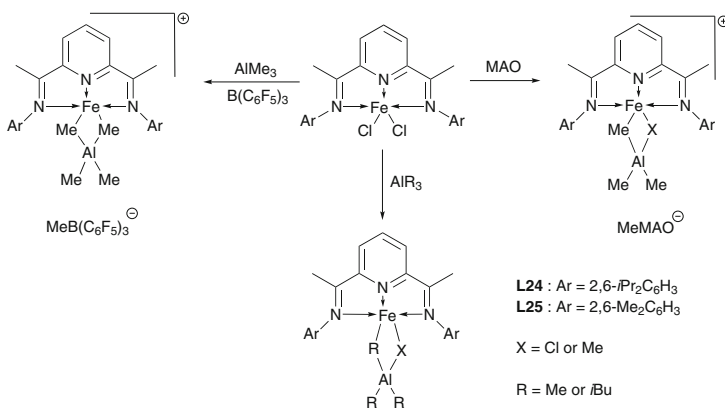
Different approaches regarding ligand unit incorporation and design for multinuclear catalysis were investigated by different groups. For the bridging [53, 54] of oligomeric [55], macrocyclic [56], or dendritic [57] structures (Fig. 11),

similar or higher activities and molecular weights were obtained compared to their monomeric analogues when activated by methylaluminoxane.

2.2 Comprehension and Characterization

As described in this chapter, bis(imino)pyridine iron-based complexes and derivatives in combination with cocatalysts such as aluminoxanes or alkylaluminum led to highly active catalytic systems for ethylene transformation. The observed product distribution, however, shows that mixtures are often obtained, e.g., linear alpha olefins accompanied by waxes or polymers from ethylene oligomerization or multimodal/broad molecular weight distribution from ethylene polymerization. This observation suggests that multiple active species and/or catalytic mechanisms are in play after activation of the well-defined iron precursors. Although the formation of the aforementioned products is believed to proceed through the well-known Cossee–Arlman mechanism [58], the formation, the nature, and the reactivity of the intermediates involved still need to be studied and validated. Major hurdles hamper a comprehensive characterization of the iron-based systems and their catalytic behavior such as the paramagnetic nature of the iron complexes, the multiple oxidation states possible, or the potential non-innocence of the ligands, although interesting progresses have been made.

Bryliakov et al. reported recently the interaction between the $[\text{FeCl}_2(\text{L24})]$ [59] and $[\text{FeCl}_2(\text{L25})]$ [60, 61] polymerization precatalysts and various aluminum-based activators such as MAO, $\text{AlMe}_3/\text{B}(\text{C}_6\text{F}_5)_3$, AlMe_3 , and $\text{Al}(\text{iBu})_3$ by ^1H NMR and EPR spectroscopy (Scheme 1). The ion pairs $[\text{Fe}(\text{L25})(\mu\text{-Cl})(\mu\text{-Me})\text{AlMe}_2]^+[\text{MeMAO}]^-$ or $[\text{Fe}(\text{L25})(\mu\text{-Cl})(\mu\text{-Me})\text{AlMe}_2]^+[\text{MeB}(\text{C}_6\text{F}_5)_3]^-$ were proposed when using MAO or $\text{AlMe}_3/\text{B}(\text{C}_6\text{F}_5)_3$, while iron(II)-aluminum-bridged neutral species were suggested with alkylaluminum. However, the species obtained



Scheme 1 Proposed reactivity of bis(imino)pyridine **L24** and **L25** iron complexes toward MAO, AlMe_3 , or $\text{AlMe}_3/\text{B}(\text{C}_6\text{F}_5)_3$

are more complex than it appears at first sight. According to the authors, the bimetallic adducts are better described with the bis(imino)pyridine ligand being non-innocent, leading to species $[(\mathbf{L24}^{(-)})\text{Fe}^{(+)}(\mu\text{-X})(\mu\text{-R})\text{Al}(\text{R})_2]$ (with $\text{X}=\text{Cl}$ or R and $\text{R}=\text{Me}$ or $i\text{Bu}$) in which the oxidation state +II is retained by the metal and one electron is being delocalized over the chelate. The debate around the oxidation state of the active species and the redox non-innocence of the bis(imino)pyridine ligand is still open and fueled by numerous spectroscopic [62–64] and theoretical [65–69] studies.

The formation, the isolation, and reactivity studies of potential intermediates [70–74] are of prime interest to provide support for the observations mentioned above, although the observed species may not be representative of the catalytic system formed under operating conditions (different activating agents, activator to catalyst ratios, pressure, temperature, etc.). An example of cationic iron(II) species as catalytic intermediates in ethylene polymerization was reported by the group of Chirik [75]. Model bis(imino)pyridine iron(II) monoalkyl cations were isolated and characterized by X-ray diffraction. $[\text{Fe}(\text{CH}_2\text{SiMe}_3)(\mathbf{L24})(\text{S})]^+[\text{BPh}_4]^-$ ($\text{S}=\text{Et}_2\text{O}$ or THF) and $[\text{Fe}(\text{CH}_2\text{SiMe}_2\text{CH}_2\text{SiMe}_3)(\mathbf{L24})(\text{S})]^+[\text{MeB}(\text{C}_6\text{F}_5)_3]^-$ were obtained from dialkylation of $[\text{FeCl}_2(\mathbf{L24})]$ followed by subsequent alkyl abstraction by boron-based compounds (Fig. 12). Upon exposure to ethylene, these isolated single-component systems exhibit a moderate catalytic activity, yielding high MW linear polymers with relatively narrow molecular weight distribution (MWD). Later, the same group demonstrated through the isolation of cationic, neutral, and anionic iron alkyl complexes that the redox non-innocence of the bis(imino)pyridine chelate allows confinement of electronic modifications to the ligand and a stable oxidation state for the metal center (iron(II)) during redox processes [76]. Recently, Cámpora et al. reported X-ray diffraction and in situ ^1H NMR characterization of the intermediates formed by reduction of $[\text{Fe}(\text{CH}_2\text{SiMe}_3)_2(\mathbf{L24})]$ by AlMe_3 [77]. A neutral monomethyl $[\text{Fe}(\text{II})\text{Me}(\mathbf{L24}^*)]$ intermediate was observed as the final product of the reaction, where the mono-electronic reduction of the chelating ligand is suspected. This species was treated with ethylene, and the reaction, monitored by ^1H NMR, led to oligomers with a Schulz–Flory distribution [78]. NMR monitoring allowed observation of the binding of the ethylene monomer to the monomethyl complex and the growth of the alkyl chain on

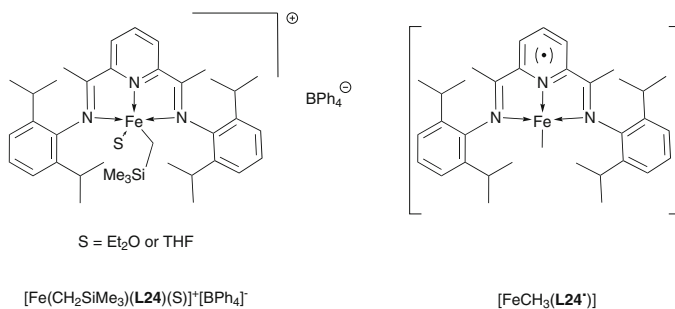


Fig. 12 Isolated bis(imino)pyridine iron alkyl complexes

the iron center via ethylene insertion. These results constitute direct evidence of a coordination–insertion mechanism when ethylene is oligomerized by such propagating species, in line with the H/D scrambling and mass spectrometry experiments, supporting a Cossee–Arlman mechanism [79]. However, considerably lower activities and product molecular weights compared to their cationic analogues question their involvement in the catalytic multicomponent ethylene polymerization process.

Recently, IFP Energies nouvelles described in a combined experimental and theoretical study the activation process of a single-site ethylene oligomerization catalyst [80]. A novel and well-defined phenoxyaluminum-based cocatalyst has been described, and its effect on the ethylene insertion and inhibition mechanisms has been compared to AlMe_3 and a MAO model. Although $[\text{PhOAlMe}_2]_2$ is clearly less active than MAO, this well-defined species presents interesting features for further characterization study and catalytic system optimization.

Important progress in synthetic and analytical chemistry recently allowed better understanding of the reactivity of aluminoxane or alkylaluminum compounds with iron complexes used in ethylene polymerization. However, if isolation of model single-component monoalkyl cationic systems has undoubtedly demonstrated that such species are able to transform ethylene, the multitude of active species accessible in a bi-/tri-component catalytic system and degradation products derived from them prevent the clear identification of each active species and the products they afford. Particularly, the reducing ability of TMA added to the redox non-innocent character of the bis(imino)pyridine ligand, whose role has still not been demonstrated as a prerequisite for polymerization activity, impedes the assignment of precise oxidation states, feeding continuation of the Fe(II)/Fe(III) active species debate. As a conclusion, the operating active species in a real, i.e., bicomponent (precatalyst and alkylaluminum activator, potentially ill defined), catalytic system still remains in the gray area, if not in a black box.

2.3 Supported Homogeneous Iron Catalysts for Oligomerization and Polymerization of Ethylene

Heterogeneous catalysts are largely employed in the polyolefin manufacturing industry to respond to a great number of economical and process engineering issues. As an example, control of particle morphology of the polymer, containment of the reaction's exothermicity, and operability in continuous slurry and gas phase processes are key features of a polymer production process. Catalyst impregnation remains the most straightforward and cheapest route to heterogenization, although other approaches have also been investigated. Attempts to immobilize highly active homogeneous single-site catalysts have flourished, aiming at maintaining high activities and selectivities and fitting into existing industrial and process constraints [81].

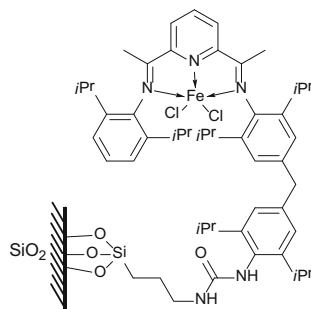
2.3.1 Impregnation

Different strategies were investigated for non-covalent immobilization of iron catalysts on supports. The iron-bis(imino)pyridine precursor may be impregnated on solids. Several examples of silica-supported iron catalysts were reported by the groups of Sivaram [82], Semikolenova [83], and Barabanov [84, 85]. The activation by methylaluminumoxane or trialkylaluminum of the immobilized polymerization precursor iron-bis(imino)pyridine generally led to lower, although steady, activity compared to the initial activities of the non-supported catalysts. The broad molecular weight distributions observed were attributed to the presence of different active species. Mesoporous zeolites as MCM-41 or SBA-15 have also been described as support for iron-catalyzed ethylene oligomerization [86] and polymerization [87–89] leading to either lower molecular weight α -olefins or higher molecular weight polyethylenes, respectively, compared to their homogeneous counterparts. MgCl_2 supports have been evaluated by the groups of Mao [90–92] and Chadwick [93, 94] for application in ethylene polymerization. They showed that temperature pretreatment of the MgCl_2 /ethanol support led to higher and steady catalytic activities, although a maximum temperature was reached when dealcoholization was performed with AlEt_3 to afford $\text{MgCl}_2/\text{AlEt}_n(\text{OEt})_{3-n}$. Spherical particles of polymers could be obtained by the impregnation method through the replication of the spherical morphology of the catalyst particles by the growing polymer chains [90, 91]. During this process, the constraint of the polymer growing into the pores of the catalyst particle leads to the fragmentation of the latter and progressively mimics its spherical shape [95].

Another strategy consists of first carrying out an ion exchange with the support, followed by the introduction of the ligand. For example, the Miura group successfully supported bis(imino)pyridine ligands on fluorotetrasilicic mica. Ion exchange between Na^+ and the desired Fe^{3+} was realized prior to intercalation of the ligand into the host support interlayers. Subsequent reaction of the ligand with Fe^{3+} ions yielded an active precatalyst for ethylene polymerization upon MAO, TEA, and TIBA activation [96]. Good activities were obtained (around 10^6 g/(mol h)). The absence of ligand or alkylaluminum activator led to inactive systems, supporting the formation of the suggested complex. The same ion-exchange strategy was also reported on montmorillonite and saponite clay supports [97]. One-pot syntheses of immobilized iron complexes in the clay mineral interlayer have recently been described [98]. Additionally, acetylaminopyridine ligand immobilized on Fe^{3+} -exchanged fluorotetrasilicic mica was claimed by the same group to promote oligomerization of ethylene in the presence of $\text{Al}(i\text{Bu})_3$, AlEt_3 , and MAO activators [99].

A relevant approach in the polymerization field is to pretreat the support (SiO_2 , calcosilicate [100], or montmorillonite [101, 102]) with methylaluminumoxane or partially hydrolyzed alkylaluminum, generally used as activators, prior to immobilization of the iron precursor. The interaction of the iron center with the supported cocatalyst is considered to ensue from the in situ formation of the active species.

Fig. 13 Selected example of a SiO₂-tethered iron precatalyst



Stable activities may be obtained along with specific polymer properties that may be tuned through various parameters such as the Al/Fe ratio.

2.3.2 Iron Catalyst Anchoring

Chemical tethering of an iron complex on a SiO₂ surface was one of the most widely explored immobilization routes. Modification of the bis(imino)pyridine ligand and subsequent reaction of the ligand/complex with the silica support allowed covalent anchoring of the precatalyst prior to ethylene polymerization. Tethering via the imino carbon atom [103–105], the central pyridine ring [106, 107], or the imino ring [108] was reported. A recent report is presented here as an example. Kim and coworkers synthesized an asymmetrical bis(imino)pyridine ligand bearing a trialkoxysilane-functionalized linker on the 4-position of the imino ring further covalently bonded to in situ formed silica gel (Fig. 13). Metalation of the anchored ligand yielded an active catalyst for ethylene polymerization upon MAO activation [109]. Moderate activities were obtained (10^4 – 10^5 g/(mol h) depending on the Al/Fe ratio and the reaction temperature). An unimodal MWD was obtained supporting the unicity of the active species.

2.3.3 Self-Immobilization

Self-immobilization relies on the copolymerization of ethylene and a polymerizable fragment of the catalyst, typically a terminal vinyl group, resulting in the insertion of the catalyst into a growing polymer chain and aggregation of the formed polymer as a particle [95]. The morphology of the starting polymer particle will be replicated by the growing polymer chains and controlled, avoiding reactor fouling. Applied to bis(imino)pyridine iron catalysts, the main strategy consisted in introducing vinyl groups on the ligand backbone. Functionalization of the central pyridine ring [110, 106], of the imino ring [111–113], or on the imino carbon atom [103, 111, 114] with a terminal vinyl moiety was reported (Fig. 14). In several cases, no self-immobilization was observed. This was rationalized by the poor ability of the

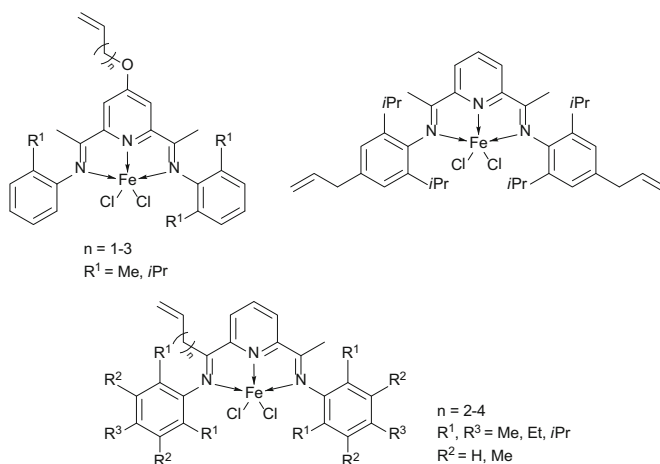


Fig. 14 Selected examples of bis(imino)pyridine iron precursors investigated in the self-immobilization approach

iron catalyst to copolymerize ethylene and α -olefins as the terminal vinyl groups. When self-immobilization was observed, no clear enhancement of the polymer properties was described.

3 Multiple Single-Site Catalysis

Multiple single-site catalysis is based on the design of catalytic systems in which at least two different single-site catalysts are operating simultaneously in a single reactor. This technology is aimed to offer tailor-made products with controlled MW, MWD, and microstructures rendering materials with suitable rheological and mechanical properties, meeting the needs of the polymer industry. Concomitantly, large initial capital investment and energy consumption devoted to multi-reactor processes could be reduced by such single reactor processes. However, using different catalysts concurrently under the same conditions (charge, temperature, pressure, solvent, cocatalyst, etc.) has its inherent difficulties. In addition to compatibility issues, each catalyst has its intrinsic properties meaning kinetics toward monomer, activation pathways, temperature response, and more.

The considerable attention devoted to metallocenes [2, 3] and post-metallocenes [115, 116] in the last decades enabled their association in multiple single-site catalysis. Their well-defined structures and ability to produce selectively polyethylene with a wide range of molecular weights (from oligomers to ultrahigh molecular weight polyethylene (UHMWPE)) and narrow molecular weight dispersity made them ideal candidates [117, 118]. In addition, they exhibit very good compatibility to each other and show stability toward cocatalysts, giving them a

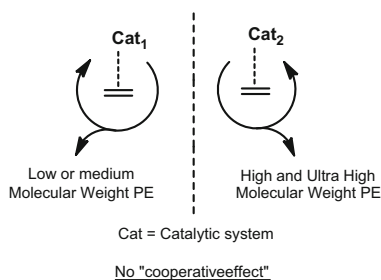
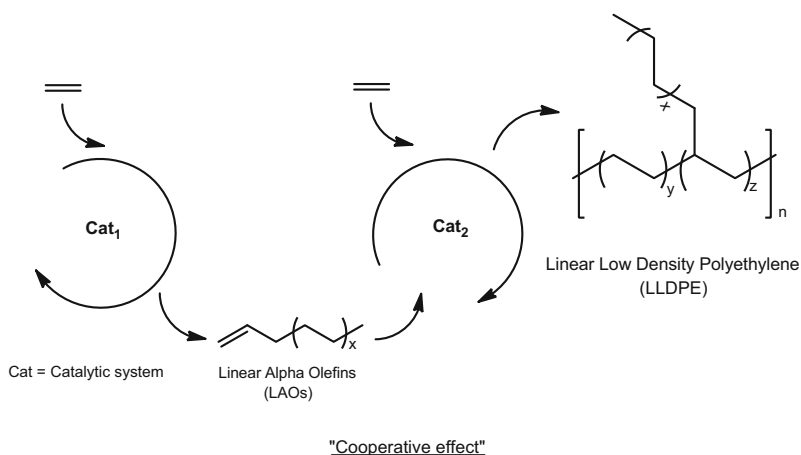


Fig. 15 Reactor blending



Scheme 2 Tandem catalysis

neat advantage compared to the traditional Ziegler-type multisite catalysts in terms of MWD control [119]. Since the discovery of the iron-bis(imino)pyridine catalysts leading to linear alpha olefins (LAOs) [120, 121] as well as to highly linear polyethylene [30, 122], a few examples are described of their use in combination with early transition metal catalysts. They can formally be divided into two families. The different catalytic centers composing the system can ensure a cooperation during the catalytic act or they operate separately. The latter case is known as *reactor blending* (Fig. 15) and the former as *tandem catalysis* (Scheme 2). Selected highlights in the application to olefin polymerization are presented.

3.1 Reactor Blending

Production of bimodal and/or broad MWD polyethylene is of premier importance for the polymer processing industry [123]. Such materials present improved impact

and processability properties. Incorporation of UHMWPE into a lower molecular weight polyethylene matrix significantly improves its mechanical properties. Indeed, long polymer chains play the role of “tie molecules” connecting crystalline regions composed by lower MW PE chains, forming thus a strengthened physical network [124]. Bimodal/broad polyethylene with a small content of UHMWPE is better suited to melt extrusion or blow molding steps. Melt blending of low molecular weight polyethylene and UHMWPE is one option to access products with the aforementioned peculiar properties [125]. Unfortunately, melt-processing issues concerning UHMWPE remain unchanged in this posttreatment step. Another widely used technology is the “cascade reactor” process in which low molecular weight PE is produced in a first reactor fed with ethylene and large quantities of hydrogen [126]. Polymerization is completed in a second reactor charged with much less hydrogen to yield high or ultrahigh molecular weight PE. Another solution for MW control of polyethylenes is the introduction of chain transfer agents into the polymerization medium. Polyethylene chain growth on dialkylzinc (typically diethylzinc) has been reported as an extremely efficient way to lower M_w and MWD of polyethylenes produced by bis(imino)pyridine catalysts [127]. Depending on the ratio of diethylzinc, a Poisson MWD with M_n and dispersity as low as 700 g/mol and 1.1, respectively, could be reached if 500 equivalents of zinc per iron are added (against $M_n = 10,000$ g/mol and $\mathcal{D} = 19.2$ in the absence of zinc). Activity is maintained in the range of the zinc-free system (10^6 g/(mol h)). Single reactor blending catalysis represents a novel alternative toward the production of bimodal/broad polyethylenes. This approach relies on using two, or eventually more, single-site catalysts with different features leading to an intimate blend of polyethylene with different M_w and MWD. Immobilization on inorganic or polymeric supports may also be envisaged to prevent reactor fouling and enable their use in slurry or gas phase polymerization processes [119].

The first iron-based reactor blending example was reported by Mecking in 1999 where the iron(II) complex $[\text{FeCl}_2(\mathbf{L24})]$ and the α -diimine nickel(II) complex $[\text{NiBr}_2(\text{ArN}=\text{C}(\text{Me})-\text{C}(\text{Me})=\text{NAr})]$ (with $\text{Ar} = 2,6\text{-Me}_2\text{C}_6\text{H}_3$) were mixed and activated by methylaluminoxane (Fig. 16) [128]. The two different catalytic systems are simultaneously active in ethylene polymerization leading to linear and branched polyethylenes for the iron and the nickel catalysts, respectively, affording a mixture with unique properties. Furthermore, the compatibility of $[\text{FeCl}_2(\mathbf{L24})]$ with the early transition metal-based system $[\text{Zr}(n\text{BuCp})_2\text{Cl}_2]$ (where

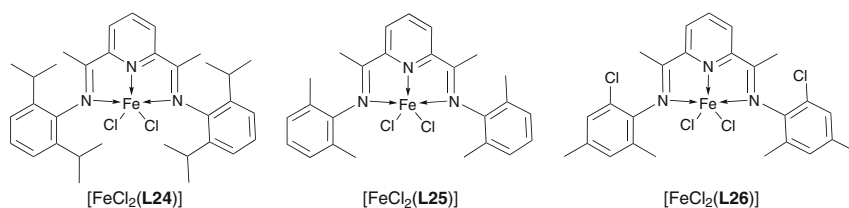


Fig. 16 Iron precatalysts evaluated in reactor blending

*n*BuCp = η -*n*-butylcyclopentadienyl) was evaluated, affording a blend of strictly linear polyethylenes with different crystallinities and molecular weights.

A combination of iron and chromium was reported by Mülhaupt and coworkers [129]. A trimodal blend of low, medium, and ultrahigh MW polyethylene with an overall ultra-broad MWD was obtained by combining two chromium(III) catalysts, a half-sandwich metallocene η^5 -[3,4,5-trimethyl-1-(8-quinolyl)-2-trimethylsilylcyclopentadienyl]CrCl₂ and a 2,6-bis-[1-(2,6-dimethylphenylimino)ethyl]pyridine CrCl₃, with [FeCl₂(L25)] (Fig. 16) co-immobilized on a silica pretreated with MAO. A UHMWPE (10⁶ g/mol) fraction was produced by the half-sandwich complex; medium (10⁵ g/mol) and low molecular weight fractions (10⁴ g/mol) were formed by the iron and chromium complexes, respectively. Overall, an MWD of 420 was reached. The molar content of each catalyst has been independently tailored resulting in the corresponding variation of the respective polyethylene fraction, thus demonstrating the flexibility and fine tuning ability of this multiple single-site system. A binary version of this system was later used by the same team to screen the influence of catalyst preparation [130]. Half-sandwich metallocene [η^5 -{3,4,5-trimethyl-1-(8-quinolyl)-2-trimethyl-silylcyclopentadienyl}CrCl₂] and [FeCl₂(L25)] were either sequentially or simultaneously supported on silica pretreated with MAO, offering different bimodal MWD patterns. Higher *M_w* and MWD values as well as a higher UHMWPE content were obtained when iron was immobilized prior to chromium. As expected, the UHMWPE content is directly connected to the ratio of chromium in the catalyst blend.

Chadwick and coworkers reported the combination of [FeCl₂(L26)] (Fig. 16) and the chromium complex [{1-(8-quinolyl)indenyl}CrCl₂], both being co-impregnated on a MgCl₂/AlEt_{*n*}(OEt)_{3-*n*} support [131]. Upon activation with Al/*i*Bu₃, a bimodal distribution of low and high MW products was obtained with good activities. It has to be noted that the overall polymer yields obtained are the sum of each catalyst taken individually, thus exhibiting the absence of cooperation of the two catalysts. Besides classical gel permeation chromatography (GPC) MW determination, differential scanning chromatography (DSC), and rheology measurements, crystallization of the polymers obtained was investigated via wide-angle X-ray diffraction (WAXD) and small-angle X-ray scattering (SAXS). The ratio of low and high MW fraction could be tailored by varying the loading of iron and chromium catalysts. The MWD varied from 5.9, when the iron catalyst was solely operated, to 1.6 for the chromium catalyst going through a maximum of 29.4 for an Fe/Cr ratio of 0.3/1.

3.2 Tandem Catalysis

Tandem catalysis is based on cooperation, also called “synergistic effect,” of two or more metals in the same reactor to offer products with peculiar microstructure and rheological properties. Linear low-density polyethylene (LLDPE) production is a perfect example of application of this relatively recent chemistry. LLDPE is a

branched polymer traditionally produced by copolymerization of ethylene with light linear alpha olefins (LAOs) as comonomer. Tandem catalysis yields LLDPE with controlled microstructure in a one-step process from the sole ethylene feedstock via the fine association of an oligomerization and a copolymerization catalyst [132]. Tandem catalysis may involve homogeneous catalysts, immobilized systems, or a combination of the two (Scheme 2).

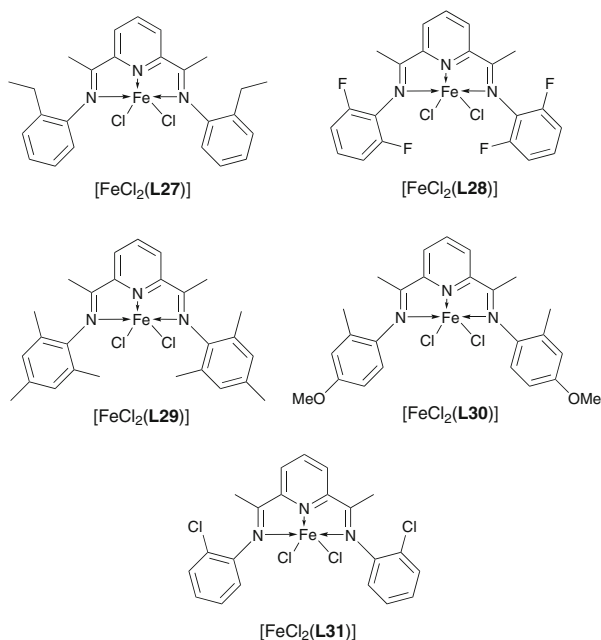
Quijada and coworkers described a homogeneous tandem system composed of the iron(II) oligomerization catalyst $[\text{FeCl}_2(\mathbf{L27})]$ and the zirconium(IV)-based catalysts $[\text{Zr}(\text{Me}_2\text{SiIn}_2)\text{Cl}_2]$ or $[\text{ZrCl}_2(\text{EtInd}_2)]$ with constrained geometry known to copolymerize ethylene with a wide range of α -olefins up to 1-octadecene [133]. The combination of $[\text{FeCl}_2(\mathbf{L27})]$ and $[\text{ZrCl}_2(\text{Me}_2\text{SiIn}_2)]$, activated by MAO, gave a polyethylene with a broad/bimodal MWD bearing short- to long-chain branches (varying from 1 to 4 branches per 100C). GPC data revealed two sets of molecular weight populations, centered around $M_w = 70,000$ and $1,500$ g/mol, which is consistent with melting point determinations by DSC. The highest molecular weight fraction is believed to be branched polyethylene resulting from the copolymerization of ethylene with α -olefins governed by the zirconium catalyst. On the other hand, the low molecular weight fraction increases with Fe/Zr ratio. In the presence of $[\text{ZrCl}_2(\text{EtInd}_2)]$, a monomodal and extremely narrow MWD polymer (around 1.6) was obtained but less branching was observed. The degree of branching increases with Fe/Zr ratio which exhibits an efficient incorporation of the in situ produced comonomers.

Titanium was also successfully combined with iron to produce branched polyethylene as reported by Xie, Zhang, and coworkers [134, 135]. Moderate molecular weights and narrow dispersities with a majority of short-chain branches were obtained using $[\text{FeCl}_2(\mathbf{L28})]$ (Fig. 17) and mono- β -diiminato or β -carbonyleneamine Ti(IV) complexes in the presence of MMAO.

A similar catalytic system but with a different feedstock was employed in the one-step production of branched polypropylene by Ye and Zhu [136]. $[\text{FeCl}_2(\mathbf{L25})]$ (Fig. 16) activated by modified methylaluminoxane (MMAO) produces atactic polypropylene (aPP) chains with low molecular weight and unsaturated end groups when used independently in propylene polymerization. The catalytic system $[\text{Zr}\{\text{rac-Me}_2\text{Si}(2\text{-MeBenz[e]Ind})_2\}\text{Cl}_2]/\text{MMAO}$ was selected to copolymerize propylene with the macromonomer formed in situ by the iron catalyst and produced PP chains in an isotactic fashion. The binary system studied yielded, as expected, polypropylene with an isotactic PP (iPP) backbone grafted with aPP side chains.

Diffusion limitation during high-density polyethylene production with supported catalysts has been studied by Chadwick and coworkers [137]. Introduction of branched polyethylene produced by the 2,3-bis(2,6-diisopropylphenylimino)butane nickel(II) dibromide complex into a high-density polyethylene matrix afforded from $[\text{FeCl}_2(\mathbf{L29})]$ (Fig. 17), where both catalysts were co-immobilized on $\text{MgCl}_2/\text{AlEt}_n(\text{OEt})_{3-n}$, was a successful approach to reduce this limitation. This was suggested to arise from the decreased crystallinity of the forming polymer due to nickel-induced branching, leading to a facilitated monomer

Fig. 17 Iron precatalysts investigated in tandem catalysis



diffusion to the iron center. Scanning electron microscopy (SEM) imaging of the more porous tandem-catalyzed polymer supported this hypothesis.

Zhang et al. reported $[\text{FeCl}_2(\text{L30})]$ (Fig. 17) and $[\text{Zr}\{\text{rac-Et}(\text{Ind})_2\}\text{Cl}_2]$ immobilized on calcosilicate CAS-1 pretreated with MAO and silica, respectively, and employed it simultaneously for in situ ethylene polymerization to LLDPE (with a branching density varying from 40 to 60 branches per 1000C) [138]. When compared to their homogeneous analogues, the supported species exhibited enhanced stability over time at elevated temperatures. According to the authors, the observed stability increase might be attributed to the confinement of the catalytic species in the support layers, preventing the bimolecular aggregation of the active species, which would result in catalyst deactivation. As a counterpart, the difficult diffusion of ethylene through the support and the forming LLDPE renders a smoothed kinetic profile of the polymerization reaction and a prolonged activation step. Additionally, the morphology of the polyethylene produced with the supported system, identified as compact particles, was significantly improved in contrast to the stacking appearance obtained with the homogeneous system, which is a result of the “duplicating effect” of the silica support particle by the growing polymer particle.

The same group supported $[\text{FeCl}_2(\text{L31})]$ (Fig. 17) and $[\text{Zr}\{\text{rac-Et}(\text{Ind})_2\}\text{Cl}_2]$ on either MAO pretreated MCM-41 or SBA-15 mesoporous materials [139]. Upon activation with AlEt_3 , in situ polymerization of ethylene at high ethylene pressure with the aforementioned system yielded products with much higher MW, broader MWD, and improved activity when compared to the MAO-activated

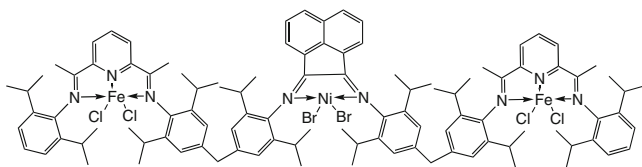


Fig. 18 Trinuclear iron–nickel complex for tandem catalysis

homogeneous catalysts. At atmospheric pressure of ethylene, the level of branching could be tailored from 20 to 50 branches per 1000C with the supported system leading to LLDPE with improved physical and mechanical properties according to rheology studies.

A bimetallic complex based on iron and nickel was reported by Kim and coworkers for ethylene polymerization [140]. Activation of this multinuclear species with various cocatalysts such as triethylaluminum, ethylaluminum sesquichloride (EASC), and MAO, the latter being the most efficient, afforded branched to linear polyethylenes, respectively, depending if Ni is present in the catalyst structure or not. A maximum of 134 branches per 1000C was observed when the system was combined with EASC due to preferential activation of the nickel center. The cooperative effect of the neighboring metals is supported by enhanced activity and stability, especially at elevated temperatures, along with lower molecular weight and broadened molecular weight distribution compared to the isolated catalysts. The bulkiness of the ligand and the proximity of growing chains on each metal center are likely to exert a strong influence on propagation rates and chain termination, leading to M_w and dispersity decrease (Fig. 18).

4 Diene Polymerization

Since the early 1990s, the field of olefin polymerization catalysis with late transition metals has witnessed a small revolution with the discovery of the nickel and palladium–diimine systems by Brookhart et al. [141, 142]. A few years later, cobalt and iron-bis(imino)pyridine precatalysts were developed [30, 122]. These systems were capable of polymerizing ethylene to high molecular weight polymers with activities comparable to the metallocene catalysts when activated with MAO (Fig. 19).

These more recent active catalysts have stimulated numerous studies for reexamining iron-based systems for diene transformations (polymerization, copolymerization, etc.). Indeed, iron-based catalysts were known for many years for diene polymerizations, but they were generally considered as being poorly active and selective compared to conventional catalysts [143]. This part of the review describes this aspect with a special focus on bidentate and tridentate nitrogen ligands.

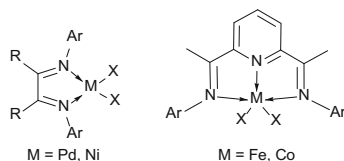
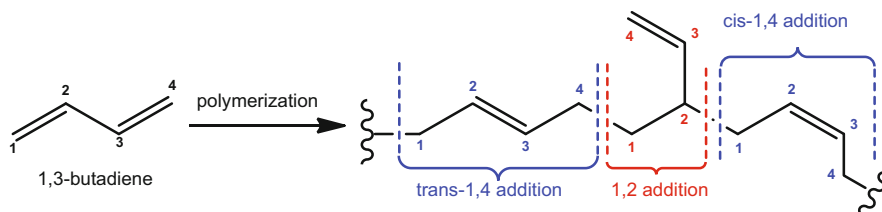


Fig. 19 From nickel and palladium–diimine to cobalt and iron-bis(iminopyridine) pre-catalysts



Scheme 3 Structure of butadiene polymers

4.1 Iron-Based Catalysts for Polymerization of Conjugated Dienes

Polymerization of conjugated dienes is largely dominated by polybutadiene and their derivatives (butadiene rubber, styrene–butadiene rubber, and acrylonitrile–butadiene–styrene), mainly used for the manufacture of automobile tires. For these applications, careful control of the microstructure of the butadiene rubber is necessary. In terms of connectivity, butadiene can polymerize in three different ways, called *cis*, *trans*, and *vinyl* (Scheme 3). The *cis* and *trans* forms arise by connecting the butadiene molecules end to end (so-called 1,4-addition), while the “vinyl” form arises from end-to-tail butadiene connection (1,2-addition).

Depending on the application and the catalyst used (Nd, Co, Ni, Ti, or Li), the polybutadiene is generally a mixture of these connectivities. For example, “high *cis*”-polybutadiene (consisting of 90% or more *cis* connections) has a high elasticity and is very popular, whereas the so-called high *trans* is a plastic crystal with no apparent applications. The vinyl content of polybutadiene is typically no more than a few percent (up to 12% but usually around 1–4%). In addition to these three kinds of connectivity, polybutadienes differ in terms of their branching and molecular weights.

The polymerization of isoprene also represents an interesting field of investigation, as polyisoprene is considered to be similar to natural rubber in structure and properties. Specifically, a very high content of the *cis*-1,4 structure is required to mimic the natural rubber. Currently synthetic polyisoprene is being used in a wide variety of applications, but its application remains limited by manufacturing capacity and monomer availability.

4.1.1 Bidentate Nitrogen-Based Ligands

In 2002, Porri et al. examined the polymerization of butadiene and other dienes with a catalyst composed of [(2,2'-bipyridine)FeEt₂]/MAO [144]. This catalyst appeared to be active for 1,3-butadiene polymerization. Polymers with a 1,2 or 3,4 structure are formed from butadiene, isoprene, (*E*)-1,3-pentadiene, and 3-methyl-1,3-pentadiene, while *cis*-1,4 polymers are derived from 2,3-dimethyl-1,3-butadiene. Importantly, an impact of the temperature on the 1,2 (3,4) polymer structure was evident in this work. Polymers obtained at 25°C were amorphous, while those obtained below 0°C were crystalline.

Ricci et al. then extended the scope of bidentate ligands (ethylenediamine **L32**, 2,2'-bipyridine **L33**, 1,10-phenanthroline **L34** derivatives, and 1,2-bis(dimethylphosphino)ethane **L35** in Fig. 20) in combination with Fe(II) precursors to examine their reactivity toward various 1,3-dienes after activation with Al(*i*Bu)₃, AlEt₃, or MAO [145]. For butadiene polymerization, the study demonstrated that when aliphatic nitrogen **L32** or diphosphine **L35** ligands are used, Fe(II) complexes exhibit very low to no activity and stereoselectivity. When aromatic diamine **L33** and **L34** ligands are used, extremely high activities were obtained with a remarkable influence of the steric hindrance of the 1,10-phenanthroline derivatives. Polybutadienes with a predominantly 1,2 structure were obtained (60–75% of 1,2). The *M_w* was very high and the molecular weight distribution (MWD) narrow. Slight deviation of the 1,2/*cis*-1,4 polymer microstructure was also observed when varying the nature of the cocatalyst. The 1,2 content of the polybutadiene was reduced from 61% with the [FeCl₂(**L33**)₂]-MAO system to 45–46% when [FeCl₂(**L33**)₂]-Al(*i*Bu)₃ or AlEt₃ was used. The catalytic [FeCl₂(N-N)₂]/MAO systems were also able to polymerize different 1,3-dienes such as isoprene (IP), (*E*)1,3-pentadiene (PD), and 2,3-dimethyl-1,3-butadiene (DMB) with a marked *cis*-1,4 stereoselectivity for DMB (99%). Interestingly, mechanistic implications of this stereoselectivity were discussed on the basis of the mechanism proposed by Porri and coworkers [143]. Some years later, the same group published a complementary study on the synthesis of syndiotactic 1,2-poly(3-methyl-1,3-pentadiene) with details on the characterization techniques used [146].

Well-defined molecular iron(II) complexes bearing bidentate iminopyridine ligands were recently described by Ritter and coworkers to polymerize isoprene and other 1,3-dienes (myrcene, farnesene) in a nonconventional, stereoselective manner (Scheme 4) [147, 148]. Initially developed for 1,4-addition reactions across

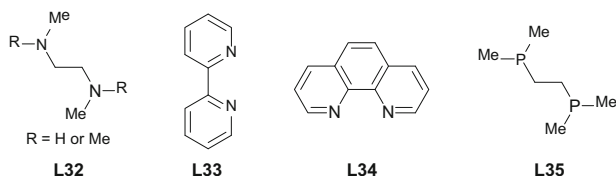
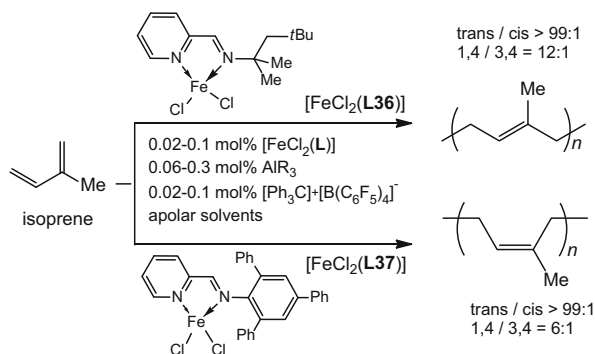


Fig. 20 Bidentate ligands evaluated in iron-catalyzed diene polymerization

Scheme 4 Polymerization of isoprene using precatalysts $[\text{FeCl}_2(\mathbf{L36})]$ and $[\text{FeCl}_2(\mathbf{L37})]$



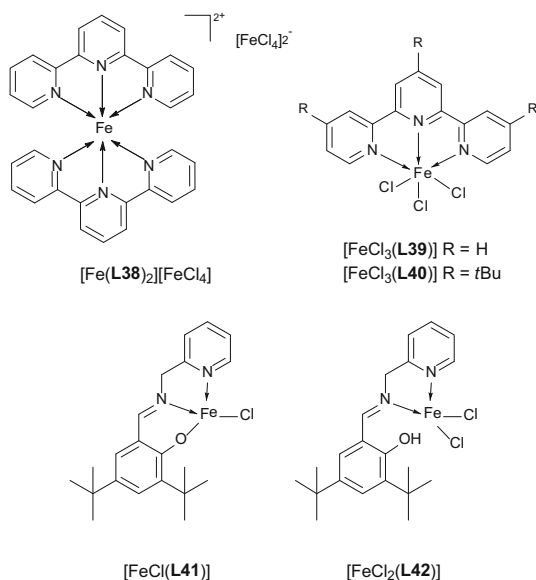
1,3-dienes [149], precatalysts $[\text{FeCl}_2(\mathbf{L36})]$ and $[\text{FeCl}_2(\mathbf{L37})]$, once activated with $\text{Al}(i\text{Bu})_3$ or AlEt_3 and $[\text{Ph}_3\text{C}]^+[\text{B}(\text{C}_6\text{F}_5)_4]^-$, provided polyisoprene with high selectivity (>85%) for *trans*-1,4 and *cis*-1,4 microstructures, respectively. Interestingly, the change in stereoselectivity is solely based on the imine substituent of the otherwise identical catalysts (Scheme 4). Even though the mechanism is not well understood, a cationic Fe(II) was proposed as active species.

More recently, Zhang et al. reported Fe(II), Ni(II), and Co(II) complexes supported by 2-(N-arylcarboximidoylchloride)quinoline ligands for the polymerization of 1,3-butadiene [150]. Using this new imine analogue, the iron-based system, once activated with MAO, presented the lowest catalytic activity and the lowest regioselectivity (*cis*-1,4 content in a range of 63–78%) compared to other Ni(II) and Co(II) catalysts. Interestingly, no polybutadiene was formed when $\text{Et}_3\text{Al}_2\text{Cl}_3$ (EASC) was used as cocatalyst. This result considerably contrasts with those obtained with phenanthroline-type ligands, indicating that electronic modification of bidentate nitrogen ligands plays an important role on both the activity and selectivity of diene polymerizations.

4.1.2 Tridentate Nitrogen-Based Ligands

In line with a study on ethylene polymerization with iron-based tridentate nitrogen ligands, Yasuda and coworkers studied the use of several Fe(II) and Fe(III) precatalysts for butadiene and isoprene polymerization [151]. Once activated with MMAO, complexes $[\text{Fe}(\mathbf{L38})_2][\text{FeCl}_4]$, $[\text{FeCl}_3(\mathbf{L39})]$, $[\text{FeCl}_3(\mathbf{L40})]$, $[\text{FeCl}(\mathbf{L41})]$, and $[\text{FeCl}_2(\mathbf{L42})]$ led to very low activities or were totally inactive toward ethylene (Fig. 21). In sharp contrast to these results, these precatalysts demonstrated their potential for controlling the activity of isoprene and 1,3-butadiene polymerizations. In the case of isoprene homopolymerization, the 3,4-microstructure (50–85%) was mainly obtained. For polybutadiene, the microstructure of the polymer seems to depend on the steric properties of the ligand used (*trans*-1,4 polymers with the less bulky systems, to equimolar *cis*-1,4/*trans*-1,4/1,2 products for bulkier ligands). During the course of their investigations, the authors also explored the potential

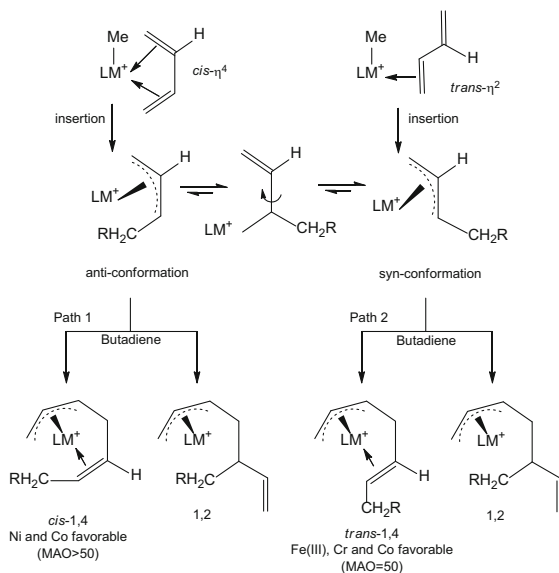
Fig. 21 Iron(II) and iron (III) precatalysts for diene polymerization



of complexes [FeCl₃(L39)] and [FeCl₃(L40)] for the random copolymerization of butadiene and isoprene to develop new materials. With a 1/1 molar ratio of 1,3-butadiene and isoprene, complex [FeCl₃(L39)] preferably performed the incorporation of 1,3-butadiene into the copolymer, whereas for complex [FeCl₃(L40)], isoprene incorporation was preferred. The increased electronegativity on the ligand via the *t*Bu group was evoked to explain this result. Microstructures observed during homopolymerization reactions did not seem to be affected by the mixture of the two dienes.

In 2009, a study conducted by Zhang and coworkers [152] attempted to demonstrate that *cis*-/*trans*-1,4 regioselectivity in 1,3-butadiene can be controlled by the nature of the metal center. Several Fe(III), Cr(III), Fe(II), Co(II), and Ni(II) chloride complexes supported by 2,6-bis[1-(iminophenyl)ethyl]pyridine were evaluated. Once activated with MAO, the activity decreased in the order of Fe(III) > Co(II) > Cr(III) ≈ Ni(II) which appeared consistent with the open space around the metal center. The microstructure of the polybutadiene varied from a high *trans*-1,4 content (88–95%) for Fe(III) and Cr(III), over a medium *trans*-1,4 and *cis*-1,4 content (55% and 35%, respectively) for Fe(II), to high *cis*-1,4 content (79–97%) for Co(II) and Ni(II). The uniquely high *trans*-1,4 selectivity observed with Fe(III) and Cr(III) catalysts was supported by a mechanism proposed for the reaction (Scheme 5). Due to less vacant sites and more crowded sterical space of the tridentate Fe(III) and Cr(III) (compared to their Fe(II) or Co(II) analogues), single *trans*-η² coordination with butadiene will be favored, giving predominantly the *syn*-π-allyl transition state. As a consequence, high *trans*-1,4 selectivity was observed.

Scheme 5 Proposed intermediates responsible for *cis*-1,4 and *trans*-1,4 polymer formation



Later, the same group also explored the role of steric hindrance of a series of 2,6-bis(imino)pyridyl iron(III) complexes for a highly *trans*-1,4 selective polymerization of 1,3-butadiene [153]. Once activated with MAO or MMAO, Fe(III) complexes exhibiting the least steric hindrance around the metal center were described as very selective for *trans*-1,4 polybutadiene (95%), while those bearing alkyl substituents at the 2-position of each *N*-aryl ring exhibit much lower catalytic activity and tunable *trans*-1,4 selectivity. Very small variations of polybutadiene microstructure were observed by varying the temperature or the cocatalyst used (MAO, MMAO, AlEt₃, or Al(*i*Bu)₃).

Structural modifications around the bis(imino)pyridine scaffold were also studied by Britovsek and coworkers by changing the substituents at the imine carbon atom [39]. Special attention has been devoted to “Thio-Pybox” **L43** and “Thio-Phebox” **L44** ligands and their corresponding Cr(III), Fe(II), Co(II), and Ni(II) complexes (Fig. 22). Once activated with MAO, they were evaluated for ethylene and butadiene polymerization. Although very low activities for ethylene polymerization were observed for most of the complexes studied, Fe(II) complexes supported by Thio-Pybox ligands revealed interesting activities for butadiene polymerization. Once again, the nature of the metal plays a predominant role on the activities, as exemplified for ligand **L43** ([CoCl₂(**L43**)] > [FeBr₂(**L43**)] ≈ [NiBr₂(**L43**)] > [CrCl₃(**L43**)]). A small variation of the polybutadiene microstructure was observed while varying the nature of the metal center (more than 73% of *cis*-1,4). The use of tridentate pincer ligands of “Phebox type” was also investigated by Mu et al. in 2012 [154]. Once activated with MAO, Fe(II) complex [FeCl(**L45**)]-[LiCl(THF)₂] showed moderate activities in butadiene polymerizations, affording the *cis*-1,4 enriched polymer as well.

Fig. 22 Bidentate ligands evaluated in iron-catalyzed diene polymerization

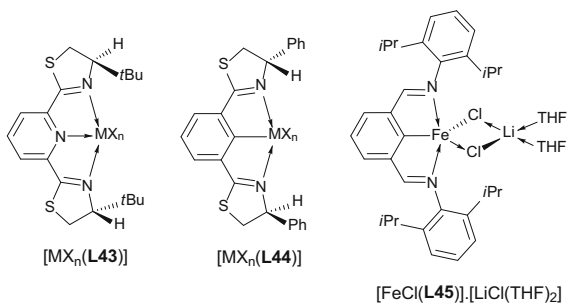
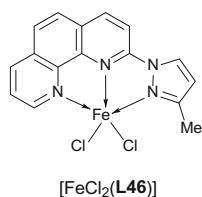


Fig. 23 Functionalized phenanthroline iron complex

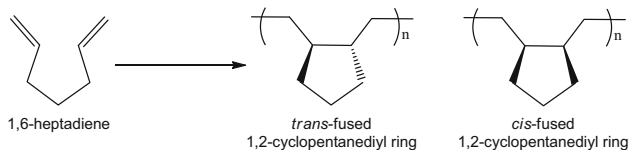


More recently, Fe(II)-bearing tridentate 2-pyrazolyl-substituted 1,10-phenanthrolines were successfully used for *trans*-1,4-specific polymerization of 1,3-butadiene (Fig. 23) [155]. The authors demonstrated for these precatalysts the huge influence of the Al-based cocatalysts, especially on the polybutadiene microstructure. The *trans*-1,4 selectivity of $[FeCl_2(L46)]$ varied in the following order: $Al(iBu)_3 > Al(Oct)_3 > AlEt_3 > AlMe_3$. Even much lower *trans*-1,4 selectivity was observed when using MAO and MMAO.

4.2 Iron-Based Catalysts for Homo- and Copolymerization of Olefins and Nonconjugated Dienes

The polymerization of nonconjugated symmetrically substituted dienes like 1,6-heptadiene or 1,5-hexadiene, known as cyclopolymerization, is also an important field of research, as it produces polymers with improved optical transparency and thermal stability [156]. This type of polymerization will produce polymers having cyclic structures in the repeating units (Scheme 6). Successful results were obtained by using early transition metal catalysts (Ti, Zr), but high selectivity for *cis* or *trans* fused rings remains scarce.

The use of late transition metals for this purpose was described by the group of Osakada in 2007 [157]. In this work, a $[FeCl_2(L47)]$ complex was reported as an efficient precatalyst for stereoselective cyclopolymerization of 1,6-heptadienes (Fig. 24). Upon activation with MMAO, complete cyclization of the diene monomer was observed during polymerization (no pendant 5-pentenyl group was detected). A majority of *cis*-1,2-cyclopentanediy rings was formed (95%).



Scheme 6 Products of 1,6-hexadiene polymerization

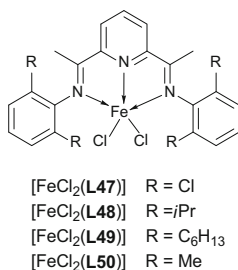
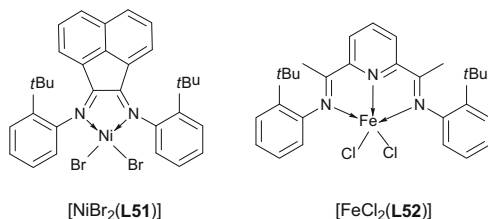


Fig. 24 Bis(imino)pyridine-based iron complexes

Interestingly, catalysts prepared from $[\text{FeCl}_2(\text{L48})]$ or $[\text{FeCl}_2(\text{L49})]$ (Fig. 24) appeared to be less active and selective than the chloride-substituted one. In a more detailed study [158], the same group reported the role of the steric hindrance of the *N*-aryl-substituted groups on the stereochemistry of cyclization in the polymer growth. Iron complexes with less bulky *N*-aryl groups gave the highest selectivity for *cis*-five-membered ring systems.

Other α,ω -dienes (9,9-diallylfluorene, 4-phenyl-1,6-heptadiene, 4-siloxy-1,6-heptadiene) were also investigated. The polymerization process occurred in a similar fashion (*cis*-selective) than that of the unsubstituted 1,6-heptadiene when $[\text{FeCl}_2(\text{L50})]/\text{MMAO}$ was used. Copolymerization of 1,6-heptadiene and ethylene with the same catalyst resulted in a mixture of the homopolymers rather than their copolymers. This result contrasts drastically with those obtained when $[\text{CoCl}_2(\text{L48})]/\text{MMAO}$ was used. In this latter case, a regular copolymer having a *trans*-five-membered ring was obtained. Limitations of iron-based catalysts to perform regular copolymerization of α,ω -dienes and ethylene were also described by Deffieux and coworkers as early as 2001 [159]. In this work, comparisons between $[\text{ZrCl}_2(\text{Cp}_2)]$, $[\text{TiCl}_2(\text{Cp}^*)\{\text{SiMe}_2(\text{N-tert-Bu})\}]$, $[\text{NiBr}_2(\text{L51})]$, and $[\text{FeCl}_2(\text{L52})]/\text{MAO}$ (Fig. 25) were described for homo- and copolymerization of ethylene with 5,7-dimethylocta-1,6-diene (5,7-DMO). Whereas nickel catalysts appeared completely inactive (5,7-DMO poisons the catalyst), zirconium and titanium performed efficiently with incorporation of the diene in the polyethylene chain. Iron complexes appeared highly active for ethylene polymerization but without any incorporation of the 5,7-DMO. Furthermore, the amount of dienes does not seem to affect the catalyst activity (i.e., no diene poisoning was observed).

Fig. 25 Nickel and iron complexes evaluated in ethylene/5,7-dimethylocta-1,6-diene copolymerization



5 Conclusion and Outlook

Since the first examples of iron-bis(imino)pyridine in combination with MAO for ethylene oligo-/polymerization more than 15 years ago, countless numbers of catalytic systems have been described covering an access to a broad range of products. Linear alpha olefins and polyethylenes are of prime interest, and ethylene is a more and more abundant feedstock, provided by the mushrooming of ethane crackers among others. However, no production unit or announcement in the press using such a technology has been built or released.

Two main considerations may arise. First, the thermal stability and lifetime of the catalysts reported in the literature likely undermine their developments. Additionally, by-product formation, often not thoroughly described, is critical for ethylene transformation. For example, polymer formation has to be avoided or at least limited in ethylene oligomerization. In the recent examples covered in this chapter, the reaction temperature remains an issue, even if interesting progress may have been observed by tuning the steric hindrance or the electronic properties of the ligand. Efforts should be increased with a careful description of the product distributions at a relevant productivity level. Heterogenization of bis(imino)-pyridine iron catalytic systems has been considered for ethylene transformation. Activation of these immobilized catalysts with MAO and activators from it led to active systems for ethylene polymerization. However, the activities exhibited by supported catalysts remain, apart from a few exceptions, lower compared to their homogeneous analogues. The selectivity might also be affected by the immobilization. The few reports found in the literature in the last 5 years denote the difficulties to overcome these activity and selectivity issues. Iron complexes still need to become competitive with actual industrial ethylene polymerization, with the goal to upgrade current catalytic systems.

Iron catalysts present interesting features for multiple single-site approaches such as reactor blending and tandem catalysis, giving access to new and unique polymers. The same limitations known for single-site catalysis have, however, to be considered in addition to compatibility issues.

Significant advances have been made in characterization and understanding at an experimental and a theoretical level. The isolation of well-defined catalyst species greatly assists the understanding of catalyst behavior. However, one major hurdle has not been surmounted so far. The activation step remains a challenge, even more so with the use of MAO in large excess. Considering the multiple oxidation states

and the ligand non-innocence possible for iron system, substantial uncertainty exists regarding the active species formed and its complex reaction landscape. This has to be considered when multiple product distributions are observed. The isolated active species and spectroscopic studies described in this chapter give only a narrow picture of the events, definitely not representative of the activation under catalytic conditions, although highly informative. Crossed reactivity study with MAO and *in operando* measurements are a means to improve our global understanding. One promising alternative to consider, even if not successful yet, is to replace MAO by well-defined species that may follow only one activation route.

Iron catalyst systems also present interesting features for diene polymerization even if both activities and selectivities remain far from those observed for conventional catalysts. Opportunities created by the development of bis(imino)pyridine-Fe(II) complexes have not been totally exploited for this application. In particular, the large versatility of these ligands lets us expect very interesting results for the discovery of highly active and selective catalysts in that field.

Acknowledgments We thank Dr. Vincent Monteil and Dr. Christophe Boisson for fruitful discussions on olefin and diene polymerization.

References

1. Nexant, LDPE, PERP Program 2013-2, 00101 0013 4102, www.nexanthinking.com
2. Kaminski W (2004) The discovery of metallocene catalysts and their present state of the art. *J Polym Sci Part A Polym Chem* 42:3911–3921
3. Hlatky GG (1999) Metallocene catalysts for olefin polymerization: annual review for 1996. *Coord Chem Rev* 181:243–296
4. Takeuchi D (2010) Recent progress in olefin polymerization catalyzed by transition metal complexes: new catalysts and new reactions. *Dalton Trans* 39:311–328
5. Leblanc A, Grau E, Broyer JP, Boisson C, Spitz R, Monteil V (2011) Homo- and copolymerizations of (meth)acrylates with olefins (styrene, ethylene) using neutral nickel complexes: a dual radical/catalytic pathway. *Macromolecules* 44:3293–3301
6. Hata G (1964) Stereospecific synthesis of 1,4-dienes. *J Am Chem Soc* 86:3903–3903
7. Hata G, Aoki D (1967) Stereospecific synthesis of 1,4-dienes. *J Org Chem* 32:3754–3758
8. Hata G, Miyake A (1968) Stereospecific synthesis of 1,4-dienes. IV. The catalytic behavior of the ethylenebis(diphenylphosphine) complex of iron(0). *Bull Chem Soc Jpn* 41:2762–2764
9. Yamamoto A, Morifujii K, Ikeda S, Saito T, Uchida Y, Misono A (1968) Diethylbis(bipyridine)iron. Butadiene cyclodimerization catalyst. *J Am Chem Soc* 90:1878–1883
10. Tom Dieck H, Dietrich J (1985) Selectivity and mechanism of diene cyclodimerization on iron(0) complexes. *Angew Chem Int Ed Engl* 24:781–783
11. Ehlers J, König WA, Lutz S, Wenz G, Tom Dieck H (1988) Gas chromatographic separation of enantiomeric olefins. *Angew Chem Int Ed Engl* 27:1556–1558
12. Tkatchenko I (1977) Catalytic reactions involving butadiene: I. Selective dimerisation to 4-vinylcyclohexene with polymetallic precursors. *J Organomet Chem* 124:C39–C42
13. Gibson VC, Solan GA (2009) Iron-based and cobalt-based olefin polymerisation catalysts. In: Guan Z (ed) *Metal catalysts in olefin polymerization*. Springer, Berlin Heidelberg, pp 107–158

14. Bianchini C, Giambastiani G, Rios IG, Mantovani G, Meli A, Segarra AM (2006) Ethylene oligomerization, homopolymerization and copolymerization by iron and cobalt catalysts with 2, 6-(bis-organylimino)pyridyl ligands. *Coord Chem Rev* 250:1391–1418
15. Boudier A, Breuil PAR, Magna L, Olivier-Bourbigou H, Braunstein P (2014) Ethylene oligomerization using iron complexes: beyond the discovery of bis(imino)pyridine ligands. *Chem Commun* 50:1398–1407
16. Abu-Surrah AS, Lappalainen K, Leskelä M, Repo T (2010) Aldimine 2,6-bis(imino)pyridine iron(II) and cobalt(II)/methyl aluminoxane catalyst systems for polymerization of tert-butylacrylate. *Transit Met Chem* 35:7–11
17. Li L, Gomes PT (2012) In: Bianchini C, Cole-Hamilton DJ, van Leeuwen PWNM (eds) *Olefin upgrading catalysis by nitrogen-based metal complexes II*, vol 36, *Catalysis by metal complexes*. Springer, Dordrecht, pp 77–197
18. Small BL, Marcucci AJ (2001) Iron catalysts for the head-to-head dimerization of α -olefins and mechanistic implications for the production of linear α -olefins. *Organometallics* 20: 5738–5744
19. Guo LH, Gao HY, Zhang L, Zhu FM, Wu Q (2010) An unsymmetrical iron(ii) bis(imino)pyridyl catalyst for ethylene polymerization: effect of a bulky ortho substituent on the thermostability and molecular weight of polyethylene. *Organometallics* 29:2118–2125
20. Wang S, Li B, Liang T, Redshaw C, Li Y, Sun WH (2013) Synthesis, characterization and catalytic behavior toward ethylene of 2-[1-(4,6-dimethyl-2-benzhydrylphenylimino)ethyl]-6-[1-(arylimino)ethyl]-pyridylmetal (iron or cobalt) chlorides. *Dalton Trans* 42:9188–9197
21. Görl C, Englmann T, Alt HG (2011) Bis(arylimino)pyridine iron(III) complexes as catalyst precursors for the oligomerization and polymerization of ethylene. *Appl Catal A Gen* 403: 25–35
22. Görl C, Beck N, Kleiber K, Alt HG (2012) Iron(III) complexes with meta-substituted bis(arylimino)pyridine ligands: catalyst precursors for the selective oligomerization of ethylene. *J Mol Catal A Chem* 352:110–127
23. Beaufort L, Benvenuti F, Noels AF (2006) Iron(II)–ethylene polymerization catalysts bearing 2, 6-bis(imino)pyrazine ligands: part I. Synthesis and characterization. *J Mol Catal A Chem* 260:210–214
24. Beaufort L, Benvenuti F, Noels AF (2006) Iron(II)–ethylene polymerization catalysts bearing 2, 6-bis(imino)pyrazine ligands: part II. Catalytic behaviour, homogeneous and heterogeneous insights. *J Mol Catal A Chem* 260:215–220
25. Britovsek GJP, Gibson VC, Hoarau OD, Spitzmesser SK, White AJP, Williams DJ (2003) Iron and cobalt ethylene polymerization catalysts: variations on the central donor. *Inorg Chem* 42:3454–3465
26. Dawson DM, Walker DA, Thornton-Pett M, Bochmann M (2000) Synthesis and reactivity of sterically hindered iminopyrrolato complexes of zirconium, iron, cobalt and nickel. *J Chem Soc Dalton Trans* 459–466
27. Gibson VC, Spitzmesser SK, White AJP, Williams DJ (2003) Synthesis and reactivity of 1,8-bis(imino)carbazolide complexes of iron, cobalt and manganese. *Dalton Trans* 2718–2727
28. Tenza K, Hanton MJ, Slawin AMZ (2009) Ethylene oligomerization using first-row transition metal complexes featuring heterocyclic variants of bis(imino)pyridine ligands. *Organometallics* 28:4852–4867
29. Appukkuttan VK, Liu Y, Son BC, Ha CS, Suh H, Kim I (2011) Iron and cobalt complexes of 2,3,7,8-tetrahydroacridine-4,5(1H,6H)-diimine sterically modulated by substituted aryl rings for the selective oligomerization to polymerization of ethylene. *Organometallics* 30: 2285–2294
30. Britovsek GJP, Gibson VC, Kimberley BS, Maddox PJ, McTavish SJ, Solan GA, White AJP, Williams DJ (1998) Novel olefin polymerization catalysts based on iron and cobalt. *Chem Commun* 849–850

31. Zhang W, Chai W, Sun WH, Hu X, Redshaw C, Hao X (2012) 2-(1-(arylimino)ethyl)-8-arylimino-5,6,7-trihydroquinoline iron(II) chloride complexes: synthesis, characterization, and ethylene polymerization behavior. *Organometallics* 31:5039–5048
32. Smit TM, Tomov AK, Gibson VC, White AJP, Williams DJ (2004) Dramatic effect of heteroatom backbone substituents on the ethylene polymerization behavior of bis(imino)pyridine iron catalysts. *Inorg Chem* 43:6511–6512
33. Archer AM, Bouwkamp MW, Cortez M, Lobkovsky E, Chirik PJ (2006) Arene coordination in bis(imino)pyridine iron complexes: identification of catalyst deactivation pathways in iron-catalyzed hydrogenation and hydrosilylation. *Organometallics* 25:4269–4278
34. Smit TM, Tomov AK, Britovsek GJP, Gibson VC, White APJ, Williams DJ (2012) The effect of imine-carbon substituents in bis(imino)pyridine-based ethylene polymerisation catalysts across the transition series. *Catal Sci Technol* 2:643–655
35. Zhang W, Sun WH, Redshaw C (2013) Tailoring iron complexes for ethylene oligomerization and/or polymerization. *Dalton Trans* 42:8988–8997
36. Zhang M, Zhang W, Xiao T, Xiang J-F, Hao X, Sun WH (2010) 2-Ethyl-ketimino-1,10-phenanthroline iron(II) complexes as highly active catalysts for ethylene oligomerization. *J Mol Catal A Chem* 320:92–96
37. Song SJ, Gao R, Zhang M, Li Y, Wang FS, Sun WH (2011) 2- β -Benzothiazolyl-6-iminopyridylmetal dichlorides and the catalytic behavior towards ethylene oligomerization and polymerization. *Inorg Chim Acta* 376:373–380
38. Hao P, Chen Y, Xiao T, Sun WH (2010) Iron(III) complexes bearing 2-(benzimidazole)-6-(1-aryliminoethyl)pyridines: synthesis, characterization and their catalytic behaviors towards ethylene oligomerization and polymerization. *J Organomet Chem* 695:90–95
39. Nobbs JD, Tomov AK, Cariou R, Gibson VC, White AJP, Britovsek GJP (2012) Thio-Pybox and Thio-Phebox complexes of chromium, iron, cobalt and nickel and their application in ethylene and butadiene polymerisation catalysis. *Dalton Trans* 41:5949–5964
40. Small BL, Rios R, Fernandez ER, Gerlach DL, Halfen JA, Carney MJ (2010) Oligomerization of ethylene using new tridentate iron catalysts bearing α -diimine ligands with pendant S and P donors. *Organometallics* 29:6723–6731
41. Small BL, Rios R, Fernandez ER, Carney MJ (2007) Oligomerization of ethylene using new iron catalysts bearing pendant donor modified α -diimine ligands. *Organometallics* 26:1744–1749
42. Zhang S, Sun WH, Xiao T, Hao X (2010) Ferrous and cobaltous chlorides bearing 2, 8-bis(imino)quinolines: highly active catalysts for ethylene polymerization at high temperature. *Organometallics* 29:1168–1173
43. Xiao T, Zhang S, Li B, Hao X, Redshaw C, Li YS, Sun WH (2011) Ferrous and cobaltous chloride complexes bearing 2-(1-(arylimino)methyl)-8-(1H-benzimidazol-2-yl)quinolines: synthesis, characterization and catalytic behavior in ethylene polymerization. *Polymer* 52:5803–5810
44. Wang L, Zhang C, Wang ZX (2007) Synthesis and characterization of iron, cobalt, and nickel complexes bearing novel *N*, *N*-chelate ligands and their catalytic properties in ethylene oligomerization. *Eur J Inorg Chem* 17:2477–2487
45. Irrgang T, Keller S, Maisel H, Kretschmer W, Kempe R (2007) Sterically demanding iminopyridine ligands. *Eur J Inorg Chem* 26:4221–4228
46. Bart SC, Hawrelak EJ, Schmisser AK, Lobkovsky E, Chirik PJ (2004) Synthesis, reactivity, and solid state structures of four-coordinate iron(II) and manganese(II) alkyl complexes. *Organometallics* 23:237–246
47. Volbeda J, Meetsma A, Bouwkamp MW (2009) Electron-deficient iron alkyl complexes supported by diimine ligand $(Ph_2CN)_2C_2H_4$: evidence for reversible ethylene binding. *Organometallics* 28:209–215
48. Spencer LP, Altwer R, Wie P, Gelmini L, Gauld J, Stephan DW (2003) Pyridine- and imidazole-phosphinimine bidentate ligand complexes: considerations for ethylene oligomerization catalysts. *Organometallics* 22:3841–3854

49. Song S, Zhao W, Wang L, Redshaw C, Wang F, Sun WH (2011) Synthesis, characterization and catalytic behavior toward ethylene of cobalt(II) and iron(II) complexes bearing 2-(1-aryliminoethylidene) quinolines. *J Organomet Chem* 696:3029–3035
50. Xiao T, Zhang S, Kehr G, Hao X, Erker G, Sun WH (2011) Bidentate iron(II) dichloride complexes bearing substituted 8-(benzimidazol-2-yl)quinolines: synthesis, characterization, and ethylene polymerization behavior. *Organometallics* 30:3658–3665
51. Boudier A, Breuil PAR, Magna L, Rangheard C, Ponthus J, Olivier-Bourbigou H, Braunstein P (2011) Novel catalytic system for ethylene oligomerization: an iron(III) complex with an anionic N, N, N ligand. *Organometallics* 30:2640–2642
52. Yankey M, Obuah C, Guzei IA, Osei-Twum E, Hearne G, Darkwa J (2014) (Phenoxyimidazolyl-salicylaldimine)iron complexes: synthesis, properties and iron catalysed ethylene reactions. *Dalton Trans* 43:13913–13923
53. Wang L, Sun J (2008) Methylene bridged binuclear bis(imino)pyridyl iron(II) complexes and their use as catalysts together with Al(*i*-Bu)₃ for ethylene polymerization. *Inorg Chim Acta* 361:1843–1849
54. Barbaro P, Bianchini C, Giambastiani G, Rios IG, Meli A, Oberhauser W, Segarra AM, Sorace L, Toti A (2007) Synthesis of new polydentate nitrogen ligands and their use in ethylene polymerization in conjunction with iron(II) and cobalt(II) bis-halides and methylaluminumoxane. *Organometallics* 26:4639–4651
55. Tolstikov GA, Ivanchev SS, Oleinik II, Ivancheva NI, Oleinik IV (2005) New multifunctional bis(imino)pyridine-iron chloride complexes and ethylene polymerization catalysts on their basis. *Dokl Phys Chem* 404:182–185
56. Liu J, Li Y, Liu J, Li Z (2005) Ethylene polymerization with a highly active and long-lifetime macrocycle trinuclear 2, 6-bis(imino)pyridyliron. *Macromolecules* 38:2559–2563
57. Zheng Z-J, Chen J, Li Y-S (2004) The synthesis and catalytic activity of poly(bis(imino)pyridyl) iron(II) metallo dendrimer. *J Organomet Chem* 689:3040–3045
58. Cossee P, Arlman EJ (1964) Ziegler-Natta catalysis III. Stereospecific polymerization of propene with the catalyst system TiCl₄-AlEt₃. *J Catal* 3:99–104
59. Bryliakov KP, Talsi EP, Semikolenova NV, Zakharov VA (2009) Formation and nature of the active sites in bis(imino)pyridine iron-based polymerization catalysts. *Organometallics* 28:3225–3232
60. Talsi EP, Babushkin DE, Semikolenova NV, Zudin VN, Panchenko VN, Zakharov VA (2001) Polymerization of ethylene catalyzed by iron complex bearing 2, 6-bis(imino)pyridyl ligand: ¹H and ²H NMR monitoring of ferrous species formed via catalyst activation with AlMe₃, MAO, AlMe₃/B(C₆F₅)₃ and AlMe₃/CPh₃B(C₆F₅)₄. *Macromol Chem Phys* 202: 2046–2051
61. Bryliakov KP, Semikolenova NV, Zakharov VA, Talsi EP (2004) Active intermediates of ethylene polymerization over 2, 6-bis(imino)pyridyl iron complex activated with aluminum trialkyls and methylaluminumoxane. *Organometallics* 23:5375–5378
62. Bryliakov KP, Semikolenova NV, Zudin VN, Zakharov VA, Talsi EP (2004) Ferrous rather than ferric species are the active sites in bis(imino)pyridine iron ethylene polymerization catalysts. *Catal Commun* 5:45–48
63. Britovsek GJP, Clentsmith GKB, Gibson VC, Goodgame DML, McTavish SJ, Pankhurst QA (2002) The nature of the active site in bis(imino)pyridine iron ethylene polymerisation catalysts. *Catal Commun* 3:207–211
64. Castro PM, Lahtinen P, Axenov K, Viidanoja J, Kotiaho T, Leskelä M, Repo T (2005) Activation of 2, 6-bis(imino)pyridine iron(II) chloride complexes by methylaluminumoxane: an electrospray ionization tandem mass spectrometry investigation. *Organometallics* 24: 3664–3670
65. Cruz VL, Ramos J, Martínez-Salazar J, Gutiérrez-Oliva S, Toro-Labbé A (2009) Theoretical study on a multicenter model based on different metal oxidation states for the bis(imino)pyridine iron catalysts in ethylene polymerization. *Organometallics* 28:5889–5895

66. Raucoules R, Bruin T, Raybaud P, Adamo C (2008) Evidence for the iron(III) oxidation state in bis(imino)pyridine catalysts. A density functional theory study. *Organometallics* 27: 3368–3377
67. Deng L, Margl P, Ziegler T (1999) Mechanistic aspects of ethylene polymerization by iron (II)-bisimine pyridine catalysts: a combined density functional theory and molecular mechanics study. *J Am Chem Soc* 121:6479–6487
68. Griffiths EAH, Britovsek GJP, Gibson VC, Gould IR (1999) Highly active ethylene polymerisation catalysts based on iron: an ab initio study. *Chem Commun* 1333–1334
69. Khoroshun DV, Musaev DG, Vreven T, Morokuma K (2001) Theoretical study on bis(imino)pyridyl-Fe(II) olefin poly- and oligomerization catalysts. Dominance of different spin states in propagation and β -hydride transfer pathways. *Organometallics* 20:2007–2026
70. Bouwkamp MW, Bart SC, Hawrelak EJ, Trovitch RJ, Lobkovsky E, Chirik PJ (2005) Square planar bis(imino)pyridine iron halide and alkyl complexes. *Chem Commun* 3406–3408
71. Fernández I, Trovitch RJ, Lobkovsky E, Chirik PJ (2008) Synthesis of bis(imino)pyridine iron di- and monoalkyl complexes: stability differences between $\text{FeCH}_2\text{SiMe}_3$ and $\text{FeCH}_2\text{CMe}_3$ derivatives. *Organometallics* 27:109–118
72. Scott J, Gambarotta S, Korobkov I, Budzelaar PHM (2005) Reduction of (diiminopyridine) iron: evidence for a noncationic polymerization pathway? *Organometallics* 24:6298–6300
73. Cámpora J, Naz AM, Palma P, Álvarez E, Reyes ML (2005) 6-Diiminopyridine iron (II) dialkyl complexes. Interaction with aluminum alkyls and ethylene polymerization catalysis. *Organometallics* 24:4878–4881
74. Scott J, Gambarotta S, Korobkov I, Budzelaar PHM (2005) Metal versus ligand alkylation in the reactivity of the (bis-iminopyridinato)Fe catalyst. *J Am Chem Soc* 127:13019–13029
75. Bouwkamp MW, Lobkovsky E, Chirik PJ (2005) Bis(imino)pyridine iron(II) alkyl cations for olefin polymerization. *J Am Chem Soc* 127:9660–9661
76. Tondreau AM, Milsmann C, Patrick AD, Hoyt HM, Loblovsky E, Wiegardt K, Chirik PJ (2010) Synthesis and electronic structure of cationic, neutral, and anionic bis(imino)pyridine iron alkyl complexes: evaluation of redox activity in single-component ethylene polymerization catalysts. *J Am Chem Soc* 132:15046–15059
77. Cartes MA, Rodríguez-Delgado A, Palma P, Alvarez E, Cámpora J (2014) Sequential reduction and alkyl exchange reactions of bis(imino)pyridine dialkyliron(II) with trimethylaluminum. *Organometallics* 33:1834–1839
78. Cartes MA, Rodríguez-Delgado A, Palma P, Sánchez LJ, Cámpora J (2014) Direct evidence for a coordination–insertion mechanism of ethylene oligomerization catalysed by neutral 2,6-bisiminopyridine iron monoalkyl complexes. *Catal Sci Technol* 4:2504–2507
79. Tomov AK, Gibson VC, Britovsek GJP, Long RJ, Meurs M, Jones DJ, Tellmann KP, Chirinos JJ (2009) Distinguishing chain growth mechanisms in metal-catalyzed olefin oligomerization and polymerization systems: $\text{C}_2\text{H}_4/\text{C}_2\text{D}_4$ co-oligomerization/polymerization experiments using chromium, iron, and cobalt catalysts. *Organometallics* 28:7033–7040
80. Boudene Z, Boudier A, Breuil PAR, Olivier-Bourbigou O, Raybaud P, Toulhoat H, de Bruin T (2014) Understanding the role of aluminum-based activators in single site iron catalysts for ethylene oligomerization. *J Catal* 317:153–157
81. Hlatky GG (2000) Heterogeneous single-site catalysts for olefin polymerization. *Chem Rev* 100:1347–1376
82. Ray S, Sivaram S (2006) Silica-supported bis(imino)pyridyl iron(II) catalyst: nature of the support–catalyst interactions. *Polym Int* 55:854–861
83. Semikolenova NV, Zakharov VA, Talsi EP, Babushkin DE, Sobolev AP, Echevskaya LG, Khysniyarov MM (2002) Study of the ethylene polymerization over homogeneous and supported catalysts based on 2, 6-bis(imino)pyridyl complexes of Fe(II) and Co(II). *J Mol Catal A Chem* 182–183:283–294
84. Barabanov AA, Bukatov GD, Zakharov VA (2008) Effect of temperature on the number of active sites and propagation rate constant at ethylene polymerization over supported bis(imino)pyridine iron catalysts. *J Polym Sci Part A Polym Chem* 46:6621–6629

85. Barabanov AA, Bukatov GD, Zakharov VA, Semikolenova NV, Mikenas TB, Echevskaja LG, Matsko MA (2006) Kinetic study of ethylene polymerization over supported bis(imino)pyridine iron(II) catalysts. *Macromol Chem Phys* 207:1368–1375
86. Guo C-Y, Xu H, Zhang M, Zhang X, Yan F, Yuan G (2009) Immobilization of bis(imino)pyridine iron complexes onto mesoporous molecular sieves and their catalytic performance in ethylene oligomerization. *Catal Commun* 10:1467–1471
87. Zhang M, Xu H, Guo C, Ma Z, Dong J, Ke Y, Hu Y (2005) Ethylene polymerization with iron-based diimine catalyst supported on MCM-41. *Polym Int* 54:274–278
88. Guo C, Jin G-X, Wang F (2004) Preparation and characterization of SBA-15 supported iron (II)-bisimine pyridine catalyst for ethylene polymerization. *J Polym Sci Part A Polym Chem* 42:4830–4837
89. Paulino IS, Schuchardt U (2004) Ethylene polymerization using iron catalysts heterogenized in MCM-41. *Catal Commun* 5:5–7
90. Huang R, Liu D, Wang S, Mao B (2005) Preparation of spherical $MgCl_2$ supported bis(imino)pyridyl iron(II) precatalyst for ethylene polymerization. *J Mol Catal A Chem* 233:91–97
91. Huang R, Liu D, Wang S, Mao B (2004) Spherical $MgCl_2$ supported iron catalyst for ethylene polymerization: effect of the preparation procedure on catalyst activity and the morphology of polyethylene particles. *Macromol Chem Phys* 205:966–972
92. Xu R, Liu D, Wang S, Mao B (2006) Preparation of spherical $MgCl_2$ -supported late-transition metal catalysts for ethylene polymerization. *Macromol Chem Phys* 207:779–786
93. Huang R, Kukalyekar N, Koning CE, Chadwick JC (2006) Immobilization and activation of 2,6-bis(imino)pyridyl Fe, Cr and V precatalysts using a $MgCl_2/AlR_n(OEt)_{3-n}$ support: effects on polyethylene molecular weight and molecular weight distribution. *J Mol Catal A Chem* 260:135–143
94. Huang R, Koning CE, Chadwick JC (2007) Effects of hydrogen in ethylene polymerization and oligomerization with magnesium chloride-supported bis(imino)pyridyl iron catalysts. *J Polym Sci Part A Polym Chem* 45:4054–4061
95. Tioni E, Monteil V, McKenna T (2013) Morphological interpretation of the evolution of the thermal properties of polyethylene during the fragmentation of silica supported metallocene catalysts. *Macromolecules* 46:335–343
96. Kurokawa H, Matsuda M, Fujii K, Ishihama Y, Sakuragi T, Ohshima MA, Miura H (2007) Bis(imino)pyridine iron and cobalt complexes immobilized into interlayer space of fluorotetrasilic mica: highly active heterogeneous catalysts for polymerization of ethylene. *Chem Lett* 36:1004–1005
97. Hiyama Y, Kawada Y, Ishihama Y, Sakuragi T, Ohshima MA, Kurokawa H, Miura H (2009) Catalytic behavior of bis(imino)pyridineiron(II) complex supported on clay minerals during slurry polymerization of ethylene. *Bull Chem Soc Jpn* 82:624–626
98. Kurokawa H, Hayasaka M, Yamamoto K, Sakuragi T, Ohshima MA, Miura H (2014) Self-assembled heterogeneous late transition-metal catalysts for ethylene polymerization; new approach to simple preparation of iron and nickel complexes immobilized in clay mineral interlayer. *Catal Commun* 47:13–17
99. Kondo T, Yamamoto K, Sakuragi T, Kurokawa H, Miura H (2012) Acetylaminopyridineiron (III) complexes immobilized in fluorotetrasilic mica interlayer as efficient catalysts for oligomerization of ethylene. *Chem Lett* 41:461–463
100. Xu H, Guo C, Xue C, Ma Z, Zhang M, Dong J, Wang J, Hu Y (2006) Novel layered calcosilicate-immobilized iron-based diimine catalyst for ethylene polymerization. *Eur Polym J* 42:203–208
101. Ray S, Galgali G, Lele A, Sivaram S (2005) In situ polymerization of ethylene with bis(imino)pyridine iron(II) catalysts supported on clay: the synthesis and characterization of polyethylene–clay nanocomposites. *J Polym Sci Part A Polym Chem* 43:304–318
102. Leone G, Bertini F, Canetti M, Boggioni L, Conzatti L, Tritto I (2009) Long-lived layered silicates-immobilized 2, 6-bis(imino)pyridyl iron(II) catalysts for hybrid polyethylene

- nanocomposites by in situ polymerization: effect of aryl ligand and silicate modification. *J Polym Sci Part A Polym Chem* 47:548–564
103. Kaul FAR, Puchta GT, Schneider H, Bielert F, Mihalios D, Herrmann WA (2002) Immobilization of bis(imino)pyridyliron(II) complexes on silica. *Organometallics* 21:74–82
 104. Han W, Niemantsverdriet H, Thüne PC (2007) A flat model approach to tethered bis(imino)pyridyl iron ethylene polymerization catalysts. *Macromol Symp* 260:147–153
 105. Han W, Müller C, Vogt D, Niemantsverdriet H, Thüne PC (2006) Introducing a flat model of the silica-supported bis(imino)pyridyl iron(II) polyolefin catalyst. *Macromol Rapid Commun* 27:279–283
 106. Kim I, Han BH, Ha CS, Kim JK, Suh H (2003) Preparation of silica-supported bis(imino)pyridyl iron(II) and cobalt(II) catalysts for ethylene polymerization. *Macromolecules* 36:6689–6691
 107. Kim I, Han BH, Kim JS, Ha CS (2005) Bis(imino)pyridyl Co(II) and Fe(II) catalysts immobilized on SBA-15 mesoporous material: new highly active supported catalysts for the polymerization of ethylene. *Catal Lett* 101:249–253
 108. Zheng Z, Liu J, Li Y (2005) Ethylene polymerization with silica-supported bis(imino)pyridyl iron(II) catalysts. *J Catal* 234:101–110
 109. Bahuleyan BK, Oh JM, Chandran D, Ha JY, Hur AY, Park DW, Ha CS, Suh H, Kim I (2010) Highly efficient supported diimine Ni(II) and iminopyridyl Fe(II) catalysts for ethylene polymerizations. *Top Catal* 53:500–509
 110. Seitz M, Milius W, Alt HG (2007) Iron(II) coordination compounds with ω -alkenyl substituted bis(imino)pyridine ligands: self-immobilizing catalysts for the polymerization of ethylene. *J Mol Catal A Chem* 261:246–253
 111. Görl C, Alt HG (2007) Iron complexes with ω -alkenyl substituted bis(arylimino)pyridine ligands as catalyst precursors for the oligomerization and polymerization of ethylene. *J Mol Catal A Chem* 273:118–132
 112. Jin G, Zhang D (2004) Micron-granula polyolefin with self-immobilized nickel and iron diimine catalysts bearing one or two allyl groups. *J Polym Sci Part A Polym Chem* 42:1018–1024
 113. Liu C, Jin G (2002) Polymer-incorporated iron catalysts for ethylene polymerization—a new approach to immobilize iron olefin catalysts on polystyrene chains. *New J Chem* 26:1485–1489
 114. Kaul FAR, Puchta GT, Frey GD, Herdtweck E, Herrmann WA (2007) Iminopyridine complexes of 3d metals for ethylene polymerization: comparative structural studies and ligand size controlled chain termination. *Organometallics* 26:988–999
 115. Gibson VC, Spitzmesser SK (2003) Advances in non-metallocene olefin polymerization catalysis. *Chem Rev* 103:283–316
 116. Ivanchev SS (2007) Advances in the development of new catalysts for ethylene and α -olefin polymerisation. *Russ Chem Rev* 76:617–637
 117. Makio H, Kashiwa N, Fujita T (2002) FI catalysts: a new family of high performance catalysts for olefin polymerization. *Adv Synth Catal* 344:477–493
 118. Barnhart RW, Bazan GC, Mourey T (1998) Synthesis of branched polyolefins using a combination of homogeneous metallocene mimics. *J Am Chem Soc* 120:1082–1083
 119. Severn JR, Chadwick JC, Duchateau R, Friederichs N (2005) “Bound but not gagged” immobilizing single-site α -olefin polymerization catalysts. *Chem Rev* 105:4073–4147
 120. Small BL, Brookhart M (1998) Iron-based catalysts with exceptionally high activities and selectivities for oligomerization of ethylene to linear α -olefins. *J Am Chem Soc* 120:7143–7144
 121. Bristovsek GJP, Mastroianni S, Solan GA, Baugh SPD, Redshaw C, Gibson VC, White AJP, Williams DJ, Elsegood MRJ (2000) Oligomerisation of ethylene by bis(imino)pyridyliron and -cobalt complexes. *Chem Eur J* 6:2221–2231
 122. Small BL, Brookhart M, Bennett AMA (1998) Highly active iron and cobalt catalysts for the polymerization of ethylene. *J Am Chem Soc* 120:4049–4050

123. Liu HT, Davey CR, Shirodkar PP (2003) Bimodal polyethylene products from UNIPOL™ single gas phase reactor using engineered catalysts. *Macromol Symp* 195:309–316
124. Böhm LL (2003) The ethylene polymerization with Ziegler catalysts: fifty years after the discovery. *Angew Chem Int Ed* 42:5010–5030
125. Boscoletto AB, Franco R, Scapin M, Tavan M (1997) An investigation on rheological and impact behaviour of high density and ultra high molecular weight polyethylene mixtures. *Eur Polym J* 33:97–105
126. Alt FP, Böhm LL, Enderle HF, Berthold J (2001) Bimodal polyethylene – Interplay of catalyst and process. *Macromol Symp* 163:135–144
127. Britovsek GJP, Cohen SA, Gibson VC, Maddox PJ, vanMeurs M (2002) Iron-catalyzed polyethylene chain growth on zinc: linear α -olefins with a Poisson distribution. *Angew Chem Int Ed* 41:489–491
128. Mecking S (1999) Reactor blending with early/late transition metal catalyst combinations in ethylene polymerization. *Macromol Rapid Commun* 20:139–143
129. Kurek A, Mark S, Enders M, Kristen MO, Mühlaupt R (2010) Mesoporous silica supported multiple single-site catalysts and polyethylene reactor blends with tailor-made trimodal and ultra-broad molecular weight distributions. *Macromol Rapid Commun* 31:1359–1363
130. Kurek A, Mark S, Enders M, Stürtzel M, Mühlaupt R (2014) Two-site silica supported Fe/Cr catalysts for tailoring bimodal polyethylenes with variable content of UHMWPE. *J Mol Catal A Chem* 383–384:53–57
131. Kukalyekar N, Balzano L, Peters GWM, Rastogi S, Chadwick JC (2009) Characteristics of bimodal polyethylene prepared via co-immobilization of chromium and iron catalysts on an $MgCl_2$ -based support. *Macromol React Eng* 3:448–454
132. Komon ZJA, Bazan GC (2001) Synthesis of branched polyethylene by tandem catalysis. *Macromol Rapid Commun* 22:467–478
133. Quijada R, Rojas R, Bazan G, Komon ZJA, Mauler RS, Galland GB (2001) Synthesis of branched polyethylene from ethylene by tandem action of iron and zirconium single site catalysts. *Macromolecules* 34:2411–2417
134. Xie G, Liu G, Li L, Li T, Zhang A, Feng J (2014) Tandem catalysis of iron and titanium non-metallocene catalysts for the production of branched polyethylene. *Catal Commun* 45: 7–10
135. Xie G, Zhang X, Li T, Li L, Liu G, Zhang A (2014) Preparation of linear low-density polyethylene from ethylene by tandem catalysis of iron and titanium non-metallocene catalysts. *J Mol Catal A Chem* 383:121–127
136. Ye Z, Zhu S (2003) Synthesis of branched polypropylene with isotactic backbone and atactic side chains by binary iron and zirconium single-site catalysts. *J Polym Sci Part A Polym Chem* 41:1152–1159
137. Huang R, Koning C, Chadwick JC (2007) Synergetic effect of a nickel diimine in ethylene polymerization with immobilized Fe-, Cr-, and Ti-based catalysts on $MgCl_2$ supports. *Macromolecules* 40:3021–3029
138. Yan FW, Xu H, Guo CY, Zhang MG, Zhang XH, Yang HJ, Yuan GQ (2009) Catalysis of ethylene to linear low-density polyethylene with iron-based diimine complex immobilized on calcosilicate and silica-supported $rac\text{-Et(Ind)}_2\text{ZrCl}_2$. *J Appl Polym Sci* 112:2298–2304
139. Guo CY, Xu H, Zhang M, Yang HJ, Yan F, Yuan G (2010) Copolymerization of ethylene and in situ-generated α -olefins to high-performance linear low-density polyethylene with a two-catalyst system supported on mesoporous molecular sieves. *Polym Int* 59:725–732
140. Bahuleyan BK, Lee KJ, Lee SH, Liu Y, Zhou W, Kim I (2011) Trinuclear Fe(II)/Ni(II) complexes as catalysts for ethylene polymerizations. *Catal Today* 164:80–87
141. Johnson LK, Killian CM, Brookhart M (1995) New Pd(II)- and Ni(II)-based catalysts for polymerization of ethylene and α -olefins. *J Am Chem Soc* 117:6414–6415
142. Kaminsky W (2000) Polymerization catalysis. *Catal Today* 62:23–34

143. Porri L, Giarrusso A (1989) Conjugated diene polymerization. In: Eastmond GJ, Ledwith A, Russo S, Sigwalt P (eds) *Comprehensive polymer science*, vol 4, Part II. Pergamon, Oxford, pp 53–108
144. Bazzini C, Giarrusso A, Porri L (2002) Diethylbis(2,2'-bipyridine)iron/MAO. A very active and stereospecific catalyst for 1,3-diene polymerization. *Macromol Rapid Commun* 23: 922–927
145. Ricci G, Morganti D, Sommazzi A, Santi R, Masi F (2003) Polymerization of 1,3-dienes with iron complexes based catalysts: influence of the ligand on catalyst activity and stereospecificity. *J Mol Catal A Chem* 204–205:287–293
146. Ricci G, Bertini F, Caterina Boccia A, Zetta L, Alberti E, Pirozzi B, Giarrusso A, Porri L (2007) Synthesis and characterization of syndiotactic 1,2-poly(3-methyl-1,3-pentadiene). *Macromolecules* 40:7238–7243
147. Raynaud J, Wu JY, Ritter T (2012) Iron-catalyzed polymerization of isoprene and other 1,3-dienes. *Angew Chem Int Ed* 51:11805–11808
148. Ritter T, Raynaud J, Wu J (2012) WO Patent 2012/109342 (President and Fellows of Harvard College)
149. Moreau B, Wu JY, Ritter T (2009) Iron-catalyzed 1,4-addition of α -olefins to dienes. *Org Lett* 11:337–339
150. Liu H, Wang F, Jia XY, Liu L, Bi JF, Zhang CY, Zhao LP, Bai CX, Hu YM, Zhang XQ (2014) Synthesis, characterization, and 1,3-butadiene polymerization studies of Co(II), Ni (II), and Fe(II) complexes bearing 2-(N-arylcarboximidoylchloride)quinoline ligand. *J Mol Catal A Chem* 391:25–35
151. Nakayama Y, Baba Y, Yasuda H, Kawakita K, Ueyama N (2003) Stereospecific polymerizations of conjugated dienes by single site iron complexes having chelating N, N, N-donor ligands. *Macromolecules* 36:7953–7958
152. Gong D, Wang B, Bai C, Bi J, Wang F, Dong W, Zhang X, Jiang L (2009) Metal dependent control of *cis-trans*-1, 4 regioselectivity in 1, 3-butadiene polymerization catalyzed by transition metal complexes supported by 2, 6-bis[1-(iminophenyl)ethyl]pyridine. *Polymer* 50:6259–6264
153. Gong D, Jia X, Wang B, Wang F, Zhang C, Zhang X, Jiang L, Dong W (2011) Highly trans-1,4 selective polymerization of 1,3-butadiene initiated by iron(III) bis(imino)pyridyl complexes. *Inorg Chim Acta* 373:47–53
154. Zhang J, Gao W, Lang X, Wu Q, Zhang L, Mu Y (2012) Ni(II) and Fe(II) complexes based on bis(imino)aryl pincer ligands: synthesis, structural characterization and catalytic activities. *Dalton Trans* 41:9639–9645
155. Wang B, Bi J, Zhang C, Dai Q, Bai C, Zhang X, Hu Y, Jiang L (2013) Highly active and trans-1,4 specific polymerization of 1,3-butadiene catalyzed by 2-pyrazolyl substituted 1,10-phenanthroline ligated iron (II) complexes. *Polymer* 54:5174–5181
156. Takeuchi D, Osakada K (2008) New polymerization of dienes and related monomers catalyzed by late transition metal complexes. *Polymer* 49:4911–4924
157. Takeuchi D, Matsuura R, Park S, Osakada K (2007) Cyclopolymerization of 1, 6-heptadienes catalyzed by iron and cobalt complexes: synthesis of polymers with trans- or cis-fused 1, 2-cyclopentenediyl groups depending on the catalyst. *J Am Chem Soc* 129:7002–7003
158. Takeuchi D, Matsuura R, Fukuda Y, Osakada K (2009) Selective cyclopolymerization of α,ω -dienes and copolymerization with ethylene catalyzed by Fe and Co complexes. *Dalton Trans* 8955–8962
159. Moniz Santos J, Rosario Ribeiro M, Farinha Portela M, Cramail H, Deffieux A (2001) Transition metal complexes as catalysts for the homo- and copolymerisation of olefins and non-conjugated dienes. *Macromol Chem Phys* 202:3043–3048

Enantioselective Iron Catalysts

Thierry Ollevier and Hoda Keipour

Abstract Synthetic organic transformations catalyzed by iron complexes have attracted considerable attention because of an enviable list of assets: iron is an ubiquitous, inexpensive, and environmentally benign metal. It has been documented that various chiral iron complexes can be used in many reactions such as oxidation, cyclopropanation, hydrogenation, hydrosilylation, and alkane hydroxylation. This chapter summarizes recent developments, mainly from 2004 to 2014, of enantioselective iron catalysts.

Keywords Alkane hydroxylation · Asymmetric catalysis · Biomimetic oxidation · Catalyst · Homogeneous catalysis · Hydrogenation · Hydrosilylation · Iron · Non-heme

Contents

1	Introduction	261
2	Chiral Iron Porphyrins	261
3	Chiral Iron Bipyridines	264
4	Chiral Schiff Base–Salen–Salan Catalysts	271
4.1	Schiff Base Catalysts	271
4.2	Salen Catalysts	273
4.3	Salan Catalysts	275
5	Bis(oxazoline) Catalysts	277
6	Pyridine <i>bis</i> (Oxazoline) Catalysts	281
7	Diamine-Derived Catalysts	285
8	Diphosphine-Derived Catalysts	291
9	Binaphthyl-Derived Catalysts	297
10	Planar-Chiral Ferrocenyl Catalysts	299

T. Ollevier (✉) and H. Keipour
Département de chimie, Université Laval, 1045 avenue de la Médecine, Québec,
QC G1V 0A6, Canada
e-mail: thierry.ollevier@chm.ulaval.ca

11 Other Catalysts	302
12 Summary and Overview	304
References	304

Abbreviations

acac	Acetylacetonate
Ad	1-Adamantyl
BAR _F	Tetrakis[3,5-bis(trifluoromethyl)phenyl] borate
binap	2,2'-Bis(diphenylphosphino)-1,1'-binaphthyl
binol	Binaphthol
bopa	Bis(oxazolinephenyl)amine
box	Bis(oxazoline)
DCE	Dichloroethane
DFT	Density functional theory
DMAP	4-Dimethylaminopyridine
DME	1,2-Dimethoxyethane
DMF	<i>N,N</i> -Dimethylformamide
DMSO	Dimethylsulfoxide
dpen	(<i>R,R</i>)-1,2-diphenylethylenediamine
dppe	1,2-Bis(diphenylphosphino)ethane
dppm	1,1-Bis(diphenylphosphino)methane
DS	Dodecyl sulfate
EPR	Electron paramagnetic resonance
H ₂ Pydic	Pyridine-2,6-dicarboxylic acid
H ₂ TAPP	5 α ,10 α ,15 α ,20 α -Tetrakis(<i>o</i> -aminophenyl)porphyrin
H ₂ TpivPP	5 α ,10 α ,15 α ,20 α -Tetrakis(<i>o</i> -pivalamidophenyl)porphyrin
HR-MS	High-resolution mass spectrometry
LASC	Lewis-acid–surfactant–combined catalyst
<i>m</i> -CPBA	<i>Meta</i> -chloroperoxybenzoic acid
NFSI	<i>N</i> -fluorobenzenesulfonimide
PDP	2-({(<i>S</i>)-2-[(<i>S</i>)-1-(pyridin-2-ylmethyl)pyrrolidin-2-yl]pyrrolidin-1-yl} methyl)pyridine
phebox	Bis(oxazoliny)phenyl
PMHS	Polymethylhydrosiloxane
PP	Porphyrin
PPN	Bis(triphenylphosphonium)iminium
pybox	Pyridine bis(oxazoline)
<i>rac</i>	Racemate
salan	2-[(phenylimino)methyl]phenolato
salen	<i>N,N'</i> -bis(salicylidene)ethylenediamine
SIPr	<i>N,N</i> -bis(2,6-diisopropylphenyl)-4,5-dihydroimidazol-2-ylidene
TBABr	Tetra- <i>n</i> -butylammonium bromide

Tf	Triflyl
TMEDA	<i>N,N,N',N'</i> -tetramethylethylenediamine
TOF	Turnover frequency
Tol	Tolyl
TON	Turnover number
TPS	<i>t</i> -Butyldiphenylsilyl
Ts	Tosyl
UHP	Urea–hydrogen peroxide adduct

1 Introduction

Metal catalysts are essential elements in organic chemists' toolbox. Iron is one of the most abundant metals on Earth; it is inexpensive, environmentally benign, and relatively nontoxic in comparison with other metals. From a green chemistry point of view, the development of new iron-catalyzed methods is of great excitement. As a matter of fact, many catalysts are derived from rare metals, and their price or toxicity prevents their use on an industrial scale. Iron, which is ubiquitous, is thus becoming one of the most versatile transition metals. Various reviews have been published in the field of iron catalysis [1–8]. The present chapter covers the most prominent uses of enantioselective iron catalysts with special emphasis on emerging applications since 2004 in terms of efficiency and novelty. Choice was made to sort the ligands and catalysts according to their structure rather than to their reactivity.

2 Chiral Iron Porphyrins

Since Collman's pioneering work on the synthesis of model iron porphyrin complexes, such as 5 α ,10 α ,15 α ,20 α -tetrakis(*o*-pivalamidophenyl)porphyrin **1** [H₂TpivPP] prepared from 5 α ,10 α ,15 α ,20 α -tetrakis(*o*-aminophenyl)porphyrin [H₂TAPP] (Fig. 1a) [9], iron porphyrins have been modified to include optically active groups. Chiral porphyrins were prepared by reacting $\alpha,\beta,\alpha,\beta$ -H₂TAPP with (*R*)-2-phenylpropanoyl chloride or the diacid chloride of 1,1'-binaphthyl-2,2'-dicarboxylic acid (Fig. 1b). Subsequent insertion of iron provided FeT($\alpha,\beta,\alpha,\beta$ -Hyd)PPCl **2** and TAPP FeT($\alpha,\beta,\alpha,\beta$ -*binap*)PPCl **3**, respectively [10]. Using these chiral iron porphyrins and iodosobenzene, styrene was oxidized to (*R*)-(+)-styrene oxide in up to 48% *ee*. Asymmetric epoxidation of alkenes was also catalyzed by iron porphyrins bearing amino acids [11] or some glycosylated groups [12]. Other chiral porphyrins were also reported for the asymmetric epoxidation reaction [13–24]. Catalytic asymmetric aziridination by iron porphyrins was also reported [25].

Other chiral modifications were studied independently by Groves [26] and Maruyama [27–29]. A chiral vaulted binaphthyl porphyrin **4** has been prepared

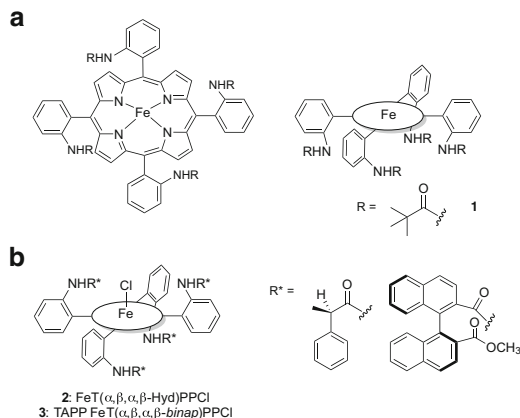


Fig. 1 Chiral Fe porphyrins

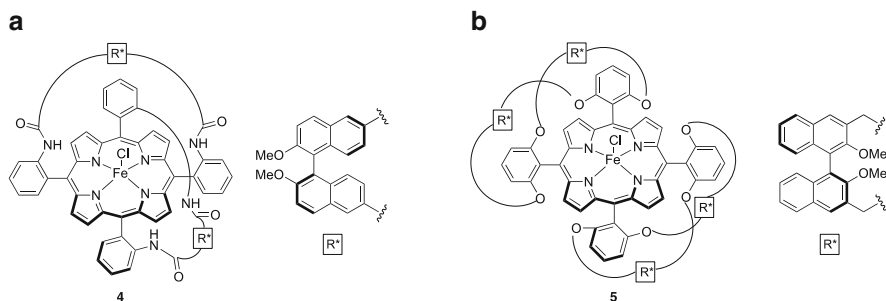
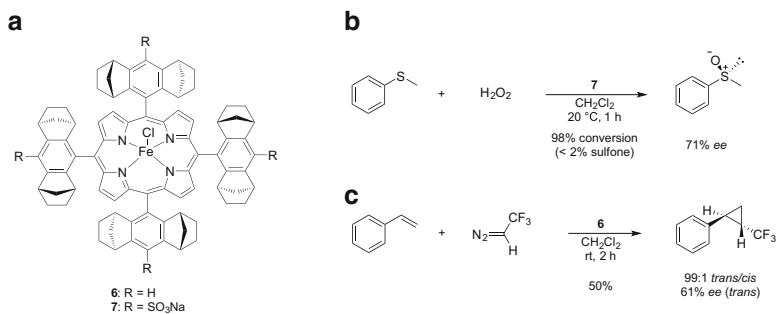


Fig. 2 Chiral Fe porphyrins including various chiral modifications

from $\alpha,\beta,\alpha,\beta$ -H₂TAPP with (*R*)-(+)-2,2'-dimethoxy-1,1'-bi-6-naphthoyl chloride (Fig. 2a) [26]. Asymmetric oxidations of alkanes, alkenes, and alkyl aryl sulfides were catalyzed with chloroiron(III) complexes. The first catalytic asymmetric hydroxylations were reported with enantiomeric excesses in the range of 40–72% [26]. For catalytic asymmetric epoxidations, enantiomeric excesses were in the range of 20–89% [27]. Oxidation of alkyl aryl sulfides led to the sulfoxides with 14–48% *ee* [26]. A different modified chiral porphyrin **5** was prepared by Naruta and Maruyama from 5,10,15,20-tetrakis(2,6-dihydroxyphenyl)porphine and enantiopure bis(bromomethyl)binaphthalene (Fig. 2b) [27–31]. Closely related porphyrins were also studied by Collman [32]. Catalytic asymmetric oxidation of sulfides with iodosobenzene as oxidant led to the sulfoxides in moderate enantioselectivities (up to 73% *ee*) and yields.

The first enantioselective iron-porphyrin-catalyzed sulfide oxidation with aqueous hydrogen peroxide was reported by Simonneaux [33]. This enantioselective oxidation of sulfides into enantiomerically enriched sulfoxides (up to 90% *ee*) was carried out in methanol/water mixtures using water-soluble iron porphyrins



Scheme 1 Halterman chiral porphyrins disclosed by Simonneaux

(Scheme 1a). The best enantioselectivities have been obtained with aryl methyl sulfides bearing electron-withdrawing groups on the aryl group. The reaction was fast and only slight overoxidation was observed (<2%) (Scheme 1b). Halterman chiral porphyrin **6** also catalyzed the cyclopropanation of styrene derivatives with 2,2,2-trifluorodiazoethane (Scheme 1c) [34]. The *trans*-cyclopropanes were obtained in moderate yields and high diastereoselectivities (up to 99:1 *trans/cis*) with up to 75% enantioselectivities for the *trans* diastereoisomer. Using ethyl diazoacetate as carbene source, styrene-type substrates were converted to cyclopropyl esters with high *trans/cis* ratios (>12) and high enantioselectivities for the *trans* isomers (74–86% *ee*) [35, 36]. The stereoselectivities were modified using axial ligand effects. Addition of organic bases such as pyridine and 1-methylimidazole led to a major increase in *trans/cis* ratios [35]. The recovery and recyclability of catalyst **7** was also studied, demonstrating that only a slight decrease of the enantioselectivity together with a maintained chemical yield of the cyclopropanation reaction was observed after four cycles [36]. Optically active cyclopropyl ketones (up to 80% *ee*) were also prepared through the asymmetric reaction of diazoacetophenone with styrene derivatives using the same catalytic system (**6**) [37]. Asymmetric cyclopropanation of styrenes was reported to be catalyzed by other Fe^{II} macrocyclic complexes [38] and Fe^{III} porphyrins [39].

More recently, Simonneaux reported the asymmetric epoxidation of styrene derivatives by H₂O₂ or UHP to give enantioenriched epoxides (up to 81% *ee*) using the abovementioned (Scheme 1) water-soluble iron porphyrin **7** as catalyst (Scheme 2a) [40]. The limitation of the process is that their system needs an excess of alkene vs. oxidant. The hydroxylation of alkanes providing secondary alcohols (up to 78% *ee*) was also reported using the same catalyst (Scheme 2b). In this case, iodobenzene diacetate converted ethylbenzene to the corresponding secondary alcohol with a better yield and much better enantioselectivity than H₂O₂.

The Fe^{III} complex **8** derived from a D₂-symmetric chiral porphyrin (Fig. 3), when used in the reaction of styrene with ethyl diazoacetate, afforded the desired cyclopropane products in low yields and poor enantioselectivities. The Co^{II} complex of the same chiral porphyrin showed its superiority over Fe^{III} in this reaction [41].

Scheme 2 Applications of water-soluble Fe porphyrin **7**

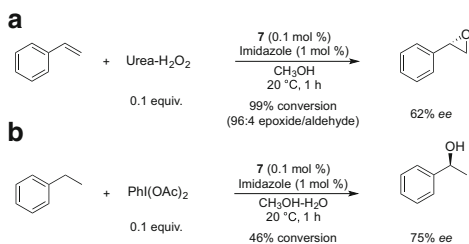
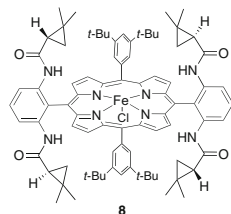


Fig. 3 *D*₂-symmetric chiral Fe porphyrin **8**

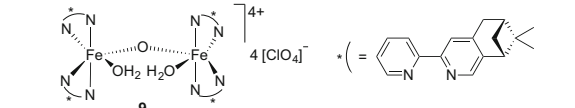


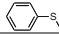
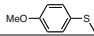
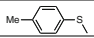
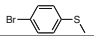
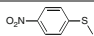
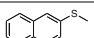
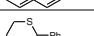
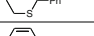
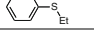
3 Chiral Iron Bipyridines

The catalytic properties of a non-heme diiron complex **9** (Table 1) derived from (–)-4,5-pinenebipyridine were studied by Fontecave [42, 43]. This dinuclear complex [Fe₂OL₄(H₂O)₂][ClO₄]₄, L = (–)-4,5-pinene-2,2′-bipyridine) efficiently catalyzed the oxidation of aryl sulfides to the corresponding sulfoxides by hydrogen peroxide in acetonitrile, with yields up to 90% based on the oxidant (Table 1). However, no oxidation at the preparative scale was reported using that system (1:600:10 Fe/substrate/oxidant ratio used in their procedure). The highest enantioselectivity (40% *ee*) was obtained with *p*-bromophenyl methyl sulfide as substrate. The catalytic properties of a mononuclear iron complex **10** ([FeL₂(MeCN)₂][ClO₄]₂, L = (–)-4,5-pinene-2,2′-bipyridine) have been compared to the related dinuclear analogue **9**. Both catalysts generate peroxo adducts, which are necessary for the oxidation of sulfides to sulfoxides. The dinuclear catalyst **9** provided better yields and enantioselectivities than its mononuclear analogue [44]. In 2007, Ménage demonstrated the ability of non-heme diferric complex **9** to catalyze the efficient epoxidation of alkenes at 0 °C by peracetic acid with high conversion (TON up to 850) [45]. However, the enantioselectivity of the process was only moderate (up to 63% *ee*).

Recently, Yamamoto described a highly efficient asymmetric epoxidation of β,β-disubstituted enones catalyzed by a combination of Fe(OTf)₂ and a phenanthroline ligand [46]. The reaction provides highly enantioenriched α,β-epoxyketones (up to 92% *ee*) that can be further converted to functionalized β-ketoaldehydes bearing an all-carbon quaternary center. The best reaction conditions involve the use of peracetic acid as the oxidant and a 2:1 ratio of ligand and Fe(OTf)₂. X-ray crystallographic analysis suggests the formation of an Fe complex

Table 1 Oxidation of prochiral sulfides by hydrogen peroxide catalyzed by dinuclear Fe complex **9**



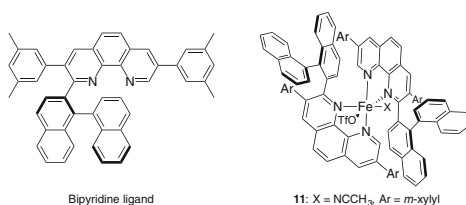
Entry	Sulfide	Yield sulfoxide (%) ^{a,b}	ee (%)
1		90	21
2		70	11
3		68	28
4		90	40
5		45	4
6		80 ^c	40
7		60	15
8		90	4
9		80	26

^aRatio of **1**/sulfide/H₂O₂ = 1:600:10

^bYield based on the oxidant after 0.15 h of reaction

^c250 equiv. of sulfide used

Fig. 4 Yamamoto's chiral Fe^{II}-bipyridine complex



in which two homochiral phenanthroline ligands coordinate the iron center in a *cis* topology, affording a pseudo-C₂-symmetric complex (Fig. 4).

Iron complex **11** coordinated by two phenanthroline ligands induces high enantioselectivity for a wide range β,β-disubstituted enones bearing different substituents of steric or electronic nature (Table 2).

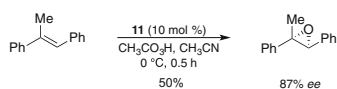
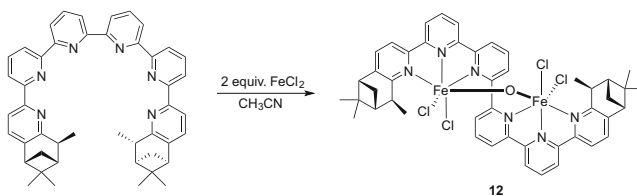
This chiral Fe^{II}-phenanthroline system **11** was also applied to a nonactivated olefin, such as *trans*-α-methylstilbene, with good enantioselectivity (Scheme 3).

A chiral Fe^{III}-sexipyridine complex **12** for epoxidation using H₂O₂ has been disclosed by Kwong in 2008 [47]. This diiron system showed excellent reactivity (3 min., up to 95% yield) and chemoselectivity toward terminal and 1,2-disubstituted aromatic alkenes (Scheme 4).

Iron complexes of chiral C₂-terpyridines **13–15** were used in catalytic asymmetric cyclopropanation of styrene (Table 3) [48]. However, the study mainly focused on the synthesis and characterization of such complexes and lacks generality and substrate scope, since only cyclopropanation of styrene with ethyl diazoacetate was described. The most effective ligands for this cyclopropanation were found to be

Table 2 Asymmetric epoxidation of β,β -disubstituted enones

Entry	R ¹	R ²	R ³	Yield (%)	ee (%)
1	Ph	Ph	Me	80	91
2	<i>p</i> -MeOC ₆ H ₄	Ph	Me	78	90
3	<i>p</i> -MeC ₆ H ₄	Ph	Me	77	92
4	<i>p</i> -FC ₆ H ₄	Ph	Me	78	92
5	<i>p</i> -CF ₃ C ₆ H ₄	Ph	Me	70	89
6	<i>m</i> -MeC ₆ H ₄	Ph	Me	67	90
7	<i>o</i> -MeC ₆ H ₄	Ph	Me	61	92
8	2-Naphthyl	Ph	Me	88	90
9	Ph	<i>p</i> -ClC ₆ H ₄	Me	88	92
10	Ph	2-Naphthyl	Me	45	92
11	Ph	<i>n</i> -C ₃ H ₇	Me	20	50
12	Ph	Ph	Et	72	92
13	Ph	Me	Ph	33	6

**Scheme 3** Asymmetric epoxidation with a nonactivated olefin**Scheme 4** Chiral Fe^{III}-sesipyridine complex **12** used for epoxidation of alkenes

the terpyridines **13–15**, **15** providing the highest enantiomeric excesses for this transformation (65 and 67% *ee* for *trans*- and *cis*-cyclopropanes, respectively). The chloride complexes [Fe(L)Cl₂] (L = **13–15**) were not active catalysts for the cyclopropanation of styrene with ethyl diazoacetate. However, active catalysts could be generated by simply stirring the chloride complexes with AgOTf in CH₂Cl₂. With some optimization of conditions; a ratio of 1:50:200 between catalyst, ethyl diazoacetate, and styrene; and slow addition of ethyl diazoacetate to the catalyst solution, fair to good yields of cyclopropanes as major products were obtained. However, the highest enantiomeric excesses (ca. 80% *ee*) were obtained using Co instead of Fe, in combination with ligand **14** (Table 3).

Table 3 Iron-catalyzed asymmetric cyclopropanation of styrene with ethyl diazoacetate

$\text{Ph-CH=CH}_2 + \text{H}_2\text{N}_2\text{COEt} \xrightarrow[\text{CH}_2\text{Cl}_2, 50^\circ\text{C}]{\text{Fe(L)Cl}_2, \text{AgOTf (2 equiv.) then filtration, catalyst (2 mol \%)}$

13: R = H
 14: R = Me
 15: R = n-butyl

Entry	Complex	Yield (%) ^a	Chemoselectivity ^b	<i>trans</i> : <i>cis</i>	<i>ee</i> (%)	
					<i>trans</i>	<i>cis</i>
1	[Fe(13)Cl ₂]	78	11.5:1	76:24	36	33
2	[Fe(14)Cl ₂]	71	8.2:1	68:32	54	54
3	[Fe(15)Cl ₂]	65	7.9:1	65:35	65	67
4	[Co(14)Cl ₂]	80	5.8:1	63:37	76	83

^aRatio of catalyst/ethyl diazoacetate/styrene = 1:50:200

^bRatio of cyclopropanes to coupling products

Our research group found that the combination of Fe(ClO₄)₂ and Bolm's ligand **16** (Table 4) provided a highly efficient chiral catalyst for enantioselective Mukaiyama aldol reactions in aqueous conditions [49–51], and for asymmetric *meso*-epoxide opening reactions [52, 53].

An enantioselective Mukaiyama aldol reaction in aqueous conditions (DME/H₂O 7:3) was developed in Kobayashi's group and in our group independently [49, 50]. Excellent yields (generally >95%), diastereo- (85:15–99:1) and enantioselectivities (90–98% *ee*) were obtained for the reaction of propiophenone-derived silyl enol ether with a wide range of aldehydes (aromatic, acetylenic, heteroaromatic, and aliphatic). The use of benzoic acid as an additive was essential to achieve such outstanding yields and selectivities (Table 4).

To the best of our knowledge, the obtained stereoselectivities are the highest found with a Lewis acid catalyst in aqueous media. Aliphatic aldehydes, which often lead to decreased enantioselectivities with other chiral catalysts, were found to undergo aldolization in high enantioselectivity (Table 4, entries 19–21). Noteworthy is that an aldehyde bearing a free alcohol can even be used without the necessity of a preliminary protection step (Table 4, entry 11). 1,2-Dimethoxyethane (DME) was found to be the best co-solvent for the reaction; however, ethanol provided excellent results as well (DME/H₂O 7:3 (97% *ee*) vs. EtOH/H₂O 7:3 (94% *ee*) for the model reaction with benzaldehyde). A silyl enol ether derived from an aliphatic ketone was also used (Table 5). In these preliminary unoptimized results, good stereoselectivities were obtained for both aldehydes tested. Given the importance of efficient methods for carbon–carbon bond-forming reactions between two aliphatic partners, the results obtained with 3-phenylpropionaldehyde are of prime importance (Table 5, entry 2).

Table 4 Catalytic asymmetric Mukaiyama aldol reaction with various aldehydes

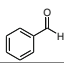
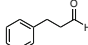
$\text{Ph-CH=C(OSiMe}_3\text{)-CH}_3 + \text{R-CHO} \xrightarrow[\text{DME:H}_2\text{O 7:3, 0 }^\circ\text{C, 16-24 h}]{\text{16 (15 mol \%), Fe(ClO}_4\text{)}_2\cdot 6\text{H}_2\text{O (5 mol \%), PhCO}_2\text{H (6 mol \%)}} \text{Ph-CH(OH)-CH}_2\text{-C(=O)-R}$

Entry	Aldehyde	R	Yield (%) ^a	<i>syn/anti</i>	<i>ee</i> (<i>syn</i>) (%)
1		H	98	97:3	97
2		4-Me	98	99:1	97
3		2-Me	96	99:1	96
4		4-MeO	96	97:3	96
5		4-Br	99	96:4	97
6		4-Cl	98	97:3	97
7		4-F	99	95:5	98
8		4-CF ₃	95	92:8	94
9		4-NO ₂	98	90:10	93
10		4-CN	99	91:9	95
11		4-CH ₂ OH	95	99:1	94
12			99	97:3	98
13			99	99:1	98
14			99	88:12	96
15		Ph	97	85:15	90
16		C ₅ H ₁₁	98	88:12	91
17			99	97:3	98
18			99	98:2	98
19			95	93:7	98
20			24	98:2	98
21			95	93:7	98

^aSilyl enol ether (1.2 equiv.), aldehyde (1.0 equiv.)

Structural evidence for the complex formed between $\text{Fe}(\text{ClO}_4)_2 \cdot 6\text{H}_2\text{O}$ and Bolm's ligand **16** was obtained by X-ray analysis [49, 54]. The structure contains a discrete monomeric $[\text{Fe}(\mathbf{16})(\text{DME})(\text{H}_2\text{O})]^{2+}$ dication and two ClO_4^- anions. It clearly appears that the bipyridine ligand is coordinated in a tetradentate fashion to the metal center. A DME molecule is also bound to the metal center, affording a slightly distorted pentagonal basis. An additional water molecule is bound to Fe in

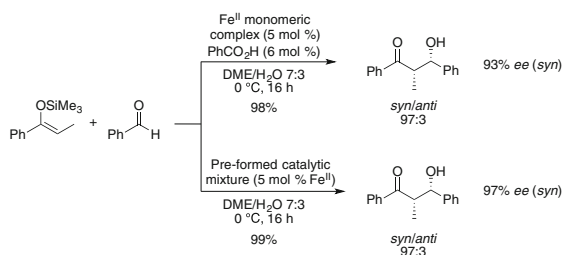
Table 5 Fe^{II}-catalyzed asymmetric Mukaiyama aldol reaction with 3-pentanone-derived silyl enol ether

Entry	Aldehyde	Yield (%) ^a	<i>syn/anti</i>	<i>ee</i> (<i>syn</i>) (%)
1		85	90:10	80
2		26 ^b	90:10	86

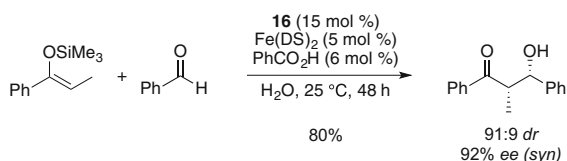
^aSilyl enol ether (*Z/E* 93:7) (1.2 equiv.), aldehyde (1.0 equiv.)

^bUnoptimized yield; 70% yield based on recovered starting material (aldehyde)

Scheme 5 Reactivity of stable isolated crystals and preformed Fe^{II} catalyst



Scheme 6 Fe(DS)₂-catalyzed Mukaiyama aldol reaction in water



axial position affording an unprecedented heptacoordinated chiral Fe^{II} complex. The catalytic efficiency of the precatalyst used as crystals was also investigated. When 5 mol% of the isolated precatalyst was used in the presence of benzoic acid, the reaction of propiophenone-derived silyl enol ether with benzaldehyde afforded the corresponding aldol in high yield (98%) and high stereoselectivities (*syn/anti* 97:3, 93% *ee* (*syn*)). These results accord with those obtained using a 1.2:1 ligand/metal ratio and confirm that this monomeric complex is catalytically active. Finally, the methodology was even made more practical by premixing the three catalyst components. The resulting orange solid was directly used as a stable preformed catalytic mixture in the model reaction. This premixed catalyst was shown to be as efficient as the *in situ*-formed catalyst since the same selectivities were obtained (Scheme 5 and Table 4, entry 1).

Catalytic asymmetric Mukaiyama aldol reaction in pure water was also carried out by using a combination of Fe^{II} dodecyl sulfate [Fe(DS)₂], chiral bipyridine ligand **16**, and benzoic acid (Scheme 6) [51]. Using the obtained Fe^{II}-derived Lewis-acid–surfactant–combined catalyst (LASC), the desired products were

afforded in good yields with high diastereo- and enantioselectivities. This efficient catalytic system proceeds in pure water and affords good yields and high enantioselectivities (up to 96% *ee*). Compared to other methods using chiral Cu^{II} or Sc^{III}, this system has the advantage of being the most efficient using a chiral Lewis acid–surfactant–combined catalyst for the Mukaiyama aldol reaction in pure water. The generality of the process was highlighted by the wide range of aldehydes that could be used in this process. Aliphatic aldehydes, such as *n*-butanal (64% yield, 72% *de*, 96% *ee* (*syn*)), were appropriate substrates as well.

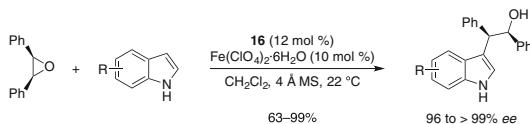
An Fe^{II}-derived catalytic system was also used for highly enantioselective *meso*-epoxide opening reactions with anilines [52]. The method allows rapid formation of chiral β -amino alcohols in good yields with excellent enantioselectivities (Table 6). Differently mono-substituted anilines, naphthylamines, and sterically hindered anilines were tested in the opening reaction of *cis*-stilbene. Yields ranging from

Table 6 Catalytic asymmetric *meso*-epoxide opening reaction with aniline derivatives

Entry	Epoxide	Aniline	R ²	Yield (%) ^a	<i>ee</i> (%)
1			H	90	95
2			2-Me	78	92
3			2-OMe	70	82
4			4-Cl	90	94
5			2-Cl	78	90
6			4-Br	87	94
7			4-CF ₃	90	96
8			4-CN	90	96
9					70
10				81	95
11				87	94
12			H	95	95
13			Br	88	96
14					79
15				80	95

^a Epoxide (1.0 equiv.), aniline (1.0 equiv.)

Scheme 7 Catalytic asymmetric *meso*-epoxide opening reaction with indoles



70 to 95% were obtained along with excellent enantioselectivities (generally $\geq 90\%$ *ee*). Excellent results were also obtained with other aromatic *meso*-epoxides.

Recently, a highly enantioselective method for the catalytic *cis*-stilbene oxide opening reaction with indole derivatives was developed by our group [53]. The scope of the reaction was studied with a selection of aromatic *meso*-epoxides and various indoles (Scheme 7), and the desired 2-(indol-3-yl)ethanol derivatives were obtained in good to excellent yields with excellent enantioselectivities (from 96 to $>99\%$ *ee*) [53].

4 Chiral Schiff Base–Salen–Salan Catalysts

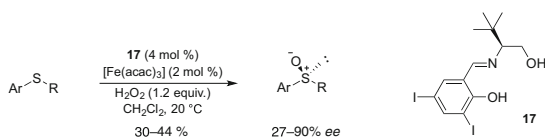
4.1 Schiff Base Catalysts

In 2003, Bolm reported a chiral Schiff base ligand **17** derived from (*S*)-*tert*-leucinol and salicylaldehyde derivatives [55]. The asymmetric sulfide oxidation using chiral ligand **17**, $[\text{Fe}(\text{acac})_3]$, and H_2O_2 provided optically active sulfoxides with up to 90% *ee* (Scheme 8). No sulfones were formed under these conditions, which indicates that the obtained enantioselectivities are only the result of the asymmetric sulfide oxidation and not of a kinetic resolution of the overoxidation to the sulfone. The best results were obtained with 0.5 equivalent of a carboxylic acid (or the carboxylate salt) relative to iron. This strongly suggests that monocarboxylate-bridged di- Fe^{III} complexes are involved in the process [56]. The best results were obtained with *para*-substituted aryl methyl sulfides leading to sulfoxides with high enantioselectivities ($>92\%$ *ee*) in moderate to good yields. The use of this catalytic system was reported for the synthesis of anti-inflammatory drug *sulindac* [57]. More challenging substrates, such as phenyl ethyl sulfide and phenyl benzyl sulfide, were oxidized with high enantioselectivities (82 and 79% *ee*, respectively). In addition, a positive nonlinear relationship between the *ee* of the product and that of the catalyst has been observed, clearly indicating that more than one ligand is involved in the stereochemistry-determining step of the process [58].

A dinuclear chiral iron complex of valinol-derived *salen* ligand **18** was used to catalyze the hydrophosphonylation of aldehydes to give α -hydroxy phosphonates in excellent yields and good enantioselectivities (Scheme 9) [59]. Either preformed **19** or prepared in situ catalysts were used in the reaction conditions and gave comparable results.

Highly enantioselective hydrophosphonylation of aldehydes was also performed using Fe^{II} -camphor-based tridentate Schiff base complexes, such as **20** (Fig. 5)

Scheme 8 Fe^{III}-catalyzed asymmetric sulfide oxidation with aqueous hydrogen peroxide



Scheme 9 Dinuclear chiral Fe complex **19** and its application in asymmetric hydrophosphonylation of aldehydes

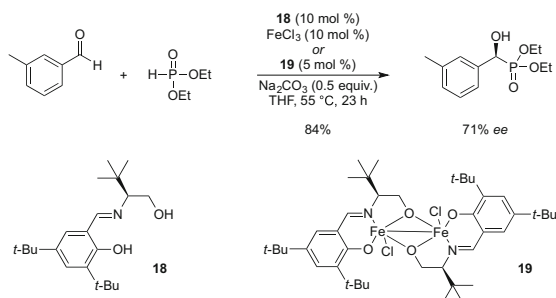
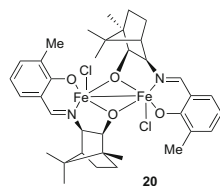
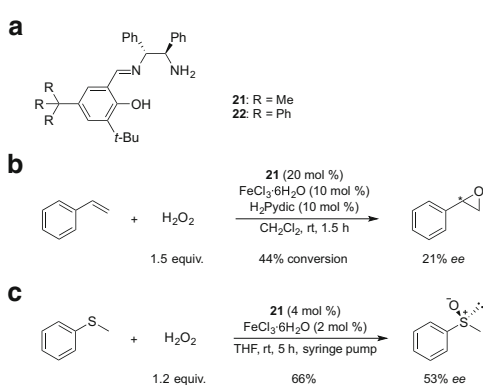


Fig. 5 Camphor-derived Fe complex for catalytic enantioselective hydrophosphonylation of aldehydes



Scheme 10 Asymmetric Fe-catalyzed oxidations using ligands **21/22**



[60]. Use of 5 mol% of these complexes derived from aminoisborneol afforded hydrophosphonylation products in good to excellent yields (up to 99%) and in excellent enantioselectivities (up to 99% *ee*).

Other chiral Schiff base ligands derived from (1*R*,2*R*)-1,2-diphenylethylenediamine and more hindered salicylaldehyde derivatives were developed (Scheme 10a) [61]. The primary amine-derived ligand **21** (R = Me) was used in combination with iron(III) chloride for the epoxidation of alkenes. In the presence

of pyridine-2,6-dicarboxylic acid (H_2Pydic) as a co-ligand, the epoxidation of styrene afforded the corresponding styrene oxide in 44% conversion and 21% enantiomeric excess (Scheme 10b). The best yield and enantioselectivity in the oxidation of thioanisole were obtained when using the ligand containing a trityl group at the 5-position of the salicylaldehyde skeleton (**22**; R = Ph). The enantioselective sulfoxidation was carried out under mild conditions and with H_2O_2 as oxidant. Moderate yields (up to 69%) and enantioselectivities (up to 54% *ee*) were obtained (Scheme 10c).

4.2 Salen Catalysts

Catalytic properties of Fe^{III} -salen catalysts in asymmetric sulfoxidation were explored by Bryliakov and Talsi [62, 63]. These catalysts were used in low loadings (0.2–2.0 mol%) with iodosoarenes as terminal oxidants and were found to efficiently catalyze the oxidation of alkyl aryl sulfides to sulfoxides in moderate to high enantioselectivities (up to 84% *ee* with isopropylthiobenzene and iodosesitylene). The influence of the electronic and steric effects of the ligand was studied through a series of Fe^{III} -salen complexes **23–25** (Fig. 6). The active intermediate was demonstrated by ^1H NMR to be a $[\text{Fe}^{\text{III}}(\text{ArIO})\text{-salen}]$ complex.

A chiral *triplesalen* ligand was developed as a C_3 -symmetric trinuclear extension of the Jacobsen ligand *salen* [64]. The complex **26** obtained with Fe^{III} was a good catalyst for the oxidation of sulfides into sulfoxides in good yields and good selectivities (Fig. 7). However, lower enantioselectivities were obtained relative to the ones obtained with $[\text{FeCl}(\text{salen})]$ **23**.

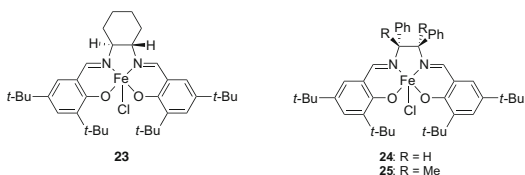


Fig. 6 Fe^{III} -salen catalysts

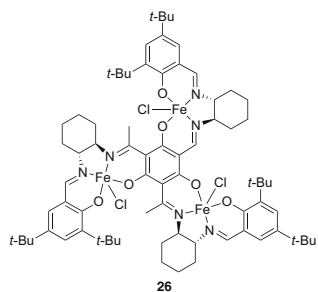
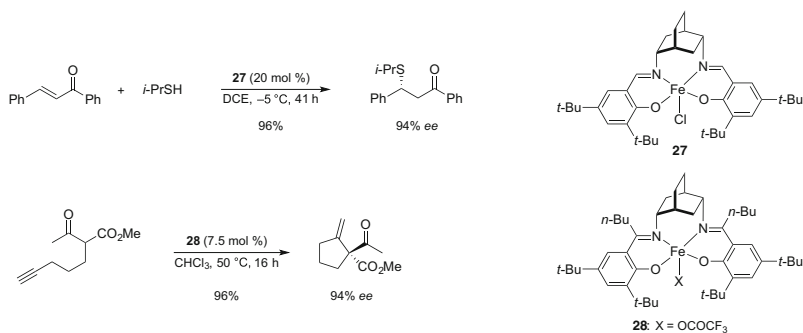


Fig. 7 Chiral trinuclear Fe^{III} -triplesalen complex



Scheme 11 *cis*-2,5-Diaminobicyclo[2.2.2]octane, as new scaffold for asymmetric synthesis via Fe-*salen*s

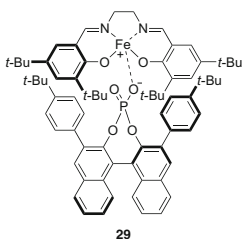


Fig. 8 Achiral Fe^{III}-*salen* cation used conjointly with a chiral phosphate counteranion

A *salen* ligand based on a chiral *cis*-2,5-diaminobicyclo[2.2.2]octane scaffold was recently developed [65]. The resulting Fe^{III} complex **27** efficiently catalyzed the asymmetric addition of thiols to α,β -unsaturated ketones and the asymmetric Conia-ene-type cyclization of α -functionalized ketones containing an unactivated terminal alkyne (Scheme 11) [66, 67]. The Michael addition produced β -thioketones in excellent yields and enantioselectivities from various aliphatic and aromatic thiols using conjugated enones as Michael acceptors. With α -substituted α,β -unsaturated ketones, the addition led mainly to the *syn* diastereoisomer. The *salen* ligand used for the Conia-ene cyclization was modified by increasing the steric bulk around the imine nitrogens by replacing the hydrogen atoms with *n*-butyl substituents (**28**). The Conia-ene carbocyclization of α -alkynyl- β -keto esters and other α -alkynyl ketones bearing an electron-withdrawing substituent were efficiently catalyzed and delivered in good yields and high enantioselectivities the *exo*-methylenecyclopentanes possessing an adjacent stereogenic quaternary center.

An achiral Fe^{III}-*salen* cation was used conjointly with a chiral phosphate counteranion as a highly active and enantioselective catalyst (**29**) for the oxidation of sulfides (Fig. 8) [68]. This novel ion-pair catalyst developed by List was used in a low loading (1 mol%) together with iodosobenzene as the terminal oxidant. The oxidation proceeded with high yields and enantioselectivities. The enantioselectivities observed, particularly for more difficult substrates such as electron-poor

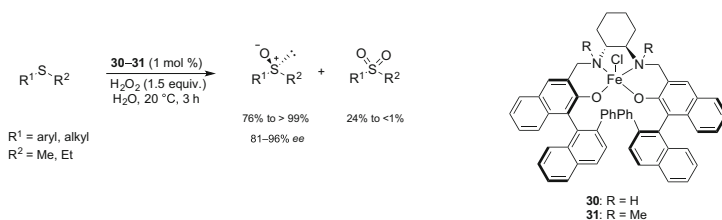
substrates and long alkyl-substituted sulfides, are the best ones obtained with an Fe-*salen* catalyst.

4.3 *Salen* Catalysts

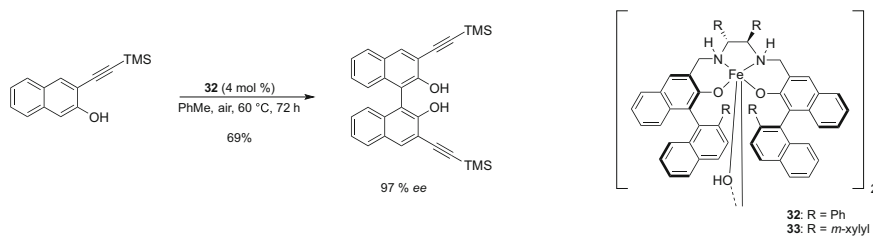
Highly enantioselective oxidation of sulfides in water in the absence of a surfactant by using Fe(*salen*) complexes **30** and **31** with H₂O₂ was reported by Katsuki (Scheme 12) [69, 70]. Not only aromatic but also aliphatic sulfides were oxidized at room temperature with high enantioselectivities. This work demonstrated the first application of the concept of asymmetric counteranion-directed catalysis to iron catalysis.

Encapsulation of chiral Fe(*salen*) complexes in the nanocage of mesoporous silicas with various microenvironments was studied by Li [71]. The influence of the chemical properties of the nanocage on the performance of the confined chiral Fe (*salen*) complex was studied using asymmetric oxidation of methylphenylsulfide as the model reaction with H₂O₂ as the oxidant. This work demonstrated the efficiency of the chemical modifications for improving the enantioselectivity and efficiency of the encapsulated chiral *salen* catalyst.

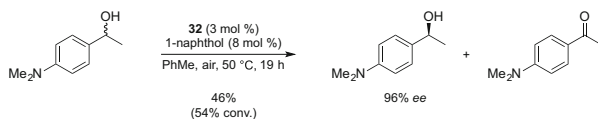
Katsuki used the same family of Fe(*salen*) complexes in asymmetric aerobic oxidative coupling of naphthols, especially 3-substituted naphthols [72, 73]. This oxidative coupling provides a general method for the synthesis of chiral 3,3'-disubstituted binaphthols with high enantioselectivities (up to 97% *ee*) (Scheme 13). The structure of the iron complex **32** was revealed to be a



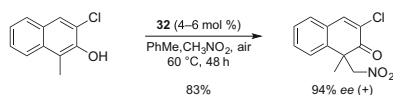
Scheme 12 Enantioselective oxidation of sulfides in water



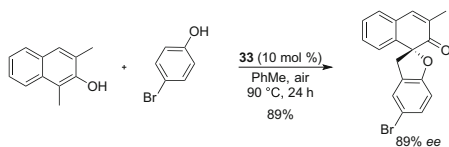
Scheme 13 Asymmetric aerobic oxidative coupling of 3-substituted naphthols



Scheme 14 Aerobic kinetic resolution of secondary alcohols using air as oxidant



Scheme 15 Oxidative dearomatization of 1,3-disubstituted 2-naphthols using nitroalkanes



Scheme 16 Asymmetric tandem synthesis of spirocyclic (2H)-dihydrobenzofurans

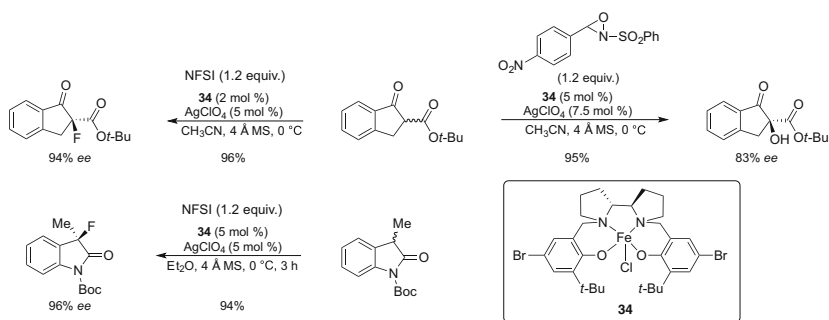
di- μ -hydroxo dimer by X-ray crystallography. Kinetic and X-ray studies indicated that the homocoupling reaction proceeds through an iron(*salan*) (2-naphthoxo) complex according to a radical anion mechanism [73].

The catalytic activity of this Fe(*salan*) complex **32** can be enhanced by coordination of a naphthoxide ligand, which is reluctant to undergo oxidative coupling, being rather oxidized to a radical cation species. The obtained complex catalyzed the aerobic kinetic resolution of secondary alcohols with air as oxidant (Scheme 14) [74, 75].

Fe(*salan*) complex **32** also catalyzed the oxidative dearomatization of 1,3-disubstituted 2-naphthols using nitroalkanes as nucleophiles, leading to the formation of an all-carbon quaternary stereocenter [76]. The dearomatized products were obtained in good to excellent yields and high enantioselectivities (up to 96% *ee*) (Scheme 15).

In 2014, Katsuki developed an Fe-catalyzed oxidative *o*-quinone methide formation/Michael addition/asymmetric oxidative dearomatization, which was inspired by the discovery of in situ aerobic oxidative *o*-quinone methide formation [77]. This strategy enables a facile synthesis of useful spirocyclic (2H)-dihydrobenzofurans with air as the hydrogen acceptor from 1-methyl-2-naphthol and phenol derivatives (Scheme 16).

Chiral Fe^{III}-*salan* complex **34** catalyzed the enantioselective α -fluorination of β -keto esters and *N*-Boc oxindoles (Scheme 17) [78]. The same complex also catalyzed the enantioselective hydroxylation of β -keto esters using 2-(phenylsulfonyl)-3-(*p*-nitrophenyl)-oxaziridine as the oxidant. Both processes gave the corresponding products in high yields and good to excellent enantioselectivities under mild reaction conditions.



Scheme 17 Fe^{III}-salan-catalyzed enantioselective α -fluorination and α -hydroxylation reactions

5 Bis(oxazoline) Catalysts

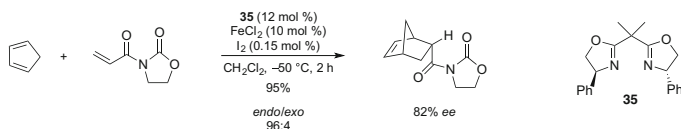
Pioneering work by Corey demonstrated the efficiency of a C_2 -symmetric chiral *bis(oxazoline)*-Fe^{III} complex for the enantioselective Diels–Alder reaction [79, 80]. The reaction of 3-acryloyl-1,3-oxazolidin-2-one and cyclopentadiene in the presence of 10 mol % of the catalyst, which was prepared from a chiral *bis(oxazoline)*, FeCl₂, and I₂, led to an excellent yield of the *endo* product (*endo/exo* 96:4) with a very good enantioselectivity (82% *ee*) for the *endo* product (Scheme 18). One cationic aqua complex prepared from a chiral dibenzofuran ligand and Fe(ClO₄)₂ was reported to be efficient in the same reaction leading to high yield and excellent stereoselectivity [81].

In 2006, Sibi disclosed the concept of chiral relay by incorporating a fluxional blocking group in the substrate. Such achiral functional additives contain multiple sites for modification and could amplify the enantioselectivity of the reaction [82]. They were used in the abovementioned Diels–Alder reaction in the presence of **35** and Fe(ClO₄)₂.

Fe-catalyzed cycloisomerization reactions have been reported using an iron catalyst obtained *in situ* via the reduction of Fe(acac)₃ with three equivalents of Et₃Al in the presence of a *bis(oxazoline)* ligand [83]. Moderate levels of stereoreinduction were obtained.

Chiral *diamino-bis(oxazoline)* ligands were prepared by Pfaltz and converted to the Fe^{II} complexes [84]. The ligands derived from *N,N'*-dimethylethane-1,2-diamine reacted with FeCl₂ in a stereoselective manner to give an octahedral mononuclear complex **36** (Fig. 9a). When the ligands are derived from *N,N'*-dimethylcyclohexane-1,2-diamine, the resulting complexes **37** and **38** showed different coordination modes depending on the diastereoisomer used: the Fe ion was either pentacoordinate or hexacoordinate (Fig. 9b).

Iron complexes of *spiro-bis(oxazoline)* ligands **39** and **40** were highly efficient catalysts for asymmetric O–H bond insertion reactions (Scheme 19) [85]. The complexes catalyze insertions into the O–H bond of a wide variety of alcohols with excellent enantioselectivities under mild reaction conditions. The iron-catalyzed



Scheme 18 Fe^{III}-catalyzed for enantioselective Diels–Alder reaction

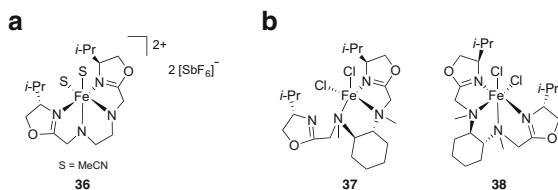
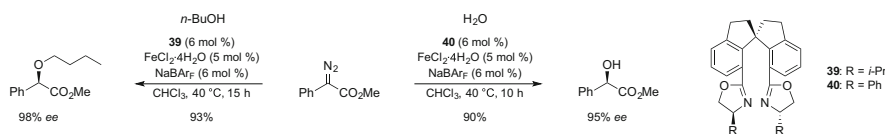
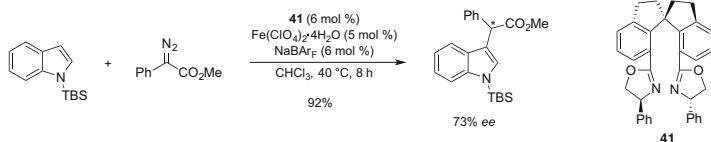


Fig. 9 Chiral *diamino-bis(oxazoline)* ligands were prepared by Pfaltz



Scheme 19 Fe^{II}-catalyzed asymmetric O–H bond insertion reactions



Scheme 20 C–H functionalization of indoles with α -aryl- α -diazoesters

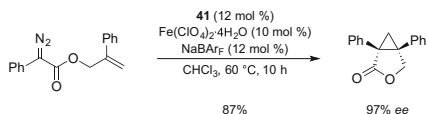
asymmetric O–H insertion reaction between water and methyl α -diazophenylacetate also led to outstanding enantioselectivities. Other transition metals, including copper and rhodium, used in the same reaction conditions, gave markedly lower enantioselectivities than the corresponding Fe catalyst.

Iron salts have also been used with chiral *spiro-bis(oxazoline)* **41** to perform the C–H functionalization of indoles with α -aryl- α -diazoesters (Scheme 20) [86]. The corresponding α -aryl α -indolylacetate derivatives were obtained in high yields and high enantioselectivities (up to 78% *ee*).

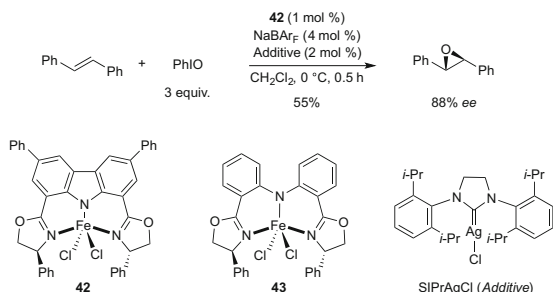
The efficiency of this Fe^{II} catalyst was also demonstrated in the asymmetric intramolecular cyclopropanation of α -diazoesters (Scheme 21) [87]. The reaction occurred in high yields and excellent enantioselectivities (up to 97% *ee*). This method is particularly useful for the synthesis of chiral [3.1.0]bicycloalkanes.

Niwa and Nakada developed a non-heme Fe^{II} complex bearing a carbazole-based tridentate ligand that displays iron porphyrin-like properties and catalyzes the asymmetric epoxidation of (*E*)-alkenes with excellent enantioselectivity [88].

Scheme 21 Asymmetric intramolecular Fe^{II}-catalyzed cyclopropanation of α -diaoesters



Scheme 22 Asymmetric epoxidations of alkene with catalytic iron complexes

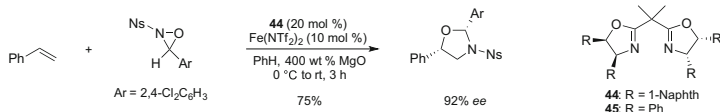


They found that complex **42**, which was prepared from $\text{FeCl}_2 \cdot 4\text{H}_2\text{O}$ and a tridentate carbazole ligand, in the presence of sodium tetrakis[3,5-bis(trifluoromethyl)phenyl] borate (NaBAR_F), catalyzed the asymmetric epoxidation of *trans*-stilbene to afford the desired chiral epoxide with moderate yield and enantioselectivity (Scheme 22). The yield was low because of the competitive formation of diphenylacetaldehyde. No epoxidation was observed in the absence of NaBAR_F . The yield and enantioselectivity were improved (55 and 88% *ee*) when 2 mol% of SIPrAgCl was used as an additive in the reaction. Also, no epoxidation occurred when Fe^{III} complex **43** was used as a tridentate *bis(oxazolinyphenyl)amine* (*bopa*) ligand, which lacks the C–C bond between the two phenyl rings in the carbazole-based tridentate system **42**.

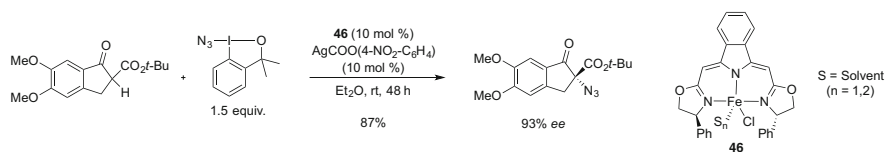
On the basis of UV-Vis and EPR studies, it was proposed that the active oxidizing species is the carbazole ligand centered π -cation radical- $\text{Fe}^{\text{IV}}=\text{O}$ complex that is generated by two-electron oxidation of the Fe^{III} catalyst. This corresponds to the largely accepted active oxidant intermediate of heme monooxygenases like cytochromes P450 and their synthetic Fe porphyrin model complexes. Thus, besides the high *ee* values, another impressive point about this unique catalyst is the fact that the ligand was found to be an efficient surrogate of porphyrins which potentially opens a new platform for the rational design of reliable catalysts for many reactions that are usually confined to the domains of metalloporphyrin catalysts.

An asymmetric oxyamination reaction of alkenes using Fe^{II} -*bis(oxazoline)* **44** has been reported [89]. The process was highly enantioselective and regioselective using *N*-sulfonyl oxaziridines (Scheme 23). This method allows the synthesis of 1,2-amino alcohols with regio- and stereochemical control.

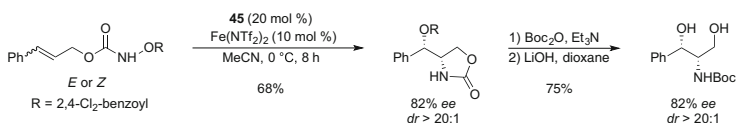
Fe -catalyzed enantioselective azidations of β -keto esters and oxindoles using complex **46** jointly with a readily available N_3 -transfer reagent were reported by



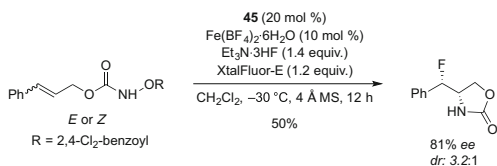
Scheme 23 Fe-catalyzed asymmetric oxyamination of olefins



Scheme 24 Enantioselective azidation of β -keto esters



Scheme 25 Fe-catalyzed asymmetric intramolecular olefin aminohydroxylation



Scheme 26 Stereoconvergent and enantioselective olefin aminofluorination

Gade in 2013 [90]. A number of α -azido- β -keto esters were obtained with up to 93% *ee* (Scheme 24). The same methodology also allowed the preparation of 3-azidooxindoles with high enantioselectivities (up to 94% *ee*).

Xu discovered a new Fe^{II}-catalyzed intramolecular olefin aminohydroxylation with functionalized hydroxylamines, where both the *N* and *O* functional groups are efficiently transferred [91, 92]. Preliminary mechanistic studies revealed that an iron nitrenoid is a possible intermediate that can undergo either olefin aziridination or aminohydroxylation (Scheme 25).

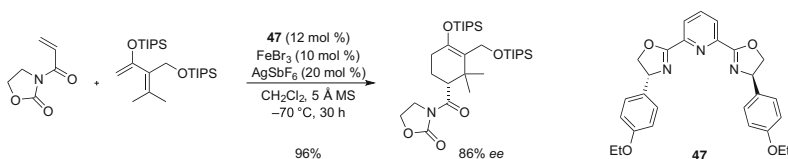
Xu also observed that the Fe-catalyzed asymmetric olefin aminofluorination is stereoconvergent: the isomeric olefins (Scheme 26) are converted to fluoro oxazolidinones with essentially the same *ee* (81%) and *dr* [93]. These results and the ligand-enabled diastereoselectivity suggest that the Fe-ligand complex is involved in the C–F and C–N bond formation process.

6 Pyridine *bis*(Oxazoline) Catalysts

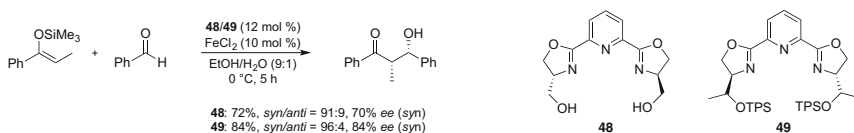
In 2004, Shibasaki developed a catalytic enantioselective Diels–Alder reaction using a cationic Fe^{III} -Ar-*pybox* **47** complex as catalyst (Scheme 27) [94]. This reaction is the first catalytic enantioselective Diels–Alder reaction of acyclic 4,4-disubstituted 1,3-dienes. It allowed the efficient and rapid synthesis of chiral polysubstituted cyclohexanones, which are difficult to access using other methods. This methodology was used later in the catalytic asymmetric total synthesis of *ent-hyperforin* [95].

Pyridine *bis*(oxazoline) ligands conjointly used with FeCl_2 were reported to be effective catalysts for the asymmetric Mukaiyama aldol reaction in aqueous media [96]. The aldol products were obtained in good yields and *syn* diastereoselectivities (Scheme 28). Moderate enantioselectivities (up to 75% *ee*) were afforded with ligand **48**. Using bulkier ligand **49** with *O*-*t*-butyldiphenylsilyl groups [97], the enantioselectivity of the process was increased (up to 92% *ee*).

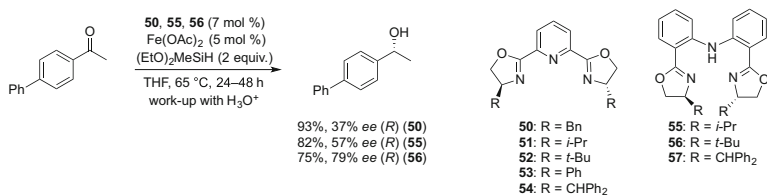
The asymmetric hydrosilylation of ketones was investigated by Nishiyama [98]. The addition of chiral tridentate *bis*(oxazoline) ligands such as *pybox* or *bis*(oxazolinephenyl)amine (*bopa*) to $\text{Fe}(\text{OAc})_2$ in THF at 65°C formed in situ a catalytically active species to hydrosilylate ketones with $(\text{EtO})_2\text{MeSiH}$ (Scheme 29). The yields were up to 93%, and the enantioselectivities of the obtained alcohols were in the 37–79% *ee* range.



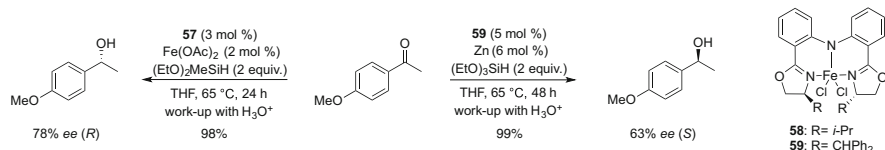
Scheme 27 Catalytic enantioselective Diels–Alder reaction



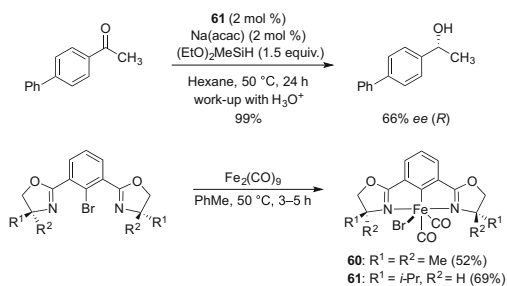
Scheme 28 Asymmetric Mukaiyama aldol reaction in aqueous media



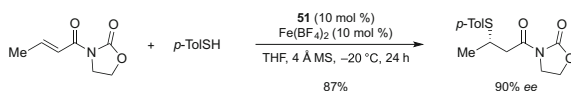
Scheme 29 Asymmetric hydrosilylation of aryl ketones catalyzed by *Fe-pybox* and *Fe-bopa* complexes



Scheme 30 Chiral Fe^{III} -*bis*(oxazolanyl) catalysts for asymmetric hydrosilylation



Scheme 31 Chiral Fe^{II} -*bis*(oxazolanyl) catalysts and their use in asymmetric hydrosilylation

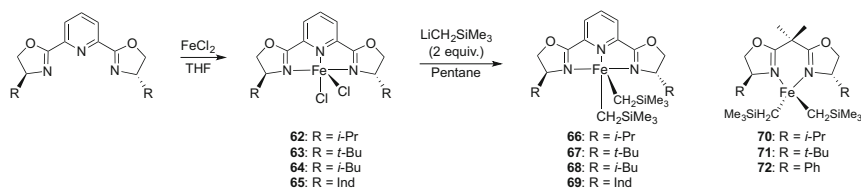


Scheme 32 Fe^{II} -catalyzed enantioselective conjugate addition of thiols

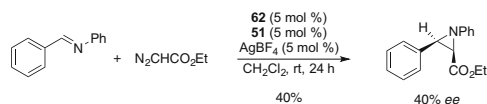
In a further study, Nishiyama was able to improve the asymmetric hydrosilylation of ketones by ligand design (Scheme 30). Bulky substituents on the oxazoline ring led to a higher enantioselectivity (up to 88% *ee*) [99]. To elucidate the mechanism of the reaction, the differences between well-defined complexes and in situ-prepared catalytic systems were investigated [100]. Interestingly, more hindered catalyst **59** (R = CHPh_2) can afford both enantiomers of the product either used as in situ-formed catalyst ($\text{Fe}(\text{OAc})_2$ /**57**) or as well-defined iron complex **59**, in conjunction with zinc as a reducing agent.

Nishiyama reported achiral **60** and chiral iron **61** complexes with *bis*(oxazolanyl) phenyl (*phebox*) ligands [101]. Interestingly, Fe^{II} complex **61** showed up to 66% *ee* with full conversion of methyl(4-phenylphenyl)ketone (Scheme 31). They have also described the synthesis and structural characterization of the first chiral iron complexes with *bis*(oxazolanyl)phenyl ligands resulting from the oxidative addition of $\text{Fe}_2(\text{CO})_9$ to *phebox*-Br. Fe^{II} -*phebox* complex **61** was used in the enantioselective hydrosilylation of ketones with $\text{HSi}(\text{OEt})_2\text{Me}$.

The enantioselective conjugate addition of thiols to (*E*)-3-crotonoyloxazolidin-2-one was catalyzed by the complex prepared from $\text{Fe}(\text{BF}_4)_2$ and *pybox* **51** (Scheme 32) [102, 103]. Michael addition products were obtained in good enantioselectivities (up to 95% *ee*).



Scheme 33 Preparation of Fe^{II} *phebox* and *pybox* ligands for asymmetric hydrosilylation



Scheme 34 Catalytic asymmetric aziridination reaction of arylimines

Chirik studied the pyridine *bis(oxazoline)* (*pybox*) and *bis(oxazoline)* (*box*) ligands in order to develop an enantioselective version of the hydrosilylation reaction (Scheme 33) [104]. These ligands are commercially available or easily synthesized from available enantiopure amino alcohols. Following the same synthetic protocol as for the *bis(imino)pyridine* Fe-dialkyl derivatives, the corresponding *pybox* and *box* Fe-dialkyl complexes have been isolated. Even though high conversions are reported for the hydrosilylation of various ketones, the chiral induction of these systems is rather poor (up to 54% *ee*).

Iron-*pybox* complexes were also used in the catalytic asymmetric aziridine-forming reaction of *N*-benzylideneaniline and ethyl diazoacetate (Scheme 34) [105]. In these conditions (complex **62** used together with an excess of ligand **51** and AgSbF₆), the corresponding *cis*-aziridine was obtained in moderate yield and enantioselectivity (up to 49% *ee*).

Asymmetric aziridination reaction of styrene using iron-derived catalysts was studied in 2008 (Table 7) [106]. Among various tridentate ligands tested in the iron (II) triflate-catalyzed conversion of styrene with *N*-(*p*-tolylsulfonyl)imino phenyliodinane to give the corresponding aziridine, ligand **51** was found to be the most effective, leading to the product with up to 40% *ee* in 72% yield. Ligands 2,6-*bis*-(*N*-pyrazolyl)pyridines **74** and **75** were also used as chiral ligands, which opens further options for ligand structure optimization.

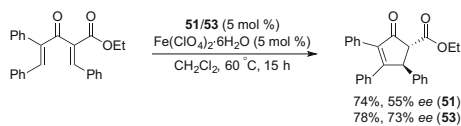
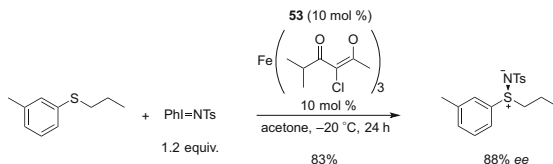
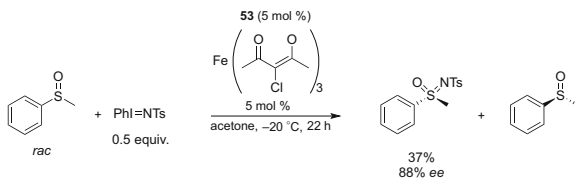
In 2010, Itoh succeeded in demonstrating that asymmetric Nazarov cyclization of divinyl ketones could be performed using Fe^{II} catalysts, which were prepared from Fe(ClO₄)₂·6H₂O and Fe(OTf)₂ (Scheme 35) [107]. Such complexes also catalyzed the tandem Nazarov cyclization–fluorination reaction of divinyl ketones in good yields and moderate enantioselectivities.

Bolm reported the first Fe-catalyzed enantioselective sulfimidation reaction using Fe^{III} salts and *pyridine bis(oxazoline)* ligand **53**, in combination with *N*-(*p*-tolylsulfonyl)imino phenyliodinane as the nitrene precursor (Scheme 36) [108]. A variety of optically active sulfimides were prepared in good yields and enantioselectivities. Interestingly, the reactions could be performed in air, without exclusion of moisture.

Table 7 Asymmetric aziridination of styrene

Entry	L	Yield (%)	ee (%)
1	51	67	15
2 ^a	51	72	40
3	52	67	15
4	53	51	25
5		75	10
6		60	20
7		40	6

^aFe(OTf)₂ (5 mol%) and chiral ligand (30 mol%) were used

**Scheme 35** Asymmetric Nazarov cyclization catalyzed by an Fe^{II} salt in the presence of a *pybox* ligand**Scheme 36** Fe^{III}-catalyzed enantioselective sulfimidation**Scheme 37** Kinetic resolution of racemic sulfoxides through catalytic asymmetric nitrene-transfer reactions

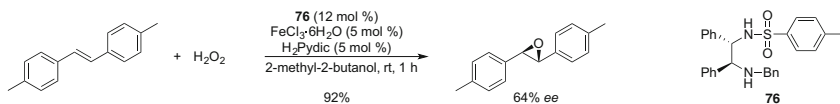
A catalyst, prepared in situ from $[\text{Fe}(\text{acac})_3]$ and *pybox* **53**, allowed the resolution of racemic sulfoxides through catalytic asymmetric nitrene-transfer reactions (Scheme 37) [109]. This method, reported by Bolm, is an attractive new method for the synthesis of sulfoximines in enantiomerically enriched form (up to 94% *ee*).

7 Diamine-Derived Catalysts

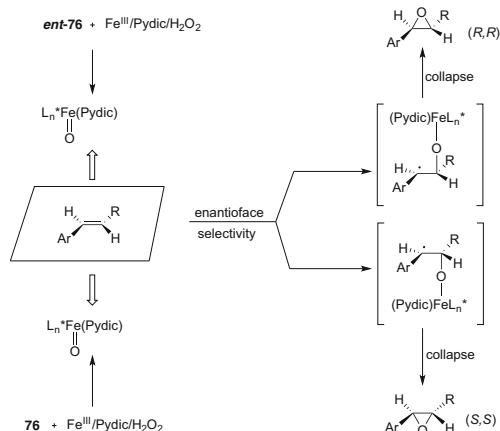
In 2007, Beller reported the first breakthrough and a promising non-heme Fe-catalyzed asymmetric epoxidation of aromatic alkenes by using hydrogen peroxide and commercially available enantiopure 1,2-diphenylethylenediamine, which not only gives good to excellent isolated yields of epoxides but also enantiomeric excess of up to 97% (Scheme 38) [110]. They have demonstrated for the first time that high enantioselectivity can be achieved in Fe-catalyzed epoxidations with hydrogen peroxide. Asymmetric epoxidation of aromatic alkenes was achieved using hydrogen peroxide and derivatives of C_2 -symmetric 1,2-diamines, such as **76**, in the presence of pyridine-2,6-dicarboxylic acid (H_2Pydic). This method provided good to excellent yields of isolated epoxides but also enantioselectivities up to 97% *ee*. This epoxidation has the advantage of using a simple 1,2-diamine and hydrogen peroxide, thus avoiding the use of iron porphyrins and iodosobenzene as oxidant.

In another report, Beller disclosed the Fe^{III} -catalyzed asymmetric epoxidation of aromatic alkenes with hydrogen peroxide as the oxygen source and a chiral Fe^{III} catalyst generated from $\text{FeCl}_3 \cdot 6\text{H}_2\text{O}$, H_2Pydic , and chiral **76** [111]. The asymmetric epoxidation of styrenes, which has been extended to sterically less demanding alkenes, gave almost complete conversions but poor *ee* values compared with larger alkenes. *cis*-Alkenes are generally poorer substrates than *trans*-alkenes for the current asymmetric epoxidation, and steric factors were more important than electronic factors in controlling the enantioselectivity, whereas larger alkenes gave high conversion and *ee* values. The enantioselectivity of alkene epoxidation was controlled by steric and electronic factors, although steric effects are more dominant. Beller also speculated on the possible mechanism of epoxidation. He presumed that initially formed $[\text{Fe}^{\text{III}}-(\mathbf{76})_2(\text{Pydic})]$ may react with H_2O_2 to generate $[\text{Fe}^{\text{III}}-(\mathbf{76})_2(\text{OOH})(\text{Pydic})]$. Homolysis or heterolysis of such a species could generate the reactive $\text{Fe}^{\text{IV}}=\text{O}$ and $\text{Fe}^{\text{V}}=\text{O}$ species. The epoxidation reaction appears to proceed via a radical intermediate as shown in Scheme 39. It is further assumed that a top-on approach of alkene is preferred over the side-on approach.

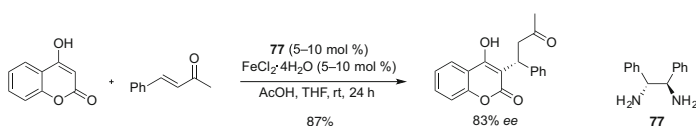
A practical approach for the anchoring of abovementioned ligands to branched carbosilane scaffolds was investigated by Klein Gebbink [112]. These molecularly



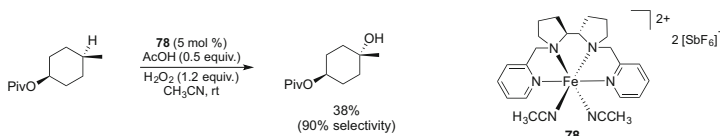
Scheme 38 Fe-catalyzed asymmetric epoxidation of various aromatic alkenes



Scheme 39 Proposed mechanistic pathway to explain the enantioselectivity of Beller's epoxidation reaction



Scheme 40 Effect of iron and primary amines on *warfarin* synthesis



Scheme 41 Selective aliphatic C–H activation

enlarged ligands were evaluated in Fe^{III} -catalyzed asymmetric *trans*-stilbene epoxidation reactions.

Iron salts were found to be effective promoters in asymmetric Michael addition of 4-hydroxycoumarin to α,β -unsaturated ketones, which resulted in excellent yields and high level of enantioselectivities (up to 91% *ee*) in the presence of low catalytic amounts of iron and simple chiral primary amine **77** (Scheme 40) [113].

Non-heme Fe complexes derived from a *bis*(pyrrolidine) core showed promising, stereospecific hydroxylation reactivities toward unactivated sp^3 C–H bonds [114]. Selective aliphatic C–H activation can be predicted. The C–H oxidation with $[\text{Fe}(S,S\text{-PDP})(\text{CH}_3\text{CN})_2][\text{SbF}_6]_2$ **78** resulted in a moderate conversion of starting material but high selectivities for the formation of tertiary hydroxylated products (Scheme 41). The functional group compatibility and substrate scope were evaluated in these catalyzed oxidations of unactivated sp^3 C–H bonds with H_2O_2 . The selectivity of this catalytic system was demonstrated and predicted based on three modes of selective oxidation (electronic, steric, and directed modes).

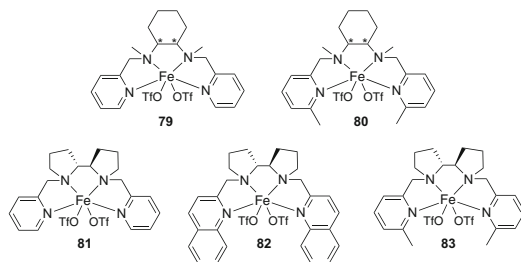


Fig. 10 Optically active Fe^{II} complexes capable of promoting asymmetric olefin *cis*-dihydroxylation

Table 8 *cis*-Dihydroxylation of olefins with H₂O₂ catalyzed by Fe^{II} complexes **79–83**

Entry	Catalyst	Olefin	<i>ee</i> (%)	Diol/epoxide	TON (% <i>de</i>)
1	79	<i>trans</i> -2-Heptene	29	1:18	0.3 (99)
2	80	<i>trans</i> -2-Heptene	79	3.2:1	3.8 (99)
3	80	1-Octene	60	5.9:1	4.1
4	80	<i>tert</i> -Butyl acrylate	23	17:1	5.1
5	81	<i>trans</i> -2-Heptene	38	1:4.6	1.1 (90)
6	82	<i>trans</i> -2-Heptene	78	4:1	3.6 (99)
7	83	<i>trans</i> -2-Heptene	97	26:1	5.2 (99)
8	83	<i>trans</i> -4-Octene	96	13:1	3.9 (93)
9	83	1-Octene	76	64:1	6.4
10	83	Allyl chloride	70	>49:1	4.9
11	83	<i>tert</i> -Butyl acrylate	68	>40:1	4.0
12	83	Ethyl <i>trans</i> -crotonate	78	>75:1	7.5 (99)

Que evaluated the Fe^{II} complexes **79** and **80** and complexes **81–83** bearing a *bis* (pyrrolidine) unit (Fig. 10), to improve the enantioselectivity for olefin *cis*-dihydroxylation (Table 8) [115, 116]. Catalyst **83** displayed high *cis*-diol selectivity and produced enantioselectivities up to 97% (Table 8, entries 7–12). By comparison to **79–83**, it is apparent that the size of the pyridine α -substituent is important, as a systematic increase in the *cis*-diol selectivities and *ee* values is observed on going from H in **81** to an *sp*²-hybridized C–H group in **82** to a CH₃ group in **83**.

The asymmetric induction provided by **83** is significantly greater than **80** (Table 8). This improvement arises from two factors: the more rigid bipyrrrolidine backbone of **83** relative to the 1,2-diaminocyclohexane backbone of **80** and *cis*- β ligand topology of **83** in contrast to the *cis*- β topology of **80**.

In 2011, Sun described the development of chiral Fe^{II} complexes of *N*₄ ligands for the asymmetric epoxidation of α,β -enones employing H₂O₂ (up to 87% *ee*) or peracetic acid as oxidant, respectively (Fig. 11) [117]. In addition, the strategy of isotopic labeling with O¹⁸ was adopted to gain rough insight into the mechanism.

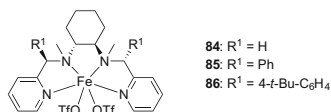
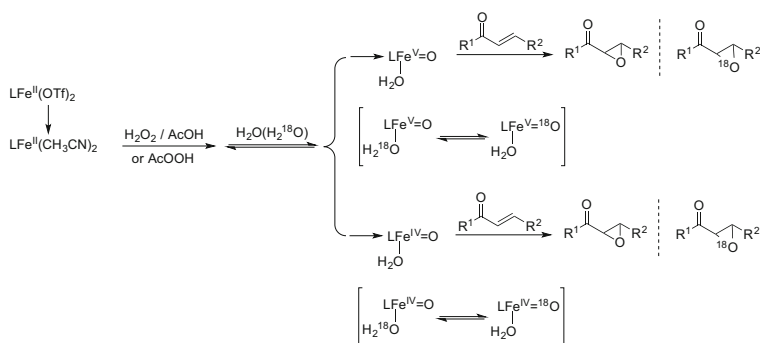
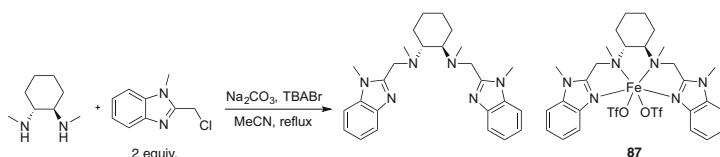


Fig. 11 Chiral Fe^{II} complexes used for epoxidation of α,β -enones



Scheme 42 Proposed mechanism using the designed catalytic system



Scheme 43 Synthesis of chiral benzimidazolymethyl-derived ligand **87**

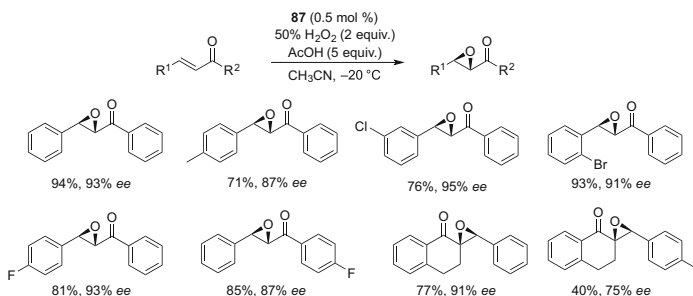
Besides, the complex $[L_2Fe^{III}(\mu-O)(\mu-CH_3CO_2)]^{3+}$, usually derived from the decay of $LFe^{IV}=O$ species or thermodynamic sinks for a number of iron complexes, was identified by HR-MS.

The authors have also proposed a possible mechanism and suggested that $LFe^V=O$ was the main active intermediate in the catalytic system (Scheme 42).

In 2013, Sun developed the synthesis and characterization of an Fe^{II} complex **87** derived from the tetradentate *N*-ligand (1*R*,2*R*)-*N,N'*-dimethyl-*N,N'*-bis(1-methyl-2-benzimidazolymethyl)cyclohexane-1,2-diamine (Scheme 43) [118]. The chiral *C*₂-symmetric tetradentate *N*-ligand was synthesized from easily available cyclohexane-1,2-diamine and 2-chloromethyl-1-methyl-benzimidazole.

Iron complex **87** was an active catalyst for asymmetric epoxidation of olefins with H₂O₂ as the oxidant and acetic acid as an additive. Up to 95% *ee* was observed for epoxidation of α,β -unsaturated ketones at -20°C (Scheme 44).

The asymmetric epoxidation of enones using **81** and hydrogen peroxide as oxygen source was described by Bryliakov and Talsi [119, 120]. The reaction requires the use of stoichiometric amounts of a carboxylic acid. In the case of chalcone, up to 80% *ee* could be achieved at -30°C with 1 mol% of catalyst **81** and using nearly one equivalent of 2-ethylhexanoic acid in acetonitrile.



Scheme 44 Enantioselective epoxidation of chalcone derivatives catalyzed by complex **87**

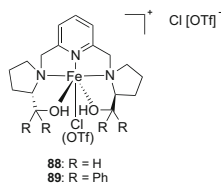


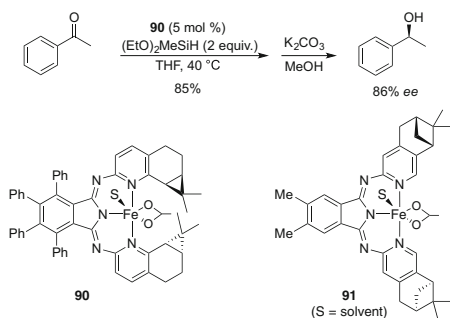
Fig. 12 Chiral Fe^{II} complexes disclosed by Klein Gebbink

Mononuclear non-heme Fe^{II} complexes of pyrrolidinyl pentadentate ligands derived from proline were disclosed by Klein Gebbink (Fig. 12) [121]. The catalytic potential of these complexes in the oxidation of alkenes and sulfides in the presence of H₂O₂ was studied. Complex **89** gave low TONs in the oxidation of alkenes but showed high activity in the oxidation of aromatic sulfides, albeit with low *ee*'s (up to 27% *ee*).

Gade described the synthesis of well-defined iron complexes containing a bidentate acetate ligand and new enantiopure tridentate *N-N-N* donor ligands (Scheme 45) [122]. The use of this iron complex in ketone hydrosilylation under conditions similar to those of Nishiyama [98] allowed the reduction, for example, of 2-acetonaphthone to the corresponding alcohol in 87% yield and 71% *ee* and of mesityl methyl ketone in 92% yield and 85% *ee*. Higher *ee* values (83 and 93%, respectively) were obtained when the temperature was decreased from 65 to 40 °C. This system also reduced dialkyl ketones, including *t*-butyl methyl ketone, to the corresponding alcohols in 59% *ee*.

Togni synthesized novel diamine ligands **92–95** (Scheme 46) and used them in association with Fe(acac)₂ to promote the asymmetric reduction of acetophenone in the presence of phenylsilane [123]. Although the conversion was quantitative, the *ee* was very low (37%). He reported that the Fe^{II} complex releases one of the oxygen-based anionic ligands, therefore becoming a cationic species which can act as a Lewis acid to activate the substrate for the reduction. The anionic oxygen ligand acts as a Lewis base and coordinates to the silicon-based reducing agent leading to the formation of the catalytically active reducing species, a pentacoordinated silicate. The silicate itself is able to transfer a hydride to the activated C=O bond. The iron complex is therefore suggested to be a chiral cation, which acts as a counterion to the catalytically active species, the silicon anion.

Scheme 45 Chiral Fe^{II} complexes used for hydrosilylation



Scheme 46 Chiral diamine ligands disclosed by Togni

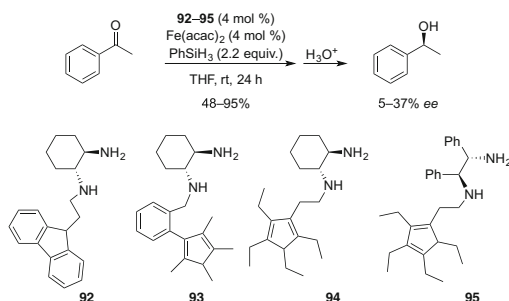
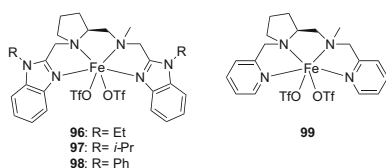


Fig. 13 Non-heme Fe^{II} catalysts



In 2012, Sun developed the asymmetric epoxidation of enones using 50% hydrogen peroxide and 2 mol% of iron complexes **96–99** (Fig. 13) [124]. These complexes were synthesized from *C*₁-symmetric tetradentate *N*-ligands (*N*₄) consisting of more rigid chiral diamine templates derived from L-proline and two benzimidazole donors. High yields and enantioselectivities were achieved in the oxidation of variously substituted chalcones and cyclic enones in the presence of 3 equiv. of acetic acid in acetonitrile. In the case of chalcone, the *N*-substituent at the benzimidazole ring of catalyst **96** and **98** significantly altered the outcome of the reactions. Superior activities and selectivities were recorded with **96** and **97** bearing *N*-ethyl and *N*-isopropyl groups, while the *N*-phenyl substitution in catalyst **98** lowered these values significantly. Catalyst **99** was found to be less active and less selective. Substitution at the aryl ring of chalcone also resulted in dramatic changes in enantioselectivities and yields, the highest *ee* and yield being obtained with *m*-chloro substitution on the alkene side of the phenyl ring, while both strongly electron-donating and electron-withdrawing groups on the carbonyl side of the aromatic ring dramatically reduced the *ee* values.

8 Diphosphine-Derived Catalysts

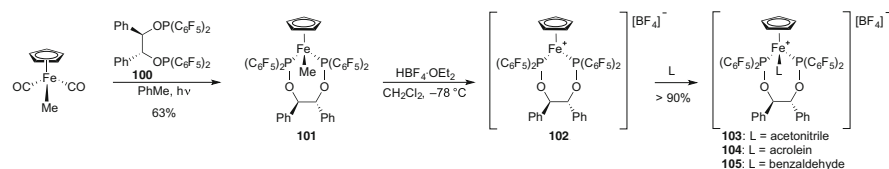
C_2 -symmetric bidentate phosphorus ligand **100** derived from (*R,R*)- or (*S,S*)-hydrobenzoin proved to be an effective ligand in the Fe^{II} -Lewis acid-catalyzed asymmetric Diels–Alder reaction of α,β -enals with dienes and its ease of synthesis merits attention for other applications in asymmetric catalysis (Scheme 47) [125–127]. Lewis acid catalyst **102** was obtained by photolytic ligand exchange from $[Fe(Cp)(Me)(CO)_2]$ followed by protolytic demethylation of complex **101**. The unsaturated Fe complex **102** was trapped in situ either by acetonitrile, acrolein, or benzaldehyde, to give complexes **103–105**, respectively.

Complex **103** is stable and is readily characterized. The acetonitrile ligand is strongly bound, and the complex does not exhibit catalytic activity in the Diels–Alder reaction between enals and dienes. Complexes **104** and **105** are stable at ambient temperature in the solid state and can be weighed in air without degradation. In CH_2Cl_2 solution, the aldehyde ligands in **104** and **105** were labile and in the absence of an excess of free aldehyde, the complexes slowly decomposed at temperatures above $-20^\circ C$. Both **104** and **105** could be used as precatalysts in Diels–Alder reactions between α,β -enals and dienes (Scheme 48). The products were obtained in good yields and excellent enantioselectivities.

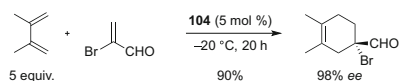
These Fe^{II} -Lewis acid catalysts can efficiently promote enantioselective 1,3-dipolar cycloadditions of nitrones with α,β -unsaturated aldehydes. This method provides rapid access to products of high synthetic potential (Scheme 49) [128].

In 2000, Imamoto prepared new *P*-chirogenic diphosphine oxide ligands, (*R,R*)-1,2-bis(alkylmethylphosphinyl)ethane, and (*S,S*)-1,1-bis(alkylmethylphosphinyl)methane, such as **107** (Ad = adamantyl) [129]. Their iron complexes were active in catalytic asymmetric Diels–Alder reactions of *N*-acrylamide dienophiles (Scheme 50). Interestingly *exo*-isomers were preferentially produced using *N*-crotonoylamides as dienophiles.

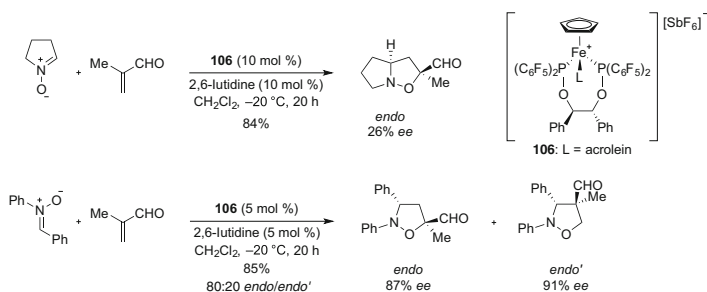
The first asymmetric transfer hydrogenation of ketones was disclosed by Gao in 2004 [130, 131]. By mixing the iron carbonyl hydride cluster complex $[NH_2Et_3][Fe_3H(CO)_{11}]$ with enantiopure phosphine ligands (Fig. 14), they formed in situ a



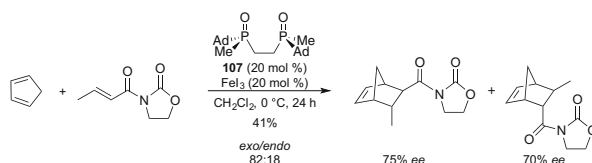
Scheme 47 Synthesis of chiral cyclopentadienyl- Fe^{II} Lewis acids



Scheme 48 Enantioselective Diels–Alder reaction using **104**



Scheme 49 Asymmetric 1,3-dipolar cycloadditions between nitrones and methacrolein



Scheme 50 Enantioselective Diels–Alder reaction using *P*-chirogenic diphosphine oxide **107**

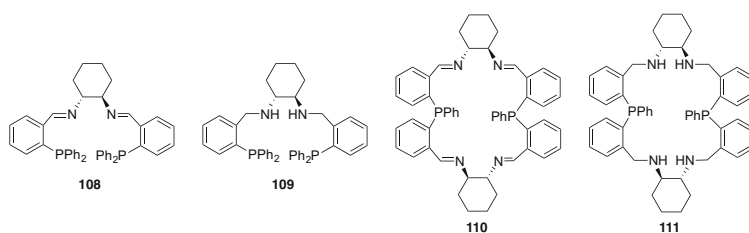


Fig. 14 Enantiopure *PNNP* ligands used for Gao's in situ-formed iron catalyst

catalytically active species which was claimed to be of trinuclear nature. The same author also reported the synthesis of chiral 22-membered macrocyclic ligands **110** and **111** and asymmetric transfer hydrogenation of selected ketones. The best enantioselectivity (98% *ee*) could be achieved using trinuclear iron carbonyl cluster $\text{Fe}_3(\text{CO})_{12}$, $[\text{NHEt}_3][\text{Fe}_3\text{H}(\text{CO})_{11}]$, or $[\text{PPN}][\text{Fe}_3\text{H}(\text{CO})_{11}]$. They examined the asymmetric reduction of a wide range of aromatic and heteroaromatic ketones using cheap and readily available $\text{Fe}_3(\text{CO})_{12}$ in combination with macrocycle **111**. These ketones have been reduced with high enantioselectivities under mild conditions using 0.5 mol% of the catalyst (Table 9).

For acetophenone and its derivatives, the catalyst system showed outstanding enantioselectivities under mild conditions (Table 9). The electronic properties of substituents on the aromatic ring had insignificant impact on the enantioselectivity, although the methoxy substituent gave the products in slightly lower enantioselectivities. More sterically hindered aromatic ketones were also reduced with excellent enantioselectivity (99% *ee*). The remarkable efficiency of the iron catalyst was

Table 9 Transfer hydrogenation of aromatic and heteroaromatic ketones with catalyst $\text{Fe}_3(\text{CO})_{12}/\mathbf{111}$

Entry	R ¹	R ²	T (°C)	t (h)	Conversion (%)	ee (%)
1	Ph	Me	55	1	97	98
2	<i>m</i> -MeC ₆ H ₄	Me	55	1	92	96
3	<i>p</i> -Cl-C ₆ H ₄	Me	65	0.5	99	97
4	<i>m</i> -MeO-C ₆ H ₄	Me	55	1	92	91
5	Ph	<i>i</i> -Pr	75	12	90	99
6	Ph	<i>n</i> -Bu	65	1	96	99
7	Ph	Cy	65	12	81	99
8	2-Naphthyl	Me	55	1	93	96
9	3-Pyridyl	Me	50	2	99	90
10	2-Thienyl	Et	75	2	87	96

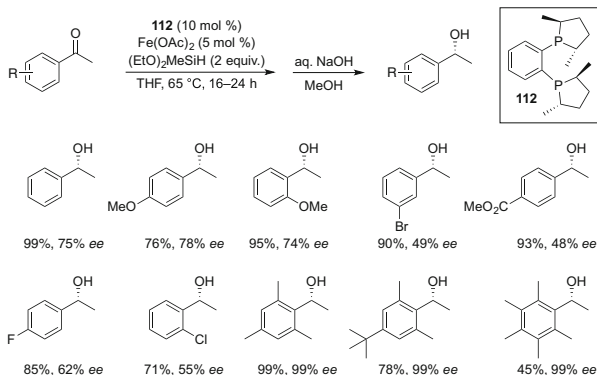
further demonstrated by its use in low loadings (0.02–0.1 mol%), giving almost identical *ee* values of products with a TOF of up to 1,940 h⁻¹ [131].

Gao also reported the hydrogenation of a wide variety of ketones by combining **111** with $\text{Fe}_3(\text{CO})_{12}$ [132]. Aromatic ketones, α -substituted aromatic ketones, and heterocyclic ketones have been hydrogenated under 50 bar H₂ at 45–65°C, affording highly valuable chiral alcohols with enantioselectivities approaching or surpassing those obtained with noble metal catalysts.

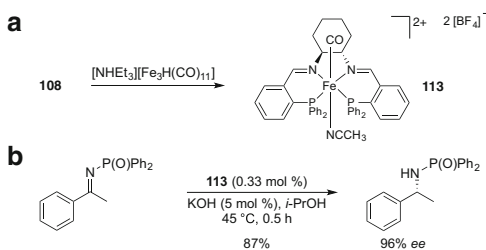
Beller developed an enantioselective reduction of ketones by selecting (*S,S*)-*Me-duphos* **112** as chiral ligand after screening a series of phosphine ligands, using $\text{Fe}(\text{OAc})_2$ (5 mol%) as catalyst and $(\text{EtO})_2\text{MeSiH}$ (2 equiv.) or PMHS (4 equiv.) as reductants (Scheme 51) [133, 134]. High enantioselectivities (up to 99% *ee*) and high yields (up to 99%) were obtained in this transformation. This new method is an important step toward general asymmetric reduction using iron catalysts. They demonstrated that the inexpensive and convenient achiral $\text{Fe}(\text{OAc})_2/\text{PCy}_3$ catalyst system is also useful for the non-enantioselective reduction of ketones with broad functional group tolerance [134]. The system provides the corresponding alcohols in good yield and selectivity with PMHS as reducing agent. Furthermore, the combination of $\text{Fe}(\text{OAc})_2$ and **112** has been applied to the stereoselective reduction of various ketones. However, it was demonstrated that high enantioselectivities can only be obtained with acetophenones bearing electron-rich substituents and sterically hindered substrates.

Beller reported the first iron-catalyzed asymmetric transfer hydrogenation of imines [135]. Several chiral ligands were tested with iron carbonyl hydride cluster complex $[\text{NHEt}_3][\text{Fe}_3\text{HCO}]_{11}$ as the catalyst precursor in the presence of KOH (Scheme 52). *Pybox*, *binap*, or *salen* ligands did not show any appreciable activity. Complex **113** showed excellent activity and enantioselectivity. The scope and limitations of the catalyst system for transfer hydrogenation of ketimines were

Scheme 51 Use of an Fe-diphosphine catalyst for asymmetric hydrosilylation of ketones



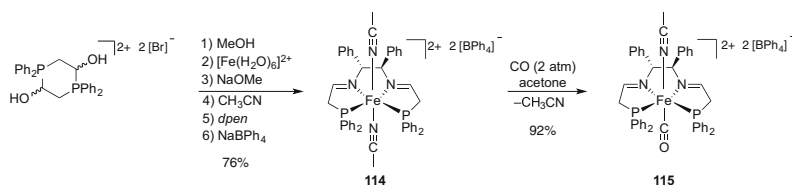
Scheme 52 Structure of iron complex **113** and asymmetric transfer hydrogenation of *N*-(diphenylphosphinyl) ketimine



explored. Excellent enantioselectivities (up to 98% *ee*) and high yields (up to 99%) were achieved upon reduction of various ketimines, including aromatic, heteroaromatic, and cyclic imines. However, lower yields and enantioselectivities were reported for imines derived from alkyl ketones.

Morris reported that a series of iron complexes bearing tetradentate ligands with two phosphorus donors and two nitrogen donors were active for asymmetric transfer hydrosilylation and asymmetric hydrogenation of ketones, once activated with KO*t*-Bu in isopropanol [136–138]. They disclosed an efficient synthesis of new catalyst precursor **115** in a facile and economical two-step process (Scheme 53). An air-stable phosphonium salt was reacted with Fe^{II} and a base and then acetonitrile, the enantiopure diamine (*R,R*)-1,2-diphenylethylenediamine (*dpen*), and finally NaBPh₄ to produce orange solid *trans*-(*R,R*)[Fe(MeCN)₂(L)][BPh₄]₂ **114** in 76% yield. Catalyst **115** was prepared by treating **114** in acetone with carbon monoxide.

Complex **115** was tested for the asymmetric transfer hydrogenation of ketones in basic isopropanol at room temperature (Table 10). It showed excellent activity for the transfer hydrogenation of acetophenone to (*S*)-1-phenylethanol in 82% *ee* (Table 10, entry 1). The addition of a strong base such as KO*t*-Bu or NaO*t*-Bu is essential for catalysis, no conversion being observed if the base is omitted. The optimal ratio of the catalyst to the base was found to be 1:8. The reduction of more hindered aromatic ketones (Table 10, entries 2 and 3) proceeded with excellent enantioselectivity, although the expected trend of a decrease in conversion for the

**Scheme 53** Synthesis of precatalyst **115****Table 10** Asymmetric transfer hydrogenation of ketones using Lewis acid **115**

$\text{R}-\overset{\text{O}}{\parallel}{\text{C}}-\text{R}' \xrightarrow[22^\circ\text{C}]{\text{115, KOt-Bu, } i\text{-PrOH}} \text{R}-\overset{\text{OH}}{\text{C}}-\text{R}'$ (S)							
Entry	R	R'	S/C/B ^a	Time (min.)	Conv. (%)	ee (%)	TOF (h ⁻¹) ^b
1	Ph	Me	600/1/8	8	75	83	3,400
2	Ph	Et	1,500/1/8	25	90	94	3,375
3	Ph	<i>t</i> -Bu	500/1/8	200	35	99	53
4	Ph	<i>c</i> -C ₆ H ₁₁	1,000/1/8	85	76	26	436
5	PhCH ₂ CH ₂	Me	1,000/1/8	30	98	14	1,960
6	<i>p</i> -Cl-C ₆ H ₄	Me	1,500/1/8	18	96	80	4,800
7	<i>p</i> -MeO-C ₆ H ₄	Me	1,000/1/8	40	65	54	930
8	<i>i</i> -Pr	Me	1,500/1/8	60	86	50	1,280

^aS/C/B = substrate/catalyst/base ratio^bTOF is calculated at the conversion and the first time noted

more bulky *t*-Bu substituent was also observed. If the methyl group of acetophenone was replaced with a bulkier cyclohexyl group (Table 10, entry 4), then the *ee* of the reaction dropped significantly. Transfer hydrogenation of the ketone with 2-phenylethyl group proceeded with reduced enantioselectivity (Table 10, entry 5). This result illustrated the importance of bulky groups next to the carbonyl for obtaining high enantioselectivity. An aromatic ketone with an electron-withdrawing group showed a higher TOF (Table 10, entry 6), while a substrate bearing an electron-donating group, on the other hand, showed lower selectivity and activity (Table 10, entry 7). Nonaromatic ketones are challenging substrates for enantioselective reduction. Catalyst **115** was found to be active for such a ketone (Table 10, entry 13) and showed moderate enantioselectivity.

Morris described highly active and well-defined iron precatalysts, such as **116** and **117** (Fig. 15) for the transfer hydrogenation of aromatic and nonaromatic ketones [139]. The iron complexes were fully characterized, including by their crystal structures. They have excellent catalytic activities at room temperature, giving TOFs of up to 2,600 h⁻¹ with low catalyst loadings (0.025–0.17%). Screening experiments showed that the precatalysts are able to produce alcohols from a wide range of simple ketones. For sterically demanding prochiral ketones, excellent

Fig. 15 Carbonyl complexes **116** and **117** for hydrogenation and transfer hydrogenation of ketones

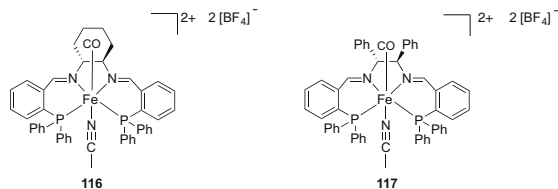
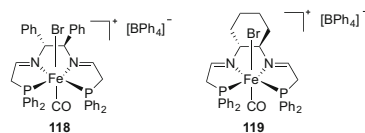


Fig. 16 Structures of chiral complexes used as precatalysts for asymmetric transfer hydrogenation reactions

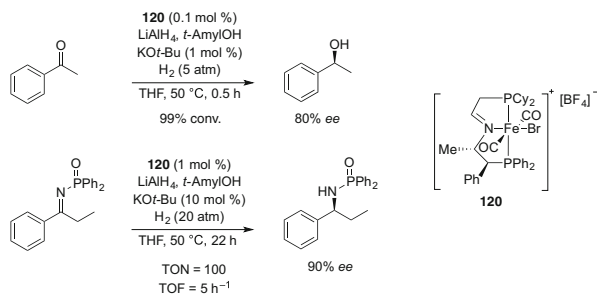


enantioselectivities were obtained (up to 96% *ee*). Upon investigating the mechanism of asymmetric transfer hydrogenation of ketones with **117**, Morris demonstrated that Fe^0 nanoparticles were being formed during catalysis [140].

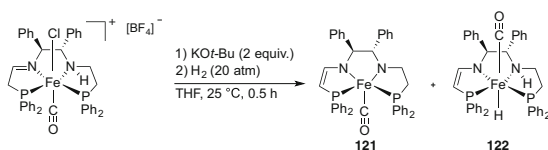
Various versatile one-pot template syntheses of Fe^{II} complexes containing various *PNNP* and *Br/CO* ligands were reported (Fig. 16) [141–145]. These complexes are highly active (TOF up to $30,000 \text{ h}^{-1}$) and enantioselective (up to 99% *ee*) in the asymmetric transfer hydrogenation of ketones when activated with an excess of base at room temperature. Successful reduction of *N*-benzylideneaniline via hydrogen transfer was reported to occur in the presence of **118** [141, 142]. However, the more difficult ketimine *N*-phenyl-(1-phenylethylidene)amine could be only partially converted to the corresponding hydrogenated amine under the same conditions using **118**.

New iron dicarbonyl complexes were developed by Morris in 2014 for the hydrogenation of ketones in THF as the solvent with a catalytic quantity of $\text{KO}t\text{-Bu}$ at 50°C and 5 atm H_2 (Scheme 54) [146]. With enantiopure complex **120**, alcohols were produced for a range of ketones with an enantiomeric excess of up to 85% *ee* (*S*) at TOFs up to $2,000 \text{ h}^{-1}$, and TONs of up to 5,000. An activated imine was also hydrogenated to the amine in 90% *ee* at a TON of 100 and a TOF of 5 h^{-1} . This is a significant advance in asymmetric pressure hydrogenation using iron.

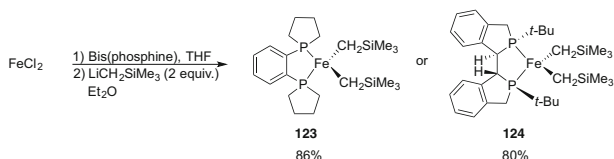
In 2014, Morris developed highly efficient catalysts for the asymmetric transfer hydrogenation of ketones [147]. Amine(imine)diphosphine iron complexes **121** and **122** (3:4 ratio of catalytic species obtained in situ from the precatalyst drawn in Scheme 55) also catalyze the H_2 hydrogenation of ketone substrates with low activity and enantioselectivity. The same structure of amine iron hydride intermediate formed by reacting the amido(ene-amido) iron complex with dihydrogen as that obtained by reacting with 2-propanol suggests a similar reaction mechanism in both hydrogenation reactions.



Scheme 54 Asymmetric hydrogenation reaction of ketones and imines



Scheme 55 Iron complexes **121** and **122** as intermediates in hydrogenation reactions



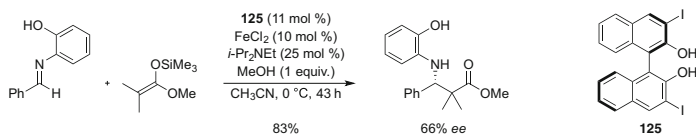
Scheme 56 Synthesis of bis(phosphine) iron dialkyl complexes **123** and **124**

Bis(isonitrile) Fe^{II} complexes derived from a C_2 -symmetric N_2P_2 macrocyclic ligand catalyze the asymmetric transfer hydrogenation of a broad scope of ketones in excellent yields and with high enantioselectivity (up to 91% *ee*) [148].

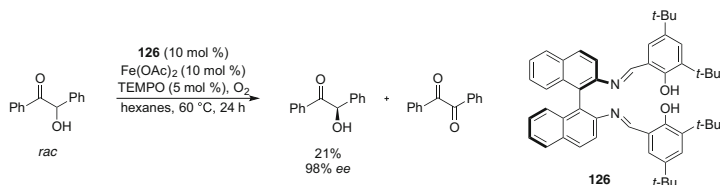
The activity of bis(phosphine) iron dialkyl complexes **123** and **124** for asymmetric hydrogenation of alkenes has been evaluated by Chirik (Scheme 56) [149]. Preparative-scale synthesis of a family of bis(phosphine) Fe^{II} -dialkyl complexes was achieved. However, no enantioselectivity was obtained in the hydrogenation of alkenes.

9 Binaphthyl-Derived Catalysts

A catalytic asymmetric Mannich-type reaction using a chiral Fe^{II} complex was developed by Kobayashi in 2002 (Scheme 57) [150]. The reactions proceeded smoothly in the presence of a catalyst prepared from iron(II) chloride, a *binaphthol* derivative, and *i*-Pr₂NEt. The desired products were obtained in good yields with



Scheme 57 Catalytic asymmetric Mannich-type reactions using a chiral Fe-*binol* catalyst



Scheme 58 Oxidative kinetic resolution of benzoin catalyzed by chiral Fe complex

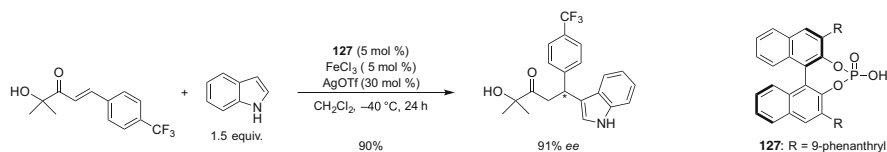
good to high enantioselectivities when 3,3'-I₂-*binol* **125** was employed as a chiral ligand. A protic additive such as methanol facilitated the reactions.

A dinuclear Fe^{III} complex containing a chiral *binaphthol* has been developed [151]. The ligand supports two Fe^{III} ions to give the dinuclear complex with (μ-oxo) (μ-carboxylato) bridges, which is close to that of non-heme diiron metalloenzymes. This complex was active in the oxidation of alkanes using *m*-CPBA. However, the enantioselectivity of the reaction and the stability of the catalyst were not satisfactory.

Sekar developed an efficient, economic, and environmentally friendly asymmetric oxidative kinetic resolution catalyzed by a chiral iron complex using molecular oxygen as stoichiometric oxidant (Scheme 58) [152]. The mild reaction conditions of the catalytic system provided access to a wide range of benzoin (α -hydroxy ketones) in good selectivities and excellent enantiomeric excesses (90–98% *ee*). This method is very versatile in that the only by-product accompanying the oxidation process is water.

Combined chiral phosphorus-based Brønsted acid and iron salts have been used as enantioselective catalysts in the asymmetric Friedel–Crafts alkylation of indoles with β -aryl α' -hydroxy enones [153]. This cooperative system developed with a chiral phosphoric acid as Brønsted acid afforded good to excellent yields and enantioselectivities, particularly for the β -aryl α' -hydroxy enones bearing electron-withdrawing groups at the *para* position of the phenyl ring (Scheme 59). The intermediacy of a phosphate salt of Fe^{III} in the catalytic system was demonstrated by the authors.

A catalytic system consisting of Fe^{III}, a chiral diphosphine such as **128**, and a diamine such as TMEDA was developed for catalytic enantioselective carbometalation with dialkylzinc reagents (Scheme 60) [154, 155]. The reaction allowed the use of functionalized alkyl, vinyl, and aryl organometallics. Although the addition of TMEDA slowed the reaction, its presence was essential for the enantioselective carbometalation.



Scheme 59 Asymmetric Friedel–Crafts alkylation of indoles

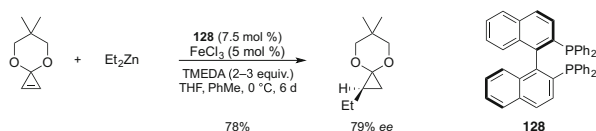
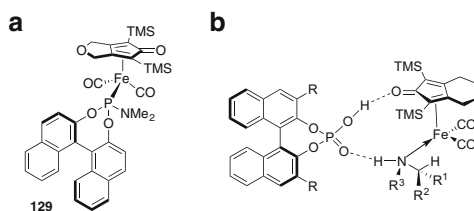
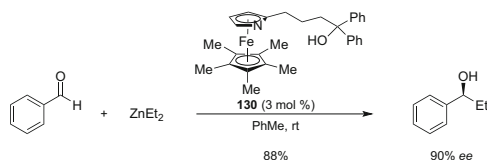
Scheme 60 Fe^{III}-catalyzed enantioselective carbometalation

Fig. 17 Knölker Fe-derived systems

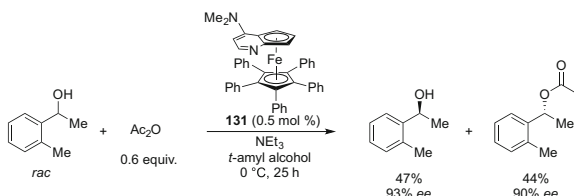
Chiral iron phosphoramidite complexes were reported by Berkessel [156]. With *monoPhos*-iron dicarbonyl complex **129** (Fig. 17a), only moderate enantioselectivity (up to 31% *ee*) was achieved in the hydrogenation of acetophenone. An enantioselective reduction reaction of imines was published by Beller [157]. The combination of Knölker's iron complex with a chiral Brønsted acid in toluene at 65 °C under 50 bar H₂ pressure smoothly catalyzed the reduction of a wide range of imines in high yields and high enantioselectivities. Various aromatic ketimines were hydrogenated smoothly in high yields and with excellent enantioselectivity by using this complex, according to the transition state proposed in Fig. 17b. Both electron-donating and electron-withdrawing substituents on the aromatic rings in the *meta* or *para* positions had little impact on the hydrogenation activity.

10 Planar-Chiral Ferrocenyl Catalysts

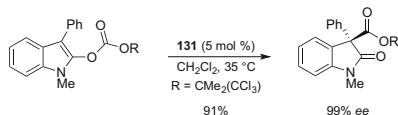
Planar-chiral heterocycles have been used in asymmetric catalysis, either as efficient chiral ligands for transition metals or as enantioselective nucleophilic catalysts [158, 159]. These 2-substituted heterocycles are chiral because they are



Scheme 61 Planar-chiral heterocycles as effective ligands for enantioselective catalysis in the addition of ZnEt₂



Scheme 62 Planar-chiral heterocycles as enantioselective nucleophilic catalysts for the kinetic resolution of alcohols



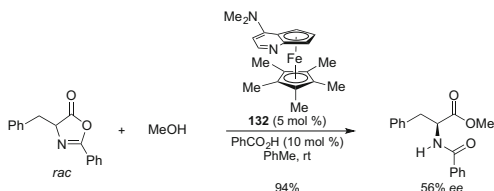
Scheme 63 Planar-chiral heterocycles for the catalytic enantioselective rearrangement of *O*-acylated oxindoles

π -bound to Fe^{II} and the asymmetric environment is due to the presence of one substituent on the heterocycle. Planar-chiral heterocycles have been demonstrated as effective ligands for the catalysis of the enantioselective addition of organozinc reagents to aldehydes [160]. Treatment of benzaldehyde with 3 mol% and 1.2 equiv. of ZnEt₂ afforded (*S*)-1-phenylethanol in good enantiomeric excess (Scheme 61).

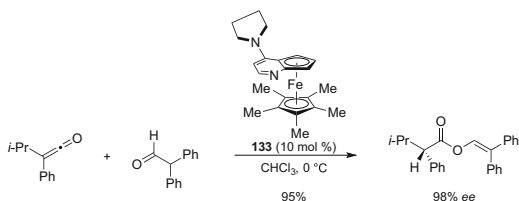
Planar-chiral heterocycles have been used as enantioselective nucleophilic catalysts for various reactions. Kinetic resolution of alcohols was developed using nonenzymatic acylation catalysts [161, 162]. Planar-chiral DMAP ferrocene derivative **131** catalyzed the kinetic resolution of aryl alkyl carbinols with high efficiency (Scheme 62). The same catalyst can also kinetically resolve a racemic diol as well as desymmetrize a *meso*-diol. High catalyst turnover and recyclability, as well as the low sensitivity of the reaction to oxygen and moisture, make this method attractive.

The same catalyst was used for the catalytic enantioselective rearrangement of *O*-acylated benzofuranones and oxindoles (Scheme 63) [163]. This efficient reaction generates a quaternary stereocenter. With the trichloro-*tert*-butoxycarbonyl

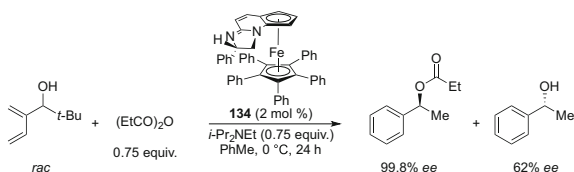
Scheme 64 Planar-chiral catalyst used in the dynamic kinetic resolution of azlactones



Scheme 65 Catalytic asymmetric synthesis of enol esters of α -arylalkanoic acids



Scheme 66
Enantioselective acyl transfer of secondary alcohols



substituent as the migrating group, the rearrangement occurred with high enantioselectivity.

A similar planar-chiral catalyst was used in the dynamic kinetic resolution in the ring opening of azlactones [162, 164]. The planar-chiral derivative catalyzed the deracemization/ring opening of azlactones, thereby affording protected α -amino acids in moderate enantioselectivity and excellent yield (Scheme 64). A catalytic asymmetric method for the preparation of tertiary α -chloroesters from ketenes using the same catalyst was also disclosed by the same author [165].

A synthesis of enantioenriched esters was also developed using planar-chiral catalyst **133** (Scheme 65) [166]. The catalytic asymmetric synthesis of enol esters of α -arylalkanoic acids from the reaction of ketenes with diphenylacetaldehyde was achieved using 10 mol% of the catalyst. The addition led to the enol esters with very good enantioselectivities. A catalytic asymmetric Staudinger reaction of these ketenes with imines was developed by the same author [167]. Various ketenes and *N*-triflyl imines reacted to afford β -lactams with good *trans* diastereoselectivity and good enantioselectivity.

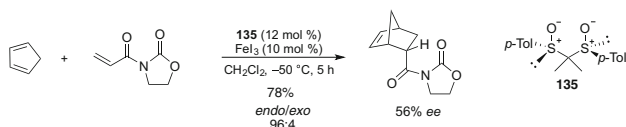
A remarkably efficient planar-chiral ferrocene nucleophilic catalyst (**134**) was developed for the enantioselective acyl transfer of secondary alcohols (Scheme 66) [168]. These novel catalysts contain both central and planar-chiral elements and are suitable for the catalytic kinetic resolution of bulky aryl alkyl alcohols to afford the corresponding esters with high enantioselectivities (up to 99.8% ee).

11 Other Catalysts

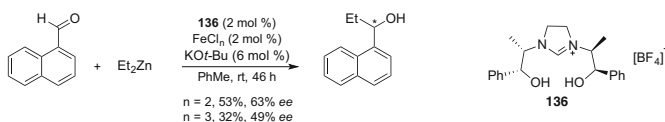
In 1993, Khiar disclosed bis(sulfoxide) ligands with C_2 -symmetry axis, as bidentate chiral controllers in a newly catalyzed Diels–Alder reaction (Scheme 67) [169]. Such ligands are very attractive as a consequence of their ease of synthesis and their availability in both enantiomeric forms from cheap starting materials. Bis(sulfoxides) as chiral ligands, such as **135**, together with iron(III) iodide, were selected as the Lewis acid catalyst in the reaction between cyclopentadiene and 3-acryloyl-1,3-oxazolidin-2-one.

A new family of enantiopure *N*-heterocyclic carbene ligands has been developed. New enantiopure imidazolium carbene ligands incorporating two hydroxy functions have been prepared from chiral amino alcohols and diamines (Scheme 68) [170]. The imidazolium salts were used in the Et_2Zn addition to 1-naphthyl carboxaldehyde. Various metal salts, including FeCl_2 and FeCl_3 , were investigated in the presence of chiral imidazolium salt **136** and 6 mol% of $\text{KO}t\text{-Bu}$. Moderate enantioselectivities were obtained.

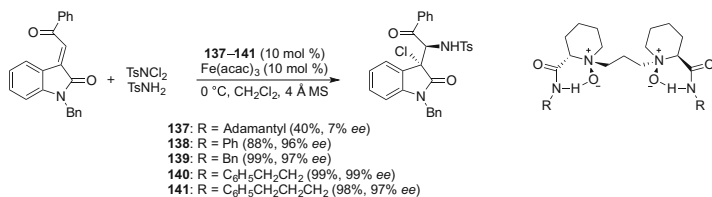
Fe^{III} -*N,N'*-dioxide complex-catalyzed asymmetric haloamination of 3-alkylidene- and 3-arylidene-indolin-2-ones was developed, affording the corresponding chiral oxindole derivatives bearing vicinal haloamine substituents with excellent results (up to 99% yield, >19:1 *dr*, 99% *ee*, Scheme 69) [171].



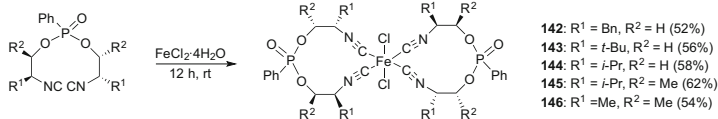
Scheme 67 Fe^{III} -bis(sulfoxide)-catalyzed Diels–Alder reaction



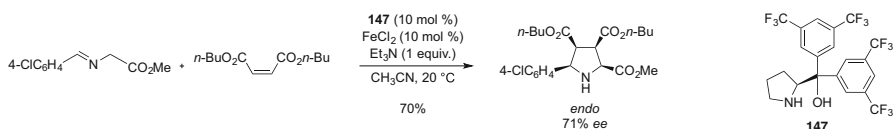
Scheme 68 Fe -*N*-heterocyclic carbene complexes for enantioselective alkylation of an aromatic aldehyde



Scheme 69 Fe^{III} -catalyzed asymmetric haloamination



Scheme 70 Synthesis of Fe^{II}-bis(isonitrile) complexes



Scheme 71 Fe-catalyzed [3 + 2] cycloaddition reaction

Fe^{III} catalysts prepared from ligands **137**–**141** also exhibit excellent enantioselectivities for chalcone derivatives.

In 2010, Reiser reported the synthesis of bidentate bis(isonitrile) ligands that could easily be synthesized from amino alcohols in two steps following the protocol developed by them earlier [172]. The corresponding Fe^{II} complexes were obtained by treatment of ligands with FeCl₂ · 4H₂O in methanol which led to the formation of [FeCl₂{bis(isonitrile)}₂] complexes in good yields (Scheme 70).

These complexes were tested as catalysts for transfer hydrogenation of acetophenone using isopropanol as the hydrogen source under basic conditions. Complex **143** was identified to be an active catalyst at room temperature affording 1-phenylethanol with 90% conversion and 64% *ee*, demonstrating for the first time the applicability of isonitrile ligands as chiral inductors in asymmetric catalysis. They have also proposed that the reaction proceeds via a Meerwein–Ponndorf–Verley-type mechanism, being different from the reported mechanisms for transfer hydrogenations with ruthenium involving achiral isonitrile ligands [172]. The authors speculate that the ketone binds via its carbonyl group or alternatively through the respective heteroatom in the case of heteroaromatic substrates to the iron center of the catalyst. Hydride transfer then occurs directly from the reduced isonitrile group acting as the hydrogen donor.

Fe^{II}-diaryl prolinol-catalyzed asymmetric 1,3-dipolar cycloaddition of azomethine ylides with alkenes was developed by Wang (Scheme 71) [173]. In the presence of FeCl₂ (10 mol%) and α,α -bis(3,5-bis(trifluoromethyl)phenyl)prolinol (**147**, 10 mol%), [3 + 2] cycloaddition of azomethine ylides with electron-deficient olefins occurred smoothly in acetonitrile at room temperature to generate the desired *endo* adducts in moderate to good yields and enantioselectivities.

An effective enantioselective Fe^{III}-1-glycyl-3-methyl imidazolium chloride complex was developed and evaluated as organocatalyst in asymmetric aldol reaction under solvent-free conditions [174]. The catalyst furnished the aldol products with excellent yields and enantioselectivities (up to 98% *ee*) and could be recycled.

12 Summary and Overview

This review compiles the applications of enantioselective iron catalysts in organic synthesis. Whereas in the 1990s only few iron-catalyzed oxidation and cyclopropanation reactions were developed, the field now comprises many major developments and appealing processes for various asymmetric transformations. In recent years, various environmentally benign chiral iron catalysts were developed for the epoxidation of alkenes, oxidation of sulfides, reduction of ketones and imines, and various C–C bond-forming reactions. The current developments demonstrate that iron chemistry truly is an emerging field. Efficient catalytic asymmetric transformations using iron are definitively high potential processes and bring very promising challenges to explore. Iron catalysts have undeniably contributed to the area of environmentally benign catalysts, known as green catalysts. Moreover, the use of iron salts as Lewis acids in aqueous conditions finally opened the door to designing catalysts and broadening the concept of hydrocompatible Lewis acids, which has since been applied to various reaction types. Given the ongoing need for new economically and green reactions, the examples presented here are the starting point for future developments in asymmetric iron catalysis. Asymmetric catalysis using iron salts will clearly be a prominent area in the forthcoming years. The development of more general enantioselective methods will demonstrate that it is possible to mimic nature by using simpler and greener catalysts.

Acknowledgments We are grateful to the Natural Sciences and Engineering Research Council of Canada (NSERC) and to the Centre in Green Chemistry and Catalysis (CGCC) for the financial support. We thank Martin Pichette Drapeau and Angela Jalba for their valuable help in proof-reading the manuscript.

References

1. Bolm C, Legros J, Le Paih J, Zani L (2004) *Chem Rev* 104:6217. doi:10.1021/cr040664h
2. Darwish M, Wills M (2012) *Catal Sci Technol* 2:243. doi:10.1039/c1cy00390a
3. Wang C, Wan B (2012) *Chin Sci Bull* 57:2338. doi:10.1007/s11434-012-5141-z
4. Srour H, Le Maux P, Chevance S, Simonneaux G (2013) *Coord Chem Rev* 257:3030. doi:10.1016/j.ccr.2013.05.010
5. Gopalaiah K (2013) *Chem Rev* 113:3248. doi:10.1021/cr300236r
6. Morris RH (2009) *Chem Soc Rev* 38:2282. doi:10.1039/b806837m
7. Sues PE, Demmans KZ, Morris RH (2014) *J Chem Soc Dalton Trans* 43:7650. doi:10.1039/c4dt00612g
8. Enthaler S, Junge K, Beller M (2008) *Angew Chem Int Ed* 47:3317. doi:10.1002/anie.200800012
9. Collman JP, Gagne RR, Reed C, Halbert TR, Lang G, Robinson WT (1975) *J Am Chem Soc* 97:1427. doi:10.1021/ja00839a026
10. Groves JT, Myers RS (1983) *J Am Chem Soc* 105:5791. doi:10.1021/ja00356a016
11. Mansuy D, Battioni P, Renaud JP, Guerin P (1985) *J Chem Soc, Chem Commun*: 155–156. doi:10.1039/c39850000155

12. Maillard P, Guerquin-Kern JL, Momenteau M (1991) *Tetrahedron Lett* 32:4901. doi:[10.1016/S0040-4039\(00\)93491-9](https://doi.org/10.1016/S0040-4039(00)93491-9)
13. Gross Z, Ini S (1997) *J Org Chem* 62:5514. doi:[10.1021/JO970463W](https://doi.org/10.1021/JO970463W)
14. Rose E, Soleilhavoup M, Christ-Tomasino L, Moreau G, Collman JP, Quelquejeu M, Straumanis A (1998) *J Org Chem* 63:2042. doi:[10.1021/JO9718713](https://doi.org/10.1021/JO9718713)
15. Gross Z, Galili N, Simkhovich L (1999) *Tetrahedron Lett* 40:1571. doi:[10.1016/S0040-4039\(98\)02647-1](https://doi.org/10.1016/S0040-4039(98)02647-1)
16. Rose E, Quelquejeu M, Pandian RP, Lecas-Nawrocka A, Vilar A, Ricart G, Collman JP, Wang Z, Straumanis A (2000) *Polyhedron* 19:581. doi:[10.1016/S0277-5387\(99\)00413-1](https://doi.org/10.1016/S0277-5387(99)00413-1)
17. Reginato G, Di Bari L, Salvadori P, Guillard R (2000) *Eur J Org Chem* 2000:1165–1171. doi:[10.1002/1099-0690\(200004\)2000:7<1165::AID-EJOC1165>3.0.CO;2-8](https://doi.org/10.1002/1099-0690(200004)2000:7<1165::AID-EJOC1165>3.0.CO;2-8)
18. Boitrel B, Baveux-Chambenoît V, Richard P (2002) *Eur J Inorg Chem* 2002:1666–1972. doi:[10.1002/1099-0682\(200207\)2002:7<1666::aid-ejic1666>3.0.co;2-](https://doi.org/10.1002/1099-0682(200207)2002:7<1666::aid-ejic1666>3.0.co;2-)
19. Boitrel B, Baveux-Chambenoît V (2003) *New J Chem* 27:942. doi:[10.1039/b212480g](https://doi.org/10.1039/b212480g)
20. Smith JRL, Reginato G (2003) *Org Biomol Chem* 1:2543
21. Rose E, Ren Q-z, Andrioletti B (2004) *Chem Eur J* 10:224. doi:[10.1002/chem.200305222](https://doi.org/10.1002/chem.200305222)
22. Nakagawa H, Sei Y, Yamaguchi K, Nagano T, Higuchi T (2004) *J Mol Catal A: Chem* 219:221. doi:[10.1016/j.molcata.2004.05.026](https://doi.org/10.1016/j.molcata.2004.05.026)
23. Ferrand Y, Daviaud R, Le Maux P, Simonneaux G (2006) *Tetrahedron: Asymmetry* 17:952. doi:[10.1016/j.tetasy.2006.03.003](https://doi.org/10.1016/j.tetasy.2006.03.003)
24. Rose E, Andrioletti B, Zrig S, Quelquejeu-Ethève M (2005) *Chem Soc Rev* 34:573. doi:[10.1039/b405679p](https://doi.org/10.1039/b405679p)
25. Simonato J-P, Pecaut J, Marchon J-C, Robert Scheidt W (1999) *Chem Commun*: 989. doi:[10.1039/a901559k](https://doi.org/10.1039/a901559k)
26. Groves JT, Viski P (1990) *J Org Chem* 55:3628. doi:[10.1021/jo00298a046](https://doi.org/10.1021/jo00298a046)
27. Naruta Y, Tani F, Ishihara N, Maruyama K (1991) *J Am Chem Soc* 113:6865. doi:[10.1021/ja00018a024](https://doi.org/10.1021/ja00018a024)
28. Naruta Y, Tani F, Maruyama K (1990) *J Chem Soc, Chem Commun* 1990:1378. doi:[10.1039/c39900001378](https://doi.org/10.1039/c39900001378)
29. Naruta Y, Tani F, Maruyama K (1991) *Tetrahedron: Asymmetry* 2:533. doi:[10.1016/s0957-4166\(00\)86106-6](https://doi.org/10.1016/s0957-4166(00)86106-6)
30. Naruta Y, Tani F, Maruyama K (1992) *Tetrahedron Lett* 33:6323. doi:[10.1016/s0040-4039\(00\)60964-4](https://doi.org/10.1016/s0040-4039(00)60964-4)
31. Naruta Y, Ishihara N, Tani F, Maruyama K (1993) *Bull Chem Soc Jpn* 66:158. doi:[10.1246/bcsj.66.158](https://doi.org/10.1246/bcsj.66.158)
32. Collman JP, Zhang X, Lee VJ, Brauman JI (1992) *J Chem Soc, Chem Commun* 1992:1647. doi:[10.1039/c39920001647](https://doi.org/10.1039/c39920001647)
33. Le Maux P, Simonneaux G (2011) *Chem Commun* 47:6957. doi:[10.1039/c1cc11675d](https://doi.org/10.1039/c1cc11675d)
34. Le Maux P, Juillard S, Simonneaux G (2006) *Synthesis* 2006:1701. doi:[10.1055/s-2006-926451](https://doi.org/10.1055/s-2006-926451)
35. Lai T-S, Chan F-Y, So P-K, Ma D-L, Wong K-Y, Che C-M (2006) *J Chem Soc, Dalton Trans*: 4845–4851. doi:[10.1039/b606757c](https://doi.org/10.1039/b606757c)
36. Nicolas I, Le Maux P, Simonneaux G (2008) *Tetrahedron Lett* 49:5793. doi:[10.1016/j.tetlet.2008.07.133](https://doi.org/10.1016/j.tetlet.2008.07.133)
37. Nicolas I, Roisnel T, Le Maux P, Simonneaux G (2009) *Tetrahedron Lett* 50:5149. doi:[10.1016/j.tetlet.2009.06.131](https://doi.org/10.1016/j.tetlet.2009.06.131)
38. Du G, Andrioletti B, Rose E, Woo LK (2002) *Organometallics* 21:4490. doi:[10.1021/om0204641](https://doi.org/10.1021/om0204641)
39. Intrieri D, Le Gac S, Caselli A, Rose E, Boitrel B, Gallo E (2014) *Chem Commun* 50:1811. doi:[10.1039/c3cc48605b](https://doi.org/10.1039/c3cc48605b)
40. Le Maux P, Srour HF, Simonneaux G (2012) *Tetrahedron* 68:5824. doi:[10.1016/j.tet.2012.05.014](https://doi.org/10.1016/j.tet.2012.05.014)
41. Chen Y, Zhang XP (2007) *J Org Chem* 72:5931. doi:[10.1021/jo070997p](https://doi.org/10.1021/jo070997p)

42. Duboc-Toia C, Ménage S, Ho RYN, Que L Jr, Lambeaux C, Fontecave M (1999) *Inorg Chem* 38:1261. doi:[10.1021/ic980958j](https://doi.org/10.1021/ic980958j)
43. Duboc-Toia C, Ménage S, Lambeaux C, Fontecave M (1997) *Tetrahedron Lett* 38:3727. doi:[10.1016/s0040-4039\(97\)00710-7](https://doi.org/10.1016/s0040-4039(97)00710-7)
44. Mekmouche Y, Hummel H, Ho Raymond YN, Que L Jr, Schünemann V, Thomas F, Trautwein Alfred X, Lebrun C, Gorgy K, Leprière J-C, Collomb M-N, Deronzier A, Fontecave M, Ménage S (2002) *Chem Eur J* 8:1196
45. Marchi-Delapierre C, Jorge-Robin A, Thibon A, Ménage S (2007) *Chem Commun*: 1166
46. Nishikawa Y, Yamamoto H (2011) *J Am Chem Soc* 133:8432. doi:[10.1021/ja201873d](https://doi.org/10.1021/ja201873d)
47. Yeung H-L, Sham K-C, Tsang C-S, Lau T-C, Kwong H-L (2008) *Chem Commun*: 3801. doi:[10.1039/b804281k](https://doi.org/10.1039/b804281k)
48. Yeung C-T, Sham K-C, Lee W-S, Wong W-T, Wong W-Y, Kwong H-L (2009) *Inorg Chim Acta* 362:3267. doi:[10.1016/j.ica.2009.02.034](https://doi.org/10.1016/j.ica.2009.02.034)
49. Ollevier T, Plancq B (2012) *Chem Commun* 48:2289. doi:[10.1039/c1cc16409k](https://doi.org/10.1039/c1cc16409k)
50. Kitanosono T, Ollevier T, Kobayashi S (2013) *Chem Asian J* 8:3051. doi:[10.1002/asia.201301149](https://doi.org/10.1002/asia.201301149)
51. Lafantaisie M, Mirabaud A, Plancq B, Ollevier T (2014) *ChemCatChem* 6:2244. doi:[10.1002/cctc.201402029](https://doi.org/10.1002/cctc.201402029)
52. Plancq B, Ollevier T (2012) *Chem Commun* 48:3806. doi:[10.1039/c2cc18032d](https://doi.org/10.1039/c2cc18032d)
53. Plancq B, Lafantaisie M, Companys S, Maroun C, Ollevier T (2013) *Org Biomol Chem* 11:7463. doi:[10.1039/c3ob41782d](https://doi.org/10.1039/c3ob41782d)
54. Plancq B, Ollevier T (2012) *Aust J Chem* 65:1564. doi:[10.1071/ch12354](https://doi.org/10.1071/ch12354)
55. Legros J, Bolm C (2003) *Angew Chem Int Ed* 42:5487. doi:[10.1002/anie.200352635](https://doi.org/10.1002/anie.200352635)
56. Legros J, Bolm C (2004) *Angew Chem Int Ed* 43:4225. doi:[10.1002/anie.200460236](https://doi.org/10.1002/anie.200460236)
57. Korte A, Legros J, Bolm C (2004) *Synlett* 2004:2397. doi:[10.1055/s-2004-832834](https://doi.org/10.1055/s-2004-832834)
58. Legros J, Bolm C (2005) *Chem Eur J* 11:1086. doi:[10.1002/chem.200400857](https://doi.org/10.1002/chem.200400857)
59. Muthupandi P, Sekar G (2012) *Org Biomol Chem* 10:5347. doi:[10.1039/c2ob25810b](https://doi.org/10.1039/c2ob25810b)
60. Boobalan R, Chen C (2013) *Adv Synth Catal* 355:3443. doi:[10.1002/adsc.201300653](https://doi.org/10.1002/adsc.201300653)
61. Stingl KA, Weiss KM, Tsogoeva SB (2012) *Tetrahedron* 68:8493. doi:[10.1016/j.tet.2012.07.052](https://doi.org/10.1016/j.tet.2012.07.052)
62. Bryliakov KP, Talsi EP (2004) *Angew Chem Int Ed* 43:5228. doi:[10.1002/anie.200460108](https://doi.org/10.1002/anie.200460108)
63. Bryliakov KP, Talsi EP (2007) *Chem Eur J* 13:8045. doi:[10.1002/chem.200700566](https://doi.org/10.1002/chem.200700566)
64. Mukherjee C, Stammler A, Boegge H, Glaser T (2010) *Chem Eur J* 16:10137. doi:[10.1002/chem.201000923](https://doi.org/10.1002/chem.201000923)
65. White JD, Shaw S (2011) *Org Lett* 13:2488. doi:[10.1021/ol2007378](https://doi.org/10.1021/ol2007378)
66. White JD, Shaw S (2014) *Chem Sci* 5:2200. doi:[10.1039/c4sc00051j](https://doi.org/10.1039/c4sc00051j)
67. Shaw S, White JD (2014) *J Am Chem Soc* 136:13578. doi:[10.1021/ja507853f](https://doi.org/10.1021/ja507853f)
68. Liao S, List B (2012) *Adv Synth Catal* 354:2363. doi:[10.1002/adsc.201200251](https://doi.org/10.1002/adsc.201200251)
69. Egami H, Katsuki T (2007) *J Am Chem Soc* 129:8940. doi:[10.1021/ja071916+](https://doi.org/10.1021/ja071916+)
70. Egami H, Katsuki T (2008) *Synlett* 2008:1543. doi:[10.1055/s-2008-1078427](https://doi.org/10.1055/s-2008-1078427)
71. Li B, Bai S, Wang P, Yang H, Yang Q, Li C (2011) *PCCP* 13:2504. doi:[10.1039/c0cp01828g](https://doi.org/10.1039/c0cp01828g)
72. Egami H, Katsuki T (2009) *J Am Chem Soc* 131:6082. doi:[10.1021/ja901391u](https://doi.org/10.1021/ja901391u)
73. Egami H, Matsumoto K, Oguma T, Kunisu T, Katsuki T (2010) *J Am Chem Soc* 132:13633. doi:[10.1021/ja105442m](https://doi.org/10.1021/ja105442m)
74. Kunisu T, Oguma T, Katsuki T (2011) *J Am Chem Soc* 133:12937. doi:[10.1021/ja204426s](https://doi.org/10.1021/ja204426s)
75. Uchida T, Katsuki T (2013) *J Synth Org Chem Jpn* 71:1126. doi:[10.5059/yukigoseikyokaishi.71.1126](https://doi.org/10.5059/yukigoseikyokaishi.71.1126)
76. Oguma T, Katsuki T (2012) *J Am Chem Soc* 134:20017. doi:[10.1021/ja310203c](https://doi.org/10.1021/ja310203c)
77. Oguma T, Katsuki T (2014) *Chem Commun* 50:5053. doi:[10.1039/c4cc01555j](https://doi.org/10.1039/c4cc01555j)
78. Gu X, Zhang Y, Xu Z-J, Che C-M (2014) *Chem Commun* 50:7870. doi:[10.1039/c4cc01631a](https://doi.org/10.1039/c4cc01631a)
79. Corey EJ, Imai N, Zhang HY (1991) *J Am Chem Soc* 113:728. doi:[10.1021/ja00002a081](https://doi.org/10.1021/ja00002a081)
80. Corey EJ, Ishihara K (1992) *Tetrahedron Lett* 33:6807. doi:[10.1016/S0040-4039\(00\)61781-1](https://doi.org/10.1016/S0040-4039(00)61781-1)

81. Kanemasa S, Oderaotoshi Y, Yamamoto H, Tanaka J, Wada E, Curran DP (1997) *J Org Chem* 62:6454. doi:[10.1021/JO970906W](https://doi.org/10.1021/JO970906W)
82. Sibi MP, Manyem S, Palencia H (2006) *J Am Chem Soc* 128:13660. doi:[10.1021/ja064472a](https://doi.org/10.1021/ja064472a)
83. Takacs JM, Boito SC (1995) *Tetrahedron Lett* 36:2941. doi:[10.1016/0040-4039\(95\)00443-g](https://doi.org/10.1016/0040-4039(95)00443-g)
84. Guillemot G, Neuburger M, Pfaltz A (2007) *Chem Eur J* 13:8960. doi:[10.1002/chem.200700826](https://doi.org/10.1002/chem.200700826)
85. Zhu S-F, Cai Y, Mao H-X, Xie J-H, Zhou Q-L (2010) *Nat Chem* 2:546. doi:[10.1038/nchem.651](https://doi.org/10.1038/nchem.651)
86. Cai Y, Zhu S-F, Wang G-P, Zhou Q-L (2011) *Adv Synth Catal* 353:2939. doi:[10.1002/adsc.201100334](https://doi.org/10.1002/adsc.201100334)
87. Shen J-J, Zhu S-F, Cai Y, Xu H, Xie X-L, Zhou Q-L (2014) *Angew Chem Int Ed* 53:13188. doi:[10.1002/anie.201406853](https://doi.org/10.1002/anie.201406853)
88. Niwa T, Nakada M (2012) *J Am Chem Soc* 134:13538. doi:[10.1021/ja304219s](https://doi.org/10.1021/ja304219s)
89. Williamson KS, Yoon TP (2012) *J Am Chem Soc* 134:12370. doi:[10.1021/ja3046684](https://doi.org/10.1021/ja3046684)
90. Deng Q-H, Bleith T, Wadepohl H, Gade LH (2013) *J Am Chem Soc* 135:5356. doi:[10.1021/ja402082p](https://doi.org/10.1021/ja402082p)
91. Liu G-S, Zhang Y-Q, Yuan Y-A, Xu H (2013) *J Am Chem Soc* 135:3343. doi:[10.1021/ja311923z](https://doi.org/10.1021/ja311923z)
92. Zhang Y-Q, Yuan Y-A, Liu G-S, Xu H (2013) *Org Lett* 15:3910. doi:[10.1021/ol401666e](https://doi.org/10.1021/ol401666e)
93. Lu D-F, Liu G-S, Zhu C-L, Yuan B, Xu H (2014) *Org Lett* 16:2912. doi:[10.1021/ol501051p](https://doi.org/10.1021/ol501051p)
94. Usuda H, Kuramochi A, Kanai M, Shibasaki M (2004) *Org Lett* 6:4387. doi:[10.1021/ol048018s](https://doi.org/10.1021/ol048018s)
95. Shimizu Y, Shi S-L, Usuda H, Kanai M, Shibasaki M (2010) *Angew Chem Int Ed* 49:1103. doi:[10.1002/anie.200906678](https://doi.org/10.1002/anie.200906678)
96. Jankowska J, Paradowska J, Mlynarski J (2006) *Tetrahedron Lett* 47:5281. doi:[10.1016/j.tetlet.2006.05.140](https://doi.org/10.1016/j.tetlet.2006.05.140)
97. Jankowska J, Paradowska J, Rakiel B, Mlynarski J (2007) *J Org Chem* 72:2228. doi:[10.1021/jo0621470](https://doi.org/10.1021/jo0621470)
98. Nishiyama H, Furuta A (2007) *Chem Commun*: 760. doi:[10.1039/b617388h](https://doi.org/10.1039/b617388h)
99. Inagaki T, Le Phong T, Furuta A, Ito J-i, Nishiyama H (2010) *Chem Eur J* 16:3090
100. Inagaki T, Ito A, Ito J-i, Nishiyama H (2010) *Angew Chem Int Ed* 49:9384. doi:[10.1002/anie.201005363](https://doi.org/10.1002/anie.201005363)
101. Hosokawa S, Ito J-I, Nishiyama H (2010) *Organometallics* 29:5773. doi:[10.1021/om1009186](https://doi.org/10.1021/om1009186)
102. Kawatsura M, Komatsu Y, Yamamoto M, Hayase S, Itoh T (2007) *Tetrahedron Lett* 48:6480. doi:[10.1016/j.tetlet.2007.07.053](https://doi.org/10.1016/j.tetlet.2007.07.053)
103. Kawatsura M, Komatsu Y, Yamamoto M, Hayase S, Itoh T (2008) *Tetrahedron* 64:3488. doi:[10.1016/j.tet.2008.01.121](https://doi.org/10.1016/j.tet.2008.01.121)
104. Tondreau AM, Darmon JM, Wile BM, Floyd SK, Lobkovsky E, Chirik PJ (2009) *Organometallics* 28:3928. doi:[10.1021/om900224e](https://doi.org/10.1021/om900224e)
105. Redlich M, Hossain MM (2004) *Tetrahedron Lett* 45:8987. doi:[10.1016/j.tetlet.2004.10.047](https://doi.org/10.1016/j.tetlet.2004.10.047)
106. Nakanishi M, Salit A-F, Bolm C (2008) *Adv Synth Catal* 350:1835. doi:[10.1002/adsc.200700519](https://doi.org/10.1002/adsc.200700519)
107. Kawatsura M, Kajita K, Hayase S, Itoh T (2010) *Synlett* 2010:1243. doi:[10.1055/s-0029-1219782](https://doi.org/10.1055/s-0029-1219782)
108. Wang J, Frings M, Bolm C (2013) *Angew Chem Int Ed* 52:8661. doi:[10.1002/anie.201304451](https://doi.org/10.1002/anie.201304451)
109. Wang J, Frings M, Bolm C (2014) *Chem Eur J* 20:966. doi:[10.1002/chem.201303850](https://doi.org/10.1002/chem.201303850)
110. Gelalcha FG, Bitterlich B, Anilkumar G, Tse MK, Beller M (2007) *Angew Chem Int Ed* 46:7293. doi:[10.1002/anie.200701235](https://doi.org/10.1002/anie.200701235)
111. Gelalcha FG, Anilkumar G, Tse MK, Bruckner A, Beller M (2008) *Chem Eur J* 14:7687. doi:[10.1002/chem.200800595](https://doi.org/10.1002/chem.200800595)
112. Yazerski VA, Orue A, Evers T, Kleijn H, Klein Gebbink RJM (2013) *Catal Sci Technol* 3:2810. doi:[10.1039/c3cy00484h](https://doi.org/10.1039/c3cy00484h)

113. Yang H-M, Gao Y-H, Li L, Jiang Z-Y, Lai G-Q, Xia C-G, Xu L-W (2010) *Tetrahedron Lett* 51:3836. doi:[10.1016/j.tetlet.2010.05.074](https://doi.org/10.1016/j.tetlet.2010.05.074)
114. Chen MS, White MC (2007) *Science* 318:783. doi:[10.1126/science.1148597](https://doi.org/10.1126/science.1148597)
115. Suzuki K, Oldenburg PD, Que L Jr (2008) *Angew Chem Int Ed* 47:1887. doi:[10.1002/anie.200705061](https://doi.org/10.1002/anie.200705061)
116. Costas M, Tipton AK, Chen K, Jo DH, Que L Jr (2001) *J Am Chem Soc* 123:6722
117. Wu M, Miao C-X, Wang S, Hu X, Xia C, Kuehn FE, Sun W (2011) *Adv Synth Catal* 353:3014. doi:[10.1002/adsc.201100267](https://doi.org/10.1002/adsc.201100267)
118. Wang X, Miao C, Wang S, Xia C, Sun W (2013) *ChemCatChem* 5:2489. doi:[10.1002/cctc.201300102](https://doi.org/10.1002/cctc.201300102)
119. Lyakin OY, Ottenbacher RV, Bryliakov KP, Talsi EP (2012) *ACS Catal* 2:1196. doi:[10.1021/cs300205n](https://doi.org/10.1021/cs300205n)
120. Lyakin OY, Ottenbacher RV, Bryliakov KP, Talsi EP (2013) *Top Catal* 56:939. doi:[10.1007/s11244-013-0058-6](https://doi.org/10.1007/s11244-013-0058-6)
121. Gosiewska S, Lutz M, Spek AL, Klein Gebbink RJM (2007) *Inorg Chim Acta* 360:405. doi:[10.1016/j.ica.2006.08.009](https://doi.org/10.1016/j.ica.2006.08.009)
122. Langlotz BK, Wadepohl H, Gade LH (2008) *Angew Chem Int Ed* 47:4670. doi:[10.1002/anie.200801150](https://doi.org/10.1002/anie.200801150)
123. Flueckiger M, Togni A (2011) *Eur J Org Chem* 2011:4353. doi:[10.1002/ejoc.201100550](https://doi.org/10.1002/ejoc.201100550)
124. Wang B, Wang S, Xia C, Sun W (2012) *Chem Eur J* 18:7332. doi:[10.1002/chem.201200992](https://doi.org/10.1002/chem.201200992)
125. Kuendig EP, Bourdin B, Bernardinelli G (1994) *Angew Chem* 106:1931
126. Bruin ME, Kündig PE (1998) *Chem Commun*: 2635. doi:[10.1039/a806445h](https://doi.org/10.1039/a806445h)
127. Kündig EP, Saudan CM, Viton F (2001) *Adv Synth Catal* 343:51. doi:[10.1002/1615-4169\(20010129\)343:1<51::aid-adsc51>3.0.co;2-n](https://doi.org/10.1002/1615-4169(20010129)343:1<51::aid-adsc51>3.0.co;2-n)
128. Viton F, Bernardinelli G, Kuendig EP (2002) *J Am Chem Soc* 124:4968. doi:[10.1021/ja017814f](https://doi.org/10.1021/ja017814f)
129. Matsukawa S, Sugama H, Imamoto T (2000) *Tetrahedron Lett* 41:6461. doi:[10.1016/s0040-4039\(00\)01030-3](https://doi.org/10.1016/s0040-4039(00)01030-3)
130. Chen J-S, Chen L-L, Xing Y, Chen G, Shen W-Y, Dong Z-R, Li Y-Y, Gao J-X (2004) *Acta Chim Sinica* 62:1745
131. Yu S, Shen W, Li Y, Dong Z, Xu Y, Li Q, Zhang J, Gao J (2012) *Adv Synth Catal* 354:818. doi:[10.1002/adsc.201100733](https://doi.org/10.1002/adsc.201100733)
132. Li Y, Yu S, Wu X, Xiao J, Shen W, Dong Z, Gao J (2014) *J Am Chem Soc* 136:4031. doi:[10.1021/ja5003636](https://doi.org/10.1021/ja5003636)
133. Shaikh NS, Enthaler S, Junge K, Beller M (2008) *Angew Chem Int Ed* 47:2497. doi:[10.1002/anie.200705624](https://doi.org/10.1002/anie.200705624)
134. Addis D, Shaikh N, Zhou S, Das S, Junge K, Beller M (2010) *Chem Asian J* 5:1687. doi:[10.1002/asia.201000064](https://doi.org/10.1002/asia.201000064)
135. Zhou S, Fleischer S, Junge K, Das S, Addis D, Beller M (2010) *Angew Chem Int Ed* 49:8121. doi:[10.1002/anie.201002456](https://doi.org/10.1002/anie.201002456)
136. Sui-Seng C, Freutel F, Lough AJ, Morris RH (2008) *Angew Chem Int Ed* 47:940. doi:[10.1002/anie.200705115](https://doi.org/10.1002/anie.200705115)
137. Mikhailine A, Lough AJ, Morris RH (2009) *J Am Chem Soc* 131:1394. doi:[10.1021/ja809493h](https://doi.org/10.1021/ja809493h)
138. Lagaditis PO, Lough AJ, Morris RH (2010) *Inorg Chem* 49:10057. doi:[10.1021/ic101366z](https://doi.org/10.1021/ic101366z)
139. Meyer N, Lough AJ, Morris RH (2009) *Chem Eur J* 15:5605. doi:[10.1002/chem.200802458](https://doi.org/10.1002/chem.200802458)
140. Sonnenberg JF, Coombs N, Dube PA, Morris RH (2012) *J Am Chem Soc* 134:5893. doi:[10.1021/ja211658t](https://doi.org/10.1021/ja211658t)
141. Mikhailine AA, Maishan MI, Lough AJ, Morris RH (2012) *J Am Chem Soc* 134:12266. doi:[10.1021/ja304814s](https://doi.org/10.1021/ja304814s)
142. Mikhailine AA, Maishan MI, Morris RH (2012) *Org Lett* 14:4638. doi:[10.1021/ol302079q](https://doi.org/10.1021/ol302079q)
143. Sues PE, Lough AJ, Morris RH (2011) *Organometallics* 30:4418. doi:[10.1021/om2005172](https://doi.org/10.1021/om2005172)
144. Zuo W, Lough AJ, Li YF, Morris RH (2013) *Science* 342:1080. doi:[10.1126/science.1244466](https://doi.org/10.1126/science.1244466)

145. Lagaditis PO, Lough AJ, Morris RH (2011) *J Am Chem Soc* 133:9662. doi:[10.1021/ja202375y](https://doi.org/10.1021/ja202375y)
146. Lagaditis PO, Sues PE, Sonnenberg JF, Wan KY, Lough AJ, Morris RH (2014) *J Am Chem Soc* 136:1367. doi:[10.1021/ja4082233](https://doi.org/10.1021/ja4082233)
147. Zuo W, Tauer S, Prokopchuk DE, Morris RH (2014) *Organometallics* 33:5791. doi:[10.1021/om500479q](https://doi.org/10.1021/om500479q)
148. Bigler R, Mezzetti A (2014) *Org Lett* 16:6460. doi:[10.1021/ol503295c](https://doi.org/10.1021/ol503295c)
149. Hoyt JM, Shevlin M, Margulieux GW, Krska SW, Tudge MT, Chirik PJ (2014) *Organometallics* 33:5781. doi:[10.1021/om500329q](https://doi.org/10.1021/om500329q)
150. Yamashita Y, Ueno M, Kuriyama Y, Kobayashi S (2002) *Adv Synth Catal* 344:929. doi:[10.1002/1615-4169\(200210\)344:9<929::aid-adsc929>3.0.co;2-z](https://doi.org/10.1002/1615-4169(200210)344:9<929::aid-adsc929>3.0.co;2-z)
151. Nagataki T, Tachi Y, Itoh S (2005) *J Mol Catal A: Chem* 225:103. doi:[10.1016/j.molcata.2004.08.032](https://doi.org/10.1016/j.molcata.2004.08.032)
152. Muthupandi P, Alamsetti Santosh K, Sekar G (2009) *Chem Commun*: 3288.
153. Yang L, Zhu Q, Guo S, Qian B, Xia C, Huang H (2010) *Chem Eur J* 16:1638. doi:[10.1002/chem.200902705](https://doi.org/10.1002/chem.200902705)
154. Nakamura M, Hirai A, Nakamura E (2000) *J Am Chem Soc* 122:978. doi:[10.1021/ja983066r](https://doi.org/10.1021/ja983066r)
155. Nakamura E, Yoshikai N (2010) *J Org Chem* 75:6061. doi:[10.1021/jo100693m](https://doi.org/10.1021/jo100693m)
156. Berkessel A, Reichau S, von der Hoeh A, Leconte N, Neudorff J-M (2011) *Organometallics* 30:3880. doi:[10.1021/om200459s](https://doi.org/10.1021/om200459s)
157. Zhou S, Fleischer S, Junge K, Beller M (2011) *Angew Chem Int Ed* 50:5120. doi:[10.1002/anie.201100878](https://doi.org/10.1002/anie.201100878)
158. Suginome M, Fu GC (2000) *Chirality* 12:318. doi:[10.1002/\(sici\)1520-636x\(2000\)12:5<318::aid-chir4>3.0.co;2-9](https://doi.org/10.1002/(sici)1520-636x(2000)12:5<318::aid-chir4>3.0.co;2-9)
159. Wurz RP, Lee EC, Ruble JC, Fu GC (2007) *Adv Synth Catal* 349:2345. doi:[10.1002/adsc.200700219](https://doi.org/10.1002/adsc.200700219)
160. Dosa PI, Ruble JC, Fu GC (1997) *J Org Chem* 62:444. doi:[10.1021/jo962156g](https://doi.org/10.1021/jo962156g)
161. Ruble JC, Fu GC (1996) *J Org Chem* 61:7230. doi:[10.1021/JO961433G](https://doi.org/10.1021/JO961433G)
162. Garrett CE, Fu GC (1998) *J Am Chem Soc* 120:7479. doi:[10.1021/ja981061o](https://doi.org/10.1021/ja981061o)
163. Hills ID, Fu GC (2003) *Angew Chem Int Ed* 42:3921. doi:[10.1002/anie.200351666](https://doi.org/10.1002/anie.200351666)
164. Liang J, Ruble JC, Fu GC (1998) *J Org Chem* 63:3154. doi:[10.1021/JO9803380](https://doi.org/10.1021/JO9803380)
165. Lee EC, McCauley KM, Fu GC (2007) *Angew Chem Int Ed* 46:977. doi:[10.1002/anie.200604312](https://doi.org/10.1002/anie.200604312)
166. Schaefer C, Fu GC (2005) *Angew Chem Int Ed* 44:4606. doi:[10.1002/anie.200501434](https://doi.org/10.1002/anie.200501434)
167. Lee EC, Hodous BL, Bergin E, Shih C, Fu GC (2005) *J Am Chem Soc* 127:11586. doi:[10.1021/ja052058p](https://doi.org/10.1021/ja052058p)
168. Hu B, Meng M, Wang Z, Du W-T, Fossey JS, Hu X-Q, Deng W-P (2010) *J Am Chem Soc* 132:17041. doi:[10.1021/ja108238a](https://doi.org/10.1021/ja108238a)
169. Khiar N, Fernandez I, Alcludia F (1993) *Tetrahedron Lett* 34:123. doi:[10.1016/s0040-4039\(00\)60073-4](https://doi.org/10.1016/s0040-4039(00)60073-4)
170. Gilani M, Wilhelm R (2008) *Tetrahedron: Asymmetry* 19:2346. doi:[10.1016/j.tetasy.2008.10.011](https://doi.org/10.1016/j.tetasy.2008.10.011)
171. Cai Y, Liu X, Zhou P, Kuang Y, Lin L, Feng X (2013) *Chem Commun* 49:8054. doi:[10.1039/c3cc44421j](https://doi.org/10.1039/c3cc44421j)
172. Naik A, Maji T, Reiser O (2010) *Chem Commun* 46:9265. doi:[10.1039/c0cc00508h](https://doi.org/10.1039/c0cc00508h)
173. Wu H, Wang B, Liu H, Wang L (2011) *Tetrahedron* 67:1210. doi:[10.1016/j.tet.2010.11.091](https://doi.org/10.1016/j.tet.2010.11.091)
174. Karthikeyan P, Muskawar PN, Aswar SA, Sythana SK, Bhagat PR (2013) *J Mol Catal A: Chem* 379:333. doi:[10.1016/j.molcata.2013.08.029](https://doi.org/10.1016/j.molcata.2013.08.029)

Molecular Iron-Based Oxidants and Their Stoichiometric Reactions

David P. de Sousa and Christine J. McKenzie

Abstract Molecular iron-based oxidants can oxidize organic substrates under relatively mild conditions, sometimes even in water. If these reactions can be converted to catalytic protocols, they hold great promise for the development of greener methods for this particularly messy class of reaction. For application in organic synthesis, the biggest question is: How selective can the reactions be? The supporting ligands in these compounds are crucial for tuning the electronic structure of a catalytically competent iron-based oxidant and its selectivity in terms of the production of a single, even enantiopure, product. A thorough understanding of the stoichiometric generation of molecular iron-based oxidants and their subsequent reactivity is an important step for the development of new iron-based catalysts. Ideally, and in analogy to many of nature's iron-based enzymes, their regeneration under catalytic conditions could involve the activation of dioxygen from air. This chapter will focus on the stoichiometric reactions of iron compounds with potential oxidizing agents including O₂, peroxides, oxygen-atom donor reagents, and even water, to form iron-based oxidizing species and the reactions of these usually very transient species with oxidizable substrates. This chapter might be especially inspiring for researchers in the field of iron catalyst design.

Keywords Bioinspired · C–H activation · Epoxidation · High-valent iron · Nonheme iron · O₂ activation · Oxidant activation · Sulfoxidation

Contents

1 Trends in the Use of Iron in Catalysis	312
2 Iron-Based Oxidations and Iron-Oxidant Species	313

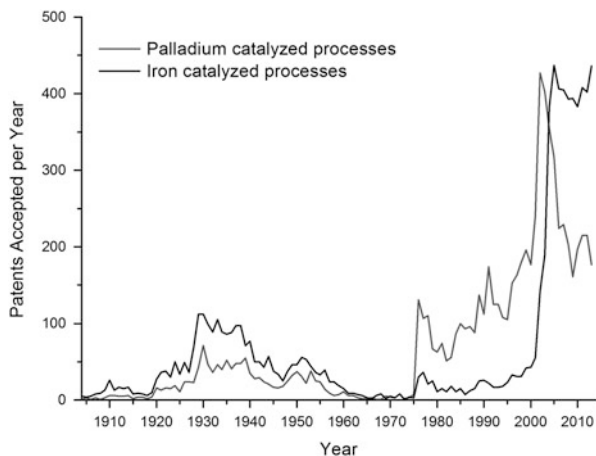
D.P. de Sousa and C.J. McKenzie (✉)
Department of Physics, Chemistry and Pharmacy, University of Southern Denmark, Odense,
Denmark
e-mail: mckenzie@sdu.dk

3	Iron in Biological Oxidations	316
4	Activation of Dioxygen by Biomimetic Iron Complexes	321
4.1	Reactions of Iron(III)-Substrate Adducts with Dioxygen	321
4.2	Binding of Dioxygen to Iron(II) Complexes	323
5	Nucleophilic Reactions of Iron Peroxide Adducts	327
5.1	Reactions with Aldehydes	329
5.2	Hydroxylation of Alkanes and Aromatic Compounds	330
6	Electrophilic Reactions of Iron-Oxo Intermediates	333
6.1	High-Valent Nonheme Iron(IV)-Oxo Complexes	334
6.2	Iron(V)Oxo and Iron(IV)Oxo-(Oxidized Radical Ligand) Complexes	337
7	Halogenation Reactions of Iron-Halide and Iron-Hypohalide Adducts	341
8	Electrophilic Reactions of Iron-Nitrido and Iron-Imido Intermediates	345
9	Intramolecular Ligand Oxidations	348
10	Conclusions and Outlook	351
	References	352

1 Trends in the Use of Iron in Catalysis

Transition metal catalysts are mainstays in modern chemistry and essential in all parts of the production chain that transforms the simple molecular building blocks provided by crude oil and agricultural feedstock into the fine chemicals, pharmaceuticals, polymers, and other advanced materials, on which we are so reliant. For the large part, the catalysts in use today are based on second and third row “coinage” metals like Ru, Rh, Pd, Pt, and Au, with their main applications in hydrogenations and carbon–carbon and carbon–heteroatom coupling reactions. With the prices for these metals already being high and only rising [1], the more abundant and cheap first row metals and even biologically tolerated metals, like manganese and iron, are in focus. The number of patents filed (Fig. 1) clearly reflect a trend. The apparent renaissance for iron represents a transition from

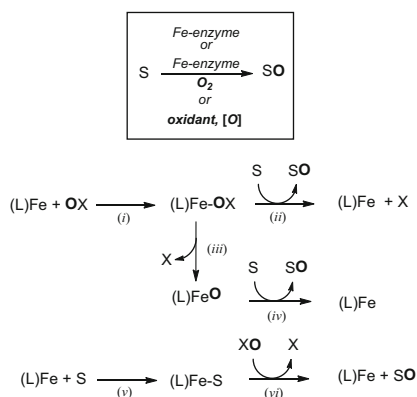
Fig. 1 Historical development in the number of patents involving iron and palladium catalyzed processes. Data extracted from the Reaxys database by searches for patents wherein the keywords iron/Fe and palladium/Pt occur categorized as catalysts



heterogeneous iron oxide catalysts, like that used in the ever so important Haber Bosch process, to an exploitation of the molecular chemistry of iron, a realm in which this particular element quite possibly offers more possible spin states, coordination numbers, and geometries than any other in the periodic table. A multitude of catalytic applications should be within our grasp if we can discover and develop the chemistry. Still, while iron is making its entrance into the catalysis of alkylations, acylations, hydrogenations, and cross-coupling reactions – largely as a replacement for the more expensive second row metals – there is still an area in which iron (and manganese for that matter) has the potential to fill a gap where catalysts traditionally have only rarely been employed – the area of oxidation catalysis.

2 Iron-Based Oxidations and Iron-Oxidant Species

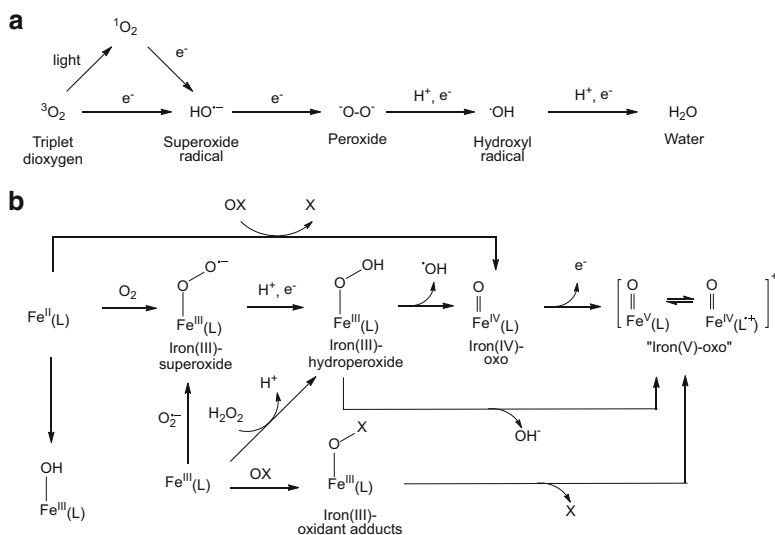
Iron complexes are capable of facilitating and accelerating the otherwise slow or kinetically hindered oxidation of a multitude of organic functional groups using a wide variety of oxidation agents. The way in which iron complexes “(L)Fe” achieve this is by activating either the oxidizing agent “[OX]” or the substrate “S”. This is generally facilitated by coordination to the iron center (Scheme 1) steps (i) and (v). Initially an iron-oxidant adduct, “(L)FeOX”, or an iron-substrate adduct, “(L)FeS”, is formed. In principle, all oxidation agents capable of coordinating to iron can be activated by forming (L)FeOX-type adducts. The iron-oxidant species, (L)FeOX, can either itself be the active oxidizing species, step (ii), or the iron center can induce either a heterolytic or homolytic cleavage of the oxidant O–X bond, step



Scheme 1 The bare bones of iron-promoted oxidations. The equation at the top is a commonly encountered and uninformative, general representation for a catalytic oxidation reaction. On the bottom, the “stoichiometric” iron-centric perspective showing generalized reactions with oxidants (steps i–vi) and substrates (steps v–vi). S = substrate, SO = oxidized substrate, and (L)Fe = a general formulation for a combination of ligand(s) and iron atom(s)

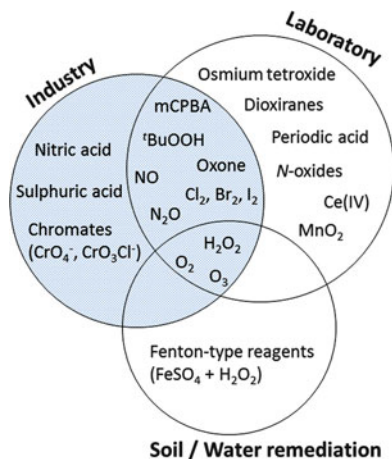
(iii), to form a highly oxidized iron-oxo species “(L)FeO” which is then capable of acting as the direct oxidant, step (iv). The processes in steps (i)–(iv) are iron-based oxidations, and in this respect quite different from oxidations carried out by oxygen- or carbon-based radicals. However, as detailed in Scheme 2, organic radicals can also be generated in the presence of paramagnetic metal ions, and oxidation processes effected by these radicals, can, depending on the oxidant, be rather difficult to separate from the metal-based processes.

The above scheme should not imply that it is requisite for an iron-based oxidant to be mononuclear or that there is only one supporting ligand “L”. It is, however, most likely true that the presence of fewer supporting ligands will predispose the system to less complicated solution speciation. Chelating multidentate ligands have intrinsically high binding constants and are expected to support metal complexes that are more robust. This is important since stability is a key factor when working under harsh oxidizing conditions. But therein lies a dichotomy, we need simultaneous stability and reactivity. Electronic, steric, and topological features are induced by the ligand(s), and this will be reflected in the iron complex in terms of activity, selectivity, or stability [2]. Multidentate ligands furnish a greater possibility of some control over the resultant complex topology compared with mono- and bidentate ligands. Especially designing complexes that are capable of activating the benign oxidants dioxygen and hydrogen peroxide, for their application in controlled



Scheme 2 (a) Dioxygen and its reduced forms. (b) Analogous iron(II)/ O_2 and iron(III)/oxidant chemistry. L = generic ligand(s), $\text{O}_2^{\cdot-}$ (e.g., KO_2), OX = generic oxidant, and X the congener reduced species. The iron complexes may have an overall charge; this depends on the L used and is not depicted here

Fig. 2 Commonly encountered oxidizing agents



and catalytic oxidation of organic molecules, remains a long-standing goal within the area of catalysis and biomimetic chemistry [2–4].

Common oxidizing agents and their main fields of use are depicted in Fig. 2. Interestingly, the most environmentally friendly oxidants with the intrinsically best atom economies (dioxygen, hydrogen peroxide, and ozone) are also the only ones whose use transverses all three domains of applied oxidation chemistry. Dioxygen and hydrogen peroxide are some of the relatively least hazardous oxidants in terms of explosion risk – a serious consideration in large-scale production settings [5]. Another attractive oxidizing/oxygenating agent, and perhaps one that is not very obvious, is water. Iron can activate water by coordination. Subsequent proton-coupled electron transfers (PCETs) can produce strongly oxidizing iron-oxo species, (L)FeO.

Well known is the prominent role of iron in biology as an essential cofactor in enzymes and proteins that bind and activate dioxygen. The example *par excellence* is hemoglobin – the protein that keeps us all alive by chemisorbing dioxygen from the air and delivering it to our tissues. A change in the endogenous donor, from histidine to cysteine, converts the reversible O_2 binding Fe-heme site into an O_2 activating site and consequently enables it to perform enzymatic oxidation catalysis.

The binding of dioxygen by iron(II) compounds is a good starting point for delving into the way in which various iron-based oxidant adducts, (L)FeOX, and iron-oxo species, (L)FeO, are generated. Dioxygen can be viewed as the fully oxidized precursor from which most oxygen-containing oxidation agents are derived. A basic overview of the activation of dioxygen and its reduced counterparts by iron is presented in Scheme 2. The scheme is simplified and crude but is useful in introducing the molecular O_2 and iron-oxido chemistry. To highlight the connection, free radical oxygen species are drawn above their iron counterparts. One important feature distinguishes the two types of species. While the reactivity of the free radicals is diffusion controlled and generally

occurs through radical-chain-based mechanisms giving rise to statistical mixtures of products [6], the iron-oxidant intermediates are potentially able to act as much more selective oxidants, principally through metal-based oxidation steps. Many analogies can be drawn to the reactivity of stoichiometric organic oxidants like 2-iodoxybenzoic acid [7, 8] and *meta*-chloroperoxybenzoic acid (*m*CPBA) [9]. However, while it is often difficult to transform systems based on stoichiometric organic oxidants into catalytically viable systems, the changes needed for converting a stoichiometric metal-based system into a catalytic one are often much smaller and easier to effect. Likewise, as discussed above, the introduction of a ligand offers a versatile synthetic handle for tuning the electronic and steric properties of the complex and its reactivity (Fig. 3).

3 Iron in Biological Oxidations

It is always good to take a look at the biological world to see if there are any biochemical processes worth mimicking. A large range of heme and nonheme iron enzymes are capable of carrying out a plethora of oxidation reactions. These include mono- and dioxygenations; hydroxylations; oxidative ring-closure reactions; cleavage reactions like C, N, S, and O-dealkylations; and oxidative halogenations [10–16]. Thus, nature does indeed furnish several iron-based oxidants, from which we can draw inspiration.

One of the most versatile iron-enzyme classes, capable of oxidizing a wide range of substrates using dioxygen as the terminal oxidant, are the cytochrome P450 enzymes (Fig. 4c). These enzymes employ an active site consisting of an iron(III)-porphyrin complex (aka heme site) often coordinated axially to a strongly donating cysteine residue (Fig. 4a). The details of the catalytic cycle (Fig. 4b) are very thoroughly studied, and spectroscopic evidence exists, often as a result of the study of stoichiometric reactions, for *all* of the proposed catalytic intermediates [15–19]. Here the catalytic hydroxylation of a hydrocarbon substrate provides an instructive example of how activation of oxygen can be achieved. The quaternary protein structure and the location of the enzyme largely determine the substrate selection; however, P450s can be promiscuous. Indeed the metabolism of substrates by this enzyme is so important that new drugs and prodrugs must be subjected to P450 activity studies. The first step (i) in the catalytic cycle (Fig. 4b) is the reduction of the active iron(III) resting state, Fe^{III}(heme). The iron(II) species formed is susceptible towards oxidative addition by dioxygen, step (ii), which leads to the formation of an iron(III)-superoxide intermediate. This intermediate is then reduced to an iron(III)-hydroperoxide adduct which is cleaved homolytically to release water and give a two-electron-oxidized species, Fe^{IV}O(heme⁺), step (iii). The redox non-innocence of the aromatic heme ligand means that the iron center is not forced to store both of the two generated oxidizing equivalents. Here, the porphyrin macrocycle accommodates one of the oxidizing equivalents by forming a π -radical anion, while the iron center accommodates the other oxidizing

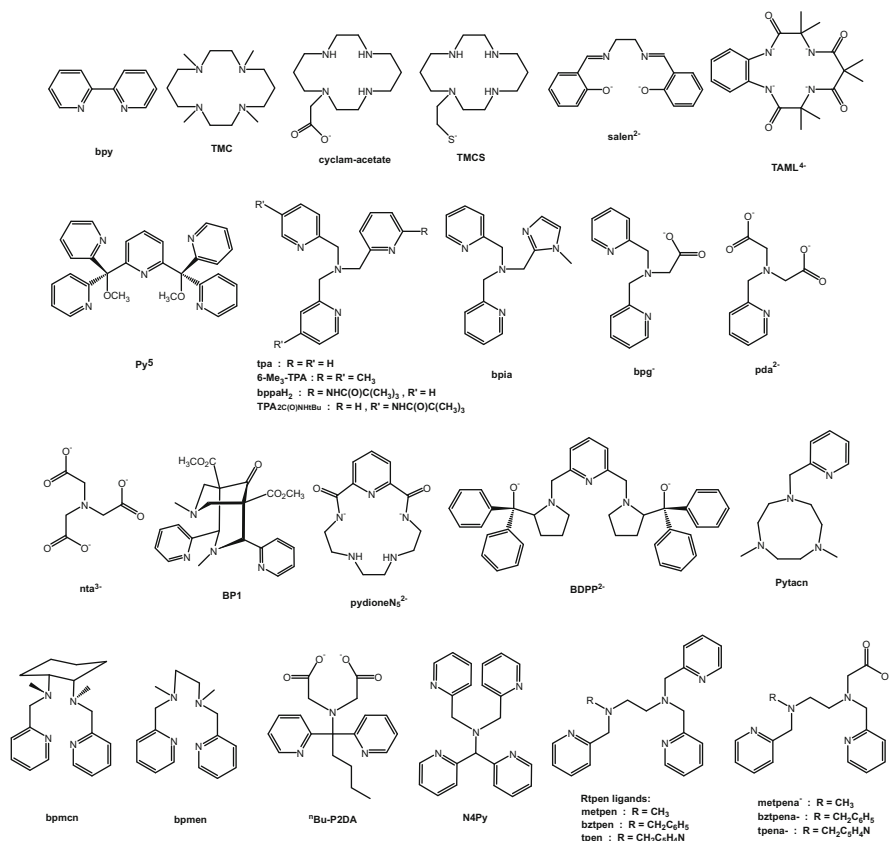


Fig. 3 Overview of commonly encountered ligands. Abbreviations: bpy=2,2'-bipyridine; TMC=1,4,8,11-tetramethyl-1,4,8,11-tetraazacyclotetradecane; salenH₂=*N,N'*-bis(salicylidene) ethylenediamine; cyclam-acetate=1,4,8,11-tetraazacyclotetradecane-1-acetate; TMCS=1-mercaptoethyl-1,4,8,11-tetraazacyclotetradecane; H₄TAML=tetraamido macrocyclic ligand; Py5=2,6-bis(methoxy(di(2-pyridyl)methyl)pyridine); tpa=tris(2-pyridylmethyl)amine; 6-Me₃-TPA=tris(6-methyl-2-pyridylmethyl)amine; bppa=bis(6-pivalamide-2-pyridylmethyl)-(2-pyridylmethyl)amine; TPA^{2C(O)NHtBu}=6,6'-(pyridine-2-ylazanediy)bis(methylene)bis(*N*-tert-butylpicolinamide)picolyl)amine; bpia⁻=bis(2-pyridylmethyl)-1-methylimidazylmethyl)amine; bpg⁻=bis(2-pyridylmethyl)iminodiacetate; pda²⁻=(2-pyridylmethyl)iminodiacetate; nta³⁻=nitritoacetate; BP1 = 3,7-dimethyl-9-oxo-2,4-bis(2-pyridyl)-3,7-diazabicyclo[3.3.1]nonane-1,5-dicarboxylate methyl ester; H₂pydioneN₅ = 3,6,9,12,18-pentaazabicyclo[12.3.1]octadeca-1(18), 14,16-triene-2,13-dione; H₂BDPP = 2,6-bis(2-(diphenylhydroxylmethyl)-1-pyridylmethyl)pyridine; Pytacn = 1-(2'-pyridylmethyl)-4,7-dimethyl-1,4,7-triazacyclononane; bpmn = *N,N'*-bis(2-pyridylmethyl)-*N,N'*-dimethylethylenediamine (also known as bispicMe₂en); bpmcn = *N,N'*-bis(2-pyridylmethyl)-*N,N'*-dimethyl-trans-1,2-diaminocyclohexane; ^tBu-P2DA = *N*-(1',1'-bis(2-pyridyl)pentyl)iminodiacetate; N₄Py = *N,N*-bis(2-pyridylmethyl)-*N*-bis(2-pyridyl)methylamine; metpen = *N*-methyl-*N,N',N'*-tris(2-pyridylmethyl)ethylenediamine (also known as trispicMeen); bztpen = *N*-benzyl-*N,N',N'*-tris(2-pyridylmethyl)ethylenediamine; tpen = *N,N,N',N'*-tetrakis(2-pyridylmethyl)ethylenediamine; mebpna⁻ = *N*-methyl-*N',N'*-bis(2-pyridylmethyl)ethylenediamine-*N'*-acetate; bzbpna⁻ = *N*-benzyl-*N,N'*-bis(2-pyridylmethyl)ethylenediamine-*N'*-acetate; tpena⁻ = *N,N',N'*-tris(2-pyridylmethyl)ethylenediamine-*N'*-acetate

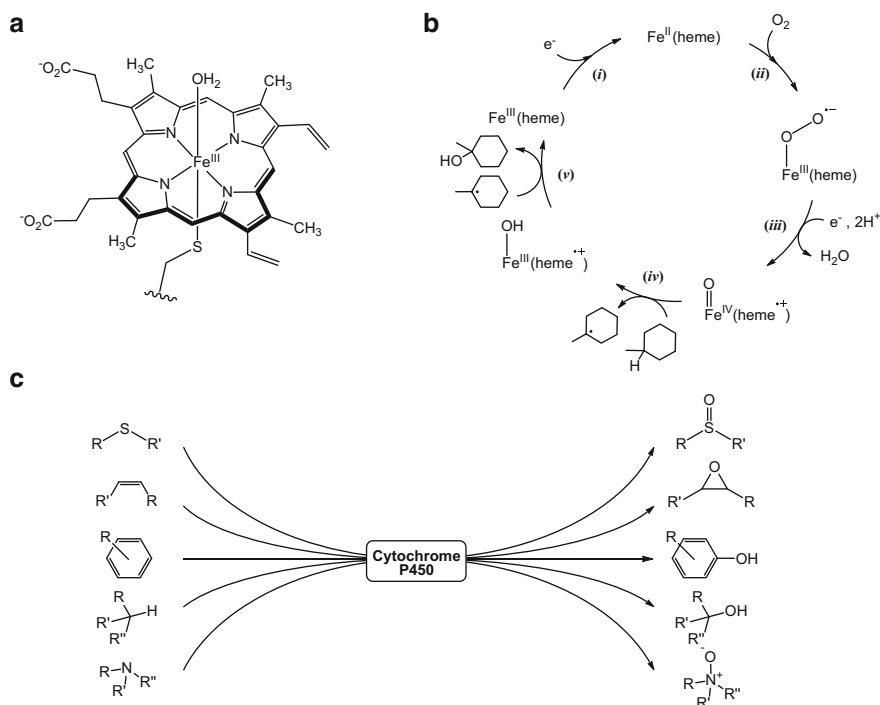
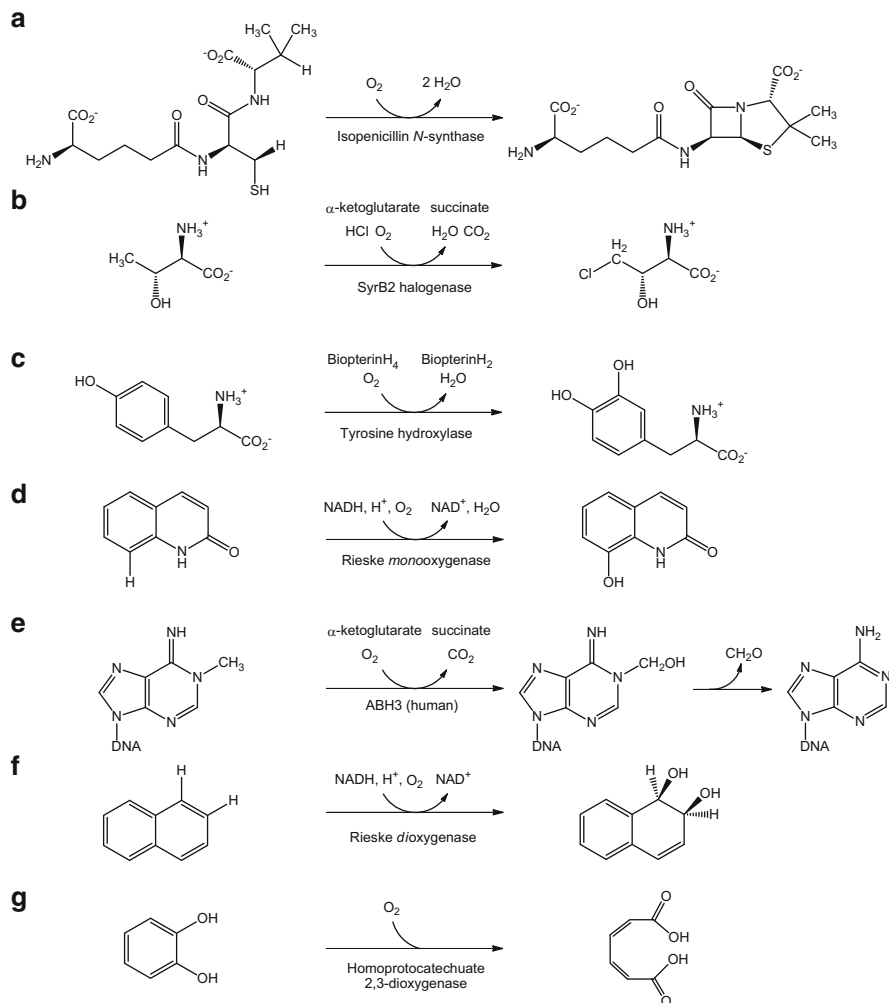


Fig. 4 (a) Active site of the monooxygenating enzyme cytochrome P450 showing its heme B-thiolate cofactor. (b) The iron speciation throughout the catalytic cycle. (c) Overview of the reactions of cytochrome P450 and peroxidase P450 enzymes

equivalent, forming an iron(IV)-oxo species. The iron-oxo intermediate has radical character and is therefore a powerful hydrogen abstractor, capable of removing hydrogens from unactivated C–H bonds, step (iv). Doing so, an iron(III)-hydroxide species and a carbon-based radical are formed. The carbon radical rebounds and abstracts the hydroxide group from the iron center, step (v), which leads to the reformation of the iron(III) active resting state and the release of a hydroxylated substrate.

Besides the O_2 -metabolizing heme enzymes, there exists a diverse class of heme enzymes, the peroxidases, capable of utilizing H_2O_2 as terminal oxidant. The other general class of iron enzymes is the nonheme iron enzymes [10–12, 14]. As their name implies, the nonheme enzymes do not employ a heme cofactor in their active sites. Rather the iron atom or atoms are bound directly by amino acid side chains like histidine, aspartate, glutamate, asparagine, cysteine, tyrosine, and other cofactors (e.g., sacrificial reductants or inorganic species like water or hydroxide, carbonate, and NO). These enzymes make for a rather diverse class of oxidoreductases, capable of utilizing O_2 as a terminal oxidant in the oxidation of a wide range of substrates. Some of the reactions carried out by nonheme iron enzymes are summarized in Scheme 3.



Scheme 3 Oxidations catalyzed by nonheme iron enzymes. Oxidases: (a) biosynthesis of penicillin, (b) chlorination of *L*-threonine. Monooxygenases: (c) hydroxylation of *L*-tyrosine by an aromatic amino acid hydroxylase to give *L*-DOPA, (d) hydroxylation of 2-oxoquinoline, (e) oxidative dealkylation of methylated DNA. Dioxygenases: (f) *cis*-dihydroxylation of naphthalene, (g) oxidative ring-opening of catechol

These reactions, in themselves, or as prototypes, are of great interest to organic chemists. Some of the steps are feasible through conventional synthesis. However, in contrast to the chemical processes, no large amounts of toxic waste are generated in the biological processes. Furthermore, while nature carries out easily 100% enantioselective oxidations, we are still a far cry from mastering this in the laboratory. One has only to examine the world of natural products to find an abundance of examples of advanced enantiopure molecules that cannot be

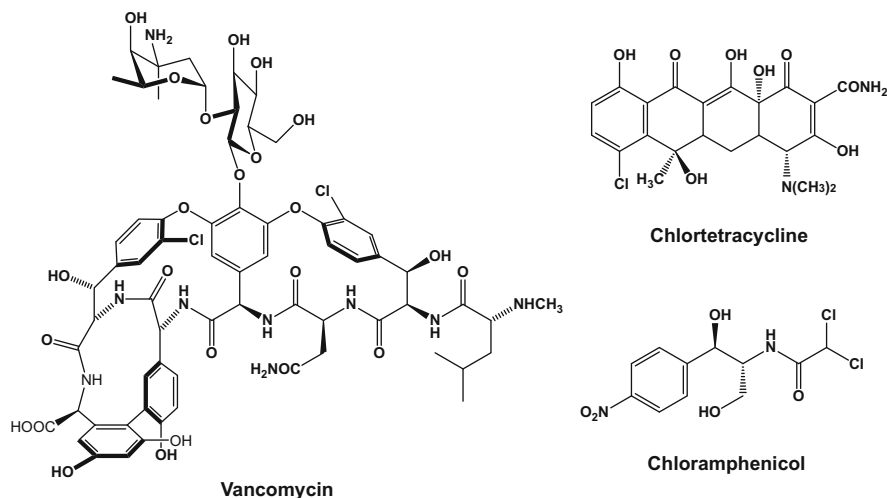


Fig. 5 Examples of natural chlorinated antibiotics

synthesized in the laboratory. Many naturally occurring antibiotics contain chloride atoms which have been inserted regio- and enantioselectively into both aliphatic and aromatic compounds at some stage during their biosynthesis. Some examples are provided in Fig. 5. A case in point is the synthesis of the Parkinson's drug L-DOPA. The industrial synthesis achieves chirality through the only tool available to the synthetic chemist – asymmetric reductive hydrogenation of a pro-chiral alkene [20] which was ultimately derived from vanillin via several prior steps. This last reaction step is carried out with 95% ee, which by all standards is an impressive feat. However, when we compare this process with the biosynthesis of L-DOPA occurring in our brains, a radically different approach is found, with the target compound being synthesized through a series of oxidations. The amino acid phenylalanine is converted to tyrosine, which is then converted to L-DOPA (Scheme 3c). L-DOPA in turn is a substrate for further oxidation reactions by which other important hormones and neurotransmitters are biosynthesized. In these reactions, dioxygen is the oxidant and the by-product is water. The requisite electron donors listed above the arrows can all be regenerated.

The production of epoxides and aziridines is a reaction of great interest in the chemical sciences. These ring-strained compounds are very susceptible to attack by nucleophilic reagents giving ring-opened substituted products and are thus versatile reaction intermediates in multistep syntheses. Likewise, a range of naturally occurring pharmaceuticals contain epoxide rings [21]. One is the cardiovascular drug eplerenone (Fig. 6). In nature, the epoxide group is usually derived from the epoxidation of a double bond by cytochrome P450, as depicted in Fig. 4. Another reaction, relatively uncommon in nature, is the monooxygenation and S-alkylation of sulfides. Several prominent pharmaceuticals and many drug leads contain a sulfoxide or a sulfonamide group. Examples of sulfoxide drugs include the

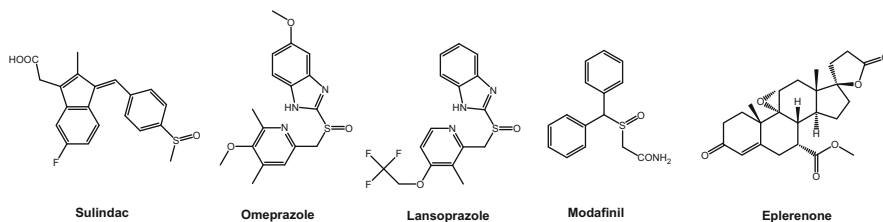


Fig. 6 Examples of pharmaceuticals containing a sulfoxide or an epoxide group

nonsteroid anti-inflammatory drug sulindac, the antiulcer agents omeprazole and lansoprazole, and the performance-enhancing drug modafinil [22, 23] (Fig. 6).

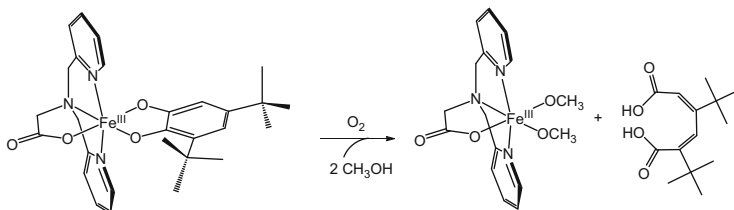
In the following sections, we will dissect the mechanisms of iron-mediated oxidation catalysis by examining the stoichiometric reactions of stable iron complexes which function as pre-catalysts, derived iron-oxidant adducts, and high-valent iron-oxo species. In recent years, several highly reactive iron-oxidant adducts and iron-oxo species have been “caught” and characterized using a battery of spectroscopic and physical methods. We will cover many of the characterization and reactivity studies and attempt to decipher the implications in terms of how the reactivity is modulated by the molecular and electronic structure of the complexes. In other words, we will examine catalysis from the point of view of the catalyst.

4 Activation of Dioxygen by Biomimetic Iron Complexes

4.1 Reactions of Iron(III)-Substrate Adducts with Dioxygen

As depicted in Scheme 2b, iron complexes can in principle activate dioxygen directly by its oxidative addition to the iron center. However, for substrates capable of coordinating to a metal center, an equally viable alternative exists: activation of the substrate. Through partial charge transfer, the coordinated substrate assumes radical character which predisposes it to attack by triplet O_2 . As we shall see in this and the next section, sometimes both oxygen activation and substrate activation processes are involved in the actual oxidation.

The enzyme homoprotocatechuate 2,3-dioxygenase (Scheme 3g) uses such a hybrid strategy to oxidize catechols to the corresponding dicarboxylic acids. Homoprotocatechuate 2,3-dioxygenase is part of the larger class of nonheme iron (III) intradiol-cleaving dioxygenases. In a series of papers some 15 years ago, Que and coworkers addressed the question of how these enzymes activate the metal-bound substrates towards O_2 [24–26] and in the process uncovered vital information regarding the influence of the ligand sphere on the O_2 reactivity. They prepared a series of heteroleptic biomimetic iron(III)-catecholato complexes using the tetradentate tripodal ligands tpa, bpia, bpg[−], pda^{2−}, and nta^{3−} (Fig. 3) and the



Scheme 4 Dioxygenation of 3,5-di-*tert*-butylcatechol (DBC) coordinated to an iron(III) center in $[\text{Fe}^{\text{III}}(\text{bpg})(\text{DBC})]$ by dioxygen

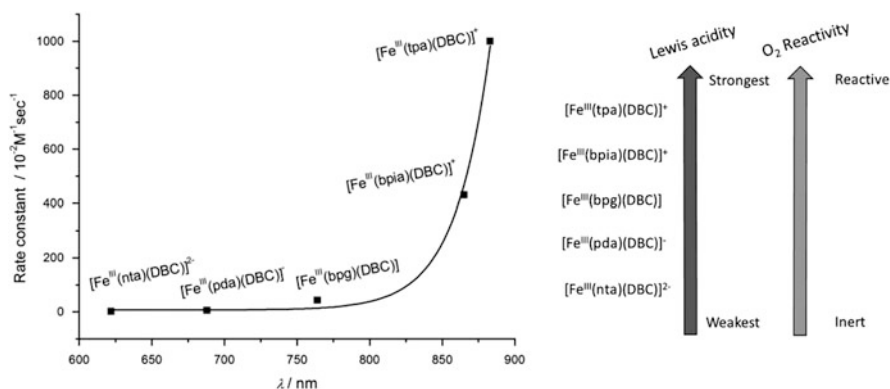
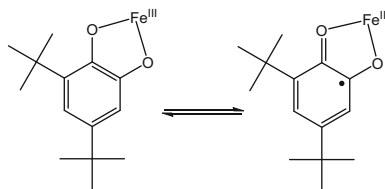


Fig. 7 Relationship between the oxygenation rates measured in methanol and the wavelength of LMCT absorption of the starting complexes in methanol. Included in the series is the $[\text{Fe}(\text{bpia})(\text{DBC})]^{+}$ complex of Krebs *and coworkers* [24]

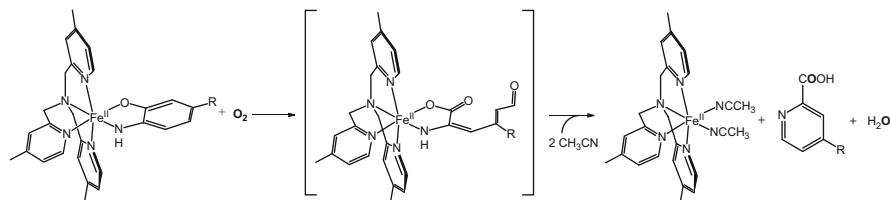
catechol 3,5-di-*tert*-butylcatechol (DBC). All the complexes are mononuclear, high spin ($S = 5/2$), and with the same general structure as $[\text{Fe}^{\text{III}}(\text{bpg})(\text{DBC})]$ depicted in Scheme 4. All complexes are air-sensitive, and if exposed to dioxygen, the coordinated catechol will spontaneously be oxidized to the corresponding ring-opened dicarboxylic acid, as illustrated in Scheme 4.

A dramatic increase in the oxygen reactivity is observed when going from the trianionic carboxylato ligand nta^{3-} to the neutral ligand tpa containing three pyridine donors. A strong and almost exponential correlation is observed between the reaction rate and the wavelength of the catecholato-to-iron(III) charge-transfer band of the complexes (Fig. 7). Phenolato-to-iron(III) charge-transfer bands are sensitive probes of the redox potential of the metal center, and a red-shift is an indicator of increased Lewis acidity of the metal center and, hence, a general decrease in the electron density at the iron center [27].

$^1\text{H-NMR}$ spectroscopy shows that in going from the carboxylato environment of $[\text{Fe}^{\text{III}}(\text{nta})(\text{DBC})]^{2-}$ to the pyridine environment of $[\text{Fe}^{\text{III}}(\text{tpa})(\text{DBC})]^{+}$, a progressive paramagnetic shift of the catecholato protons takes place as the iron(III)-DBC bonding becomes more covalent. This effects a “radicalization” (Scheme 5) of the



Scheme 5 Electronic conformers: iron(III)-catecholate and iron(II)-“semiquinolate.” The supporting tripodal ligand is not drawn



Scheme 6 Oxidation of iron-coordinated aminophenols

coordinated catechol which effectively eliminates the spin barrier for reaction with triplet O_2 [13] and provides rationale for why the complexes with the strongest Lewis acidity are those that react fastest with O_2 .

Newer work by Paine and coworkers from 2014 [28], aimed at modeling the recently discovered aminophenol dioxygenases, shows that analogous oxygenations occur for iron-coordinated aminophenols. When $[Fe^{II}(6\text{-Me}_3\text{-TPA})(\text{HAP})]^+$ type-complexes (HAP=4-methylaminophenol, 4,6-ditertbutylaminophenol or 4-nitroaminophenol) is exposed to dioxygen, the coordinated aminophenols are spontaneously oxidized to the corresponding ring-opened deoxygenated products. Subsequently these undergo spontaneous dehydrative ring closure to give the corresponding picolinic acids (Scheme 6). $^{18}O_2$ -labeling experiments verified that one of the oxygen atoms from molecular oxygen is incorporated into the cleavage products – just as expected.

It is clear that there is a great potential in these dioxygen insertion reactions. It is not unlikely that the substrate scope can be extended to practically any aromatic molecule containing two vicinal functional groups, as long as both groups are capable of coordinating to an iron center.

4.2 Binding of Dioxygen to Iron(II) Complexes

One question still remains: How do a dioxygen molecule and a coordinated substrate actually react with one another? Does dioxygen react directly with the substrate without iron being involved, i.e., is the role of iron that of a Lewis acid

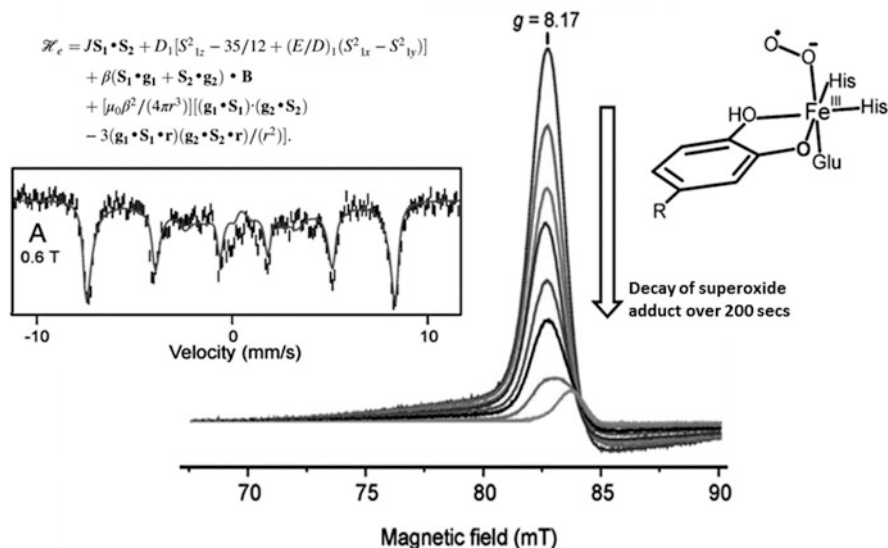
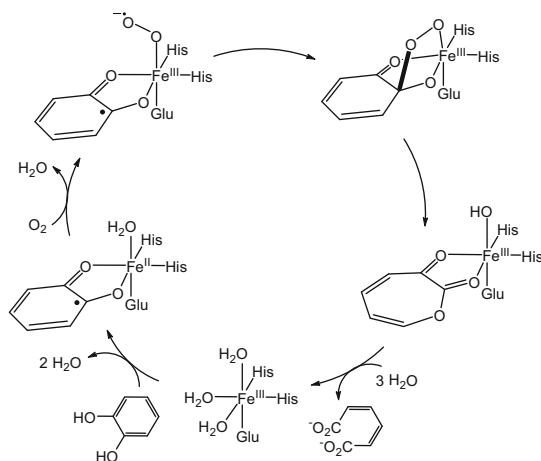


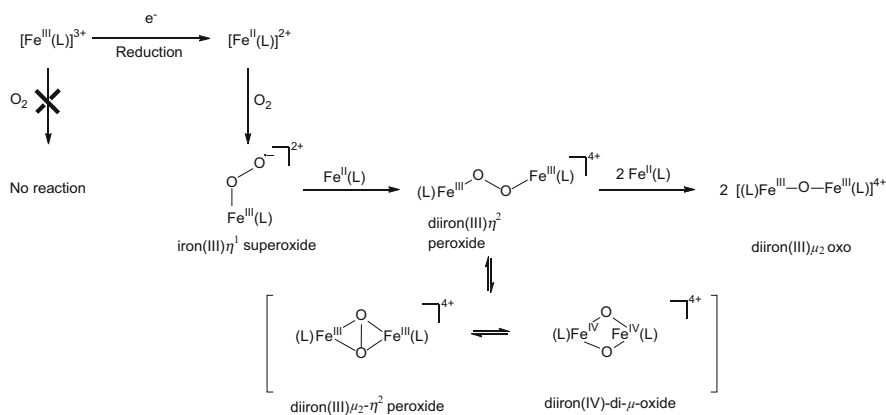
Fig. 8 A trapped iron(III)-superoxide enzymatic intermediate. On the left side is the frozen solution Mössbauer spectrum recorded in an applied magnetic field and its best fit superimposed as solid curve. On the right side is the solution state EPR spectrum recorded at 4°C showing the gradual decay of the superoxide adduct. Modified from Mbughuni et al. with permission from the National Academy of Sciences [32]

only? Or does dioxygen first coordinate to the iron atom to create an iron-superoxo intermediate, as introduced in Scheme 2, which then attacks the coordinated substrate? For heme systems, it is well established that O₂ can bind to the metal site in an “end-on” fashion, and crystal structures showing this arrangement for oxymyoglobin [29] and picked-fence porphyrin models [30, 31] have even been obtained. Recent work by Lipscomb and coworkers [32] provides clues as to how dioxygen is activated: When cooled anaerobic solutions of homoprotocatechuate 2,3-dioxygenase, saturated with substrate, are exposed to dioxygen, a short-lived intermediate is observed. By using a mutated enzyme, in the presence of the reagent 4-nitrocatechol, the intermediate can be trapped for several minutes. This enabled a thorough characterization by Mössbauer and Electron Paramagnetic Resonance (EPR) spectroscopies. The spectra are fitted satisfactorily with a spin Hamiltonian for a system consisting of two coupled paramagnetic centers. It can therefore be concluded that the transient species comprises of a high-spin iron(III) center ($S = 5/2$) antiferromagnetically coupled to a superoxide radical ($S = 1/2$) (Fig. 8). Thus, at least in the enzymatic case, there seems to be evidence for iron having a double role: It activates both substrate and oxidant. Scheme 7 gives an overview of the proposed catalytic cycle for the enzyme.

The kinetics of reactions of iron(II) complexes with dioxygen has been studied extensively [33]. In spite of this, until recently, the elusive Fe-superoxide adducts had only been detected for iron-porphyrin complexes [31]. Even when using



Scheme 7 Catalytic cycle for the intradiol catechol cleaving dioxygenases



Scheme 8 The reaction of iron(II) complexes with dioxygen. Here the superoxide ligand is shown coordinating in an “end-on” fashion. A “side-on” coordination mode is equally viable

cryogenic stopped-flow techniques (with temperatures as low as -40 and -90°C), the most commonly detected products are diiron(III)-peroxo-bridged species, $\text{Fe}(\text{III})-\text{O}-\text{O}-\text{Fe}(\text{III})$, Scheme 8. These dinuclear species are themselves also transient and decay to give diiron(III) oxo-bridged species (the coordination chemistry equivalent to rust) [33, 34] especially in protic solvents. The precursor iron (II) complexes can also be dinuclear, however, and only one of the iron centers is involved in the initial binding of dioxygen.

Four examples (besides the enzymatic intermediate) of plausible nonheme iron (III)-superoxide adducts exist in the literature. All of them have been generated in aprotic solvents. The earliest example was reported by Shan and Que in 2005 [35]. They exposed anaerobic dichloromethane solutions of the diiron

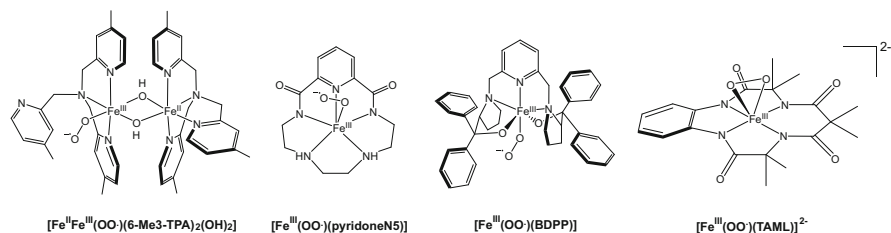
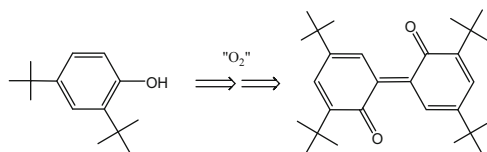


Fig. 9 Proposed iron(III)-superoxide adducts

(II) dihydroxo-bridged complex $[(6\text{-Me}_3\text{-TPA})\text{Fe}^{\text{II}}(\text{OH})_2\text{-Fe}^{\text{II}}(6\text{-Me}_3\text{-TPA})]$ (Fig. 3) to O_2 at -80°C and detected a green intermediate using UV-Vis spectroscopy. The species is only short-lived and quickly rearranges to a (relatively) more stable diiron(III)-peroxo-bridged species, as expected from Scheme 8. Frozen-solution resonance Raman experiments were carried out in the search for characteristic O–O and Fe–O stretches. When ^{18}O -labeled dioxygen was used, a shift in a resonance assigned to $\nu(\text{O}-\text{O})$ at $1,310\text{ cm}^{-1}$ to $1,231\text{ cm}^{-1}$ was observed. By comparing the result to similar O–O stretching frequencies observed for the better characterized iron(III)-heme-superoxo species, it can be concluded that the green species is a dinuclear iron-superoxo intermediate (Fig. 9). In 2007 Rybak-Akimova and coworkers [36] detected a short-lived mononuclear nonheme iron species by UV-Vis spectroscopy after exposing $[\text{Fe}^{\text{II}}(\text{pyridoneN5})]$ to O_2 at -40°C in a mixture of DMF/acetonitrile. This was tentatively formulated as the superoxo complex, $[\text{Fe}^{\text{III}}(\text{OO}^*)(\text{pyridoneN5})]$. This species has a half-life of around $\tau_{1/2} = 0.5\text{--}5\text{ s}$ before it reacts with a second $[\text{Fe}^{\text{II}}(\text{pyridoneN5})]$ to give the (relatively) more stable diiron(III)-peroxo-bridged species, $[(\text{pyridoneN5})\text{Fe}^{\text{III}}\text{-OO-Fe}^{\text{III}}(\text{pyridoneN5})]$. No other characterization besides optical spectroscopy was reported. Very recently (2014) Chiang et al [37] reported a possible mononuclear iron(III)-superoxide intermediate, $[\text{Fe}^{\text{III}}(\text{OO}^*)(\text{BDPP})]$, generated by bubbling O_2 through an anaerobic solution of the iron(II) precursor complex, $[\text{Fe}^{\text{II}}(\text{BDPP})]$. The intermediate proved difficult to analyze, with the complex being both EPR silent and displaying a messy Mössbauer spectrum together with an almost featureless resonance Raman spectrum. Not long after, however, Sastri and coworkers reported the crystal structure of $[\text{Fe}^{\text{III}}(\text{OO}^*)(\text{TAML})]^{2-}$ generated from the reaction of potassium superoxide with $[\text{Fe}^{\text{III}}(\text{TAML})]^-$. Interestingly, the O_2^{*-} moiety is coordinated not in an “end-on” fashion, but instead in a “side-on” fashion. To rule out that the species was not a Fe(III)-peroxide species, *vide infra*, magnetic susceptibility measurements, and Mössbauer spectroscopy were carried out. The magnetic studies reveal that the species consists of a $S = 3/2$ iron(III) center coupled antiferromagnetically to a $S = 1/2$ superoxide moiety. Solution-state infrared spectroscopy reveals a vibration at $1,260\text{ cm}^{-1}$ that shifted to $1,183\text{ cm}^{-1}$ upon exposure to K^{18}O_2 , cementing the Fe(III)-superoxo assignment.

The reactivity of $[\text{Fe}^{\text{III}}(\text{OO}^*)(\text{TAML})]^{2-}$ in stoichiometric reactions with various substrates has been tested [38]. No reactivity is observed towards aliphatic molecules with weak C–H bonds. The complex however does exhibit both electrophilic and nucleophilic properties and can both dehydrogenate activated

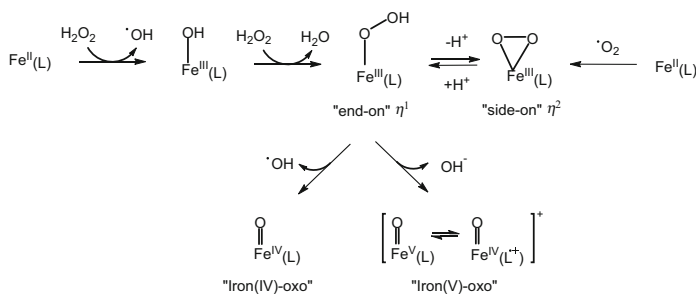


Scheme 9 Oxidation of 2,6-di-*tert*-butylphenols

2,6-di-*tert*-butylphenols while also being able to deformylate *para*-substituted 2-phenylpropionaldehydes in a nucleophilic fashion. The products of the methylaldehyde oxidations are reported to be the corresponding one-carbon shortened carbonyls (i.e., acetophenone in the case of native 2-phenylpropionaldehyde (Scheme 11)). Consistently UV–Vis spectroscopy shows that the precursor $[\text{Fe}^{\text{III}}(\text{TAML})]^-$ complex is regenerated after reaction completion. In the case of the phenol oxidations, no product characterization was reported. It is however known from previous studies with oxoiron(IV) species [38] and from autooxidation studies that the oxidation of sterically hindered phenols usually yields complicated mixtures of dimerized diphenoquinones [39–41], e.g., as illustrated in Scheme 9.

5 Nucleophilic Reactions of Iron Peroxide Adducts

While only few iron(III)- O_2 adducts have been identified, adducts formed in the reaction of iron complexes with reduced forms of O_2 are relatively more common. Heme and nonheme iron complexes are capable of reacting with dihydrogen peroxide and alkyl hydroperoxides (like *tert*-butyl hydroperoxide) to form spectroscopically detectable peroxide adducts and secondary products like high-valent oxides (Scheme 1 steps (i) and (iii)). The first iron(III)- η^1 -alkyl peroxide adduct, based on tpa, was reported in 1993 [42]. A short time later, the first iron(III)- η^1 -hydroperoxide and iron(III)- η^2 -peroxo adducts were spectroscopically identified [43, 44] using the neutral pentadentate ligand metpen (Fig. 3). Since then, several iron(III)-hydroperoxo [45–60], iron(III)-peroxo [55, 60–63], and iron(III)-alkylperoxo adducts [51, 64–68] have been reported. All these complexes are thermally unstable and can only be detected for short times at low temperatures. The hydroperoxo and alkylperoxo adducts are typically generated by exposing the precursor iron(II) (Scheme 10) or iron(III) complex to a somewhat large excess of H_2O_2 or alkyl hydroperoxide in order to attain reasonable concentrations of the species. When Fe(II) is used, the cleavage of H_2O_2 is promoted and an intermediate Fe(III)-hydroxide is formed with concurrent production of hydroxyl radicals. The intrinsic mechanistic details of these reactions have been examined by Hazell et al. for a series of iron(II) complexes of the Rtpen ligand family, $[\text{Fe}^{\text{II}}(\text{Rtpen})\text{Cl}]^+$ ($\text{R}=\text{CH}_3, \text{CH}_2\text{C}_6\text{H}_5$). They have shown that the formation occurs in a two-step process. The first and fastest step is the oxidation of the starting chloride complexes, $[\text{Fe}^{\text{II}}\text{Cl}(\text{Rtpen})]^+$ to $[\text{Fe}^{\text{III}}(\text{Rtpen})(\text{OH})]^{2+}$ (or $[\text{Fe}^{\text{III}}(\text{Rtpen})(\text{OCH}_3)]^{2+}$ when



Scheme 10 Generation and generic structures of iron(III)-hydroperoxo and iron(III)-peroxo adducts and secondary products, high-valent iron-oxo species

methanol is present). The second step is a much slower substitution, where a hydroperoxide molecule substitutes the OH^- group as auxiliary ligand and thus forms the iron(III)-hydroperoxide adduct, $[\text{Fe}(\text{Rtpen})-(\eta^1\text{-OOH})]^{2+}$ [59, 69].

Peroxo adducts usually are generated by the deprotonation of a hydroperoxo adduct. However, they can also be generated from the direct reaction of superoxide with an iron(II) complex [50] (Scheme 10). The time span for the decomposition of iron(III) peroxides ranges from seconds to several hours at room temperature depending on the supporting ligand system. Several decay routes have been shown. In some cases, the decay occurs by homolytic cleavage of the O–O bond to give the corresponding iron(IV)-oxo complexes, which are in themselves also potential oxidants (Scheme 1 and Sects. 2, 6 and 7).

Both high-spin ($S = 5/2$) and low-spin ($S = 1/2$) iron(III)-hydroperoxo adducts have been reported, with the majority being low spin. In both cases, a rather diagnostic hydroperoxo-to-iron(III) charge-transfer band is observable in the optical spectra around 500–600 nm. So far no single crystal X-ray structures are known; however, there are two reports of isolated powders [47, 58]. In spite the absence of structural data, much knowledge has been gleaned regarding the coordination mode of the $-\text{OOR}$ ($\text{R}=\text{H}$ or *tert*-butyl) moiety from resonance Raman and Extended X-ray Absorption Fine Structure (EXAFS) studies. These clearly point towards the only mode of coordination for the mononuclear complexes being the “end-on” η^1 fashion [50, 53, 56, 70]. With respect to the spin state of mononuclear iron(III)-peroxo adducts, there is less flexibility, and so far, all those reported are high spin ($S = 5/2$). Resonance Raman studies and EXAFS point towards the peroxo moiety coordinating in a bidentate “side-on” η^2 fashion [56], so the complexes are probably mostly 7-coordinated. A $d-d$ transition appears in the vicinity of 500–700 nm. Two crystal structures of mononuclear iron-peroxo adducts are known. One is of the nonheme iron(III) complex, $[\text{Fe}^{\text{III}}\text{O}_2(\text{TMC})]^+$ [45] (Fig. 10), and the other is an impressive model for the active site of cytochrome c oxidase: an iron(III)-porphyrin complex linked to a $[\text{Cu}^{\text{II}}(\text{TPA})]^+$ moiety, where the peroxide group bridges the Fe and Cu atoms in an end-on/side-on bridging fashion [61].

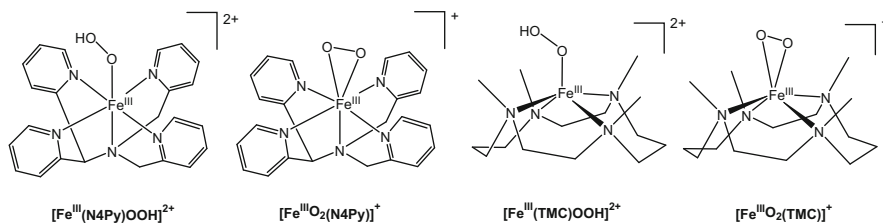
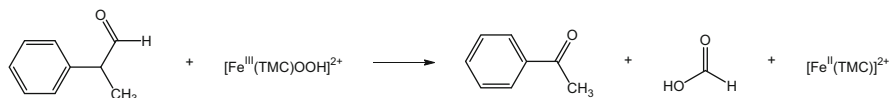


Fig. 10 Structures of two iron(III)- η^1 -hydroperoxide complexes and their conjugate bases iron(III)- η^2 -peroxide adducts

The reactivity patterns of iron-hydroperoxides and iron-peroxides are at present not completely understood. One of the difficulties faced when performing reactivity studies of these adducts is the problems that arise from the excess H_2O_2 in solutions necessary for maintaining reasonable concentrations of the species. Blatant in Scheme 10 is that the mixing iron(II) complexes with H_2O_2 will inevitably lead to the simultaneous generation of oxygen-based HO^\bullet radicals and a mixture of iron intermediates (viz., Fe(III)-hydroxo, Fe(III)-hydroperoxo, Fe(III)-peroxo, and Fe(IV)-oxo species). Furthermore, these systems can catalyze the disproportionation of H_2O_2 to O_2 and H_2O , and this can be the dominating reaction. In this case, substrate oxidations, even if they are present, may go unnoticed. There are several reports showing that substrate oxidations have been observed using Fe(II) complexes and H_2O_2 ; however, statistical mixtures of products are often obtained [71] presumably due to organic radical-chain reactions proliferated by HO^\bullet radicals [72]. Despite the difficulties, investigations of stoichiometric reactions with potential substrates are essential for fine tuning this chemistry, so that it can be implemented for catalysis. Thus, the iron-based oxidants need to be distinguished from each other and from hydroxyl radicals. In the following, we will discuss some studies that have been performed, either by using isolated powders [47, 58] or by employing low temperatures in combination with stopped-flow techniques [45, 62, 73].

5.1 Reactions with Aldehydes

Nam and coworkers [45, 62, 74] have probed the reactive nature of the high-spin peroxide and hydroperoxide adducts $[\text{Fe}^{\text{III}}\text{O}_2(\text{TMC})]^+$, $[\text{Fe}^{\text{III}}\text{O}_2(\text{N4Py})]^+$, and $[\text{Fe}^{\text{III}}(\text{TMC})\text{OOH}]^{2+}$ (Fig. 10) by using stopped-flow techniques to mix the complexes with a range of different substrates while measuring the decay of their chromophores by UV-Vis spectroscopy. The high-spin hydroperoxo adduct $[\text{Fe}^{\text{III}}(\text{TMC})\text{OOH}]^{2+}$ and both peroxo complexes, $[\text{Fe}^{\text{III}}\text{O}_2(\text{TMC})]^+$ and $[\text{Fe}^{\text{III}}\text{O}_2(\text{N4Py})]^+$, are capable of acting as nucleophiles in the oxidative cleavage of aldehydes like 2-phenylpropionaldehyde, pentanal, 2-methylbutanal, and pivaldehyde. The hydroperoxo adduct reacts fairly quickly, whereas the reactions



Scheme 11 Oxidative splitting of 2-phenylpropionaldehyde by an iron(III)-hydroperoxide adduct

of two peroxo adducts are more than two orders of magnitude slower – a clear indication of their poorer ability to act as oxidants. Similar observations have been made for iron-porphyrin complexes, where species like [Fe^{III}O₂(TMP)][−] (Scheme 17) despite their negative charge are widely regarded as unreactive [75, 76]. In the case of the oxidation of 2-phenylpropionaldehyde promoted by the Fe-TMC complexes, the cleavage products are acetophenone and formic acid (Scheme 11). UV–Vis spectroscopy shows that a diamagnetic iron(II) complex, likely to be [Fe^{II}(TMC)]²⁺, is formed after the reaction is complete.

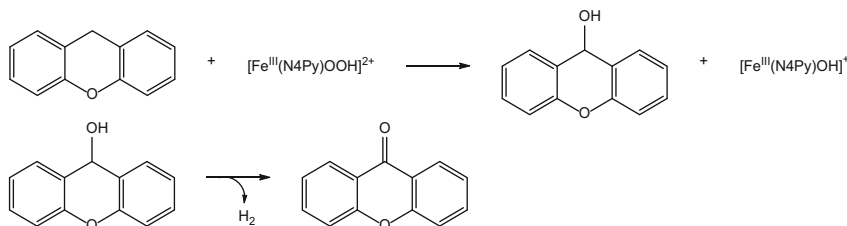
5.2 Hydroxylation of Alkanes and Aromatic Compounds

It is generally accepted that the initial step in the metal-mediated hydroxylation of aliphatic and aromatic hydrocarbons is the abstraction of a hydrogen atom from the weakest C–H bond in the substrate. Common test substrates include molecules on the brink of aromaticity (i.e., molecules that achieve aromaticity if hydrogen atoms are removed). Examples are cyclohexadiene (bond-dissociation energy, BDE = 74 kcal mol^{−1}) and dihydroanthracene (77 kcal mol^{−1}). A good diagnostic test for a hydrogen-atom abstraction pathway is to plot the natural logarithm of the initial rates for the reactions of the iron species with a series of substrates against the C–H bond-dissociation energies of the substrates. If a linear correlation is seen, it is fair to conclude that the rate-determining step in the oxidations is a hydrogen-atom abstraction and that the mechanism is the same for all substrates in the series. The basis for this test is the Evans–Polanyi relationship, which is often obeyed for a series of reactions with similar reagents (i.e., the assumption is that a direct correlation exists between the activation energy and the enthalpy change for the rate-determining step for a series of related reactions (Scheme 12)). It should be noted that the relationship is rather empirical and that the parameters obtained should not be subjected to overinterpretation.

In line with this, Nam and coworkers compared [Fe^{III}O₂(TMC)]⁺ and the two hydroperoxides, [Fe^{III}(TMC)OOH]²⁺ and [Fe^{III}(N4Py)OOH]²⁺, in potential hydrogen-abstraction reactions with xanthene (BDE = 76 kcal mol^{−1}) and dihydroanthracene. Only the hydroperoxide adducts shows activity and that this was roughly on the same scale as the corresponding high-valent iron-oxo complex [Fe^{IV}O(TMC)]²⁺ (see Sect. 6). The major oxidation products are xanthone and anthracene, respectively. In both cases, it is likely that products formed initially are unstable hydroxides. These are oxidized further, either spontaneously or by a

The Evans–Polanyi relationship:	$E_a = E_0 + \alpha \cdot \text{BDE}$
The Arrhenius equation:	$k = A \cdot e^{-E_a/RT}$
$\ln(k) = [\ln(A) - E_0/RT] - (\alpha/RT) \cdot \text{BDE}$	

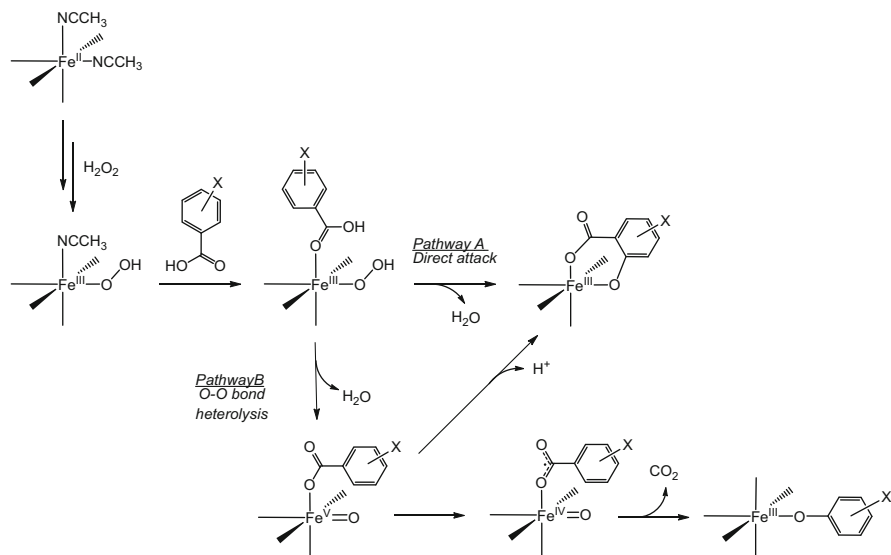
Scheme 12 The Evans–Polanyi relationship and the Arrhenius equation. k = the rate constant, E_a = activation energy, α = transition-state factor, A = pre-exponential factor, R = gas constant, T = temperature



Scheme 13 The steps in the oxidation of xanthene to xanthone

metal-based oxidation, to give the observed products (Scheme 13). A similar reactivity trend has been observed by Wada et al. [47] for the high-spin adduct $[\text{Fe}^{\text{III}}(\text{bppaH}_2)(\text{OOH})]^{2+}$. The complex gives only a low yield of hydroxylated product when reacted with cyclohexane ($\text{BDE} = 96 \text{ kcal mol}^{-1}$), whereas when exposed to cyclohexene, a greater yield of cyclohexenol (BDE of $\alpha\text{-C-H}$ bond = 75 kcal mol^{-1}) is obtained with no epoxide or diol products detected. Oxidation of the electron-rich dimethylsulfide on the other hand proceeds only very poorly, whereas the reaction with the more electrophilic dimethylsulfoxide gives a good yield. Thibon et al. [73] observed that the low-spin $[\text{Fe}^{\text{III}}(\text{metpen})\text{OOH}]^+$ is capable of giving low yields of phenol when reacted with benzene ($\text{BDE} = 112 \text{ kcal mol}^{-1}$) and slightly higher yields of *ortho*- and *para*-hydroxyanisole when reacted with anisole. The iron speciation in the product mixtures was monitored by EPR spectroscopy and the final complex identified as $[\text{Fe}^{\text{III}}(\text{metpen})\text{OH}]^{2+}$.

A last example is provided by Rybak-Akimova, Que, and coworkers [77, 78] who used the complexes $[\text{Fe}^{\text{II}}(\text{bpmen})(\text{CH}_3\text{CN})_2]^{2+}$ and $[\text{Fe}^{\text{II}}(\text{tpa})(\text{CH}_3\text{CN})_2]^{2+}$ to activate H_2O_2 and promote either an *ortho*-hydroxylation of benzoic acids to produce the corresponding salicylic acids or their decarboxylation and concomitant *ipso*-hydroxylation to give phenol products. By first mixing the iron(II) complexes with benzoic acids under anaerobic conditions, iron(II)-benzoate adducts are generated. Subsequent addition of a slight excess of H_2O_2 leads to the formation of oxidized iron(III)-salicylate complexes and occasionally iron(III)-phenolate adducts (see Scheme 14). The authors identified the products through observation of strong phenolato-to-iron charge-transfer bands ($\lambda \sim 600\text{--}700 \text{ nm}$, $\epsilon \sim 2,000 \text{ M}^{-1} \text{ cm}^{-1}$) in the UV–Vis spectra of the reaction solutions and by the appearance of distinctive Fe–O stretches ($\nu \sim 540\text{--}660$ and $860\text{--}960 \text{ cm}^{-1}$) in the



Scheme 14 Mechanistic proposal for the oxidation and possible decarboxylation of iron(III)-coordinated benzoates to salicylates or phenols

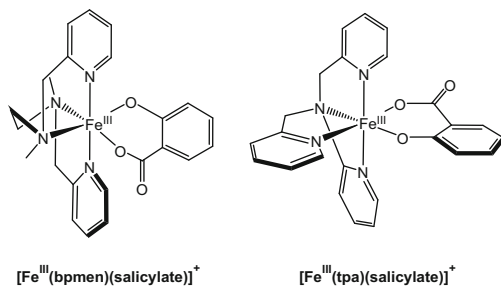


Fig. 11 Structures of iron(III)-salicylate complexes

resonance Raman spectra of the solutions. By removing the iron from the complexes using the strong chelator EDTA^{4-} , the presence of liberated salicylic acids could be confirmed by NMR spectroscopy. Using esterification protocols, yields and product distributions were determined by GC analyses. In the case of the Fe-bpmen system, exposure to benzoic acid and H_2O_2 leads to the quantitative formation of $[\text{Fe}^{\text{III}}(\text{bpmen})(\text{salicylate})]^+$. The corresponding reaction for $[\text{Fe}^{\text{II}}(\text{tpa})(\text{CH}_3\text{CN})_2]^{2+}$ on the other hand gives a mixture of the corresponding iron(III)-salicylate (51%) and iron(III)-phenolate (21%) complexes (Fig. 11).

For both complexes, reactions with substituted benzoic acids, like 3-methyl and 3-chlorobenzoic acids, give rise to mixtures of salicylic acid isomers. While the collective yields for the Fe-bpmen system consistently is around 90–95%, the

Fe-tpa system only gives collective yields of around 50–60%. With activated methoxy-substituted benzoic acids, the yields drop and decarboxylated phenol products are generated with both complexes. Likewise, reactions with deactivating nitro-substituted benzoic acids also give lower yields. To determine if the active oxidant is an iron(III)-hydroperoxide adduct or a high-valent Fe(IV)-oxo adduct, the authors generated both reactive intermediates independently with Fe-tpa system in the absence of substrate and examined their reactivity when exposed to substrate. Interestingly $[\text{Fe}^{\text{IV}}\text{O}(\text{tpa})(\text{NCCH}_3)]^{2+}$ does not react with any of the benzoic acids, whereas $[\text{Fe}^{\text{III}}(\text{tpa})(\text{NCCH}_3)\text{OOH}]^{2+}$ does. When using oxygen-18 labeled $\text{H}_2\text{}^{18}\text{O}_2$, it was repeatedly observed that only one of the oxygen-18 atoms is incorporated into the product. The pathways in Scheme 14 were proposed.

6 Electrophilic Reactions of Iron-Oxo Intermediates

While by far the most common and stable oxidation states of iron are the +2 and +3 states, iron can be forced into higher oxidation states. A common feature of high-valent complexes of any metal ion is the presence of an auxiliary oxo (O^{2-}) group, and this is also the case for iron(IV) and iron(V) species. More rarely, the auxiliary group can also be a nitrido (N^{3-}) or an imido (NR^{2-}) group. Somewhat unique for iron, these high-valent oxidation states are very unstable and will act as strong oxidizing agents by both inner sphere and outer sphere mechanisms. The characterization of ferryl ($\text{Fe}^{\text{IV}}=\text{O}$) [80–86] and perferryl ($\text{Fe}^{\text{V}}=\text{O}$) [87] complexes are important steps towards the discovery of robust catalysts. Their potential strong electrophilic nature will facilitate formal O-atom transfer reactions with electron rich substrates such as sulfides and phosphines [39, 84, 88–91, 91–93]. High-valent iron species are far too unstable to be put into a bottle and so must be generated in situ, ideally using benign less reactive terminal oxidants. As covered briefly in Sect. 3, it is widely believed that many heme and nonheme iron enzymes employ transient iron-oxo species as the direct oxidants in their catalytic cycles, and evidence for these species has been found through the use of advanced techniques such as freeze-quench Mössbauer spectroscopy and stopped-flow low-temperature UV–Vis spectroscopy [93].

The most common strategy for generating iron(IV)-oxo and iron(V)-oxo species is to oxidize a precursor iron(II) and iron(III) complex with a two-electron oxidant like iodosylbenzene (PhIO) or *m*CPBA (Fig. 12b). An alternative strategy is to use peroxides like hydrogen peroxide and TBHP [45, 94, 95]; however, this requires that the intermediate iron(III)-alkyl peroxide or iron(III)-hydroperoxide species decays spontaneously to give an iron(IV)-oxo complex (Scheme 10). As discussed above, these reactions face the risk of being rather complicated, and the chemistry can be difficult to control. Most Fe(IV)-oxo complexes have been prepared using PhIO, or a derivative, as oxidant. This strategy has also commonly been employed for the preparation of the “high-valent” complexes of other first row transition metal ions, e.g., Cr(V)oxo [96], Co(IV)oxo [97], Mn(IV)oxo [98], and Mn(V)oxo

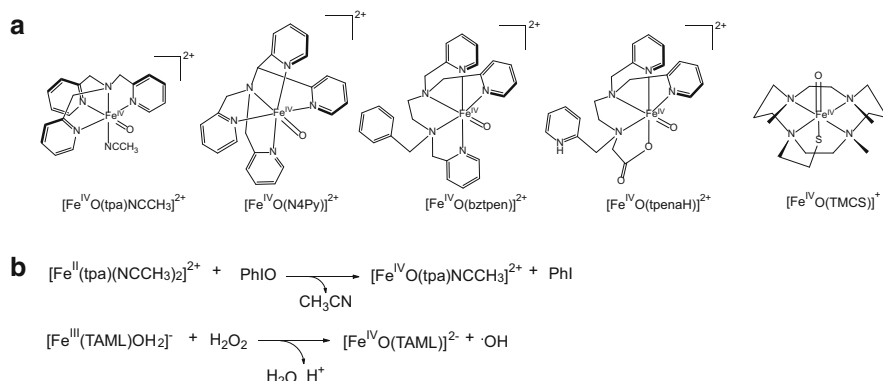


Fig. 12 (a) Examples of nonheme iron(IV)-oxo complexes. (b) Preparation of iron(IV)-oxo complexes

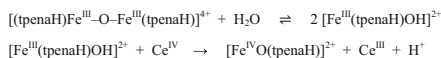


Scheme 15 Formation of high-valent iron-oxo species from intermediate iron-iodosylbenzene adducts

[99]. All these species are formed in accordance to the general reaction Scheme 15. This reaction implies the intermediate formation of a metal oxidant adduct (e.g., “(L)FeOX” in Scheme 1), which in this case is a complex in which iodosylbenzene (PhIO) is coordinated.

6.1 High-Valent Nonheme Iron(IV)-Oxo Complexes

Examples of non-porphyrinic iron(IV)-oxo complexes are shown in Fig. 12a. The first three, one based on a neutral tetradentate ligand the other two on pentadentate ligands, $[\text{Fe}^{\text{IV}}\text{O}(\text{tpa})(\text{CH}_3\text{CN})]^{2+}$, $[\text{Fe}^{\text{IV}}\text{O}(\text{N4py})]^{2+}$, and $[\text{Fe}^{\text{IV}}\text{O}(\text{bztpen})]^{2+}$, are generated using PhIO according to Scheme 15. An obvious strategy for increasing the oxidation state of iron is to use more electron-donating ligands. Appending negative charge to the ligand through the introduction of a carboxylate, amide, phenolate, or a sulfide donor is a way to achieve this. In the case of the biomimetic carboxylato complex, $[\text{Fe}^{\text{IV}}\text{O}(\text{tpenaH})]^{2+}$, and the thiolato complex, $[\text{Fe}^{\text{IV}}\text{O}(\text{TMCS})]^+$, however, only iron(IV)-oxo species have been obtained so far. The contrast in their preparation, compared to the first three complexes, is however worth noting. While the generation of iron-oxo intermediates is usually performed in organic solvents, these two species are among a few recent examples of iron(IV)-oxo complexes generated in water through oxidation with Ce(IV) [100–103]. In



Scheme 16 Formation of an aqueous iron(IV)-oxo complex through cerium(IV) oxidation

recent work, iron-oxo species have even been generated electrochemically [104, 105] and photoelectrochemically [106] also in aqueous solvents.

As discussed in detail in Sect. 4.2, iron(II) complexes of the classes of ligands described here are usually not stable in aerobic solutions. This is especially true in aqueous media, where iron(II) compounds are usually oxidized rapidly by O₂ to form μ -oxo-bridged complexes. Likewise monomeric iron(III) complexes often undergo hydrolysis and oligomerization in the presence of water. Therefore, if a complex shows this propensity, reversibility is essential. The synthesis of [Fe^{IV}O(tpenaH)]²⁺ is an example (Scheme 16) [100]. [Fe^{IV}O(tpenaH)]²⁺ is an aggressive H-atom abstractor and no selective oxidation of a particular substrate has been reported. This result offers interesting perspectives with respect to the use of water as a solvent and as O-atom donor.

Likely due to their very short life times (minutes to hours even at low temperatures), only a handful of Fe(IV)-oxo complexes have been crystallized (one of which includes [Fe^{IV}O(N4Py)]²⁺ (Fig. 12a)). However, while their isolation is often very nearly impossible, their identification in solution is relatively straightforward since nonheme iron(IV)-oxo species exhibit a range of diagnostic spectroscopic features. The most prominent is perhaps a near-infrared optical $d-d$ transition between 800 and 900 nm, which, in the case of nonheme complexes, gives these species a pale green color [93]. In heme complexes, these optical transitions often are obscured by the much stronger ligand transitions [107]. The Fe=O moiety also gives rise to distinctive vibrations in resonance Raman spectra between 750 and 850 cm⁻¹ [93]. The oxidation state of the iron center can be determined with great certainty with advanced techniques such as Mössbauer and X-ray absorption near-edge spectroscopy (XANES), while structural details can also be obtained from fitting of the EXAFS part of the X-ray absorption spectrum. The pre-edge energy of a complex determined from its Fe-K-edge XAS spectrum is a useful indicator of the oxidation state of the iron center, when compared to other complexes of the same (or a related) ligand with iron in different oxidation states (Fig. 13). As a rule of thumb, a one-step increase in the oxidation state of iron will increase the pre-edge energy by 1 eV [108, 109]. Likewise, a good correlation can often be found between the oxidation states for a series of similar complexes and the Mössbauer isomer shifts of the complexes. An excellent example of this has been reported by Wieghardt and coworkers [110] (Fig. 14).

Both the nonheme oxoiron(IV) species [Fe^{IV}O(N4Py)]²⁺ and [Fe^{IV}O(TMC)]²⁺ (Fig. 12a) and the fluorinated porphyrin complex [Fe^{IV}O(TPFPP)]²⁺ (Fig. 15) have been proven capable of dealkylating electron-rich *N,N*-dialkylanilines. The porphyrin complex is by far the most reactive, but in all three cases kinetic studies strongly indicate that the likely mechanism is a PCET pathway. Likewise all three iron(IV)-oxo species have been found to be acting as strong electrophiles in the reactions (with negative Hammett constants – $\rho > 2$) [87]. [Fe^{IV}O(N4Py)]²⁺ and [Fe^{IV}O(bztpen)]²⁺

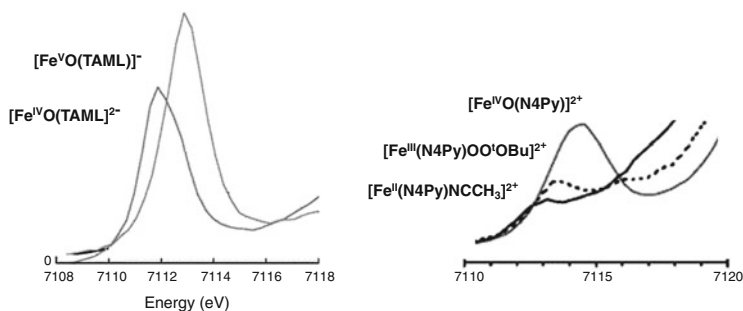


Fig. 13 Pre-edge features in Fe–K-edge X-ray absorption spectra of iron complexes. On the *left-hand side*: High-valent Fe-TAML complexes. Adapted from DeBeer and coworkers [108] with permission of The Royal Society of Chemistry. On the *right-hand side*: iron(II), iron(III), and iron(IV)-oxo species of N4Py. Adapted from Que and coworkers [70] with permission from the American Chemical Society. Copyright (2004) American Chemical Society

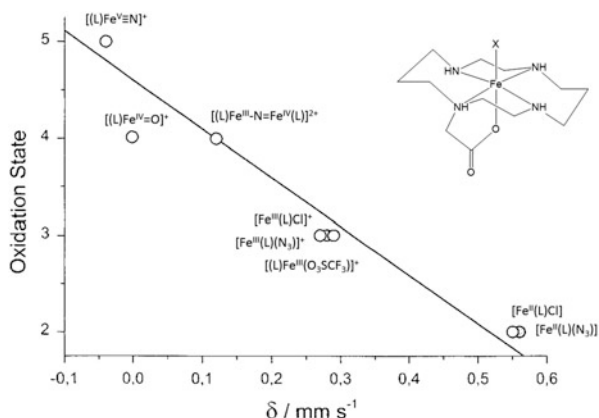


Fig. 14 Correlation between the oxidation state and the Mössbauer isomer shift for a series of iron complexes with the ligand L = cyclam-acetato. Adapted from Wieghardt and coworkers [110] with permission from the American Chemical Society. Copyright (2000) American Chemical Society

(Fig. 12) have also proven capable of oxidizing a range of sulfides, such as thioanisoles and the more difficult dibenzothiophene [89, 91, 92]. Interestingly, titration studies by Park et al. have shown that these reactions can be greatly accelerated through the addition of redox-inactive metal ions like $M^{3+} = Lu^{3+}, Y^{3+},$ and Sc^{3+} . Kinetic studies revealed that the acceleration is due to interactions with the trivalent ion which somehow switch the mechanism from an oxygen–atom transfer pathway to a faster tunnelling–driven PCET pathway [92, 93].

Iron(IV)-oxo species are capable of reacting in hydrogen-atom transfer reactions (also covered in Sect. 5.2). In a comparative study, a series of Fe-TMC complexes, $[Fe^{IV}O(TMC)(X)]^{2+/+}$ ($X = CH_3CN, CF_3COO^-, N_3^-$) and $[Fe^{IV}O(TMCS)]^+$, were compared in their capability to abstract hydrogen atoms from both C–H and O–H bonds [38, 83, 88]. A strong correlation was revealed between the reactivity and the

donor strength of the axial auxiliary ligand “X”: the stronger the donor, the faster the reaction. The introduction of the strong axial donors also has the effect of increasing the reduction potential of the species. [38]. An explanation for the rate acceleration could therefore simply be an enhanced stabilization of the high-valent species. The same trend is also observed for iron porphyrins [111] as covered in the next section.

6.2 Iron(V)Oxo and Iron(IV)Oxo-(Oxidized Radical Ligand) Complexes

The chemistry of synthetic biomimetic iron-porphyrin complexes is very well developed, and as a consequence, the cytochrome P450 enzymes (Sect. 3) are presently one of the most well-understood classes of metalloenzymes. The most commonly encountered synthetic porphyrinato ligands are tetraphenylporphyrinates (TPP²⁻) and their substituted analogues tetrafluorophenylporphyrinates (TFPP²⁻) (Fig. 15). Iron(III)-porphyrin complexes like [Fe^{III}(TPP)Cl] and [Fe^{III}(TFPP)Cl] are capable of undergoing one- or two-electron oxidation to give iron(IV)-oxo species and formal “iron(V)oxo” species – where one oxidizing equivalent is located on the iron center as a Fe(IV)oxo moiety while the second is

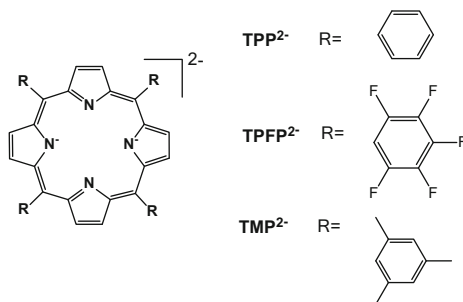
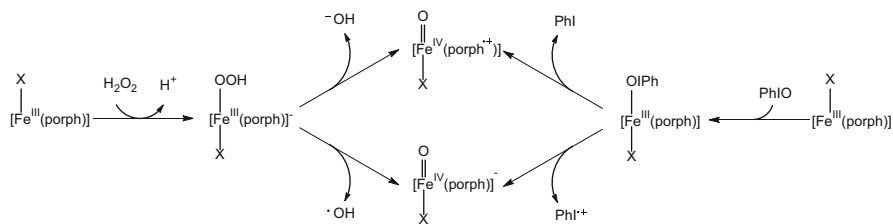


Fig. 15 Illustrations of the TPP²⁻, TFPP²⁻, and the TMP²⁻ porphyrinate ligands



Scheme 17 Generation of iron(IV)-oxo and “iron(V)-oxo” intermediates from H₂O₂ or PhIO oxidation of an iron(III) porphyrin complex. Here porph²⁻ is a generic porphyrin ligand

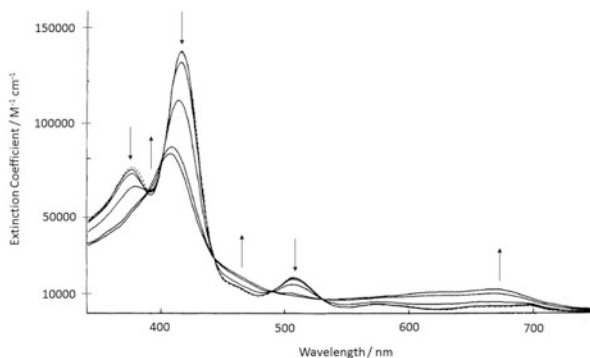


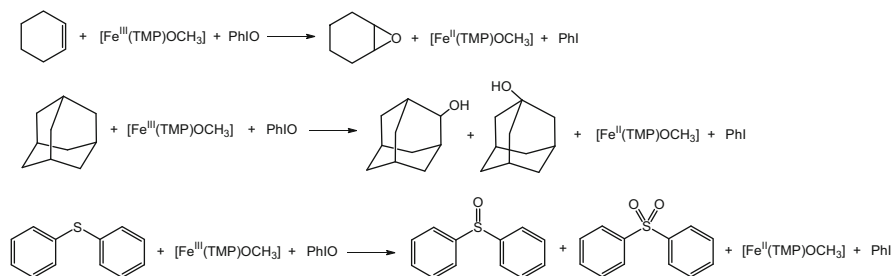
Fig. 16 Optical spectrum showing the oxidation of $[\text{Fe}^{\text{III}}(\text{TMP})\text{Cl}]$ by *m*CPBA to form $[\text{Fe}^{\text{IV}}\text{O}(\text{TMP}^{\bullet+})\text{Cl}]$. Adapted from Groves and Watanabe [114] with permission from the American Chemical Society. Copyright (1988) American Chemical Society

supported by the porphyrinato ligand which forms a π -radical, i.e., $[\text{Fe}^{\text{IV}}\text{O}(\text{TMP}^{\bullet-})]\text{Cl}$ (Scheme 17).

The first high-valent iron-oxo complex was generated in 1981 by Groves and coworkers [112]. They were trying to solve a long-standing question in the field of porphyrin chemistry: The nature of the mysterious Intermediate I of cytochrome P450 – a transient species observed to be the active oxidizing species in these enzymes [113]. By oxidizing the porphyrin complex $[\text{Fe}^{\text{III}}(\text{TMP})\text{OCH}_3]$ with *m*CPBA at $-78\text{ }^\circ\text{C}$, the high-valent $[\text{Fe}^{\text{IV}}\text{O}(\text{TMP}^{\bullet+})\text{OCH}_3]$ was generated. The complicated electronic structure of this green intermediate was deduced by subjecting it to a battery of spectroscopic techniques.

When following the reaction with optical spectroscopy [114], a dramatic change in the intense porphyrin Soret band around 420 nm is observed, accompanied by a new broad Q band around 600 nm (Fig. 16). The resulting spectrum is rather reminiscent of that for Intermediate I in the cytochrome enzymes. This together with the revelation of a spin $S = 3/2$ ground state from Mössbauer, NMR, and EPR studies leads to the conclusion that the Fe(III) system as a whole has undergone a two-electron oxidation – with one oxidation equivalent situated on the iron center and the other on the porphyrin ligand, forming a spin $S = 1$ Fe(IV)-oxo moiety ferromagnetically coupled to a $S = 1/2$ porphyrin-radical ligand. Thus, the conjugated macrocyclic ligand behaves in a redox non-innocent manner and supports the iron center by donating an electron. The oxoiron(IV)-porphyrin- π -radical species is a competent oxidant capable of epoxidizing alkenes and hydroxylating alkanes [112]. Interestingly when PhIO is used as the oxygen-atom donor, the red species $[\text{Fe}^{\text{IV}}\text{O}(\text{TMP})]^-$ is generated instead. The combination of $[\text{Fe}^{\text{III}}(\text{TMP})\text{Cl}]$ and PhIO in methanol is a good catalytic system for olefin epoxidation, hydrocarbon hydroxylation [115], and sulfoxidation of sulfides [116] (Scheme 18).

As depicted in Scheme 17, the product obtained from PhIO is not general, and it has been observed that with other porphyrins, or other supporting axial ligands, the two-electron-oxidized oxoiron(IV)-porphyrin- π -radical can indeed be generated

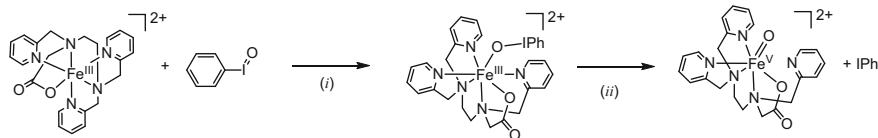


Scheme 18 Epoxidation of cyclohexene, hydroxylation of adamantane, and sulfoxidation of diphenyl sulfide with $[\text{Fe}^{\text{III}}(\text{TMP})\text{OCH}_3]$ and PhIO

[117]. This puzzled researchers for quite some time until Nam and coworkers carried out a systematic study of the factors that influence this selection [118–121]. When axial ligands like $\text{X}^- = \text{OH}^-$, CH_3CO_2^- , F^- , Cl^- are present, the oxidation with PhIO yields the red one-electron-oxidized product Fe(IV)oxo, whereas if weakly coordinating anions like $\text{X}^- = \text{NO}_3^-$, ClO_4^- , CF_3SO_3^- are employed, the same reaction generates the green two-electron-oxidized “Fe(V)oxo” species [119]. Rather dramatic differences are found in the iron(II)/iron(III) redox potentials of the $[\text{Fe}^{\text{III}}(\text{TMP})\text{X}]$ complexes, with stronger donor anions leading to larger shifts compared with the weakly coordinating anions.

X^- :	OH^-	CH_3CO_2^-	F^-	Cl^-		NO_3^-	ClO_4^-	CF_3SO_3^-
$E_{1/2}$ (vs. Fc):	1,200	820	780	770		420	350	330

Competitive reactivity studies have been performed [122] where a mixture of *cis*-stilbene and *trans*-stilbene is epoxidized with PhIO using as catalysts the iron complexes of the related, unmethylated, tetraphenyl ligand TPP^{2-} and its electron-deficient fluorinated analogue TPFP^{2-} . Interestingly, dramatically different product selectivities are seen when $[\text{Fe}(\text{TPP})\text{Cl}]$ and $[\text{Fe}(\text{TPP})\text{CF}_3\text{SO}_3]$ are used as pro-catalysts. Not only are the yields using the triflate complex slightly better, with a total yield of 60% (against 54% for the chloride complex), the reactions are also much more selective with a 56% yield of *cis*-stilbene oxide and only 4% *trans*-stilbene oxide. In contrast, the reactions using the chloride complex produce an isomeric mixture of 26% *cis*-stilbene oxide and 28% *trans*-stilbene oxide. The same reactivity trends are also observed for the analogous electron-deficient porphyrin complexes, $[\text{Fe}^{\text{III}}(\text{TPFP})\text{X}]$. Impressively, the electron-poor porphyrin systems are also capable of activating H_2O_2 [122–124] (however, as always with H_2O_2 , selectivity is a problem). The results can be rationalized with the notion of two different species acting as the active oxidants in the case of the chloride adducts, $[\text{Fe}^{\text{IV}}\text{O}(\text{porph})\text{Cl}]^-$ and $[\text{Fe}^{\text{III}}(\text{porph})(\text{OR})\text{Cl}]^{0/-}$ ($\text{OR} = \text{OIPh}$ or $^- \text{OOH}$), whereas in the case of the triflate adduct, only $[\text{Fe}^{\text{IV}}\text{O}(\text{TMP}^{*+})\text{CF}_3\text{SO}_3]$ is acting as oxidant. Support for the Fe(III)–OIPh intermediate hypothesis was later provided, when the same group spectroscopically detected Fe(III)–OIPh adducts and found that these exist in equilibrium with the corresponding $[\text{Fe}^{\text{IV}}\text{O}(\text{porph}^{*+})]$



Scheme 19 Generation of the iron(III)-OIPh adduct of tpena^- and its possible subsequent heterolytic cleavage to yield an iron(V)oxo derivative

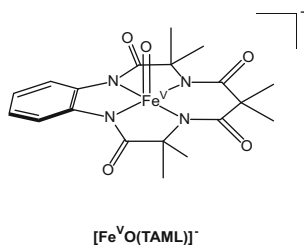


Fig. 17 Structure of the Fe(V)oxo intermediate of TAML^{4-}

[120]. Generally, it has been observed that oxidative power increases when the porphyrinic scaffold is decorated with electron-withdrawing substituents [117, 118]. Somewhat counterintuitively, it has also been shown that the reactivity of $[\text{Fe}^{\text{IV}}\text{O}(\text{TMP})(p\text{-OPyY})]^+$ complexes towards the electrophilic epoxidation of olefins and hydroxylation of aromatic and aliphatic substrates increases, when Y is an electron-donating group [111]. DFT calculations indicate that a complicated trans-effect is at play.

While iron(III)-OIPh adducts have been proposed or implied numerous times, and spectroscopically trapped with porphyrin ligands, only one example of a structurally characterized iron complex of OIPh exists. The complex, $[\text{Fe}^{\text{III}}(\text{tpena})\text{OIPh}](\text{ClO}_4)_2$, was generated using the hexadentate monoanionic nonheme ligand tpena^- in 2012 [125]. The complex is capable of oxidizing the sulfide thioanisole chemoselectively to its sulfoxide. The reaction must occur either by the direct oxygen-atom transfer to the thioether S atom from $[\text{Fe}^{\text{III}}(\text{tpena})\text{OIPh}]^{2+}$ or from a putative $[\text{Fe}^{\text{V}}\text{O}(\text{tpena})]^{2+}$ derivative (Scheme 19).

There is some evidence that nonheme complexes of negatively charged ligands are capable of supporting iron(V)-oxo species. Despite this, no true “iron(V)-oxo” species has been detected for porphyrin systems. However, one iron(V)-oxo species has been generated and thoroughly characterized using the macrocyclic nonheme amido ligand TAML^{4-} [86] (Fig. 17). Somewhat surprisingly, stoichiometric reactivity studies have revealed that $[\text{Fe}^{\text{V}}\text{O}(\text{TAML})]^-$ is only a mediocre oxidant in the oxidation of alkenes and alkanes, when compared to the analogous Fe(IV)oxo species [86, 126]. Regardless, the Fe-TAML system and its derivatives (especially systems where the ligand is decorated with electron-withdrawing fluoride substituents) are effective catalysts in the nonselective oxidation of sulfides, hydrocarbons, and chlorinated aromatic compounds with H_2O_2 [127–129] and in the

selective *N*-dealkylation of tropane alkaloids [130, 131]. A key feature of the Fe-TAML systems is that despite being extremely good catalase mimics (17 L O₂ per g catalyst per second vs. 22 L/(g s) for beef liver catalase), when substrate is present, the substrate oxidation pathway dominates over the catalase pathway [94]. This is especially true when the substrate concentration is kept higher than the H₂O₂ concentration. [Fe^{IV}O(TAML)]²⁻ has been shown by Popescu and coworkers [95] to be the dominating species when [Fe^{III}(TAML)]⁻ complexes are exposed to aqueous H₂O₂ or ^tBuOOH, with no traces of [Fe^VO(TAML)]⁻.

7 Halogenation Reactions of Iron-Halide and Iron-Hypohalide Adducts

In biology, the halogenation of aromatic and aliphatic biomolecules is a common reaction catalyzed by vanadium, heme, and nonheme iron enzymes. Examples of chlorinated natural products are shown in Fig. 5. Generally, the enzymes catalyze these reactions by organizing the reactants and generating oxidizing OX⁻ equivalents (X=Cl, Br, I), using simple halide ions and O₂ or H₂O₂, to generate the active oxidants. While the heme enzymes are capable of halogenating activated/electron-rich aromatic substrates, the nonheme iron enzymes are also capable of halogenating difficult aliphatic substrates. Only a few synthetic iron complexes have been reported able to carry out such reactions. The earliest example is given by Kojima et al. in 1993 [132], who, in fact, prior to the discovery of the nonheme halogenases, showed that the complexes [Fe^{III}(tpa)X₂]ClO₄ (X=Cl⁻, Br⁻) (Fig. 18b) are capable of halogenating the aliphatic substrates cyclohexane and adamantane using *tert*-butyl

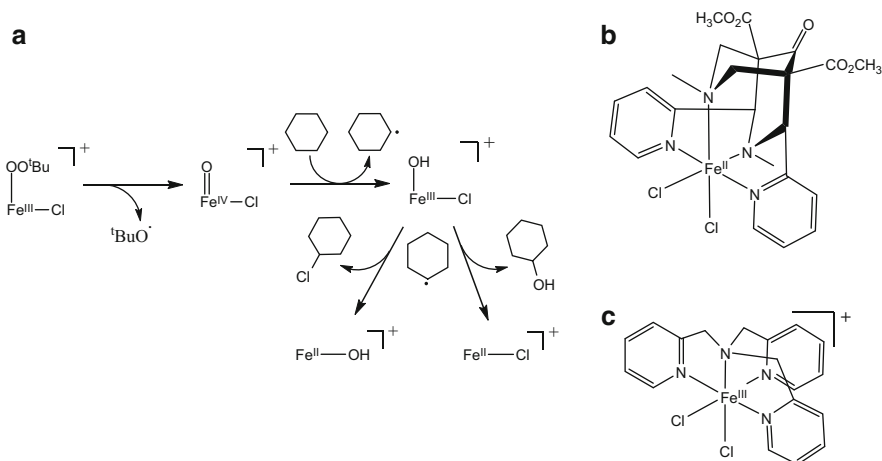
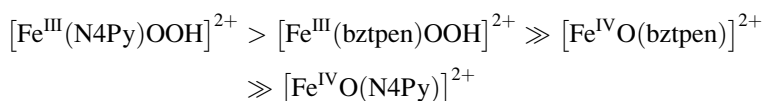


Fig. 18 Concurrent halogenation and hydroxylation of alkanes. (a) The proposed mechanism for the chlorination of cyclohexane by *tert*-butyl hydroperoxide and nonheme iron(III) complexes, explaining why competing hydroxylation also takes place. (b) Structure of [Fe^{II}(BP1)Cl₂]. (c) Structure of [Fe^{II}(tpa)Cl₂]⁺

hydroperoxide (TBHP) as the terminal oxidant. The reactions could not be made catalytic, as the necessary amounts of the halide source (added as *tert*-butylammonium salts) rendered the complexes inactive. Furthermore, problems are encountered when using an excess of TBHP. Under such conditions mainly the oxygenated products, cyclohexanol and cyclohexanone, are formed and with an alcohol/ketone ratio of 9/13 (close to 1) indicative of a free radical-based and not a metal-centered oxidation mechanism [2, 133]. In 2010, Comba and Wunderlich [134] tested the halogenation activity of iron(II)-bispidine complexes (Fig. 18c) probing TBHP, H₂O₂, and PhIO as terminal oxidants. They obtained a near 50/50 ratio of halogenated-to-hydroxylated product when using TBHP, while H₂O₂ and PhIO gave almost exclusively halogenated products, albeit in much lower yields. Again attempts to convert the stoichiometric reaction to a catalytic reaction failed, as no additional halogenated product was obtained beyond the first turnover. Similar mechanistic considerations were made (Fig. 18a).

In both cases, DFT calculations support these “rebound-type” mechanisms [134, 135]. The iron(IV)-oxo species abstracts a hydrogen from one of the substrate carbons, forming an organic radical which in turn abstracts a chloride (or hydroxide) from the iron(III) center. This mechanism can be experimentally justified in that it accounts for the concurrent formation of hydroxylated and halogenated products. A Fe(III)-OO^tBu adduct [64] has been identified for the tpa system. Likewise iron(IV)-oxo complexes are known for both systems [104, 136]. A fundamental issue with the mechanisms however is the a priori assumption of homolytic O–O bond cleavage of the Fe(III)-OOR adduct to form a Fe(IV)oxo species. It appears that no attempt has been made to test if the alkyl peroxide adducts themselves could be the active oxidants.

Recently, de Visser and coworkers [90, 137] have taken a new approach to this topic and in two communications performed comparative studies. They compared the low-spin [Fe^{III}(N4Py)OOH]²⁺ and [Fe^{III}(bztpen)OOH]²⁺ adducts (Fig. 10) with the low-spin iron(IV)-oxo analogues, [Fe^{IV}O(N4Py)]²⁺ and [Fe^{IV}O(bztpen)]²⁺ (Fig. 14a), in the ability to oxidize simple halide X[−] ions (X=Cl, Br, I). It turns out that the iron(III)-hydroperoxo adducts are generally much faster at oxidizing the halide anions than the iron(IV)-oxo adduct. The order is presented below:



For all the complexes, a linear correlation between the rate of oxidation and the oxidation potential of the halide anions is observed. Such linearity can be interpreted within the framework of the Marcus theory of electron transfer. This means that the processes are driven predominantly by electron transfer from the halide ion to the iron complex. Consequently the rates observed are mainly determined by the electrochemical potentials of the reagents [138]. In the case of [Fe^{III}(N4Py)OOH]²⁺, addition of Br[−] (added as a TBA salt) leads to the formation of [Fe^{III}(N4Py)OH]²⁺ – according to UV–Vis and mass spectrometry. No attempt to

analyze the reaction products for the reactions of the iron(IV)-oxo species has been reported, rather it is hypothesized that either X^{\bullet} or X^{-} is formed. The findings have been rationalized by DFT calculations on the N4Py systems with bromide. BDEs for the bonds have been calculated and found to be high. This rejects the notion that the hydroperoxo adduct could have undergone homolytic O–O cleavage. The nature of the transition states determined for the two intermediates are quite different. An early transition state was calculated for the reaction with the iron(IV)-oxo intermediate, with a nearly complete $1e^{-}$ electron transfer from Br^{-} to the FeO moiety. In contrast to this, a late transition state was established for the Fe(III)-OOH intermediate, with only minor charge transfer. It can therefore be concluded that for $[Fe^{IV}O(N4Py)]^{2+}$ a one e^{-} transfer takes place, while in the case of $[Fe^{III}(N4Py)OOH]^{2+}$ a $2e^{-}$ transfer (most likely oxygen-atom transfer) occurs, Scheme 20.

Non-heme iron complexes have also been tested for somewhat more useful reactions. When exposing $[Fe^{III}(N4Py)OOH]^{2+}$ and $[Fe^{IV}O(N4Py)]^{2+}$ to anisole and tert-butylammonium chloride, chlorinated anisole products are observed. The Fe(III)-OOH system turns out to be the most selective, with the main products being *para*- and *ortho*-chloroanisole, while the Fe(IV)-oxo systems is less selective and also yields 2,4-dichloroanisole and chloromethylbenzene. No absolute yields have been reported and, somewhat surprisingly no co-formed hydroxylated products are reported either. A reasonable rationalization for the observed trends in the reactivity can be deduced on the basis of the redox potentials of the iron complexes. It is known that the redox potential for the reversible Fe^{2+}/Fe^{3+} couple for the precursor iron(II) complex $[Fe^{II}(bztppen)NCCH_3]^{+}$ is around +80 mV higher than that of the corresponding $[Fe^{II}(N4Py)NCCH_3]^{2+}$ ($E_{1/2} = +690$ and +610 mV, respectively). The same trend is observed in the electrochemical generation of the iron(IV)oxo species, where the $Fe^{III}-OH_2/Fe^{IV}O$ couple has been estimated to be some +170 mV higher for the bztppen system than for the N4Py system ($E_{1/2} = +1,070$ and +900 mV, respectively) [104]. The electrochemistry suggests that it is harder to oxidize iron in the bztppen systems compared to the N4Py systems. This is a good indicator that there is less electron density on the iron center in the bztppen systems than in the N4Py systems. Thus, it is expected that $[Fe^{IV}O(bztppen)]^{2+}$ will be reduced faster than $[Fe^{IV}O(N4Py)]^{2+}$. Likewise the increased Lewis acidity of the iron center in $[Fe^{III}(bztppen)OOH]^{2+}$ should stabilize the hydroperoxide moiety, making it less likely to undergo O–O bond cleavage.

Another system capable of chlorinating substrates are the fluorinated hypochlorite porphyrin complexes, $[Fe^{III}(TPFP)(OCl)_2]^{-}$ and $[Fe^{III}(TPFP)(OCl)(1-Me-Im)]$ (1-Me-Im = 1-methylimidazol (Fig. 15 and Fig. 19). Fujii and coworkers [139] tested both complexes in their ability to chlorinate the primed substrate 1,3,5-trimethoxybenzene at $-60^{\circ}C$. Interestingly, only the dihypochlorite complex is active. The reactivity of $[Fe^{III}(TPFP)(OCl)_2]^{-}$ and the lack-hereof for

Scheme 20 Reactions of iron(IV)-oxo and iron(III)-OOH adducts with bromide

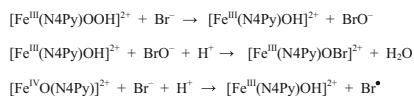
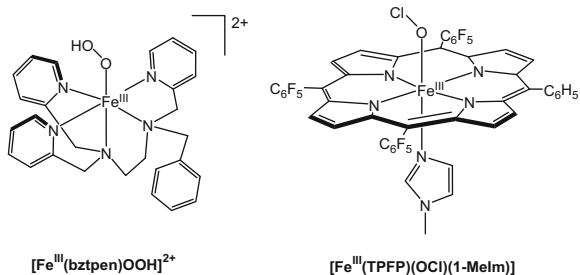
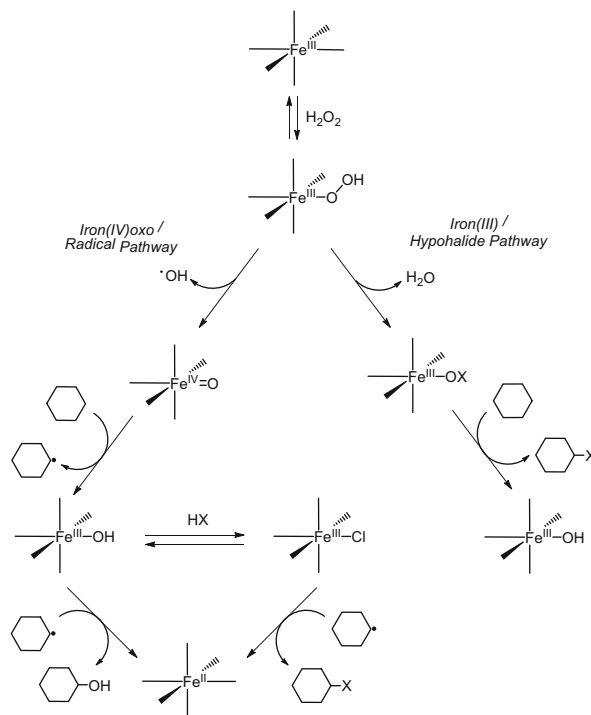


Fig. 19 Complexes used in the chlorination of hydrocarbon substrates



the imidazole-substituted complex is accompanied by a much enhanced stability of the latter. By monitoring the decay of both species by UV–Vis spectroscopy, it is seen that the Fe(III)-hypochlorite adducts decay to give $\text{Fe}^{\text{IV}}\text{O}(\text{porph}^{+})$ species. In a related study, the authors took another approach and first, using ozone, generated a porphyrin- π -cation radical, $[\text{Fe}^{\text{IV}}\text{O}(\text{TPFP}^{+})(\text{NO}_3)]^{2+}$, which was then exposed to a mixture of chloride and trifluoroacetic acid. This system is also active in the chlorination of aromatic and aliphatic substrates [140]. The related manganese(III) complex $[\text{Mn}^{\text{III}}(\text{TPP})\text{Cl}]$ has likewise been shown capable of catalyzing rather selective chlorinations and fluorinations of a wide range of aromatic and aliphatic substrates, using ClO^- and AgF/PhIO , respectively [141, 142].

From the existing literature in the field, it seems appropriate to suggest two candidates for the active oxidant in the halogenation of hydrocarbons by iron complexes. Either the active halogenating agent is a putative iron(III)-hypohalide adduct – generated directly with added hypochloride or hypobromide – or generated in situ from hydrogen peroxide and a halide source. Alternatively, the active oxidant is an iron(IV)-oxo species with a co-coordinated halide as second auxiliary ligand. In the first case, a concerted transition state is to be expected where the role of the iron center is to act as a polarizing Lewis acid that activates the oxygen atom, without undergoing any spin state changes. In the case of an iron(IV)-oxo adduct as the active oxidant, a rebound mechanism as detailed previously must be at play. This will explain the co-formation of hydroxylated products. It is not unlikely that in the case of $\text{H}_2\text{O}_2/\text{Cl}^-$ systems both mechanisms can potentially be active, but that the dominating pathway is dependent on the specific iron system, and thus a matter of choosing the right supporting ligand. In this respect, it should be reiterated that some iron(III)-hydroperoxide complexes decay spontaneously to give iron(IV)-oxo species, while others do not. Summarizing these mechanistic considerations, Scheme 21 is proposed.



Scheme 21 A collective mechanistic proposal for the halogenation of C–H bonds by iron(III)/ $\text{H}_2\text{O}_2/\text{X}^-$ systems

8 Electrophilic Reactions of Iron-Nitrido and Iron-Imido Intermediates

Just as iron can be stabilized in high-valent oxo states ($\text{Fe}^{\text{IV}}=\text{O}$ and $\text{Fe}^{\text{V}}=\text{O}$) in complexes of a wide variety of ligands, so are analogous iron-nitrido ($\text{Fe}^{\text{V}}\equiv\text{N}$) and iron-imido ($\text{Fe}^{\text{IV}}=\text{NR}$) species accessible [107]. Some examples are shown in Fig. 20. While the chemistry of iron nitride/imido systems is much less developed, it is obvious that there are many parallels due to their common electrophilic nature [90]. The electrophilicity of these high-valent species translates into an ability to react with electron-rich substrates, and in the same ways as iron-oxo adducts are capable of epoxidizing alkenes and oxygenate sulfides and sulfoxides, so are iron-nitrido and iron-imido adducts capable of inserting an imido group into alkenes and sulfides/sulfoxides to generate the analogous aziridines and sulfimides/sulfoximides. An overview of O- and N-oxidized sulfide derivatives is given in Scheme 23. The parallels can be illustrated with an example. In Scheme 22, an epoxidation of *trans*-stilbene by a hypothetical iron(IV)-oxo complex together with an analogous aziridination of *trans*-stilbene by an iron(IV)-imido adduct is shown. In both cases, the high-valent iron complexes are generated from the reaction of an

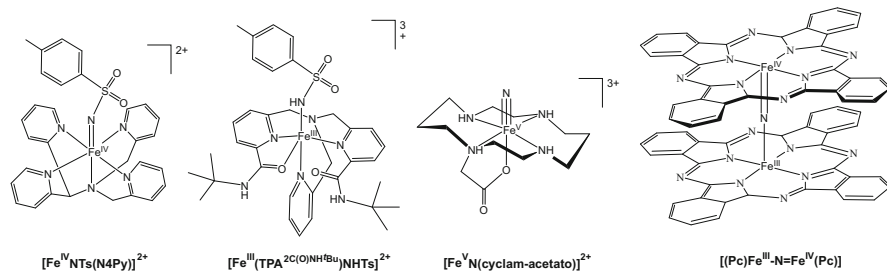
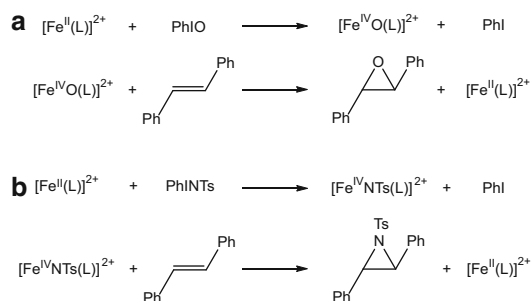
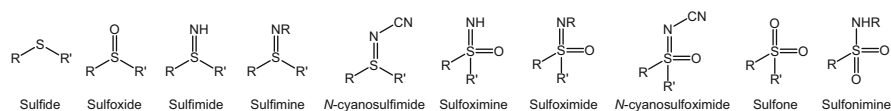


Fig. 20 Examples of iron-imido and iron-nitrido complexes



Scheme 22 Generalized reaction schemes for the (a) epoxidation and (b) aziridination of the alkene trans-stilbene by iron(IV) = X complexes (X=O, NTs)



Scheme 23 Sulfide and its oxygen and nitrogen oxidated derivatives

iron(II) precursor complex with a hypervalent iodine transfer reagent, in this example PhIO and *N*-tosyliodinane (PhINTs), respectively.

Just as iron(IV)-oxo intermediates are very strong hydrogen abstractors capable of removing hydrogens from unactivated hydrocarbons, so are iron(IV)-imido intermediates. An example of this is provided by Chang and coworkers [143] who reacted the iron(II) compound $[\text{Fe}^{\text{II}}(\text{TPA}^{2\text{C}(\text{O})\text{NHtBu}})]^{2+}$ with PhINTs at $-40\text{ }^\circ\text{C}$, leading to the generation of a transient chromophore – likely the corresponding iron(IV)-imido complex $[\text{Fe}^{\text{IV}}\text{NTs}(\text{TPA}^{2\text{C}(\text{O})\text{NHtBu}})]^{2+}$. Upon warming to ambient temperatures, the species reacted with an unknown substrate in a hydrogen-abstraction reaction to give an iron(III)-NHTs species, $[\text{Fe}^{\text{III}}(\text{TPA}^{2\text{C}(\text{O})\text{NHtBu}})(\text{NHTs})]^{2+}$ (Fig. 20). Sorokin and coworkers have demonstrated that the high-valent diiron phthalocyanine species $[(\text{Pc})\text{Fe}^{\text{III}}-\text{N}=\text{Fe}^{\text{IV}}(\text{Pc})]$ (Fig. 20) is capable of activating H_2O_2 and TBHP towards the defluorination of fluorinated aromatic

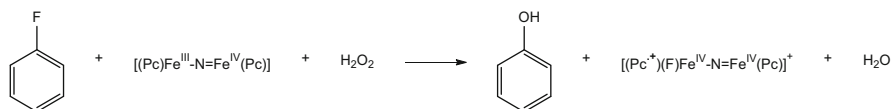
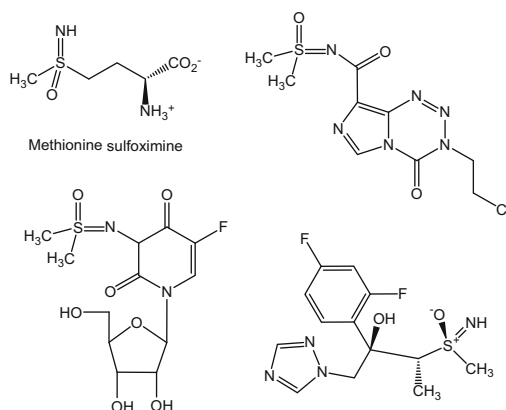


Fig. 21 Defluorination of fluorobenzene by an diiron(III)-nitrido bridged species



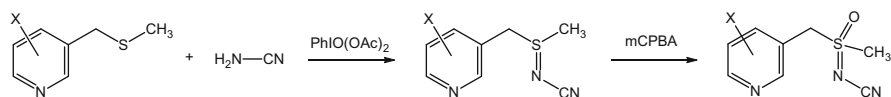
Scheme 24 Examples of biologically active molecules containing the S=N motif

compounds [144]. This reaction was subsequently successfully converted to a catalytic reaction. Carbon-fluoride bonds are some of the strongest known, which makes this an impressive achievement (Fig. 21).

In another recent study, Vardhaman et al. [90] compared the two high-valent species $[\text{Fe}^{\text{IV}}\text{O}(\text{N4Py})]^{2+}$ and $[\text{Fe}^{\text{IV}}\text{NTs}(\text{N4Py})]^{2+}$ (Fig. 20) in their ability to act as oxidants in heteroatom transfer reactions with the sulfide thioanisole and as hydrogen-atom abstractors with xanthene, dihydroanthracene, and cyclohexadiene. The nitrido species is found to be much faster than the oxo species in all reactions, suggesting that the iron-nitrido species is a stronger electrophile. This is confirmed by the Hammett plot for a series of *para*-substituted thioanisoles, which gives a much more negative slope for the iron-nitrido species than for the iron-oxo species.

Sulfimides ($\text{R}_2\text{S}=\text{NH}$) and sulfines ($\text{R}_2\text{S}=\text{NR}$) and their derivatives, like *N*-cyanosulfimides ($\text{R}_2\text{S}=\text{N}-\text{C}\equiv\text{N}$) and sulfoximides ($\text{O}=\text{S}(\text{R}_2)=\text{N}$), are not uncommon in pharmaceutical and agrochemical lead compounds. Some examples of biologically active sulfoximines and sulfoximides [145], including the phosphorylase inhibitor methionine sulfoximine, are shown in Scheme 24.

A representative example of the state-of-the-art in industry for the production of *N*-oxidized sulfides in a synthetic route for *N*-cyanosulfimides and *N*-cyanosulfoximides is illustrated in Scheme 25, and described in a recent patent from Dow AgroSciences. [146]. The sulfide is first oxidized to *N*-cyanosulfimide using cyanamide as *N*-donor and $\text{PhI}(\text{OAc})_2$ as oxidant (possibly with $\text{PhI}=\text{N}-\text{CN}$ or $\text{PhI}(\text{NHCN})_2$ as the active oxidant [147]). The *N*-cyanosulfimide is then oxygenated using the peracid *m*CPBA. This process could be a future target for a significant



Scheme 25 Conventional synthesis of N-oxidized sulfides

improvement in atom economy if a Fe-catalyst/ O_2 /reductant or Fe-catalyst/ H_2O_2 regime could be implemented in place of the stoichiometric use of $PhI(OAc)_2$ and mCPBA.

9 Intramolecular Ligand Oxidations

The self-degradation of the ligand in metal complexes during exposure to large excesses of oxidants under catalytic conditions should not be ignored. A helpful mental exercise is to inspect the ligands in Fig. 3. It is not difficult to imagine the various alkyl and aryl C–H bonds which could be subjected to oxidative attack. They may in fact be even more activated to do just that when the ligands are coordinated. Endogenous ligand oxidation may however not always detrimental. In some special cases an in situ activation of the complex might be a requisite activating step. For example, the posttranslational oxygenation of the cysteine donors to the nonheme iron atom occurs in the activation of nitrile hydratase [158]. An obvious method for addressing the potential instability of a supporting ligand and/or complex is to study the reactions of the pro-catalysts with oxidants and identify the resultant iron species. A true catalyst should of course not be consumed. The insights gained from examination the degradation products are twofold: Firstly the observation of the cleavage or oxygenation of certain parts of the ligand scaffold gives direct information on the vulnerabilities of the ligand and thereby hints at how ligand design can be improved. Secondly, the characterization of “degraded” complexes can be informative for gleaning mechanistic details [72, 100, 148–157]. Particularly interesting with the view to greener oxidation chemistry are those reactions which imply O_2 activation. Degradation products can give clues for the next iteration in rational catalyst design.

The vulnerability of the often present methylene groups linking amine and pyridine donors towards oxidation by TBHP in basic organic solvent was demonstrated for the iron complexes of tpa and related di(2-pyridylmethyl)amine (dpa) in the presence of ca. 33 equivalents of TBHP [72]. After removal of iron by cyanide and workup, together with unaffected tpa, several of its oxidized derivatives were identified (Fig. 22). Chemically equivalent products were obtained in analogous experiments using $[Fe(dpa)_2](OTf)_2$. Complex robustness will however depend on reaction conditions and even the actual presence of substrate. These results illustrate the importance of checking catalyst integrity after reactions.

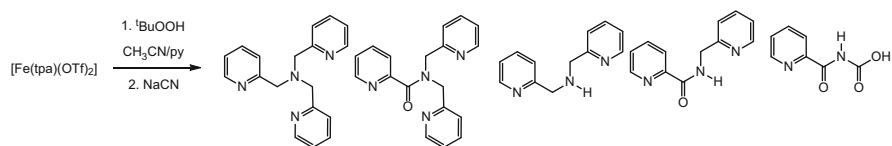


Fig. 22 Products from the oxidation of the aminopyridyl ligand in $[\text{Fe}(\text{tpa})(\text{OTf})_2]$ when treated with an excess TBHP in acetonitrile/pyridine under conditions simulating catalytic reactions, however without the presence of substrate

The removal or replacement of the oxidatively susceptible part of a ligand may inhibit suicidal self-oxidation and thereby preserve the activity of the iron catalyst during the harsh working conditions. Bpmen (Fig. 3) is used for both manganese- and iron-based oxidation catalysts [160]. Britovsek and coworkers compared $[\text{Fe}^{\text{II}}(\text{bpmen})(\text{OTf})_2]$ with the iron complex of the parent non-methylated ligand and found that the unmethylated complex was significantly less catalytically active [157]. The reason for this is likely to be that the amine NH groups are susceptible to oxidative conversion to imines [161] or amides [72]. Methylation of the amine groups effectively prevents this reaction and endows some steric constraints. $[\text{Fe}^{\text{II}}(\text{bpmen})X_2]$ complexes however are still susceptible to deactivation through μ -oxo formation (see Sect. 4.2), especially in the presence of aqueous oxidants like H_2O_2 [155, 157].

N-Dealkylations make the ubiquitous amine connector a potential weak link. As outlined by Britovsek and coworkers, an adjacent CH_2 group can be oxidized to form a hemiaminal ($\text{N}-\text{CH}-\text{OH}$) group [157]. An *N*-bound hemiaminal complex can isomerize easily to the corresponding *O*-bonded ($\text{NH}-\text{CH}-\text{O}^-$) complex. Examples of such rearranged systems have been isolated several times [148, 149, 151, 162]. Alternatively if the amine group is linked to a methylpyridine or a methylbenzyl group, a cleavage reaction can occur with the formation of an amide complex, or it can perhaps further oxidized to a picolinate complex. Formation of stable picolinate complexes of transition metal ions derived from more elaborate ligands have been reported on several occasions [152, 153, 163, 164]. There is no reason to assume that iron complexes will be immune to this particular ligand degradation. Indeed, ligand degradation reactions via oxidative *N*-dealkylation has recently been observed for $[\text{Fe}^{\text{II}}(\text{bpmcn})\text{Cl}_2]^{2+}$ during catalytic toluene oxidation with H_2O_2 [155]. Further examples of endogenous amine linker oxidations are shown in Fig. 23. In the first example the dangling benzyl groups on the classic bpmen scaffold are subject to different ligand oxidations, dependent on the presence or not of chloride as co-ligand in the starting iron(II) complex. In their presence, the benzene moiety is *C*-*H* hydroxylated, while in their absence *N*-dealkylation occurs (Fig. 23a) [150]. The methoxylation of the amide containing PaPy3 ligand in Fig. 23b is initiated by the formation of a hydroperoxide complex which was spectroscopically characterized [53]. Nucleophilic attack by methanol on the carbon $\text{C}=\text{N}$ bond to the amide would seem to be aided by the heterolytic *O*-*O* cleavage and possible the transient formation of a strong Lewis acidic iron(V)oxo

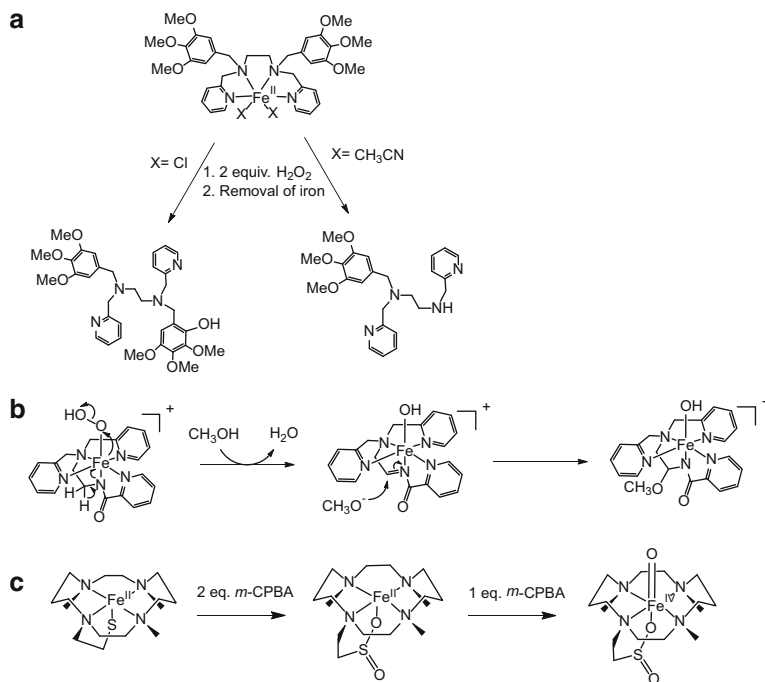


Fig. 23 (a) Different ligand oxidation reactions depending on the type of auxiliary ligand. (b) Methoxylation of a Fe(III) amide complex. (c) Stepwise oxygen atom addition to the thiolato ligand in an Fe(II) complex

species. Sulfur donors are particularly prone to conversion into sulfoxides and sulfones. The complex $[\text{Fe}^{\text{II}}(\text{TMCS})]^{2+}$, which has a pendant thiolate group attached to its cyclam ligand, can be sulfoxidized if exposed to *m*CPBA (Fig. 23c). If, however, base is added before the addition of *m*CPBA, the sulfur oxygenation is prevented and the Fe(IV)oxo species in Fig. 12a is formed instead [159].

The involvement of an undetected Fe(V)oxo species in an intramolecular O-atom transfer is entirely credible for the complexes of the pentadentate carboxylato ligands, *bzbpna*⁻ and *mebpna*⁻. Both ligands form stable Fe(III) complexes; however, these can activate O₂ and peroxides. In the case of $[\text{Fe}(\text{bzbpna})\text{OH}]^+$, the dangling benzene group is hydroxylated in the presence of air when ascorbic acid is provided as the reductant [151]. Solutions change from yellow to dark blue over a few hours, indicating the formation of an iron(III)-phenolato complex, as depicted in Fig. 24a. Thus, it seemed obvious that the removal of this sensitive part of the ligand might be a way of trapping an iron(V) oxo species. Instead, the use of the homologue *metpna*⁻ gives an unexpected outcome: the regioselective oxygenation of one of the amine N atoms (Fig. 24b). The crystallographically characterized product seems rather unfavorable, given its

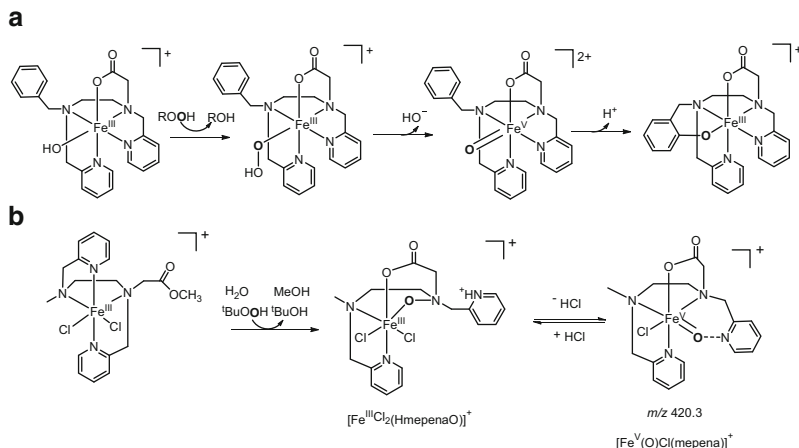


Fig. 24 (a) Intramolecular oxygenation of the dangling benzene moiety in $[\text{Fe}^{\text{III}}(\text{bztpena})\text{OH}]^+$ via a putative Fe(V)oxo generated by heterolytic O–O cleavage of a precursor hydroperoxo species to give $[\text{Fe}^{\text{III}}(\text{btpenaO})]^+$ (b) Regioselective amine N-oxygenation of $[\text{Fe}^{\text{III}}(\text{metpena})\text{Cl}_2]$ and the structural assignment of an ion in its ESI mass spectrum which can be related to the isolated product by intramolecular O-atom transfer and loss of neutral HCl

7-membered chelate ring. It is indeed quite unexpected that if an oxygen atom is to be inserted regioselectively into one of the iron-ligand bonds of a complex such as this, it is inserted into a particular amine-iron bond rather than a pyridine-iron bond (to give a coordinated pyridine N-oxide) or the carboxylato-iron bond (to give a coordinated peracid). The observation of an ion in the mass spectra of the reactions solutions, assignable as “ $[\text{Fe}^{\text{V}}(\text{O})\text{Cl}(\text{mepena})]^+$,” gives some clues to the formation of this unusual molecule. This apparent iron(V)oxo complex could potentially be formed by an intramolecular O-atom migration and reformation of a Fe–N bond concurrent with deprotonation and coordination of the dangling pyridine associated with neutral HCl loss. Similarly to the *I*-oxide complex, Fe(III)-OIPh of the related hexadentate ligand, Scheme 19, the N-oxide complex, $[\text{Fe}^{\text{III}}\text{Cl}_2(\text{HmepenaO})]^+$ might be regarded as a latent Fe(V)oxo species.

10 Conclusions and Outlook

Iron-based oxidation chemistry is incredibly rich and currently in a state of rapid expansion. We have attempted to provide a comprehensive coverage of the most important findings from the viewpoint of stoichiometric reactions in the solution phase.

From our survey of the literature, it is clear that tremendous progress has been made in identifying pertinent iron-based oxidants and the types of ligand systems which can support them. These ligands will be expected to withstand chemically

harsh conditions, for example, the presence of excess oxidants, and an awareness of their potential weak points is increasing. Over the years, focus has moved away from the iron porphyrins and onto the nonheme systems. However, other conjugated systems like the corroles have been somewhat neglected and deserve more attention. The prevalence in nature of metalloenzymes for neutralizing aggressive reactive oxygen species like superoxide shows us that oxidative resistance of the supporting ligands of a catalyst is possible to achieve.

What is especially pleasing is the significant progress made in the understanding of how the environmentally attractive, but difficult, oxidants O_2 and H_2O_2 , are activated. Iron does indeed seem to possess some unique qualities here. We predict that within the next couple decades that the art of harnessing and controlling the oxidizing powers of the ultimate green terminal oxidant – dioxygen will have been mastered. Another highlight, and an area for which we anticipate great growth, is the dawning research topic of iron-nitrido and iron-sulfido chemistry. Here oxidative chemistry is taken in a new direction and is moved away from the traditional oxygen-atom insertions, and onto more elaborate oxidative coupling chemistry – in analogy with the reductive couplings well-known from modern organic chemistry.

References

1. Enthaler S, Junge K, Beller M (2008) *Angew Chem Int Ed* 47:3317–3321
2. Talsi EP, Bryliakov KP (2012) *Coord Chem Rev* 256:1418–1434
3. Punniyamurthy T, Velusamy S, Iqbal J (2005) *Chem Rev* 105:2329–2363
4. Srour H, Le Maux P, Chevance S, Simonneaux G (2013) *Coord Chem Rev* 257:3030–3050
5. Caron S, Dugger RW, Ruggeri SG, Ragan JA, Ripin DHB (2006) *Chem Rev* 106:2943–2989
6. Sun X (2013) *Organic mechanisms: reactions, methodology, and biological applications*. Wiley, Hoboken
7. Nicolaou KC, Baran PS, Zhong Y-L, Barluenga S, Hunt KW, Kranich R, Vega JA (2002) *J Am Chem Soc* 124:2233–2244
8. Nicolaou KC, Montagnon T, Baran PS, Zhong Y-L (2002) *J Am Chem Soc* 124:2245–2258
9. Bach RD, Canepa C, Winter JE, Blanchette PE (1997) *J Org Chem* 62:5191–5197
10. Lange SJ, Que L Jr (1998) *Curr Opin Chem Biol* 2:159–172
11. Van der Donk WA, Krebs C, Bollinger JM (2010) *Curr Opin Struct Biol* 20:673–683
12. Abu-Omar MM, Loaiza A, Hontzeas N (2005) *Chem Rev* 105:2227–2252
13. Costas M, Mehn MP, Jensen MP, Que L (2004) *Chem Rev* 104:939–986
14. Bruijninx PCA, van Koten G, Gebbink R (2008) *Chem Soc Rev* 37:2716–2744
15. Suslick K (2000) *Porphyr Handb* 4:41–60
16. Torres Pazmiño DE, Winkler M, Glieder A, Fraaije MW (2010) *J Biotechnol* 146:9–24
17. Rittle J, Green MT (2010) *Science* 330:933–937
18. Svastits EW, Dawson JH, Breslow R, Gellman SH (1985) *J Am Chem Soc* 107:6427–6428
19. Sono M, Roach MP, Coulter ED, Dawson JH (1996) *Chem Rev* 96:2841–2888
20. Vineyard BD, Knowles WS, Sabacky MJ, Bachman GL, Weinkauff DJ (1977) *J Am Chem Soc* 99:5946–5952
21. Yudin AK (2006) *Aziridines and epoxides in organic synthesis*. Wiley, Weinheim
22. Wojaczyńska E, Wojaczyński J (2010) *Chem Rev* 110:4303–4356
23. Legros J, Dehli JR, Bolm C (2005) *Adv Synth Catal* 347:19–31
24. Jang HG, Cox DD, Que L Jr (1991) *J Am Chem Soc* 113:9200–9204

25. Cox DD, Benkovic SJ, Bloom LM, Bradley FC, Nelson MJ, Que L, Wallick DE (1988) *J Am Chem Soc* 110:2026–2032
26. Cox DD, Que L (1988) *J Am Chem Soc* 110:8085–8092
27. Pyrz JW, Roe AL, Stern LJ, Que L (1985) *J Am Chem Soc* 107:614–620
28. Chakraborty B, Bhunya S, Paul A, Paine TK (2014) *Inorg Chem* 53:4899–4912
29. Phillips SEV (1978) *Nature* 273:247–248
30. Collman JP, Gagne RR, Reed CA, Robinson WT, Rodley GA (1974) *Proc Natl Acad Sci* 71:1326–1329
31. Momenteau M, Reed CA (1994) *Chem Rev* 94:659–698
32. Mbughuni MM, Chakrabarti M, Hayden JA, Bominaar EL, Hendrich MP, Munck E, Lipscomb JD (2010) *Proc Natl Acad Sci U S A* 107:16788–16793
33. Feig AL, Lippard SJ (1994) *Chem Rev* 94:759–805
34. Korendovych IV, Kryatov SV, Rybak-Akimova EV (2007) *Acc Chem Res* 40:510–521
35. Shan X, Que L (2005) *Proc Natl Acad Sci U S A* 102:5340–5345
36. Korendovych IV, Staples RJ, Reiff WM, Rybak-Akimova EV (2004) *Inorg Chem* 43:3930–3941
37. Chiang C-W, Kleespies ST, Stout HD, Meier KK, Li P-Y, Bominaar EL, Que L, Münck E, Lee W-Z (2014) *J Am Chem Soc* 136:10846–10849
38. Sastri CV, Lee J, Oh K, Lee YJ, Lee J, Jackson TA, Ray K, Hirao H, Shin W, Halfen JA, Kim J, Que L, Shaik S, Nam W (2007) *Proc Natl Acad Sci* 104:19181–19186
39. Horswill EC, Ingold KU (1966) *Can J Chem* 44:269–277
40. Wei M, Musie GT, Busch DH, Subramaniam B (2004) *Green Chem* 6:387–393
41. Çimen Y, Türk H (2007) *J Mol Catal A Chem* 265:237–243
42. Zang Y, Elgren TE, Dong Y, Que L (1993) *J Am Chem Soc* 115:811–813
43. Bernal I, Jensen IM, Jensen KB, McKenzie CJ, Toftlund H, Tuchagues JP (1995) *J Chem Soc-Dalton Trans* 3667–3675
44. Jensen KB, McKenzie CJ, Nielsen LP, Pedersen JZ, Svendsen HM (1999) *Chem Commun* 1313–1314
45. Cho J, Jeon S, Wilson SA, Liu LV, Kang EA, Braymer JJ, Lim MH, Hedman B, Hodgson KO, Valentine JS, Solomon EI, Nam W (2011) *Nature* 478:502–505
46. Hashimoto K, Nagatomo S, Fujinami S, Furutachi H, Ogo S, Suzuki M, Uehara A, Maeda Y, Watanabe Y, Kitagawa T (2002) *Angew Chem Int Ed* 41:1202–1205
47. Wada A, Ogo S, Nagatomo S, Kitagawa T, Watanabe Y, Jitsukawa K, Masuda H (2002) *Inorg Chem* 41:616–618
48. Zang Y, Kim J, Dong YH, Wilkinson EC, Appelman EH, Que L (1997) *J Am Chem Soc* 119:4197–4205
49. Ho RYN, Roelfes G, Feringa BL, Que L (1999) *J Am Chem Soc* 121:264–265
50. Shearer J, Scarrow RC, Kovacs JA (2002) *J Am Chem Soc* 124:11709–11717
51. Widger LR, Jiang Y, McQuilken AC, Yang T, Siegler MA, Matsumura H, Moënné-Loccoz P, Kumar D, de Visser SP, Goldberg DP (2014) *Dalton Trans* 43:7522–7532
52. Rowland JM, Olmstead M, Mascharak PK (2001) *Inorg Chem* 40:2810–2817
53. Bukowski MR, Zhu S, Koehntop KD, Brennessel WW, Que L (2004) *J Biol Inorg Chem* 9:39–48
54. Lubben M, Meetsma A, Wilkinson EC, Feringa B, Que L (1995) *Angew Chem Int Ed Engl* 34:1512–1514
55. Ho RYN, Jr LQ, Roelfes G, Feringa BL, Hermant R, Hage R (1999) *Chem Commun* 2161–2162
56. Roelfes G, Vrajmasu V, Chen K et al (2003) *Inorg Chem* 42:2639–2653
57. Simaan AJ, Döpner S, Banse F, Bourcier S, Bouchoux G, Boussac A, Hildebrandt P, Girerd J-J (2000) *Eur J Inorg Chem* 2000:1627–1633
58. Martinho M, Dorlet P, Riviere E, Thibon A, Ribal C, Banse F, Girerd JJ (2008) *Chemistry* 14:3182–3188

59. Hazell A, McKenzie CJ, Nielsen LP, Schindler S, Weitzer M (2002) *J Chem Soc Dalton Trans* 310–317
60. Horner O, Jeandey C, Oddou J-L, Bonville P, McKenzie CJ, Latour J-M (2002) *Eur J Inorg Chem* 2002:3278–3283
61. Chishiro T, Shimazaki Y, Tani F, Tachi Y, Naruta Y, Karasawa S, Hayami S, Maeda Y (2003) *Angew Chem Int Ed* 42:2788–2791
62. Annaraj J, Suh Y, Seo MS, Kim SO, Nam W (2005) *Chem Commun* 4529–4531
63. Neese F, Solomon EI (1998) *J Am Chem Soc* 120:12829–12848
64. Kim J, Larka E, Wilkinson EC, Que L (1995) *Angew Chem Int Ed Engl* 34:2048–2051
65. Jensen MP, Costas M, Ho RYN, Kaizer J, Payeras AMI, Munck E, Que L, Rohde JU, Stubna A (2005) *J Am Chem Soc* 127:10512–10525
66. Krishnamurthy D, Kasper GD, Namuswe F, Kerber WD, Sarjeant AAN, Moenne-Loccoz P, Goldberg DP (2006) *J Am Chem Soc* 128:14222–14223
67. Lehnert N, Ho RYN, Que L, Solomon EI (2001) *J Am Chem Soc* 123:12802–12816
68. Gosiewska S, Permentier HP, Bruins AP, Koten G van, Gebbink RJMK (2007) *Dalton Trans* 3365–3368
69. Nebe T, Beitat A, Würtele C, Dücker-Benfer C, van Eldik R, McKenzie CJ, Schindler S (2010) *Dalton Trans* 39:7768–7773
70. Rohde JU, Torelli S, Shan XP, Lim MH, Klinker EJ, Kaizer J, Chen K, Nam WW, Que L (2004) *J Am Chem Soc* 126:16750–16761
71. Bryliakov KP, Talsi EP (2014) *Coord Chem Rev* 276:73–96
72. Lenze M, Martin ET, Rath NP, Bauer EB (2013) *ChemPlusChem* 78:101–116
73. Thibon A, Jollet V, Ribal C, Senechal-David K, Billon L, Sorokin AB, Banse F (2012) *Chem Eur J* 18:2715–2724
74. Liu LV, Hong S, Cho J, Nam W, Solomon EI (2013) *J Am Chem Soc* 135:3286–3299
75. Ohta T, Liu J-G, Naruta Y (2013) *Coord Chem Rev* 257:407–413
76. McCandlish E, Miksztal AR, Nappa M, Sprenger AQ, Valentine JS, Stong JD, Spiro TG (1980) *J Am Chem Soc* 102:4268–4271
77. Makhlynets OV, Das P, Taktak S, Flook M, Mas-Balleste R, Rybak-Akimova EV, Que L (2009) *Chem Eur J* 15:13171–13180
78. Taktak S, Flook M, Foxman BM, Lawrence Que J, Rybak-Akimova EV (2005) *Chem Commun* 5301–5303
79. Rohde J-U, In J-H, Lim MH, Brennessel WW, Bukowski MR, Stubna A, Müncker E, Nam W, Que L Jr (2003) *Science* 299:1037–1039
80. Klinker EJ, Kaizer J, Brennessel WW, Woodrum NL, Cramer CJ, Que L Jr (2005) *Angew Chem Int Ed Engl* 44:3690–3694
81. Thibon A, England J, Martinho M, Young VG, Frisch JR, Guillot R, Girerd J-J, Münck E, Que L, Banse F (2008) *Angew Chem Int Ed* 47:7064–7067
82. Lacy DC, Gupta R, Stone KL, Greaves J, Ziller JW, Hendrich MP, Borovik AS (2010) *J Am Chem Soc* 132:12188–12190
83. England J, Martinho M, Farquhar ER, Frisch JR, Bominaar EL, Münck E, Que L (2009) *Angew Chem Int Ed* 48:3622–3626
84. Donald WA, McKenzie CJ, O’Hair RAJ (2011) *Angew Chem Int Ed* 50:8379–8383
85. Fukuzumi S, Morimoto Y, Kotani H, Naumov P, Lee Y-M, Nam W (2010) *Nat Chem* 2:756–759
86. Tiago de Oliveira F, Chanda A, Banerjee D, Shan XP, Mondal S, Que L, Bominaar EL, Munck E, Collins TJ (2007) *Science* 315:835–838
87. Nehru K, Seo MS, Kim J, Nam W (2007) *Inorg Chem* 46:293–298
88. Lee Y-M, Hong S, Morimoto Y, Shin W, Fukuzumi S, Nam W (2010) *J Am Chem Soc* 132:10668–10670
89. Vardhaman AK, Sikdar S, Sastri CV (2011) *Indian J Chem* 50A:427–431
90. Vardhaman AK, Barman P, Kumar S, Sastri CV, Kumar D, de Visser SP (2013) *Angew Chem Int Ed* 52:12288–12292

91. Park J, Morimoto Y, Lee Y-M, Nam W, Fukuzumi S (2014) *Inorg Chem* 53:3618–3628
92. Park J, Morimoto Y, Lee Y-M, Nam W, Fukuzumi S (2011) *J Am Chem Soc* 133:5236–5239
93. McDonald AR, Que L (2013) *Coord Chem Rev* 257:414–428
94. Ghosh A, Mitchell DA, Chanda A, Ryabov AD, Popescu DL, Upham EC, Collins GJ, Collins TJ (2008) *J Am Chem Soc* 130:15116–15126
95. Popescu D-L, Vrabel M, Brausam A, Madsen P, Lente G, Fabian I, Ryabov AD, van Eldik R, Collins TJ (2010) *Inorg Chem* 49:11439–11448
96. Groves JT, Kruper WJ, Haushalter RC, Butler WM (1982) *Inorg Chem* 21:1363–1368
97. Pfaff FF, Kundu S, Risch M et al (2011) *Angew Chem Int Ed* 50:1711–1715
98. Wu X, Seo MS, Davis KM, Lee Y-M, Chen J, Cho K-B, Pushkar YN, Nam W (2011) *J Am Chem Soc* 133:20088–20091
99. Collman JP, Chien AS, Eberspacher TA, Zhong M, Brauman JI (2000) *Inorg Chem* 39:4625–4629
100. Vad MS, Lennartson A, Nielsen A, Harmer J, McGrady JE, Frandsen C, Morup S, McKenzie CJ (2012) *Chem Commun* 48:10880–10882
101. Sastri CV, Seo MS, Park MJ, Kim KM, Nam W (2005) *Chem Commun* 1405–1407
102. Fillol JL, Codola Z, Garcia-Bosch I, Gomez L, Pla JJ, Costas M (2011) *Nat Chem* 3:807–813
103. Codolà Z, Gómez L, Kleespies ST, Que L Jr, Costas M, Lloret-Fillol J (2015) *Nat Commun* 6:5865. doi:10.1038/ncomms6865
104. Wang D, Ray K, Collins MJ et al (2012) *Chem Sci* 4:282–291
105. Collins MJ, Ray K, Que L (2006) *Inorg Chem* 45:8009–8011
106. Kotani H, Suenobu T, Lee Y-M, Nam W, Fukuzumi S (2011) *J Am Chem Soc* 133:3249–3251
107. Hohenberger J, Ray K, Meyer K (2012) *Nat Commun* 3:720
108. Chandrasekaran P, Stieber SCE, Collins TJ, Que L, Neese F, DeBeer S (2011) *Dalton Trans* 40:11070–11079
109. George SD, Petrenko T, Neese F (2008) *J Phys Chem A* 112:12936–12943
110. Grapperhaus CA, Mienert B, Bill E, Weyhermüller T, Wieghardt K (2000) *Inorg Chem* 39:5306–5317
111. Kang Y, Chen H, Jeong YJ, Lai W, Bae EH, Shaik S, Nam W (2009) *Chem Eur J* 15:10039–10046
112. Groves JT, Haushalter RC, Nakamura M, Nemo TE, Evans BJ (1981) *J Am Chem Soc* 103:2884–2886
113. Hrycay EG, Bandiera SM (2012) *Arch Biochem Biophys* 522:71–89
114. Groves JT, Watanabe Y (1988) *J Am Chem Soc* 110:8443–8452
115. Groves JT, Nemo TE, Myers RS (1979) *J Am Chem Soc* 101:1032–1033
116. Ando W, Tajima R, Takata T (1982) *Tetrahedron Lett* 23:1685–1688
117. Nam W (2007) *Acc Chem Res* 40:522–531
118. Goh YM, Nam W (1999) *Inorg Chem* 38:914–920
119. Nam W, Lim MH, Oh SY (2000) *Inorg Chem* 39:5572–5575
120. Nam W, Choi SK, Lim MH, Rohde JU, Kim I, Kim J, Kim C, Que L (2003) *Angew Chem Int Ed* 42:109–111
121. Song WJ, Sun YJ, Choi SK, Nam W (2006) *Chem Eur J* 12:130–137
122. Nam W, Jin SW, Lim MH, Ryu JY, Kim C (2002) *Inorg Chem* 41:3647–3652
123. Nam W, Goh YM, Lee YJ, Lim MH, Kim C (1999) *Inorg Chem* 38:3238–3240
124. Traylor TG, Tsuchiya S, Byun YS, Kim C (1993) *J Am Chem Soc* 115:2775–2781
125. Lennartson A, McKenzie CJ (2012) *Angew Chem Int Ed* 51:6767–6770
126. Kwon E, Cho K-B, Hong S, Nam W (2014) *Chem Commun* 50:5572–5575
127. Brown VJ (2006) *Environ Health Perspect* 114:A656–A659
128. Mondal S, Hangun-Balkir Y, Alexandrova L, Link D, Howard B, Zandhuis P, Cugini A, Horwitz CP, Collins TJ (2006) *Catal Today* 116:554–561
129. Shen LQ, Beach ES, Xiang Y, Tshudy DJ, Khanina N, Horwitz CP, Bier ME, Collins TJ (2011) *Environ Sci Technol* 45:7882–7887

130. Do Pham DD, Kelso GF, Yang YZ, Hearn MTW (2012) *Green Chem* 14:1189–1195
131. Pham DDD, Kelso GF, Yang Y, Hearn MTW (2014) *Green Chem* 16:1399–1409
132. Kojima T, Leising RA, Yan SP, Que L (1993) *J Am Chem Soc* 115:11328–11335
133. Gozzo F (2001) *J Mol Catal A Chem* 171:1–22
134. Comba P, Wunderlich S (2010) *Chem Eur J* 16:7293–7299
135. Noack H, Siegbahn PEM (2007) *J Biol Inorg Chem* 12:1151–1162
136. Lim MH, Rohde JU, Stubna A, Bukowski MR, Costas M, Ho RYN, Munck E, Nam W, Que L (2003) *Proc Natl Acad Sci U S A* 100:3665–3670
137. Vardhaman AK, Sastri CV, Kumar D, de Visser SP (2011) *Chem Commun* 47:11044–11046
138. Fukuzumi S (2013) *Coord Chem Rev* 257:1564–1575
139. Cong Z, Yanagisawa S, Kurahashi T, Ogura T, Nakashima S, Fujii H (2012) *J Am Chem Soc* 134:20617–20620
140. Cong Z, Kurahashi T, Fujii H (2012) *J Am Chem Soc* 134:4469–4472
141. Liu W, Groves JT (2010) *J Am Chem Soc* 132:12847–12849
142. Liu W, Huang X, Cheng M-J, Nielsen RJ, Goddard WA, Groves JT (2012) *Science* 337:1322–1325
143. Soo HS, Sougrati MT, Grandjean F, Long GJ, Chang CJ (2011) *Inorg Chim Acta* 369:82–91
144. Colomban C, Kudrik EV, Afanasiev P, Sorokin AB (2014) *J Am Chem Soc* 136 (32):11321–11330
145. Reggelin M, Zur C (2000) *Synthesis* 2000:1–64
146. Babcock JM, Young CD, King JE, Kubiszak ME (2013) US Patent Application No. 0288897
147. Zhdankin VV, Stang PJ (2008) *Chem Rev* 108:5299–5358
148. Arulsamy N, Hodgson DJ (1994) *Inorg Chem* 33:4531–4536
149. Ugalde-Saldívar VM, Sosa-Torres ME, Ortiz-Frade L, Bernès S, Höpfl H (2001) *J Chem Soc Dalton Trans* 3099–3107
150. Mekmouche Y, Ménage S, Toia-Duboc C, Fontecave M, Galey J-B, Lebrun C, Pécaut J (2001) *Angew Chem Int Ed* 40:949–952
151. Nielsen A, Larsen FB, Bond AD, McKenzie CJ (2006) *Angew Chem Int Ed* 45:1602–1606
152. Lonnon DG, Craig DC, Colbran SB (2006) *Inorg Chem Commun* 9:887–890
153. Pijper D, Saisaha P, de Boer JW et al (2010) *Dalton Trans* 39:10375–10381
154. Mandon D, Jaafar H, Thibon A (2011) *New J Chem* 35:1986–2000
155. Canals M, Gonzalez-Olmos R, Costas M, Company A (2013) *Environ Sci Technol* 47:9918–9927
156. Sahu S, Quesne MG, Davies CG, Dürr M, Ivanović-Burmazović I, Siegler MA, Jameson GNL, de Visser SP, Goldberg DP (2014) *J Am Chem Soc* 136:13542–13545
157. Grau M, Kyriacou A, Martinez FC, de Wispelaere IM, White AJP, Britovsek GJP (2014) *Dalton Trans* 43:17108–17119
158. Hopmann KH (2014) *Inorg Chem* 53:2760–2762
159. McDonald AR, Bukowski MR, Farquhar ER et al (2010) *J Am Chem Soc* 132:17118–17129
160. Lyakin OY, Ottenbacher RV, Bryliakov KP, Talsi EP (2013) *Top Catal* 56:939–949
161. Saucedo-Vázquez JP, Kroneck PMH, Sosa-Torres ME (2015) *Dalton Trans* 44 (12):5510–5519
162. Yi C, Jia G, Hou G, Dai Q, Zhang W, Zheng G, Jian X, Yang C-G, Cui Q, He C (2010) *Nature* 468:330–333
163. Groni S, Dorlet P, Blain G, Bourcier S, Guillot R, Anxolabéhère-Mallart E (2008) *Inorg Chem* 47:3166–3172
164. Vad MS, Nielsen A, Lennartson A, Bond AD, McGrady JE, McKenzie CJ (2011) *Dalton Trans* 40:10698–10707

Index

A

3-Acryloyl-1,3-oxazolidin-2-one, 302
Acylsulfonamides, 120
Adamantane, 52, 341
 hydroxylation, 339
 oxidation, 163
Addition reactions, 67, 83, 242
Adiponitrile, 203
Aldehydes, 205, 329
 hydrophosphonylation, 271
 reduction, 183
Alkanes, epoxidation, 10
 hydroxylation, 158, 178, 259, 263, 330, 341
 oxidation, 10, 155, 159, 166, 298, 340
Alkenes, 173
 aminochlorination, 110
 hydroboration, 210
 reduction, 175
Alkenyl thioethers, 131
Alkenylations, 23
Alkynes, 173
 addition, 132
 aminochlorination, 111
 chlorosulfonation, 133
 chlorosulfonation, 133
 hydroboration, 210
 reduction, 175
Allenyl triazoles, 125
Allylic amination, 90, 95
Allylic amines, 88
Allylic substitution, 88, 133
Allylic sulfones, 134
Allylic thioethers, 134

Amides, 120, 202
Amination, cross-dehydrogenative, 92
Aminohydroxylation, 106
Aminopyridines, 115
2-Aminopyrimidines, 117
Amoco process, oxidation of p-xylene, 153
Anilines, 200
Antibiotics, chlorinated, 320
Arcyriarubin, 103
Aryl allyl sulfones, 134
Aryl sulphamates, 33
Arylaluminates, 41
Arylammonium triflate salts,
 cross-coupling, 24
Arylimines, aziridination, 283
Arylmagnesium chloride, 41
Arylsulfonation, 133
Asymmetric catalysis, 259
Autooxidation, metal-ion catalysed, 153
Azaferracycloheptatriene, 117
Azide adamantane, 95
Azides, 95, 101
Aziridination, 95, 98, 261
Aziridines, 320
Azomethine ylides, 303

B

Benzaldehydes, DRA, 201
Benzimidazoles, 101
Benzothiazoles, 135
Benzylic imidazoles, 92
Binaphthyl-derived catalysts, 297

Bioinspired, 311
 Biomimetic oxidation, 259
 alkanes, 145
 Bipyridines, 264
 2,6-Bis(arylimino)pyridyl iron(II)
 complexes, 12
 Bisboryloxide, 79
 Bis(diethylphosphino)ethane, 31
 Bis(imino)pyridine, 222
 Bis(isonitrile), 303
 Bis(oxazoline) catalysts, 277
 Bis(oxazolyl)phenyl (phebox), 282
 Bis(oxazolyl)phenylamine (bopa), 279, 281
 Bis(N-pyrazolyl)pyridines, 283
 Bleomycin, 150, 151
 Boron-based nucleophiles, 38
tert-Butyl hydroperoxide (TBHP), 340

C

C–C, 7
 C–H, 90
 activation, 286, 311
 N-arylation, 94
 cross-dehydrogenative coupling, 90
 functionalization, 83
 C–N, 83, 85
 C–P, 83, 137
 C–S, 83, 128
 C–X, 9, 83
 Carbon dioxide, reduction, 202
 Carbonyl derivatives, 173
 Carboxylic acids, 173, 206
 reduction, 202
 Carboxylic esters, 204
 Catalases, 147
 Catalysis, asymmetric, 259
 enantioselective, 13
 heterogeneous, 4, 15, 231, 313
 homogeneous, 5, 15, 112, 231, 240, 259
 Chloramphenicol, 320
 Chlorostyrenes, 24
 Chlorosulfonation, 133
 Chlorosulfonation, 133
 Chlortetracycline, 320
 Cinnamylloxycarbonyl azides, 109
 Cross-coupling, 19, 83, 131
 dehydrogenative, 8, 47
 Cross-dehydrogenative coupling (CDC), 49
 Cycloaddition, 83, 103
 Cycloalkenoxycarbonyl azides, 109
 Cyclohexane, 331
 alkylation, 52

 chlorination, 341
 hydroxylation, 158
 oxidation, 157, 159
 Cyclohexanone, 130, 188, 191, 194
 Cyclohexadiene, 330, 347
 Cyclohexene, 130, 331
 epoxidation, 166, 339
 Cyclohydroamination, 111
 Cyclopentadiene, 302
 Cyclopentadienyl-Fe(II) Lewis acids, 291
 Cytochrome c oxidase, 328
 Cytochrome P450, 102, 147, 154, 279, 316,
 320, 337

D

Davies' reagent, 13
 Diamine-derived catalysts, 285
 Diamino-bis(oxazoline), 277
 Diaminobicyclo[2.2.2]octane, 274
 Dichloroanisole, 343
 2,3-Dichloro-5,6-dicyano-1,4-benzoquinone
 (DDQ), 8
 Diels–Alder, enantioselective, 281, 291
 Diene carboxylates, 22
 Dienes, 23, 73, 90, 181, 210, 219, 281, 291
 polymerization, 240
 Dienol phosphates, 23
 Dihydropyrroles, 105
 Dihydroquinazolines, 118
 Dihydroquinoline, 89
 Dinitriles, 203
 Diolefins, 217, 220
 Dioxygen, 10, 146
 activation, 311, 321–325
 Dioxygenases, 155, 319
 Diphenylquinones, 327
 Diphenyl sulfide, sulfoxidation, 339
N-(Diphenylphosphinyl)ketimine, transfer
 hydrogenation, 294
 Diphosphine ligands, 30
 Diphosphine-derived catalysts, 291
 Di(2-pyridylmethyl)amine, 348
 Dipyrromethene iron, 95
 Direct reductive amination (DRA), 201
 DOPA, 320
 Doyle–Kirmse reaction, 136

E

E–E bond, 74
 Enzymes, iron-based, 146
 Epoxidation, 311

- Epoxides, 320
 ring opening, 119
- Esters, hydrogenation, 205
- Ethylene, oligo-/polymerization, 221
- F**
- Fenton chemistry, 3, 10, 153
- Ferrocenyl catalysts, planar-chiral, 299
- Ferryl, 10
- Fischer–Tropsch process, 5
- Formaldehyde, 207
- Formic acid, 207
- G**
- Gif chemistry, 10
- Grignard reagents, cross-coupling, 8, 22
- H**
- Halogenation, 316, 341–344
- Heme, 10, 147
- Heme peroxidases, 147
- Heteroatom–heteroatom bonds, 9
- N*-Heterocyclic carbene (NHC), 32
- 2-His-1-carboxylate facial triad, 149
- Homogeneous catalysis, 259
- Homoprotocatechuate 2,3-dioxygenase, 321
- Hydroamination, 111
- Hydroboration, 173, 210
- Hydrodehalogenation, 23
- Hydrogen peroxide, hydroxyl radicals, 153
- Hydrogen transfer, 173
- Hydrogenation, 11, 173, 175, 183, 259
- Hydrophosphination, 137
- Hydrosilylation, 11, 173, 178, 192, 259
- Hydroxycoumarin, 286
- Hydroxyphosphonates, 138
- I**
- Imidazoles, 93
- Imines, 100, 198, 301, 349
 hydrogenation, 293, 297
 reduction, 198, 299
- Indoles, aminohydroxylation, asymmetric
 intramolecular, 110
 synthesis, 112
- Iodosylbenzene, 10
- Iron, abundance, 1
 high-valent, 311
 reduction, 173
 toxicity, 1
- Iron bipyridines, chiral, 264
- Iron catalysis, 1
 metal impurities, 1
- Iron hydride, 11
- Iron nitride/imido systems, 345
- Iron peroxide adducts, nucleophilic
 reactions, 327
- Iron porphyrins, chiral, 261
- Iron-halide, 3412
- Iron-hypohalide adducts, 341
- Iron-imido, 345
- Iron-nitrido, 345
- Iron-oxo intermediates, 333
- Iron(III) tris(acetylacetonate), 22
- Iron(III)-salicylate, 332
- Isochromans, 93
- Isopenicillin N synthase, 151
- K**
- Kabachnik–Fields reaction, 139
- Ketimines, 103, 198, 293, 299
- β -Ketoesters, azidation, 125
- Ketones, reduction, 183
- Kumada couplings, 8
- L**
- Lactones, 206
- Lansoprazole, 321
- Lewis acid, 4
- Ligands, pentadentate, 159
 tetradentate, 155
- Linear alpha olefins (LAOs), 219
- Lipoxygenases, 151
- M**
- Metalloenzymes, 150
- Methane, 207
 conversion, 15
 oxidation, 146, 152
- Methane monooxygenase (MMO), 147,
 149, 151
- Methyl 2-phenylethyl ether, 204
- Michael addition, 55, 128, 138, 274, 286
- Modafinil, 321
- Monoxygenases, 319
- (*R*)-Montelukast, 129
- Mukaiyama aldol reaction, 281

N

- N*-methylpyrrolidone (NMP), 8, 22
- Nitrenes, 95, 100, 123, 283
- Nitriles, hydrogenation, 203
 - reduction, 200
- Nitroarenes, hydrogenation, 200
- Nitrogenated heterocycles, 98
- Nitroso-ene reaction, 92
- Nonheme, 10, 145, 149, 259

O

- Olefins, 217
 - aminofluorination, 280
 - aminohydroxylation, 106
 - aziridination, 98
 - oxyamination, asymmetric, 280
- Oligomerization, 12, 217, 335
- Omeprazole, 321
- Organoaluminium, 41
- Organoboronates, 210
- Oxazolidinones, 109
- Oxidants, 10, 47, 313
 - activation, 311
- Oxidases, 319
- Oxidation, 145, 154, 313
 - biomimetic oxidation, 259
- Oximes, 127
- Oxindoles, polycyclic, 130
 - Togni's reagent, 125
- β -Oxosulfones, 136
- Oxygen, activation, 311
- Oxygenases, α -keto acid dependent, 149

P

- Parkinson's disease, 23
- Peroxidase P450, 318
- Phenanthroline, 224
- 2-Phenylethanol, 204
- Phosphine donors, 30
- Polymerization, 12, 217
- Polymethylhydrosiloxane (PMHS), 192
- Porphyryns, 261
- Propargyl sulfides, 126
- Pterin, 149
- Pudovik reaction, 138
- 2-Pyranones, 22
- Pyridine bis(oxazoline) catalysts, 281
- Pyridines, synthesis, 112
- Pyrido[1,2-*a*] indoles, 94
- Pyrroles, 104

Q

- Quinolines, 72, 119, 226
- o*-Quinone methide, 276
- Quinoxalines, 198

R

- Radicals, 47
- Reduction, 11, 173, 183, 202
- Rieske dioxygenases, 149, 151

S

- Safety concern, 3
- Salan catalysts, 275
- Salen catalysts, 273
- Salicylaldehyde, 271
- Schiff base-salen-salan catalysts, chiral, 271
- Self-degradation, 348
- Si-O-B bonds, 79
- Spiro-bis(oxazoline), 277
- ST1535, 23
- Styrene, 27, 62, 65, 98, 107
 - aziridination, 284
- Succinimides, 103
- Sulfides, N-oxidized, 348
- Sulfimidation, 284
- Sulfimides, 347
- Sulfonamides, 120
- Sulfones, 134
- Sulfoxidation, 311
- Sulfoxides, reduction, 209
- Sulfoximines, 93
- Sulfur donors, 30

T

- Tetrahydropyrans, 88
- Tetrahydroquinolines, 67, 95, 118, 130, 198
- Tetramethyldisiloxane (TMDS), 192, 200
- Thio-Michael additions, 130
- Thioanisole, 347
- Thioarylation, 132
- Thioesters, 121
- Thiol synthon, 130
- Thiols, 77, 78, 128, 134, 282
 - alkenylation, 131
 - asymmetric addition, 274
- Thiovinylation, 132
- Toxicity, 2
- Transfer hydrogenation, 12, 175, 187, 291, 303
 - catalysis, 11

Triazolines, 105

Trifluoroacetic esters, 205

U

Ureas, iron-catalyzed hydrosilylation, 207

V

Vancomycin, 320

Vinyl halides, 23

2-Vinyl-piperidines, 88

W

Water, oxidation, 15

X

Xantphos, 31, 39, 131

Z

Zinc-based nucleophiles, 35